Fibrin and fibrinogen-induced signalling pathways in microglia – Implications for Neurodegeneration

Thomas Michael Piers

UCL Institute of Neurology

A thesis submitted for the degree of

Doctor of Philosophy (Ph.D)

I, Thomas Michael Piers confirm that the work presented in this thesis is my own. Where information has been derived from other sources, I confirm that this has been indicated in the thesis.

Acknowledgements

I would firstly like to thank my supervisors, Dr Jennifer Pocock and Professor Simon Heales for their support, guidance and genuine enthusiasm throughout my PhD. I would also like to further express my gratitude to Jenny for initially giving me the opportunity to work in her laboratory and I am very grateful to the Medical Research Council for providing the funding for the research.

Many thanks also go to my colleagues and peers, past and present that have helped and guided me whenever it was asked of them. In particular I'd like to thank Dr Ioanna Sevastou, Dr Claudie Hooper, Ms Emma Mead, Mrs Ulrike Traeger, Professor Sarah Tabrizi, Mr Joseph Jebelli and Ms Helen Crehan.

Finally, I would like to express my utmost thanks and gratitude to my family: Mum, Dad, Adam, Sarah and Molly and my friends: Mat, Jon and Emma who have always provided help and support, financially, emotionally and alcoholically whenever it was required. In particular I would like to thank my Mum and Dad, who painstakingly instilled a belief in me that I was capable of much more than I gave myself credit for, and last but by no means least, my fiancée Claire for her effortless patience, tolerance and humility throughout the long process. Thanks Peg.

Abstract

Blood brain barrier dysfunction and breakdown is increasingly implicated in neurodegenerative disease (NDD) pathogenesis. Recently, the blood borne protein fibrinogen and the cleaved form fibrin were shown to be involved in neuroinflammatory pathways in animal models of NDDs, with microglia, the immune cells of the central nervous system playing a central role. Studies have identified binding sites on microglia for fibrinogen and induction of an activated phenotype has been reported. Studies performed here using primary microglial and cerebellar granule cell (CGC) cultures aimed to elucidate the signalling pathways induced in microglia by fibrinogen and fibrin, and specifically how these signals affected neuronal integrity. Fibrin induced microglial death after prolonged exposure with both fibrinogen and fibrin capable of inducing significant release of the pro-inflammatory cytokines TNFα and IL-6. However, this was dependent on culture serum conditions, which also affected iNOS expression after treatment with fibrinogen. Non-apoptotic induction of caspase-3/7 expression in microglia was also proposed after treatment with fibrinogen. Characterisation of the CGCs identified the presence of a population of microglia and development of a microglial depletion technique suggested the observed population was involved in fibrinogen- and fibrin-mediated neuronal death. Further manipulation using pharmacology, microglial depletion and conditioned medium suggested that microglial TNFα release and caspase activation were specifically involved in fibrinogen- and fibrin-mediated neuronal death. Endoplasmic reticulum stress and calcium dyshomeostasis in the form of calpain activation were coupled to the microglial activation pathway as well as being associated with neuronal death after fibrinogen exposure. Neuroprotection from fibrinogen and fibrin treatment was found by co-activating specific metabotropic glutamate receptors on either microglia or neurons. Finally, translation of specific findings to a human phagocyte culture model provides strong support for the induction of the same pathways in humans.

Table of Contents

List of Figures

3. Initial characterisation of fibrinogen- and fibrin-mediated effects on microglia in different culture systems

4. Identifying and coupling a role for Endoplasmic Reticulum Stress in fibrinogen-mediated neuronal apoptosis

5. Characterisation of mGluR agonist-mediated neuroprotection from fibrinogen-mediated toxicity

List of Tables

Page

2. Materials and Methods

Abbreviations

°C - Degrees Celsius

$^{-ve}$CTR - Negative control

A_{260} - Absorbance at 260 nm

A_{280} - Absorbance at 280 nm

Aβ - Amyloid-β

AD - Alzheimer's Disease

AFU - Arbitrary fluorescence units

ALS - Amyotrophic lateral sclerosis

AMPA - (2-amino-3-(5-methyl-3-oxo-1,2-oxazol-4-yl)propanoic acid)

AMT-HCl - 2-Amino-5,6-dihydro-6-methyl-4H-1,3-thiazine hydrochloride

ANOVA - Analysis of variance

APO - Apocynin

APP - Amyloid precursor protein

APS - Ammonium persulphate

AraC - Cytosine arabinosuranoside

ATF6 - Activating transcription factor 6

ATP - Adenosine triphosphate

BAPTA-AM - 1,2-*Bis*(2-aminophenoxy)ethane-*N*,*N*,*N*',*N*'-tetraacetic acid tetrakis(acetoxymethyl ester)

BBB - Blood-brain barrier

BCL-2 - B-cell lymphoma 2

BSA - bovine serum albumin

Ca^{2+} - Calcium Ion

CAA - Cerebral amyloid angiopathy

Cal - Calpastatin

CD11b - MAC-1 Integrin receptor

cDNA - transcribed DNA

CDPPB - 3-Cyano-*N*-(1,3-diphenyl-1*H*-pyrazol-5-yl)benzamide

CgA - Chromogranin A

CGC - Cerebellar granule cell

CNS - Central nervous system

CO_2 - Carbon dioxide

CSF - Cerebrospinal fluid

CTR - Control

g - gram

Cy3 - Cyanine-3

DAPI - 4',6-diamidino-2-phenylindole

DCGIV - (2S,2'R,3'R)-2-(2',3'-dicarboxycyclopropyl) glycine

ddH_2O - Endotoxin free pure distilled water

DHE - Dihydroethidium

DHPG - (S)-3,5-dihydroxyphenylglycine

DIV - Days *in vitro*

DMEM - Dulbecco's modified eagle medium

DMSO - Dimethyl sulfoxide

DNA - Deoxyribonucleic acid

EAE - Experimental autoimmune encephalitis

EBSS - Earle's balanced salts solution

EC_{50} - 50% of effective concentration

ECL - Enhanced chemiluminescence

EDTA - Ethylene diamine tetraacetic acid

EGF - Epidermal growth factor

EGTA - Ethylene glycol tetraacetic acid

eIF2α - Eukaryotic translation initiation factor 2α

ELISA - Enzyme-linked immunosorbent assay

ER - endoplasmic reticulum

ERK1/2 - Extracellular signal-regulated kinase1/2

FACs - Fluorescence activated cell sorting

FALS - Familial amyotrophic lateral sclerosis

FAM-DEVD-FMK - Carboxyfluorescein-labelled caspase-3/7 inhibitor

FasL - Fas ligand

FBS - Foetal bovine serum

FG - Fibrinogen

FITC - Fluorescein isothiocyanate

FITC-ATAD-FMK - Carboxyfluorescein-labelled caspase-12 inhibitor

fMRI - functional Magnetic resonance imaging

FN - Fibrin

Fu - Fucoidan

g - acceleration due to gravity

MAPK - mitogen-activated protein kinase

GABA - gamma amino butyric acid

GAPDH - Glyceraldehyde 3-phosphate dehydrogenase

GFAP - glial fibrillary acidic protein

GM-CSF - Granulocyte-Macrophage Colony Stimulating Factor

GPCR - G-protein coupled receptor

h - hour

HEPES - 4-(2-hydroxyethyl)-1-piperazineethanesulfonic acid

Hi - Hirudin

hMΦ - human Monocyte-derived macrophages

Hoechst-33342 - 2´-(4-Ethoxyphenyl)-5-(4-methyl-1-piperazinyl)-2,5´-bi-1H-benzimidazole

HRP - Horse radish peroxidise

I-B_4 - *Bandeiraea simplicifolia* isolectin B_4

ICC - Immunocytochemistry

IFNγ - Interferon-γ

IgG - Immunoglobulin G

IL - interleukin

iNOS - inducible nitric oxide synthase

Ion - Ionomycin

IP_3 - Inositol trisphosphate

IRE1α - Inositol-requiring 1 homologue

JNK - c-Jun N-terminal kinase

K^+ - Potassium ions

KCl - Potassium Chloride

kDa - kiloDalton

L - litre

L-AP4 - L-(+)-2-amino-4-phosphonobutyric acid

LDH - Lactate dehydrogenase

LME - L-Leucine methyl ester

LOAD - Late onset Alzheimer's disease

LPS - Lipopolysaccharide

M - molar

PAMP - pathogen-associated molecular pattern

MEM - minimum essential medium

MG - microglia

mg - milligrams

MGCM - microglial-conditioned medium

mGluR - metabotropic glutamate receptor

MHC - Major histocompatibility complex

min - minute

ml - millilitre

mM - millimolar

mRNA - messenger ribonucleic acid

MS - multiple sclerosis

MTEP - 3-((2-Methyl-4-thiazolyl)ethynyl)pyridine

mV - milliVolt

MW - molecular weight

µg - microgram

µl - microlitre

µM - micromolar

Na^+ - Sodium Ions

NAAG - N-acetylaspartylglutamate

NADPH - nicotinamide adenine dinucleotide phosphate

NDD - Neurodegenerative disease

NFκB - nuclear factor kappa-lightchain-enhancer of activated B cells

ng - nanogram

NGS - normal goat serum

nM - nanomolar

NMDA - N-Methyl-D-aspartic acid

nNOS - neuronal nitric oxide synthase

NO - nitric oxide

NRbS - Normal Rabbit serum

ns - not statistically significant

$O_2^{\bullet-}$ - Superoxide

$ONOO^-$ - Peroxynitrite

OPC - oligodendrocyte precursor cell

p - probability value

PAGE - polyacrylamide gel electrophoresis

TGFβ - Transforming growth factor β

Th - Thapsigargin

PBMCs - Peripheral blood mononuclear cells

PBS - Phosphate buffered saline

PD - Parkinson's Disease

PDL - Poly-D-lysine

PERK - Protein kinase R-like endoplasmic reticulum kinase

pg - picogram

pH - Hydrogen ion concentration

PI - Propidium iodide

PI3K - Phosphoinositide 3-kinase

PKC - Protein kinase C

PMA - Phorbol 12-myristate 13-acetate

PMSF - Phenylmethylsulfonyl fluoride

PMX - polymyxin B

PNS - Peripheral nervous system

PRR - Pattern recognition receptors

PS1 - Presenilin-1

ROS - Reactive oxygen species

rpm - Revolutions per minute

RT - Room temperature

RT-PCR - Reverse transcription-Polymerase chain reaction

Sal - Salubrinal

SBTI - Soy bean trypsin inhibitor

SC - serum-containing

SDS-PAGE - Sodium dodecyl sulphate-Polyacrylamide gel electrophoresis

SEM - standard error of the mean

SF - serum-free

SOD1 - Superoxide dismutase 1

siRNA - Short interfering ribonucleic acid

SR-A - Scavenger receptor-A

SR-B1 - Scavenger receptor-B1

STS - Staurosporine

T_A - Annealing temperature

TEMED - N, N, N', N'-tetramethylethylenediamine

Thal - Thalidomide

TLR - Toll-like receptor

T_M - Melting temperature

TNFα - Tumour necrosis factor α

TNFR - Tumour necrosis factor receptor

tPA - Tissue-type plasminogen activator

TRITC - Tetramethyl rhodamine isothiocyanate

TTBS - Tween-20 Tris-buffered saline

Tu - Tunicamycin

uPA - Urokinase-type plasminogen activator

UPR - Unfolded protein response

Wort - Wortmannin

w/v - weight/volume

z-ATAD-FMK - carbobenzoxy -Ala-Thr-Ala-Asp(OME)-fluoromethylketone

z-VAD-FMK - carbobenzoxy-Val-Ala-Asp(OME)-fluoromethylketone

1. Introduction

1.1. Cells of the Central Nervous System

It is estimated that the human mammalian brain contains 85 billion neurons supported, maintained and protected by a further 85 billion non-neuronal cells including glia. It is becoming increasingly evident that elucidation of the neuron-glial connections and interactions will not only play a key role in our future understanding of the human nervous system but also our understanding of neurodegenerative disease progression.

1.1.1. Neurons

Neurons are specialised cells in the nervous system responsible for the sending and receiving of chemically mediated electrical signals. The nature of the signals and whether they are excitatory or inhibitory depends on the ratio of neurotransmitter released (Seal & Edwards 2006).

The morphological diversity of neuronal morphology at first glance would suggest a particularly heterogeneous population however, these structural characteristics have a great dependence on the relative cellular location, and basic neuronal anatomy and physiology tends to be relatively uniform. A typical neuron consists of the cell body, or soma, that contains the nucleus, branched cellular extensions known as dendrites that receive the vast majority of the cells excitatory or inhibitory input, and the axon, an extension from the axon hillock responsible for neuronal signal output (**Figure 1.1.1**). Signalling between neurons depends primarily on ion exchange in the axon which is mediated through voltage-gated ion channels and ion pumps including the Na^+/K^+-ATPase transversing the plasma membrane. Broadly, neurons have a negative resting membrane potential of -70 mV due to the specific permeability of neuronal membranes to K^+, leading to extracellular leakage. Transmission of a neural signal occurs when the membrane potential reaches a voltage-dependent threshold upon which time an action potential is fired leading to a brief depolarisation of the cell,

normally to a value of approximately +40 mV, followed by repolarisation and a refractory period, all of which occurs in under 1 ms (Purves 2008).

The action potential is chemically propagated to other neurons via specialised structures called synapses composed of the pre-synaptic terminal, the post-synaptic terminal, the synaptic cleft and glial terminals. Upon neuronal depolarisation, chemicals known as neurotransmitters are released from the pre-synaptic nerve terminal into the synaptic cleft, ligating relevant neurotransmitter receptors on the post-synaptic neuron, leading to propagation of the excitatory or inhibitory signals.

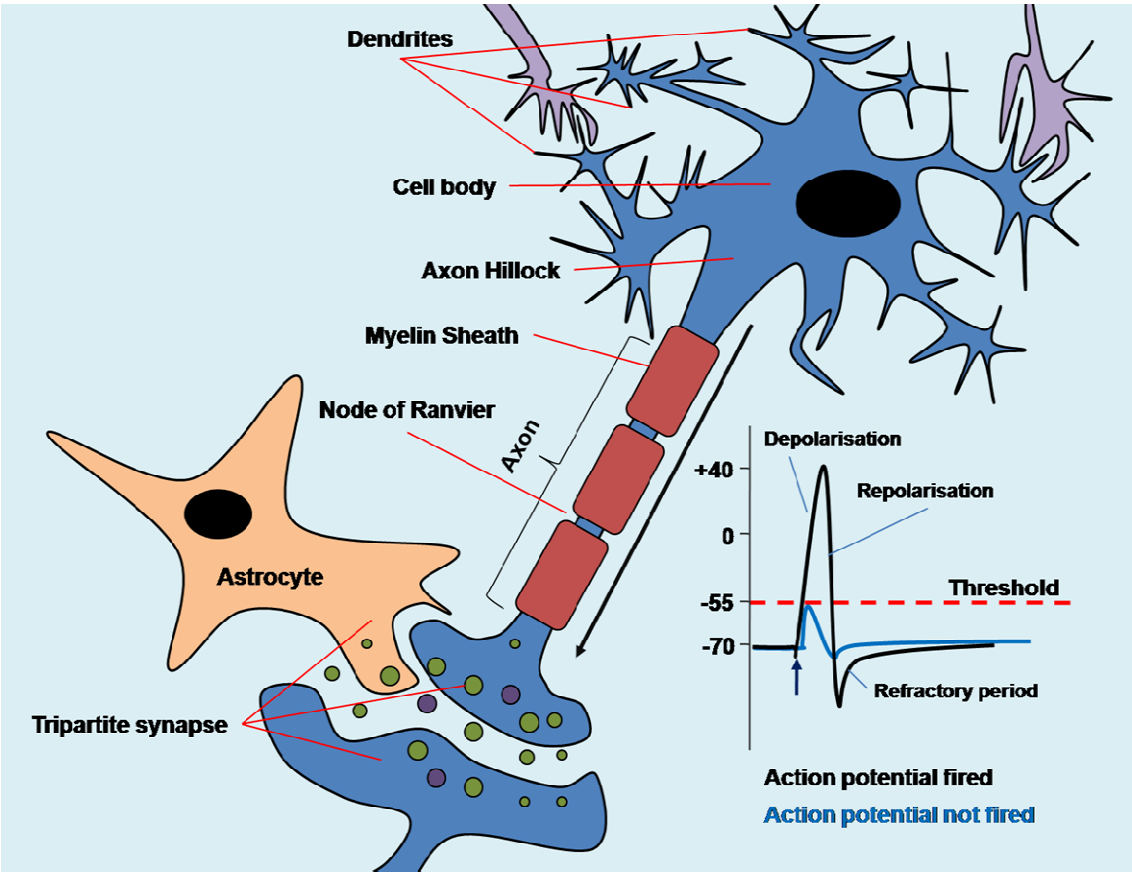

Figure 1.1.1. Basic neuronal anatomy

Classic anatomy of a neuron including the main extracellular connections such as afferent nerves (purple) synapsing with the dendritic tree surrounding the cell body and the tripartite synapse showing the involvement of astrocytes during synaptic transmission induced through the firing of an efferent action potential, after supra-threshold stimulation, down the axon (black arrow and graph).

1.1.1.1. The cerebellum and cerebellar granule neurons

The cerebellum is generally considered as the motor element of the brain, maintaining equilibrium and coordinating muscle contractions, ensuring appropriate muscle contraction occurs at the appropriate time. More recent studies however, suggest the cerebellum additionally contributes to cognitive and sensory functions (Strick et al. 2009; Timmann et al. 2010). The gross anatomy of the cerebellum consists of a cortex, of gray matter contained in transverse folds or folia and a central region of white matter (**Figure 1.1.2**), providing the distinctive and unmistakable anatomy. There are four pairs of intrinsic central nuclei (dentate, globose, emboliform and fastigial) embedded in the cerebellar white matter and three pairs of central peduncles (superior, middle and inferior) connecting the cerebellum with the midbrain, pons and medulla, respectively (Kiernan 2009).

More than 90% of the cerebellum is composed of granule neurons, or CGCs, and they constitute the largest homogenous neuronal population in the mammalian brain (Contestabile 2002). Neurogenesis of granule cells is largely postnatal, which led to the idea that explanted cerebella could provide an uncomplicated source of primary neurons, *in vitro,* and since the development of the culture nearly 40 years ago (Gallo et al. 1982), hundreds of labs have utilised it for all nature of neuronal experimental models. Furthermore, CGCs are glutamatergic neurons, the most prevalent neuronal type in the mammalian brain and in culture they mature and express synaptic connections and a wide range of receptors including the NMDA receptor, the primary receptor implicated in excitotoxicity, a phenomena linked to acute and chronic neurodegenerative disease processes (Salińska et al. 2005; Lau & Tymianski 2010). Also, recent studies (Kaushal & Schlichter 2008) using embryonic cortical neurons have replicated previous studies in our laboratory performed on CGCs (Taylor et al. 2005), supporting the physiological similarities of differing neuronal subtypes in culture.

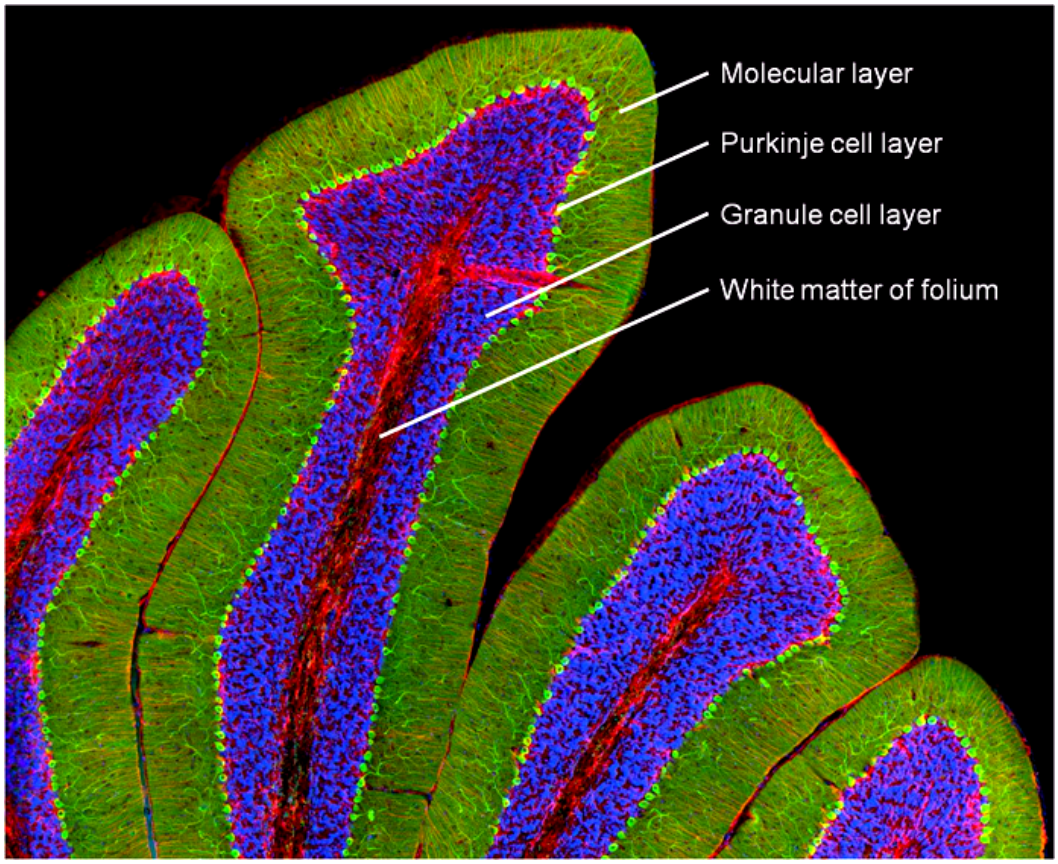

Figure 1.1.2. Rat cerebellar anatomy

A multi-photon fluorescence image of rat cerebellum in which the Purkinje cells were labelled green (anti-IP_3R marked with 488 nm cadmium selenide/zinc sulphide quantum dots), glia were marked red (anti-GFAP marked with 568nm cadmium selenide/zinc sulphide quantum dots) and cell nuclei marked blue (using Hoechst DNA stain). Permission to use the image was granted by Mr Thomas Deerinck at the *National Centre for Microscopy and Imaging Research* (*NCMIR*) located at the University of California San Diego (UCSD).

1.1.1.2. Circuitry of the cerebellum

The cerebellum is organised into three distinct layers as shown in **Figure 1.1.2 and 1.1.3**. There is a Purkinje cell layer consisting of a single row of Purkinje cell bodies which project their dendrites superficially into a synaptic zone known as the molecular layer. Finally there is the granule cell layer, the deepest layer of the cerebellum, consisting of densely packed interneurons with axons that extend into the molecular layer. Other cerebellar interneurons such as Basket cells and Golgi cells have their cell bodies in the molecular and granule layers (Kiernan 2009). With respect to afferent fibres into the cerebellum, climbing fibres originate in the inferior olivary complex of nuclei and synapse with proximal elements of the Purkinje cell dendritic trees in the molecular layer. Other afferent fibres, not originating from the inferior olivary nuclei are known as mossy fibres and synapse with neurons in the granule layer (**Figure 1.1.3**) (Kiernan 2009).

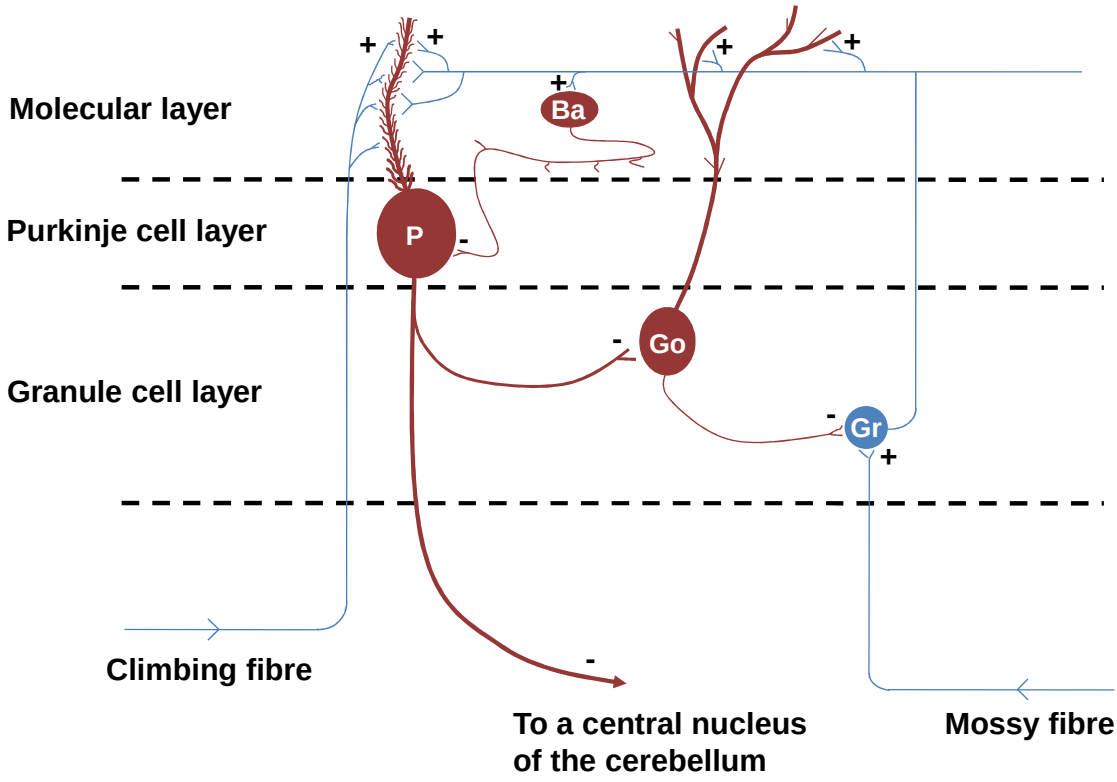

Figure 1.1.3. Cerebellar circuitry

A longitudinal representation of the neurons of the cerebellar cortex, showing excitatory (+) and inhibitory (-) synapses. Purkinje cell (P), Granule cell (Gr), Golgi cell (Go), Basket cell (Ba). Adapted from Kiernan (2009).

1.1.2. Astrocytes

Astrocytes, or astroglia, are the most numerous and diverse glial cell population in the CNS. The ‘true’ astrocytes have a unique ‘astro/stellate’ morphology due to the arrangement of intermediate filament proteins (**Figure 1.1.4**), including glial fibrillary acidic protein (GFAP; used as an astrocytic marker in immunofluorescence) and vimentin (Verkhratsky & Butt 2007). Astrocytes can be further sub-classified based on location. Proteoplasmic astrocytes are located in the grey matter and fibrillary or fibrous astrocytes located in the white matter, and it is therefore not surprising, based on their locations, that they associate with neuronal cell bodies and synapses or with axons, respectively.

Radial glia, another population of astrocytes, are bipolar cells with an ovoid cell body and elongated processes. They are involved in the formation of the neurovascular unit and produce two main processes with one forming astrocytic end-feet (**Section 1.2.1**) on ventricular walls and the other at the pial surface (Verkhratsky & Butt 2007). These cells also form scaffold to assist neuronal migration during early embryonic stages of development and also contribute to the oligodendrocyte progenitor cell (OPC) population (Nishiyama et al. 2009). After CNS maturation, radial glia generally disappear from the majority of brain regions, transforming into stellate astrocytes. However, in certain brain regions some do remain, such as the Müller cells of the retina and Bergmann glia, the most abundant astrocyte of the cerebellum (Haydon 2001). Other smaller populations of specialised astrocytes also exist after maturation including velate astrocytes in cerebellum and tanycytes in periventricular organs and raphe part of spinal cord (Verkhratsky & Butt 2007).

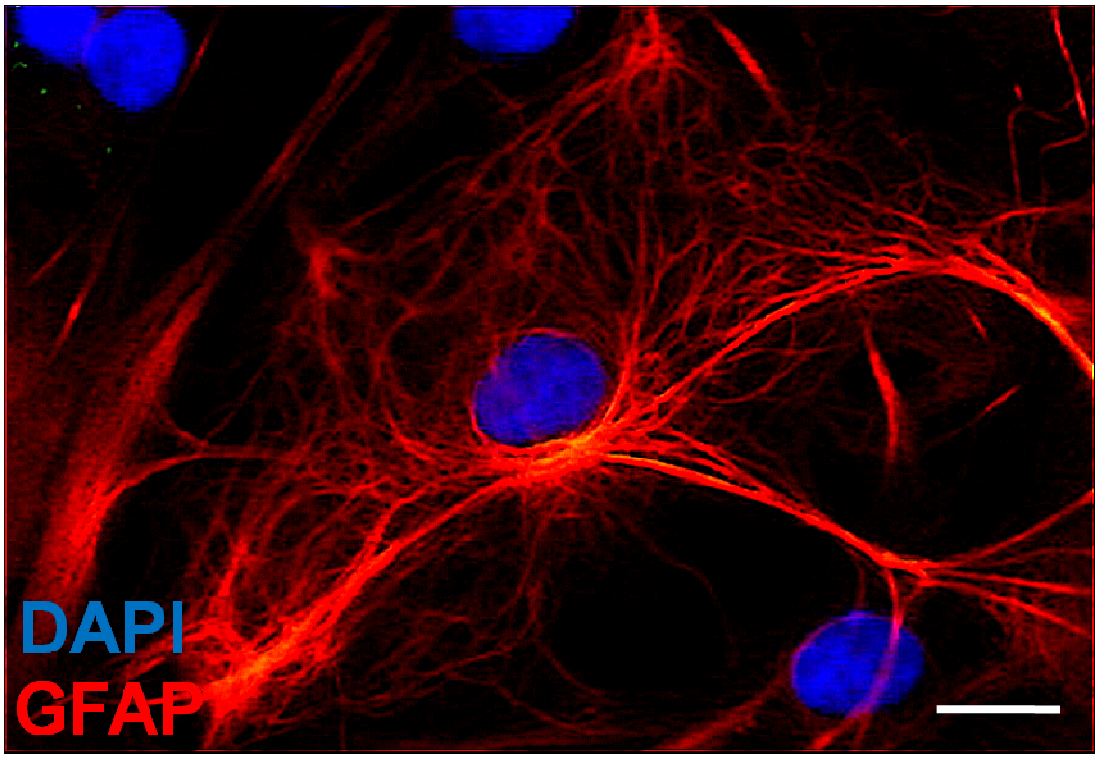

Figure 1.1.4. Astrocyte morphology

A standard fluorescence image of primary rat astrocyte cultures showing the classical stellate astrocytic morphology using immunofluorescent tagging of the astrocyte-specific marker glial fibrillary acid protein (anti-GFAP marked with anti-Cy3; red) and cell nuclei (DAPI; blue). Scale bar = 15 µm.

Astrocytes tile the entire CNS in an essentially non-overlapping orderly manner communicating with each other distally through gap-junctions (Sofroniew & Vinters 2010). These individual region-specific astrocytes are in contact with thousands of neuronal synapses formed between many different neurons, prompting the idea of significant involvement of astrocytes in neuronal function. Astrocytic involvement in neuronal activity was supported by studies identifying the expression of potassium and sodium ion channels and that they exhibit evoked inward currents suggesting excitability yet, they do not fire or propagate action potentials (Lalo et al. 2006). This does not however make them excitably redundant with the discovery that regulated changes in intracellular calcium represent astrocytic excitability (Cornell-Bell et al. 1990; Charles et al. 1991). These regulated changes are functionally significant in astrocyte-astrocyte and astrocyte-neuronal communication and occur as intrinsic oscillations resulting from intracellular calcium store release that propagate over large

distances (Sofroniew & Vinters 2010). Furthermore, via expressed neurotransmitter receptors, changes in astrocytic intracellular calcium concentrations can be triggered by neurotransmitter release from neurons at the synapse inducing the release of neuroactive substances from the astrocytes, which in turn signal back to the neurons creating a feedback loop that either enhances or inhibits neuronal activity (Haydon 2001; Barres 2008).

The integral importance of astrocytes in the development and regulation of neuronal activity was first alluded to by Pfieger and Barres (1997). Retinal ganglion neurons can be highly purified and cultured in serum-free medium with a high survival rate in the total absence of glia. Pfieger and Barres used these cultures to identify the significance of astrocytes in relation to neuronal firing. The cultured neurons had dendrites and axons and were electrically excitable but little spontaneous synaptic activity was observed. However, if these neurons were co-cultured with astrocytes, or conditioned medium from astrocyte cultures was administered, the frequency and amplitude of spontaneous postsynaptic currents were significantly enhanced (Pfrieger & Barres 1997). These data suggested that developing neurons in culture formed inefficient synapses requiring glial signals to become fully functional, and following on from these studies it is now widely accepted that astrocytes are intrinsically involved in modulating synaptic transmission (Perea & Araque 2010), to the extent that, anatomically, the synapse is now termed the tri-partite synapse, which includes the pre- and post-synaptic clefts and an astrocytic element.

Astrocytes maintain tight control of local ion and pH homeostasis, deliver glucose, provide metabolic substrates, and clear neuronal waste (Nedergaard et al. 2003). Through two-photon-imaging of calcium signals, studies also show that astrocytes regulate blood flow with respect to neuronal activity (Schummers et al. 2008), further identifying the fundamental involvement of these cells in normal brain function. However, this integral involvement in normal function suggests that in dysfunctional

conditions astrocytes would also be significantly affected. Reactive astrocytes termed astrogliosis is a common pathological hallmark of dysfunctional and diseased CNS tissue where the astrocytes demarcate the injury site from healthy tissue by forming a glial scar (Schachtrup et al. 2010), and it has been suggested that dysfunctions in astrogliosis or scar formation could contribute to, or be the primary cause of, CNS disease mechanisms (Sofroniew & Vinters 2010).

1.1.3. Oligodendrocytes

This population of glia have few processes, hence the prefix ‘oligo’, their main function being the myelination of axons between the nodes of Ranvier for electrical insulation and saltatory nerve conduction. The population was initially described by Del Rio Hortega in 1928 who classified them into four phenotypes dependent on morphology and location, descriptions of which are given below:

Type I: Have a small rounded cell body with four to six primary processes that branch and myelinate 10-30 thin (<2 µm diameter) axons. Each secondary process forms a single internodal myelin segment approximately 100-200 µm in length. Present in forebrain, cerebellum and spinal cord

Type II: Morphologically similar to type I but are only present in the white matter, for example, the optic nerve.

Type III: Have a much larger cell body than types I and II, with several thick primary processes with the ability to myelinate up to five thick axons (4 -15 µm diameter). These cells produce sheaths that range from 200 - 500 µm in internodal length. Present in medulla oblongata and spinal cord

Type IV: Have no processes and form a single long myelin sheath up to 1000 µm in internodal length around the largest diameter axons.

These are present almost exclusively around the nerve root entrances into the CNS

The four morphological phenotypes are likely to originate from common oligodendrocyte progenitor cells (OPCs), which have been shown to derive in particular areas of the CNS including the ventral ventricular zone of the spinal cord, the ventral forebrain, and the ganglionic eminences (Bradl & Lassmann 2010). Differentiation of OPCs into oligodendrocytes is dependent on the Notch 1 receptor (Genoud et al. 2002), γ-secretase and astrocytes (Watkins et al. 2008). Also, their ability to myelinate axons is regulated by neuronal activity (Gyllensten & Malmfors 1963) and is brief, occurring early during differentiation (Watkins et al. 2008). As previously mentioned, oligodendrocytes myelinate the axons to provide electrical insulation, however they also induce sodium channel clustering at the nodes of Ranvier, an important requirement for saltatory nerve conduction (Kaplan et al. 1997; Kaplan et al. 2001).

Oligodendrocyte death and subsequent demyelination occurs in multiple sclerosis leading to some of the characteristic symptoms associated with the disease (**Section 1.3.2**). The cells also express AMPA, kainite and NMDA receptors, exposing them to glutamate toxicity, a pathological mechanism associated with a number of neurodegenerative diseases, and also the purinergic $P2X_7$ receptor that exposes them to potential damage from high extracellular concentrations of ATP (Bradl & Lassmann 2010).

1.1.4. NG2-positive cells or Polydendrocytes

NG2-positive cells were the most recent major glial population to be discovered in the CNS and are defined as CNS parenchymal cells expressing the NG2 proteoglycan. They are classically known as oligodendrocyte progenitor cells (OPCs) however the name polydendrocyte has recently been proposed due to their multi-processed morphology, lineal relationship to oligodendrocytes and observations that they are in fact multi-potential progenitors (Nishiyama et al. 2009).

Reports from *in vitro* studies suggested these cells could differentiate into oligodendrocytes and astrocytes if serum was absent or present, respectively (Raff et al. 1983), and were thus initially proposed as bipotential progenitors. At first these studies were alluded to as *in vitro* artefacts however studies *in vivo* showed a purified OPC cell line (CG-4) could differentiate into oligodendrocytes and astrocytes when transplanted into a glial-depleted environment (Franklin et al. 1995). Although this supported the bipotentiality of these cells, a heterogeneous population consisting of distinct committed progenitor cells of oligodendrocyte and astrocyte lineage or cellular changes due to the artificial immortality of the cell line can't be ruled out.

Further observations suggested the polydendrocytes were multi-potential progenitors with the generation of neurons from OPCs excised from postnatal rat optic nerve and treated with bone morphogenetic protein 2 (BMP2) and platelet derived growth factor AA (PDGF AA). This led to the generation of multi-potent neural stem cell-like cells that were capable of generating neurons, astrocytes and oligodendrocytes (Kondo & Raff 2000).

Distinctive physiological properties for polydendrocytes have been observed using electrophysiology on hippocampal slice preparations identifying these cells as distinct from mature astrocytes (Nishiyama et al. 2009). These cells are also able to generate ionotropic glutamate and GABA receptor currents, again discovered using slice preparations (Berger et al. 1992). Further studies led to the concept of neuron-polydendrocyte synapses, which in the hippocampus have been shown to undergo long term potentiation demonstrated by increasing excitatory post-synaptic current amplitudes (Ge et al. 2006). These neuron-glia synapses have also been identified in the molecular layer of the cerebellum, where the polydendrocytes were shown to respond to multiple climbing fibre inputs with coordination of the response with Purkinje cells (Lin et al. 2005).

The complete functional significance of these cells is still being intensely researched, with the synaptic involvement a very hot topic. The general suggestion at present is that these neuronal synaptic inputs are involved in the classical functions attributed to the OPCs, such as proliferation, differentiation into mature glia and migration to demyelinated regions (Nishiyama et al. 2009).

1.1.5. Microglia

Microglia as a single population was first introduced by Pio del Rio-Hortega in 1932 after development of a silver carbonate staining technique provided the first high quality images of these cells (Rio-Hortega 1932). Limited breakthroughs in the physiology of microglia occurred until the development of the facial nerve lesion model (Blinzinger & Kreutzberg 1968), which enabled the study of microglial responses to injury in CNS tissue with an intact blood brain barrier.

Microglia are the innate immune cells of the CNS, are of mononuclear phagocyte lineage and their underlying role is to monitor the environment and act to maintain homeostasis (Perry et al. 2007; Kettenmann et al. 2011). They are derived mainly from leptomeningeal mesenchymal cells, which enter the brain during development and transform into microglia (Bechmann et al. 2007). Elegant studies with rat bone marrow chimeras demonstrated that a subset of microglia, termed ‘perivascular’ microglia was derived from bone marrow (Hickey & Kimura 1988). It is assumed that in the healthy brain, microglia exist as a stable population however, after axonal degeneration and blood brain barrier disruption it has been shown that a subpopulation of monocytes can infiltrate the CNS and transform into microglia (Bechmann et al. 2005; Mildner et al. 2007).

The varying derivations of microglia could contribute to the observed heterogeneity of the population with studies suggesting regional differences in microglia *in situ* and in culture, demonstrated by selective expression of mRNAs or proteins (including TNFα, IL-6, integrins and iNOS) or differences in proliferative potential (Kettenmann et al.

2011). Furthermore, variations in neurotransmitter exposure and proximity to blood vessels could also be contributing to the heterogeneity.

1.1.5.1. Phenotypes

The resting phenotype of microglia is characterised by ramified morphology displaying a small cell body, long slender processes with secondary fine cellular branching (**Figure 1.1.5**). Little is known about the mechanism by which the infiltrating progenitors morphologically change to this state however, some experiments suggest purines including ATP and adenosine and certain unknown astrocytic factors induce the resting phenotype (Wollmer et al. 2001).

Until recently this 'resting' phenotype was considered quiescent however *in vivo* imaging studies have shown the fine cellular processes are highly dynamic, suggesting constant surveillance is performed by the microglia (Nimmerjahn et al. 2005; Davalos et al. 2005). This observation coupled with the idea that the little known general daily functions of microglia in healthy subjects are likely to involve restrained activation due to sub-inflammatory threshold changes in brain homeostasis, there is now a general consensus that microglia have shifts in activation states from a surveillance mode to other states dependent on the intensity of the inflammatory insult (Kettenmann et al. 2011).

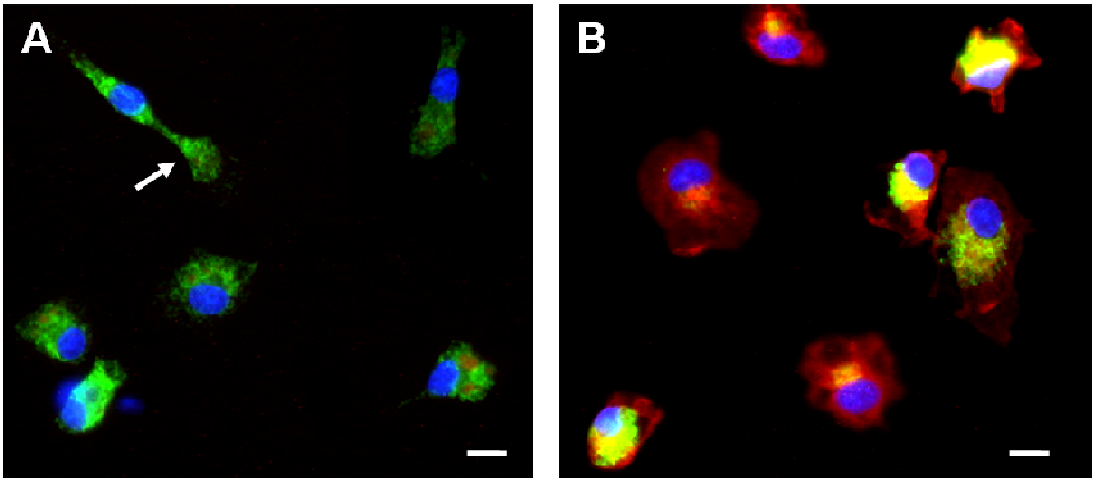

Figure 1.1.5. Changes in microglial morphology

Standard immunofluorescence imaging of primary rat microglial cultures with microglia presenting with small cell bodies and slender processes identified as a 'resting' morphology (arrow; **A**) or presenting with the classic activated morphology identified by large cell bodies with amoeboid characteristics (**B**). Immunofluorescence was performed with an IB_4-FITC conjugation to label microglia (green), anti-iNOS to label activated microglia after LPS treatment (marked with anti-Cy3; red) and cell nuclei (DAPI; blue). Scale bars = 10 µm.

Classical 'full' activation seen during infection, trauma, ischemia and neurodegenerative disorders can be characterised by an increase in cell volume, an amoeboid-like morphology, and the increased expression of cell-surface molecules including CD14, major histocompatibility complex (MHC) molecules and chemokine receptors, that are involved in a broad range of inflammatory responses from antigen-presentation to cell migration (Block et al 2007). The amoeboid morphology coupled with chemokine gradients creates motile microglia that are able to migrate to immune-compromised and damaged areas of the CNS and actively attempt to return homeostasis. This congregation of microglia to the injured area of the CNS is termed microgliosis and is seen during neuroinflammation (Carbonell et al. 2005) and in chronic neurodegeneration (Ladeby et al. 2005).

Activated microglia are the phagocytes of the CNS and engulf tissue debris and dead cells in an attempt to return homeostasis, as well as being involved in the phenomenon

of ‘synaptic stripping’ (Graeber et al. 1993; Schiefer et al. 1999), a mechanism by which the synapses of injured neurons are pruned from their cell bodies in an attempt to promote growth and survival, although a recent review argues against microglial involvement (Perry & O’Connor 2010). In the presence of immobilised fibrinogen and fibrin deposits in models of MS and AD, microglia are activated to a phagocytic phenotype (Adams et al. 2007a; Paul et al. 2007) and have also been shown to phagocytose myelin (Pinteaux-Jones et al. 2008) and β-amyloid (Aβ) deposits (Fiala et al. 2007). With a focus on AD, a specific cell surface receptor complex (CD36/$\alpha_6\beta_1$ integrin/CD47) has been identified that mediates phagocytosis of fibrous Aβ by microglia, *in vitro*, that differs from the complex used by the classical phagocytic receptors, i.e. the immunoglobulin or complement receptors (Koenigsknecht & Landreth 2004). Interestingly, recent studies have suggested that this observed microglial-mediated phagocytosis of fibrous Aβ can be inhibited if oligomeric Aβ is present suggesting a further enhancement of inflammation (Pan et al. 2011).

1.1.5.2. Signalling – Receptors and released factors

Microglia express a vast array of receptors and channels ranging from ion channels and receptors involved with inflammatory responses, to neuropeptide and classical neurotransmitter receptors. This section will focus on the receptors relevant to this thesis, which includes a subset of the receptors involved in inflammatory and phagocytic mechanisms and the metabotropic glutamate receptors (mGluRs). This will be followed by an overview of classical inflammatory responses after microglial activation.

1.1.5.2.1. Pattern recognition receptors

The evolution of microglia to express multiple, diverse membrane receptors that identify and bind pathogen-associated molecular patterns (PAMPS) known as pattern recognition receptors (PRR) allows them to be activated by a diverse array of stimuli. However, activation of these receptors can have unwanted effects. In the case of

microglial-mediated neurotoxicity, PRRs responsible for host defence and phagocytosis have often been observed mediating neuronal damage in the absence of a known pathogen, suggesting that non-pathogenic stimuli could be misinterpreted with neurotoxic consequences (Block et al 2007).

Toll-like receptors (TLRs) are the most studied group of PRRs. Microglia regulate the expression of TLRs throughout development and in response to pathogens (McKimmie & Fazakerley 2005). TLRs initiate innate immune responses on interaction with infectious agents but have also been implicated in detrimental microglial activation and neurotoxicity through the induction and release of neurotoxic factors (Block et al 2007). The recognition of particular PAMPs by particular TLRs leads to transcriptional upregulation of distinct genes, dependent on the TLRs and cell types involved, with differing signalling cascades dependent on the adaptor molecules recruited. Generally speaking TLR signalling can be divided into usage of either the MyD88 or TRIF adaptor molecules (Takeuchi & Akira 2010).

Microglia are reported to express TLRs 1-9 (Jack et al. 2005) and it is generally accepted that TLR4 is the primary lipopolysaccharide (LPS) receptor (Lien et al. 2000) reported to be a crucial contributor to the microglial response to LPS, mediating LPS-induced neurodegeneration *in vitro* (Lehnardt et al. 2003). LPS is a major constituent on the outer membrane of Gram-negative bacteria. It acts as a potent endotoxin and elicits strong immune responses in mammals making it an excellent tool to induce microglial activation (**Section 1.1.5.2.4**). Upon ligand stimulation, TLR4 recruits the adapter protein MyD88 which subsequently forms a complex leading to the translocation of the transcription factor NFκB (nuclear factor kappa-light-chain-enhancer of activated B cells) to the nucleus driving cytokine production. Simultaneously, MAPK cascades are activated leading to activation of nuclear AP-1 which is also critical for the induction of cytokine genes (Takeuchi & Akira 2010). TLR4 has been shown to be upregulated during brain inflammation (Bsibsi et al. 2002)

however the receptor has also been implicated in beneficial repair processes including improved remyelination and cerebral tissue protection (Glezer et al. 2006).

Recently, non-apoptotic, orderly activation of caspase-8 and -3/7 via a protein kinase C (PKC)-δ-dependent pathway has been shown to specifically regulate microglial activation after treatment with LPS and other inflammogens including lipoteichoic acid (LTA, TLR2 agonist) and PamC3sk4 (synthetic lipopeptide TLR1/2 agonist) (Burguillos et al. 2011). These data further elucidate TLR-associated activation pathways providing interesting evidence for intracellular pathway convergence in microglia after diverse extrinsic pathogen exposure.

Interestingly, fibrinogen-(FG)-mediated secretion of macrophage inflammatory protein-1α, (MIP-1α), MIP-1β, MIP-2, and monocyte chemoattractant protein-1 from a macrophage cell line as well as primary murine peritoneal macrophages, has been shown to be dependent on TLR4 signalling (Smiley et al. 2001). This suggests that LPS and FG could have a similar evolutionary conserved binding motif for TLR4, potentially explaining the involvement of FG in inflammatory responses (Adams et al. 2007b).

1.1.5.2.2. Integrin and Scavenger receptors

The integrin family of molecules have roles in cell adhesion, tissue specific homing and cellular trafficking during development and infection. The four β_2-integrin members of this family are best known for their roles in leukocyte trafficking during inflammation and contributing to leukocyte activation in immune responses and phagocytosis (Ley et al. 2007). The β_2-integrins are heterodimeric receptors that share a common β-chain (CD18) and are known as CD11a/CD18 ($\alpha_L\beta_2$, LFA-1), CD11b/CD18 ($\alpha_M\beta_2$, Mac-1, CR3), CD11c/CD18 ($\alpha_X\beta_2$, p150,95, CR4) and CD11d ($\alpha_D\beta_2$). The α and β chains are composed of multiple protein domains that contribute to ligand binding and subsequent signalling. In the inactive state, these protein domains are masked by a 'folded' conformation inhibiting any interactions with ligands however upon activation by

cytokines or other inflammatory factors the intracellular domains are exposed after conformational changes to an open, active state, allowing ligand-receptor interactions (Abram & Lowell 2009; Hu et al. 2010).

Activation tends to induce rapid multimerisation of the receptors followed by assembly of an intracellular signalling platform resulting in gene expression modulation via Akt, ERK and/or JNK signalling pathways. Cytoskeletal rearrangements also occur upon activation with dependence on Rap-GTPases (Abram & Lowell 2009).

CD11b is one of the more characterised members of the β_2-integrin sub-family and has been shown to participate in signalling cascades that result in the transmigration of leukocytes into lymphoid organs and to sites of infection and inflammation as well as involvement in complement-mediated phagocytosis (Hu et al. 2010). The β_2-integrins have been identified on human brain microglia, and have been shown to be upregulated during AD (Akiyama & McGeer 1990). Interestingly, soluble fibrinogen has been shown to interact with CD11b in a competitive manner (Benimetskaya et al. 1997). Furthermore, 'immobilised' fibrinogen has been shown to induce a phagocytic microglial phenotype that was dependent on CD11b binding, with competitive inhibitory binding significantly attenuating EAE disease progression (Adams et al. 2007a).

The scavenger receptors are another group of microglial-associated receptors that mediate cell adhesion to, and endocytosis of, various native and pathologically modified substances (Husemann et al. 2002). The group can be pooled with other 'multi-ligand receptors' such as the receptor for advanced glycation end products (RAGE) and the LDL-like receptor related protein (LRP), but the classical scavenger receptor members are scavenger receptor class A (SR-A, CD204), scavenger receptor class B type I (SR-BI) and CD36. Here, the emphasis will be on SR-A, the scavenger receptor that was investigated in this thesis.

SR-A and SR-BI seem to be developmentally regulated with observable expression in neonatal microglia but little or no expression in the adult brain (Husemann & Silverstein

2001). However, during AD pathogenesis, a significant increase in microglial-associated SR-A expression is observed (Christie et al. 1996; Honda et al. 1998) with *in vitro* studies suggesting microglial SR-A mediates adhesion and endocytosis of fibrillar Aβ by microglia (El Khoury et al. 1996). Interestingly, studies have shown that fibrillar Aβ activates signal transduction in microglia via two parallel pathways involving either p38 MAPK or ERK1/2 (McDonald et al. 1998). However, activation of scavenger receptors failed to induce these pathways, suggesting fibrillar Aβ interactions with SR-A induce an alternative pathway although performing simple competitive binding assays would have provided stronger evidence for this differential SR-A activation.

Inflammation also seems to modulate scavenger receptor expression with studies showing an increase in SR-A mRNA and protein in microglia after treatment with LPS, IFNγ and IL-1α, but not with TGF-β1, *in vitro* (Grewal et al. 1997). Furthermore, SR-A ligands including fucoidan and polyinosinic acid have been shown to block chromogranin-A-(CgA)-mediated responses in MG including iNOS expression, mitochondrial depolarisation, glutamate release and apoptosis, as well as attenuating CgA-induced microglial-mediated neurotoxicity (Hooper et al. 2009a).

Interestingly, the use of animal models of AD, identified that SR-A expression was localised to microglia associated with parenchymal and vascular deposits of Aβ (Bornemann et al. 2001), suggesting roles for the receptor in AD pathology. However, it was shown previously using SR-A$^{-/-}$ human APP mice that the receptor was not required for development of AD-like pathology in these mice (Huang et al. 1999), suggesting possible compensatory effects by other family members. A complete knockout of the three known members would provide greater insight into the role of these receptors in AD pathogenesis.

Briefly, CD36 has been shown to be present in microglia throughout CNS development with variable expression observed in a number of neurodegenerative diseases including high expression in the microglia of AD patients. Furthermore it has been

shown to mediate ROS production from microglia in response to fibrillar Aβ (Coraci et al. 2002)

1.1.5.2.3. Neurotransmitter receptors – focus on mGluRs

Studies identifying the expression of neurotransmitter receptors on microglia, coupled with the proposal of volume transmission as a signalling mechanism in parallel with the classical wiring transmission (Agnati et al. 1995), brought about the idea that neuron-microglial communication could occur through these receptors. Microglia express many groups of neurotransmitter receptors including metabotropic and ionotropic glutamate receptors, GABA, purinergic and dopaminergic to name a few (Pocock & Kettenmann 2007; Kettenmann et al. 2011). Here, the focus will be on the metabotropic glutamate receptors (mGluRs) and their involvement in microglial activation and subsequent neurotoxicity or protection.

The mGluRs are members of the g-protein coupled receptor (GPCR) superfamily, which is the most abundant receptor gene family in the human genome. They are membrane bound proteins with seven transmembrane domains that are activated by extracellular ligands, which in turn transduce intracellular signals via interactions with g-proteins (a heterotrimeric complex of α, β and γ subunits) with subsequent modulation of various effector molecules such as enzymes, ion channels and transcription factors (Niswender & Conn 2010). The mGluRs are sub-classified into three groups based on sequence homology, g-protein coupling and ligand selectivity.

Group I mGluRs (mGluR1 and 5) are predominantly coupled to G_q/G_{11} proteins and activate phospholipase C_β, resulting in the hydrolysis of phosphotinositides and generation of inositol 1,4,5-trisphosphate (IP_3) and diacylglycerol, which leads to calcium mobilisation and activation of protein kinase C (Niswender & Conn 2010). Two independent studies have suggested that only mGluR5 from group I is expressed in microglia (Biber et al. 1999; Byrnes et al. 2009a). The latter study further suggested that agonism of mGluR5 could attenuate LPS-mediated microglial activation with

significant decreases in nitric oxide, reactive oxygen species, TNFα and galectin-3 observed (Byrnes et al. 2009a). Furthermore, this specific activation of microglial mGluR5 was able to attenuate microglial-mediated neurotoxicity after LPS treatment, suggesting a neuroprotective role through microglial mGluR5 activation (Byrnes et al. 2009a). This was further alluded to by the same group using rat spinal cord injury models *in vivo* to show mGluR5 activation downregulated ED-1, Iba-1 and Galectin-3 expression with decreases in NADPH oxidase components, TNF release and iNOS expression also shown (Byrnes et al. 2009b). Further studies by the same group using siRNA techniques identified that the mGluR5-mediated decrease in microglial reactivity and subsequent neurotoxicity was due to NADPH oxidase inhibition (Loane et al. 2009).

Group II (mGluR2 and 3) and group III (mGluR4, 6, 7 and 8) are predominantly coupled to $G_{i/o}$ proteins, which are classically coupled to the inhibition of adenylyl cyclase with a subsequent decrease in cAMP levels (Niswender & Conn 2010). Work completed and ongoing in our laboratory has provided and continues provide insight into the differential roles of group II and III mGluRs on microglia, ranging from direct and indirect toxicity to the induction of neuroprotective phenotypes (Kingham et al. 1999; Taylor et al. 2002; Taylor et al. 2003; Taylor et al. 2005; Pinteaux-Jones et al. 2008). Initial studies by Kingham et al (1999) identified that the microglial apoptosis induced by chromogranin A (CgA), a peptide associated with AD senile plaques, could be significantly attenuated by broad antagonism of group II and III mGluRs, suggesting a role for this class of receptor in regulating the toxicity of disease-associated deposits (Kingham et al. 1999).

These findings were taken forward by subsequent studies firstly identifying the functional expression of both group II mGluRs on microglia, activation of which induced significant microglial death whereas antagonism attenuated microglial-mediated neurotoxicity after treatment with CgA (Taylor et al. 2002). Secondly, Taylor et al (2003) identified functional group III (mGluR4, 6 and 8 but not mGluR7) mGluRs on

microglia, which when activated attenuated CgA and LPS-mediated microglial activation, the opposite to that observed after group II activation. Furthermore, specific activation of the group III receptors on microglia was able to attenuate microglial-mediated neurotoxicity after treatment with CgA or LPS (Taylor et al. 2003). Finally, it was identified that mGluR2 activation, and not mGluR3 of the group II receptors was responsible for the observed microglial-mediated toxicity. Microglial mGluR2-mediated TNFα release was shown to be responsible for the observed neurotoxicity, in concert with the pro-apoptotic factor Fas ligand (Taylor et al. 2005).

Support for the detrimental activation of microglial group II mGluRs was observed in an *in vitro* model of stroke penumbra. Glutamate released from oxygen and glucose deprived stressed embryonic rat neurons stimulated co-cultured microglial group II mGluRs triggering the activation and induction of neurotoxicity mediated through microglial release of TNFα (Kaushal & Schlichter 2008). This mechanism could also be mimicked by administration of a group II mGluR agonist. Interestingly, the mGluR-dependent microglial activation involved NFκB signalling, but in contrast to LPS-induced microglial activation, no MAPK signalling or NO production and release was observed (Kaushal & Schlichter 2008).

The old view of neurotransmitters as molecules solely for communication between synapses is being tested with discoveries showing receptors present on non-neuronal cells with diverse functionality. Further studies into the roles and functions of these neurotransmitter receptors on microglia will help us to understand the seemingly vast signalling capacity these cells have, which could lead to further breakthroughs in our understanding of neuron-glial relationships.

1.1.5.2.4. Microglial-mediated cytokine and ROS signalling

The final subsection will focus on the factors released from microglia during activation. This is a vast and complicated subject, some of which has already been covered in previous sections. Therefore, this will be an overview of the inflammatory factors

released after classical LPS-mediated microglial activation and those associated with Alzheimer's disease pathogenesis.

For over twenty years, microglial activation has been modelled *in vitro* with LPS, a component of gram-negative bacteria (Hetier et al. 1988). It is now widely accepted that chronic microglial activation results in deleterious & neurotoxic consequences with contributions from the chronic release of pro-inflammatory factors that can lead to neuronal toxicity and death (Block et al. 2007). *In vitro*, LPS exposure induces prolonged classic (M1) microglial activation (Porcheray et al. 2005), characterised by the release of pro-inflammatory factors, which is used to mimic the chronic activation identified to be detrimental *in vivo*. These studies have enabled researchers to identify the profile of released factors that could potentially drive disease pathogenesis.

The most intensely studied group of factors shown to be released from microglia during activation is the cytokines. These are small proteins ranging in size from 8 – 40 kDa that are able to be synthesised by nearly all nucleated cells. Interestingly, there is no obvious amino acid sequence motif or 3D structural similarities linking this family, it is rather their biological activities that provide the sub-classification into either pro- or anti-inflammatory, based on the evoked ligand-receptor signalling and subsequent up- or down-regulation of pro- or anti-inflammatory gene products (Dinarello 2000). As described in **section 1.1.5.2.1**, microglia, upon activation with LPS via TLR4, mediate signalling through the MyD88 adapter system complex that activates downstream kinases such as IκB and MAPKs, which in turn control the activities of signal-dependent transcription factors such as NFκB that regulate hundreds of genes, including cytokines (Glass et al. 2010). LPS has been shown to induce microglial release of pro-inflammatory cytokines including TNFα, IL-1α, IL-1β and IL-6 (Hetier et al. 1988; Lee et al. 1993), on numerous occasions. In support of the *in vitro* modelling of LPS-induced microglial activation, the cytokine release profile has been shown to translate to AD pathology where microglia surrounding AD plaques stained positive for

TNFα, IL-1β and IL-6, as well as monocyte chemotactic protein-1 (MCP-1, CCL2), a pro-inflammatory chemokine (Akiyama et al. 2000). Interestingly, fibrinogen and fibrin have also been shown to induce the production of pro-inflammatory cytokines including IL-1β, IL-6 and TNFα from human monocytes, *in vitro* (Perez et al. 1999; Jensen et al. 2007).

Focussing on TNFα, the pro-inflammatory cytokine is a member of the TNF superfamily of ligands, many of which promote inflammatory signalling (Wajant et al. 2003). TNFα is synthesised as a monomeric transmembrane protein (tmTNFα) that is inserted into the membrane as homotrimers, cleavage of which releases the 51 kDa soluble TNFα trimer (solTNFα) that circulates during an inflammatory response. Both forms of TNFα are biologically active and synthesis can occur in microglia, astrocytes, and some populations of neurons (McCoy & Tansey 2008). Cell signalling with TNFα occurs via TNFR1 and TNFR2 with solTNFα preferentially binding to TNFR1 leading to subsequent activation of a number of signal transduction pathways, including ERK, NFκB, p38 MAPK and c-Jun N-terminal kinase (JNK) (McCoy & Tansey 2008). Activation of these various pathways leads to an array of outcomes, ranging from pro-survival to apoptosis with dependence thought to derive from acute or chronic TNFα-induced JNK activation (Sato et al. 2005; Tobiume et al. 2001).

TNFR2 is not as widely expressed as TNFR1 and does not couple to an intracellular death domain. The transmembrane form of TNFα is the preferential ligand for TNFR2 activation, which can lead to pro-inflammatory and pro-survival signalling pathways through recruitment of adapter proteins and activation of the NFκB pathway. TNFR2 signal transduction has been shown to promote neuronal survival via activation of phosphatidylinositol-3-kinase-(PI3K)-dependent signalling (McCoy & Tansey 2008). Also, it has been suggested that the primary contribution of TNFR2 to TNFα-mediated signal transduction is through the promotion of TNFR1 signalling by enhancement of

the solTNFα binding affinity for TNFR1, a mechanism known as 'ligand passing' (Tartaglia et al. 1993).

Finally, as well as microglial-induced paracrine signalling of TNFα through the described receptors, microglial-mediated TNFα release has been shown to act in an autocrine fashion through activation of TNF receptors on microglia contributing to self-perpetuating microglial activation (Kuno et al. 2005; Kettenmann et al. 2011) (**Figure 1.1.6**). Furthermore, microglial-mediated TNFα release can activate astrocytes leading to the release of astrocytic factors that can lead to further microglial activation (Saijo et al. 2009).

With respect to modelling microglial activation in rodent models, it is now well established that activation promotes expression of the inducible nitric oxide synthase (iNOS) enzyme. However, there is still a debate over whether human cells utilise the enzyme as prominently as their rodent counterparts (Peterson et al. 1994; Ding et al. 1997; Panaro et al. 2003). Expression of iNOS occurs in response to inflammatory cytokines and promotes the production of nitric oxide (NO), a pleiotropic cell signalling molecule and free radical released from microglia that combats pathogen invasion. It has been consistently shown that NO release from microglia is mediated by the p38 and p42/44 MAPK pathways resulting in NFκB-mediated transcription of the iNOS gene (Bhat et al. 1998). Nitric oxide interacts with superoxide ($O_2^{\bullet -}$) free radicals to form peroxynitrite ($ONOO^-$), a potent toxin that can cause DNA breakage, lipid peroxidation and protein nitration (Pacher et al. 2007). However, NO has also been shown to protect neurons from excitotoxicity by downregulating NMDA receptor activity through nitrosylation of the receptors redox groups and it is in fact the conversion of NO to $ONOO^-$ that induces the significant neurotoxicity, implicating another enzyme called NADPH oxidase (Pacher et al. 2007). NADPH oxidase is a multi-subunit protein involved in the production of reactive oxygen species (ROS) through catalysis of the formation of $O_2^{\bullet -}$ from oxygen which in turn can lead to the production of $ONOO^-$ and

hydrogen peroxide (H_2O_2) through reactions involving NO. Glial NADPH oxidase has been implicated in NDDs with microglial NADPH oxidase shown to be involved in AD-associated oxidative stress (Wilkinson & Landreth 2006). Furthermore, Aβ-mediated microglial activation has been shown to involve TNFα-dependent expression of iNOS, subsequently leading to neuronal death (Combs et al. 2001).

It must not be forgotten that first and foremost the microglial population is present to maintain CNS homeostasis. Microglia are not auto-aggressive cells, with their main function being to protect damaged neurons and not cause damage themselves (Streit 2004). For example, anti-inflammatory cytokines such as TGFβ and IL-10 that can suppress NO or $O_2^{\bullet -}$ radical generation are also released from microglia during inflammatory responses to counteract the inflammation (Gebicke-Haerter 2001).Thus, it is likely that the combination of chronic inflammation, microglial senescence, genetic and epigenetic factors lead to microglial dysfunction including a loss of pro- and anti-inflammatory factor equilibrium, which contributes to neurodegenerative disease progression.

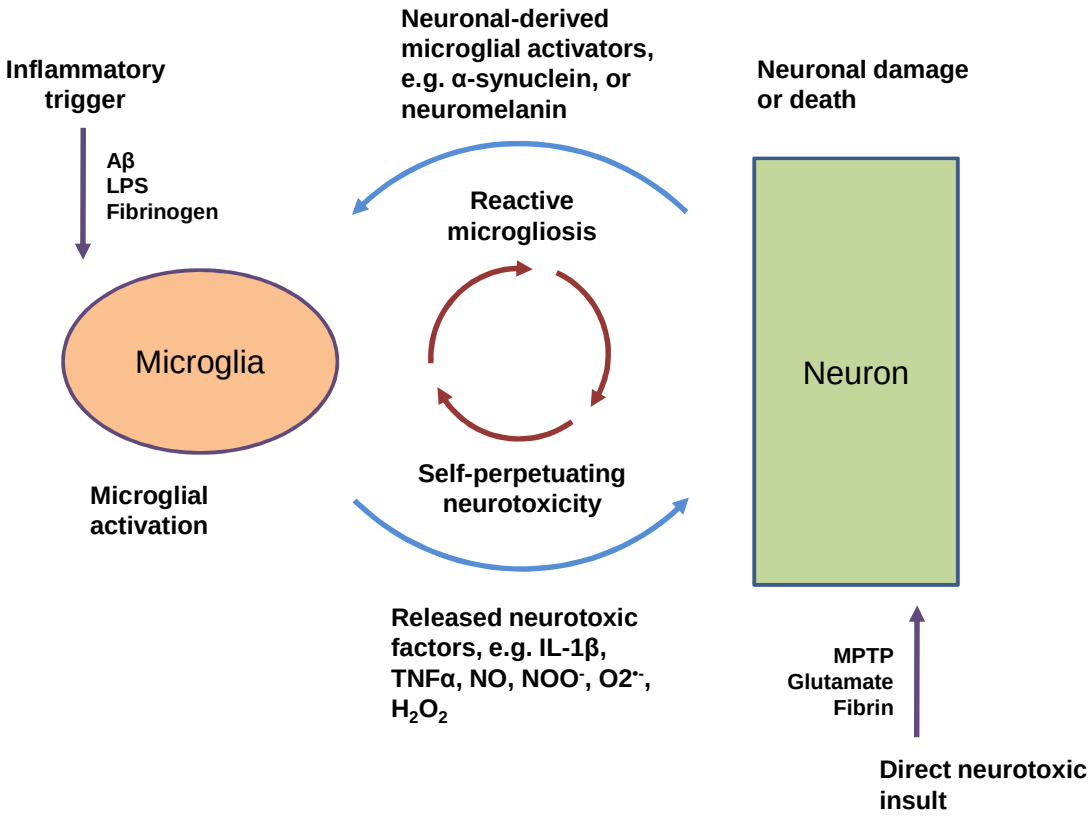

Figure 1.1.6. Activated microglia in self-perpetuating neurotoxicity

The mechanism through which microglia are activated is either via a direct stimulus or inflammatory trigger such as LPS or due to neuronal damage from toxins such as MPTP and the release of neuronal-derived microglial activators such as α-synucelin leading to reactive microgliosis. This can also induce the subsequent release microglial-derived neurotoxic factors including cytokines and reactive oxygen and nitrogen species. In chronic neurodegeneration these mechanisms could lead to self-perpetuating neurotoxicity through sustained activation of microglia.

1.2. The blood brain barrier – structure, function and dysfunction

The bacteriologist Paul Ehrlich was first to touch on the concept of a barrier separating the brain from the rest of the body in the early 20th century. He noticed that after intravenous injection of a range of dyes, staining was observed in all tissues except for the brain. However at first he assumed the reason for lack of staining was due to a low affinity for the dyes in CNS tissue (Ehrlich 1904). It was not until a student of Ehrlich's, Edwin Goldmann, injected the same dyes into the cerebrospinal spinal fluid and observed the opposite to Erhlich's conclusions that the concept of the barrier was proposed (Goldmann 1913).

1.2.1. Structure and Function

Today the blood brain barrier (BBB) can be defined by its functions of limiting the entry of plasma components, red blood cells and leukocytes into the CNS, and maintaining the chemical composition of the neuronal environment, which is required for the proper functioning of neuronal circuits, synaptic transmission, angiogenesis, and neurogenesis in the adult brain (Zlokovic 2008). The human brain receives approximately 20% of cardiac output and if cerebral blood flow stops or slows, brain functions can stop in seconds leading to neuronal damage occurring within minutes (Girouard & Iadecola 2006). Thus neuronal-vascular relationships are critical for normal brain function.

In simplistic terms the BBB is composed of a tightly sealed monolayer of brain endothelia, which precludes free exchange of solutes between the blood and brain and visa versa (Abbott et al. 2006; Zlokovic 2008). Brain endothelial cells are functionally different from peripheral vascular endothelial cells. They contain an increased number of mitochondria, lack fenestrations, have minimal pinocytotic activity, and very importantly, form tight junctions (Desai et al. 2007) with proteins such as occludins and claudins, which confer the low paracellular permeability and high electrical resistance of the barrier (Zlokovic 2008). Transport across the barrier is therefore via active rather than passive mechanisms, which can be classified into 5 main categories: carrier-

mediated transport, ion transport, active efflux transport, receptor-mediated transport and caveolae-mediated transport. These mechanisms transport nutrients and ions, expel metabolites, transport large proteins, and regulate endocytosis, respectively.

In partnership with the monolayer of brain endothelia, neurons, pericytes, astrocytes and microglia form a functional unit referred to as the neurovascular unit (**Figure 1.2.1**) creating an interface between the brain and vasculature (Bell & Zlokovic 2009). Pericytes are from vascular smooth muscle lineage (Zlokovic 2008). Their processes wrap the brain endothelium and communicate directly through the specialized synapse-like "peg-socket" contacts (Bell & Zlokovic 2009), contributing to the stability of the microvessels (von Tell et al. 2006). These cells regulate endothelial growth and migration through release of growth factors and angiogenic molecules such as TGFβ (Desai et al. 2007; Dore-Duffy & LaManna 2007). Recent studies have suggested pericytes are vital for the formation of the BBB, regulating functional aspects including the formation of tight junctions between the brain endothelia (Daneman et al. 2010).

Astrocytes communicate with other cells of the neurovascular unit through 'end feet' which contact the capillary surface providing the brain with physical support, with an important role in regulating brain water-electrolyte metabolism (Zlokovic 2008). Factors released from the astrocytes such as TGFβ and IL-6 enhance expression of endothelial signalling proteins and tight junction proteins leading to improved BBB function (Desai et al. 2007). Furthermore, astrocytes contribute to brain communication pathways, for example by modulating synaptic transmission (Newman 2003).

Microglia under inflammatory conditions release cytokines and chemokines that enable recruitment to the CNS of peripheral mononuclear cells that are able to penetrate the healthy BBB by a process of diapedesis directly through the cytoplasm of the brain endothelia cells and not via a paracellular route (Abbott et al. 2010). Microglia also form end feet connections with the brain endothelia and along with the astrocytic end feet are termed the glia limitans. This part of the barrier coupled with the basement

membrane forms the final obstacle for the mononuclear cell entry into the brain (Man et al. 2007). Finally, the basement membrane separates the brain endothelium from the pericytes and astrocytes in the neurovascular unit (Zlokovic 2008). It is composed of extracellular matrix proteins including collagen type IV, heparin, sulphate proteoglycans, laminin and fibronectin, and provides mechanical support for the neurovascular unit (Desai et al. 2007).

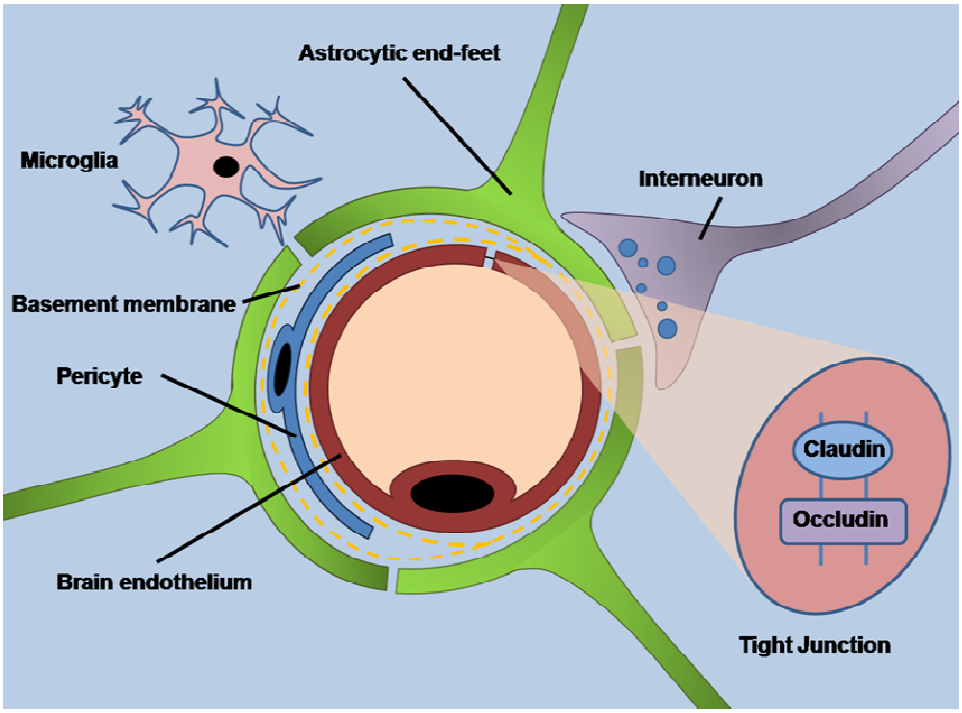

Figure 1.2.1. Components of the neurovascular unit and blood brain barrier

The blood brain barrier at the immediate vasculature interface is formed from brain endothelia that are secured together by tight junctions that are composed of proteins including the claudins and occludins. This initial barrier is surrounded by the basement membrane, composed of extracellular matrix proteins, such as fibronection, as well as pericytes and astrocytic endfeet, which provide the cellular link to neurons. Perivascular microglia also contribute to the neurovascular units integrity.

1.2.2. Dysfunction

Dysfunction and disruption of the BBB and trans-endothelial migration of activated leukocytes are among the earliest pathological hallmarks seen in MS brains, with release of pro-inflammatory cytokines and chemokines contributing to the observed BBB disruption (Kermode et al. 1990; Minagar & Alexander 2003). With the use of EAE animal models of MS, it has been shown that auto-aggressive CD4+ T lymphocytes are activated outside the CNS and accumulate in the CNS by crossing the BBB due to cytokine signalling (Ransohoff et al. 2003) contributing to neuronal death. Furthermore using the same animal models, decreased expression of claudin-3 was observed, suggesting either breakdown or rearrangement of tight junctions (Wolburg et al. 2003) potentially contributing to the loss of BBB integrity. Finally, blood borne proteins including fibrinogen, normally excluded from the CNS parenchyma, have been localised to lesion sites in MS apparently prior to significant cerebral tissue injury and demyelination (Akassoglou et al. 2004) further supporting early significant breakdown of the BBB in MS. These data have been supported in house by immunohistochemical studies performed on EAE spinal cord tissue, showing significant extravascular fibrinogen staining (**Figure 1.2.2**).

In AD pathology, the role of BBB dysfunction is relatively novel in comparison to MS. A commonly accepted view, until discoveries with functional magnetic resonance imaging (fMRI) (Drake & Iadecola 2007), was that the barrier was in fact intact in AD patients when compared with 'non-demented' elderly (Alafuzoff et al. 1987). Now, it is widely accepted, as a result of information obtained from brain imaging studies in humans and animal models, that cerebrovascular dysfunction may precede cognitive decline and the onset of neurodegenerative changes in human AD and animal AD models (Bell & Zlokovic 2009). Changes in the brain capillary unit, degeneration of the brain capillaries, reduction in resting cerebral blood flow (CBF), or a combination of the aforementioned, may be the first indications of a disease process prior to the better

characterized neuronal changes and loss (Zlokovic 2008). It is now generally accepted that vascular dysfunction has a critical role in Alzheimer's disease and is discussed in further detail in **section 1.3.1**. The accumulation of Aβ on blood vessels and in the brain parenchyma can cause a decrease in CBF (Zlokovic 2008). This negatively affects the synthesis of proteins required for memory and learning, and could eventually lead to neuronal injury or death (Bell & Zlokovic 2009).

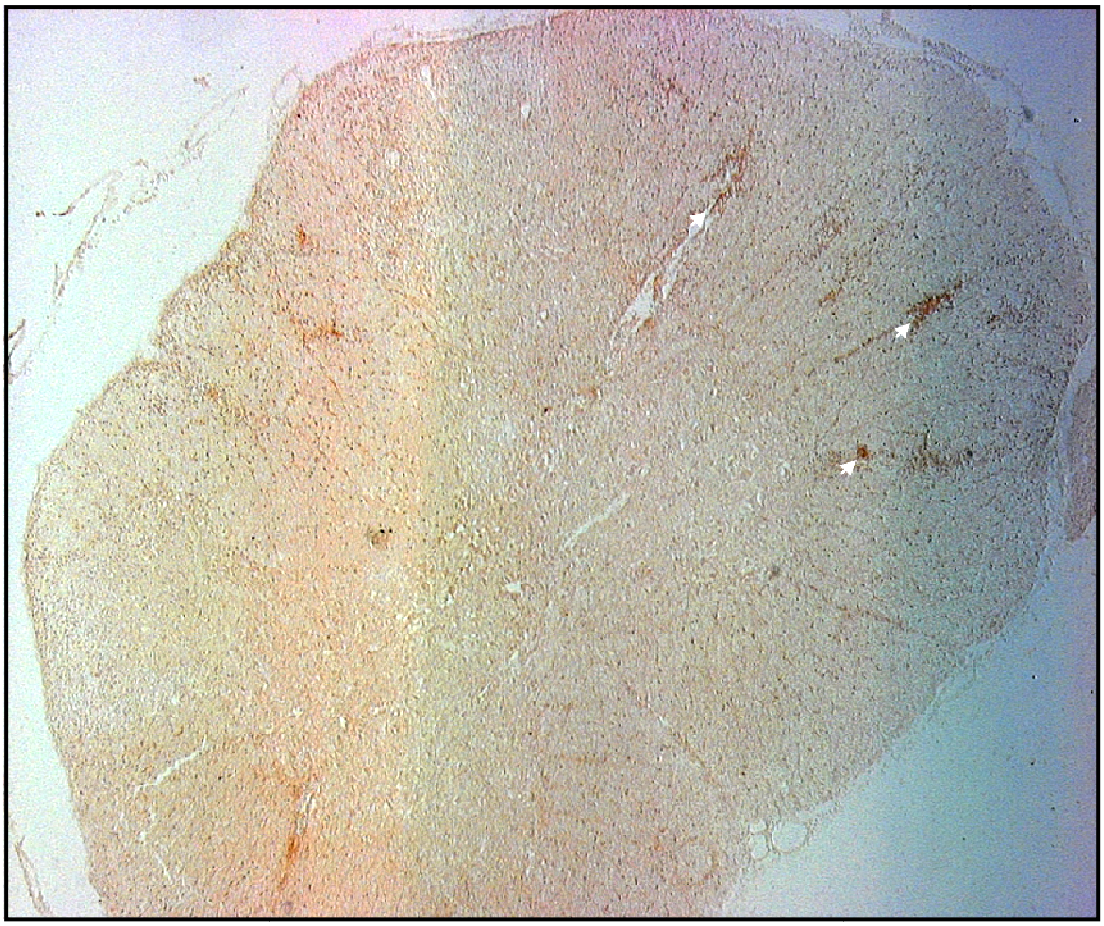

Figure 1.2.2. Fibrinogen extravasation in an animal model of blood brain barrier breakdown

Immunohistochemistry with anti-fibrinogen-HRP on symptomatic EAE rat spinal cord sections showing significant extravascular deposits of fibrinogen in the perivascular areas of the CNS (dark brown; prominent areas shown with arrow heads).

Expression of the major Aβ-influx transporter, RAGE, has been shown to increase in affected cerebral vessels, microglia and neurons, suggesting peripheral Aβ could be transported back into the CNS. Furthermore, expression of low-density lipoprotein receptor related protein-1 (LRP), a key Aβ clearance receptor at the BBB and along the cerebrovascular system, is suppressed early in AD (Zlokovic 2008; Bell & Zlokovic 2009), with decreased expression of the major efflux transporter p-glycoprotein also observed (Lee & Bendayan 2004). Other changes in the expression of key vascular genes and receptors in brain capillaries and small cerebral arteries are also likely to compromise BBB functionality, causing an increase in Aβ accumulation and a neuroinflammatory response (Zlokovic 2008; Abbott et al. 2010). The neuroinflammatory hallmark of AD is likely to have an impact on barrier integrity and function, with pro-inflammatory cytokines TNFα and IL-1β, both elevated in AD, being well-known disruptors of BBB integrity in sepsis (Desai et al. 2007).

Other functional abnormalities likely to have an effect on BBB integrity in AD are changes in the organization and expression of tight junction proteins after Aβ deposition (Marco & Skaper 2006). Furthermore, studies on institutional and ambulatory patients with AD have shown an increase in serum proteins within the CSF, suggesting increased permeability of the BBB (Elovaara et al. 1985; Kalaria & Kroon 1992). The detrimental impact of this increase in serum proteins in the CNS has been studied in animal models of AD, where significant deposition of fibrinogen accelerated neurovascular damage and enhanced neuroinflammation (Paul et al. 2007).

Limited data has been published on BBB dysfunction in Parkinson's disease (PD) however it has been suggested that absorption and metabolism of putative PD toxins and faulty elimination of these toxins from the CNS, across the BBB, may play a role in disease pathogenesis (Zlokovic 2008). Interestingly, studies suggesting a polymorphism in the p-glycoprotein efflux transporter gene *MDR1* may predispose carriers to damaging effects of pesticides leading to a PD-like phenotype (Drożdzik et

al. 2003). Further studies expanded the number of polymorphisms in the *MDR1* gene found to be associated with the risk of developing PD in a Chinese population (Lee et al. 2004a). Functional support for this genetic risk factor was provided by PET studies that indirectly observed a decrease in the p-glycoprotein efflux transporter in the midbrain of people at a risk of developing PD (Kortekaas et al. 2005). However, further studies identified limited changes in p-glycoprotein expression in early PD (Bartels et al. 2008a), although significant decreases were observed in later stages of the disease (Bartels et al. 2008b), suggesting loss of the p-glycoprotein efflux transporter is not a primary event in the pathogenesis of PD.

The occurrence of BBB disruption in ALS was initially suggested due to studies that observed abnormally high levels of IgG and albumin in the CSF of ALS patients (Leonardi et al. 1984). These studies were supported by subsequent observations of an increased level of IgG in the spinal cord of ALS patients (Engelhardt & Appel 1990). Furthermore, the same group showed IgG from the sera of ALS patients could induce death in an *in vitro* culture of the motor neuron cell line VSC4.1 (Smith et al. 1994).

The use of G93A SOD1 mutation mice as a model of ALS has showed functional impairment of the BBB, demonstrated by Evans blue extravasation into the spinal cord at the early stages of disease onset (Garbuzova-Davis et al. 2007). Furthermore this study observed significant decreases in the expression of glutamate transporter-1 and CD146, which suggested endothelia damage or loss. These observations were subsequently supported by Zhong et al (2008), in a number of animal models of ALS, who also detected significant decreases in tight junction proteins that preceded significant expression of inflammatory markers and disease onset, suggesting pre-symptomatic BBB dysfunction occurs very early in ALS disease progression (Zhong et al. 2008).

The decrease in tight junction proteins was translated to the human disease with studies quantifying mRNA levels of the proteins in post-mortem samples (Henkel et al.

2009). These abnormalities in tight junction protein expression were confirmed by studies on post mortem human spinal cord from ALS patients (Miyazaki et al. 2011) with further observations including changes in basement membrane component levels and a significantly higher dissociation of astrocytic end feet from the neurovascular unit, supporting a loss of BBB integrity in ALS.

BBB dysfunction in neurodegeneration is clearly an extremely important pathological event. It seems the loss of integrity observed in the disorders described can be divided into three general areas:

- The inefficient clearance of toxins
- Increased transport of auto-aggressive immunocompetent cells across the BBB
- A physical loss of barrier integrity partly due to loss of tight junctions

1.3. Neurodegenerative diseases – focussing on inflammation and microglial involvement

Inflammation is an underlying component of a diverse range of neurodegenerative diseases (NDDs) and their associated neuropathology and it is believed by many that microglia are a causative factor in this process (Block et al 2007). Here, descriptions of the main NDDs focussed on in this thesis will be provided with an emphasis on the involvement of inflammation and microglia.

1.3.1. Alzheimer's disease

Alzheimer's disease (AD) can be broadly characterised by progressive cognitive decline associated with neurovascular dysfunction (Iadecola 2004; Zlokovic 2005), accumulation of neurotoxic Aβ in vasculature and the brain parenchyma (Hardy 2006), and intraneuronal fibrillar tangles (Santacruz et al. 2005; Qiang et al. 2011).

Aβ has been at the centre of Alzheimer's disease research since the proposal of the amyloid cascade hypothesis (Hardy & Allsop 1991) due to the discovery of a mutation in the amyloid precursor protein gene in familial AD patients (Goate et al. 1991). Furthermore, levels of Aβ have been shown to be increased in the interstitial fluid of familial and sporadic AD sufferers, leading to the formation of neurotoxic Aβ oligomers (Haass & Selkoe 2007).

Only around 1% of AD cases are familial with approximately 99% of AD patients presenting with sporadic late onset AD (LOAD), which is defined as being over the age of 65 years with no evidence of Mendelian genetic transmission (Tanzi & Bertram 2005). Twin studies into genetic risk factors for the development of LOAD have however shown sporadic AD to be highly heritable with genes involved in more than 60% of disease susceptibility with mutations in the *APOE* gene accounting for as much as 50% of this genetic susceptibility (Gatz et al. 2006).

Familial mutations in APP have been shown to increase the production of $A\beta_{42}$ compared with the shorter $A\beta_{40}$ (Suzuki et al. 1994). This longer form more readily forms insoluble amyloid fibrils suggesting a possible mechanism for enhanced Aβ deposition. Interestingly however, no increase in Aβ production is observed in LOAD and current concepts suggest that Aβ accumulates in the sporadic form due to faulty clearance (Tanzi et al. 2004), contributing to neurovascular accumulation and vascular deposition of Aβ leading cerebral amyloid angiopathy (CAA) (Greenberg et al. 2004), a significant risk factor in dementia (Zlokovic 2008) and a prominent feature in the alternative vascular hypothesis of AD (de la Torre 2004). Furthermore, recent studies have identified that fibrinogen contributes to this faulty clearance of Aβ (Cortes-Canteli et al. 2010). Recent data has identified new genetic risk factors for LOAD, namely clusterin and complement receptor 1 (*CLU* and *CR1*, respectively) (Harold et al. 2009; Lambert et al. 2009). The protein products of these genes are associated with cellular clearance pathways, with clusterin previously being shown to be involved in the regulation of microglial-mediated phagocytosis of Aβ (Cole & Ard 2000).

Extensive evidence has been published suggesting that Aβ deposition provokes microglial-mediated inflammatory responses that significantly contribute to cell loss and cognitive decline (Akiyama et al. 2000). Levels of the pro-inflammatory cytokine TNFα are shown to increase in the brains and plasma of AD patients (Fillit et al. 1991; Tarkowski et al. 1999). Furthermore TNFα has been shown to induce neuronal death (Venters et al. 1999; Taylor et al. 2005), with *in vitro* studies identifying microglial signalling pathways induced by Aβ subsequently lead to the release of this pro-inflammatory cytokine (Combs et al. 2000; Combs et al. 2001).

Chromogranin A (CgA) is an AD plaque-associated peptide. Studies published from our laboratory have identified CgA-mediated toxicity of both microglia and neurons (Kingham et al. 1999; Kingham & Pocock 2000; Taylor et al. 2002; Taylor et al. 2003; Hooper & Pocock 2007). Recent studies have also identified the microglial scavenger receptor class A (SR-A) as the putative receptor for the observed CgA-mediated

neurotoxicity (Hooper et al. 2009a) with regulation by the transcription factor p53 also observed (Davenport et al. 2010).

Further *in vitro* studies coupled with *in vivo* studies have identified the CD11b (MAC-1, CR3, $\alpha_M\beta_2$ integrin) receptor and PI3K pathway to be essential in fibrillar Aβ-mediated microglial activation leading to superoxide production and neuronal loss (Zhang et al. 2011)

Clinical data to identify the role of microglia in AD has been advanced with PET studies using ^{11}C-R-PK11195, a marker for activated microglia (Banati 2002). Initial studies suggest that the ^{11}C-R-PK11195 signal is significantly enhanced in particular areas of the brain in AD patients when compared with controls, mostly correlating with a significant increase in amyloid load. Interestingly, along with the microglial association with amyloid deposition, a negative correlation between microglial activation and Mini Mental State Examination (MMSE) test results was observed, suggesting microglial activation in an attempt to decrease the amyloid burden could be contributing to neuronal dysfunction and cognitive deficits (Edison et al. 2008).

Epidemiological studies have demonstrated that people prescribed non-steroidal anti-inflammatory drugs (NSAIDs) for relatively long periods of time were less inclined to develop AD (Etminan et al. 2003; Vlad et al. 2008), and limited evidence suggests that they may attenuate AD progression (Weggen et al. 2007). Although clinical trials with NSAIDs failed to show any significant efficacy in AD (possibly due to inhibition of only one inflammatory pathway in microglia), the epidemiological studies coupled with new genetic risk factor data support a prominent role for inflammation in AD, which would subsequently involve the immune-competent cells of the CNS. With this in mind, any significant breakthrough in our understanding of how microglia are involved in the cognitive decline observed in AD could provide a leap forward in our therapeutic strategies for this disease.

1.3.2. Multiple sclerosis

Multiple sclerosis (MS) involves the chronic destruction of the protective myelin sheath around nerve axons via degradation of its cellular components, (oligodendrocytes in the CNS, Schwann cells in the PNS) and subsequent loss of neuronal functionality. Symptoms can vary significantly from patient to patient but include: visual disturbances, muscle weakness, co-ordination and balance issues, numbness and prickling sensations and cognitive issues. The majority of patients (80%) suffer from relapsing-remitting MS where symptoms typically evolve over a period of several days, stabilise and then often improve, either spontaneously or after administration of corticosteroids, within weeks. It typically begins in the 2^{nd} – 3^{rd} decade of life with a female predominance of 2:1 (Noseworthy et al. 2000). Secondary progressive MS occurs in patients suffering from the relapsing-remitting disease and is identified by persistent signs of CNS dysfunction developing after a relapse, with disease progression occurring between relapses. Finally, the other 20% of patients suffer from primary progressive MS, which is characterised by a gradually progressive clinical score.

The pathological hallmark of chronic MS is the demyelinated plaque which can be characterised by a hypocellular region due to demyelination, relative preservation of neurons and astrocytic scars (Compston et al. 2005). It is broadly believed to be an immune-mediated disorder that occurs in genetically susceptible people (Noseworthy et al. 2000). However, despite the obvious immunological features of the disorder other researchers believe it is primarily a neurodegenerative disease (Hemmer et al. 2002; Chaudhuri & Behan 2004) arguing amongst other things that many NDDs have immunological elements. Given the considerable clinical, genetic, MRI and pathological heterogeneity of the disease, it is most likely that more than one molecular mechanism contributes to the significant tissue injury observed (Noseworthy et al. 2000).

Along with infiltrating lymphocytes, microglia play important roles throughout the pathogenesis of MS. In the early stages of disease, prior to significant BBB disruption

or myelin sheath degradation activated microglia have been observed in MS lesion tissue (Gay et al. 1997), and along with the oligodendrocytes have been proposed to drive MS pathology with identification in pre-active lesions (van der Valk & Amor 2009). Furthermore, activated microglia have been shown adhering to damaged myelin sheaths and axons in acute MS lesions, suggesting a role for these cells in the destructive process (Trapp et al. 1998). Finally, laser confocal microscopy of post-mortem MS patient tissue showed significant iNOS expressing cells in chronically active lesions with a sub-population identified as microglia (Hill et al. 2004).

In an EAE model of MS, dendritic microglia have been demonstrated to present myelin antigens to infiltrating T cells within the brain suggestive of a critical role in driving the progression observed in this model (Miller et al. 2007). Furthermore, studies using *in vivo* pharmacogenetic and bone marrow chimera techniques identified that microglial paralysis could substantially repress the development of EAE disease progression (Heppner et al. 2005).

The ability of microglia to phagocytose myelin has been demonstrated *in vitro*. Initial studies found human microglia-mediated phagocytosis of myelin induced significant release of IL-1, IL-6 and TNFα after 12 – 24 hours (Williams et al. 1994). Interestingly, earlier studies suggest that peritoneal macrophage-mediated myelin phagocytosis was dependent on the MAC-1 receptor, with increased TNFα concentrations significantly reducing the cells' ability to phagocytose myelin (Brück et al. 1992). Later studies suggest microglia are more efficient than peritoneal macrophages at phagocytosing myelin (Mosley & Cuzner 1996). Furthermore, myelin-mediated microglial activation has been shown to lead to neurotoxicity, *in vitro* (Pinteaux-Jones et al. 2008).

Microglia are clearly actively involved throughout MS disease progression. Their roles in pre-active lesions with oligodendrocytes, as antigen-presenting cells within the CNS, in initiating and propagating immune responses, in phagocytosis of myelin debris and apoptotic cells, and in the production of pro-inflammatory factors potentially

exacerbating tissue injury, suggests manipulation of microglia could provide an avenue of therapeutic benefit.

1.3.3. Parkinson's disease

Parkinson's disease (PD) is a chronic movement disorder affecting the dopaminergic neurons, specifically in the substantia nigra and locus coeruleus, with one hypothesis suggesting an initial locus in the dorsal motor nucleus of the vagus nerve (Braak et al. 2006). The neuronal loss is accompanied by three distinctive intraneuronal inclusions: the Lewy body, the pale body, and the Lewy neurite, with the main component of Lewy bodies being the aggregated form of the presynaptic protein α-synuclein (Lees et al. 2009). Typically PD sufferers have lost over 80% of their dopaminergic neurons before symptoms appear which include tremors, rigidity, slow movement (bradykinesia), balance issues and the Parkinsonism gait.

PD is generally considered as a sporadic disease with ageing as the major risk factor. Incidence of the disease rises steeply from 17.4 in 100,000 between the ages of 50 and 59 years to 93.1 in 100,000 between the ages of 70 – 79 years, with a total lifetime risk of 1.5% (Lees et al. 2009). However, approximately 10% of cases develop before the age of 45. Due to the sporadic nature of the disease, environmental factors are assumed to take a prominent role. To date, certain environmental toxins have been identified including 1-methyl-4-phenyl-1,2,3,6-tetrahydropyridine (MPTP), cyanide, rotenone and toluene, which can produce a similar but not identical models of the disorder (Tanner & Aston 2000).

Investigations into genetic factors have identified a number of genes with mutations associated with Parkinsonism or PD, including *α-synuclein, LRRK-2, GBA, MAPT,* HLA-*DRA*, *Parkin, PINK1, DJ-1 and ATP13A2* (Lees et al. 2009; Simón-Sánchez et al. 2009; Hamza et al. 2010). The most interesting risk factor with respect to inflammation and microglia in PD is the latest factor to be identified, *HLA-DRA* (Hamza et al. 2010), a gene that partly codes for the class II HLA-DR antigen protein expressed by antigen-

presenting cells such as microglia, enabling interaction with inflammatory T cells (Kreutzberg 1996). Interestingly, mutations in this gene have also been associated with multiple sclerosis (Noseworthy et al. 2000).

Microglial inflammation is thought to underpin the tissue damage in PD (Halliday & Stevens 2011) with a neuroprotective phenotype in early PD followed by a switch to a neurotoxic phenotype as the disease progresses (Sawada et al. 2006), although this hypothesis has been brought into question (Graeber & Streit 2009). Modelling dopaminergic neuronal loss with the neurotoxin MPTP has identified microglial activation as a contributing factor to MPTP-mediated toxicity. MPTP induces its neurotoxic effects after conversion to MPP^+, catalysed by the mostly astrocytic enzyme monoamine oxidase B (Lobsiger & Cleveland 2007). In MPTP-treated mouse models of PD, significant microgliosis and enhancement of iNOS expression in microglia has been observed after treatment. Furthermore $iNOS^{-/-}$ mice were shown to be more resistant to MPP^+ toxicity (Liberatore et al. 1999), and therefore, taken with the microglial-associated iNOS expression, these data suggest an important mechanistic contribution from microglia in the MPP^+-mediated toxicity. *In vivo* studies and *in vitro* co-cultures have provided support for the inflammatory microglial involvement in MPP^+-mediated neurotoxicity. Studies using the inflammatory modulator minocycline reduced MPP^+-mediated iNOS expression in BV2 microglia and MPP^+ induced neurotoxicity could only be attenuated by minocycline if glia were present (Du et al. 2001).

The major constituent of Lewy bodies, mutated α-synuclein, has been shown to more potently stimulate microglia to a pro-inflammatory phenotype than the normally folded protein, with increased levels of IL-1β and TNFα observed (Klegeris et al. 2008). Recently, wildtype α-synuclein has been shown to alter TLR expression on microglia (Béraud et al. 2011), suggesting the protein contains a pathogen-associated molecular pattern (PAMP), required for recognition by TLRs (**Section 1.5.1.2.1**).

These models specifically target one aspect of PD pathology, whether it's neuronal loss or Lewy body constituents. The development of more comprehensive models utilising α-synuclein mutants in conjunction with chemically induced loss of neurons, or the use of rotenone, another dopaminergic neurotoxin which also aggregates α-synuclein (Betarbet et al. 2000; Sherer et al. 2003) would, in my view, provide more relevant data to the human disorder, some of which is starting to appear (Mount et al. 2007).

1.3.4. Amyotrophic lateral sclerosis

Motor neurone disease or amyotrophic lateral sclerosis (ALS) is a chronic neurodegenerative disorder of vulnerable motor neurons in the brain, brainstem and spinal cord. Symptoms include fasciculation, muscle wasting and weakness, increased spasticity, hyper-reflexia and respiratory complications, which usually occur in advanced disease causing death through paralysis of the respiratory muscles and diaphragm after 2 – 5 years from disease onset (Boillée et al. 2006a; Glass et al. 2010). The majority (90%) of patients suffer from sporadic ALS, whereas the remaining 10% suffer from familial ALS, a quarter of which are associated with genetic mutations in superoxide dismutase-1 (*SOD-1*), an enzyme involved in the destruction of the reactive oxygen species, superoxide ($O_2^{\bullet -}$). To date over 115 disease-associated mutations have been found in the *SOD-1* gene and the emerging general consensus suggests that the disease results from a toxic gain of function in the mutant protein, not loss of enzymatic activity (Lobsiger & Cleveland 2007). In support of this, complete absence of functional SOD-1 does not compromise life-span in mice or promote motor neurone disease (Boillée et al. 2006a).

Studies have suggested that SOD-1 is a central contributor to disease initiation but not disease progression. The use of short interfering RNA (siRNA) to specifically silence mutant SOD-1 in motor neurons substantially delayed disease onset but did not significantly delay progression after onset (Ralph et al. 2005), suggesting other non-cell autonomous mechanisms are involved. Thus, the observed role for inflammation in

ALS could provide answers to this mechanistic shortfall. Both ALS animal models and patients develop prominent features of neuroinflammation including astrogliosis and microgliosis (Boillée et al. 2006a; Lobsiger & Cleveland 2007). Interestingly however, treatment of ALS mutant mice with minocycline significantly extended survival by delaying disease onset (Zhu et al. 2002), suggesting a prominent role for inflammation, as well at mutant SOD-1, in disease initiation.

Later more elegant studies strongly suggested that microglia were significantly involved in ALS disease progression. Boillée and colleagues (2006) used a CD11b-promoter driven Cre transgene to specifically knockdown mutant SOD-1 in cells of the myeloid lineage (including microglia) in a LoxSOD1^{G37R} mouse model of ALS. These animals showed no delay in disease onset, suggesting a microglial SOD-1-independent mechanism in disease initiation. However survival was greatly enhanced due to slowing of disease progression (Boillée et al. 2006b), suggesting microglial-specific mutant SOD-1 contributes significantly to ALS progression. A similar outcome was observed in another study using differing techniques. Using a double mutant mouse SOD1^{G93A}/PU.1$^{-/-}$ (PU.1 is a transcription factor vital for production of myeloid derived cells) bone marrow transplantation was performed to provide a donor-derived microglial population (Beers et al. 2006). If SOD1^{G93A}/PU.1$^{-/-}$ mutants received wild-type donor-derived microglia after bone marrow transplantation, motor neuron loss was significantly slowed and disease duration was prolonged, when compared with mice receiving SOD1^{G93A} donor-derived microglia (Beers et al. 2006).

A number of microglial associated inflammatory factors have been proposed as key mediators in this motor neuron loss including TNFα, enhanced synthesis of which has been shown by SOD^{G93A} mutant microglia (Weydt et al. 2004). However, deletion of the TNFα gene did not affect the lifespan or the extent of motor neuron loss in either SOD^{G93A} or SOD1^{G37R} ALS mouse models (Gowing et al. 2006), suggesting other inflammatory mediators are involved. NADPH oxidase-dependent reactive oxygen

species were found to be the likely component of the microglial-mediated non-cell autonomous ALS progression. Studies showing genetic knockdown of the $gp91^{phox}$ catalytic subunit of the NADPH oxidase significantly extended survival in SOD^{G93A} ALS models, although like previous studies (Zhu et al. 2002), this seems to be due to delay of disease onset rather than slowing disease progression, suggesting little correlation can be made here with the mutant microglial-ablation studies (Boillée et al. 2006b; Beers et al. 2006).

In each of the diseases described, distinct pathways are involved in the generation of the inducers of inflammation, such as Aβ, myelin, α-synuclein or SOD-1, that occurs in distinct brain regions. However, once these disease-associated inducers of inflammation are present, remarkable convergence in the effector mechanisms is observed leading to the amplification of inflammation and subsequent neurotoxicity and neuronal death, with activation of microglia as the universal component. Attenuating neuroinflammation may not prevent disease initiation or alter the underlying cause, but by specifically targeting microglial-mediated release of neurotoxic factors there are suggestions that progression could be slowed, potentially providing a clinical benefit.

1.4. Cell Death

Cell death is defined as irreversible loss of plasma membrane integrity (Kroemer et al. 2009). In broad terms, there are three specific types of cell death that have been characterised extensively based on morphological criteria. The first type of cell death termed apoptosis by Kerr and colleagues in 1972 can be morphologically identified by characteristic changes in nuclear morphology, including chromatin condensation (pyknosis) and fragmentation (karyorrhexis), minor changes in cytoplasmic organelles, and overall cell shrinkage, blebbing of the plasma membrane and formation of apoptotic bodies that contain nuclear or cytoplasmic material (Kroemer et al. 2009), with these changes occurring prior to loss of plasma membrane integrity. The second type of cell death is characterized by the presence of large autophagic vacuoles in the cytoplasm, hence the commonly used nomenclature, autophagy-mediated cell death. The final form of cell death termed necrosis is often defined as an unregulated form of cellular destruction. Necrosis is determined morphologically by early plasma membrane rupture and dilatation of cytoplasmic organelles, in particular mitochondria and nuclei (Kroemer et al. 2009). In recent years a regulated form of necrosis has been suggested with data proposing death receptor activation can occur in apoptotic-'deficient' conditions, termed necroptosis (Hitomi et al. 2008).

This thesis focuses on mainly characterising apoptotic cell death in cell cultures after exposure to fibrinogen and fibrin, therefore the focus of this chapter will be on apoptotic pathways, with particular attention paid to ER stress-mediated apoptosis.

1.4.1. Apoptosis

Apoptosis is an evolutionary conserved form of cell death. As previously stated it is characterised morphologically by nuclear and cytoplasmic condensation, nuclear membrane breakdown, DNA cleavage, plasma membrane blebbing and creation of apoptotic bodies (Kerr et al. 1972). Apoptosis occurs via two execution programs downstream of a death signal. The first is via caspase pathways and the second is due

to organelle dysfunction, such as mitochondrial or endoplasmic reticulum dysfunction (Danial & Korsmeyer 2004), with some convergence of the two pathways usually occurring. The process is highly regulated by members of the B-cell leukaemia/lymphoma-2 (Bcl-2) family (Pettmann & Henderson 1998) preventing uncontrolled apoptosis from occurring. Within the central nervous system it follows a specialized highly ordered sequence of signalling cascades. These cascades can be initiated by intrinsic factors such as calcium dyshomeostasis or chronic production of reactive oxygen species (ROS) (Benn & Woolf 2004). Induction can also occur via an extrinsic pathway involving death receptors and pro-inflammatory cytokines (Degterev & Yuan 2008).

1.4.1.1. The role of the caspases

Caspases are a family of cysteine protease enzymes that are triggered in response to pro-apoptotic signals and result in the cleavage of protein substrates, causing disassembly of the cell (Gross et al. 1999). With respect to apoptosis, they are divided into two sub-groups named initiator caspases and executioner caspases. They are synthesised as catalytically inactive zymogens that require proteolytic activation to induce apoptosis (Shi 2002). Caspases have a cysteine residue at the active site and are cleaved after aspartic acid (Asp) residues, hence the name, **C**-**ASP**-ase. As summarised in **Figure 1.4.1**, procaspases contain an N-terminal prodomain, as well as sequences that encode the large (p20) and small (p10) subunit of the activated protease. These subunits form a heterodimer, with two such dimers assembling to for the active tetramer (Alberts 2008). The initiator caspases can be characterised by a long prodomain (>90 amino acids), containing a caspase recruitment domain (CARD) that serves as a platform for the recruitment of activating adapter proteins, such as Apaf-1 (Kurokawa & Kornbluth 2009) inducing activation and the subsequent amplifying, irreversible caspase cascade (**Figure 1.4.2**).

Caspase-1, or mammalian interleukin-1β-converting enzyme (ICE), was the first caspase hypothesized to be involved in apoptosis because of the enzyme's homology with CED-3, the product of a gene (*ced-3*) required for death in the nematode *C-elegans* (Slee et al. 1999). It has now been identified that caspase-1 is primarily involved in the induction of inflammation (Yuan et al. 1993). However, caspase-1 involvement in chromogranin-A-induced microglial apoptosis has been observed in our laboratory (Kingham et al. 1999; Kingham & Pocock 2000)

As well as caspase-1, other homologues of the *C- elegans* protein CED-3 in mammals have been characterized including caspase-3, and caspase-9, which have been identified as major components in mammalian cell death cascades (Thornberry 1998). To date 14 distinct mammalian caspases have been identified, eight of which have been found to be involved in apoptosis (Shi 2002).

The use of *C- elegans* also identified homologues in mammals of the genes *ced-4* and *ced-9* as Apaf-1 and members of the Bcl-2 family, respectively (Danial & Korsmeyer 2004). The adaptor protein Apaf-1 has been shown to interact with cytochrome *c*, released from mitochondria during initiation of the intrinsic pathways of apoptosis, forming a heptomeric mega-complex called the 'apoptosome', which in turn induces cleavage of initiator caspases, such as procaspase-9 (Shi 2002) with subsequent activation of executioner caspases (**Figure 1.4.3 & 1.4.4**). The requirement for multi-component complexes to proteolytically cleave initiator caspases is a good example of the tight regulation of caspase activation.

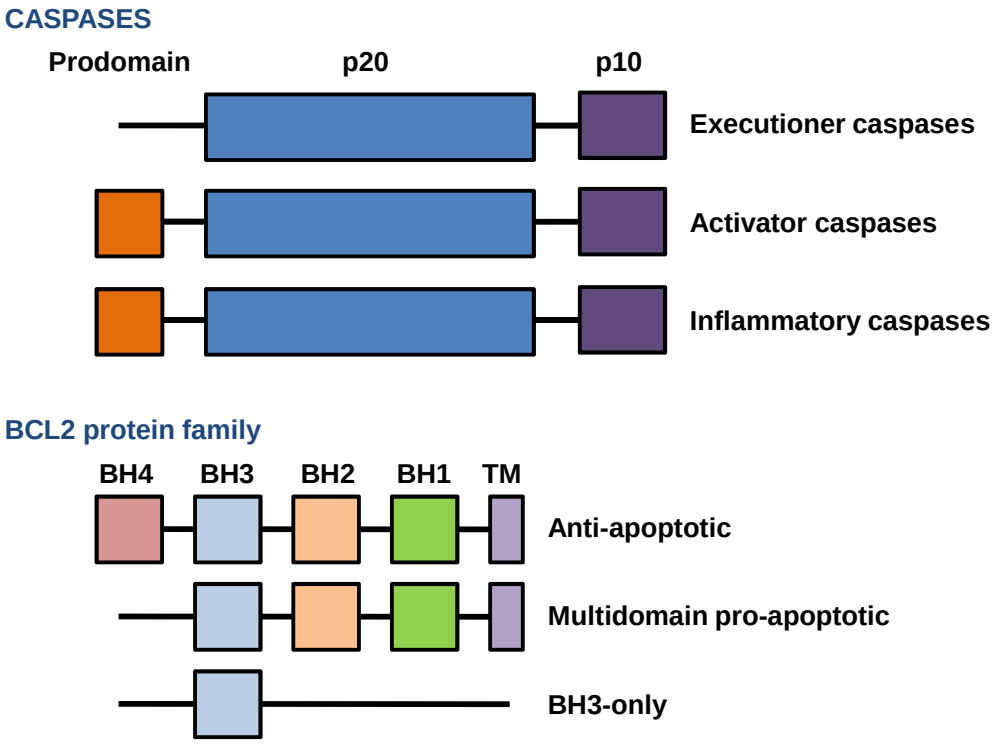

Figure 1.4.1. The main protein domains of the regulators of apoptosis

Caspases contain three main domains: a prodomain and large (p20) and small (p10) catalytic domains. The large domain contains the active Cys residue with activation of caspases involving proteolytic cleavage including the removal of the prodomain and separation of the p20 and p10 subunits.

BCL-2 family proteins are sub-divided into three classes based on domain homology: anti-apoptotic (such as Bcl-2 and Bcl_{XL}), multidomain pro-apoptotic (BAX and BAK) and BH3-only (such as BIM, BID, BAD, PUMA).

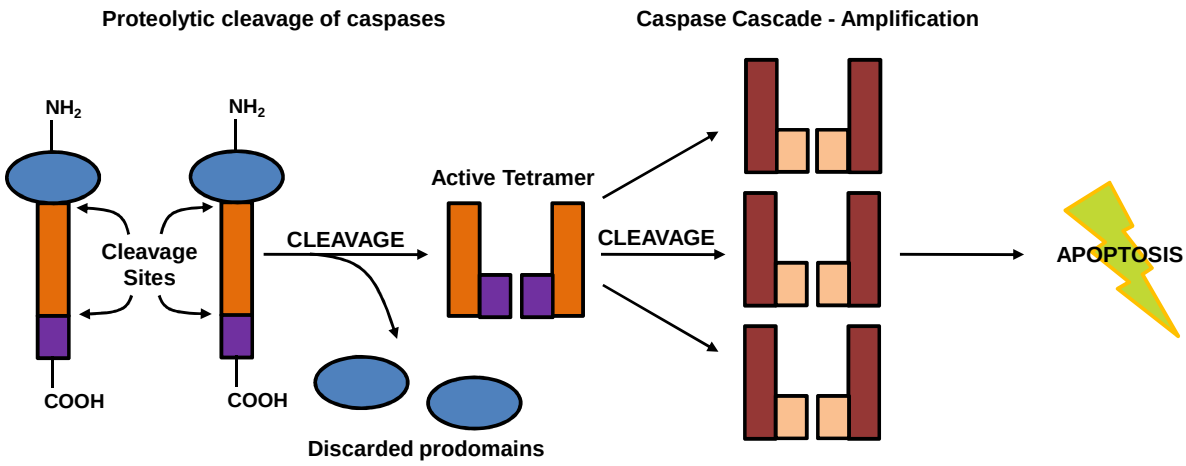

Figure 1.4.2. Classical activation of caspase zymogens during the apoptotic cascade

After discarding of the caspase prodomain, the p20 (orange) p10 (purple) domains are cleaved and form an active caspase tetramer with two other domains. The initiator caspases, once cleaved, can themselves activate many executioner caspases leading to an amplification of the signal transduction. The executioner caspases can then cleave a variety of key proteins in the cell leading to programmed cell death. Adapted from Alberts 2008.

1.4.1.1.1. Emerging non-apoptotic roles for caspases

In the last few years, caspases have been shown to be involved in non-apoptotic cellular processes. These range from a vital requirement for caspase-3 in long term depression (Li et al. 2010), and synaptic pruning and internalisation of AMPA receptors leading to early synaptic dysfunction in AD models (D'Amelio et al. 2011). Caspase-3 has also been shown to be involved in $A\beta_{1-42}$-mediated inhibition of long term potentiation (Jo et al. 2011). However, most interestingly with respect to this thesis, caspase-8 and -3/7 have now been shown to be intrinsic in LPS-mediated microglial activation (Burguillos et al. 2011; Venero et al. 2011). These new findings will be taken into consideration when critically analysing the data presented here.

1.4.1.2. The intrinsic pathway of apoptosis

The intrinsic pathway of apoptosis can be initiated by DNA damage, loss of cell adherence, or ER stress (Lindsten et al. 2005), to name a few. It involves caspase

cascade activation and is tightly regulated by the Bcl-2 family of proteins. The family, consisting of anti- and pro-apoptotic members, is divided into three main subclasses based on the homology shared within four conserved domains termed 'Bcl-2 homology (BH) 1-4 domains (Danial & Korsmeyer 2004) (**Figure 1.4.1**). The families namesake, Bcl-2, was the first member to be discovered. It was shown to block cell death following treatment with an array of physiological and pathological stimuli and was therefore the first of the anti-apoptotic members of the family to be discovered. Bax was the first pro-apoptotic member to be discovered (Oltvai et al. 1993) after interactions with Bcl-2 were observed. The inactive form of Bax resides in the cytosol or loosely anchored to membranes. On induction of a death signal the protein complexes into homooligomerised multimers that form pores in the outer mitochondrial membrane allowing efflux into the cytosol of cytochrome *c* (Lauber et al. 2001), leading to apoptosome formation and subsequent cellular breakdown. Upstream of these signals lay the BH3-only members of the Bcl-2 family. These proteins selectively respond to specific death/survival signals, serving as cellular sentinels (**Figure 1.4.3**).

Focussing on neurodegenerative disease, the exact mechanisms of mitochondrial injury is relatively unknown; however it is likely to include input from reactive oxygen species (ROS), excitotoxins and/or toxic proteins. Intracellular Ca^{2+} is of the utmost importance for many neuronal functions including cell death and it has been shown that changes in the calcium homeostasis within cells can initiate intrinsic pathways leading to apoptosis. When intracellular levels of calcium exceed physiological levels, neuronal death can occur (Degterev et al. 2001). Furthermore, with the endoplasmic reticulum being the largest store of calcium in the mammalian cell, much emphasis is now focussed on the involvement of the ER-associated activation of the intrinsic pathway of apoptosis in neurodegenerative disorders, which will be discussed in more detail in **section 1.4.1.4**.

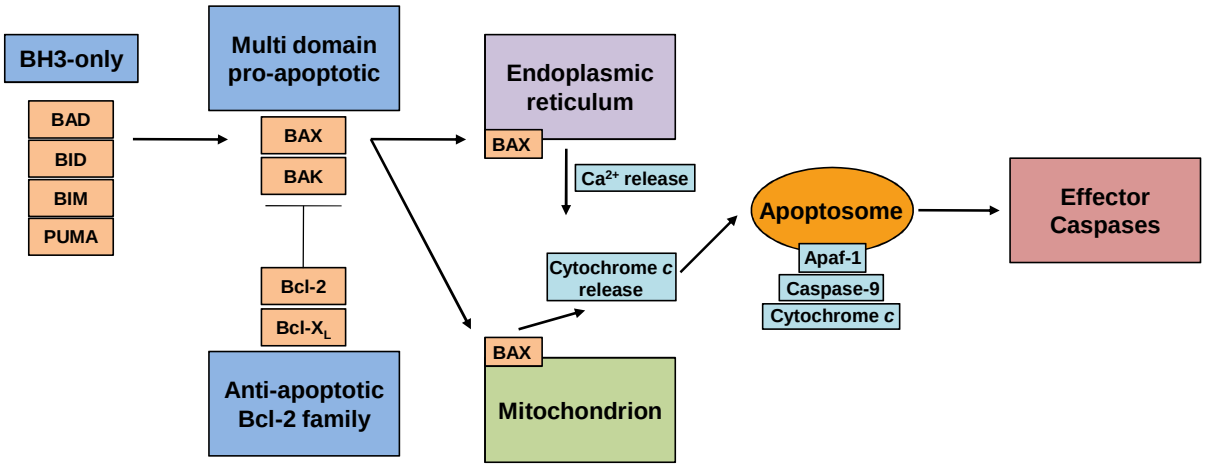

Figure 1.4.3. The intrinsic pathway of apoptosis

Initiation of the intrinsic pathway of apoptosis occurs after DNA damage, loss of cell adherence or ER stress. BH3-only Bcl-2 proteins activate the multi-domain pro-apoptotic family of Bcl-2 proteins leading to cytochrome c release from the mitochondria and ER stress-mediated Ca^{2+} dyshomeostasis. Cytochrome *c* completes the apoptosome which initiates effector/executioner caspase-mediated apoptosis Adapted from Degterev and Yuan 2008.

1.4.1.3. The extrinsic pathway of apoptosis

The extrinsic pathway is initiated through activation of death receptors on the cell surface. These contain a ligand binding domain, a single transmembrane domain, and an intracellular death domain. The receptors are homotrimers and belong to the TNF receptor family. The ligands that activate the death receptors are also structurally related homotrimers that belong to the TNF family of signal proteins (Alberts 2008). The receptors include FAS-Receptor (FAS-R; also known as Apoptosis antigen-1), tumour necrosis factor receptor 1 (TNFR1), TNFR2, and TNF-related-apoptosis inducing ligand receptor 1 (TRAILR1). Activation of these receptors, particularly TNFR1 and FAS-R can cause apoptosis independently or the cascades can converge with intrinsic pathways at the mitochondria (Cecconi et al. 1998), via the recruitment of BH3-only proteins (Danial & Korsmeyer 2004) .

FAS-R is a major death receptor in apoptosis relating to neurological disorders. Under normal physiological conditions FAS expression is relatively low; however during

chronic neurodegenerative disorders, such as AD, expression is significantly enhanced (Lukiw 2004). Taylor et al. 2005 reported that TNF-α required the presence of the Fas receptor ligand, FasL, to induce neurotoxicity after activation of the microglial metabotropic glutamate receptor 2 (mGluR2) with the group I agonist DCGIV.

The FAS-FASL interaction, extracellularly, can lead to cell death by recruitment of the Fas-associated death domain (FADD), which complexes with caspase-8 inducing activation (Benn & Woolf 2004). This complex is known as the death inducing signalling complex (DISC) (**Figure 1.4.4**). Caspase-8 in turn can stimulate downstream caspase-3 activation via an apoptosome-independent mechanism and/or initiate intrinsic apoptotic pathways via association with the BH3-only protein Bid (Danial & Korsmeyer 2004).

TNFα, a pro-inflammatory cytokine associated with microglial activation and neurodegenerative disorders can bind and activate death receptors including TNFR1 and TNFR2. Activation of TNFR1 initiates recruitment to the intracellular complex of TNF receptor associated death domain (TRADD). TRADD functions as a platform for the binding of two mediators, FADD and receptor interacting protein (RIP-1) (Micheau & Tschopp 2003). The addition of these proteins to the complex defines whether a death or survival pathway is initiated, respectively (**Figure 1.4.4**). Interestingly, RIP-1 has also been identified in another type of cell death termed necroptosis, a regulated form of necrosis (Holler et al. 2000; Hitomi et al. 2008). As suggested for FAS-R-associated extrinsic apoptosis, FADD recruitment to the DISC can induce activation of procaspase-8 which in turn can trigger amplification of downstream caspase cascades (Benn & Woolf 2004).

The cytokine TNFα not only has the capacity to directly kill cells via receptor-mediated activation of caspases, but also indirectly via the upregulation of apoptotic factors such as nitric oxide and α-chemokines (Benn & Woolf 2004). However, TNFα activation and the subsequent pathways do not always end with programmed cell death.

Observations have shown a TNFα pro-survival pathway via NFκB and activation of TNFR2 (Benn & Woolf 2004).

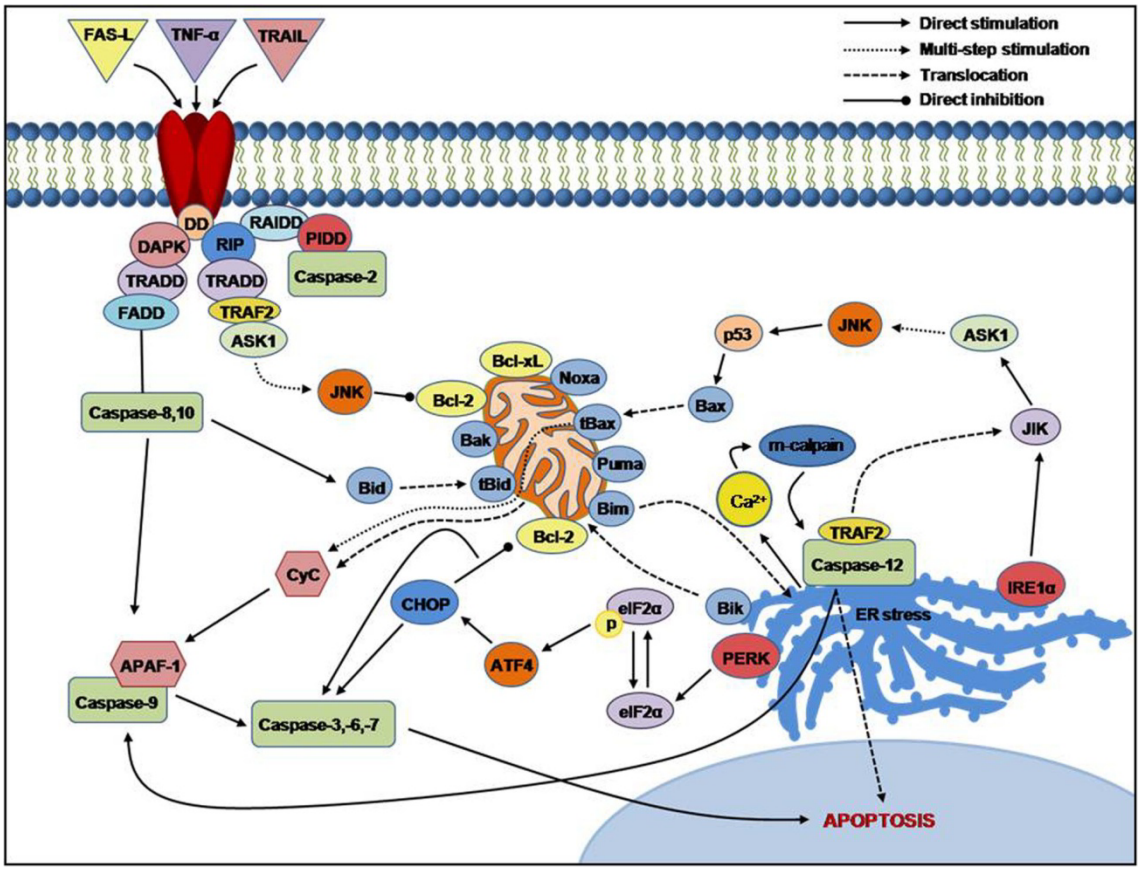

Figure 1.4.4. An overview of the extrinsic and ER stress-mediated pathways of apoptosis

Initiation of the extrinsic pathway of apoptosis occurs through death receptors such as TNFR1, FAS and TRAIL. This activation leads to intracellular recruitment of death domain proteins such as RIP, TRADD, FADD, TRAF2 and ASK1 that form a death inducing signalling complex (DISC). This in turn can activate caspases including caspase-8 and-10 that amplify the signal transduction either through the apoptosome, which includes caspase-9 and APAF-1 and cytochrome c, or through convergence with the intrinsic pathway of apoptosis via the BH3-only protein, Bid. Bid translocates to the mitochondria upon activation where it can regulate the release of cytochrome c, thus inducing formation of the apoptosome and subsequent apoptosis via caspase-3, -6, and -7 activation. ER stress-mediated apoptosis can occur through the PERK-eIF2α-ATF4-CHOP axis that leads to activation of caspase-3, -6, and -7. ER stress can also induce apoptosis via an IRE1α-ASK-p53 depedent pathway that leads to the BCL-2 protein Bax translocating to the mitochondria leading to release of cytochrome c and subsequent apoptosome formation. Furthermore caspase-12-dependent ER stress mediates its effects after calcium dyshomestasis and cleavage by m-calpain, via convergence with the apoptosome or by translocation to the nucleus. Finally, BH3-only proteins Bim and Bik have been identified as mediators of crosstalk between the mitochondria and the ER during apoptosis, with Bim translocating from the mitochondria to the ER and Bik translocating in the opposite direction.

1.4.1.4. ER stress and it's role in apoptosis

Interest in the role of the endoplasmic reticulum (ER) in apoptosis after cell stress induction has increased over the last decade with the identification of ER-localised caspases (caspase-12 and -4), involved in Aβ-mediated neurotoxicity in mouse models (Nakagawa et al. 2000; Hitomi et al. 2004). Also, identification of a pro-apoptotic Bcl-2 family protein, Bik, shown to be localised to the ER whilst having pro-apoptotic effects on the mitochondria (Germain et al. 2002) further supported ER involvement in some forms of cellular apoptosis. Another pro-apoptotic member of the Bcl-2 family, Bim, has also been shown to translocate to the ER membrane and is important for ER stress-mediated cell death (Puthalakath et al. 2007).

The ER is a subcellular organelle with a luminal volume equating to approximately 10% of total cell volume. Under normal physiological conditions, the ER is the cellular area where the majority of secretory and transmembrane proteins are glycosylated and correctly folded (Alberts 2008). A number of stresses can disturb ER homeostatic functions including calcium dyshomeostasis, hypoxic or ischaemic conditions, the loss of an oxidising environment and protein overload (Szegezdi et al. 2003). These conditions can promote accumulation of unfolded proteins, leading to an induction of the unfolded protein response (UPR).

Upon activation, the UPR essentially shuts down protein manufacture in the ER allowing an ER-associated protein degradation system (ERAD) to remove any accumulated mis-folded proteins. The UPR is mediated by three molecules known as the inositol-requiring-1 homologue (IRE1α), activating transcription factor 6 (ATF6), and protein kinase R-like endoplasmic reticulum kinase (PERK). These molecules are localised in the ER membrane and sense protein aggregation, triggering the UPR (Szegezdi et al. 2003). During acute dyshomeostasis, induction of the UPR is a pro-survival mechanism. However, with chronic ER stress the UPR is able to initiate apoptosis. Of the three main arms of the UPR, it is generally thought that ER-mediated

apoptosis can occur via the IRE1α-associated branch and the PERK-associated branch (Benn & Woolf 2004) (**Figure 1.4.4**). A third, caspase-associated, pathway can also be activated in cells undergoing ER stress-mediated apoptosis via cleavage and processing of caspase-12 (Nakagawa et al. 2000; Szegezdi et al. 2003).

1.4.1.4.1. CHOP and Caspase-12 in ER stress-mediated apoptosis

CHOP (or GADD153) is a 29 kDa protein with 169 amino-acid residues, expression of which is mainly regulated at the transcriptional level (Oyadomari & Mori 2003). During ER stress all arms of the UPR induce transcription of CHOP. However, for CHOP protein translation to occur, the PERK-eIF2α-ATF4 branch of the UPR is essential (Szegezdi et al. 2006). Previous studies have shown that over expression of CHOP can lead to growth arrest and apoptosis (Kawahara et al. 2001). Also, $CHOP^{-/-}$ fibroblasts have shown resistance to ER stress mediated death (Oyadomari et al. 2001). Furthermore, inhibition of eIF2α dephosphorylation by salubrinal protects against excitotoxic neuronal death (Sokka et al. 2007). These data suggest a strong association between the PERK-eIF2α-ATF4 branch of the UPR, CHOP expression and ER stress-induced apoptosis. Limited association of ER stress with microglial activation has been published. Depletion of microglial calcium stores by increased levels of nitric oxide has been shown to induce CHOP-associated stress responses leading to apoptosis (Kawahara et al. 2001). Further support for CHOP-associated microglial apoptosis was observed in our laboratory, with published data suggesting a correlation between an increase in CHOP expression after treatment of primary microglial cultures with LPS, chromogranin A or Aβ peptide, and subsequent microglial apoptosis (Davenport et al. 2010).

Caspase-12 is a member of the group I family of 'ICE'-like caspases, initially suggesting an inflammatory role. However, identification and localisation of caspase-12 to the ER and its subsequent involvement in ER stress-mediated apoptosis identified an alternative pathway to the ER transcription factor-mediated death pathways

(Nakagawa et al. 2000). More recent studies have shed controversy on the role of caspase-12 in humans. Of the 9 different, alternatively spliced mRNA species for caspases-12, all have acquired frame shift mutations and premature stop codons, potentially inhibiting translation of a fully functional protein (Fischer et al. 2002). However, mRNA editing and post-translational modifications enabling synthesis of a functional protein cannot be ruled out. This hypothesis is supported by data from a variety of disease models, including cancer (Mandic et al. 2003), Prion disease (Hetz et al. 2003), and recently Alzheimer's disease (Lee et al. 2010) suggesting involvement of a functional human caspase-12 protein in ER stress-mediated apoptosis. Proposals have also been made for human caspase-4 as the direct homolog of rodent caspase-12. It has been localised to the ER and is involved in Aβ-mediated neurotoxicity using human cell lines (Hitomi et al. 2004)

With regards to the execution of apoptosis by caspase-12, differing mechanisms have been published. A mitochondrial-independent mechanism for caspase-12 induction has been proposed by Morishima and colleagues (2002). They show caspase-12 translocates from the ER to the cytosol directly cleaving procaspase-9 which turn cleaves procaspase-3 (Morishima et al. 2002). These data have been supported by studies using *Apaf*$^{-/-}$ mouse fibroblasts, which were still able to undergo ER stress-mediated apoptosis (Rao et al. 2002). Conversely, other laboratories have suggested close links between the ER & mitochondria, in particular, with respect to calcium dyshomeostasis and downstream cascades (Nakamura et al. 2000) with regulation of cytosolic calcium homeostasis from ER stores shown to utilise mitochondrial associated Bcl-2 family proteins (Bcl-2 and Bcl-x_L to inhibit release, and Bax and Bak to promote release) via ER located calcium channels such as IP_3R (Lindholm et al. 2006). Further involvement of calcium in caspase-12-mediated apoptosis has been suggested through crosstalk between the calcium activated cysteine proteases, the calpains, and caspase-12 in Aβ-mediated apoptosis (Nakagawa & Yuan 2000). Nakagawa and colleagues show calcium dyshomeostasis due to Aβ exposure leads to m-calpain-

dependent processing of caspase-12 into the p10 and p20 subunits leading to an executioner caspase cascade via procaspase-9.

1.4.1.4.2. ER stress in neurodegeneration

The accumulation of mis-folded proteins is a pathological hallmark of many neurodegenerative disorders, for example Alzheimer's disease, where there is an association with the pathological accumulation of Aβ aggregates. Significant induction in PERK and eIF2α expression has been observed in AD patients, however no significant increase in these immediate response ER stress markers was observed in Prion diseases, unless neurofibrillary tangle pathology was also present (Unterberger et al. 2006). Interestingly, Lee and colleagues (2010) also found significant upregulation of markers associated with ER stress-mediated cell death in AD patient samples. However, no significant induction was observed in samples taken from the aged transgenic AD mouse model, Tg2576 (Lee et al. 2010), which has significant plaque burden but no tangle pathology (Richardson & Burns 2002). These data suggest a prominent role for neurofibrillary tangles in transcription factor-associated ER stress, with limited involvement from Prion protein or Aβ aggregates. Interestingly, caspase-12- and caspase-4-associated ER stress pathways in rodents and humans, respectively, seems to be responsible for inducing Aβ-mediated apoptosis in neurons (Nakagawa et al. 2000; Hitomi et al. 2004), suggestiing that differential ER stress pathways are activated by differing pathologies. This is further supported with respect to Prion diseases with studies suggesting Prion protein toxicity is dependent on caspase-12 activity (Hetz et al. 2003).

Finally, with respect to AD and ER stress, the presenilin-1 (PS1) protein potentially links ER stress to pathogenesis of the disease. PS1 is an ER transmembrane protein, mutations in which are present in cases of autosomal dominant familial Alzheimer's disease (FAD) (Berezovska et al. 2005). PS1 and its homolog PS2 are part of the multiprotein γ-secretase complex that mediates cleavage of amyloid precursor protein

(APP). Mutations in PS1 have been shown to alter APP processing leading to an increased ratio of toxic $A\beta_{42}$ to $A\beta_{40}$ (Lindholm et al. 2006), leading to plaque burden and early age of onset. Cells with PS1 mutations have been shown to have altered calcium homeostasis and an enhanced sensitivity to ER stress-mediated apoptosis. Furthermore, mutant PS1 inhibits IRE1α, suppressing UPR activation, causing a decrease in the cells sensitivity to ER stress (Lindholm et al. 2006).

Again using genetic models of neurodegenerative diseases, the study of rare familial forms of Parkinson's disease (PD) has provided elucidation of cellular pathways and mechanisms suggested to be important in disease progression. Of the genetic risk factors identified, the ubiquitin ligase, Parkin, has been of most interest with respect to ER stress pathways evoked in PD pathogenesis (Lindholm et al. 2006). Parkin is frequently mutated in early onset PD (Imai & Takahashi 2004) with loss of function mutations shown to be responsible for the majority of autosomal recessive Parkinsonism cases (Lindholm et al. 2006). Functional Parkin suppresses ER stress-mediated death (Imai et al. 2000), whereas loss of Parkin has been shown to cause ER stress via accumulation of cytotoxic fibrils and protein aggregates (Imai & Takahashi 2004). Recently, studies by Bouman and colleagues showed functional Parkin to be stress protective with a role in interorganellar crosstalk between the ER and mitochondria, promoting survival in cells undergoing stress (Bouman et al. 2011). These data further support the idea that ER stress could contribute to the pathogenesis of Parkinson's disease. Finally, the use of compounds to model the selective loss of dopaminergic neurons observed in PD (such as 6-hydroxy-dopamine (6-OHDA) and N-methyl-4-phenyl-1,2,3,6-tetrahydropyridine (MPTP)), shows a significant induction of ER stress in cell cultures of dopaminergic neurons leading to increases in CHOP expression and phosphorylation of PERK and IRE1α (Ryu et al. 2002).

Studies into motor neurone disease pathogenesis have suggested roles for ER stress mediated neuronal death, in particular in familial amyotrophic lateral sclerosis (FALS)

(Atkin et al. 2006) where significant expression of ER stress related markers were observed. Further support for a role for ER stress in ALS was provided by Nagata and colleagues (2007) who also found a significant induction in ER stress-related markers in lysates from lumbar spinal cord of transgenic mice carrying a mutation (G93A) in the SOD1 gene. The paper suggests that due to an observed disproportionate increase in pro-apoptotic markers in comparison to anti-apoptotic markers, such as GRP78, an imbalance occurs leading to ER stress prone cells (Nagata et al. 2007). Following on from these suggestions interesting studies into motor neurone disease using three separate mouse models of FALS show a subset of 'vulnerable' motor neurons are more susceptible to ER stress, showing an upregulation of ER stress markers from birth. Inhibition of ER stress using salubrinal attenuated disease and it is suggested that these vulnerable neurons, susceptible to ER stress, influence progressive manifestations of weakening and paralysis (Saxena et al. 2009).

Finally, very limited data has been published on the role of ER stress in multiple sclerosis (MS) lesions. However, increased expression of ER stress markers including CHOP, XBP-1 and BiP has been observed in oligodendrocytes, astrocytes and microglia in active MS lesions (Mháille et al. 2008; Cunnea et al. 2011).

1.5. Fibrinogen and Fibrin – structure and evidence for prominent roles in neurodegenerative disease pathogenesis

The role fibrinogen and fibrin in the progression of NDDs has received increasing attention since BBB barrier dysfunction and vascular abnormalities were shown to be common features of some NDDs. Elevated levels of fibrinogen in blood plasma have been shown to correlate with an increased risk for Alzheimer's disease (AD) and dementia (van Oijen et al. 2005; Xu et al. 2008). Furthermore, in the pursuit for biomarkers to enable early diagnosis of Alzheimer's disease, the level of fibrinogen-γ-A chain precursor was shown to be raised in the cerebrospinal fluid of AD patients when compared with aged matched controls (Lee et al. 2007).

Separate from classical involvement in the coagulation cascade, fibrinogen and fibrin can bind and activate mononuclear cells, including microglia, with increased cytokine release observed (Fan & Edgington 1993; Perez & Roman 1995; Perez et al. 1999; Smiley et al. 2001; Adams et al. 2007a; Jensen et al. 2007; Hodgkinson et al. 2008), supporting a role for the protein in the inflammatory responses now considered key to the pathogenesis of many NDDs. Furthermore, detrimental association with classical NDD peptides such as Aβ (Cortes-Canteli et al. 2010) only promotes further evidence of an involvement in progressive neurodegeneration. Here, the structure of fibrinogen and the cleavage product fibrin will be briefly described, followed by published evidence on the significant contributions from these blood borne protein products in NDDs, in particular AD and MS. An emphasis on studies suggesting fibrinogen-mediated activation of microglia will be presented.

1.5.1. Structure of fibrinogen and its cleaved product fibrin

Fibrinogen (FG) is a 340 kDa soluble glycoprotein synthesized by hepatocytes which under normal physiological conditions circulates at a concentration of approximately 3 mg/ml (Schachtrup et al. 2007). FG molecules are 45 nm elongated protein dimers,

which consist of two outer D-domains connected to a central E-domain by coiled coil segments (**Figure 1.5.1**) (Mosesson 2005). The domains consist of duplicate Aα-, Bβ- and γ-chains derived from separate genes coupled by multiple disulphide bridges primarily at the N-terminals in the 'E' domain of the molecule (**Figure 1.5.1**). Each Aα chain contains an N-terminal fibrinopeptide A sequence that is cleaved by the protease thrombin, initiating assembly of fibrin (FN) (Mosesson 2005).

The cleavage of FG by thrombin exposes polymerisation sites that have affinity for complementary binding pockets located in the γ-chains present in the D domain of neighbouring FG molecules. This initially creates staggered overlapping protein binding, generating double stranded fibrils, known as fibrinogen polymers (Adams et al. 2007a). These polymers are further stabilised and cross-linked by Factor XIII (transglutaminase) of the coagulation cascade, leading to creation of an insoluble FN clot. When no longer required, the clot is degraded and cleared via proteolysis by the enzyme plasmin (East et al. 2008). Plasmin is produced from cleavage of the precursor protein plasminogen with regulation by either tissue-type plasminogen activator (tPA) or urokinase-type (uPA) (Akassoglou & Strickland 2002). The tPA has been shown to be constitutively expressed in the rodent brain (Sappino et al. 1993), and microglia have been shown to express uPA (Cunningham et al. 2009). Furthermore, both activators have been shown to be over-expressed in microglia after brain injury (Dietzmann et al. 2000).

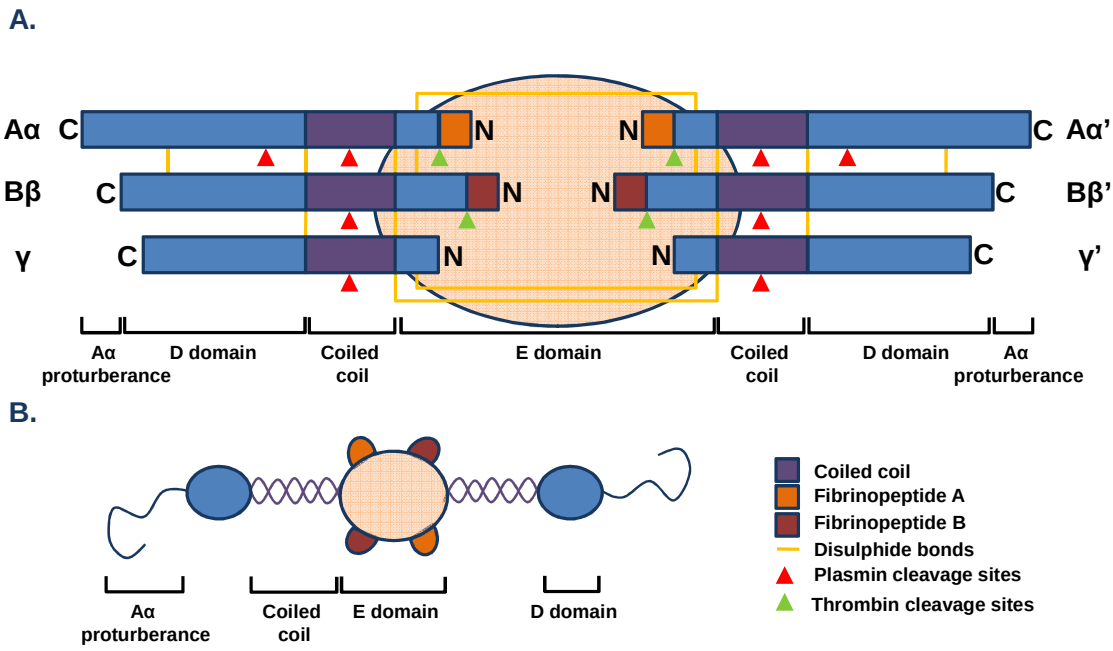

Figure 1.5.1. The structure of fibrinogen

Fibrinogen molecules are composed of elongated protein dimers consisting of duplicate Aα-, Bβ- and γ-chains derived from separate genes coupled by multiple disulphide bridges (**A**). The molecule is segregated into two outer D-domains connected to a central E-domain by coiled coil segments (**B**).

1.5.2. The functions of fibrinogen and fibrin in chronic neurodegenerative disease pathogenesis

Vascular pathology has been identified as an important factor in Alzheimer's disease. Cerebral amyloid angiopathy (CAA) is the deposition of Aβ peptide in the vasculature and is important in the severity of AD disease pathology (Cortes-Canteli et al. 2010). CAA has been shown to promote degradation of vessel wall components, negatively affect cerebral blood flow leading to chronic brain hypoperfusion and enhance cognitive decline (Greenberg et al. 2004; de la Torre 2006; Thal et al. 2008). Epidemiological studies provide further evidence for a strong vascular component in AD, with vascular diseases such as stroke, atherosclerosis and hypertension associated with an increased risk for dementia and AD (de la Torre 2002). Moreover, neuronal loss and memory deficits have also been proposed as secondary to the vascular component in

AD (Cortes-Canteli et al. 2010).

FN deposition is observed in the vessels and CNS parenchyma of AD mice (Cortes-Canteli et al. 2010; Paul et al. 2007). Furthermore FG has been shown to accumulate in the extravascular space in AD patients (Fiala et al. 2002; Ryu & McLarnon 2009). Inhibition of plasmin fibrinolytic activity, increased levels of prothrombotic molecules (Arai et al. 2006) and BBB dysfunction present in AD brains have been proposed as contributors to this FG accumulation and subsequent FN deposition (Zlokovic 2008; Cortes-Canteli et al. 2010). As previously described in **section 1.2**, BBB dysfunction has been shown to occur in many neurodegenerative disorders, including acute events such as ischaemic stroke (Sandoval & Witt 2008), and chronic diseases such as AD, PD, ALS and MS (Zlokovic 2008; Quaegebeur et al. 2011). This dysfunction enables FG and other components of blood to extravasate into the CNS parenchyma with subsequent haemorrhage and neuronal damage occurring (Adams et al. 2004). Interestingly some blood borne molecules have been shown not to cross into the parenchyma in AD (Sagare et al. 2007) suggesting specific interactions are still required to permit extravasation of FG into the CNS.

Paul and colleagues (2007) have shown fibrin deposition in animal models of AD accelerated neurovascular damage. Inhibition of plasmin, thus preventing FN clot degradation, significantly enhanced the extravasation of Evans blue into the CNS, which could be attenuated if prior depletion of fibrinogen was performed (Paul et al. 2007). Furthermore the paper shows a positive correlation between blood brain barrier damage induced by inhibition of FN clot degradation, and microgliosis, which could again be attenuated if prior depletion of FG was performed, suggesting FN deposition enhances neuroinflammation in these models (Paul et al. 2007).

Studies by Cortes-Canteli and colleagues (2010) propose a direct link between FG, Aβ and CAA-associated physiology. *In vitro* and *in vivo* experiments showed FN clots formed in the presence of Aβ peptide were structurally abnormal and resistant to

degradation. Interestingly, stereotactic administration of FG into the CNS parenchyma of 6 month old AD mice was not cleared efficiently, when compared with younger transgenics or wildtype mice of the same age, suggesting a negative correlation between FG clearance and Aβ plaque burden. Furthermore, this delayed clearance seemed to be specific to FG as bovine serum albumin (BSA) administration was cleared with no significant loss of efficiency when plaque burdened AD mice and wildtype litter mates were compared (Cortes-Canteli et al. 2010). Finally, the paper provides physiological evidence to suggest the presence of FG contributes to CAA-associated cognitive decline in AD mouse models. Together these data provide significant evidence that FG extravasation and FN deposition in the CNS, and FN deposition in the vasculature, contributes to AD disease pathogenesis.

One of the earliest events coupled to the observed BBB dysfunction in MS (van Horssen et al. 2007) is the leakage of FG into the CNS resulting in perivascular deposition of FN (Adams et al. 2007a). A significant volume of research, utilising *in vitro* and *in vivo* models, suggests a link between MS disease severity, FG and the subsequent FN deposition (Kwon & Prineas 1994; Akassoglou et al. 2000; Akassoglou et al. 2002; Akassoglou et al. 2004; East et al. 2005; Adams et al. 2007a; Adams et al. 2007b; East et al. 2008; Yang et al. 2011a).

In animal models of MS, genetic knockdown or pharmacological depletion of FG was shown to decrease inflammation and delay demyelination (Akassoglou et al. 2004; Yang et al. 2011a). An indirect correlation between FN deposition and aggressiveness of MS disease progression can also be taken from studies performed by East and colleagues. Induction of experimental allergic encephalomyelitis (EAE), an animal model for MS, in tPA genetic knockout mice ($tPA^{-/-}$) was performed in parallel with EAE induction in wildtype mice. The $tPA^{-/-}$ EAE mice showed an enhanced, early and more severe onset of acute disease with an incomplete recovery when compared with the wild-type controls (East et al. 2005), suggesting a decrease in FN clot degradation

efficiency can enhance disease severity, again implicating FG and FN in disease pathogenesis. However, although enhanced FN accumulation was observed in these mice, a tPA-dependent mechanism independent of FN could be responsible and should not be overlooked. Interestingly, increases in tPA expression observed in MS studies are matched by a significant increase in the tPA inhibitor, plasminogen activator inhibitor-1 (PAI-1), suggesting inefficient clearance of fibrin would still occur (East et al. 2008).

Limited data has been published on involvement of FG in PD. One study shows no significant increase in circulating FG levels, used as a biomarker for inflammation (Chen et al. 2008). However, it must be noted that the sample size was very small (84 cases, compared with 165 matched controls), and a later, larger study (>8000 participants) showed an association between increased FG levels and prevalence of PD in patients over 75 years of age (Wong et al. 2010). This epidemiological study suggests possible involvement of FG in late stage PD but no *in vitro* or *in vivo* animal model studies have been performed to identify whether FG has any specific signalling capacity in the observed dopaminergic neuron degeneration, either directly or via inflammation.

Similarly, little evidence has been published for FG involvement in ALS. One study to date has shown significantly enhanced serum FG levels in 80 ALS patients compared with age-matched controls (Keizman et al. 2009) but no specific involvement in motor neuron weakening or paralysis has been suggested.

1.5.3. Cellular interactions and signalling with fibrin and fibrinogen

Fibrin(ogen) has been shown to have a vast signalling capacity with involvement in inflammatory mechanisms of a wide range of disorders including rheumatoid arthritis, sepsis, myocardial infarction, infection and MS (Adams et al. 2007b). Aside from the well-documented role in the coagulation cascade, FG can mediate leukocyte

proliferation and inhibit apoptosis (Whitlock et al. 2000). Furthermore FG and FN can induce the release of pro-inflammatory cytokines from a human monocytic cell line (Perez et al. 1999) or primary human isolated peripheral blood monocytes (Fan & Edgington 1993; Jensen et al. 2007).

As previously described (**Section 1.1.5.2.2**), the CD11b/CD18 ($\alpha_M\beta_2$, MAC-1, CR3) receptor is a member of the β-integrin family of receptors and orchestrates the innate immune response by regulating phagocyte adhesion, migration and engulfment of potentially harmful factors (Ehlers 2000). The receptor is expressed on microglia cells, and upregulation has been observed in AD brains post mortem (Akiyama & McGeer 1990). The receptor has also been shown to mediate LPS-induced production of superoxide in microglia (Pei et al. 2007). FG association with CD11b/CD18 on many immune cells suggests an important role for the receptor in FG-induced inflammatory responses. FG-mediated TNFα release in isolated peripheral blood mononuclear cells (PBMCs) was dependent on CD11b (Fan & Edgington 1993). Furthermore, FG treatment of the human monocytic cell line U937 induced significant IL-1β expression via CD11b and NFκB signalling (Perez et al. 1999).

To date, only one *in vitro* signalling paper has been published identifying FG-mediated activation of microglia (Adams et al. 2007a). FG was shown to induce a phagocytic phenotype in microglia via a CD11b signalling pathway dependent on PI3K and RhoA, two major downstream signals from CD11b that mediate cytoskeletal rearrangements associated with changes in cell morphology (Adams et al. 2007). Interestingly, the paper uses what they term 'immobilised' FG to induce this interaction. This is due to studies undertaken into the mechanism of fibrinogen ligation to CD11b. These studies suggested that FG contains a masked, cryptic binding site in the γ-chains that is not able to associate with CD11b until the protein has become immobilised, i.e. in a polymerised form (Lishko et al. 2002). However, as previously shown, soluble FG can induce cytokine release from PBMCs (Perez & Roman 1995; Perez et al. 1999; Jensen

et al. 2007) including human macrophages (Hodgkinson et al. 2008), and subsequently the same group involved in the identification of the cryptic binding site in FG published further data suggesting multiple binding domains in the FG molecule with an ability to ligate CD11b (Lishko et al. 2004).

Another integrin receptor CD11c/CD18, associated with dendritic cells, has been shown to interact with FG inducing activation (Ugarova & Yakubenko 2001). Moreover, FG has been associated with the $\alpha_v\beta_3$ integrin receptor on CGCs causing inhibition of neurite outgrowth via phosphorylation of the epidermal growth factor (EGF) receptor (Schachtrup et al. 2007). Studies using the RAW264.7 mouse macrophage-like cell line and primary peritoneal macrophages, have also shown FG can induce chemokine secretion with dependence on toll-like receptor 4 (TLR4) (Smiley et al. 2001).

Finally, FG has been shown to serve as an early signal in glial scar formation via the TGFβ/Smad signalling pathway in astrocytes. It was shown that FG can act as a carrier of latent TGFβ and induces phosphorylation of Smad2 in astrocytes leading to an inhibition of cortical neurite outgrowth potentially due to FG-mediated release of the chondroitin sulphate proteoglycan, neurocan, from astrocytes (Schachtrup et al. 2010).

Together these data show the capabilities of the FG molecule through interactions with an array of receptors on differing cell types as well as providing a pool of TGFβ to induce inhibitory signalling. This broad receptor signalling capacity leads to differential induction of cytokines and chemokines suggesting FG may be able to promote diverse responses during different stages of inflammation as well as having a role in the inhibition of adult neurogenesis.

1.6. Aims and Objectives

The role of microglia in neurodegeneration is an increasing area of research and roles for blood borne proteins in CNS disease progression are being continually implicated. Little research has been performed to identify how microglia respond in the presence of fibrinogen and fibrin at a molecular level. Here, the main aim was to try and elucidate members of signalling cascades involved in fibrinogen and fibrin-mediated microglial activation. This was performed using *in vitro* culture models with pharmacological manipulation where required. The research for this thesis was performed to identify answers to the following questions:

- How do microglia respond to the presence of soluble fibrinogen and insoluble fibrin?
- Is there a difference in microglial response to these factors and if so, how do the profiles differ?
- Can fibrinogen and/or fibrin interact directly with neurons, *in vitro*?
- Is it possible to manipulate observed responses with pharmacological interaction?
- Do these data translate to human models?

2. Materials and Methods

2.1. Materials

Sprague Dawley pups for primary cultures were obtained from Central Biological Services, UCL, London, UK. The BV2 cell line was a kind gift from Dr Claudie Hooper (MRC Centre for Neurodegenerative Research, Institute of Psychiatry, Kings College London, UK). CO_2 gas cylinders were obtained from BOC gases (Guilford, UK). Foetal bovine serum (FBS), Dulbecco's Modified Eagle's Medium (DMEM) powder (52100-039), Minimum Essential Medium (MEM) powder (11700-077), RPMI culture medium (21875-091), Earle's balanced salts solution (EBSS) (14155-048), Neurobasal® medium (21103-049), B27® neuronal supplement (17504-044) and Trizol® reagent (15596018) were obtained from Invitrogen (Paisley, UK). MACS® multistand with QuadroMACS™ (130-091-051), MACS® LS columns (130-042-401) and human anti-CD14 MicroBeads (magnetic beads conjugated to monoclonal human CD14 antibodies; 130-050-201) were kindly provided by Professor Sarah Tabrizi (Department of Neurodegeneration, UCL Institute of Neurology) and were originally purchased from Miltenyi Biotec Ltd (Surrey, UK).

Tissue culture plasticware were obtained from Appleton Woods (Buckinghamshire, UK) or VWR (Leicestershire, UK) and 13 mm coverslips (MIC3336) were obtained from Scientific Laboratory Supplies (Nottingham, UK). N,N,N',N'-tetramethylethylenediamine (TEMED, 20-3000-25) and 30% w/v acrylamide (20-2100-05) were obtained from Severn Biotech (Worcestershire, UK). ECL Plus™ Western Blotting Reagents (RPN2106) and Amersham™ Hyperfilm ECL (28-9068-37) were purchased from GE Healthcare (Buckinghamshire, UK) and Immobilion® P polyvinylidene difluoride (PVDF) membranes (IPVH00010) were from Millipore (Watford, UK).

FITC-ATAD-FMK caspase-12 staining kit (PK-CA577-K172-100), z-ATAD-FMK (caspase-12 inhibitor; PK-CA577-1079) and z-VAD-FMK (caspase-3 inhibitor; PK-CA577-1010) were purchased from Promokine (Heidelberg, Germany) and

CaspaTag™ FAM-DEVD-FMK caspase-3/7 staining kit (APT423) was purchased from Millipore (Watford, UK). Annexin V-FITC apoptosis detection kit (ab140585) was procured from AbCam (Cambridge, UK).

N-(2,6-dioxo-3-piperidinyl)phthalimide (Thalidomide, #0652), 2-Amino-5,6-dihydro-6-methyl-4H-1,3-thiazine hydrochloride (AMT-HCl, #0871), (S)-3,5-Dihydroxyphenylglycine (DHPG, #0805), 3-Cyano-*N*-(1,3-diphenyl-1*H*-pyrazol-5-yl)benzamide (CDPPB, #3235), 3-((2-Methyl-1,3-thiazol-4-yl)ethynyl)pyridine hydrochloride (MTEP, #2921), (2S,2'R,3'R)-2-(2',3'-Dicarboxycyclopropyl) glycine (DCGIV, #0975), L-(+)-2-Amino-4-phosphonobutyric acid (L-AP4, #0103), Thapsigargin (#1138), PD98059 (#1213) SB203580 (#1202), Ionomycin (#1704), BAPTA-AM (#2787), and Calpastatin (#2950) were purchased from Tocris Bioscience (Bristol, UK). Salubrinal (ALX-270-428) was procured from Enzo Life Sciences (Exeter, UK) and apocynin (178385), Suc-Leu-Tyr-AMC (fluorogenic calpain substrate, 208731) and m-calpain (208718) were from Calbiochem (Merck, Middlesex, UK).

TNF-α (RTA00) and IL-6 (R6000B) Quantikine® ELISA kits, human recombinant GM-CSF (215-GM) and IFNγ (585IF) were purchased from R&D Systems (Oxford, UK). GoTaq® DNA polymerase kits (M3175) were purchased from Promega (Southampton, UK) and Superscript® II Reverse Transcriptase kits (18064-014) were purchased from Invitrogen (Paisley, UK). A broad-range protein molecular weight marker (2-212 kDa, P7702) and a Quick-Load® 100 bp DNA ladder (N0464) were purchased from New England BioLabs (Hertfordshire, UK).

Goat anti-TNFα (sc1351), mouse anti-GADD153 (CHOP; sc7351), rabbit anti-total-p38 MAPK (sc535), donkey anti-goat-IgG-HRP (sc2020) and goat anti-mouse-IgG-HRP (sc2055) were purchased from Santa Cruz Biotechnology (Heidelberg, Germany). Mouse anti-ED1 (MCA341) and mouse anti-CD11b (MCA275EL) were obtained from AbD Serotec (Oxford, UK). Rabbit anti-iNOS (610333) and rabbit anti-bNOS (N31030) were obtained from BD Transduction Lab (Oxford, UK). Rabbit anti-phospho-p38

MAPK (9211), mouse anti-phospho-p42/44 MAPK (9106), rabbit anti-total-p42/44 MAPK (9102) and rabbit anti-cleaved caspase-3 (9664) antibodies were obtained from Cell Signaling Technology (New England BioLabs, Hertfordshire, UK). Rabbit anti-caspase-12 (ab18766), goat anti-mouse-FITC (ab6785) and rat IgG serotype control (ab37361) were purchased from AbCam (Cambridge, UK) and goat anti-rabbit-Cy3 (A10520) was from Invitrogen (Paisley, UK). Mouse anti-NeuN (MAB377) was from Millipore (Watford, UK), mouse anti-CD68 (clone EBM11; M0718) was from DAKO (Ely, UK) and goat anti-rat-fibrinogen-HRP (GARa-Fbg-HRP) was from Source Bioscience (Nottingham, UK). TRITC-conjugated calnexin was kindly provided by Dr Adamantios Mamais (Department of Molecular Neuroscience, UCL Institute of Neurology). Mouse anti-β_{III}-tubulin (T5076), mouse anti-β-actin clone AC-15 (A5441), rabbit anti-GFAP, (G4546), goat anti-rabbit-TRITC (T6778), and goat anti-rabbit-IgG-HRP (A0545) were purchased from Sigma-Aldrich (Dorset, UK).

Finally, Dulbecco's Phosphate buffered saline without $CaCl_2$ or $MgCl_2$ (PBS; D5652) powder, LPS (Lipopolysaccharides from *Escherichia coli*; serotype 026:B6; L2762), fibrinogen (F4883), fibrin (F5386), Phenylmethylsulfonyl fluoride (PMSF, P7626), L-glutamine (G3126), Leucine-methyl-ester (LME, L1002), N-acetylaspartylglutamate (NAAG, A5930), Bradford protein assay reagent (B6916), Tween-20 (P7949), ammonium persulphate (APS, A3678), photographic developer (P7042) and fixer (P7167), polymyxin B (PMX, P4932), Hirudin (94581), Fucoidan (F5631), Staurosporine (STS, 54400), Phorbol 12-myristate 13-acetate (PMA, P1585), Wortmannin (W1628), Tunicamycin (T7765), 4',6-diamidino-2-phenylindole (DAPI, D8417), 2´-(4-Ethoxyphenyl)-5-(4-methyl-1-piperazinyl)-2,5´-bi-1H benzimidazole (Hoechst-33342, B2261), propidium iodide (P4170), FITC-isolectin-B4 (L2895), DNAase (D5025), soybean trypsin inhibitor (T9003), bovine trypsin (T9935), cytosine arabinofuranoside (Ara-C, C1768), poly-*D*-lysine (PDL, P1149), freezing medium (C6164), 4-(2-hydroxyethyl)-1-piperazineethanesulfonic acid (HEPES, H0891),

ampicillin (A2804), gentamicin (G1397), penicillin-streptomycin solution (P4333), ACCUSPIN™ System-Histopaque®-1077 tubes (A7054), and all bench grade chemicals were obtained from Sigma-Aldrich (Dorset, UK).

2.2. BV2 cell culture and maintenance

Limited studies were performed using the BV2 murine microglial cell line, generated by infecting primary microglial cell cultures with the v-raf/v-myc oncogene carrying retrovirus J2 (Blasi et al., 1990). The cells exhibit similar morphological, phenotypical and functional properties to primary microglia, however some studies have shown significant differences in activation, in particular with respect to cytokine release profiles (Horvath et al. 2008). Even so, the BV2 cell line is an extremely useful tool for *in vitro* microglia researchers, in particular as primary microglia culture yield is generally quite limited.

BV2 microglia were maintained in T175 culture flasks in Dulbecco's modified Eagle's medium (DMEM) with 10% foetal bovine serum (FBS), supplemented with 2 mM L-glutamine, 100 U/ml penicillin and 100 mg/ml streptomycin at 37℃ in a humidified atmosphere with 6% CO_2. Cryopreservation of cells was routinely performed to increase longevity of the cell line. The BV2 microglia, at a density of 1 x 10^6/ml were suspended in Sigma freezing medium (DMEM, 20% foetal bovine serum (FBS), 2 mM L-glutamine, 100 U/ml penicillin, and 10% DMSO – to prevent membrane rupture) and stored at -80℃. Once required, a frozen vial of cells was thawed and added to pre-warmed BV2 medium in a T25 culture flask. The cells were maintained at 37℃ in a humidified atmosphere with 6% CO_2 and medium was replaced at 1 day in vitro (DIV) to remove the cytotoxic components of the freezing medium.

For experimental procedures and passaging, BV2 microglia were harvested from the culture flasks enzymatically by incubation for 5 minutes at 37℃ with ~ 10 ml of 0.5 mg/ml trypsin (1:10 dilution of 5 mg/ml stock). Neutralisation of trypsin was performed by adding at least an equal volume of medium to the flask. The cells were then pelleted by centrifugation at 3645 *g* for 5 minutes at room temperature (Eppendorf Centrifuge

5804R) and resuspended in 5 ml of fresh warm medium. For quantification of cell number, 20 µl of the cell suspension was administered to a haemocytometer, and cells in four quadrants were counted, which equated to the number of cells present in 0.1 µl of the suspension volume.

The BV2 cell line was utilised for Western blotting (**section 2.7**) and calpain activity assay (**section 2.9**) lysates. The cells were plated on 6 well plates at a density of 1 x 10^5/well. With respect to the preparation of Western blotting lysates, at least two hours prior to activation, serum-containing (SC) medium was replaced with serum-free (SF) medium (DMEM, 2 mM L-glutamine, 100 U/ml penicillin and 100 µg/ml streptomycin), this was due to observations made previously in the laboratory that the cultures appeared more ramified and responded better to stimuli in SF conditions.

2.3. Primary cell cultures

The majority of the studies performed in this thesis used primary cell cultures. Whilst these cultures are much more sensitive to technique, the data produced represents a more physiological picture in an *in vitro* setting when compared with an immortalised cell line.

2.3.1 Rat microglia

Primary microglia were isolated from 5-6 day old Sprague Dawley rat pups as previously described (Kingham et al. 1999). Rats were killed by cervical dislocation and decapitation in accordance with the United Kingdom Animals (Scientific Procedures) Act, 1986. Whole brains, minus the cerebellum, which was required for neuronal culture preparation (**Section 2.3.3**), were dissected and placed into to a phosphate buffered saline solution, on ice, (137 mM NaCl, 5.37 mM KCl, 5.65 mM $NaH_2PO_4.H_2O$, 13.3 mM $Na_2HPO_4.7H_2O$), supplemented with 11.1 mM D-glucose, 0.02% bovine serum albumin (BSA), 100 units/ml penicillin, 100 µg/ml streptomycin, and 3 µg/ml ampicillin. The solution was prepared using filtered, UV-treated, autoclaved dH_2O, pH 7.4. Brains were then gently homogenised using 10 – 15 strokes of a Potter-Elvehjem tissue grinder with a Teflon pestle (VWR, Leicester, UK). The smooth homogenate was

halved and transferred to two 50 ml tubes (no more than the equivalent of 4 brains per tube) and centrifuged at 500 *g* for 5 min (Eppendorf Centrifuge 5804R). The resulting supernatant was discarded and the pellet was resuspended in 10 ml 70% Percoll. A gradient was then produced by overlaying the cell containing 70% Percoll solution with 10 ml of 30% Percoll solution, followed by 10 ml of sterile PBS (**Figure 2.3.1**). Addition of each overlaying solution took place with the upmost care, so as not to disturb the layer below. The Percoll gradient was then centrifuged at 1250 *g* (Eppendorf Centrifuge 5804R), with no acceleration or braking, for 50 min to allow dissociation of the microglia from the other brain tissue, which could be collected at the 70%/30% Percoll gradient interface (**Figure 2.3.1 B**).

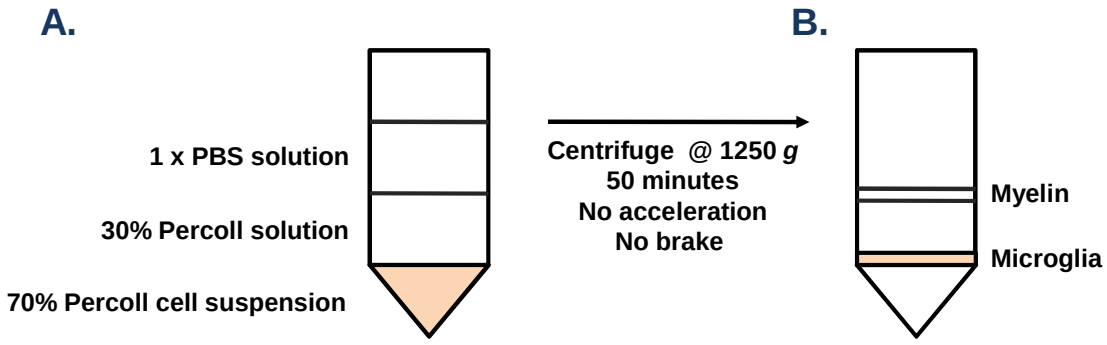

Figure 2.3.1. Graphical representation of the Percoll gradient preparation

A. Creation of the Percoll gradient was performed by addition of 70 % Percoll solution containing the tissue homogenate that was overlaid by 30% Percoll solution followed by 1 x PBS solution. **B.** Following centrifugation, myelin collected at the 30%/PBS interface was removed and discarded, and microglia were collected from the 70%/30% gradient interface.

Microglia were collected and washed in 50 ml of sterile PBS to dilute the Percoll concentration. The solution was then centrifuged at 500 *g* with medium acceleration and brake (Eppendorf Centrifuge 5804R) for 5 min. The resulting 'microglia' pellet was resuspended in 1 ml of pre-warmed medium (Minimal Essential Medium (MEM) supplemented with 10% FBS, 20 mM KCl, 30 mM D-glucose, 2 mM L-glutamine, 25 mM $NaHCO_4$, 50 U/ml penicillin, 50 µg/ml streptomycin, and 6 µg/ml ampicillin) and were quantified using a haemocytometer as previously described (See BV2 method). It is worth noting that microglia were cultured in the same medium as the cerebellar

granule cell (CGCs) cultures to enable microglial conditioned medium (MGCM) to be added to the CGCs as a treatment.

It was previously observed in the laboratory that primary microglia did not adhere well to tissue culture plastic. Therefore, cells were always plated on sterile 13 mm glass coverslips at a density of $5x10^4$/well in 24 well plates. Cell density per well was calculated so that the microglia were initially plated in a volume of 100 µl to provide optimum adherence conditions. After 30 minutes incubation at 37℃ in a humidified atmosphere with 6% CO_2, culture medium well volume was increased to 500 µl and plates were returned to the incubator and left for approximately 24 h before being washed 3 times in pre-warmed medium to remove debris. Finally, cultures were exposed to SF medium (MEM supplemented with 20 mM KCl, 30 mM D-glucose, 2 mM L-glutamine, 25 mM $NaHCO_4$, 50 U/ml penicillin, 50 µg/ml streptomycin, and 6 µg/ml ampicillin) and left to rest for a further 3 h before treatment. Microglia were always used within 48 h of isolation.

Microglia were characterised following the Percoll method of isolation. Staining using the microglial specific marker isolectin-B_4 (**Figure 2.3.2**) and OX-42 have shown that cultures routinely contain >90% microglia (Kingham et al. 1999). Furthermore, previous studies in our laboratory, as well as my own showed that at 2 DIV only ~20% of microglia stain positive for ED-1 (Morgan et al. 2004). This suggests basal activation in the microglial cultures used here is relatively low.

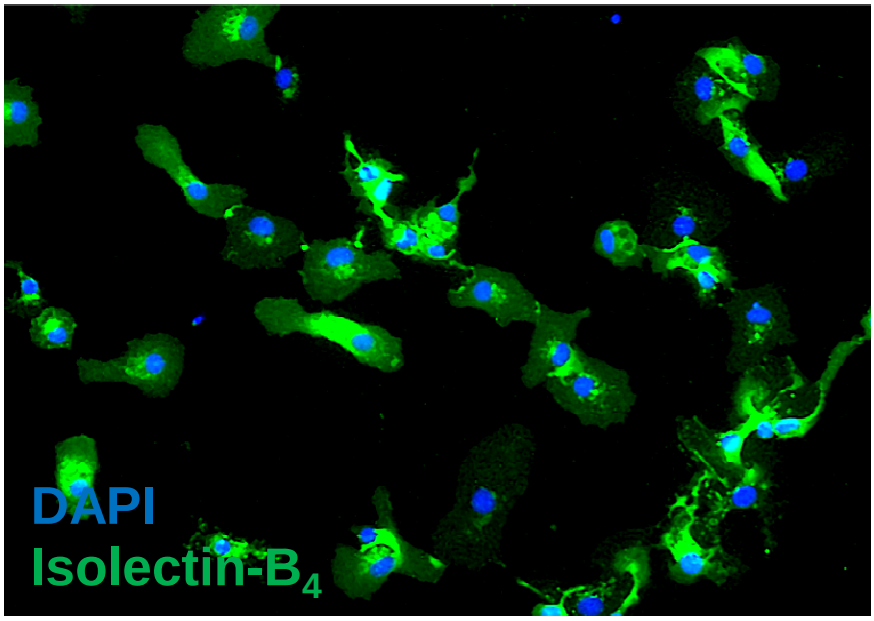

Figure 2.3.2. Characterisation of primary microglial cultures with Isolection-B_4

Live cell staining of primary microglial cultures with the microglia marker Isolectin-B_4 (IB_4; Streit 1990) shows a highly pure culture, with >90% of cells positively stained.

2.3.2 Rat mixed glia

To obtain primary astrocytic cultures, a modified shaking method was performed (McCarthy & De Vellis 1980). The method was optimised for the isolation of microglia as well as oligodendrocytes from the astrocytic layer, which were required by other members of the laboratory. To acquire a relatively pure astrocyte culture, 2 shaking steps were performed on the mixed glia cultures. Initially, 5-6 day old Sprague-Dawley rat pups were killed by cervical dislocation and decapitation in accordance with the United Kingdom Animals (Scientific Procedures) Act, 1986. Brains were dissected and placed into a sterile Petri dish containing minimum essential medium (MEM) with 25 mM 4-(2-hydroxyethyl)-1-piperazineethanesulfonic acid (HEPES), 100 U/ml penicillin, and 100 mg/ml streptomycin (HEPES-MEM). Cortical hemispheres were dissected and placed into a new Petri dish with fresh HEPES-MEM and homogenised by trituration through syringe needles of decreasing gauge (19-, 23- and 25-gauge, respectively) until full dissociation of the tissue had occurred. The tissue homogenate was then transferred to a tube containing 45 ml HEPES-MEM and centrifuged at 230 *g* for 10 minutes (Eppendorf Centrifuge 5804R). The resulting pellet was resuspended in pre-warmed medium (DMEM, 10% FBS, 1 mM sodium pyruvate, 25 mg/ml gentamycin) and the suspension was seeded into a T175 tissue culture flask pre-coated with 100 mg/ml poly-*D*-lysine (PDL) and maintained in an incubator at 37°C in a humidified atmosphere with 6% CO_2. The suspension seeded in each flask was a volume equivalent to two brains. The medium was replaced with fresh, pre-warmed medium every 3 DIV, being extremely careful not to disturb the growing surface. After at least 10 days DIV a confluent astrocytic monolayer was present on the growth surface, with easily distinguishable microglia and cell clusters identified as oligodendrocytes precursor cells (OPCs). Initially, microglia were shaken off by particular lab members for their personal use followed by the OPCs. This left an enriched astrocytic monolayer, which was utilised purely for optimisation of the leucine-methyl-ester (LME) microglia depletion technique (**Section 2.5**). The astrocytes were enzymatically dissociated from

the growth surface using 0.5 mg/ml trypsin (1:10 dilution of 5 mg/ml stock) and quantified, as described previously (**Section 2.2**). The cells were plated on sterile 13 mm glass coverslips in 24 well plates at a density of 1 x 10^5/well and treated after a further 3 DIV.

2.3.3 Rat cerebellar granule neurons

Cerebellar granule cells (CGCs), are excitatory neurons found within the granular layer of the cerebellum (**Section 1.1.1.1 and 1.1.1.2**) and receive excitatory input from mossy fibres (Kiernan 2009), express excitatory amino acid receptors such as N-methyl-D-aspartate (NMDA) receptors and release glutamate (D'Mello et al. 1993). Survival in culture was limited until the discovery by Gallo and colleagues that the cells require high extracellular concentrations of potassium (K^+), i.e. depolarising concentrations, to survive (Gallo et al. 1987). Experimental procedures suggested that the requirement of these depolarising concentrations *in vitro* mimicked physiological stimulation of NMDA receptors, involving Ca^{2+} entry, *in vivo,* if one was to compare the timing of the differentiation and innervations of the post-mitotic granule cells (Gallo et al. 1987).

CGCs were cultured from the cerebella of 5-6 day old Sprague-Dawley rat pups, as previously described (Kingham et al. 1999). As previously stated, pups were killed by cervical dislocation and decapitation in accordance with the United Kingdom Animals (Scientific Procedures) Act, 1986. The cerebella were dissected and placed into a sterile Petri dish containing ice cold 100 mM phosphate buffer saline (PBS), 0.3 % bovine serum albumin (BSA), 10 mM D-glucose and 0.38% $MgSO_4.7H_2O$. This solution was referred to as solution B (BASE) and was, as the name suggests used to prepare all subsequent solutions needed for the CGC preparation. After collection, the tissue was mechanically diced with a sterile razor blade. The resulting suspension was then enzymatically dissociated further by addition of 10 ml of solution B containing 0.5 mg/ml trypsin (Solution T). The tissue was incubated in a water bath at 37℃ for 5 minutes with gentle agitation every 1-2 minutes to enhance the enzymatic reaction.

Neutralisation of the extracellular matrix digestion by trypsin was then performed by administration of 20 ml solution B containing 8 units/ml DNAase and 8 µg/ml soybean trypsin inhibitor (SBTI). Several inversions were performed to fully neutralise the enzyme then the suspension was centrifuged at 65 *g* for 5 minutes at room temperature. The supernatant was discarded and the pelleted cells were resuspended in 4 ml of solution B containing 50 units/ml DNAase and 50 µg/ml SBTI by trituration with three fire-polished Pasteur pipettes of decreasing diameter, forming a homogeneous suspension. Perikarya were then collected by underlying the suspension with 5 ml 4% BSA in Ca^{2+}-free Earle's Balanced Salts Solution (EBSS) and centrifuging for 5 min at 100 *g*. The resulting soft pellet of enriched perikarya was then resuspended in 1 ml of culture medium consisting of minimum essential medium (MEM) with 10% FBS, 20 mM KCl, 25 mM $NaHCO_3$, 30 mM D-glucose, 2 mM L-glutamine, 100 U/ml penicillin, 100 µg/ml streptomycin and 6 µg/ml ampicillin. Quantification of cell number was then performed using a 1:20 dilution of the 1 ml suspension, as described in previous cell culture methods (**Section 2.2**). Cells (100 µl in volume) were plated onto sterile PDL (100 µg/ml) coated 13 mm coverslips at a density of 8 x 10^5/coverslip. After 1 hour in the incubator at 37℃ in a humidified atmosphere with 6% CO_2, to allow adherence to the coverslip, 500 µl of pre-warmed culture medium was carefully administered. The cultures were returned to the incubator and after 1 DIV the cells were washed and half the culture medium was replaced with fresh medium supplemented with 10 µM cytosine arabinofuranoside (Ara-C), an anti-mitotic (Politis & Houle 1985), to prevent glial cell proliferation. Treatment of CGCs was performed from 6 DIV.

2.3.3.1. Serum-free Neuronal Medium

Where serum-free neuronal culture conditions were required (**Section 3.3.9**), the CGC preparation was performed in an identical manner as described above but the neuronal medium was composed of Neurobasal® medium supplemented with 2% B27®

neuronal supplement, 20 mM KCl, 30 mM D-Glucose, 2 mM L-Glutamine, 50 U/ml penicillin, and 50 µg/ml streptomycin.

2.3.4 Human monocyte-derived-macrophages (hMΦ)

To translate findings from the BV2 cell line and primary rat culture data to a human *in vitro* model, culturing of human macrophages was performed. It has been suggested that peripheral blood monocytes are a valuable model for investigating the innate immune dysfunction in AD (Fiala et al. 2007; Schulz et al. 2007), and previous studies have utilized hMΦ alongside primary rat or human microglia to strengthen their findings (Vegeto et al. 2001; Coraci et al. 2002). Furthermore, early studies identified that hMΦ share similar morphological and immunological features with microglia, including ruffled cell membrane and the expression of MHC class II and complement receptor 3 (CR3; MAC-1, CD11b) (Bauer et al. 1991).

Initially, monocytes were isolated from healthy human volunteers as previously described (Björkqvist et al. 2008). All human experiments were performed in accordance with the declaration of Helsinki (2008) and approved by University College London (UCL)/UCL Hospitals Joint Research Ethics Committee. All subjects gave informed written consent.

Phlebotomy was performed within the National Hospital for Neurology and Neurosurgery (Queen Square) with 50 ml of blood being taken from each subject into Heparin treated tubes. The blood tubes were then transferred to the laboratory. The isolation of mononuclear cells was performed by transferring blood to ACCUSPIN™ System-Histopaque®-1077 tubes (Sigma-Aldrich, Dorset, UK) that had been warmed to room temperature (RT). Initially, the empty tubes were centrifuged at 1000 *g* for 1 minute at RT, followed by transfer of the blood to the tubes (25 ml/tube) and further centrifugation at 1000 *g* for 10 minute at RT to separate the blood components (**Figure 2.3.3 A**). The peripheral blood mononuclear cell (PBMC) layer was transferred to a sterile 50 ml tube and washed with sterile PBS by dilution to a volume of 50 ml. The

tube containing the PBMCs was then centrifuged at 300 *g* for 5 minutes at 4℃, and the resulting pellet was resuspended in 10 ml of PBS and quantified using a haemocytometer, as previously described (**Section 2.2**), to determine the volume of antibody required in the following steps. The suspension was centrifuged at 300 *g* for 5 minutes at 4℃ and the supernatant was discarded. The pellet was resuspended in a volume of MACS® buffer (1 x PBS supplemented with 0.5% BSA and 2 mM EDTA, pH 7.4) containing magnetic anti-CD14 beads, dependent on cell density (i.e. 90 µl of MACS® buffer and 10 µl of magnetic anti-CD14 beads was required per 1 x 10^7 cells). The suspension was incubated in a fridge at 4℃ (not on ice) for 15 minutes, during which time the column apparatus for $CD14^+$ cell separation was assembled (**Figure 2.3.3 Bi**). After the incubation, cells were washed by dilution in 4 ml of MACS ® buffer, followed by centrifugation at 300 *g* for 5 minutes at 4℃, and finally resuspended in 500 µl of MACS® buffer. Each column used in the apparatus setup was initially washed through with 500 µl of MACS® buffer prior to the addition of the cell suspension containing cell-bound magnetic-CD14 antibody (**Figure 2.3.3 Bii**). After the samples had been filtered the column was washed through three times with 500 µl of MACS® buffer to remove any contaminants. Finally, each column was removed from the apparatus setup (and the magnetic field) and 2 ml of MACS® buffer was added. A plunger was then applied to each column to remove the CD14-positive cells (**Figure 2.3.3 Biii**).

The cell density of the suspension was again quantified and an aliquot containing 1 x 10^6 cells was collected to allow monocyte purity to be calculated by FACs analysis using a FACs Calibur high speed cell sorter and CellQuestPro software (BD Biosciences). This was kindly performed by Ulrike Traeger in Professor Sarah Tabrizi's Laboratory and after analysis using FlowJo software (Treestar Inc., San Carlos, CA), the preparations of monocytes were shown to be 90-95% pure, consistent with previously reported data (Björkqvist et al. 2008) (**Figure 2.3.4 A**).

The monocytes were seeded at a density of 2 x 10^6/ well in sterile 6 well plates for gene expression experiments, or at 7.5 x 10^4 cells/well on sterile 13 mm glass coverslips in 24 well plates for ICC experiments in RPMI culture medium supplemented with 10% FBS, 2 mM L-glutamine, 50 U/ml penicillin, and 50 µg/ml streptomycin.To induce differentiation of the monocytes to macrophages, cell medium was supplemented with 20 ng/ml GM-CSF (Martinez et al., 2006), and replaced at 3 DIV. Macrophages were viable for use at 7 DIV, when medium was changed to serum-free, prior to treatment. Macrophage purity ($CD14^+/CD206^+$ cells) by FACs analysis was again kindly performed by Ulrike Traeger and cultures were shown to be 95-99% pure, suggesting near complete differentiation (**Figure 2.3.4 B**).

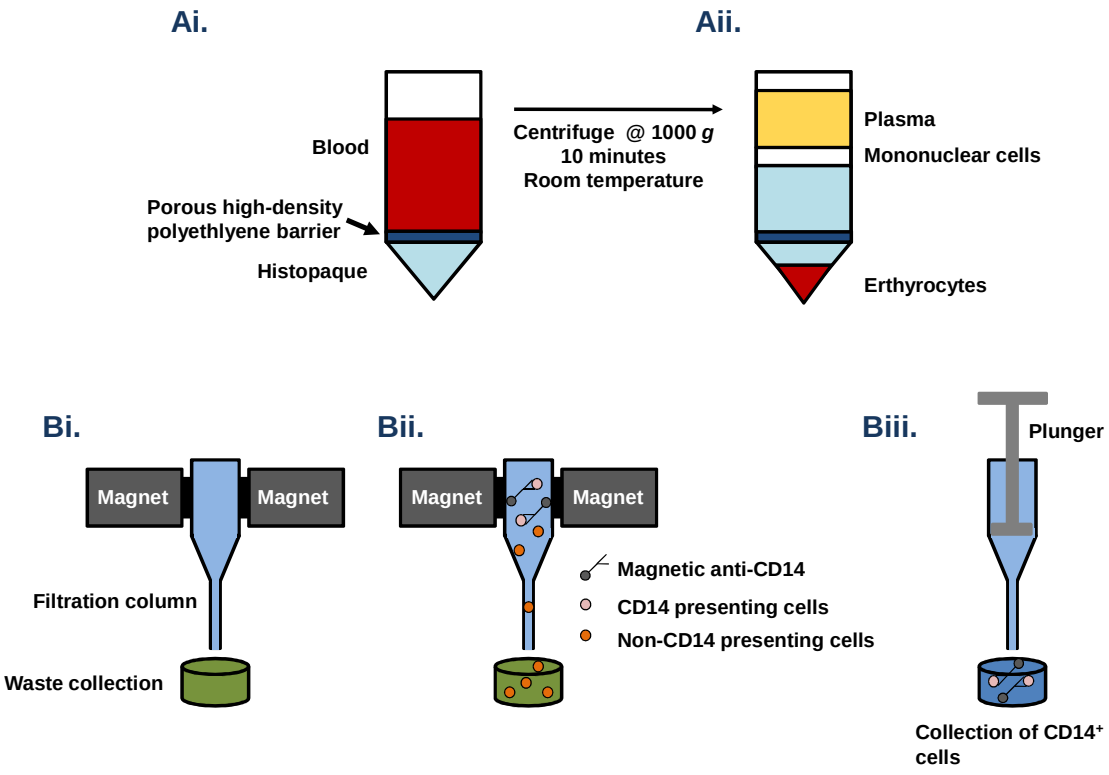

Figure 2.3.3. Schematic representation of specific steps in the human macrophage cell culture preparation

A. Blood was transferred to a histopaque-containing tube (**Ai**). After centrifugation the layer of mononuclear cells could be collected (**Aii**). **B.** Filtration of the sample to remove non-$CD14^+$ cells with the initial apparatus setup shown in **Bi**. $CD14^+$-cells bound to the magneticly tagged anti-CD14 antibodies were retained in the column whilst non-CD14 presenting cells filtered out and discarded (**Bii**). The column was then removed from the magnetic field and the CD14+ cells (monocytes) were collected (**Biii**).

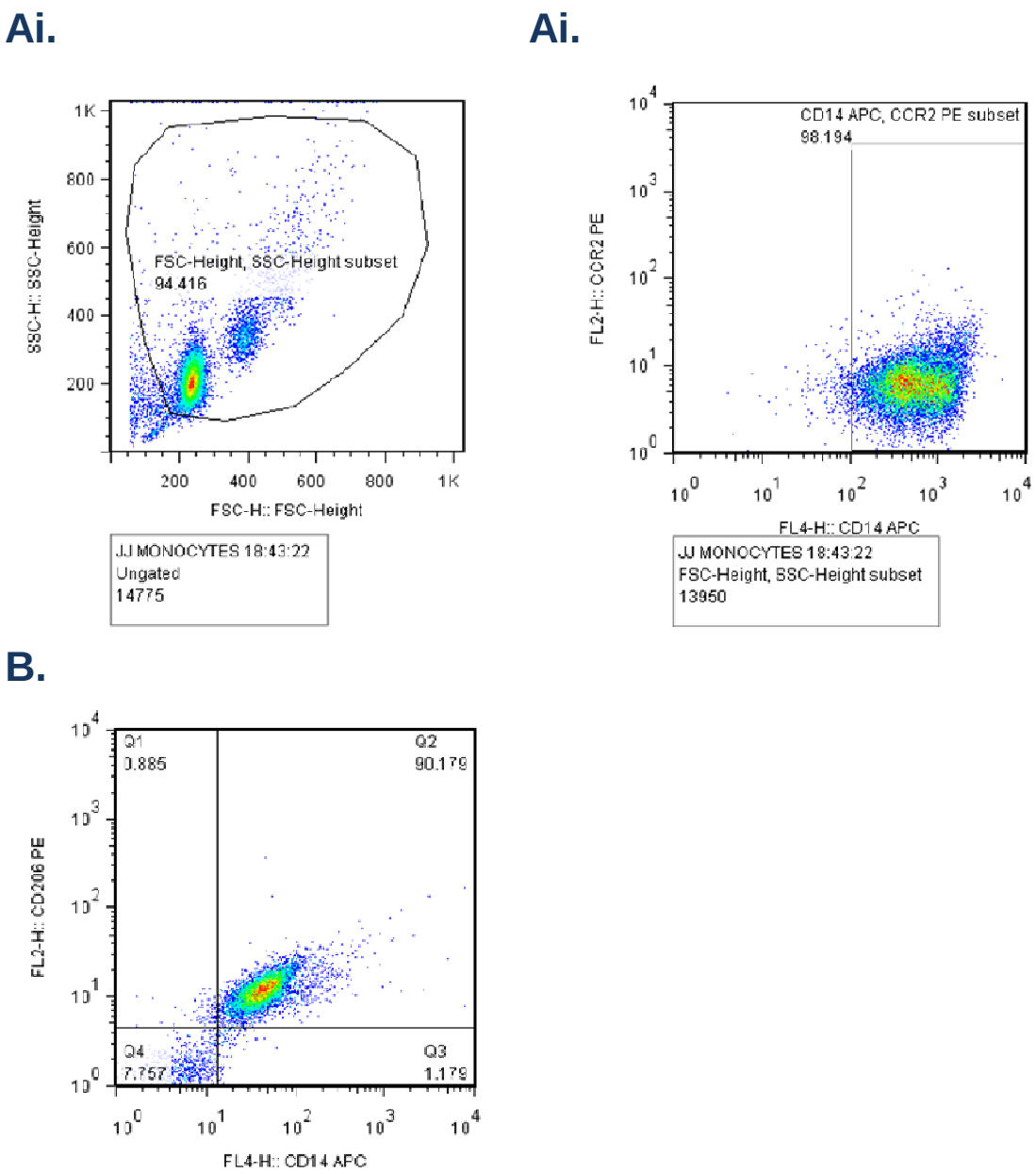

Figure 2.3.4. FACs analyses of monocytes and differentiated macrophages

Representative plots of FACs analysis performed on monocyte and macrophage preparations. **Ai.** Cell sorting by size and granularity was initially performed using front and side scatter analysis. This initial gated area was deemed to contain cells corresponding to the size and granularity associated with mononuclear cells. **Aii.** Further purity calculations were performed using two fluorescent probes, anti-CD14-APC and anti-CCR2-PE, specific for monocytes, in this specific instance showing over 98% purity, with respect to CD14 staining. CCR2 staining shown here is low, which can occur as monocytes express viable levels of this chemokine receptor. Gating of these analyses was performed with respect to a negative control population of T and B cells that are CD14-negative. **B.** Following differentiation in culture to macrophages, the cell preparation purity was calculated using anti-CD14-APC and CD206-PE probes. Here the culture purity is shown as >90%.

2.4. Cell Treatments

2.4.1. Direct treatment of cultures

Primary microglia and the BV2-microglial cell line were routinely plated 24 hours prior to treatment with substitution of the cell medium to serum-free medium at least 3 hours before treatment, unless otherwise stated. Microglia and CGC cultures were activated with LPS alone, or in combination with IFNγ, fibrinogen and fibrin for 1 – 48 hours. For inhibition of endotoxin-mediated responses cultures were treated with PMX 1 hour before activation. Depletion of microglia was performed by administration of LME 24 hours before activation, described in detail in **section 2.5.2**. Thrombin catalysis was inhibited by pre-treating cultures with Hirudin, 1 hour before activation. For TNFα synthesis inhibition prior to activation, cultures were pre-treated with thalidomide (Thal), 1 hour before. Inhibition of iNOS activity was performed in the same manner by pre-treating cultures 1 hour before activation with AMT-HCl. Inhibition of scavenger receptor A was performed by administration of fucoidan to cultures 1 hour prior to activation. Induction of cellular apoptosis was performed by administering staurosporine (STS) to cultures for 4 – 8 hours. Anti-CD11b and rat-IgG were administered to CGC cultures 12 hours before activation.

Superoxide induction via NADPH oxidase was induced by administration of PMA to CGC cultures for 24 hours. Inhibition of this induction was performed by co-treatment of cultures with apocynin. Inhibition of p38, p42/44 (ERK1/2) and PI3K MAPK pathways was performed by pre-treating cultures 1 hour before activation with SB203580, PD98059 and Wortmannin, respectively.

For induction of ER stress, CGC cultures were treated with thapsigargin (Th) or tunicamycin (Tu) for 1 – 24 hours. Inhibition of ER stress was performed by pre-treating cultures with salubrinal (Sal), 1 hour before induction. Inhibition of pan-caspase activation was performed by pre-treating cultures with z-VAD-FMK 12 hours before induction. For specific inhibition of caspase-12 activation, z-ATAD-FMK was

administered to cultures 12 hours before activation was performed. For release of intracellular calcium from BV2 microglia, Ionomycin (Ion) was administered for 0.25 – 1 hours. Chelation of calcium in primary microglial cultures was performed with BAPTA-AM (BAPTA) for 24 hours alone or co-treated with activators shown above. Inhibition of calpains was performed by administration of calpastatin 1 hour prior to activation. All compounds and antibodies with concentrations used to treat cultures are provided in **Table 2.4.1**. The concentrations selected are justified in the corresponding result chapters and were either selected based on previous studies or selected following titration of the proteins or inhibitors used.

Agonists and antagonists of metabotropic glutamate receptors (mGluRs) were used alone or as a co-treatment with the above activators. All the mGluR agonists and antagonists used are listed in **Table 2.4.2**. The concentrations of the mGluR agonists or antagonists used in this study were based on previous studies on the effect of mGluR manipulation on microglia or published EC_{50} values (Macek et al. 1996; Taylor et al. 2003; Taylor et al. 2005; Stauffer 2011).

Compound	Description	Concentration	Catalogue Number
LPS	Gram-negative bacterial wall component: microglial activator	1 µg/ml	Sigma L2762 Serotype: 026:B6
IFNγ	Pro-inflammatory cytokine: microglial activator	100 U/ml	R&D systems 585IF
Fibrinogen	Blood borne protein	0.1 – 2.5 mg/ml	Sigma F4843
Fibrin	Insoluble matrix of fibrinogen	0.05 – 1 mg/ml	Sigma F5386
LME	Lysosomatropic agent that depletes microglia	5 – 75 mM	Sigma L1002
Hirudin	Thrombin inhibitor	50 U/ml	Sigma 94581
Polymyxin B	Endotoxin inhibitor	100 nM	Sigma P4932
Fucoidan	Scavenger receptor A ligand	100 µg/ml	Sigma F5631
Anti-CD11b	CD11b receptor blocking antibody	10 µg/ml	Serotec MCA27EL
Thalidomide	TNFα synthesis inhibitor	10 µg/ml	Tocris 0652
AMT-HCl	iNOS activity inhibitor	150 nM	Tocris 0871
Staurosporine	Apoptotic inducer	0.5 µM	Sigma 54400
PMA	NADPH oxidase	10 ng/ml	Sigma P1585
Apocynin	NADPH oxidase inhibitor	10 µM	Calbiochem 178385
PD98059	ERK1/2 inhibitor	10 µM	Tocris 1213
SB203580	p38-MAPK inhibitor	10 µM	Tocris 1202
Wortmannin	PI3K inhibitor	100 nM	Sigma W1628
Thapsigargin	ER stress inducer	2 µM	Tocris 1138
Tuncamycin	ER stress inducer	1 µg/ml	Sigma T7765
Salubrinal	ER stress inhibitor	100 nM	Enzo Life Sciences ALX-270-428
z-VAD-FMK	Pan-caspase inhibitor	1 µg/ml	Promokine PK-CA577-1010
z-ATAD-FMK	Caspase-12 inhibitor	1 µg/ml	Promokine PK-CA577-1079
Ionomycin	Calcium ionophore	2 µM	Tocris 1704
BAPTA-AM	Calcium chelator	5 – 10,000 nM	Tocris 2787
Calpastatin	Calpain inhibitor	1 – 10,000 nM	Tocris 2950

Table 2.4.1. Compounds and antibodies used to treat cultures

Abbreviations: LPS, lipopolysaccharide; IFNγ, interferon-gamma; LME, leucine-methyl-ester; AMT-HCl, 2-Amino-5,6-dihydro-6-methyl-4*H*-1,3-thiazine hydrochloride; PMA, phorbol 12-myristate 13-acetate; PD98059, 2-(2-Amino-3-methoxyphenyl)-4*H*-1-benzopyran-4-one; SB203580, 4-[5-(4-Fluorophenyl)-2-[4-(methylsulfonyl)phenyl]-1*H*-imidazol-4-yl]pyridine; z-VAD-FMK, carbobenzoxy-Val-Ala-Asp(OME)-fluoromethylketone; z-ATAD-FMK, carbobenzoxy -Ala-Thr-Ala-Asp(OME)-fluoromethylketone; BAPTA-AM, 1,2-*Bis*(2-aminophenoxy)ethane-*N*,*N*,*N*',*N*'-tetraacetic acid tetrakis(acetoxymethyl ester).

Compound	Description	Concentration	Catalogue Number
DHPG	Selective Group I mGluR agonist (mGluR1/5)	100 µM	Tocris 0805
CDPPB	Selective mGluR5 agonist	100 nM	Tocris 3235
MTEP	Selective mGluR5 antagonist	100 µM	Tocris 2921
DCGIV	Selective Group II mGluR agonist (mGluR2/3)	500 nM	Tocris 0975
NAAG	Selective mGluR3 agonist	50 µM	Sigma A5930
L-AP4	Selective Group III mGluR agonist (mGluR4/6/7/8)	100 µM	Tocris 0103

Table 2.4.2. Metabotropic glutamate receptor agonists and antagonists used to treat cultures

Abbreviations: DHPG, (*S*)-3,5-Dihydroxyphenylglycine; CDPPB, 3-Cyano-*N*-(1,3-diphenyl-1*H*-pyrazol-5-yl)benzamide; MTEP, 3-((2-Methyl-1,3-thiazol-4-yl)ethynyl)pyridine hydrochloride; DCGIV, (2*S*,2'*R*,3'*R*)-2-(2',3'-Dicarboxycyclopropyl)glycine; NAAG, *N*-Acetyl-L-aspartyl-L-glutamic acid; L-AP4, L-(+)-2-Amino-4-phosphonobutyric acid.

2.4.2. Microglial conditioned medium administration to neuronal cultures

Microglial cultures were treated as required and incubated for 24 hours. Medium was then classed as microglial conditioned medium (MGCM) and collected into 1500 µl Eppendorf tubes and placed immediately on ice. MGCM was centrifuged (Eppendorf 5415R benchtop centrifuge) at 15,800 *g* at 4℃ for 5 minutes to remove debris and immediately snap frozen with dry ice, followed by storage at -20℃. Administration of MGCM to CGC cultures was performed after depletion of microglia from the cultures with LME as shown in **Section 2.5.2**. Half the CGC medium (250 µl) was removed, discarded and replaced with the relevant MGCM and incubated at 37℃.

In the case of fibrinogen-treated MGCM, to identify if resulting observations were due to factors released from microglia or cross-transfer of fibrinogen in the medium an experiment was performed using concentrated MGCM. Initially, MGCM from FG treated cultures (FG-MGCM) was concentrated using centrifugal filter units (Amicon Ultra, Millipore, Watford, UK) that allowed removal of media components below a molecular weight of 10 kDa. FG-MGCM was concentrated in the spin columns by centrifugation (Eppendorf 5415R benchtop centrifuge) at 4 ℃ for 15 minutes at 14000 *g* resulting in a concentrated solution (~ 15 µl), which was collected by centrifugation at 4℃ for 5 minutes at 1000 *g*. The concentrated sample was resolved through a 10% gel (**Table 2.7.2**) and Western blotting (**Section 2.7**) with anti-FG conjugated to HRP was performed to identify the presence of FG in MGCM, controlled with known concentrations (**Figure 2.4.1**). As expected, a strong concentration dependent expression was observed when known concentrations were resolved. Concentrated MGCM however showed much lower expression of FG at concentrations lower than those able induce significant toxicity (require >100 µg/ml; E. East unpublished observations), suggesting any cross transfer was limited and not able to induce significant toxicity alone.

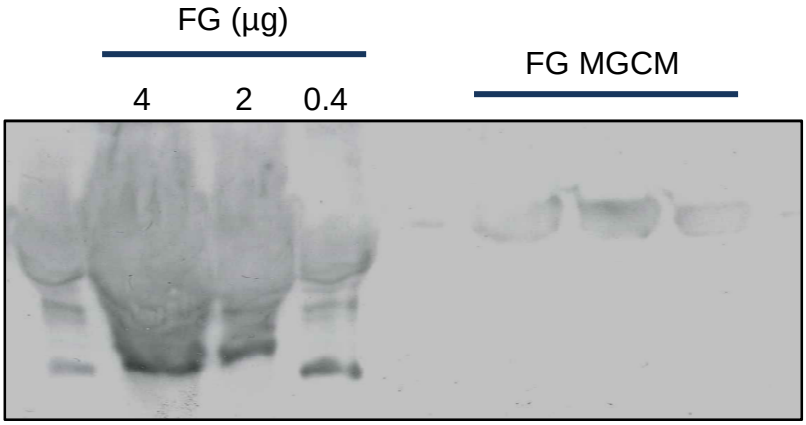

Figure 2.4.1. Only low level transfer of FG occurs in MGCM experiments

Western blot analysis was performed on concentrated MGCM from cultures treated with FG, with comparison to known masses of FG. Limited transfer of FG was observed in MGCM, when compared with the known masses, suggesting only low levels of FG remain in MGCM after 24 hours of treatment. Lane 1 contains overflow from lane containing 4 µg FG (lane 2). Anti-FG-HRP (1:500) was incubated with membranes for 2 hours at RT.

2.5. Development and optimisation of microglia depletion from neuronal cultures

Due to the observation that LPS treatment could induce significant toxicity in neuronal cultures, it was hypothesised that a small population of microglia present in the cultures was responsible. Therefore, a protocol to selectively deplete microglia from the CGC cultures was optimised, guided by previously published methodology (Giulian et al. 1993; Morgan et al. 2004; Hamby et al. 2006). Initially the methodology followed previously published studies from our laboratory (Morgan et al. 2004), however this protocol required further adaption to increase neuronal survival, and methodology that was shown previously to deplete microglia from astrocyte cultures (Hamby et al. 2006) was modified for use on the CGC cultures used here.

2.5.1. Initial optimisation

Following previously described methodology (Morgan et al. 2004), depletion of microglia from CGC cultures was initially attempted using *L*-leucine-methyl-ester (LME) treatment for 24 h. LME is a lysosomatropic agent originally employed to selectively deplete macrophages (Thiele et al. 1983), however a number of research groups have used it to selectively deplete microglia from astrocyte or oligodendrocytes cultures (Giulian et al. 1993; Hewett et al. 1999; Hamby et al 2006). Previous studies suggested a concentration range of 1 – 10 mM LME could significantly deplete microglia from neural cultures. Therefore, at 6 DIV culture medium on CGCs was changed to medium containing 1 – 10 mM LME and cultures were fixed and analysed after 24 h. To quantify microglia and apoptosis, cultures were stained with Isolectin-B_4 (IB_4) and DAPI (**See section 2.6.5**), respectively.

Only treatment with medium containing 10 mM LME could significantly decrease microglia number in the CGC cultures. However, significant apoptosis also occurred, that was concluded to be due to LME treatment rather than the cell culture media change, as no significant difference was observed between control cultures +/- a media change (**Figure 3.3.4**). Furthermore, it had been suggested that this concentration

range and exposure time to LME was optimal in low density cultures (Hamby et al. 2006). CGC cultures are at high density, so a differing approach was performed using higher concentrations of LME coupled with a shorter exposure time.

At 6 DIV, CGCs were treated with LME but this time using a concentration range of 25 – 75 mM for 1 h. Initially, LME was dissolved in culture medium, pH was returned to 7.4 using 1 M sodium hydroxide (NaOH), followed by filter sterilisation. The LME concentration dissolved in the medium was equal to twice the concentration required (2 x LME). Half the culture medium was removed from each CGC-containing well and retained at 37℃, followed by administration of 2 x LME to the CGC-containing wells, i.e. diluted 1:1 giving the desired concentration. The cultures were then incubated at 37℃ in a humidified atmosphere with 6% CO_2 for 1 h. LME was removed from the cultures following two washes with pre-warmed fresh CGC medium. The retained cell medium plus an equal volume of fresh CGC medium was then added to the corresponding wells. Cultures were left to rest for 24 h then fixed and analysed as previously described with IB_4 and DAPI staining. Control cultures were treated in an identical fashion but CGC medium without LME was used instead. The highest LME concentrations tested (50 -75 mM), deemed necessary to deplete microglia in astrocyte cultures (Hamby et al. 2006), significantly depleted microglia in the CGC cultures used here, but also significantly increased observed toxicity (**Figure 3.3.5**). Treatment with 25 mM LME, significantly decreased microglia number without a significant increase in toxicity being observed in the CGC cultures (**Figures 3.3.5**). Further characterisation of this concentration, showed neuronal and astrocytic morphology was not significantly altered (**Figure 3.3.6 and 3.3.7**). Therefore this concentration was utilised for all future LME experiments following the protocol provided in **section 2.5.2**.

2.5.2. Optimised protocol

CGC cultures were treated with 25 mM LME for 1 h after 6 DIV. A fresh stock concentration of LME (150 mM) was produced in CGC medium prior to each experiment. The pH of the LME stock solution was return to 7.4 and the solution filter

sterilised using a 28 mm Polyether Sulfone (PES) 0.2 µm syringe filter (Corning, Bucks, UK). The stock was then diluted to a concentration of 50 mM (2 x LME) in CGC medium and warmed in a waterbath set to 37℃ for 10 minutes. Half the culture medium (250 µl) was removed from each CGC-containing well and retained at 37℃. Wells were then treated with CGC medium containing 2 x LME (250 µl), i.e. diluted 1:1 giving a well concentration of 25 mM, or with pre-warmed CGC medium without LME (250 µl) for control cultures. Cultures were incubated at 37℃ in a humidified atmosphere with 6% CO_2 for 1 h. Wells were then washed twice in fresh pre-warmed CGC medium to remove LME-containing media followed by the addition of the retained culture medium and an equal volume of fresh pre-warmed CGC medium to the corresponding wells. Cultures were then returned to the incubator (humidified with 6% CO_2 at 37℃) and left to rest for 24 h before any furth er treatment.

2.6. Fluorescence microscopy

2.6.1. The fluorescence microscope

A Zeiss Axioskop 2 fluorescence microscope (Oberkochen, Germany) was used to obtain images from immunocytochemistry (ICC) to identify protein expression and live and fixed cellular staining to assess caspase activation, superoxide production and cell death. In all cases, cells were viewed with x20 and x40 Neofluar objectives or x100 Neofluar oil immersion objective. Images were captured using a Zeiss AxioCam HRc camera and analysed using Zeiss Axiovision 4.8 software.

2.6.2. Measurement and quantification of apoptotic morphology in cultures

Apoptosis is programmed cell death. When cells are chronically stressed, deprived of nutrients or injured, apoptosis can occur to induce death. The term apoptosis was proposed for programmed cell death with classic morphological features including membrane blebbing and bright pyknotic nuclei, due to chromatin condensation (Kerr et al. 1972). These morphological features can be simply identified in PFA fixed cultures using the nuclear stain 2´-(4-Ethoxyphenyl)-5-(4-methyl-1-piperazinyl)-2,5´-bi-1H-benzimidazole (Hoechst-33342) or with 4',6-Diamidino-2-Phenylindole (DAPI) in ICC

experiments. Hoechst-33342 is lipophilic, readily crosses plasma membranes, and binds DNA allowing for quantification of cells displaying apoptotic morphology.

Cultures were plated on 13 mm coverslips in 24 well cell culture plates, treated as required, fixed for 30 minutes in 4% PFA then stored until use at 4℃ in PBS. Hoechst-33342 (final concentration of 4 $\mu g.ml^{-1}$) was administered directly to the PBS and incubated at room temperature in the dark for 15 minutes. Coverslips were then removed from plates and gently rinsed in PBS before mounting on a slide with a drop of PBS being used as the mountant. Hoechst-33342 stained nuclei were excited with light at a wavelength of 365 nm, with emission over 490 nm, to visualise Hoechst-33342 staining. At least three fields from each coverslip were captured using the fluorescence microscope, with treatments being performed in duplicate or triplicate, and experiments repeated three times to allow for statistical analysis. Quantification was performed without blinding of the treatments. However, in an attempt to avoid objectivity, random datasets were quantified in parallel by other members of the lab that were blinded to the treatments. These quality control measures were performed in all of the large quantified datasets including the fixed and live cell staining and ICC.

2.6.3. Live cell staining for the determination of cellular death, caspase activation and superoxide production

Methods for quantifying cell death with less objectivity are desirable. This can be performed with the use of specific markers of death in parallel with Hoechst-33342 staining. For example, the use of propidium iodide, a nuclear stain, that can only bind DNA if there is loss of membrane integrity due to the compounds lipophobicity, allows for quantification of total cell death. Staining of cultures with FITC-conjugated annexin V can be used to quantify cells in the early stages of apoptosis. This is due to a published observation that soon after initiating apoptosis, cells ‘flip’ phosphatidylserine (PS) from the inner face of the plasma membrane to the extracellular surface as a phagocytic signal to macrophages and microglia (Fadok et al. 1992). Once PS is on the

extracellular surface it can be detected by staining with FITC-conjugated annexin V, a protein with a strong, natural affinity for PS (Zhang et al. 1997).

As described in **section 1.4.1.1**, caspase activation occurs during classical apoptosis. Therefore, the use of fluorescently tagged peptides that covalently bind to the activated form of specific caspases, allows for quantification of cells undergoing apoptosis. However recent studies suggesting non-apoptotic roles for caspases (Li et al. 2010; Jo et al. 2011; D'Amelio et al. 2011; Burguillos et al. 2011) suggests this staining should be undertaken in parallel with other markers of cell death. Finally, quantification of superoxide production in microglia present in the CGCs also provides a good marker for microglial activity.

Cultures were plated on 13 mm coverslips in cell culture plates, treated as required, then incubated with fluorescent dyes for varying times (**Table 2.6.1**) at 37℃ in the dark. Coverslips were then mounted on slides in warmed basic medium (153 mM NaCl, 3.5 mM KCl, 0.4 mM KH_2PO_4, 20 mM N-Tris(hydroxymethyl)methyl-2-aminoethanesulphonic acid (TES), 5 mM $NaHCO_3$, 1.2 mM Na_2SO_4, 1.2 mM $MgCl_2$, 2.6 mM $CaCl_2$, 5 mM glucose) and viewed immediately. For dye excitation and emission wavelengths, see **Table 2.6.1**. Initially, Hoechst-33342 staining of cell nuclei was captured to focus on a particular plane of cells, followed by other fluorescent markers. At least three fields from each coverslip were captured, with treatments being performed in duplicate or triplicate, and experiments repeated three times to allow for statistical analysis

2.6.4. Immunocytochemistry

Primary rat microglia or human monocyte-derived macrophages (hMΦ) were cultured on 13 mm glass coverslips and treated as required. The cultures were fixed with 4% paraformaldehyde (PFA) in phosphate-buffered saline (PBS; 154 mM NaCl, 1.84 mM KH_2PO_4, 9.81 mM $K_2HPO_4.3H_2O$, pH adjusted to 7.4 with further addition of $KH_2PO_4/K_2HPO_4.3H_2O$ as necessary) for at least 30 minutes at room temperature. Cultures were then washed three times with PBS and permeabilised in 100% ice cold

Fluorescent Dye	Target	Excitation (nm)	Emission (nm)	Final Concentration	Incubation times (min)
Hoechst-33342	Total Nuclei	365	490	4 µg/ml	15
Propidium Iodide (PI)	Dead Nuclei	541	572	1 µg/ml	30
Annexin V-FITC	Early apoptotic – phosphatidylserine 'flip'	485	530	5 µg/ml	60
FAM-DEVD-FMK	Active caspase-3/7	485	530	1 µg/ml	60
FITC-ATAD-FMK	Active caspase-12	485	530	1 µg/ml	60
Dihydroethidium (DHE)	Produced Superoxide	541	572	5 µM	45
Fluorescently conjugated antibody	**Target**	**Excitation (nm)**	**Emission (nm)**		**Incubation times (min)**
Goat anti-Rb-TRITC	1°Abs raised in Rabbit	541	572	1:500	120
Goat anti-Rb-Cy3	1°Abs raised in Rabbit	541	572	1:500	120
Goat anti-Ms-FITC	1°Abs raised in Mouse	485	530	1:1000	120
Isolectin-B_4-FITC	Microglial-specific lectins	485	530	2 µg/ml	120
pAb-Calnexin-TRITC	Cellular Calnexin	541	572	2 µg/ml	120

Table 2.6.1. Summary of fluorescent markers and fluorescently tagged antibodies

Fluorescent markers and antibodies used in fixed and live cell staining and immunocytochemistry experiments. Excitation and Emission wavelengths, final well concentrations and relative incubation times are also provided.

methanol for 20 minutes at -20ºC or 0.1% Triton-X100 for 10 minutes at room temperature (NeuN staining only) followed by three further washes with PBS. Cells were then blocked with 4% normal goat serum (NGS) for 30 minutes at room temperature. The choice of block was due to the species the secondary antibodies were raised in, i.e. the secondary antibodies used were raised in goat. The use of species-specific serum combats non-specific binding of the secondary antibody. Following the block of non-specific binding, 200 µl of a primary antibody diluted in PBS (**Table 2.6.2**) was incubated with the cultures overnight at 4℃ in a dark, humidified atmosphere. Negative controls were performed in all experiments where the primary antibody was omitted and replaced with PBS to identify any non-specific secondary antibody binding. Cultures were then washed three times with PBS and incubated with 200 µl of a relevant secondary antibody-conjugated to fluorescein isothiocyanate (FITC), tetramethylrhodamine-5-(and 6)-isothiocyanate (TRITC) or Cyanine-3 (Cy3) (**Table 2.6.1**) diluted in PBS for 2 hours in the dark at room temperature. If microglia identification and quantification was required, FITC-conjugated lectin from *Griffonia simplicifolia* ($I\text{-}B_4$) (Streit 1990) was administered at the secondary antibody stage. Cultures were then again washed with PBS in the dark and incubated with 200 µl of 1:1000 4',6-Diamidino-2-Phenylindole (DAPI; final concentration 300 ng/ml) in PBS for 1 minute in the dark at room temperature to identify nuclear morphology. Finally cultures were washed once more with PBS, rinsed with ddH_2O and mounted on a glass slide with Vectashield mountant. The edges of each coverslip were sealed to prevent the cells drying out and slides were stored in the dark at -20℃ until viewing on the Zeiss Axioskop 2 fluorescence microscope. Brightness, contrast and colour balance were adjusted identically across treatments to allow quantification.

Antibody	Species	Relevant Reactivity	Target	Dilution
pAb-iNOS	Rabbit	Rat	Inducible nitric oxide synthase	1:250
mAb-bNOS	Mouse	Rat	Neuronal nitric oxide synthase	1:250
mAb-ED-1	Mouse	Rat	Lysosomal-glycoprotein in microglia	1:500
pAb-Cleaved caspase-3	Rabbit	Rat, Human	Activated caspase-3	1:500
mAb-NeuN	Mouse	Rat	Neuronal specific protein	1:200
mAb-GADD153/CHOP	Mouse	Rat	ER stress-associated transcription factor	1:250
mAb-CD68	Mouse	Human	Human homologue of ED-1	1:100
mAb-CD11b	Mouse	Rat	MAC-1 integrin receptor on microglia	1:100
mAb-β-III-tubulin	Mouse	Rat	Neuron-specific microtubule protein	1:100
pAb-GFAP	Rabbit	Rat	Astrocyte-Glial fibrillary acidic protein	1:100

Table 2.6.2. Summary of primary antibodies used in ICC experiments

Host species, relevant reactivity, target information and relative dilutions are provided.

2.7. Western blotting

The development of a method that allowed transfer of resolved proteins to a membrane enabling detection of small quantities of protein in a sample occurred in two separate labs around the same time (Towbin et al., 1979; Burnette et al., 1981). However, it was Burnette and colleagues' more simple methodology that went on to be named Western blotting, a play on the name of the molecular genetics tool, Southern blotting, that allows for the immobilisation of electrophoretically fractionated DNA onto nitrocellulose filters (Burnette et al., 1981).

Proteins in a prepared sample are separated using gel electrophoresis. The most common type of gel electrophoresis is sodium dodecyl sulphate polyacrylamide gel electrophoresis, or SDS-PAGE. The proteins are stabilised in a denatured state with the application of strong reducing agents, normally present in the initial lysis buffer. The resulting polypeptides are coated in the negatively charged SDS present in the protocol buffers, allowing migration through the acrylamide gel mesh towards a positive electrode in the gel tank. The lower the molecular weight, the faster the polypeptides migrate through the mesh, yielding separation on the basis of size. The following steps involve transfer of the resolved proteins in the gel to a membrane, again using an electric field, which then allows semi-quantification of proteins using specific antibodies targeted at the protein of interest and visualised using chemiluminescence.

Western blotting was used to identify changes in cytosolic protein expression in cell lines and primary cultures, after treatment.

2.7.1. Sample collection and preparation

BV2s, primary microglia, and neuronal cultures (density ranging from 3 x 10^5 – 2.4 x 10^6) were harvested into lysis buffer (30 – 45 µl, dependent on density) and incubated on ice for at least 20 minutes. Lysis buffer (pH 7.4) composition and relative component function is given in **Table 2.7.1**. Cell lysates were centrifuged at 15,800 *g* to pellet nuclear and membrane fractions, as well as cellular debris. All identified proteins of

interest were cytosolic so the resulting cytoplasmic fraction in the supernatant was collected and stored at - 20℃ until use.

2.7.2. Determination of protein concentration

The protein concentration of the cytoplasmic fraction was determined by the Bradford protein assay (Bradford 1976) using bovine serum albumin (BSA) as a standard. To a 96 well plate, 1 µl of each cytoplasmic lysate was added in triplicate, alongside a BSA standard curve. To this, 200 ml of Bradford reagent was added and mixed using an EASIA orbital shaker (Medgenix Diagnostics, Fleurus, Belgium) set to 60 rpm for 5 minutes. The absorbance was measured on a GeniOS™ plate reader (Tecan Group, Reading, UK) at a wavelength of 595 nm. The acidic environment of the Bradford reagent induces protein binding to the Coomassie dye present in the reagent. This causes a spectral shift in absorbance from the brown form of the dye to the blue form of the dye, i.e. the more protein present, the more intense to shift from brown to blue. **Figure 2.7.1** shows a representative BSA standard curve that allowed analysis of protein concentration in the lysed samples, by plotting known BSA concentrations against sample absorbance at 595 nm.

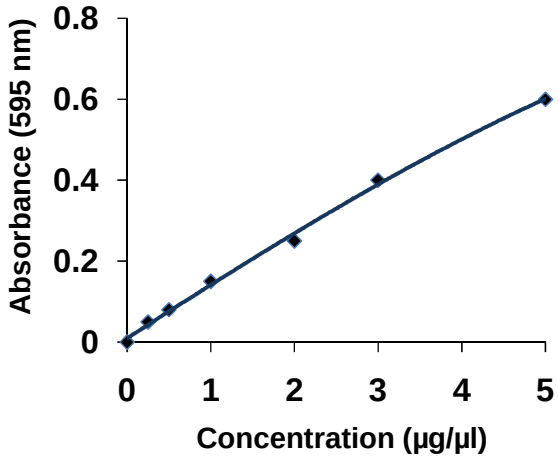

Figure 2.7.1. Example standard curve generated for Bradford identification of the protein concentration in cell lysates

2.7.3. Pouring acrylamide gels

Acrylamide gels for SDS-PAGE were prepared using mini gel apparatus (Bio-Rad, Hertfordshire, UK). The compositions of the protein resolving gels and protein stacking gel are provided in **Table 2.7.2**. Depending on the molecular weight of the targeted protein, the percentage of acrylamide in the resolving gel was altered. To target high molecular weight proteins (>100 kDa; e.g. iNOS and ED-1), 10% acrylamide gels were used, and to target lower molecular weight proteins (<100 kDa; e.g. Caspase-12 and TNFα), 12% acrylamide gels were used. The resolver gel was poured between two 100% ethanol washed glass plates to a level 2.5 cm below the top of the front plate, and covered with 100% ethanol until the acrylamide had polymerised. The ethanol was removed and the stacker gel (4% acrylamide) was then poured onto the resolver gel, and a lane comb inserted.

2.7.4. SDS-PAGE electrophoresis

The volume of protein lysate sample equivalent to 30-45 µg of protein was diluted 1:1 in sample buffer (2% SDS, 10% glycerol, 2.5% β-mercaptoethanol, 125 mM Tris-Base (pH 6.8) and bromophenol blue crystals) (Laemmli 1970) and boiled for 5 minutes to further denature the proteins. The samples were mixed, centrifuged at 1000 rpm for 15 seconds, and loaded into the stacker gel wells submerged in a Bio-Rad mini gel tank filled with running buffer (125 mM Tris-Base, 1 M glycine, 0.01% SDS). Where possible, protein of interest standards and a broad-range protein molecular weight marker (2-212 kDa, New England BioLabs, Hertfordshire, UK) were loaded on the gel. The protein samples were then electrophoresed using a voltage of 130-165 V, until the 'gel front' (a combination of contaminating cell media and bromophenol blue) and the molecular weight marker had reached the bottom of the resolver gel.

2.7.5. Transfer of resolved proteins to membrane using electrophoresis

The gel was carefully removed from the glass plates and equilibrated in ice-cold transfer buffer for 20 minutes (25 mM Tris-Base, 192 mM glycine, 20% methanol, 0.01% SDS). During this time Immobilon-P-polyvinylidene difluoride (PVDF) membrane

was cut to the shape of the gel, activated in ice-cold 100% methanol for 1 minute, washed in ddH_2O for 5 minutes, and equilibrated in ice-cold transfer buffer for 15 minutes. A sandwich of transfer buffer soaked fibre pads, 3MM Chromatography paper (Whatman, Kent, UK), the gel and the PVDF membrane was constructed on a cassette as shown in **Figure 2.7.2**. After rolling out any trapped air-bubbles, the cassettes were placed in the Bio-Rad mini gel transfer apparatus with an ice pack and magnetic stirrer, making sure the sandwich was inserted in the correct orientation. The proteins were transferred to the PVDF membrane with 80 V of electricity for 1 hour.

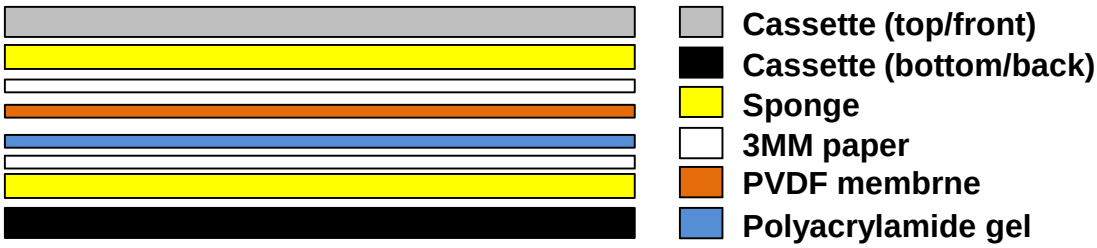

Figure 2.7.2. Setup of the gel/membrane sandwich required for transfer of resolved proteins to a membrane using electrophoresis

2.7.6. Immuno-blotting

Membranes were removed from the cassette and washed with Tween 20-Tris-buffered saline (T-TBS; 10 mM Tris-Base, 150 mM NaCl, and 0.5% Tween 20, pH 7.4) for 10 minutes and blocked for at least 1 h at room temperature (RT) in blocking buffer (T-TBS plus 5% non-fat dried milk or 1% BSA). Membranes were then incubated with the primary antibody diluted in blocking buffer for either 2 hours at room temperature or overnight at 4°, dependent on the antibody manufacturer's recommendations (**Table 2.7.3**). After 3 x 10 minute washes with T-TBS, the membranes were incubated for 1 hour at RT with HRP-conjugated secondary antibodies with specificity for the primary antibody in question (**Table 2.7.3**), followed by 3 x 10 minute washes with T-TBS. The membranes were then gently blotted and incubated for 1 minute in a 1:1 solution of reconstituted ECL (enhanced chemiluminescence solutions 1 and 2). The membranes were lightly blotted again, wrapped in thin transparent film (Saran Wrap) and secured in an X-ray film cassette. In the dark room membranes were exposed to photographic film (Amersham™ Hyperfilm) for 1-30 minutes depending on signal intensity, immersed in developing solution followed by fixing solution, and finally washed in H_2O. After being air-dried, the banded films were subjected to densitometry using MacBioPhotonics Image J software (NIH Image, Bethesda, USA) for semi-quantification of relative protein expression. Standard blots for caspase-12 induction using lysates from CGCs treated with positive controls are shown in **Figure 2.7.3**. In most cases, treatments and conditions were replicated 3 times and quantified for statistical analysis.

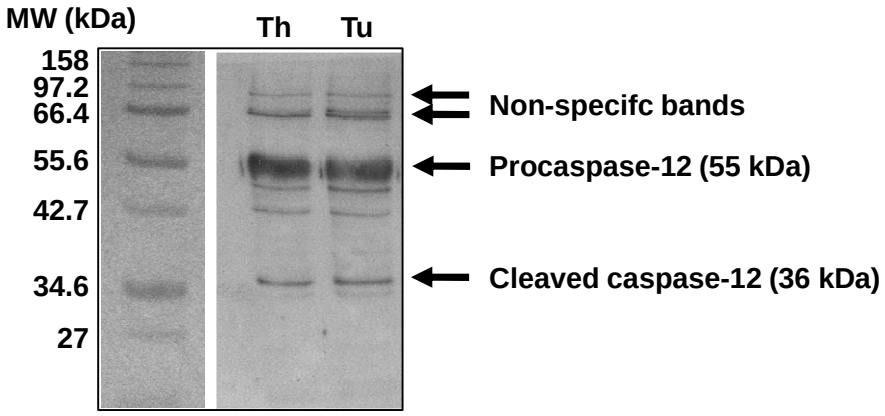

Figure 2.7.3. Sample Caspase-12 blots with MW marker

Western blot analysis of caspase-12 expression in CGC lysates treated with thapsigargin (Th; 2 µM) or Tunicamycin (Tu; 1 µg/ml). The molecular weight marker provides identification of the large band associated with pro-caspase-12 at approximately 55 kDa and the cleaved active form at approximately 36 kDa. Non-specific banding is also observed.

2.7.7. Checking secondary antibody specificity

Observations were made that suggested the secondary antibody used to identify caspase-12 expression by Western blotting could be directly binding to transferred fibrinogen. Therefore control experiments were performed using a combination of standard Western blotting technique and Coomassie blue membrane staining.

Initially, Coomassie blue experiments were performed on gels loaded with 4 µg of fibrinogen (from fresh and frozen stocks) prepared in standard Western blotting lysis buffer. This provided identification of the molecular weights of relative subunits of fibrinogen in the preparations used here. An 8% resolver gel (**Table 2.7.2**) was set-up and the fresh or frozen preparations of fibrinogen were loaded into a standard stacker gel, resolved for 1 h at 165 V and transferred onto PVDF membrane as previously described.

In line with a previously published protocol (Houen et al. 1997), transferred membranes were blocked in a 1% Tween-20 solution for 30 minutes. Membranes were then stained by immersion in a 0.01% Coomassie blue solution for 10 – 20 minutes and air-dried. **Figure 2.7.4 A** shows both fresh and frozen stocks of fibrinogen give the same banding pattern with a main band showing at a molecular weight of ~ 56 kDa, corresponding to the β-chain. Other bands above and below correspond to the α-chain (63 kDa) and γ-chain (47 kDa), respectively.

To control for secondary antibody binding to resolved fibrinogen transferred from the cell lysates, another experiment was performed using a range of fibrinogen concentrations (4 ng – 400 µg) prepared in lysis buffer. Fibrinogen was loaded into an 8% resolver gel alongside a 4% Normal Rabbit Serum (NRbS) positive control lane. Protein was resolved and transferred as previously described and the goat anti-rabbit-HRP secondary antibody was incubated with the membrane in 5% blocking buffer (T-TBS plus 5% non-fat dried milk) for 1 h at room temperature. Chemiluminescence was performed and **Figure 2.7.4 Bi** shows the antibody bound only to NRbS and not to any

of the fibrinogen concentrations tested, shown to be present using the Coomassie blue protocol **Figure 2.7.4 Bii**.

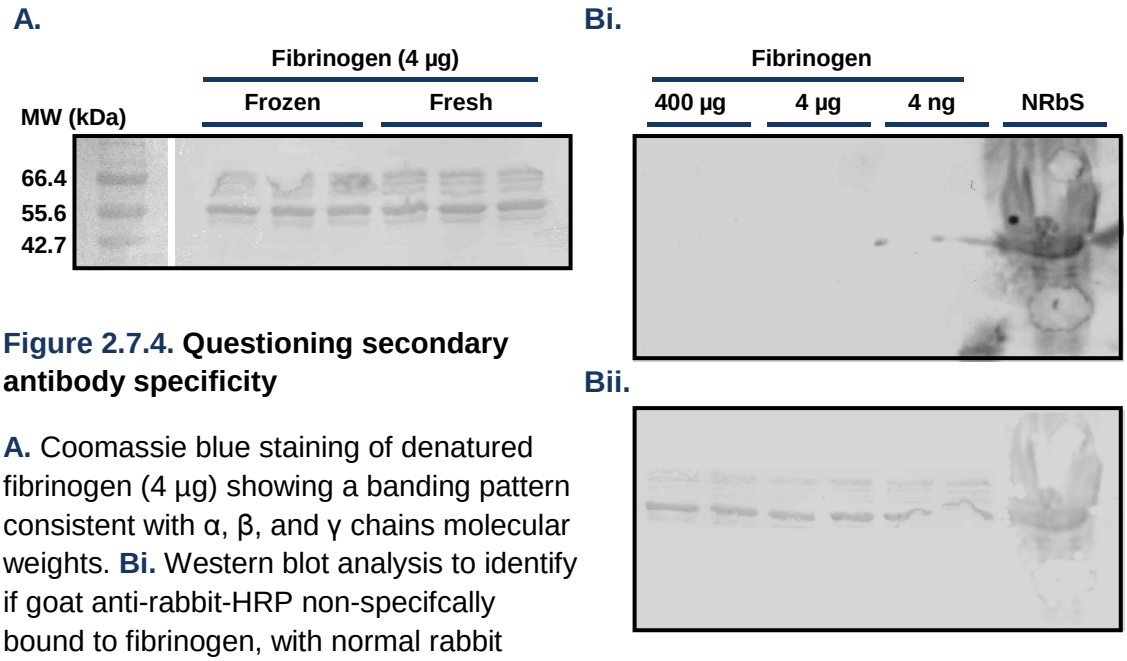

Figure 2.7.4. Questioning secondary antibody specificity

A. Coomassie blue staining of denatured fibrinogen (4 µg) showing a banding pattern consistent with α, β, and γ chains molecular weights. **Bi.** Western blot analysis to identify if goat anti-rabbit-HRP non-specifcally bound to fibrinogen, with normal rabbit serum (NRbS) used as a positive control. No significant binding was observed and fibrinogen was shown to be present after coomassie staining was performed (**Bii**).

Component	Final Concentration	Function
Tris-acetate	20 mM	Buffer
Ethylene diamine tetraacetic acid (EDTA)	1 mM	Calcium chelator
Ethylene glycol tetraacetic acid (EGTA)	1 mM	Magnesium chelator
Sodium-β-glycerophosphate	10 mM	False phosphatase substrate
Sodium orthovanadate	1 mM	Tyrosine phosphatase inhibitor
Glycerol	5 %	Cryo-protectant
Triton X-100	1 %	Solubilises membranes
Sucrose	0.27 M	Increases osmolarity, stabilises membranes
Benzamidine	1 mM	Protease inhibitor
Leupeptin	4 µg/ml	Lysosomal protease inhibitor
Phenylmethylsulfonyl fluoride (PMSF)	1 mM	Cysteine protease inhibitor
Microcystin - LR	1 µM	Phosphatase inhibitor
β-mercaptoethanol	0.1 %	Reducing agent

Table 2.7.1. Western blotting lysis buffer components

Components of lysis buffer required for Western blotting as previously published (Kingham & Pocock 2000) with the addition of PMSF for caspase-specific studies.

Resolver Gel (8%)	Resolver Gel (10%)	Resolver Gel (12%)	Stacker Gel (4 %)
2.4 ml 30% acrylamide	3.33 ml 30% acrylamide	4 ml 30% acrylamide	1.33 ml 30% acrylamide
2.5 ml Resolver buffer (1.15 M Tris-HCl, 0.1% SDS, pH 8.8)	2.5 ml Resolver buffer	2.5 ml Resolver buffer	2.5 ml Stacker buffer (0.38 M Tris-HCl, 0.1% SDS, pH 6.8)
5.1 ml ddH_2O	4.17 ml ddH_2O	3.5 ml ddH_2O	6.17 ml ddH_2O
50 µL 10 % Ammonium persulphate (APS)	50 µL 10 % APS	50 µL 10 % APS	50 µL 10 % APS
5 µL TEMED	5 µL TEMED	5 µL TEMED	5 µL TEMED

Table 2.7.2. Compositions of all used protein resolving gels and protein stacking gel

Primary Antibody	Host	Target	Dilution	Blocking buffer
pAb-iNOS	Rabbit	Inducible nitric oxide synthase	1:5000	5% non-fat milk
mAb-ED-1	Mouse	Lysosomal-glycoprotein in microglia	1:1000	5% non-fat milk
pAb-Cleaved caspase-3	Rabbit	Activated caspase-3	1:1000	5% non-fat milk
pAb-Caspase-12	Rabbit	Activated caspase-12	1:1000	5% non-fat milk
mAb-phospho-ERK1/2	Rabbit	Phosphorylated extracellular signal-regulated kinases-1/2	1:1000	1% BSA
mAb-total-ERK1/2	Mouse	Total extracellular signal-regulated kinases-1/2	1:2000	1% BSA
mAb-phospho-p38 MAPK	Mouse	Phosphorylated p38-mitogen-activated protein kinase	1:1000	5% non-fat milk
pAb-total-p38 MAPK	Rabbit	Total p38-mitogen-activated protein kinase	1:1000	5% non-fat milk
pAb-TNFα	Goat	Pro-inflammatory cytokine TNFα	1:500	5% non-fat milk
mAb-β-actin	Mouse	Cytoskeletal protein β-actin	1:5000	5% non-fat milk
Anti-Rb-HRP	Goat	1℃Abs raised for Rabbit	1:1000	5% non-fat milk
Anti-Ms-HRP	Goat	1℃Abs raised for Mouse	1:1000	5% non-fat milk
Anti-Gt-HRP	Donkey	1℃Abs raised for Goat	1:1000	5% non-fat milk
Anti-Rt-FG-HRP	Goat	1℃Abs targeting rat fibrinogen	1:500	5% non-fat milk

Table 2.7.3. Summary of primary and HRP-conjugated secondary antibodies used in Western blotting experiments

Host species, target information, relative dilutions and blocking buffer requirements are provided.

2.8. Enzyme-linked immunosorbent assay for cytokine quantification

The enzyme-linked immunosorbent assay (ELISA) is a method that allows for specific protein concentration quantification in a given sample. Interestingly, the assay was developed independently and simultaneously in 1971 by Peter Perlmann and Eva Engvall at Stockholm University and by Anton Schuurs and Bauke van Weemen in The Netherlands (Lequin 2005). The technique is extremely useful for the quantitative analysis of functional cytokine release, a consequence of microglia activation. Quantitative sandwich ELISA kits (R&D Systems) for the measurement of classical pro-inflammatory cytokines, tumour necrosis factor-α (TNFα) (Taylor et al. 2005) and Interleukin-6 (IL-6) were utilised to measure the concentration of TNFα and IL-6 released from treated and non-treated microglia and CGC cultures. The sandwich ELISA is a methodological upgrade on the standard ELISA technique. In a classical ELISA system, the antigen binds directly to the plate surface allowing for potentially high levels of non-specific binding. The sandwich ELISA combats this by coating the plate with a monoclonal antibody to capture the antigen under investigation, almost completely diminishing non-specific binding (Schuurs & Van Weemen 1977) . The bound antigen can then be traced using a second, usually polyclonal, antigen-specific antibody with a HRP conjugation providing an indirect concentration-dependent signal that can be quantified (**Figure 2.8.1**).

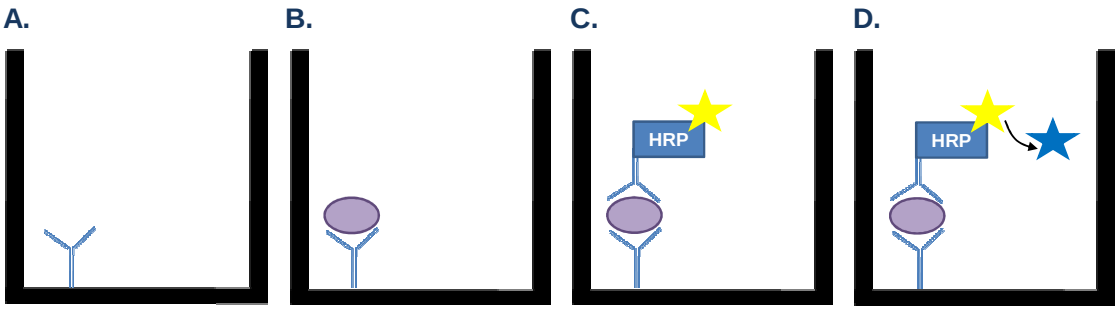

Figure 2.8.1. Graphical representation of an ELISA system

A. Plate wells are coated in an antibody specific for the antigen of interest.

B. Antigen binds to antibody and all other factors are removed.

C. A second HRP-conjugated antibody to the same target is added.

D. The HRP signal is converted to an absorbance signal using a specific solution and read on a plate reader. The absorbance signal is converted to concentration of protein by use of a standard curve (**Figure 2.8.2**).

2.8.1. Sample collection and preparation

Primary microglia or CGC cultures were treated as required. Media was collected from the treated cultures into sterile 1500 µl Eppendorf tubes and placed immediately on ice. Samples were then centrifuged at 800 *g* in an Eppendorf 5415R benchtop centrifuge for 5 minutes at 4℃, to remove any debris present in the collected medium. Samples were then immediately snap frozen on dry ice and stored at -20℃ until required. Sample preparation and storage was performed as quickly as possible to prevent significant degradation of released cytokines, furthermore, samples were used within 1 month of collection.

2.8.2. Tumour necrosis factor-α sandwich ELISA

The assay was performed following the manufacturer's instructions (RTA00, R&D Systems). 96 well plates pre-coated with a monoclonal rat anti-TNFα specific antibody were used. To each well, 50 µl of assay diluent were added. To allow for determination of the concentration in the unknown samples, rat TNFα standards (50 µl) in a concentration range were added to a section of the plate. A TNFα internal kit control (50 µl; a TNFα containing sample that had to fall within a particular concentration

range) was also administered to a section of the plate and 50 µl of the medium samples were added to the final section of the plate. After gentle agitation on an EASIA orbital shaker (Medgenix Diagnostics, Fleurus, Belgium) set to 60 rpm for 1 minute, wells were incubated for 2 hours at room temperature and then washed six times with 1 x wash buffer. A solution (100 µl) containing the second rat anti-TNFα antibody (polyclonal) conjugated to horseradish peroxidise (TNFα conjugate) was then added to the plate and incubated for 2 hours at room temperature. After six washes with 1 x wash buffer, 100 µl of substrate solution was added to the wells for 30 minutes at room temperature in the dark. The substrate solution reacts with the HRP conjugate and provides a luminescent signal. Finally, 100 µl of hydrochloric acid solution (stop solution) was added to each well to terminate the substrate solution colour reaction. The plate was gently shaken at 60 rpm for 1 minute and well-specific optical density was measured with a microplate reader (Anthos htII, Salzburg, Austria) set to 450 nm with the reference filter set to 540 nm to correct for optical imperfections. The plate optical density was measured within 30 minutes of the stop solution reaction termination. The optical density readout in the cell culture medium samples was then converted to a released TNFα concentration using the standard curve produced from the same plate. Examples of typical standard curves are shown in **Figure 2.8.2**. Samples were run in duplicate from three independent experiments to allow for statistical analysis.

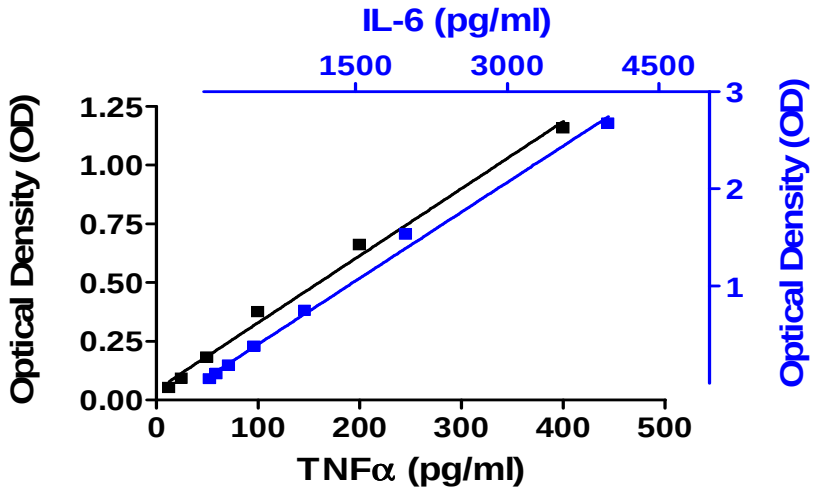

Figure 2.8.2. ELISA system example standard curves

Examples of standard curves generated for TNFα (black) and IL-6 (blue) ELISA assays.

2.8.3. Interleukin-6 sandwich ELISA

The IL-6 ELISAs were again performed following the manufacturer's instructions (R6000B, R&D Systems). The methodology was identical to that provided for the TNFα ELISA, with the all corresponding additions being of the same volume and incubation time.

2.9. Calpain activity assay

During cellular stress, particularly stress of the endoplasmic reticulum, a family of cysteine proteases called calpains are activated (Saido et al. 1994; Nakagawa & Yuan 2000). Calpains are activated by differing calcium concentrations that occur during cellular stress and it has been suggested that m-calpain, a family member activated by millimolar concentrations of calcium, may be responsible for procaspase-12 cleavage to the active form and that disturbances in intracellular calcium storage as a result of amyloid-β peptide cytotoxicity may induce apoptosis through calpain-mediated caspase-12 activation (Nakagawa & Yuan 2000). From these published observations, coupled with the unfortunate loss of calcium imaging equipment, it was decided that an assay to quantify calpain activity could be used to identify not only if these proteases were activated but also whether treatments induce calcium dyshomeostasis.

2.9.1. Optimisation

Initially, the fluorogenic calpain substrate (Suc-Leu-Tyr-AMC) was tested against pure calpain, using methodology previously described (Sun et al. 1999). Calpain II (m-calpain, 5 µg/ml), alone or pre-incubated for 2 h with the calpain antagonist calpastatin (1 nM – 10 µM), was added to 1 ml of assay buffer (50 mM Tris-HCl, 150 mM NaCl, 5 mM $CaCl_2$, 1 mM DTT, and 2 mM Suc-Leu-Tyr-AMC) and incubated for 5 minutes. The reaction was stopped by the addition of 10 mM ethylene glycol tetraacetic acid (EGTA). Aliquots (100 µl) were added to a flat bottomed clear 96-well plate (NUNC) and fluorescence associated with calpain activity due to Suc-Leu-Tyr-AMC binding, was read on a microplate spectrophotometer (GeniOS™, Tecan Group, Reading, UK) with an excitation wavelength of 360 nm and an emission wavelength of 460 nm. Calpain II addition significantly increases activity associated fluorescence when compared with control aliquots (identically treated, minus calpain II addition). Significant inhibition of calpain II-associated fluorescence occurred when calpain II was pre-incubated with at least 1 µM calpastatin (**Figure 4.4.4 A**). Therefore, for experiments involving inhibition of calpain, 1 µM calpastatin will be administered.

To optimise a calpain activity assay using cell lysates, methodology previously published by D'Amelio et al (2011) was modified for use here. This paper utilises a fluorometric assay for quantification of caspase-3 activity using a caspase-3-specific fluorogenic substrate with an AMC-conjugation (D'Amelio et al. 2011). Therefore, the method was simply modified to use a calpain-specific fluorogenic substrate. To test whether the methodology would allow us to identify if significant calcium dyshomeostasis could induce calpain II activation after treatment, assay optimisation was performed with the calcium ionophore, ionomycin, which elevates cytoplasmic calcium concentrations (Pocock & Nicholls 1992). BV2 microglia were plated at a density of 1 x 10^5 and treated after 1 DIV. Cultures were treated with 2 µM ionomycin time dependently (0 – 2 h). Medium was aspirated and cultures were homogenised in assay lysis buffer (100 mM HEPES, 0.1% Chaps (wt/vol), 1 mM EDTA, 10 mM DTT and 1 mM PMSF). Lysis occurred by freezing in liquid nitrogen and thawing at 37℃ three times. Lysates were centrifuged at 11,500 *g* for 5 minutes to pellet debris and the nuclear fraction. The protein concentration of each resulting supernatant was then determined using the Bradford analysis method previously described (**Section 2.7.2**) and an equal mass of protein was incubated with 50 µM Suc-Leu-Tyr-AMC for 1 h at 37℃ for calpain activity determination. Fluorogeni c substrate activity was then read on a microplate spectrophotometer (GeniOS™, Tecan Group, Reading, UK) with an excitation wavelength of 360 nm and an emission wavelength of 460 nm. **Figure 4.4.4 B** shows calpain activity-associated fluorescence is greatest after 30 minutes of ionomycin treatment, therefore this incubation period will be used in future assays as a positive control for calcium-mediated calpain II activity.

Finally, to optimise the signal window, the incubation period of the fluorogenic substrate and the well position of the fluorescence readout were tested. Cultures were treated with ionomycin for 30 minutes and lysed as previously described. Incubation with Suc-Leu-Tyr-AMC was performed at 37℃ for either 1 or 1 6 h, and fluorescence readouts were taken from the bottom and the top of each well. Incubation of the fluorogenic

substrate with the cell lysates for 16 h significantly increased the fluorescent signal. Furthermore, the signal window was at its greatest when the fluorescent readout was taken from the bottom of the well (**Figure 4.4.4 C**). Therefore all subsequent calpain activity assays used a 16 h incubation of the fluorogenic substrate and the fluorescent signal was taken from the bottom of each well.

2.9.2. Optimised protocol

BV2 microglia were plated at a density of 1 x 10^5 in sterile six well plates in BV2 medium and treated. After the required incubation, cultures were lysed in assay lysis buffer (100 mM HEPES, 0.1% Chaps (wt/vol), 1 mM EDTA, 10 mM DTT and 1 mM PMSF). Lysis occurred using a freeze-thaw process with liquid nitrogen and thawing at 37℃ three times. Lysates were centrifuged at 11,500 *g* for 5 minutes and the protein concentration of the resulting supernatant was determined using Bradford analysis as previously described (**Section 2.7.2**). An equal mass of protein (50 µg) was incubated with 50 µM Suc-Leu-Tyr-AMC in assay lysis buffer (final volume of 100 µl) for 16 h at 37℃ in a sterile 96 well plate (NUNC). Relevant plate and fluorescence controls were also performed, i.e. protein lysate alone, Suc-Leu-Tyr-AMC alone, and pure assay lysis buffer. Fluorogenic substrate activity was then read on a microplate spectrophotometer (GeniOS™, Tecan Group, Reading, UK) with an excitation wavelength of 360 nm and an emission wavelength of 460 nm. Data were plotted as a percentage of non-treated control calpain activity, with control levels set at 100% activity.

2.10. Lactate dehydrogenase release assay

The CGC cultures were tested for levels of cell stress after treatment by measurement of lactate dehydrogenase (LDH) activity released into the culture medium using a method essentially as previously described (Kim et al. 2010). LDH is a ubiquitous cytoplasmic oxidoreductase which converts pyruvate to lactate in the presence of reduced nicotinamide adenine dinucleotide (NADH) (**Figure 2.10.1**) (Koh & Choi 1987). LDH activity was measured by monitoring the production of NAD^+ from NADH during the conversion of pyruvate to lactate. Aliquots (50 µl) of cell culture medium were incubated at room temperature with 0.26 mM NADH, 2.87 mM sodium pyruvate, and 100 mM potassium phosphate buffer (pH 7.4) in a total volume of 200 µl. The rate of NAD^+ formation was monitored for 5 min at 2-s intervals at 340 nm using a microplate spectrophotometer (GeniOS™, Tecan Group, Reading, UK). The percentage of LDH released into medium was calculated from three separate preparations as follows: (treatment-induced LDH release into medium/Total LDH in medium after cell lysis with 1% Triton-X) x 100. The concentration of Triton-X used has previously been shown to induce maximal cell lysis in CGCs (Yabe et al. 2001).

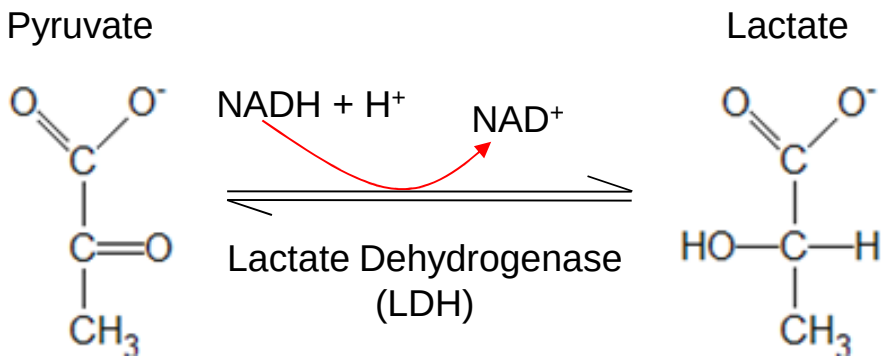

Figure 2.10.1. Lactate dehydrogenase-mediated conversion of pyruvate to lactate

LDH-mediated conversion of pyruvate to lactate, requiring the presence of reduced nicotinamide adenine dinucleotide (NADH)

2.11. Quantification of gene expression by evaluation of mRNA levels using reverse transcription-polymerase chain reaction

Reverse transcription-polymerase chain reaction (RT-PCR) allows for the investigation of gene expression through quantitative analysis of mRNA expression. The method consists of four distinct steps:

1. RNA extraction and isolation from cells or tissue of interest
2. Reverse transcription of all isolated RNA back to complementary DNA (cDNA), also known as transcribed DNA and is performed using an RNA-dependent DNA polymerase enzyme (reverse transcriptase; EC 2.7.7.49).
3. PCR involving the amplification of specific cDNA using oligonucleotide primers complimentary to a section of the cDNA, initiating synthesis. The use of primers designed specifically to compliment base sequence existing only within the cDNA of interest makes the PCR highly specific for the gene of interest.
4. Visualisation of the amplified cDNA produced during the PCR, and comparison between samples. PCR products are run through an agarose gel containing ethidium bromide, a compound that intercalates into DNA and fluoresces under UV light. The densities of the bands correspond directly to the amount of mRNA extracted from the original sample, allowing for quantification of gene expression after treatments or differing conditions.

The invention of the polymerase chain reaction over 23 years by Kary Mullis and Fred Faloona revolutionised the capture and manipulation of DNA. The theory behind PCR is simple and involves cyclical temperature changes optimal for DNA replication. Initially a denaturing or dissociation phase is performed at 92-95℃ depending on the protocol used. As the name suggests, this separates the double stranded cDNA to allow the primer pairs specific for the gene of interest to anneal, also known as the

second phase. Annealing temperatures (T_A) can vary quite substantially and is dependent on the relative cytosine (C)/guanine (G) and adenine (A)/thymine (T) nucleotide content of the primers used and is given by:

$$\mathbf{T_A = T_m - 4℃}$$

Where T_m is the melting temperature, given by:

$$\mathbf{T_m = 4(G+C) + 2(T+A)\ ℃}$$

The final step is the elongation of the cDNA sequence between the primer pairs. This utilises a DNA polymerase (EC 2.7.7.7) from *Thermophilus aquaticus (Taq),* a bacterium first discovered in thermal springs, with the ability to withstand high temperatures, including those used in the initial dissociation phase. The elongation phase is conducted at 72℃, the characterised, opti mum temperature for *Taq* DNA polymerase. A complimentary strand of cDNA is synthesised for each existing strand, therefore, exponential growth of the cDNA of interest occurs after each cycle of dissociation, annealing and elongation. This process is only slowed when consumption of vital reagents has occurred.

2.11.1. Extraction of mRNA

RNase-free consumables were used throughout and surfaces and gloves were frequently sprayed with RNase inhibitor. Extraction was performed using a modified acid guanidinium thiocyanate-phenol-chloroform extraction method (Chomczynski & Sacchi 1987). Medium was aspirated from cells, rinsed with PBS and then lysed into 1 ml Trizol® using a continuous solution aspiration/explusion technique. The Trizol®-containing cell lysate was transferred to autoclaved RNase-free safelock tubes and incubated at room temperature for at least 5 minutes. The nucleic acids were isolated by adding 200 µl of chloroform to each tube and shaking vigorously for 15 seconds followed by incubation at room temperature for a further 3 minutes. The tubes were spun at 11,600 *g* in an Eppendorf 5415R benchtop centrifuge for 15 minutes at 4℃ and the clear upper aqueous phase containing the nucleic acids was transferred into new tubes, taking care not to contaminate with material from the lower phases. RNA

was precipitated from the aqueous phase by the addition of 500 µl of isopropyl alcohol followed by incubation at room temperature for 10 minutes. Precipitated RNA was pelleted by centrifugation at 11,600 *g* for 10 minutes at 4℃. The supernatant was discarded and the pelleted RNA was washed with 1 ml 75% ethanol, vortexed and pelleted after centrifugation at 6200 *g* for 5 minutes at 4℃. The supernatant was removed and the RNA pellet was air-dried before dissolution into an appropriate volume (10-50 µl, dependent on pellet size) of ddH_2O treated with the nuclease inhibitor diethyl pyrocarbonate (DEPC). Tubes were incubated at 70℃ for 10 minutes to aid dissolution. RNA concentration of the resulting solutions was then calculated using absorbance readouts at 260 nm (A_{260}) and at 280 nm (A_{280}) on a Pharmacia Biotech Ultraspec 2000 spectrophotometer. The ratio A_{260} / A_{280} indicates the purity of the RNA, where pure RNA gives a ratio of 2:1, respectively.

The standard equation to calculate the concentration of RNA from the absorption at 260 nm is Beer's law:

$$\mathbf{A_{260} = e\ C\ l}$$

Where $\mathbf{A_{260}}$ is the measured absorption at 260 nm

e is the extinction coefficient (25 µl.µg^{-1}.cm^{-1} for RNA)

C the RNA concentration

and **l** is the pathlength (1 cm)

Rearrangement gives:

$$\mathbf{C = A_{260} / (e\ l) = A_{260} \times 40\ \mu g/ml}$$

However, this is the concentration of the diluted solution and the dilution factor needs to be taken in to account to calculate the sample concentration:

$\mathbf{C_{(sample)} = C_{(measured)}}$ **x dilution factor** (for example: 303/3 = **101**)

For example, if $\mathbf{A_{260} = 0.1}$, **then** $\mathbf{C_{(measured)} = 0.1 \times 40\ \mu g/ml = 4\ \mu g/ml}$

and $\mathbf{C_{(sample)} = 4\ \mu g/ml \times 101 = 404\ \mu g/ml =}$ **<u>0.404 µg/ul</u>.**

2.11.2. Reverse transcription of mRNA

Reverse transcription of RNA was carried out using Superscript® II Reverse Transcriptase (RT) developed from the polymerase (*pol*) gene of Moloney murine leukaemia virus (M-MLV). Reverse transcription of 1 µg of RNA in 10 µl of DEPC-treated ddH_2O was performed. The first reaction consisted of the RNA solution, 1 µl of 0.25 µg/µl oligo$(dT)_{12\text{-}18}$ primer, (the classic primer mix used to prime synthesis of the first strand cDNA by reverse transcriptase using poly A^+ mRNA***** as a template) and 1 µl of 10 mM deoxynucleotide triphosphates (dNTPs; required for elongation of sequence). This reaction was incubated at 65℃ for 5 minutes then immediately quenched on ice. During this incubation a mastermix was prepared containing (per reaction) 4 µl of 5X buffer (supplied with Superscript® II RTase), 2 µl 0.1 M dithiothreitol (DTT; a reducing agent that breaks disulphide bonds disrupting the secondary structure of the RNA, helping to facilitate RT enzyme initiation of reverse transcription), and 40 units/ml (1 µl) of RNaseOUT (a ribonuclease inhibitor). Seven microlitres of the mastermix was added to each reaction and incubated at 42℃ for 2 minutes before final addition of 200 units of Superscript® II RTase (1 µl) for 50 minutes at 42℃. Reactions were terminated by heating to 70 ℃ for 15 minutes. Samples were transferred to ice and stored at -20℃.

2.11.3. Polymerase Chain Reaction

A PCR was run on the product of 0.1 µg reverse transcribed RNA (2 µl). To each sample 48 µl of a PCR mastermix was added, containing: 10 µl 5X Flexi buffer (supplied with the *Taq* polymerase enzyme), 2.5 mM $MgCl_2$ (concentration optimised by previous PhD student), 2.5 µM of forward and reverse primers, 0.2 mM dNTPs, 1.25 units *Taq* DNA polymerase (0.25 µl of 5 units/µl) and DEPC-treated ddH_2O to make up to 48 µl. The reaction consisted of an initial denaturing step at 94℃ for 5 minutes, followed by an optimised number of cycles (see **Table 2.11.1**) of dissociation at 94℃, annealing (calculated and optimised for each primer, see **Table 2.11.1**), and elongation at 72℃. All reactions were terminated after a furt her 7 minute elongation phase at

72℃ through storage at 4℃. To control for human e rror and varying RNA concentrations a house keeper gene, glyceraldehyde 3-phosphate dehydrogenase (GAPDH) was analysed in parallel with the genes of interest.

2.11.4. Agarose gel electrophoresis

After reserve transcription of RNA and PCR, 15 µl of each PCR product was loaded a 1% w/v agarose gel in Tris/borate/EDTA buffer, containing 0.5 µg/ml ethidium bromide. Where possible 10 µl of a Quick-Load® 100 base pair DNA ladder (New England BioLabs) was loaded alongside. The gel was run for approximately 1-2 hours at 80-120 V, dependent on tank size, and then viewed under UV light using a Gel-Pro Imager system. Images were captured using a CoolSNAP-Pro camera and densitometry was subsequent performed using ImageJ software.

Gene Product	**Forward Primer Sequence (5'-3')**	**Reverse Primer Sequence (5'-3')**	**Cycle No.**	**T_A (℃)**
Rat Prothrombin	ATGAGGAGGGCGTGTGGT GCTATGT	CCGTCGATGTAGGATTCC AGGAGCT	35	60
Rat GAPDH	TGGTGCCAAAAGGGTCAT CATCTCC	GCCAGCCCCAGCATCAAA GGTG	35	60
Human iNOS	ACCAGTACGTTTGGCAAT GG	TCAGCATGAAGAGCGATT TCT	30	58
Human TNFα	CAGCCTCTTCTCCTTCCTG AT	GCCAGAGGGCTGATTAGA GA	30	58
Human CHOP	CAGAGCTGGAACCTGAGG AG	TGGATCAGTCTGGAAAAG CA	30	58
Human GAPDH	AGCCACATCGCTCAGACA C	GCCCAATACGACCAAATC C	30	58

Table 2.11.1. Primer sequences and associated PCR cycle number and annealing temperatures

2.12. Statistical Analysis

To directly compare single treatments, two tailed un-paired Student's *t*-tests were performed. If comparisons were to be made between basal or control treatments with other treatments, one way analysis of variance (ANOVA) was used in combination with the Dunnett's post hoc test. Where data are presented as percentages, statistical analyses were performed on the raw data and only transformed post analysis for presentation purposes. Throughout data are presented as mean ± standard error (SEM). Where data were shown to be statistically significant, *p* values of *<0.05, **<0.01 and ***<0.001 were given, non significant data (ns) was shown as *p* >0.05.

3. Initial characterisation of fibrinogen- and fibrin-mediated effects on microglia in different culture systems

3.1. Introduction

In this chapter, initial characterisation of microglia and neuronal cultures after treatment with fibrinogen (FG) and fibrin (FN), *in vitro,* was performed. The induction of death after treatment was investigated to identify whether the protein preparations were toxic. The expression and release of proteins implicated in microglial activation and toxicity were quantified in primary microglial cultures but also neuronal cultures, after treatment. Pharmacological inhibition of particular pathways was also investigated as potential therapeutic interventions, with the role of microglia in any significant observation being prioritised.

3.1.1. Microglia activation, *in vitro*

Whether *in vitro* models of any sort can truly mimic an *in vivo*, physiological setting is an area of intense debate. Microglia in culture have been shown to be more sensitive than *in situ* and it can be easily perceived that without down-regulatory signals from other neural cells, changes in homeostasis *in vitro*, e.g. treatment, are likely to cause microglial activation. However, numerous studies have shown this not to be the case (Taylor et al. 2005; Ifuku et al. 2007; Klintworth et al. 2009; Maezawa et al. 2011). Differences in 'resting' microglial morphology *in vitro* when compared with histological slices, including an increase in microglia presenting amoeboid/activated characteristics rather than the classical ramified morphology, suggest that activation observed after treatment could be attributed, at least in part, to the un-physiological setting the cells find themselves in. However, neuronal morphology *in vitro* can also be dissimilar to the morphology observed *in vivo* but the cultures display similar physiology to that observed in situ suggesting that evolutionarily conserved signalling pathways in microglia may not dramatically change when the cell is isolated. Furthermore, initial *in vitro* experimentation to discover parallelism with the *in vivo* setting can save vast

amounts of money and studies that pursue the identification of factors required to down-regulate microglia will only add to the usefulness of *in vitro* culturing. These points coupled with the fact that many cellular and molecular responses induced after microglial activation by pathogens or protein aggregates associated with disease, at present, are not accessible *in vivo*, makes *in vitro* modelling an extremely useful tool.

3.1.2. Activation of microglia by blood-borne proteins

Disorders involving blood brain barrier dysfunction allow infiltration of blood-borne proteins into the CNS parenchyma providing potential for microglia interaction. Previous studies have identified microglial activation in the presence of albumin (Hooper et al. 2009b), fibrinogen (Adams et al. 2007a; Paul et al. 2007), and thrombin (Möller et al. 2000; Choi et al. 2003), although, more recently, certain thrombin-mediated activation factors, including cytokine release, have been attributed to unknown high molecular weight contaminants in the protein preparations (Hanisch et al. 2004; Möller et al. 2006).

It is hypothesised that microglia are primarily activated to clear or phagocytose the infiltrating proteins, but the chronic presence of these proteins causes hyperactivity and the release of factors at concentrations great enough to induce toxicity, not only in surrounding neural cells but also in an autocrine fashion. This thesis focuses on fibrinogen and the insoluble matrix, fibrin that is deposited during proteolytic cleavage by thrombin (Adams et al. 2004). Previous studies have identified receptors on microglia (Adams et al. 2007a) and neurons (Schachtrup et al. 2007), that interact with fibrinogen, in an immobilised form, to induce a phagocytic microglia phenotype and inhibit neurite outgrowth, respectively. Adams et colleagues (2007a) failed to show effects with soluble fibrinogen, however other studies have identified significant macrophage activation, including cytokine release, after treatment with the soluble form of the protein (Kajikawa et al. 1986; Hodgkinson et al. 2008). The initial characterisation of primary microglia after fibrinogen and fibrin treatment supports activity with both soluble and insoluble forms of the protein, with the observation of

differential toxicity. A non-apoptotic induction of caspases was also observed, supporting new literature suggesting caspase-3, -7 and -8 is primarily involved in microglia activation after LPS treatment rather than apoptosis (Burguillos et al. 2011).

3.1.3. Modelling microglia activation in neuronal cultures

As previously stated, pure *in vitro* cultures of primary microglia are useful tools for elucidating signalling pathways, however models that allow manipulation of microglial responses in a more physiological setting, i.e. in the presence of other cell types, are more attractive. Characterisation of cerebellar granule cultures (**Section 2.5**) identified the presence of glia including microglia, at a density similar to that observed in situ (~ 12%). This provided an ideal preparation to model microglial involvement in fibrinogen- and fibrin-mediated toxicity in a more physiological environment. Previous observations showing that the presence of contaminating microglia in astrocyte cultures are responsible for iNOS expression after LPS treatment (Saura 2007) suggests that the population identified in the neuronal cultures used here could also mediate inflammatory responses. Modification and optimisation of a protocol to specifically deplete microglia (Hamby et al. 2006) from the neuronal cultures (**Section 2.5.2**) allowed the study of the involvement of microglia in fibrinogen and fibrin mediated responses. These studies were then compared with studies involving the administration of microglial-conditioned medium to neuronal cultures initially depleted of microglia to identify whether responses were due to released soluble factors from microglia or cell-cell contact.

3.2. Effects of direct exposure of primary microglial cultures to fibrinogen and fibrin

To assess any obvious morphological changes in the primary microglial cultures after treatment with FG or FN, immunocytochemistry (ICC) with IB_4 was performed. Treatment of cultures with FG or FN for 24 hours did not significantly increase the percentage of pyknotic and condensed nuclei, a classic morphological hallmark of cells undergoing apoptosis, when compared with control (CTR; **Figure 3.2.1**). Conversely, this morphological change was shown to be significantly increased in cultures treated with staurosporine (STS), when compared with control levels. Cultures treated with FN showed a significant increase in the percentage of enlarged nuclei, a hallmark for necrotic cell death, when compared with CTR. However, treatment with FG or the classical microglial activator, lipopolysaccharide (LPS) did not replicate these findings, suggesting differential effects of these treatments when compared with FN (**Figure 3.2.1**).

The MAC-1 integrin receptor (CD11b) is a marker of microglial activation and expression has been shown to be upregulated in AD brains (Akiyama & McGeer 1990). This receptor has also been shown to mediate FG-induced phagocytic activity, *in vitro* (Adams et al. 2007a). Here it is shown that treatment of primary microglial cultures with FG or FN for 24 hours significantly increases the microglial expression of CD11b, to a level similar, or in the case of FG, greater, than the increase observed after LPS treatment (**Figure 3.2.2 A**). This was quantified for statistical analysis by calculating fluorescence intensity/cell in each field with ImageJ software (NIH, USA) and plotted as an arbitrary fluorescence unit (AFU) (**Figure 3.2.2 B**).

Figure 3.2.1

A.

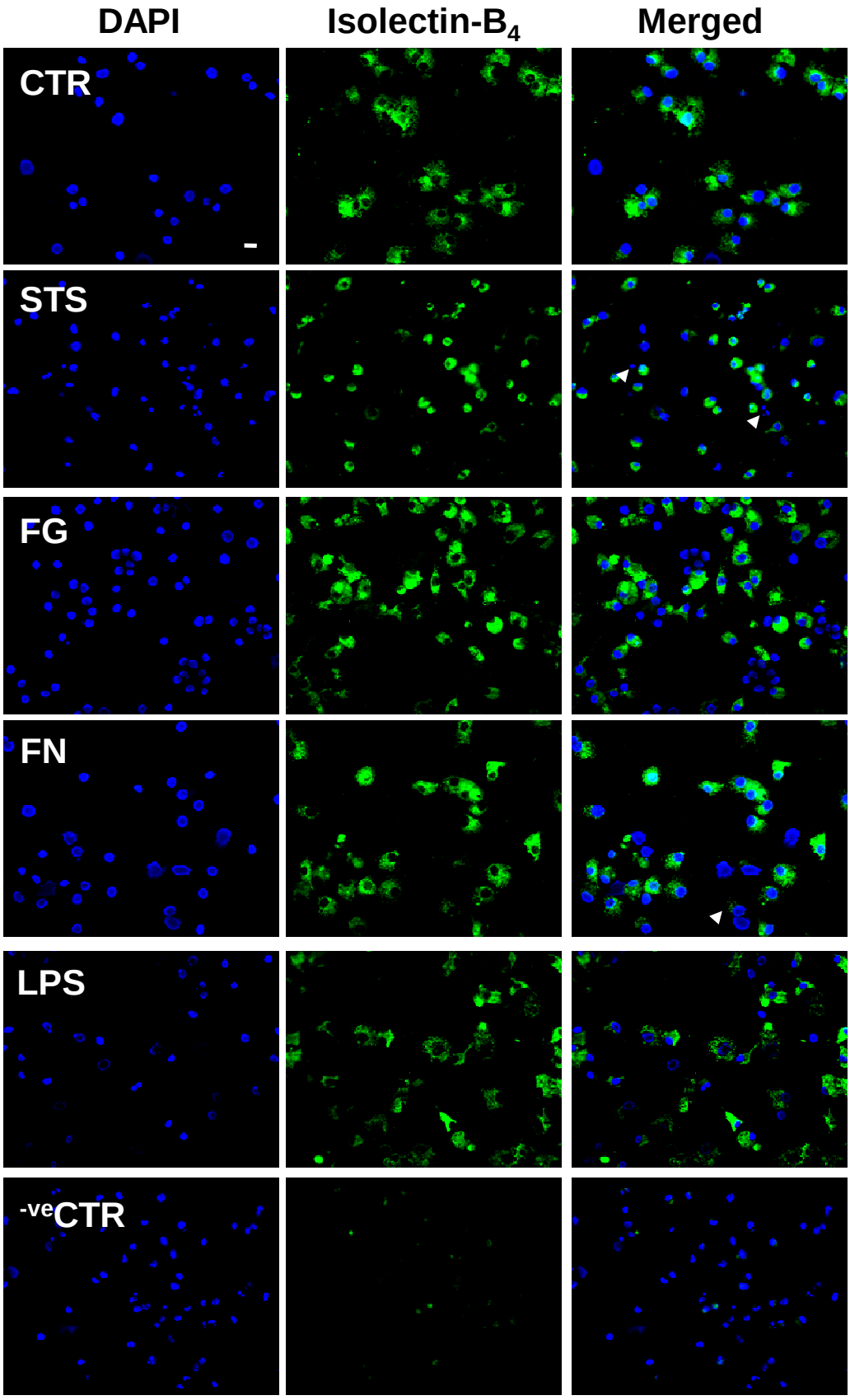

Figure 3.2.1

B.

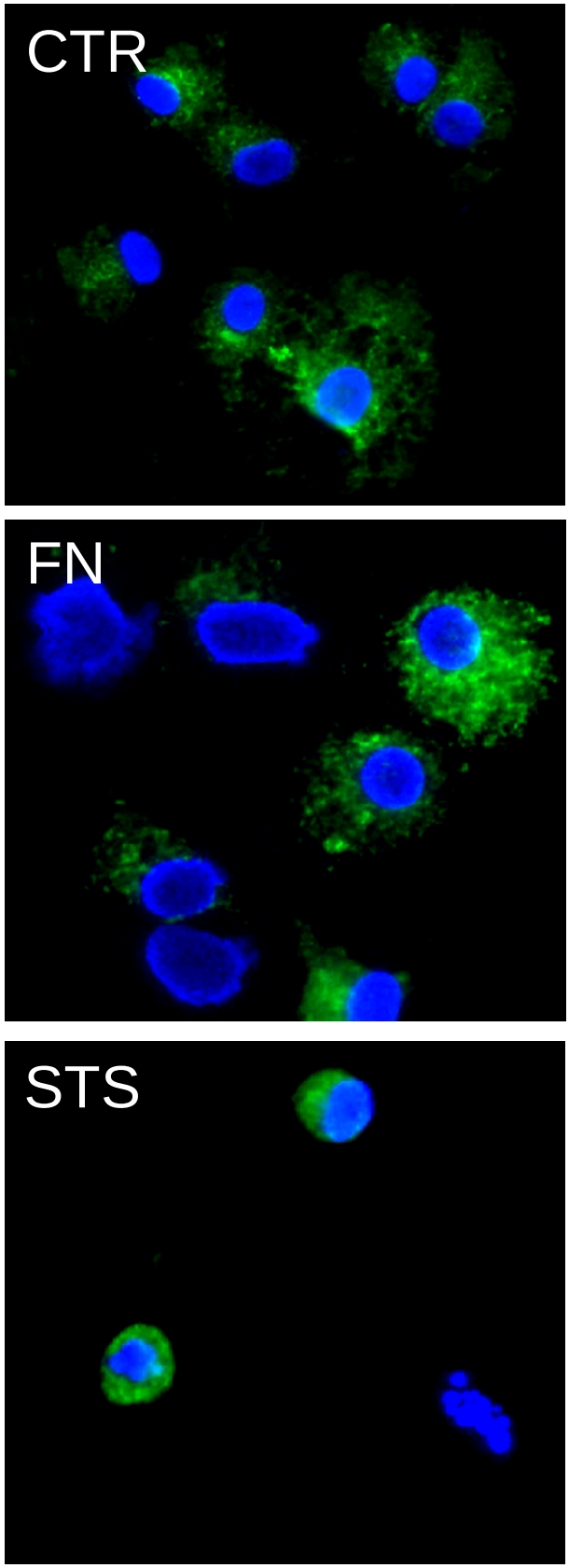

C.

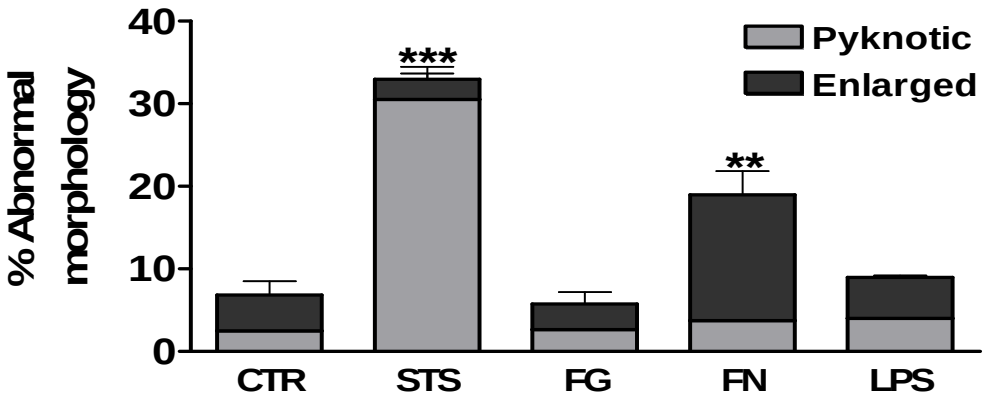

Figure 3.2.1. FN but not FG induces cytotoxic changes in microglia

A. Representative images of microglial cultures after treatment with STS (0.5 µM) for 4 hours, or FG (2.5 mg/ml), FN (1 mg/ml) or LPS (1 µg/ml) for 24 hours. Cultures were stained with DAPI for quantification of changes in nuclear morphology and Isolectin-B_4 for microglial identification (Streit 1990), except in negative control cultures. Original magnification: x40, scale bar: 10 µm. **B.** Sample sections of fields of particular interest at higher resolution, including CTR cultures, and FN- or STS-treated cultures, with the latter two showing microglial necrosis and apoptosis, respectively. **C.** Quantification of apoptotic and necrotic nuclear morphology in microglial cultures after administration of treatments given above. Data are presented as the mean ± SEM. Treatments were in duplicate in each experiment and data were analysed from 3 independent experiments. Paired two-tailed Student's *t*-tests were performed between control and each treatment. Levels of significance were: non-significant $p>0.05$, ** $p<0.01$, *** $p<0.001$.

Figure 3.2.2

A.

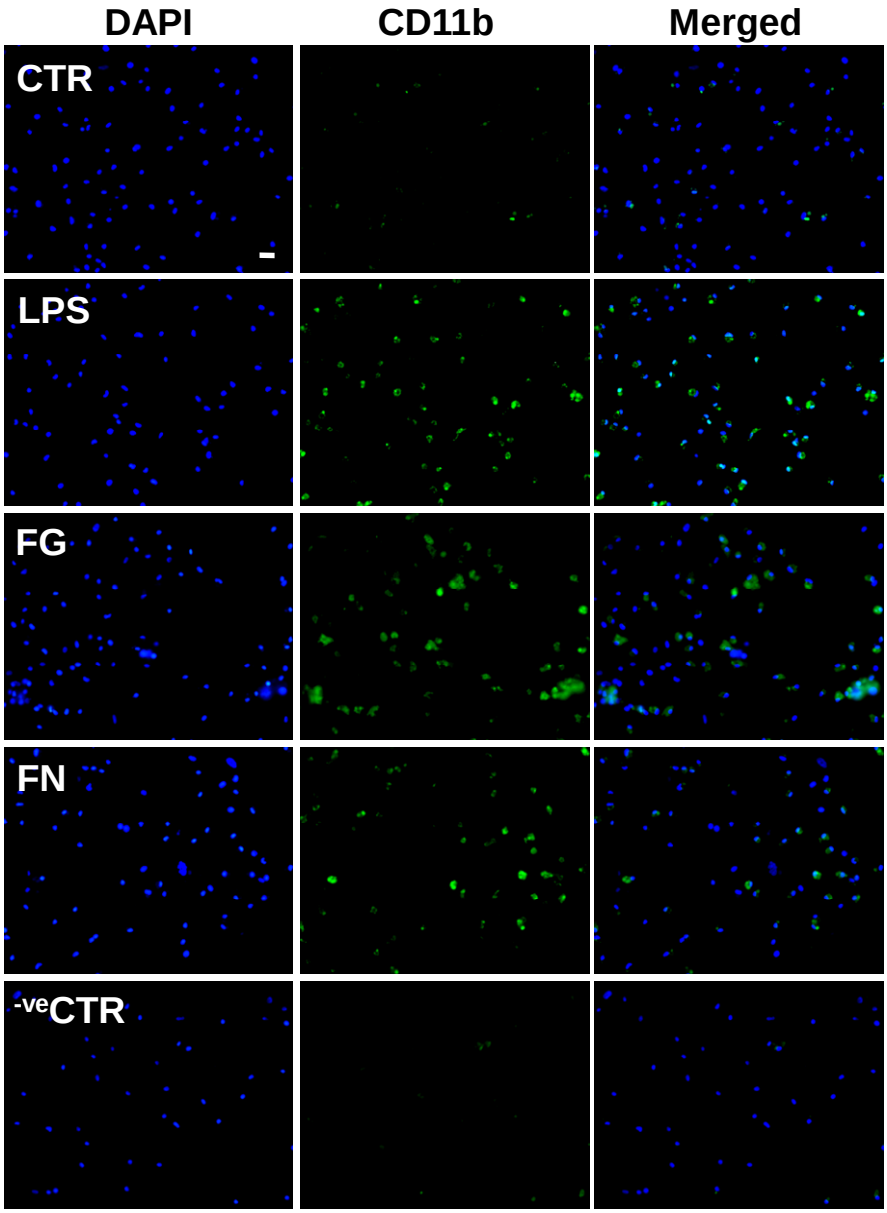

B.

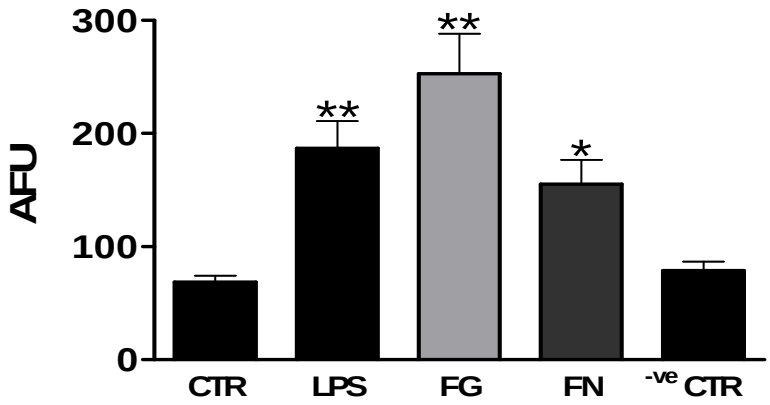

Figure 3.2.2. FG and FN induce significant expression of CD11b

A. Representative images of primary microglial cultures after treatment with FG (2.5 mg/ml), FN (1 mg/ml) or LPS (1 µg/ml) for 24 hours. Cultures were stained with DAPI for quantification of cell number and probed with anti-CD11b (green) for identification of microglial activation state, except in negative control cultures, where anti-CD11b was omitted. Original magnification: x20, scale bar: 30 µm. **B.** Quantification of relative fluorescence intensity/cell in microglial cultures after administration of the treatments stated above. Data are presented in arbitrary fluorescence units (AFU). Treatments were in duplicate in each experiment and data were analysed from 3 independent experiments. Paired two-tailed Student's *t*-tests were performed between control and each treatment. Levels of significance were: non-significant $p>0.05$, * $p<0.05$, ** $p<0.01$.

3.2.1. Fibrinogen and fibrin treatment causes TNFα release from microglia

Activation of microglia can cause significant release of pro-inflammatory cytokines, which are able to induce upregulation of pro-apoptotic factors in surrounding cells as well as the host cell (Kingham et al. 1999; Nguyen et al. 2002; Taylor et al. 2005). Treatment of primary microglial cultures with FG or FN significantly induced TNFα release, a classical pro-inflammatory cytokine. Treatment with the positive control, LPS, for 8 hours induced a highly significant increase in release, compared with non-treated control cultures (CTR). This was followed by a significant drop in release after 16 hours, when compared with levels of release after 8 hours. After 16 hours of LPS treatment, TNFα release rose significantly until 48 hours, the final time-point assayed, with no plateau (**Figure 3.2.3 A**). FN treatment induced an earlier significant rise in release in comparison to LPS-treated cultures. This was followed by a plateau until 16 hours from where a steady significant increase in release was observed until 48 hours exposure, following a similar profile to that observed in LPS-treated cultures. FG treatment however, showed a different profile of TNFα release. Significant release was still observed after 8 hours of treatment. However, unlike LPS and FN treatment, release peaked at 24 hours, when compared with control levels, followed by a significant drop in TNFα release by 48 hours, when compared with levels of release after 24 hours (**Figure 3.2.3 A**). Furthermore, the FG- and FN-mediated TNFα release was concentration dependent at both 24 and 48 hours (**Figure 3.2.3 B and C**).

Due to the observation that LPS or FN-induced TNFα release profiles were similar, it was questioned whether endotoxin contamination of FN was an issue. Previously it has been reported that only 40 pg/ml (or 0.4 EU/ml; 10EU/ng) of endotoxin is required to induce microglial proliferation, NO production and cytokine release (Weinstein et al. 2008). Therefore, cultures were pre-treated with polymyxin B (PMX), an antibiotic that binds to the biologically active portion of the endotoxin-(LPS)-macromolecule known as lipid A (Morrison & Jacobs 1976) and potently abolishes LPS responses (Jacobs & Morrison 1977). PMX (100 nM) pre-treatment significantly attenuated LPS-mediated

TNFα release after 24 hours but did not affect FG- or FN-mediated release suggesting insignificant or no LPS contamination in the protein preparations used here (**Figure 3.2.4**). Finally, to control against false-positive ELISA readouts, cultures were pre-treated with thalidomide, a potent inhibitor of TNFα synthesis (Lopez-Talavera et al. 1996). Inhibition of TNFα synthesis significantly attenuated the LPS-mediated TNFα release. Also, thalidomide pre-treatment significantly attenuated FG- and FN-mediated TNFα release (**Figure 3.2.4**).

In an attempt to further elucidate pathway factors upstream of TNFα release after FG exposure, ELISAs were performed after pre-treatment with Mitogen-activated protein kinase (MAPK) inhibitors. LPS-mediated TNFα release from microglia is dependent on activation of the p38-MAPK pathway (Nakajima et al. 2004). In addition the phosphoinositide 3-kinase (PI3K) pathway has been shown to be involved in microglial-mediated neurotoxicity after Aβ treatment (Zhang et al. 2011). Both pathways were pharmacologically inhibited to identify possible involvement in FG-mediated TNFα release. Pre-treatment of microglia with the potent, cell permeable, specific inhibitor of p38-MAPK, SB203580 (10 µM; the EC_{50} value), significantly decreased FG-mediated TNFα release after 24 hours by approximately 50% (**Figure 3.2.5**), suggesting FG-mediated TNFα release is dependent on the p38-MAPK pathway. Conversely, the PI3K pathway was not involved in FG-mediated TNFα release since inhibition of the PI3K pathway with wortmannin (100 nM), a highly selective and potent inhibitor, did not attenuate the FG-mediated TNFα release (**Figure 3.2.5**).

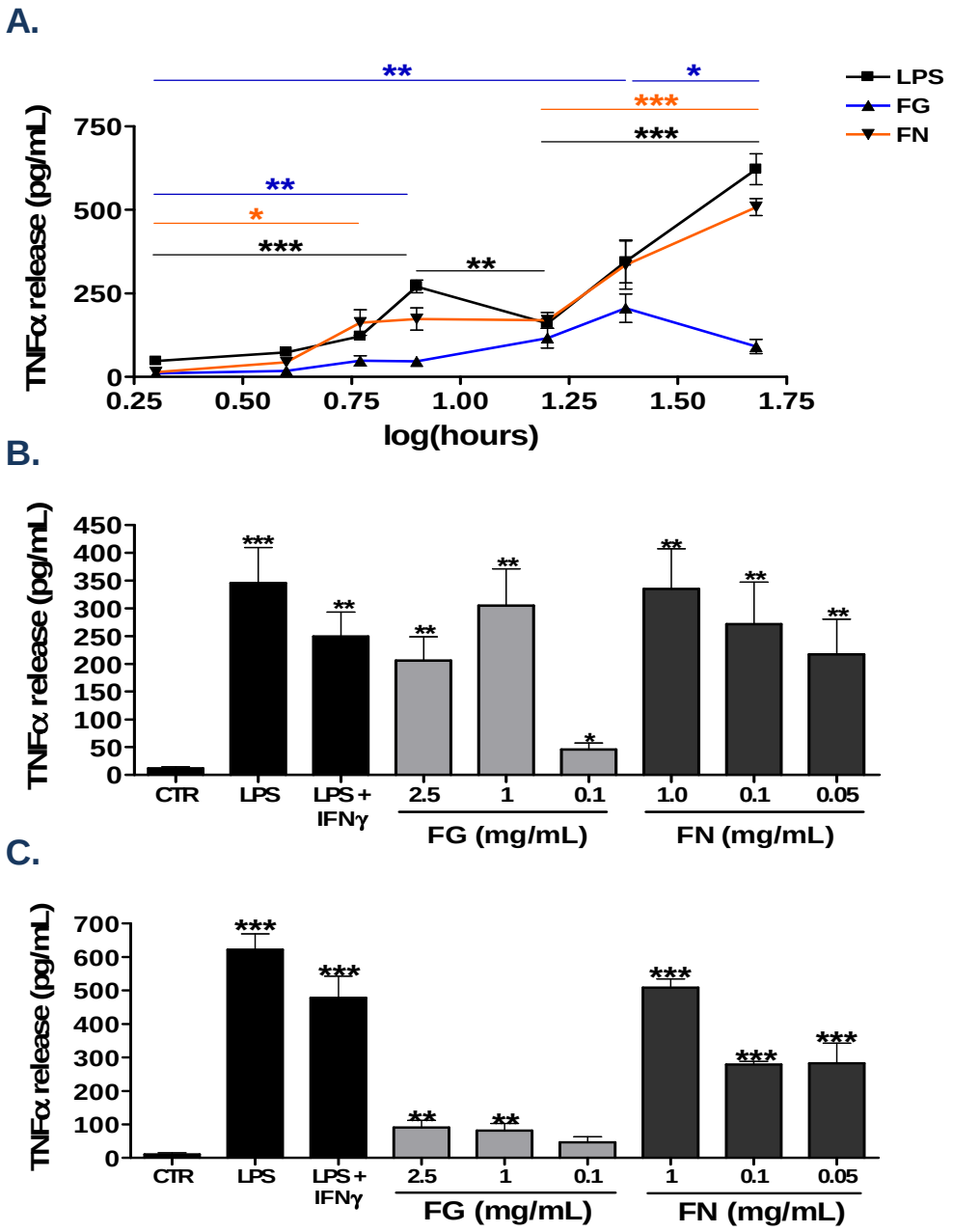

Figure 3.2.3. FG and FN induce significant TNFα release from microglia

A. Log timecourse analysis of TNFα release using an ELISA system after treatment of primary microglia with FG (2.5 mg/ml), FN (1 mg/ml) or LPS (1 µg/ml). **B.** Analysis of TNFα release after treatment for 24 hours with FG (0.1-2.5 mg/ml), FN (0.05-1 mg/ml), LPS (1 µg/ml) or LPS and IFNγ (100U/ml). **C.** Analysis of TNFα release after treatment for 48 hours with FG (0.1-2.5 mg/ml), FN (0.05-1 mg/ml), LPS (1 µg/ml) or LPS and IFNγ (100U/ml). Treatments were in duplicate in each experiment and data were analysed from 3 independent experiments. For timecourse analysis, paired two-tailed Student's *t*-tests were performed between specific time-points as indicated by coloured lines. In concentration dependent studies a one-way analysis of variance (ANOVA) was performed with Dunnett's post-test. Levels of significance were: non-significant $p>0.05$, * $p<0.05$, ** $p<0.01$, *** $p<0.001$.

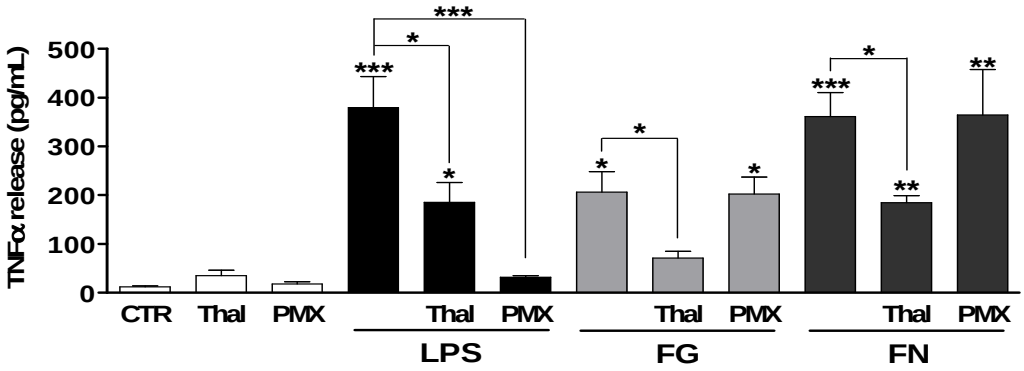

Figure 3.2.4. FG- and FN-mediated TNFα release was not due to endotoxin contamination

Analysis of TNFα release was performed using an ELISA system after treatment of primary microglia cultures for 24 hours with FG (2.5 mg/ml), FN (1 mg/ml) or LPS (1 µg/ml), co-treated with either thalidomide (Thal; 10 µg/ml) or polymyxin-B (PMX; 100 nM). Treatments were in duplicate in each experiment and data were analysed from 3 independent experiments. To compare induction of TNFα release in multiple treatments with control levels a one way ANOVA was performed with Dunnett's post-test. Direct comparison of specific treatments was analysed using paired two-tailed Student's *t*-tests. Levels of significance were: non-significant $p>0.05$, * $p<0.05$, ** $p<0.01$, *** $p<0.001$.

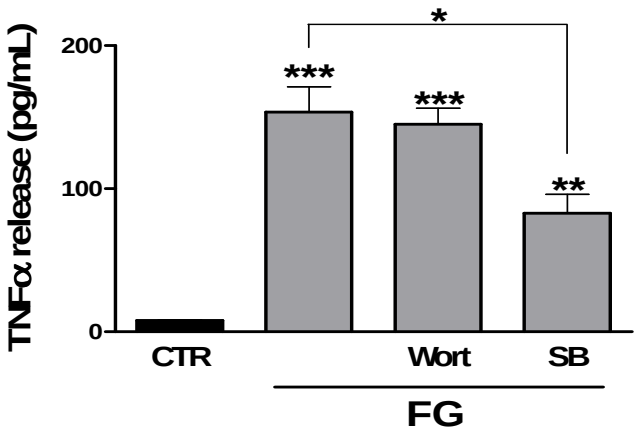

Figure 3.2.5. FG-mediated TNFα release was dependent on p38-MAPK pathway activation

Analysis of TNFα release was performed using an ELISA system after treatment of primary microglia cultures for 24 hours with FG (2.5 mg/ml) and co-treated with either wortmannin (Wort; 100 nM) or SB203580 (SB; 10 µM). Treatments were in duplicate in each experiment and data were analysed from 3 independent experiments. To compare induction of TNFα release in multiple treatment groups with control levels a one way ANOVA was performed with Dunnett's post-test. Direct comparison of specific treatments was analysed using paired two-tailed Student's *t*-tests. Levels of significance were: non-significant $p>0.05$, * $p<0.05$, ** $p<0.01$, *** $p<0.001$.

3.2.2. Differential iNOS expression is observed in microglia after treatment with fibrinogen or fibrin

To further assess microglial reactivity in the presence of FG or FN, iNOS expression was assayed using ICC. The expression of iNOS is a classic marker of activated microglia (Ferretti et al. 2011). These experiments were again performed in the presence of PMX, to control for endotoxin contamination. In serum-free conditions FG and FN treatment for 24 hours significantly induced expression of iNOS to a level similar to that observed after LPS treatment for 24 hours, when compared with control levels. PMX pre-treatment of FG- and FN-treated cultures had no significant effect on the percentage of microglia presenting iNOS expression, however LPS-mediated expression was significantly inhibited (**Figure 3.2.6**).

Interestingly, when iNOS expression was quantified in primary microglia cultured and treated in medium that still contained serum, FG-induced expression disappeared. Expression of ED-1 however, a classical marker of activated/phagocytic microglia, was still significantly higher than observed in control cultures. This suggests that although iNOS expression was lost, the FG-treated cells were still activated in an iNOS-independent fashion (**Figure 3.2.7**). Furthermore this serum-masking effect caused no significant difference to the iNOS expression in FN- or LPS-treated cultures, with significant expression above control levels being observed (**Figure 3.2.7**).

A.

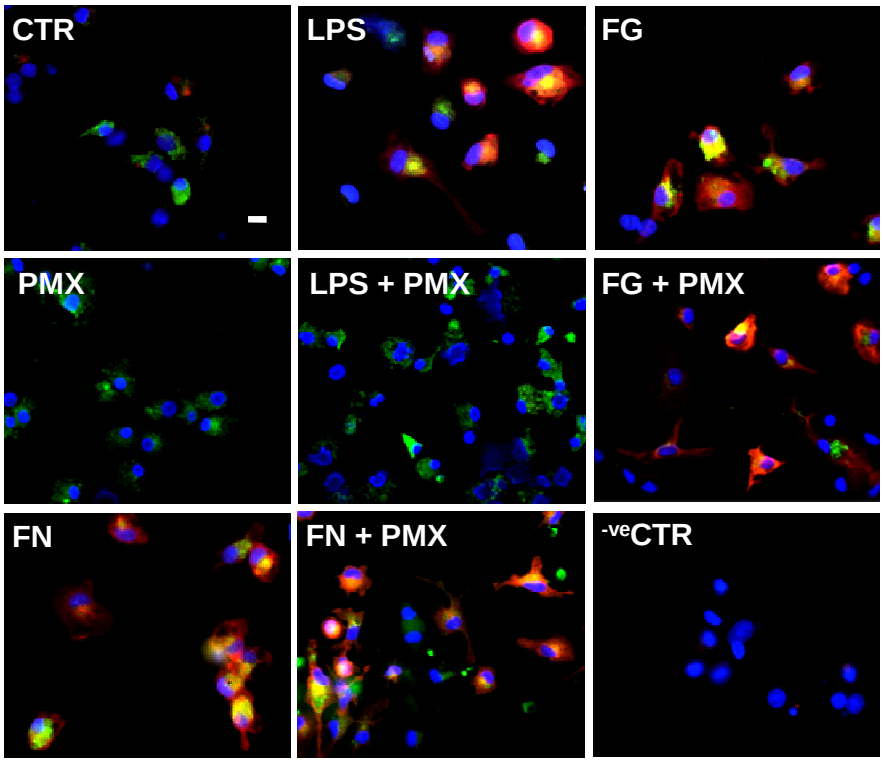

B.

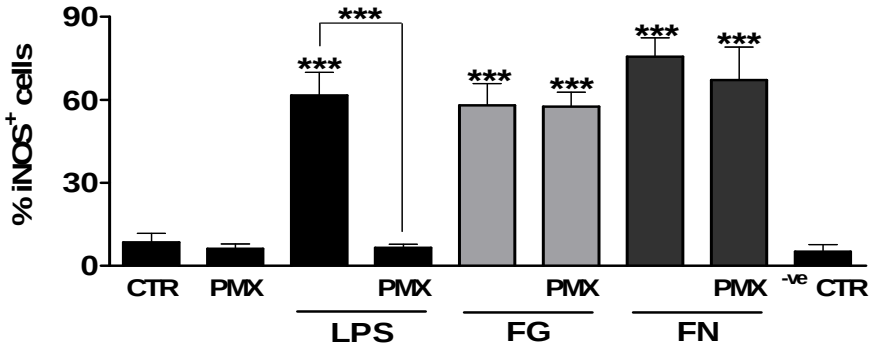

Figure 3.2.6. FG and FN induced microglial iNOS expression in serum-free conditions

A. Representative images from serum-free microglial cultures after 24 hours of treatment with FG (2.5 mg/ml), FN (1 mg/ml) or LPS (1 µg/ml), and co-treatment with PMX (100 nM). Cultures were co-stained with DAPI for quantification of cell number, and probed with anti-ED1 (green) for identification of activated microglia and anti-iNOS (red), except in negative control cultures, where primary antibodies were omitted. Original magnification: x40, scale bar: 10 µm. **B.** Quantification of $iNOS^+$ microglia after administration of treatments given above. Data are presented as a percentage of total microglial number. Treatments were in duplicate in each experiment and data were analysed from 3 independent experiments. To compare the expression of iNOS in multiple treatment groups with control levels a one way ANOVA was performed with Dunnett's post-test. Direct comparison of specific treatments was analysed using paired two-tailed Student's *t*-tests. Levels of significance were: non-significant $p>0.05$, * $p<0.05$, ** $p<0.01$, *** $p<0.001$.

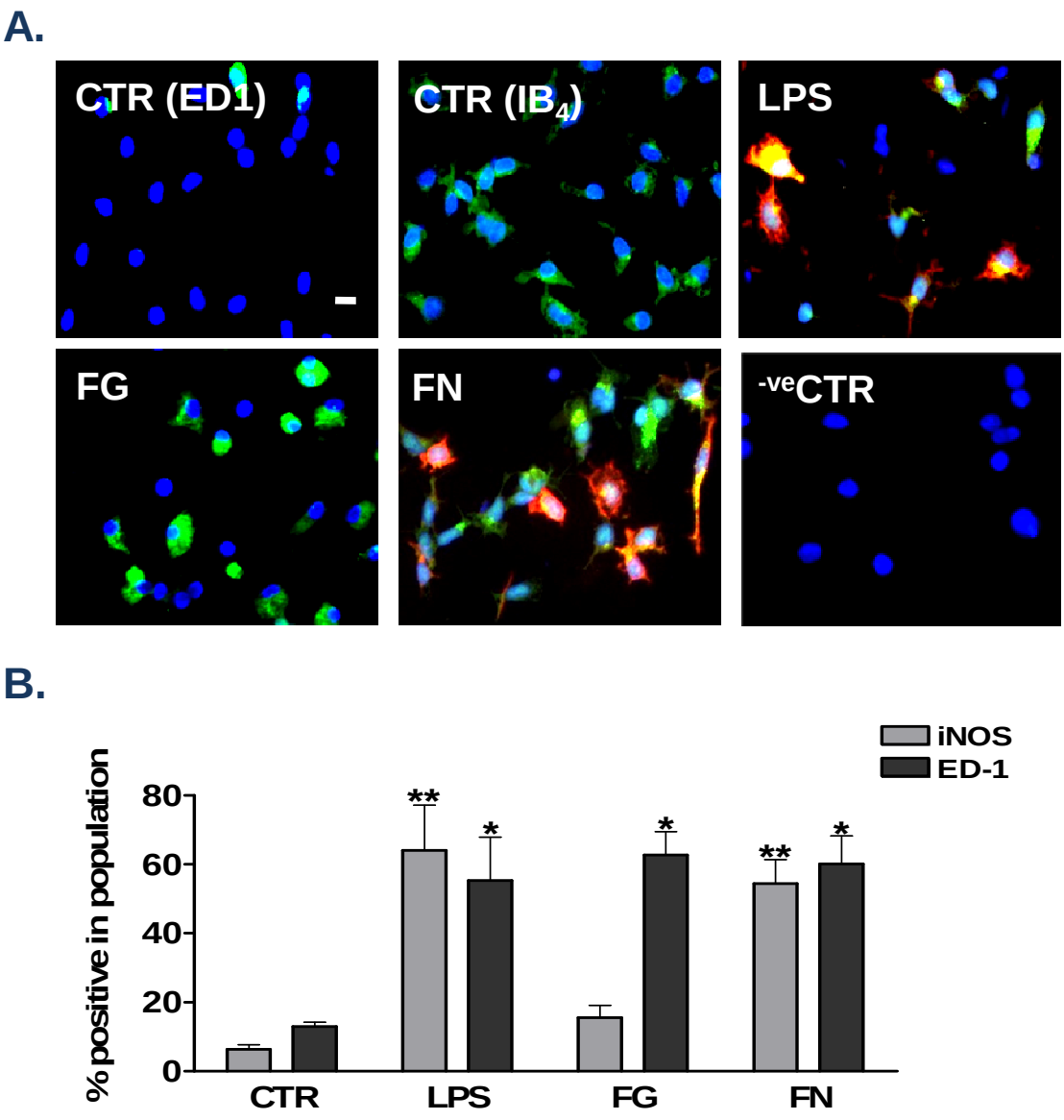

Figure 3.2.7. FN but not FG induced microglial iNOS expression in serum-containing conditions

A. Representative images of serum-containing primary microglial cultures after 24 hours of treatment with FG (2.5 mg/ml), FN (1 mg/ml) or LPS (1 µg/ml). Cultures were co-stained with DAPI for quantification of cell number, and probed with anti-ED1 (green) for identification of activated microglia and anti-iNOS (red), except in negative control cultures, where primary antibodies were omitted. Some non-treated controls were stained with isolectin-B_4 (IB_4, green; Streit 1990) to identify culture purity. Original magnification: x40, scale bar: 10 µm. **B.** Quantification of $iNOS^+$ and $ED1^+$ microglia after administration of treatments stated above. Data are presented as a percentage of total microglial number. Treatments were in duplicate in each experiment and data were analysed from 3 independent experiments. To compare the expression of iNOS or ED1 in multiple treatment groups to control levels a one way ANOVA was performed with Dunnett's post-test. Levels of significance were: non-significant $p>0.05$, * $p<0.05$, ** $p<0.01$.

3.2.3. A non-apoptotic expression of cleaved caspase-3 after fibrinogen treatment of microglia

To further support the initial finding that treatment with FG or FN did not induce significant or observable apoptosis, ICC targeting the expression of the cleaved form of the classic apoptotic executioner caspase, caspase-3, was performed (**Figure 3.2.8**). As expected, treatment of cultures with STS for 8 hours induced significant expression of the cleaved form of caspase-3, when compared with control levels. However, treatment of cultures for 24 hours with LPS also induced significant cleavage of caspase-3, when compared with that in control cultures. This was unexpected as previous findings (**Figure 3.2.1**) suggested that LPS treatment did not induce significant apoptosis in primary cultures, again replicated in this experiment. Similarly, treatment with FG or FN for 24 hours significantly induced caspase-3 cleavage, when compared with control levels, and in the case of FG-treatment, no significant apoptotic cell death was seen, when compared with control, which again supported previous findings (**Figure 3.2.8 B**). Significant death was observed FN-treated cultures, which also supported previous findings. Certainly, in the case of FG or LPS, these data suggest that treatment can induce cleavage of caspase-3 in a non-apoptotic role.

Figure 3.2.8

A.

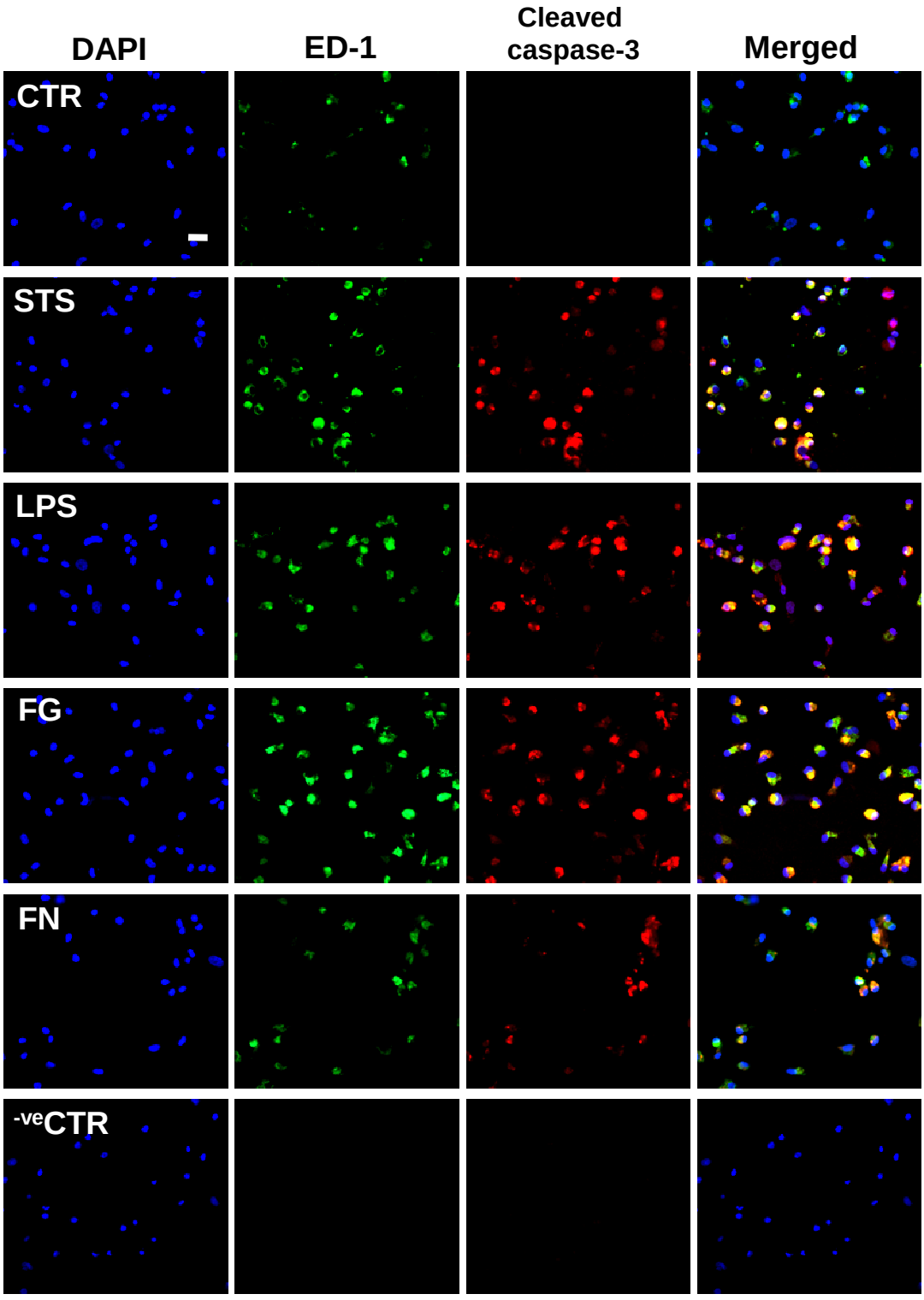

B.

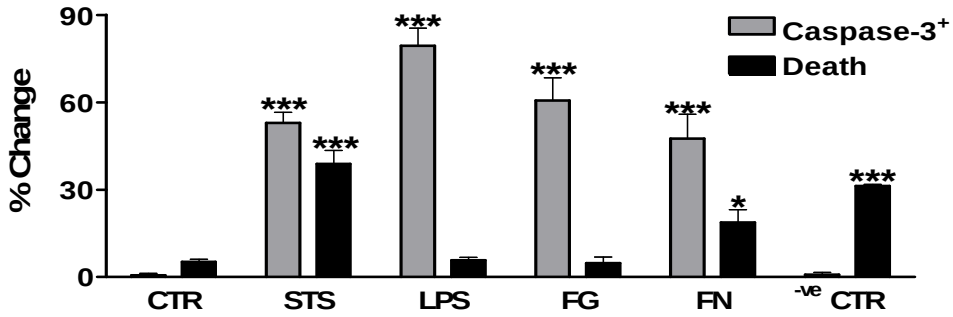

Figure 3.2.8. FG induces microglial cleaved caspase-3 expression, independent of death

A. Representative images of primary microglial cultures after STS treatment (0.5 µM; 4 hours) or 24 hours of treatment with FG (2.5 mg/ml), FN (1 mg/ml) or LPS (1 µg/ml). Cultures were co-stained with DAPI for quantification of cell number, and probed with anti-ED1 (green) for identification of activated microglia and anti-cleaved caspase-3 (red), except in negative control cultures, where cultures were treated with STS and primary antibodies were omitted. Original magnification: x40, scale bar: 30 µm. **B.** Quantification of apoptotic/necrotic (death) morphology and cleaved caspase-3^+ microglia after administration of treatments given above. Data are presented as a percentage of total microglial number. Treatments were in duplicate in each experiment and data were analysed from 3 independent experiments. To compare % death or expression of cleaved caspase-3 in multiple treatment groups to control levels a one way ANOVA was performed with Dunnett's post-test. Levels of significance were: non-significant $p>0.05$, * $p<0.05$, *** $p<0.001$.

3.3. Effects of direct exposure of enriched cerebellar granule cell cultures to fibrinogen and fibrin

3.3.1. Characterisation of fibrinogen- and fibrin-mediated death

To ascertain whether exposure of enriched cerebellar granule cultures (CGCs) to FG or FN caused any significant apoptosis, cultures were treated with either FG or FN for 24 and 48 hours, fixed and stained with Hoechst-33342. The cultures were then observed under a fluorescence microscope and cells with classic apoptotic morphology, i.e. pyknotic nuclei showing chromatin condensation, and membrane blebbing (Kerr et al. 1972) were quantified against total cell number/field. Staurosporine (STS) treatment for 8 hours was used as a positive control, and as expected, caused a significant increase in the number of cells displaying apoptotic nuclear morphology (**Figure 3.3.1 Ai & Aii**). Interestingly, treatment with FG induced a significant increase in cell nuclei displaying apoptotic morphology after 24 hours, but FN-treatment for the same time period did not, similar to that seen after LPS treatment (**Figure 3.3.1 B & D**). However, after cultures were exposed to LPS for 48 hours significant apoptotic morphology was observed. The same observation was made after FG and FN exposure for 48 hours (**Figure 3.3.1 B & D**). LPS induces its neurotoxicity primarily through activation of microglia, with a positive correlation being observed between abundance of microglia and sensitivity to LPS-induced neurotoxicity (Kim et al. 2000). Therefore, it is likely that contaminating microglia present in these enriched neuronal cultures are responsible for the significant increase in LPS-mediated neuronal death after 48 hours.

Exposure of cell cultures to charged proteins with a high molecular weight, such as FG can cause nuclear shrinkage due to alteration of the osmotic equilibrium. Administration of such a protein produces a hypertonic ‘extracellular’ culture medium that causes water diffusion down the gradient, in this case, intracellular to extracellular, causing cell shrinkage (Horie et al. 1989). Therefore, administration of proteins like FG could appear to induce apoptosis if quantification depended solely on morphological changes. Therefore, to provide support for the morphological quantification of

apoptosis, live cell staining using an Annexin V-FITC conjugate was performed (**Figure 3.3.1 C**). Similar to the Hoechst-33342 apoptotic morphology findings significant Annexin V-FITC staining was observed after 24 hours treatment with FG and 48 hours after both FG and FN treatment, comparable to treatment of CGCs with STS for 8 hours, supporting the original data from Hoechst-33342 quantification (**Figure 3.3.1 C & D**).

Further support for FG- and FN-mediated neuronal apoptosis was provided with ICC for cleaved caspase-3 expression and live cell staining for caspase-3/7 activation in CGCs (**Figures 3.3.2 & 3.3.3**). As expected, treatment with STS for 8 hours significantly induced cleavage of caspase-3 in ICC (**Figure 3.3.2**) and caspase-3/7 in live cell staining experiments, shown by the significant increase in FAM-DEVD-FMK fluorescence, quantified using Image J (**Figures 3.3.3 A & B**). Treatment with FG for 24 hours and FN and LPS for 48 hours also significantly increased the cleavage of caspase-3 in ICC experiments that was associated with NeuN staining, suggesting the apoptotic cells were neuronal (**Figure 3.3.2**). Live cell staining for caspase-3/7 cleavage after the same treatments was also significantly enhanced further supporting the hypothesis that these protein preparations can induce neuronal toxicity and apoptosis (**Figure 3.3.3 A & B**).

A lactate dehydrogenase (LDH) assay was also performed for biochemical analysis of cellular integrity. As cell death and toxicity can be evaluated by quantification of plasma membrane damage, the use of an assay to assess the level of damage can be extremely informative. The LDH assay is one of the most commonly used forms of membrane damage quantification assay due to LDH being present in relatively high abundance in all cell types. The enzyme is also rapidly released from the cell upon membrane damage making it an ideal candidate for sensitive quantification of toxicity. As expected, treatment of the CGC cultures with STS significantly increased LDH release from membrane compromised cells into the culture medium after 8 hours (**Figure 3.3.3 C**). Treatment with FG for 24 hours also significantly increased the

release of LDH, when compared with non-treated control cultures. Furthermore, treatment for 48 hours with FN also significantly increased LDH release, again similar to the release induced by LPS treatment for 48 hours.

Figure 3.3.1

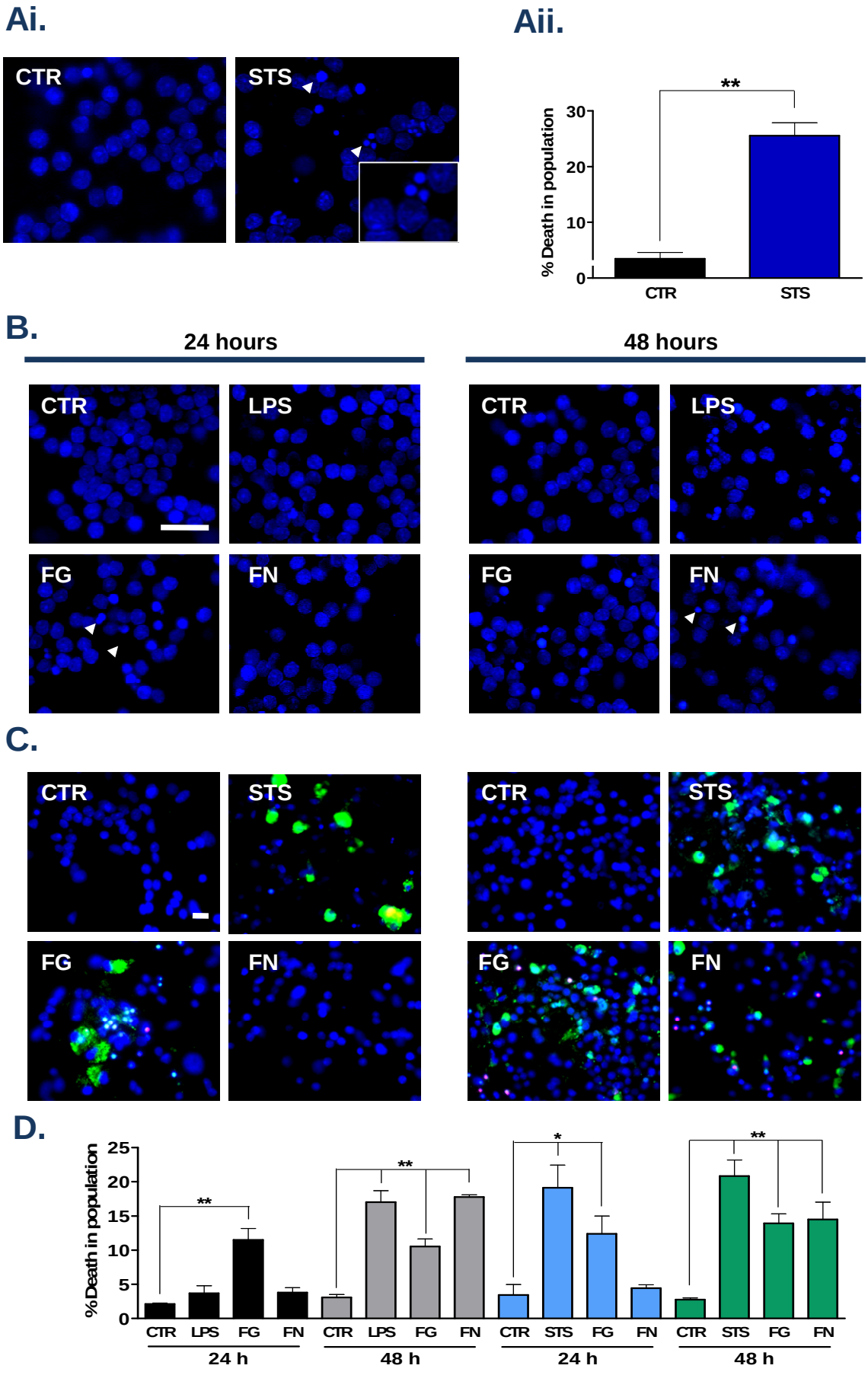
Ai.
Aii.
CTR
STS
**
% Death in population
30
20
10
0
CTR
STS
B.
24 hours
48 hours
CTR
LPS
FG
FN
C.
D.
% Death in population
25
20
15
10
5
0
CTR LPS FG FN CTR LPS FG FN CTR STS FG FN CTR STS FG FN
24 h
48 h
24 h
48 h

Figure 3.3.1

E.

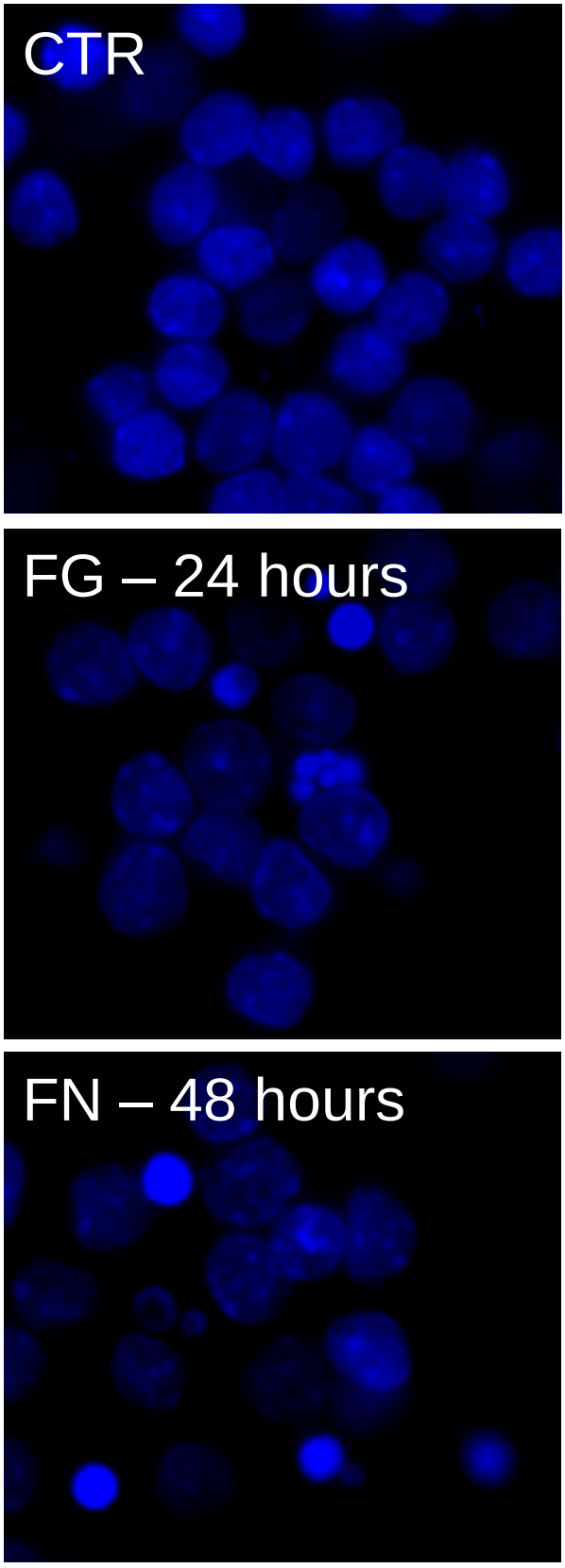

Figure 3.3.1. FG and FN induce significant death in CGC cultures

Ai. Representative images of CGC cultures after STS treatment (0.5 µM; 8 hours). Inset shows classic apoptotic morphology, indicated throughout the figure with arrowheads. Cultures were fixed, stained with Hoechst-33342 and apoptotic morphology was quantified (**Aii**). **B.** Representative images of CGC cultures after FG (2.5 mg/ml), FN (1 mg/ml) or LPS (1 µg/ml) treatment for 24 and 48 hours. As above, cultures were fixed, stained with Hoechst-33342 and apoptotic morphology quantified. **C.** Representative images of CGC cultures, treated as outlined in **B**, with LPS being substituted for STS (8 hours), and subjected to live cell staining with Hoechst-33342 and Annexin-V-FITC (green). **D.** Quantification of **B** (black, 24 hours; grey, 48 hours, Hoechst-33342) and **C** (blue, 24 hours; green, 48 hours, Annexin-V). **E.** Sample fields of interest from the Hoechst-33342 fixed cell staining experiments at higher resolution for easier identification of FG and FN-mediated apoptosis in the CGC cultures when presented on the printed page. Data are presented as a percentage of total death in the CGC culture. All images were captured using x40 magnification, and all scale bars = 40 µm. Treatments were in triplicate in each experiment and data were analysed from 3 independent experiments. To compare death at each time-point in both protocols between control levels and treatments, a one way ANOVA was performed with Dunnett's post-test. Levels of significance were: non-significant $p>0.05$, * $p<0.05$, ** $p<0.01$, *** $p<0.001$.

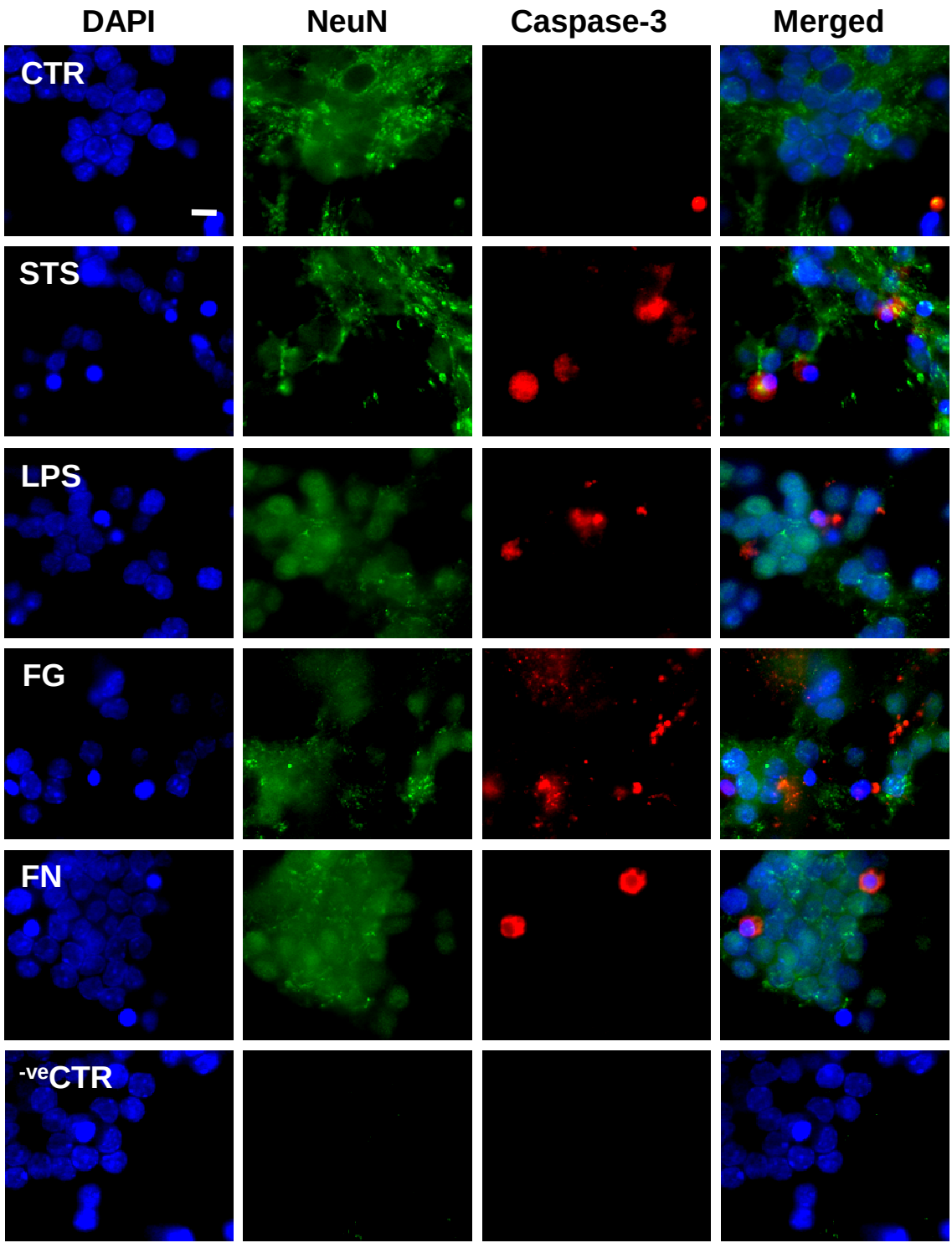

Figure 3.3.2. FG and FN treatment induces neuronal caspase-3 cleavage

Representative images from ICC experiments on CGC cultures after STS (0.5 µM; 8 hours), FG (2.5 mg/ml; 24 hours), FN (1 mg/ml; 48 hours) or LPS (1 µg/ml; 48 hours) treatment are shown. Cultures were co-stained with DAPI for nuclear identification, and probed with anti-NeuN (green) for identification of neurons and anti-cleaved caspase-3 (red), except in negative control cultures, where primary antibodies were omitted. All images were captured using x100 magnification, and scale bar = 10 µm. Treatments were in duplicate.

Figure 3.3.3

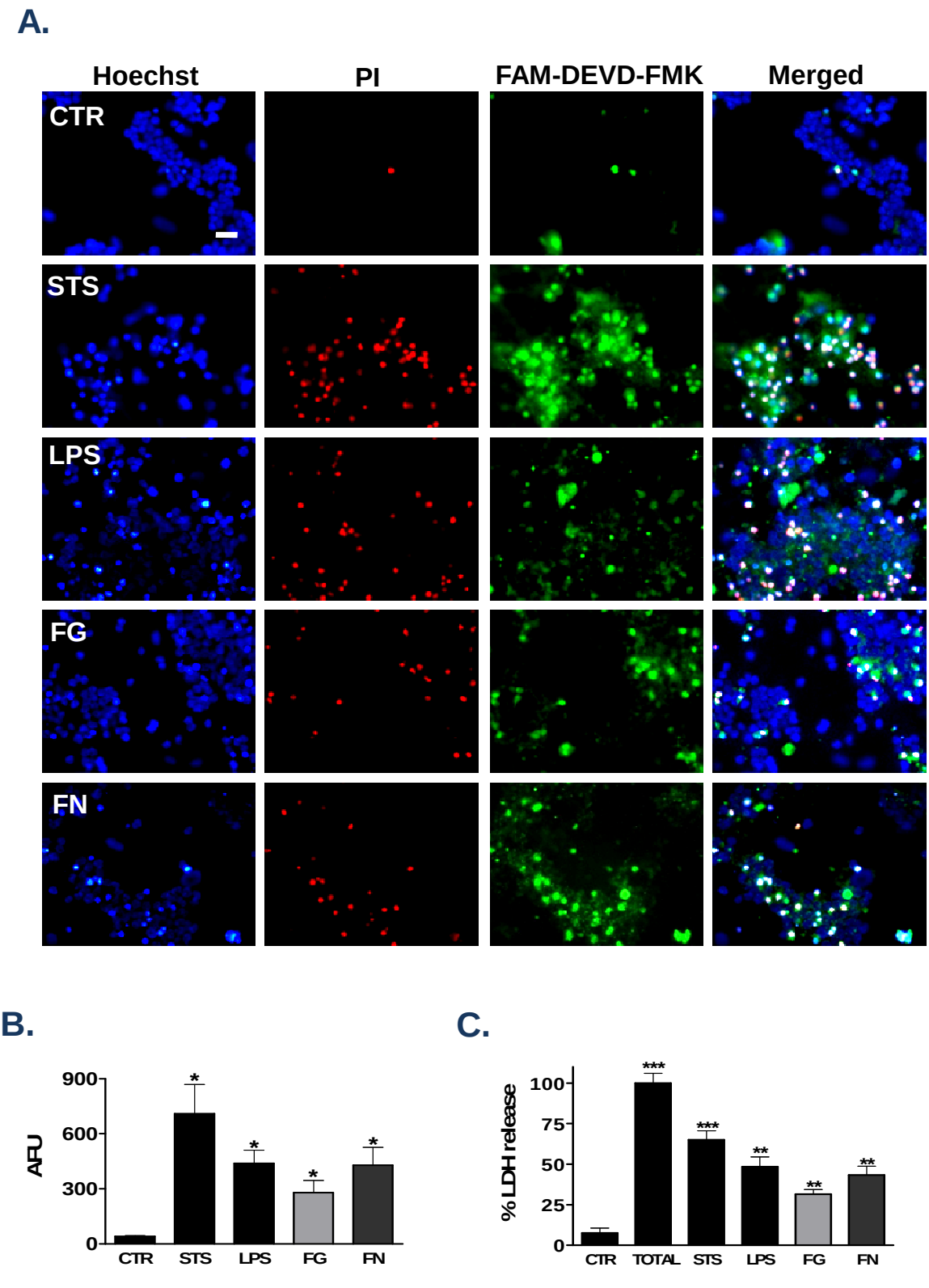
A.
Hoechst
PI
FAM-DEVD-FMK
Merged
CTR
STS
LPS
FG
FN
B.
ARU
900
600
300
0
CTR
STS
LPS
FG
FN
C.
% LDH release
100
75
50
25
0
CTR
TOTAL
STS
LPS
FG
FN

Figure 3.3.3. FG and FN induce caspase-3/7 cleavage and LDH release in CGC cultures

A. Panel of representative images of live cell staining experiments in CGC cultures after treatment with STS (0.5 µM; 8 hours), FG (2.5 mg/ml; 24 hours), FN (1 mg/ml; 48 hours) or LPS (1 µg/ml; 48 hours). Live cell staining was performed with Hoechst-33342 for nuclear identification, propidium iodide (PI; red) for total cell death, and FAM-DEVD-FMK (green) for active caspase-3/7. Original magnification: x40, scale bar: 40 µm. **B.** Quantification of the relative active caspase-3/7 fluorescence intensity/cell in CGC cultures after administration of treatments stated above. Data are presented in arbitrary fluorescence units (AFU). **C.** LDH release assay after treatment of CGCs as stated above. Data are presented as a percentage of total LDH release provided by cell lysis. Treatments were in triplicate for both live cell staining experiments and LDH assays, and data were analysed from 3 independent experiments. To compare AFU or LDH release between control levels and treatments, a one way ANOVA was performed with Dunnett's post-test. Levels of significance were: non-significant $p>0.05$, * $p<0.05$, ** $p<0.01$, *** $p<0.001$.

3.3.2. Differential involvement of microglia in fibrinogen- and fibrin-mediated neuronal death

Due to the observation that LPS could induce neuronal death in the CGCs after 48 hours of exposure, a method to specifically ablate microglia present in the cultures was optimised (**Section 2.5.2; Figure 3.3.4 – 3.3.7**). The use of leucine-methyl-ester (LME) as a phagocyte-specific executioner has been previously published for use on microglial (Morgan et al. 2004) and astrocyte (Hamby et al. 2006) cultures, and an adaptation of these methods were optimised for use on the neuronal cultures used here.

As shown previously, CGC cultures exposed to LPS for 48 hours present a significant increase in cells displaying apoptotic morphology, when compared with non-treated controls (**Figure 3.3.8 Aii & B**). However, cultures pre-treated with LME then exposed to LPS for 48 hours did not show the same significant increase in apoptotic morphology (**Figure 3.3.8 Aii & B**), supporting the essential role of microglia in LPS-mediated neurotoxicity. Interestingly, the observed increase in apoptotic morphology seen after 24 hours exposure of the cultures to FG was also attenuated to control levels after microglia depletion. This also suggests a significant role for microglia in FG-mediated neuronal apoptosis, after 24 hours (**Figure 3.3.8 Ai & B**). By 48 hours however, cultures exposed to FG had a significant number of cells with apoptotic morphology even if microglia had been depleted from the cultures. This suggests either FG has direct neurotoxic capabilities, or that the protein is cleaved in culture to FN (**Section 3.3.4**), which in turn could have direct neurotoxic effects.

When microglia were depleted from cultures exposed to FN for 24 hours, the number of cells displaying apoptotic morphology significantly increased (**Figure 3.3.8 Ai & B**). This suggests microglia protect the neurons from 24 hours of FN exposure. However, this observed ‘protective’ effect must be time-dependent, because as previously shown (**Figure 3.3.1**), FN exposure for 48 hours with microglia present in the CGC cultures caused a significant increase in apoptotic morphology (**Figure 3.3.8 Aii & B**). These

findings suggest that microglia are able to efficiently clear ‘acute’ (<24 h) FN exposure, but not ‘chronic’ (>24 h) exposure, possibly due to FN-mediated microglial toxicity which indirectly causes neuronal death.

3.3.3. Differential expression of ED-1 is observed in CGC cultures after FG or FN treatment

To support the hypothesis that FN induces microglial death in the CGC cultures, ED-1 expression in the cultures was assayed. FN increased ED-1 expression after 2 h. This was followed a slow decline until 24 h when a significant decrease was observed at 48 h (**Figure 3.3.9 Ai & B**), supporting the suggestion that FN is directly toxic to microglia. Interestingly, FG induced a bi-phasic expression of ED-1 in the CGC cultures, with decreases being observed after 4 h and 48 h (**Figure 3.3.9 Aii & B**).

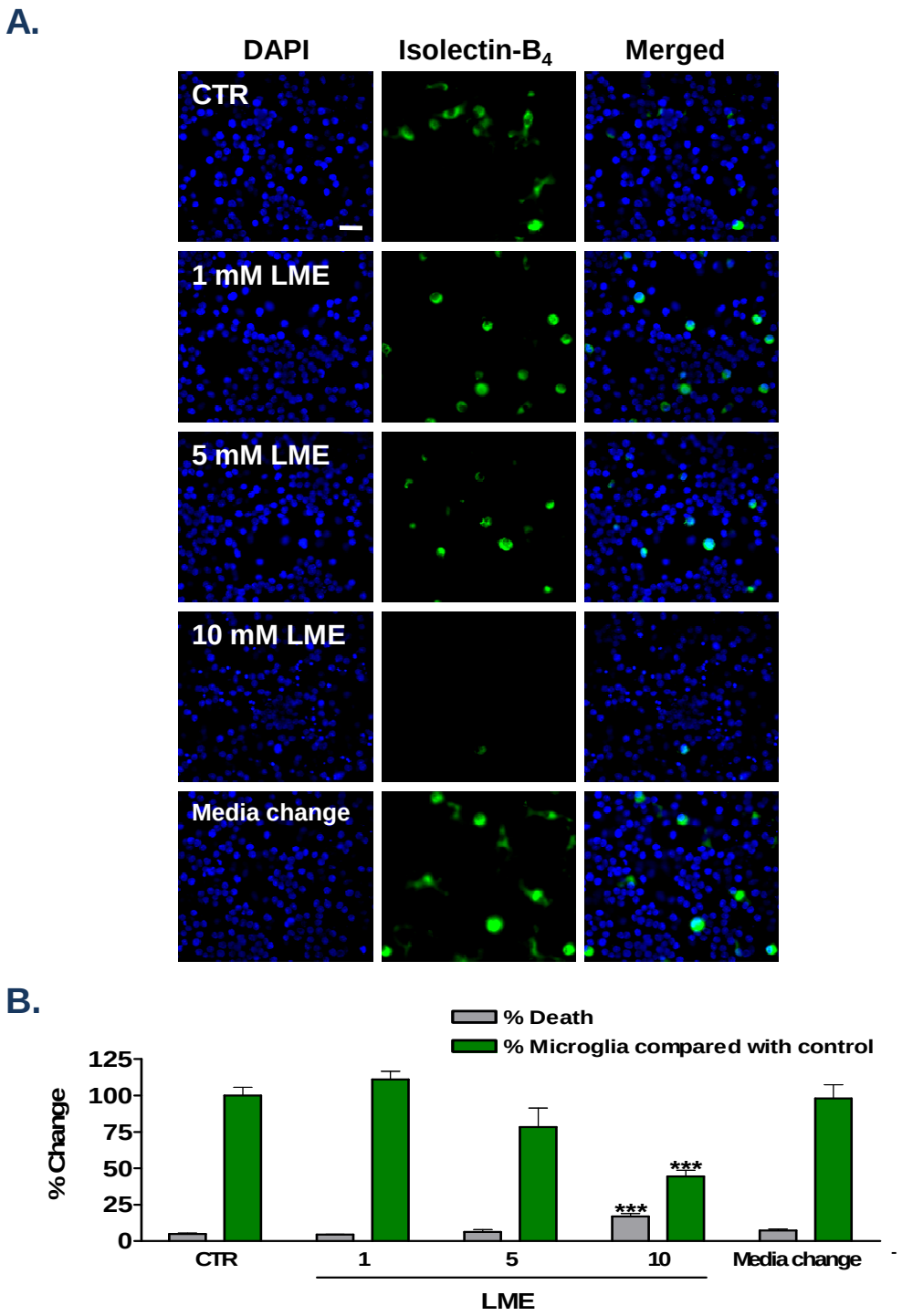

Figure 3.3.4. Initial characterisation of LME treatment of CGCs

A. Representative images from ICC experiments performed on CGC cultures after treatment with 1-10 mM LME for 24 hours. ICC was performed with DAPI (blue) for quantification of total cell number and those displaying apoptotic morphology, and IB_4 (green) for microglial identification and quantification. Scale bar = 30 µm. **B.** Quantification of cells displaying apoptotic morphology (% of total cell number in the field) and microglial number, as a percentage of control levels. Paired two-tailed Student's *t*-tests were performed between controls and specific treatments. Levels of significance were: non significant $p>0.05$, *** $p<0.001$. N = 3.

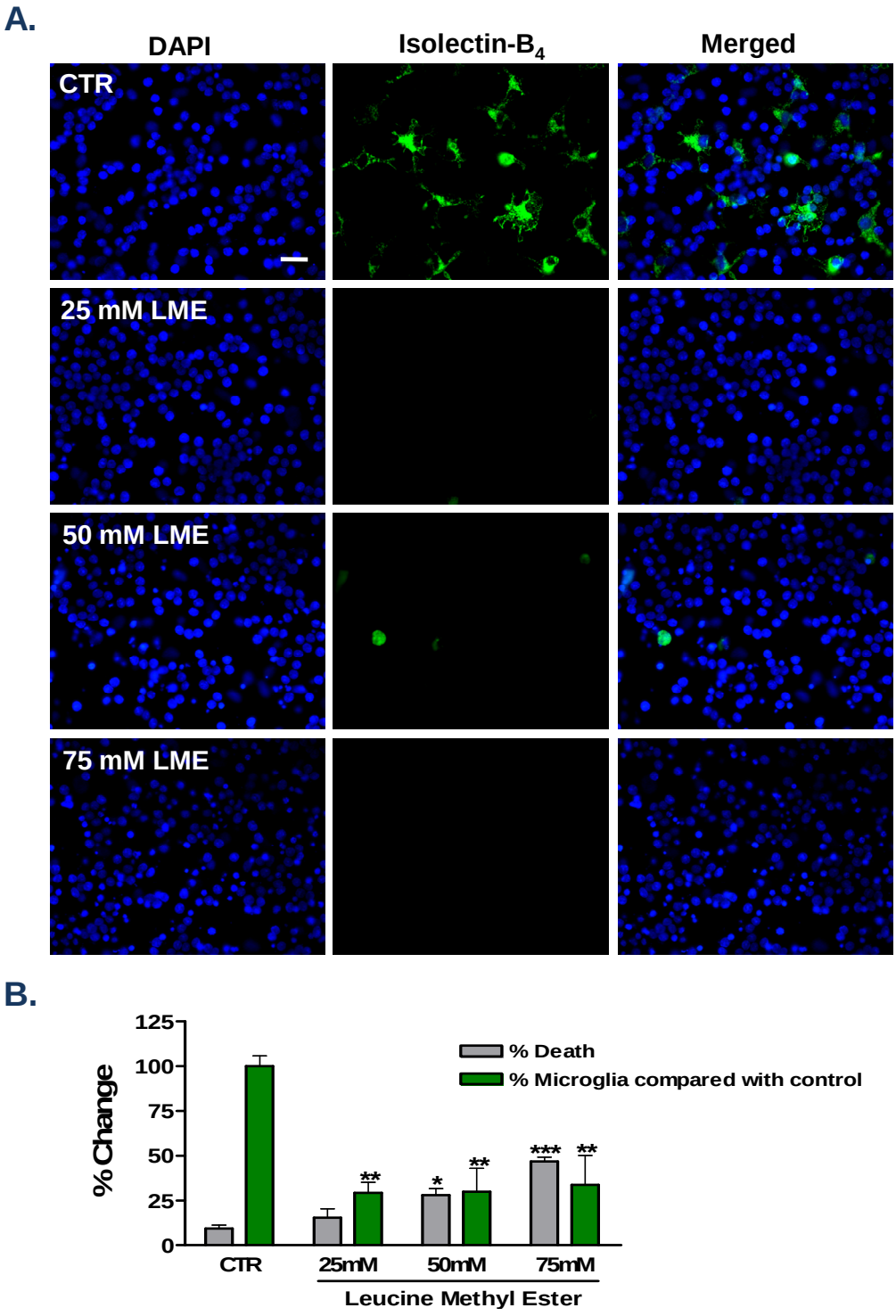

Figure 3.3.5. Secondary characterisation of LME treatment of CGCs

A. Representative images from ICC experiments performed on CGC cultures after treatment with 25-75 mM LME for 1 hour, followed by wash-off. ICC was performed with DAPI (blue) for quantification of total cell number and those displaying apoptotic morphology, and IB_4 (green) for microglial identification and quantification. Scale bar = 30 µm. **B.** Quantification of cells displaying apoptotic morphology (% of total cell number in the field) and microglial number, as a percentage of control levels. Paired two-tailed Student's *t*-tests were performed between controls and specific treatments. Levels of significance were: non significant $p>0.05$, * $p<0.05$, ** $p<0.01$, *** $p<0.001$. N = 3.

Figure 3.3.6

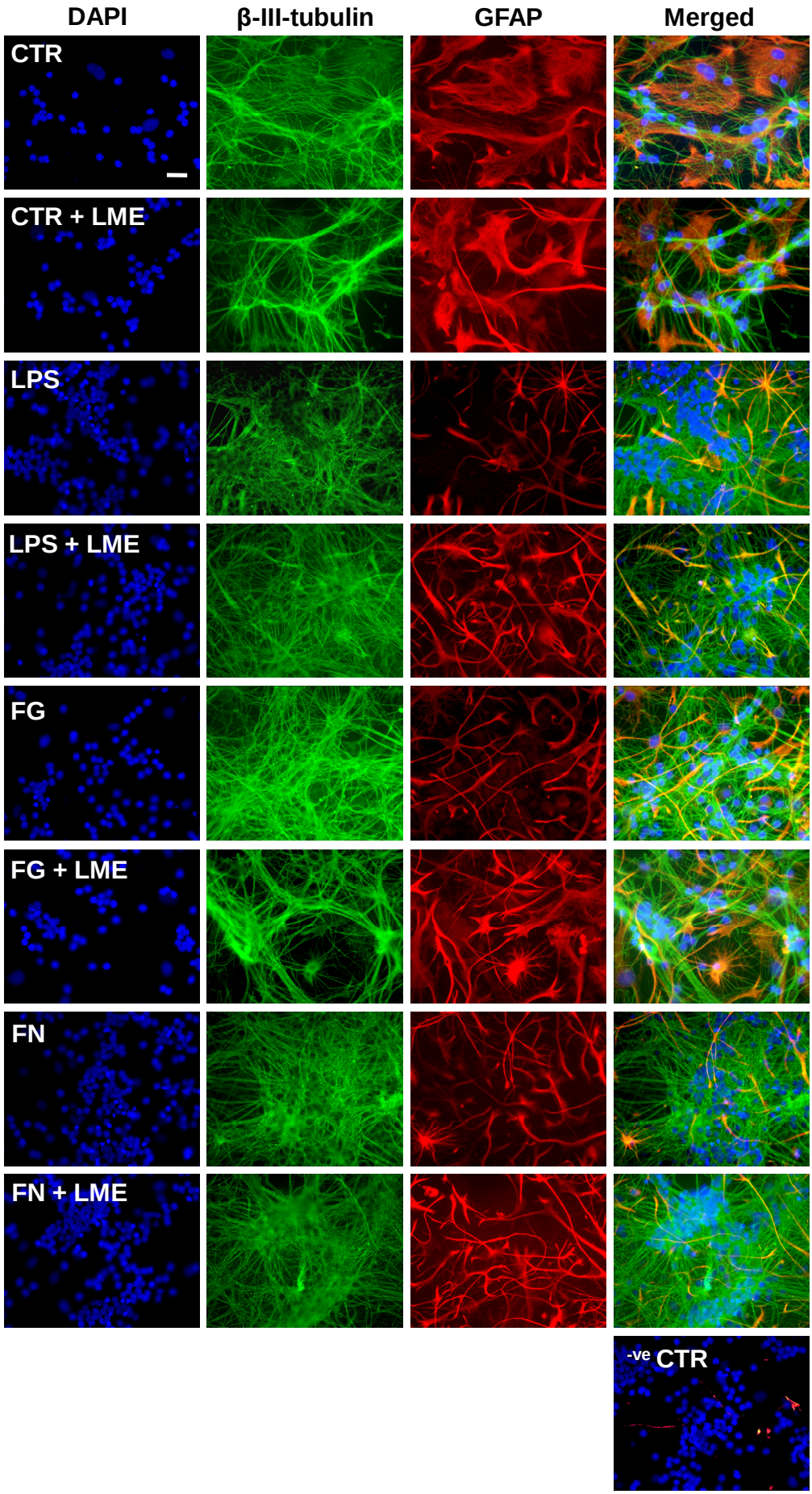
DAPI
β-III-tubulin
GFAP
Merged
CTR
CTR + LME
LPS
LPS + LME
FG
FG + LME
FN
FN + LME
-ve CTR

Figure 3.3.6. Characterisation of the effects of 25 mM LME treatment on neurons and astrocytes in CGC cultures

Panel of representative images from ICC experiments performed on CGC cultures after treatment with LPS (1 µg/ml; 48 hours), FG (2.5 mg/ml; 24 hours) or FN (1 mg/ml; 48 hours) and pre-treatment with 25 mM LME for 1 hour. No observable changes to astrocyte and neuronal density and morphology were recorded with respect to each main treatment group. Importantly, no significant change in neuronal or astrocytic morphology were observed when cultures were treated with LME alone, supporting a microglial-specific action of the compound. ICC was performed with DAPI (blue), anti-β-III-tubulin (green) for identification of changes in neuronal density and anti-GFAP (red) for identification of changes in astrocytic density and morphology. Scale bar = 30 µm.

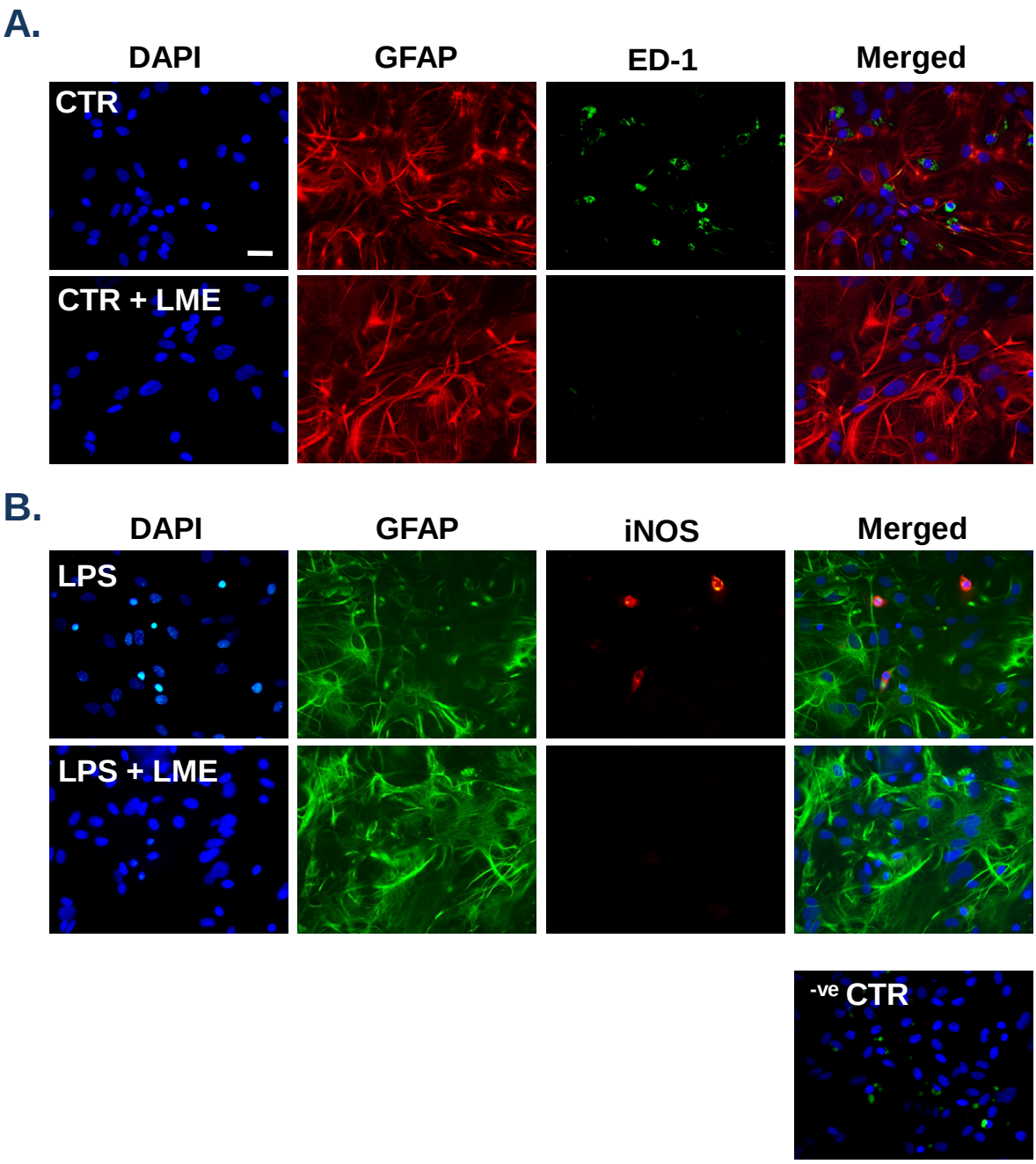

Figure 3.3.7. Further characterisation of the effectiveness of 25 mM LME treatment in the removal of microglia from astrocytic cultures

A. Panel of representative images from ICC experiments performed on primary astrocyte cultures after pre-treatment with 25 mM LME for 1 hour showing no observable changes in astrocyte density and morphology, but an observable loss of contaminating microglia. ICC was performed with DAPI (blue), anti-GFAP (red) for identification of changes in astrocytic density and morphology, and anti-ED1 (green) for identification of microglial number. **B.** Representative images from ICC experiments performed on primary astrocyte cultures after treatment with LPS (1 µg/ml) for 24 hours following pre-treatment with 25 mM LME for 1 hour. ICC was performed as described in **A** but with anti-GFAP (green) and anti-iNOS (red) to identify activated microglia. As in **A** no changes in astrocyte density and morphology were observed, however a loss in contaminating microglial number/reactivity was identified. Scale bar = 30 µm.

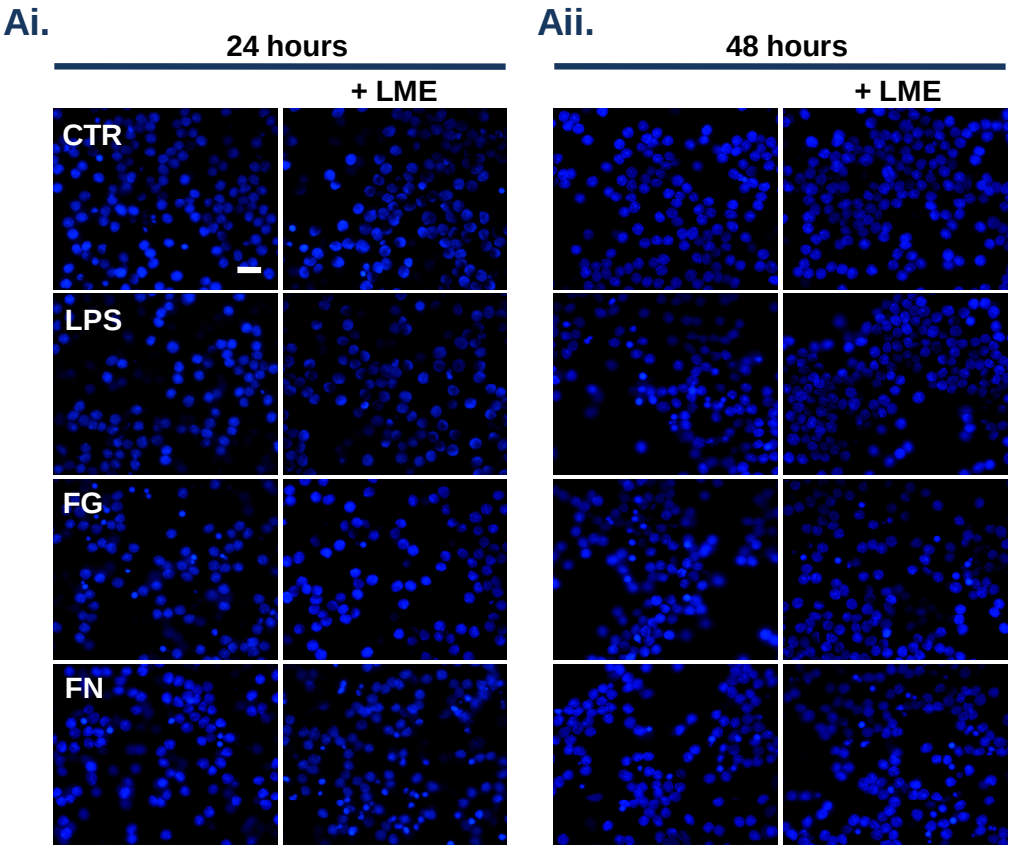

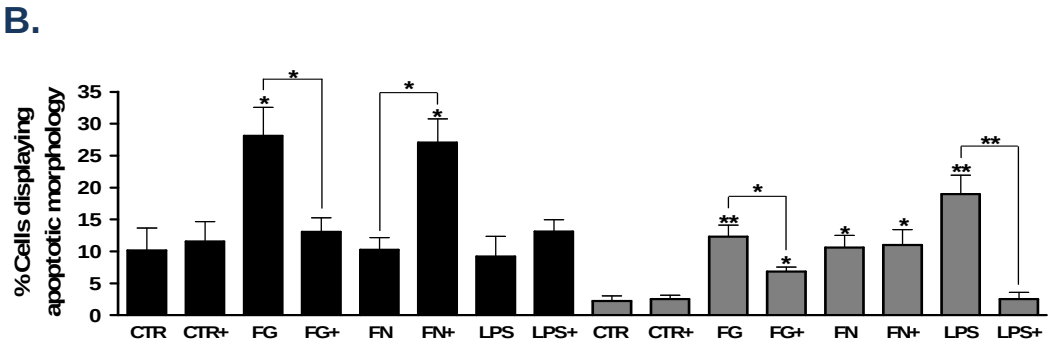

Figure 3.3.8. FG- and FN-mediated neuronal death is differentially dependent on microglia

A. Panel of representative images from fixed cell staining experiments in CGC cultures, in some cases, treated with leucine-methyl-ester (LME; 25 mM) to deplete microglia, prior to treatment with FG (2.5 mg/ml), FN (1 mg/ml) or LPS (1 µg/ml) for 24 hours (**Ai**) or 48 hours (**Aii**). Cell staining was performed using Hoechst-33342 for nuclear morphology analysis. Original magnification: x40, scale bar: 20 µm. **B.** Quantification of apoptotic morphology in the CGC cultures in the presence and absence of microglia. Data are presented as the percentage of the total population displaying apoptotic morphology. Treatments were in triplicate and data were analysed from 3 independent experiments. To compare between control levels and treatments, a one way ANOVA was performed with Dunnett's post-test. For direct comparison between treatment in the presence and absence of microglia, paired two-tailed Student's *t*-tests were performed. Levels of significance were: non-significant $p>0.05$, * $p<0.05$, ** $p<0.01$, *** $p<0.001$.

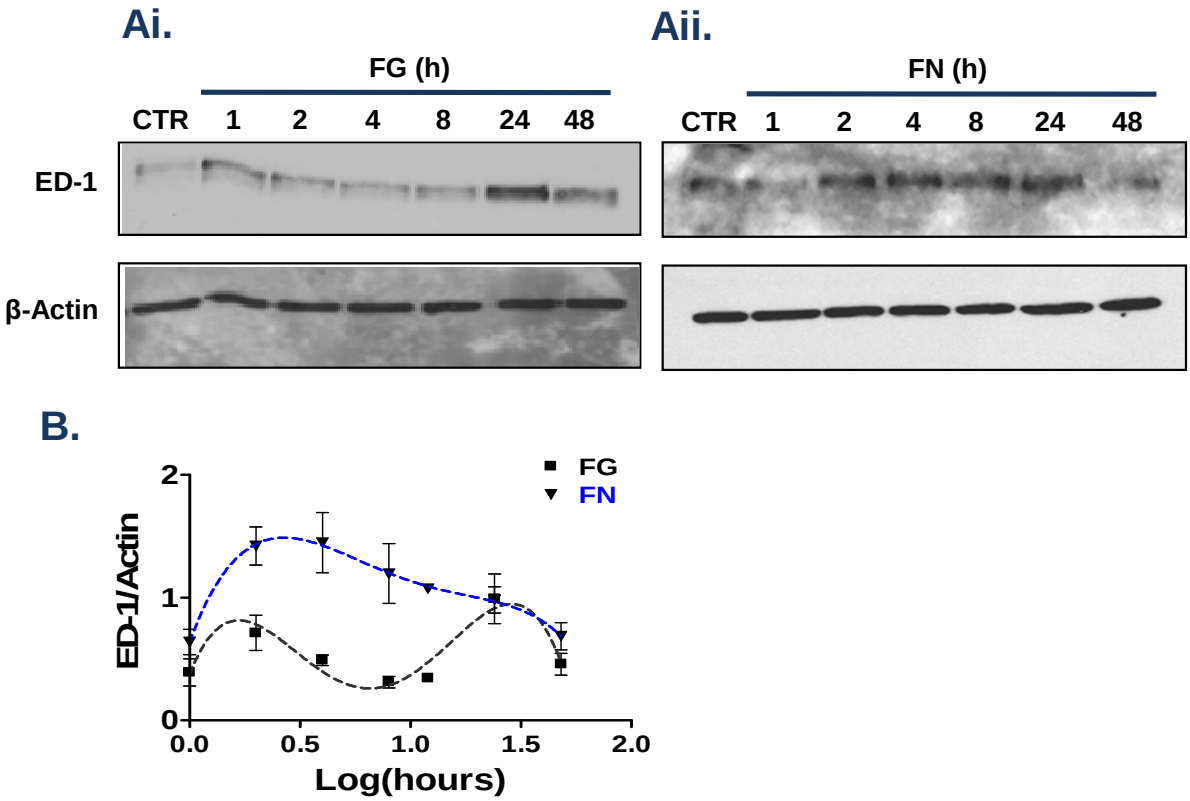

Figure 3.3.9. FG and FN induce differential, time-dependent expression of ED1 in CGC cultures

A. Representative Western blots for ED1 and β-actin expression in CGC cultures after timecourse treatment with FG (2.5 mg/ml; **Ai**) or FN (1 mg/ml; **Aii**). **B.** Quantification of ED1 expression (log scale) with respect to protein-loading control, β-actin. Western blots were repeated once (n = 2).

3.3.4. Fibrinogen is cleaved to fibrin in culture and is responsible for late neuronal death

If FG is cleaved to FN in culture and this reaction mediates the 'direct', non-microglial neurotoxicity, the serine protease thrombin that is responsible for the cleavage reaction (Möller et al. 2006) would have to be present in the culture. To identify whether prothrombin was expressed in the CGC cultures used here and whether FG treatment increased or modulated this expression, RNA was extracted from CGCs, which had been time-dependently exposed to FG, and reverse transcribed to cDNA. Polymerase chain reaction (PCR) was performed and constitutive expression of prothrombin in the CGC cultures was not observed, however a significant increase in prothrombin gene expression was seen after 48 hours exposure with FG (**Figure 3.3.10 A**), suggesting that the chronic (>24 h) presence of FG can induce expression of the enzyme required for conversion of the protein to FN. These data do not confirm that FG is converted to FN but do suggest and further support the idea that FG could be converted to FN and induce direct neurotoxicity.

To further elucidate whether FG is converted to FN in the CGC cultures, which in turn induces direct or non-microglial mediated neurotoxicity, a thrombin activity inhibitor, hirudin (Hi) was administered to the cultures prior to 24 or 48 hours of FG exposure, in the presence or absence of microglia (**Figure 3.3.10 B**). Inhibition of thrombin activity had no effect on FG-mediated increases in apoptotic morphology after either 24 or 48 hours of treatment, when microglia were present. However, if microglia were depleted from the cultures prior to thrombin inhibition, 'FG'-mediated neuronal toxicity after 48 hours was significantly inhibited (**Figure 3.3.10 Bii**), which strongly suggests that FG is indeed cleaved in culture to FN which in turn is responsible for the late neuronal toxicity.

Figure 3.3.10

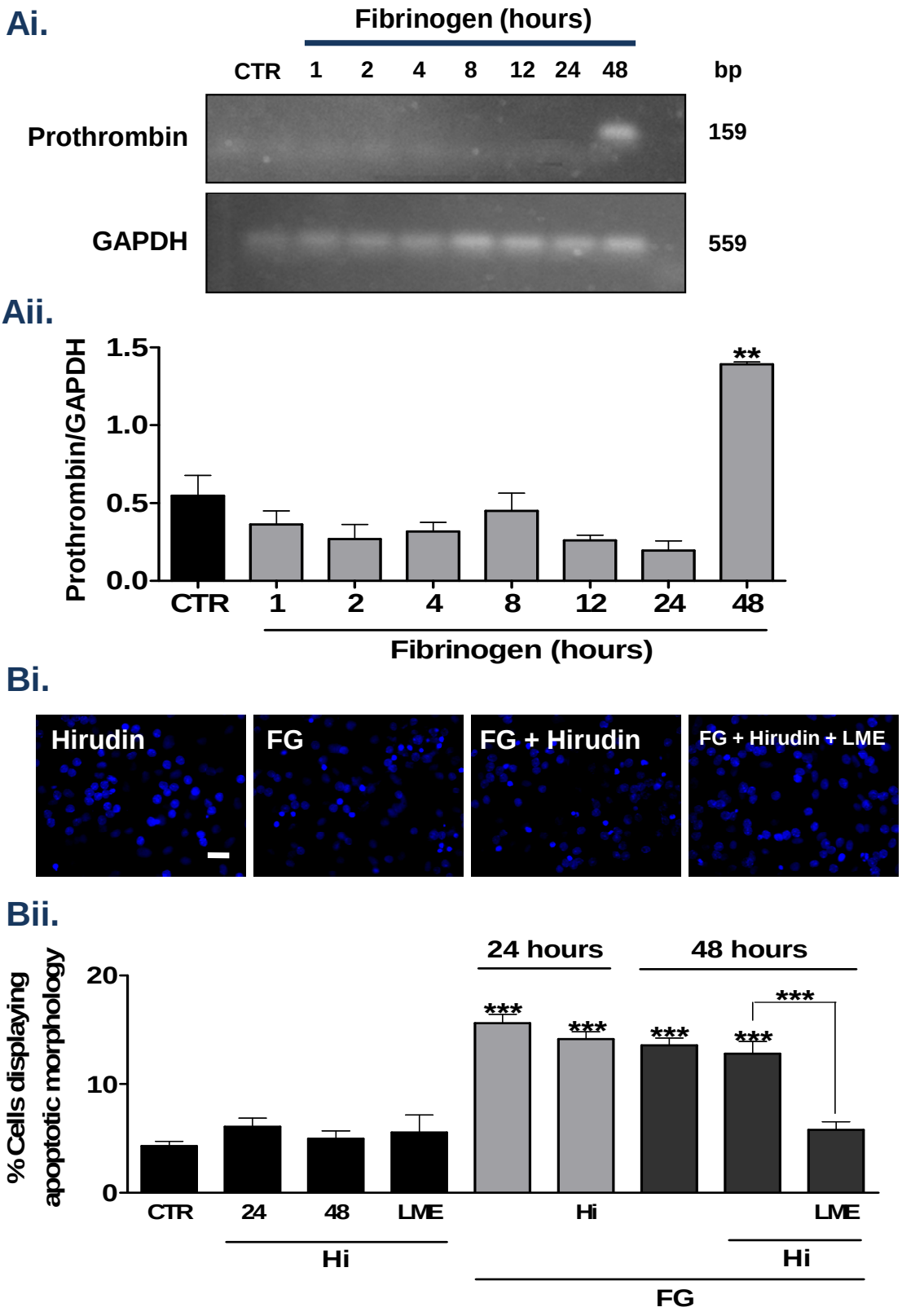
Ai.
Fibrinogen (hours)
CTR 1 2 4 8 12 24 48 bp
Prothrombin
159
GAPDH
559
Aii.
Prothrombin/GAPDH
1.5
1.0
0.5
0.0
**
CTR 1 2 4 8 12 24 48
Fibrinogen (hours)
Bi.
Hirudin
FG
FG + Hirudin
FG + Hirudin + LME
Bii.
% Cells displaying apoptotic morphology
24 hours
48 hours
20
10
0
***
CTR 24 48 LME Hi LME
Hi
Hi
FG

Figure 3.3.10. 'Chronic' FG treatment induces prothrombin gene expression in CGCs leading to cleavage of FG to FN

Ai. A representative PCR gel identifying prothrombin gene expression in CGC cultures after FG (2.5 mg/ml) timecourse treatment. **Aii.** Quantification of thrombin gene expression in CGC cultures with respect to expression of the house-keeper gene, GAPDH. **Bi.** Panel of representative images from fixed cell staining experiments in CGC cultures treated with FG (2.5 mg/ml), Hirudin (Hi; 50 U/ml) or in combination, after LME-treatment (25 mM) for 48 hours. Cell staining was performed using Hoechst-33342 to assess nuclear morphology. Original magnification: x40, scale bar: 20 µm. **Bii.** Quantification of apoptotic morphology in the CGC cultures after administration of treatments stated in **Bi** after 24 or 48 hours incubation. The PCR experiment quantification is presented as the relative thrombin gene expression with respect to GAPDH expression. The fixed cell staining data were presented as the percentage of nuclei in the total population displaying apoptotic morphology. Treatments were in triplicate and data were analysed from 3 independent experiments. To compare between control levels and treatments, one way ANOVA were performed with Dunnett's post-test. For direct comparison between treatments in the presence and absence of microglia after 48 hours, a paired two-tailed Student's *t*-test was performed. Levels of significance were: non-significant $p>0.05$, ** $p<0.01$, *** $p<0.001$.

3.3.5. Differential induction of Map Kinase pathways after fibrinogen and fibrin treatment of CGCs

The p38-MAPKs, of which there are four, were first defined trying to identify drugs to inhibit TNFα-mediated inflammatory responses (Lee et al. 1994), and have been shown to be activated when cells are under stress by a vast array of stimuli (Johnson & Lapadat 2002). Furthermore, persistent activation of the p38-MAPK signalling pathway has been suggested to mediate neuronal apoptosis in AD, PD, and ALS (Kim & Choi 2010). Therefore, to identify whether activation of this stress pathway was induced in CGCs after FG or FN treatment, Western blotting for expression of the phosphorylated form of p38 was performed.

Expression of phospho-p38-MAPK after FG treatment was time dependent, increasing over time until 24 hours of exposure, with significant expression compared with control being reached after 4 hours (**Figure 3.3.11 A**). A slight decrease in phosphor-p38-MAPK was observed after 48 hours of treatment when compared with that seen at 24 hours, however this was not significant. Treatment with FN did not induce a similar profile to that observed after FG exposure, with an earlier significant expression of phospho-p38-MAPK, after 2 hours exposure (**Figure 3.3.11 B**). However, expression of phospho-p38-MAPK at later time-points did not reach significance when compared with non-treated control levels, suggesting an earlier role for the p38-MAPK pathway in FN-mediated stress, when compared with FG-mediated induction of the pathway.

Figure 3.3.11

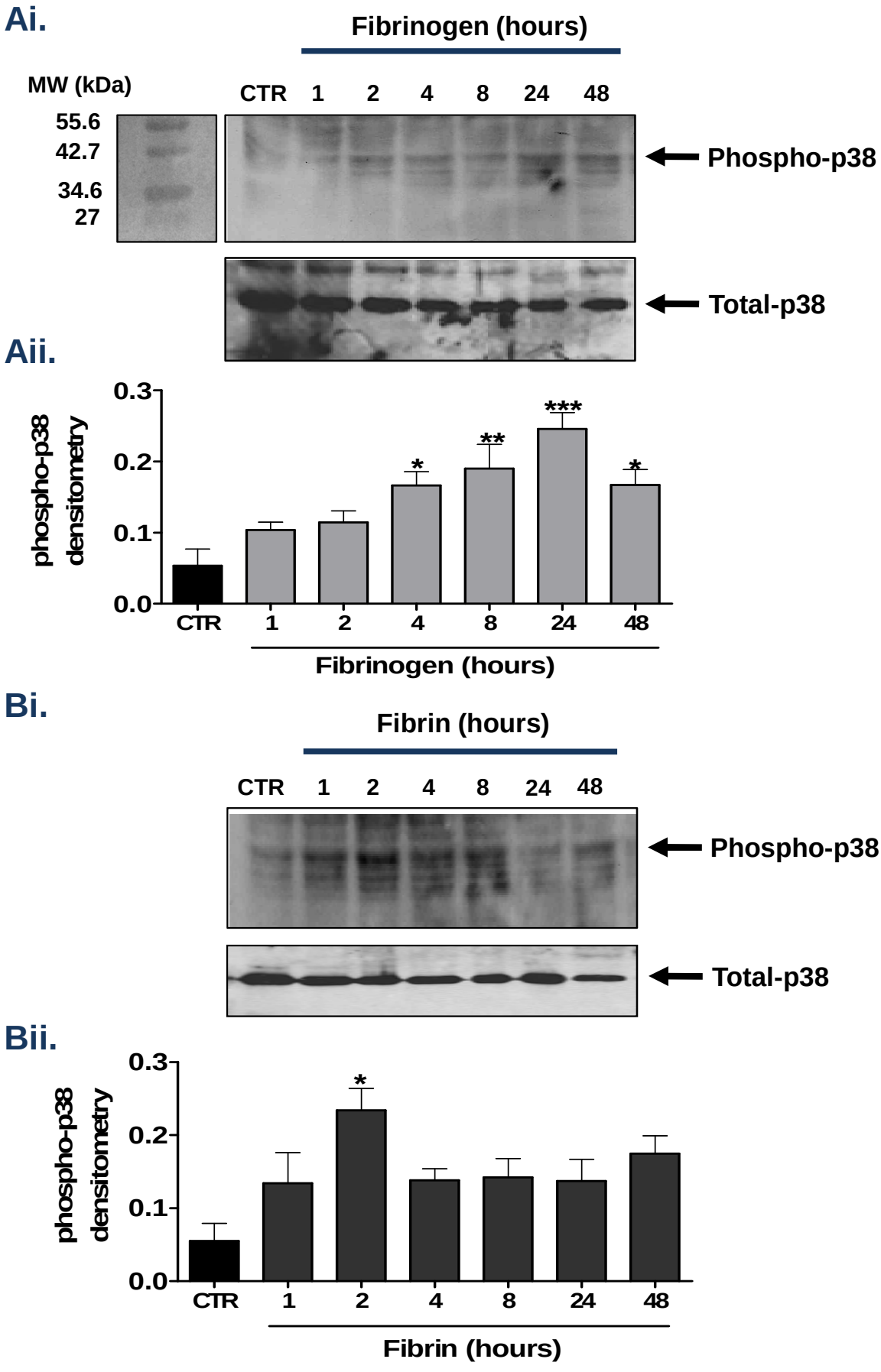
Ai.
Fibrinogen (hours)
MW (kDa)
CTR 1 2 4 8 24 48
55.6
42.7
34.6
27
Phospho-p38
Total-p38
Aii.
phospho-p38 densitometry
0.3
0.2
0.1
0.0
*
**
***
*
CTR 1 2 4 8 24 48
Fibrinogen (hours)
Bi.
Fibrin (hours)
CTR 1 2 4 8 24 48
Phospho-p38
Total-p38
Bii.
phospho-p38 densitometry
0.3
0.2
0.1
0.0
*
CTR 1 2 4 8 24 48
Fibrin (hours)

Figure 3.3.11. FG and FN induce differential, time-dependent expression of phosphorylated p38-MAPK in CGC cultures

Ai. Representative Western blots for phosphorylated p38-MAPK and total p38-MAPK expression in CGC cultures after timecourse treatment with FG (2.5 mg/ml), presented with the molecular weight marker allowing identification of the specific phosphorylated p38-MAPK band. **Aii.** Densitometric quantification of phosphorylated p38-MAPK expression in CGC cultures after timecourse treatment with FG, with respect to background intensity. **Bi.** Representative Western blots for phosphorylated p38-MAPK and total p38-MAPK expression in CGC cultures after timecourse treatment with FN (1 mg/ml). **Bii.** Densitometric quantification of phosphorylated p38-MAPK expression in CGC cultures after timecourse treatment with FN, with respect to background intensity. Blots are representative of n = 3 experiments. To compare between control levels and all treatment time-points, one way ANOVAs were performed with Dunnett's post-test. Levels of significance were: non-significant $p>0.05$, * $p<0.05$, ** $p<0.01$, *** $p<0.001$.

3.3.6. Fibrinogen and fibrin treatment of CGCs induces TNFα release, dependent on microglia

As previously shown with primary microglial cultures (**Figure 3.2.3**), TNFα release is a prominent feature when cells are exposed to FG or FN. Therefore, similar experiments were performed in the CGCs, known to have microglia present, to identify whether these cells behaved in a similar manner in a more physiological setting.

Initially a time-course was performed to observe whether the treatment of the CGCs following a similar pattern to that seen in primary microglial cultures (**Figure 3.3.12 A**). LPS treatment as a positive control, significantly increased TNFα release from as early as 4 hours. Treatment of CGCs with LPS saw a significant drop in release, at 8 hours, compared with release at 6 hours. Finally, LPS treatment saw a significant rise in TNFα release, after 8 hours, which peaked at 24 hours before dropping significantly at 48 hours (**Figure 3.3.12 A**).

TNFα release due to FN treatment did not reach significance until 24 hours. Similar to LPS treatment, a significant drop at 48 hours was observed in the FN-treated cultures when compared with 24 hour release levels (**Figure 3.3.12 A**). Treatment with FG saw further stunted TNFα release profile in comparison to LPS-mediated release, however significant release was observed at 24 hours with a significant drop in release at 48 hours when compared with 24 hour release levels (**Figure 3.3.12 A**).

To identify whether the microglia present in the cultures were responsible for the observed TNFα release, LME depletion of the cells was performed prior to treatment with FG, FN or LPS (**Figure 3.3.12 B**). As expected, LPS-mediated TNFα release after 24 hours was significantly reduced in cultures where microglia had been depleted (**Figure 3.3.12 Bi**). Co-treatment of cultures with LPS and Interferon-γ (IFNγ) did not significantly enhance TNFα release, when compared with sole treatment with LPS. Treatment with the two highest concentrations of FG tested significantly induced TNFα release that was dependent on microglia present. The same observation was also made with the two highest concentrations of FN administered (**Figure 3.3.12 Bi**). The

depletion of microglia had a similar effect on LPS-mediated TNFα release after 48 hours of treatment. The same was true for TNFα release mediated by the top two FG concentrations administered and also the two highest concentrations of FN administered (**Figure 3.3.12 Bii**).

Cultures were also co-treated with LPS and FG or FN to identify whether the same pathways were being induced. Co-treatment of cultures with FG and LPS significantly enhanced TNFα release when compared with treatment of FG only. Similarly, treatment of cultures with FN and LPS significantly enhanced TNFα release when compared with treatment of FN only (**Figure 3.3.13**). These data suggest that the pathways and mechanisms by which FN and FG mediate their TNFα release differ from those utilised by LPS.

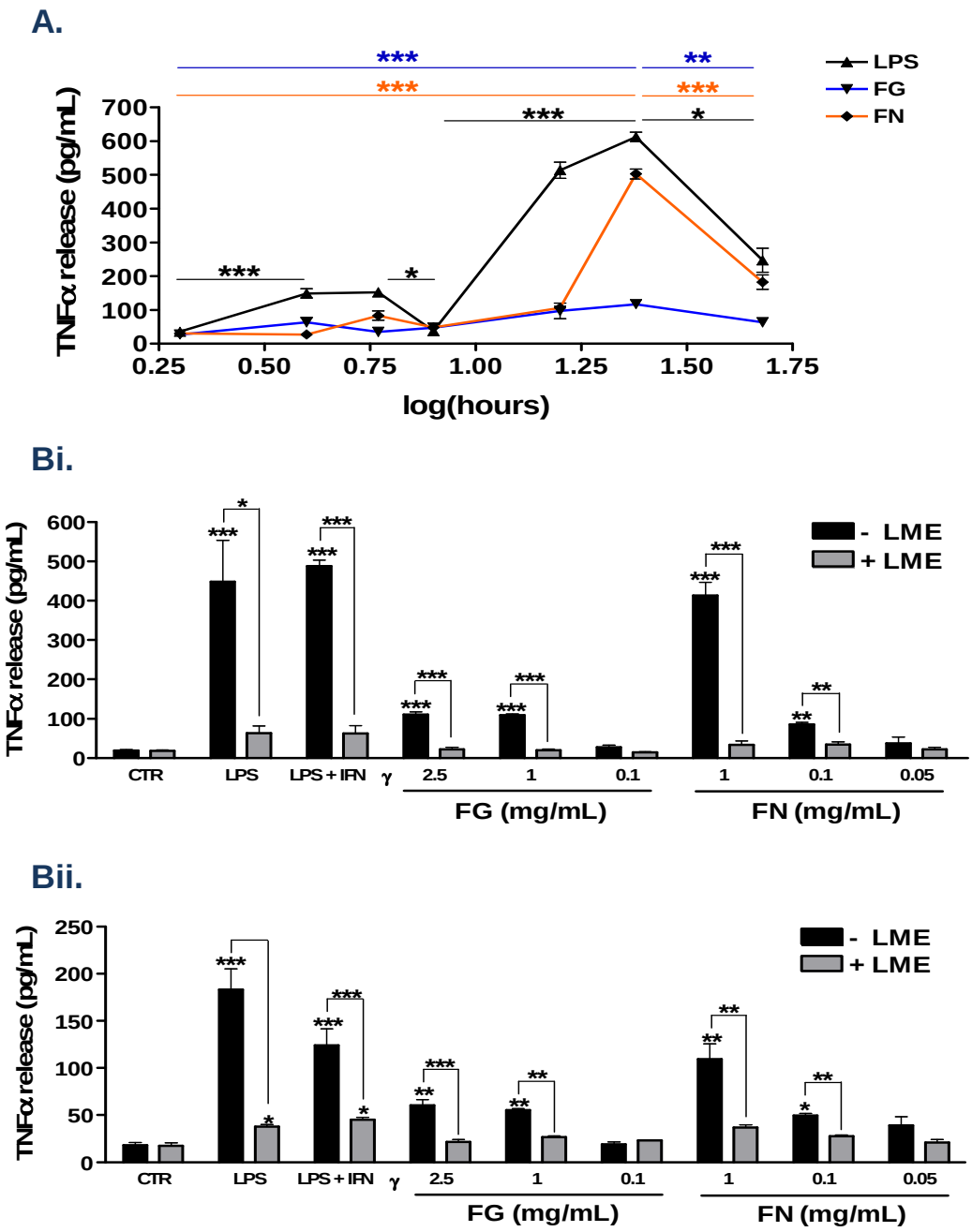

Figure 3.3.12. FG and FN induce significant TNFα release in CGC cultures, dependent on microglia

A. Timecourse analysis of TNFα release using an ELISA system after treatment of CGC cultures with FG (2.5 mg/ml), FN (1 mg/ml) or LPS (1 µg/ml). **B.** Analysis of TNFα release in CGC cultures after treatment for 24 hours (**Bi**) and 48 hours (**Bii**) with FG (0.1-2.5 mg/ml), FN (0.05-1 mg/ml), LPS (1 µg/ml) or LPS and IFNγ (100U/ml), in the presence (-LME) or absence (+LME) of microglia. Treatments were in duplicate in each experiment and data were analysed from 3 independent experiments. Paired two-tailed Student's *t*-tests were performed for direct comparisons between time-points (as in **Figure 3.2.3**) or for comparison of treatments in the presence and absence of microglia. In concentration dependent studies a one-way ANOVA was performed with Dunnett's post-test. Levels of significance were: non-significant p>0.05, * p<0.05, ** p<0.01, *** p<0.001.

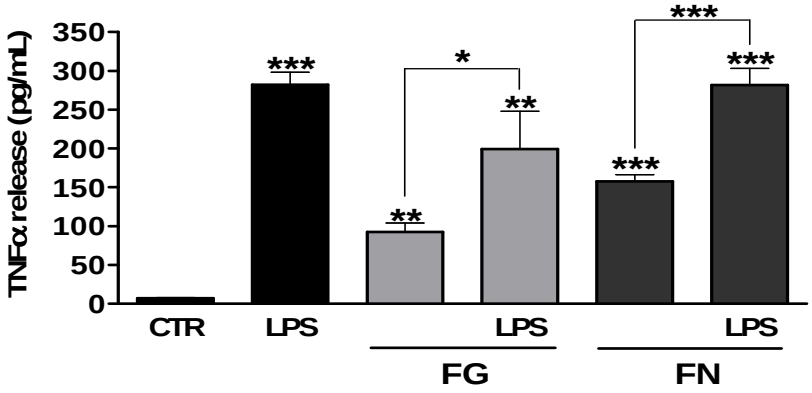

Figure 3.3.13. FG and FN induce significant TNFα release in CGC cultures via a different mechanism to LPS

Analysis of TNFα release in CGC cultures using an ELISA system after treatment for 24 hours with LPS (1 µg/ml), FG (2.5 mg/ml), FN (1 mg/ml), or FG and FN in combination with LPS. Treatments were in duplicate in each experiment and data were analysed from 3 independent experiments. For comparisons between control levels and all treatments a one way ANOVA was performed with Dunnett's post-test. Paired two-tailed Student's *t*-tests were performed for direct comparisons between treatments alone or in combination with LPS. Levels of significance were: non-significant $p>0.05$, * $p<0.05$, ** $p<0.01$, *** $p<0.001$.

3.3.7. Fibrin- but not fibrinogen-mediated responses are regulated by CD11b and scavenger receptor-A

To further attempt to elucidate the signalling pathways contributing to FN- and FG-mediated neuronal toxicity, antibody block of the CD11b (Mac-1) integrin receptor was performed prior to treatment with FN and FG for 24 hours and ELISA analyses of TNFα release. Antibody block of CD11b prior to LPS treatment did not significantly modulate TNFα release. Also, FG-mediated TNFα release was not attenuated by antibody block of the receptor (**Figure 3.3.14 A**). However FN-mediated TNFα release was significantly reduced in the presence of CD11b blocking antibody (**Figure 3.3.14 A**), suggesting differential receptor binding affinity for soluble fibrinogen and its insoluble cleavage product fibrin.

Following on from these data suggesting contributions from other receptors, pharmacological inhibition of scavenger receptor A (SRA) was performed. Roles for SRA in microglial-mediated responses have been published on numerous occasions (Husemann et al. 2002; Hooper et al. 2009a; Yang et al. 2011b), so it was therefore deemed a reasonable target to pursue with respect to FG- and FN-mediated cellular interactions. Western blotting for iNOS expression in CGCs was performed after LPS, FG, or FN treatment for 24 hours in the presence or absence of the SRA inhibitor, fucoidan (Hooper et al. 2009a). As shown previously, in serum-containing conditions, FG failed to induce significant iNOS (**Figure 3.3.14 Bii**). However FN induced iNOS expression to a level similar to that observed after LPS treatment. Furthermore this FN-mediated induction of iNOS could be significantly attenuated if cultures were pre-treated with fucoidan, suggesting a possible role for this receptor. LPS-induced expression of iNOS was not modulated significantly by fucoidan pre-treatment (**Figure 3.3.14 Bii**).

As FG-treatment failed to induce iNOS expression in the serum-containing conditions used for CGC culturing, TNFα release was performed on supernatants collected from cultures pre-treated with fucoidan (**Figure 3.3.14 C**). Interestingly no significant

modulation of TNFα release occurred after any of the treatments, including FN-treated cultures, suggesting TNFα release after LPS, FN, or FG treatment is not dependent on ligand-SR-A binding (**Figure 3.3.14 C**).

Figure 3.3.14

A.

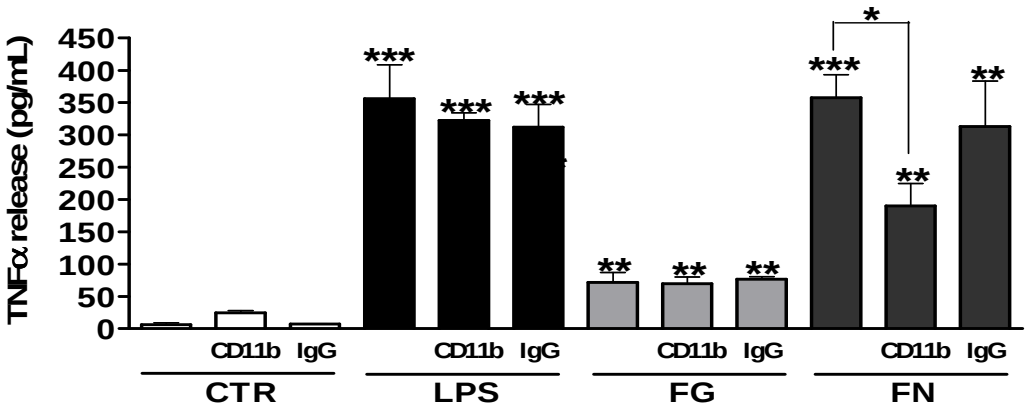

Bi.

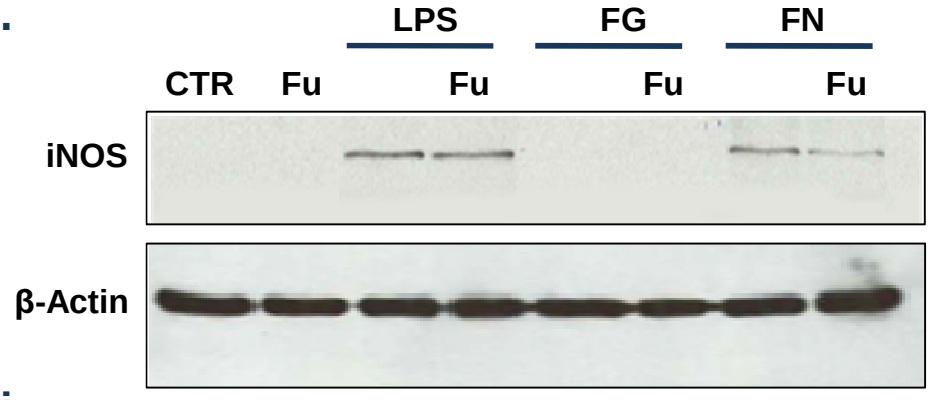

Bii.

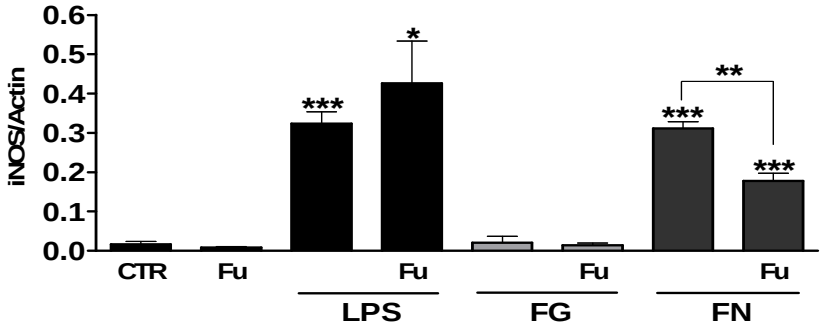

C.

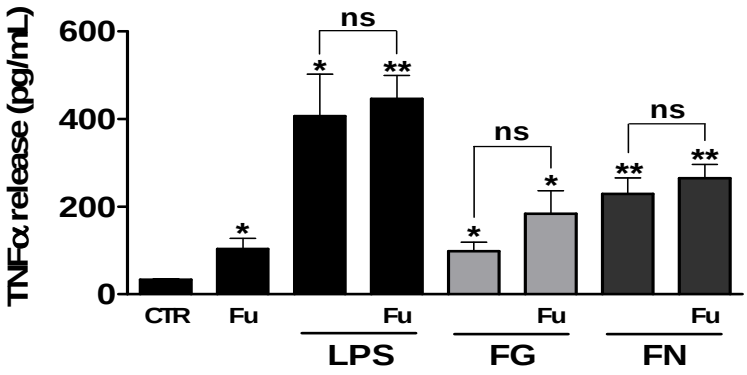

Figure 3.3.14. FN- but not FG-mediated responses are regulated by CD11b and scavenger receptor class A

A. Analysis of TNFα release in CGC cultures using an ELISA system after treatment for 24 hours with LPS (1 µg/ml), FG (2.5 mg/ml), FN (1 mg/ml), or LPS, FG and FN in combination with CD11b blocking antibody (10 µg/ml) or rat IgG as a serotype control (10 µg/ml). **B.** Western blot analysis of iNOS expression in CGC cultures after treatment for 24 hours with LPS (1 µg/ml), FG (2.5 mg/ml), FN (0.05-1 mg/ml) alone or in combination with Fucoidan (Fu; 100 µg/ml). A representative blot is shown in **Bi** and quantification of 3 independent experiments in **Bii**. **C.** Analysis of TNFα release in CGC cultures using an ELISA system after treatment for 24 hours as outlined in **B**. For each ELISA experiment, treatments were assayed in duplicate and data were analysed from 3 independent experiments. For comparisons between control levels and all other treatments, a one way ANOVA was performed with Dunnett's post-test. Paired two-tailed Student's *t*-tests were performed for direct comparisons between treatments alone or in combination inhibitors or serotype controls. Levels of significance were: non-significant $p>0.05$, * $p<0.05$, ** $p<0.01$, *** $p<0.001$.

3.3.8. Fibrinogen and fibrin treatment induces microglial superoxide production in CGCs, dependent on NADPH oxidase

To further characterise the microglia present in these CGC cultures, live cell staining for superoxide production was performed. Cultures were co-stained with isolectin-B4 (IB_4) and dihydroethidium (DHE) which stain microglia and produced superoxide, respectively (Streit 1990; Park & Jin 2008). Superoxide-positive microglia were identified by obvious red staining of the cell nucleus, and quantified.

Treatment of cultures with the positive control PMA, induced superoxide production in microglia, which could be significantly attenuated if cultures were pre-treated with apocynin (APO), an inhibitor of NADPH oxidase activity (Park & Jin 2008). Only the top concentration of FG significantly increased superoxide production in microglia, which could be attenuated by pre-treatment with APO (**Figure 3.3.15 A**). Treatment with lower concentrations of FG also induced significant superoxide production in the microglia present when compared with control levels, however pre-treatment with APO did not inhibit the superoxide production. Pre-treatment with APO caused significant attenuation of the superoxide produced by the highest concentration or FN (**Figure 3.3.15 A**).

This observed superoxide production was not involved in the FG- or FN-mediated TNFα release, as treatment of the CGCs with APO prior to FG or FN treatment for 24 hours did not significantly modulate release of the cytokine (**Figure 3.3.15 B**). Interestingly treatment with PMA for 24 hours significantly increased TNFα release in these cultures, and this also could not be attenuated by APO (**Figure 3.3.15 B**), suggesting NADPH oxidase-independent effects of PMA were responsible or the concentration used wasn't sufficient to attenuate the release. Finally, Hoechst-33342 staining on fixed CGC cultures to identify nuclear morphology was performed. Cultures treated with PMA for 24 hours showed no significant increase in cells displaying apoptotic morphology, when compared with control levels. Also, pre-treatment with APO did not induce any PMA-mediated effects. In line with previous findings, treatment

with FG for 24 hours induced a significant increase in apoptotic morphology, when compared with control levels, however pre-treatment with APO did not modulate this effect. Similarly, LPS administration for 48 hours caused a significant increase in apoptotic morphology when compared with control levels, with pre-treatment of cultures with APO having no significant effect (**Figure 3.3.15 C**). However, treatment with FN in the presence of APO caused a significant increase in cells displaying apoptotic morphology, suggesting some protective effects are mediated via NADPH oxidase activity (**Figure 3.3.15 C**).

Figure 3.3.15

Ai.

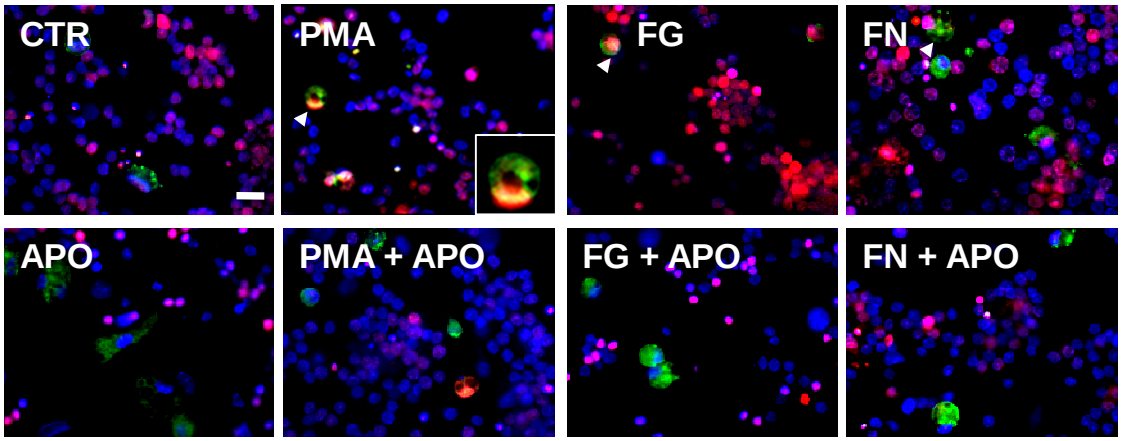

Aii.

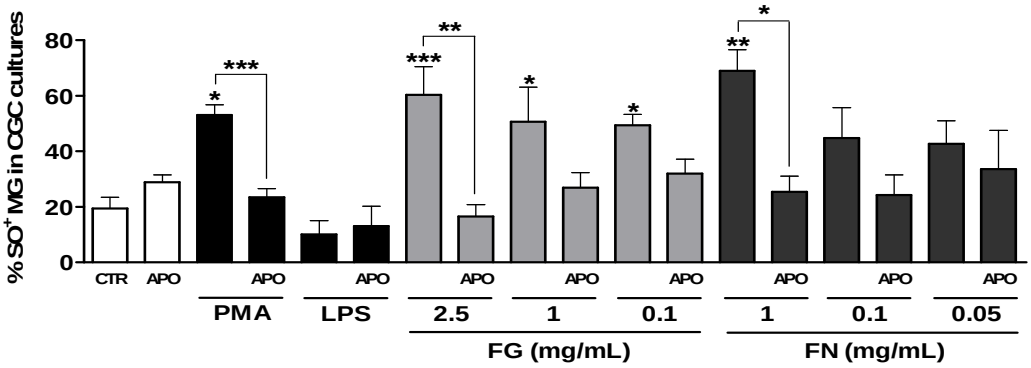

B.

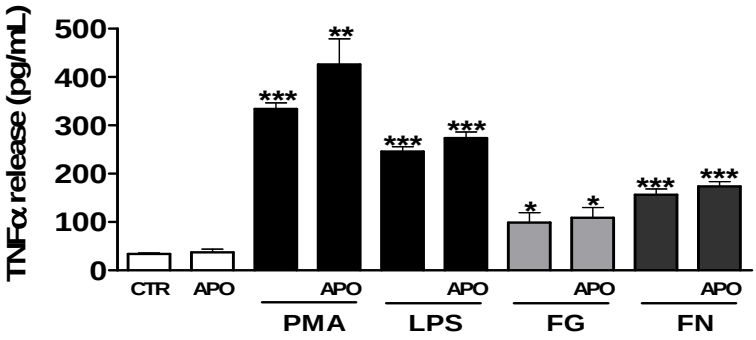

C.

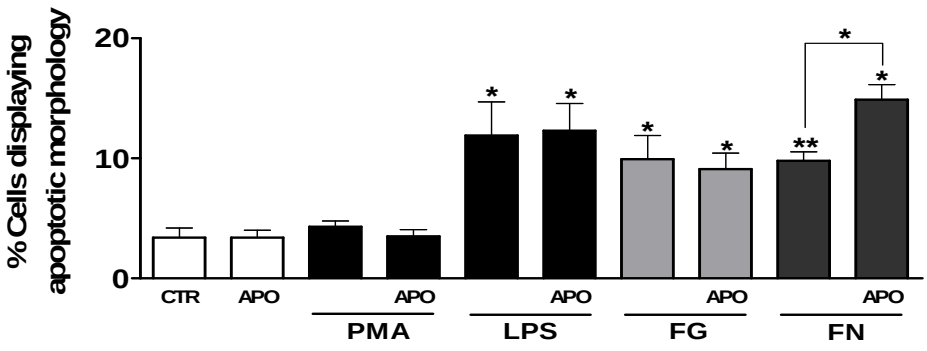

Figure 3.3.15. FG and FN induce superoxide production, but it is not involved in TNFα release or apoptosis

Ai. Representative images of live cell staining experiments performed on CGC cultures after treatment with PMA (10 ng/ml), FG (2.5 mg/ml), FN (1 mg/ml) or LPS (1 µg/ml), in the absence or presence of apocynin (APO; 10 µM), for 24 hours. Cell staining was performed with Hoechst-33342 for total cell number quantification, dihydroethidium (DHE; 5 µM) for the presence of superoxide (red), and IB_4 for the identification of microglia (green). Inset shows enlarged DHE^+ cell nuclei with arrowheads identifying other positively stained microglia. Original magnification: x40, scale bar: 20 µm. **Aii.** Specific quantification of the superoxide-positive microglia present in the CGC cultures with data presented as a percentage of total microglia displaying nuclear DHE staining. Treatments were in triplicate and data were analysed from 3 independent experiments. **B.** Analysis of TNFα release in CGC cultures using an ELISA system after treatment as outlined in **Ai**. **C.** Quantification of cells displaying apoptotic morphology after treatment as outlined in **Ai**. To compare between control levels and treatments, one way ANOVA tests were performed with Dunnett's post-test. For direct comparison between treatments in the absence and presence of inhibitors, paired two-tailed Student's *t*-tests were performed. Levels of significance were: non-significant $p>0.05$, * $p<0.05$, ** $p<0.01$, *** $p<0.001$.

3.3.9. The presence of serum causes differential release of pro-inflammatory cytokines

Interleukin-6 (IL-6) is another pro-inflammatory cytokine released from activated microglia (Horvath et al. 2008). Therefore, CGC cultures were assayed for IL-6 release by ELISA to identify whether this cytokine is released after treatment with FG and FN. Some cultures were pre-treated with LME to remove microglia, a CD11b blocking antibody, or rat IgG as an isotype control. Cultures were then treated with LPS, FG or FN for 24 hours and supernatants were assayed for IL-6 release. LPS treatment significantly induced IL-6 release after 24 hours, compared with control levels. Pre-treatment of cultures with LME, significantly attenuated the LPS-mediated release of IL-6, suggesting microglia are required for IL-6 release (**Figure 3.3.16**). Interestingly, FG treatment did not significantly induce IL-6 release, when compared with control levels. However, FN-treatment caused a significant induction in IL-6 release, which was significantly attenuated if microglia were depleted from the cultures prior to treatment (**Figure 3.3.16**). Also, in line with TNFα release data, CD11b block, caused significant attenuation of FN-mediated IL-6 release, however, as with TNFα release, no significant block was observed in LPS-treated cultures (**Figure 3.3.16**).

To identify if the lack of IL-6 release after FG treatment was due to the presence of serum in the cultures as previously suggested with respect to iNOS expression (**Figure 3.2.6 & 3.2.7**), a serum-free CGC culture medium was developed (**Section 2.3.3.1**). In serum-free conditions FG-treatment induced significant IL-6 release after 24 hours, when compared with control levels (**Figure 3.3.17 A**). Also pre-treatment of cultures with LME significantly attenuated the observed FG-mediated IL-6 release, supporting the requirement of microglia for IL-6 secretion in these cultures. Interestingly, LPS-induced IL-6 release in serum-free conditions (SF) is not significantly different from LPS-mediated release in serum-containing conditions (SC). However FN-mediated release in SF conditions is significantly lower than release observed in SC conditions. These data show differential effects of serum in all treatment groups.

Serum-free conditions were then subsequently tested in a TNFα release ELISA (**Figure 3.3.17 B**). Interestingly only a small insignificant increase in release was observed in FG treatment cultures when compared with release in conditions containing serum. Again, no significant modulation was seen in LPS-induced release. However, FN-mediated TNFα release was again significantly decreased in SF conditions compared with SC conditions (**Figure 3.3.17 B**).

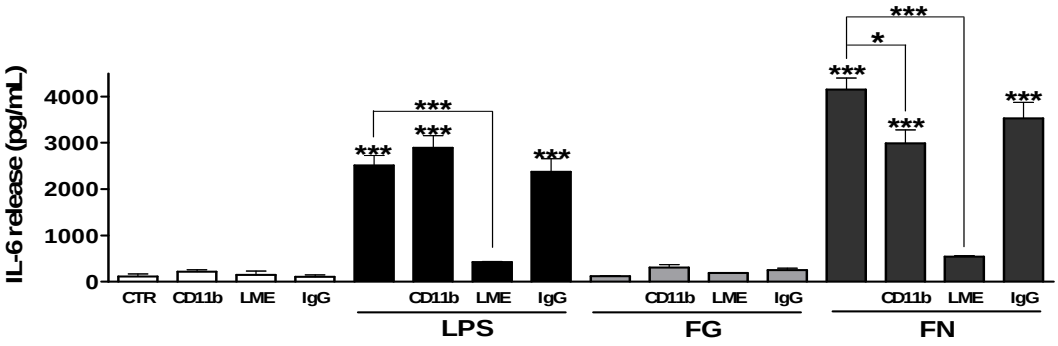

Figure 3.3.16. FN but not FG induces IL-6 release in serum-containing CGC cultures, dependent on microglia

Quantification of IL-6 release from CGC cultures after treatment with FG (2.5 mg/ml), FN (1 mg/ml) or LPS (1 µg/ml) alone or in combination with anti-CD11b blocking antibody (10 µg/ml) or rat IgG, as a serotype control (10 µg/ml), for 24 hours. In some instances, LME pre-treatment was performed to deplete microglia (LME). Treatments were in duplicate in each experiment and data were analysed from 3 independent experiments. A one-way ANOVA was performed with Dunnett's post-test to compare control levels with all treatments. Paired two-tailed Student's *t*-tests were performed for direct comparisons between treatments in the absence or presence of inhibitors or microglia. Levels of significance were: non-significant $p>0.05$, * $p<0.05$, *** $p<0.001$.

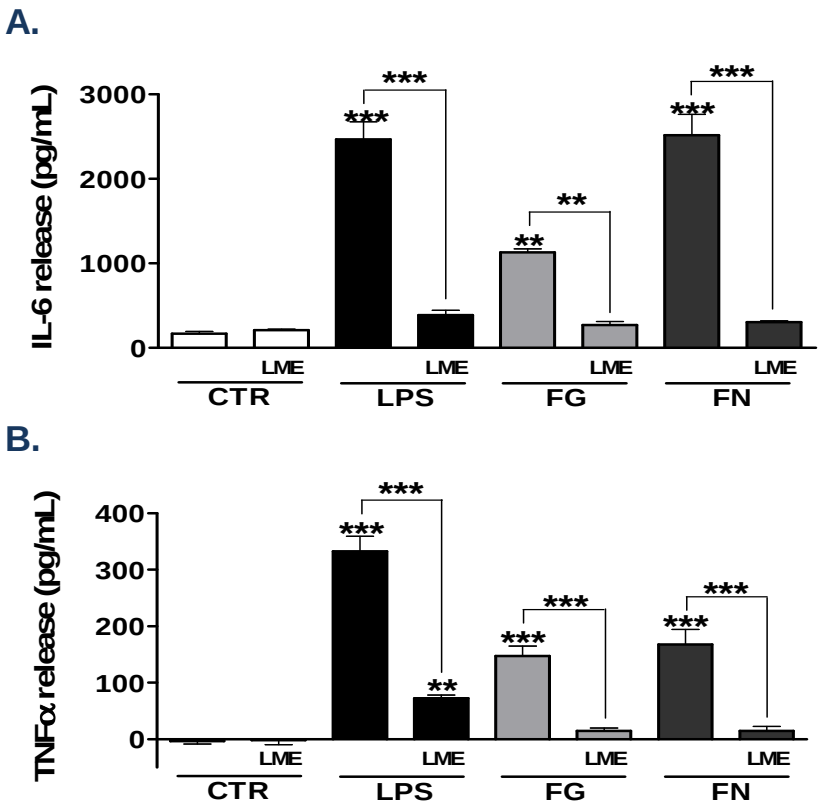

Figure 3.3.17. FG and FN induce IL-6 and TNFα release in serum-free CGC cultures, dependent on microglia

A. Quantification of IL-6 release using an ELISA system after treatment of serum-free CGC cultures with FG (2.5 mg/ml), FN (1 mg/ml) or LPS (1 µg/ml), +/- LME pre-treatment to deplete microglia (LME). **B.** Quantification of TNFα release using an ELISA system after treatment of serum-free CGC cultures as stated in **A**. Treatments were in duplicate in each experiment and data were analysed from 3 independent experiments. A one-way ANOVA was performed with Dunnett's post-test to compare control levels with all treatments. Paired two-tailed Student's *t*-tests were performed for direct comparisons between specific treatments in the absence or presence of microglia. Levels of significance were: non-significant $p>0.05$, ** $p<0.01$, *** $p<0.001$.

3.3.10. Expression of inducible, but not constitutive nitric oxide synthase is modulated by fibrin treatment of CGCs with dependence on TNFα synthesis

Changes in neuronal NOS (nNOS, bNOS, or NOS1), the constitutively expressed isoform, after treatment was initially characterised due to studies suggesting constitutive NOS isoforms can contribute to the activation of apoptotic pathways in the brain during inflammation (Czapski et al. 2007). Cultures were treated for 24 hours with FG, FN or LPS and ICC was performed (**Figure 3.3.18**). No obvious increase in nNOS expression was observed, suggesting a limited role for nNOS at 24 hours of treatment. However, these data are preliminary.

The inducible form of NOS (iNOS or NOS2) is a common marker for rodent microglial activation (Ferretti et al. 2011). Treatment for 24 hours with LPS or FN increased the number of microglia in culture expressing iNOS (**Figure 3.3.19**). FG caused the lowest increase in iNOS positive microglia, supporting earlier studies in primary microglial cultures (**Figure 3.2.7**). To further support these findings, Western blotting for iNOS expression was performed on the cultures. Some cultures were pre-treated with LME or AMT-HCl, a specific iNOS activity inhibitor (Combs et al. 2001). In support of the ICC data, significant iNOS expression was observed in LPS- and FN-treated cultures with no significant expression in FG-treated cultures (**Figure 3.3.19 B**). LME pre-treatment of cultures showed that the observed LPS- and FN-mediated iNOS expression depended on the presence of microglia due to the near complete attenuation of expression. Pre-treatment with AMT-HCl had no significant effect on expression (**Figure 3.3.19 B**).

Finally, to identify whether there is a convergence of iNOS and TNFα pathways after FN treatment, Western blotting for iNOS expression in cultures pre-treated with thalidomide was performed. Treatment with FG again showed no modulation of iNOS expression. Treatment with LPS and FN showed increased levels of iNOS expression which was down-regulated in the cultures pre-treated with thalidomide (**Figure 3.3.20**).

These data suggest LPS- and FN-mediated iNOS expression is dependent on TNFα synthesis. However, these data are preliminary.

Figure 3.3.18

A.

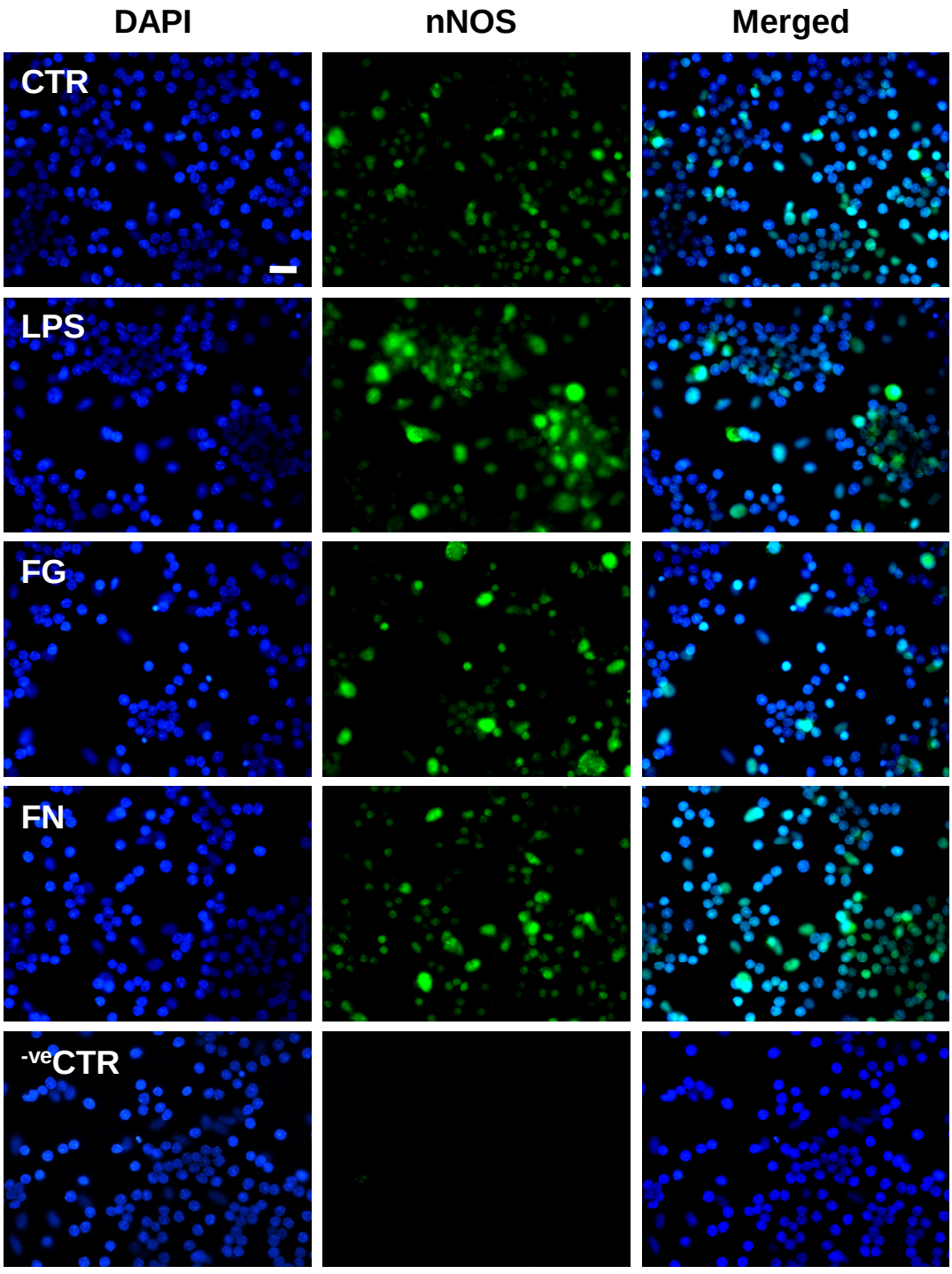

Figure 3.3.18. FG or FN treatment does not modulate nNOS expression in CGC cultures

A. Representative images of CGC cultures after 24 hours of treatment with FG (2.5 mg/ml), FN (1 mg/ml) or LPS (1 µg/ml). Cultures were co-stained with DAPI for quantification of cell number and probed with anti-nNOS (green), except in negative control cultures, where the primary antibody was omitted. Original magnification: x40, scale bar: 20 µm. N = 1.

Figure 3.3.19

A.

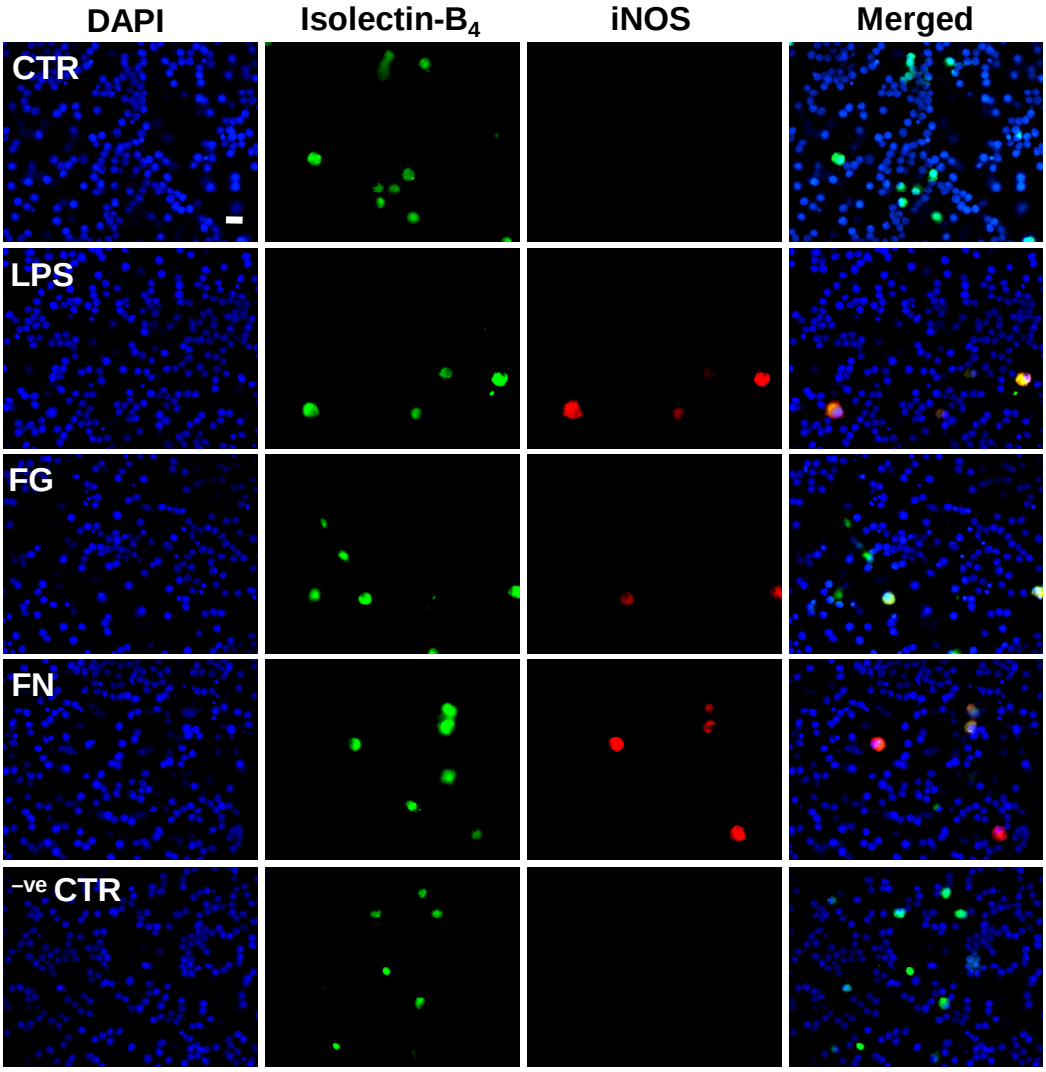

Bi.

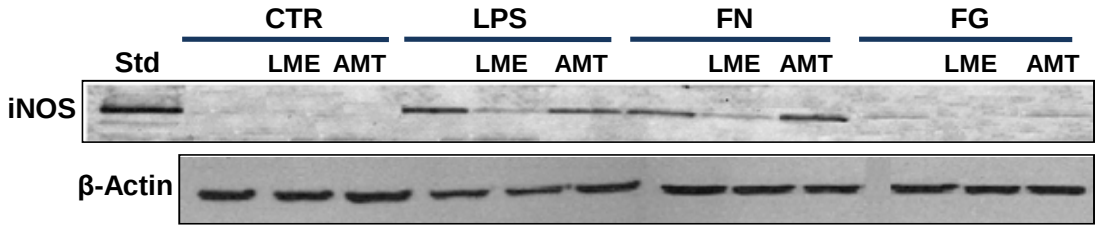

Bii.

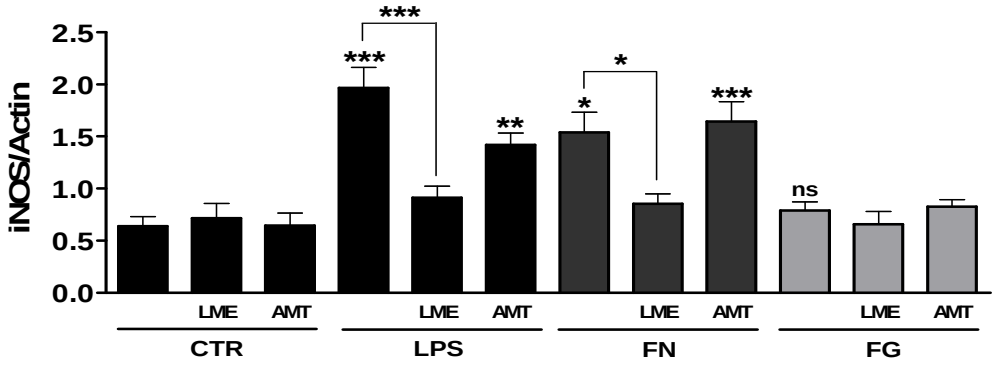

Figure 3.3.19. FN but not FG treatment increases microglial-associated iNOS expression in CGC cultures

A. Representative images of CGC cultures after treatment with FG (2.5 mg/ml; 24 hours), FN (1 mg/ml; 48 hours) or LPS (1 µg/ml; 48 hours). Cultures were co-stained with DAPI for quantification of cell number, IB_4 for microglial identification (green) and probed with anti-iNOS (red), except in negative control cultures, where IB_4 and anti-iNOS were omitted. Original magnification: x40, scale bar: 20 µm. **Bi.** Representative Western blots for iNOS and β-actin expression in CGC cultures after treatment as stated in **A**, alone or in combination with AMT-HCl (AMT; 150 nM), +/- LME depletion of microglia (LME). **Bii.** Quantification of iNOS expression with respect to protein-loading control, β-actin. For ICC experiments, treatments were in duplicate in each experiment and data were analysed from 2 independent experiments. For Western blotting experiments treatments were repeated in 3 independent experiments. One way ANOVA with Dunnett's post-test was performed to compare control levels with all other treatments. For specific comparisons paired two-tailed Student's *t* tests were performed. Levels of significance were: non-significant $p>0.05$, * $p<0.05$, ** $p<0.01$, *** $p<0.001$.

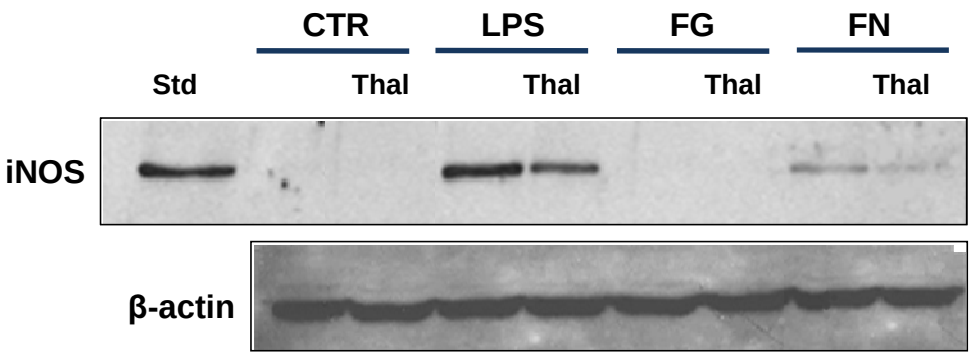

Figure 3.3.20. FN-mediated iNOS expression in CGC cultures is attenuated by thalidomide pre-treatment

Representative Western blots for iNOS and β-actin expression in CGC cultures treated with FG (2.5 mg/ml; 24 hours), FN (1 mg/ml; 48 hours) or LPS (1 µg/ml; 48 hours) alone or in combination with Thalidomide (Thal; 10 µg/ml). N = 1.

3.4. The effects of modulating microglial function on fibrinogen- and fibrin-induced cerebellar granule cell toxicity

Polymyxin B (PMX) does not inhibit FG- or FN-mediated responses in microglia (**Figure 3.2.4 & 3.2.6**). To further support this hypothesis, Hoechst-33342 fixed cell staining was performed on cultures after treatment with PMX prior to exposure to FG or FN for 24 and 48 hours, respectively, and apoptotic morphology was quantified. As expected, 48 hours of LPS treatment induced significant apoptotic morphology, which could be significantly inhibited by pre-treating cultures with PMX (**Figure 3.4.1**). Also, in support of previous findings, FG-induced a significant increase in apoptotic morphology, when compared with control, which could not be inhibited by pre-treatment of cultures with PMX. Similarly, FN induced a significant increase in apoptotic morphology compared with control levels, which could not be significantly inhibited by pre-treatment with PMX (**Figure 3.4.1**).

Ai

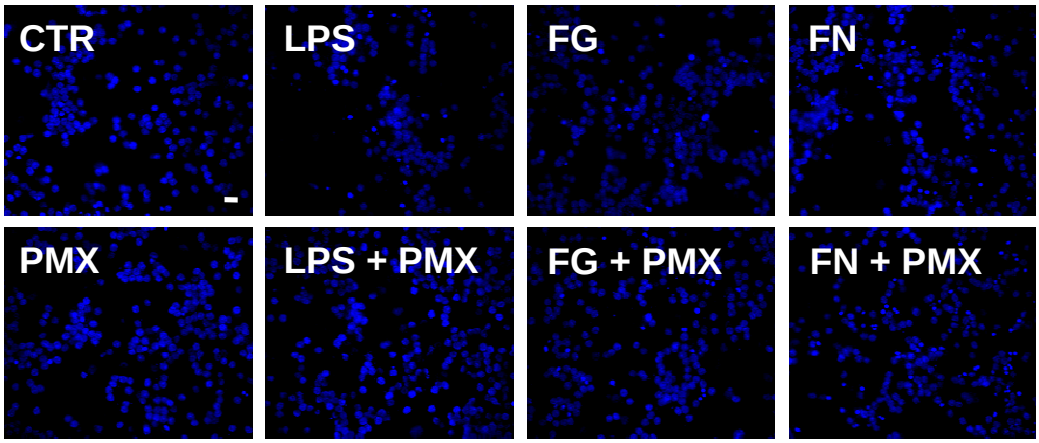

Aii

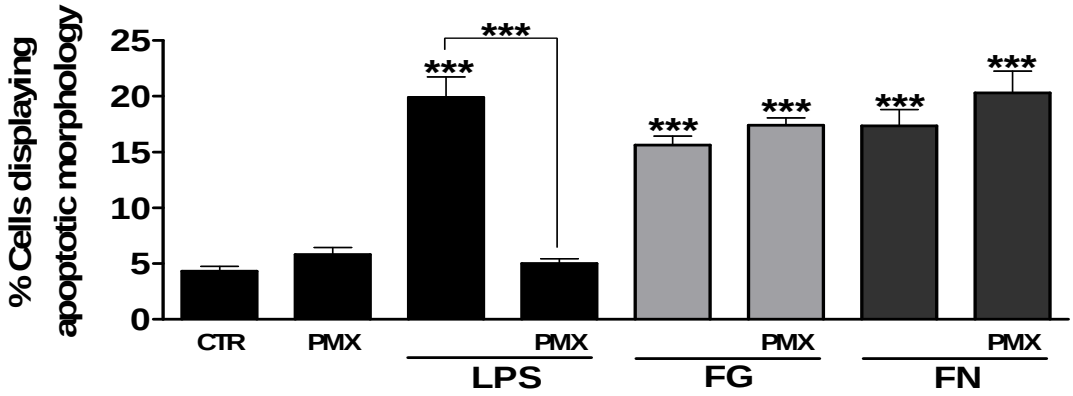

Figure 3.4.1. FG- and FN-mediated neuronal death is not due to endotoxin contamination

Ai. Panel of representative images of fixed cell staining experiments in CGC cultures after treatment with FG (2.5 mg/ml; 24 hours), FN (1 mg/ml; 48 hours) or LPS (1 µg/ml; 48 hours) alone or in combination with PMX (100 nM). Cell staining was performed with Hoechst-33342 for nuclear morphology analysis. Original magnification: x40, scale bar: 20 µm. **Aii.** Quantification of apoptotic morphology in CGC cultures treated as stated in **Ai**. Data are presented as a percentage of the total population displaying apoptotic nuclear morphology. Treatments were in triplicate and data were analysed from 3 independent experiments. To compare between control levels and treatments, a one way ANOVA was performed with Dunnett's post-test. For direct comparison between specific treatments, paired two-tailed Student's *t*-tests were performed. Levels of significance were: non-significant $p>0.05$, *** $p<0.001$.

3.4.1. Pharmacological inhibition of TNFα synthesis, but not iNOS activity protects against fibrinogen- and fibrin-mediated toxicity

TNFα release was a prominent feature of both FG- and FN-treated cultures, suggesting a role for this cytokine in observed neuronal toxicity. Therefore, CGC cultures were treated with TNFα synthesis inhibitor, thalidomide prior to FG treatment for 24 hours or FN treatment for 48 hours. Pre-treatment was also performed with AMT-HCl (**Figure 3.4.2**).

Inhibition of TNFα synthesis, caused a significant reduction in observed apoptotic morphology in LPS-treated, however cells displaying apoptotic morphology was still significantly above control levels. Similarly, pre-treatment of LPS-treated cultures with AMT-HCl, significantly reduced apoptotic morphology, however, as with thalidomide pre-treatment, levels of apoptotic morphology were still significantly above that observed in control cultures (**Figure 3.4.2**). Pre-treatment with thalidomide also caused significant attenuation of FG-induced increases in apoptotic morphology, however, AMT-HCl pre-treatment had no significant effect. Following a similar profile, FN-induced increases in apoptotic morphology could be significantly attenuated by thalidomide pre-treatment, with AMT-HCl pre-treatment having no effect (**Figure 3.4.2**). Pre-treatment with thalidomide did not completely attenuate FN-mediated death. Finally, as expected, depletion of microglia prior to treatments caused an attenuation of the protective effect mediated by thalidomide pre-treatment in cultures exposed to FN, further supporting the prominent role for microglia in the TNFα-dependent death.

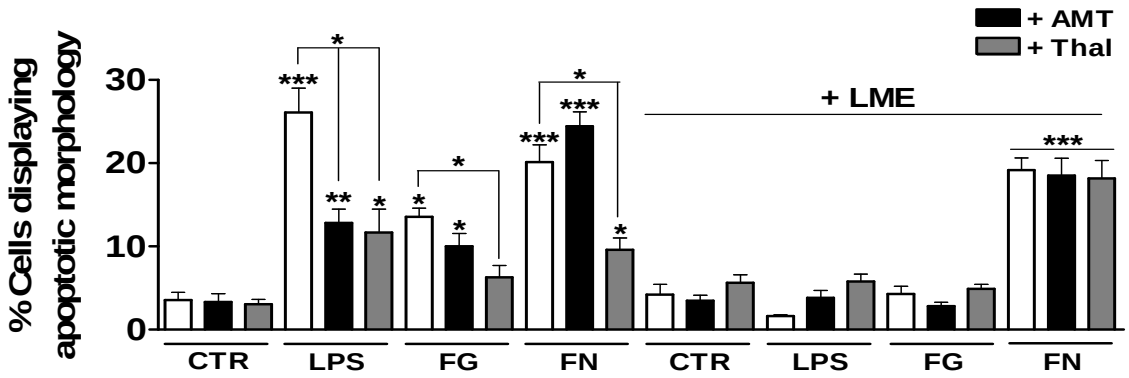

Figure 3.4.2. FG- and FN-mediated neuronal death involves TNFα synthesis, but not iNOS activity

Quantification of fixed cell staining experiments in CGC cultures after direct treatment with FG (2.5 mg/ml; 24 hours), FN (1 mg/ml; 48 hours) or LPS (1 µg/ml; 48 hours) alone or in combination with AMT (150 nM) or Thal (10 µg/ml), +/- LME depletion of microglia. Cell staining was performed with Hoechst-33342 for nuclear morphology analysis. Treatments were in duplicate and data were analysed from 3 independent experiments. Data are presented as the percentage of the total population displaying apoptotic nuclear morphology. To compare between control levels and all other treatments, a one way ANOVA was performed with Dunnett's post-test. For direct comparison between specific treatments, paired two-tailed Student's *t*-tests were performed. Levels of significance were: non-significant $p>0.05$, * $p<0.05$, ** $p<0.01$, *** $p<0.001$.

3.4.2. Microglia are responsible for the release of neurotoxic factors after fibrinogen and fibrin treatment

To support the role for microglia in mediating the observed neuronal toxicity, experiments were performed using microglial-conditioned medium (MGCM). Primary microglial cultures were treated with thalidomide or AMT-HCl prior to exposure to LPS, FG, or FN for 24 hours. The MGCM was collected from these cultures and administered to CGCs that had been depleted of microglia and incubated for a further 24 hours (**Figure 3.4.3**). Exposure of the CGCs to MGCM from LPS-treated microglia induced a significant increase in apoptotic morphology, compared with cultures exposed to non-treated control MGCM. Furthermore, exposure of CGCs to MGCM from LPS-treated cultures pre-treated with thalidomide or AMT-HCl, significantly reduced the LPS-mediated increase in apoptotic morphology (**Figure 3.4.3**). Again, in line with the direct treatment of neuronal cultures, exposure of CGCs to MGCM from FG-treated microglia induced a significant increase in cells displaying apoptotic morphology. Exposure of CGCs to MGCM from FG-treated cultures pre-treated with thalidomide, significantly reduced the FG-mediated increase in apoptotic morphology, however, MGCM from FG-treated cultures pre-treated with AMT-HCl could not significantly reduce FG-mediated increases in apoptotic morphology (**Figure 3.4.3**). Similarly, exposure of the neuronal cultures to MGCM from FN-treated microglia induced a significant increase in apoptotic morphology with MGCM pre-treated with thalidomide attenuating the FN-induced effect and AMT-HCl pre-treatment having no effect.

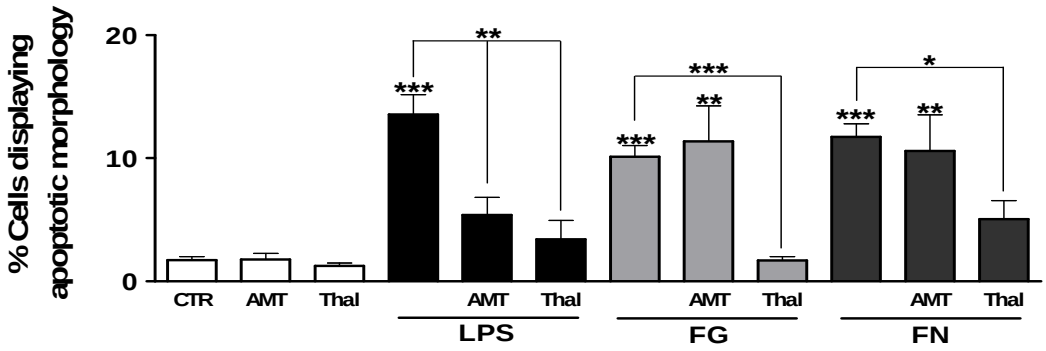

Figure 3.4.3. FG and FN mediate neuronal death via microglia, with significant dependence on TNFα synthesis

Quantification of fixed cell staining experiments on CGC cultures after exposure to microglial condition medium (MGCM) from primary cultures treated with FG (2.5 mg/ml), FN (1 mg/ml) or LPS (1 µg/ml) alone or in combination with AMT (150 nM) or Thal (10 µg/ml), for 24 hours. Cell staining was performed using Hoechst-33342 for nuclear morphology analysis. Treatments were in duplicate and data were analysed from 3 independent experiments. Data are presented as the percentage of the total population displaying apoptotic nuclear morphology. To compare between control levels and all other treatments, a one way ANOVA was performed with Dunnett's post-test. For direct comparison between specific treatments, paired two-tailed Student's *t*-tests were performed. Levels of significance were: non-

3.4.3. Inhibition of caspase-3 activation in microglia attenuates fibrin- and fibrinogen-mediated neurotoxicity

Due to the observation in primary microglial cultures, that cleavage of caspase-3 was significantly induced after FG and FN treatment for 24 hours with little or no significant death, MGCM assays using the pan-caspase inhibitor, z-VAD-FMK, were performed. As in the thalidomide and AMT-HCl MGCM assays, primary microglial cultures were treated with z-VAD-FMK prior to treatment with LPS, FG or FN for 24 hours. The MGCM was then administered to CGCs depleted of microglia and incubated for a further 24 hours (**Figure 3.4.4**). As shown previously, CGCs exposed to MGCM from LPS-, FG- and FN-treated cultures have a significantly higher number of cells displaying apoptotic morphology, when compared with control cultures. Furthermore, MGCM from LPS-, FG-, or FN-treated cultures pre-treated with z-VAD-FMK significantly attenuated the increases in apoptotic morphology when compared with relevant treatment groups (**Figure 3.4.4 Aii**). Finally to be noted, CGCs treated with MGCM from FN + z-VAD-FMK cultures still had a significant number of cells displaying apoptotic morphology compared with control levels (**Figure 3.4.4 Aii**), suggesting a caspase-3 independent mechanism for some FN-mediated neurotoxicity or possible transfer of FN in the medium.

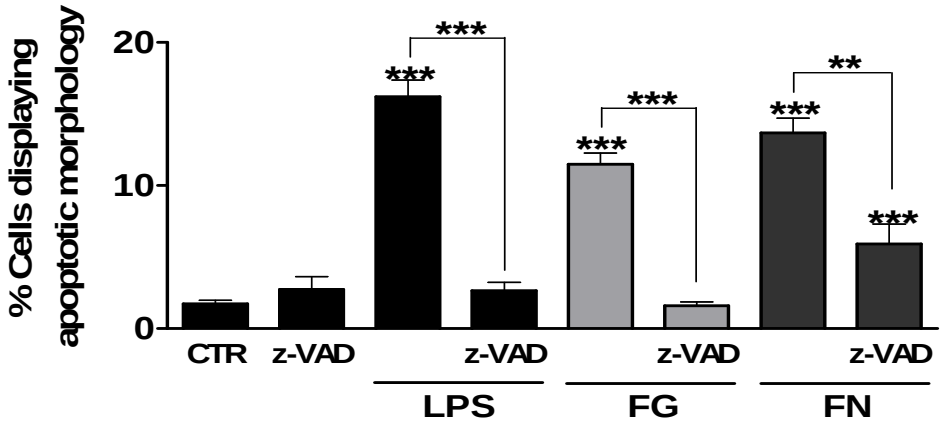

Figure 3.4.4. FG- and FN-mediated neuronal death via microglia can be attenuated by microglial-specific caspase inhibition

Quantification of apoptotic morphology in CGC cultures after exposure to MGCM from primary cultures treated with FG (2.5 mg/ml), FN (1 mg/ml) or LPS (1 µg/ml) alone or in combination with z-VAD-FMK (1 µg/ml) for 24 hours. Cell staining was performed using Hoechst-33342 for nuclear morphology analysis. Data are presented as the percentage of the total population displaying apoptotic nuclear morphology. Treatments were in triplicate and data were analysed from 3 independent experiments. To compare between control levels and treatments, a one way ANOVA with Dunnett's post-test was performed. For direct comparison between specific treatments, paired two-tailed Student's *t*-tests were performed. Levels of significance were: non-significant $p>0.05$, ** $p<0.01$, *** $p<0.001$.

3.5. Discussion

This chapter characterises microglia and neuronal culture responses after exposure to FG and FN. Pharmacological manipulation of the FG and FN responses were characterised using either direct or indirect administration of inhibitors. Initially, toxicity was quantified and differential observations after FG or FN treatment were observed. Furthermore, expression of iNOS, ED-1 and CD11b and cytokine release were characterised, again with differences between the treatments being observed. Development of methodology, here, to deplete microglia from the cerebellar granule cultures supports significant differential roles for microglia in FG and FN-mediated neurotoxicity, *in vitro*, with further support from indirect conditioned medium experiments.

3.5.1. FG and FN can induce microglial activation, but only FN is toxic

It has been suggested that FN deposition contributes to pathology (Paul et al. 2007). Therefore the toxic effect of FN and the soluble precursor FG on primary microglial cultures was quantified by assessing morphological changes associated with different forms of death. Apoptosis or programmed cell death in a culture can be characterised by quantification of cells displaying classic morphological features including membrane blebbing and bright pyknotic nuclei, due to chromatin condensation (Kerr et al. 1972). Necrosis is a passive form of cell death lacking the regulatory mechanisms characteristic of apoptosis. Although necrotic cell death morphology is more diverse than apoptotic morphology, due to its unregulated nature, some characteristics are common. These include early membrane permeability and nuclear dilation (Ziegler & Groscurth 2004). Nuclear dilation is a simple morphological change to quantify, and was therefore used for this initial analysis of FN and FG toxicity.

Apoptotic morphology in microglia treated with FG or FN for 24 hours was almost non-existent unlike microglia treated with staurosporine (STS), a classic inducer of apoptosis (Kingham & Pocock 2000). Furthermore data presented here suggest that

exposure to LPS, the classic treatment to model microglia inflammatory responses (Block et al. 2007; Saijo et al. 2009; Burguillos et al. 2011), also failed to induce significant apoptotic morphology after 24 hours of treatment. Previously published literature, including work in our lab has shown LPS treatment of microglia can induce significant apoptosis (Lee et al. 2001; Taylor et al. 2003). However, recent work suggests LPS does not induce significant apoptosis until chronic treatment is reached (>48 h) (Burguillos et al. 2011). These differences in LPS-mediated effects are possibly due to variations in the LPS serotype used. It has been shown previously that prostacyclin synthesis from human endothelial cells differs depending on the LPS serotype administered (Watanabe & Jaffe 1993). However, differences in culture preparation and media composition could also contribute to this variation and timecourse analyses of apoptotic induction after treatment would provide a clearer picture.

Cultures treated with FN, but not FG showed a significant increase in the percentage of cells displaying enlarged, dilated nuclei, the morphological change used here to quantify necrosis. No direct link between FN and microglial necrosis has previously been shown. However, leakage of factors from necrotic cells, due to increased membrane permeability, initiates or potentiates pro-inflammatory responses (Hirt & Leist 2003), and studies that deplete fibrin from animal models of multiple sclerosis and Alzheimer's disease have shown significant attenuation of inflammation (Akassoglou et al. 2004; Paul et al. 2007). This suggests FN deposition in the CNS is capable of activating an inflammatory response, which could be due to the FN-mediated induction microglial death observed here.

Previous studies have identified CD11b as a marker of microglial activation which is upregulated in AD brains (Akiyama & McGeer 1990). Furthermore, the receptor has been identified as key to FG-mediated phagocytosis by microglia, *in vitro* (Adams et al. 2007a). Therefore, changes in CD11b receptor expression were deemed a relevant

marker of microglial activation after FG or FN treatment. Significantly increased microglial surface expression of CD11b, similar to that observed after LPS treatment, which has been shown to rapidly increase surface expression of CD11b on monocytes by 2 - 3 fold (Fan & Edgington 1991) is shown after FG and FN treatment. These data support previous findings and suggest that FG and FN can induce an activated microglial phenotype.

3.5.2. FG and FN induce TNFα release from microglia

Further characterisation of the activated microglia phenotype was performed by analysis of TNFα release after treatment with FG and FN. TNFα is a well characterised pro-inflammatory cytokine involved in many neuroinflammatory cascades, including autocrine microglia activation (Kuno et al. 2005) and direct apoptosis via activation of extrinsic pathway-associated TNF receptors (Kaul et al. 2001; Taylor et al. 2005). It is shown that treatment of primary microglial cultures, but also CGC cultures, with FG or FN significantly induced TNFα release, with differential profiles. It is also shown, in CGC cultures, that FG- and FN-induced TNFα release is dependent on microglia. Furthermore, the concentrations released were similar or above previously published concentrations shown to be sufficient to induce neurotoxicity (Taylor et al. 2005). As previously reported (Nguyen et al. 2002), and supported here, LPS can significantly induce TNFα release from microglia. FN-, but not FG-mediated induction of TNFα release in both cultures followed a similar pattern of release to that observed after LPS treatment. Possible contamination of the FN preparations with endotoxin (LPS) was therefore suggested. Published literature states that only 40 pg/ml of LPS is required to induce microglial proliferation, NO production and cytokine release (Weinstein et al. 2008). Cultures treated with polymyxin B (PMX), an antibiotic that binds to the biologically active portion of the LPS macromolecule known as lipid A (Morrison & Jacobs 1976) and potently abolishes LPS responses (Jacobs & Morrison 1977), prior to FG and FN exposure were still able to induce significant TNFα release comparable to PMX-negative cultures. Furthermore, support for the induction of differing pathways

in microglia after FG or FN treatment compared with LPS was found by co-treating CGC cultures with either FG or FN and LPS. If LPS, FG and FN are inducing TNFα release via the same pathway, co-treatment of cultures would not significantly enhance release when compared with sole-treatment of cultures. However, significant increases in release were observed in both FG-LPS and FN-LPS treated cultures. Additionally, pre-treatment with PMX did not attenuate FG- or FN-mediated neuronal apoptosis. These data suggest that FG- or FN-mediated responses are not due to endotoxin contamination and induce TNF release via differing pathways to LPS.

3.5.3. Involvement of the p38-MAPK pathway in FG-mediated responses

It was decided at an early stage to focus mainly on FG-mediated signalling over FN. This was mainly due to solubility issues with FN which prevented exact concentration dependent analysis, but was also because focussing on the earlier event, i.e. FG extravasation into the CNS parenchyma, would be more interesting and significant from a disease progression viewpoint. However, wherever possible FN treatment was performed in parallel with FG treatment.

LPS-mediated TNFα release has been shown to be dependent on activation of the p38-MAPK pathway (Nakajima et al. 2004). Also the PI3K pathway has been shown to be involved in FG-mediated microglial phagocytosis (Adams et al. 2007a) and microglial-mediated neurotoxicity after amyloid-β treatment (Zhang et al. 2011). Data presented here suggests that pre-treatment of primary microglial cultures with SB203580, an inhibitor of p38-MAPK, using a previously published concentration (Kim et al. 2002), significantly decreased FG-mediated TNFα release after 24 hours. However inhibition of PI3K with the specific inhibitor wortmannin, at a previously published concentration (Morgan et al. 2004), could not attenuate FG-mediated TNFα release. In CGC cultures, p38-MAPK phosphorylation significantly increased, time-dependently after FG treatment until 24 hours, whereas FN treatment only induced an early significant increase in phosphorylation. These data suggest FG-mediated TNFα

release is dependent on the p38-MAPK pathway, which was shown to be significantly phosphorylated over time. However no role for the PI3K pathway was observed in FG-mediated TNFα release suggesting the role of other MAPKs should be investigated.

3.5.4. FG-mediated iNOS expression was dependent on serum conditions

The expression of iNOS is a classic marker of activated microglia (Ferretti et al. 2011). Previous studies in our laboratory had given differential expression of iNOS after FG treatment (E. East, unpublished observations; I. Sevastou, unpublished observations). Interestingly the FG-mediated iNOS expression in microglial cultures seemed to be dependent on the presence or absence of serum. In serum-free conditions both FG and FN treatment significantly induced expression of iNOS to a level similar to that observed after LPS treatment. However, in serum-containing conditions, FG-induced iNOS expression was non-existent, with no significant change in FN- or LPS-mediated expression. Interestingly, the same loss of FG-induced iNOS expression when serum was present was observed in CGC cultures. However in primary microglial cultures and CGCs treated with FG, increased expression of ED-1, a marker of phagocytic, activated microglia (Damoiseaux et al. 1994; Pinteaux-Jones et al. 2008), was observed. It is also shown that TNFα and IL-6 release is differentially induced after FG treatment of CGCs. These data suggest that serum can preferentially mask FG-mediated iNOS expression and cytokine release but microglial activation still occurs. In a physiological situation, other serum factors are likely to extravasate from vasculature into the CNS parenchyma, subsequently suggesting that iNOS expression and IL-6 release may not be important in FG-mediated toxicity. Many human studies suggest macrophage and microglial activation is independent of significant iNOS expression and NO release (Peterson et al. 1994; Denis 1994; Colton et al. 2000; Carter & Dick 2003). Interestingly, published data have suggested both TNFα and IL-6 production can be induced by FG treatment of PBMCs, *in vitro* (Jensen et al. 2007). These studies however use serum-free conditions. TNFα release by LPS stimulation however, has been shown to be markedly enhanced in the presence of FG, in serum-containing

conditions (Fan & Edgington 1993), supporting a significant role for TNFα in FG-associated inflammation. Here, it is also shown that iNOS expression after FN and LPS treatment is coupled to TNFα synthesis with thalidomide treatment attenuating iNOS expression although inhibition of iNOS activity had no significant effect on FN-mediated neurotoxicity. No significant modulation in the constitutively expressed NOS isoform, nNOS was observed, further suggesting that NOS enzymes are not significantly involved in FG- or FN-mediated toxicity

Inhibition of FG binding to microglial CD11b down-regulates iNOS expression in a model of MS, in vivo (Adams et al. 2007a). Nitric oxide (NO), the product of an iNOS-catalysed reaction has been shown to induce neuronal death by inhibiting the mitochondrial respiratory chain (Bal-Price & Brown., 2001). These findings suggest iNOS expression could be important in disease progression. Analyses of the FG structure have suggested that for FG-CD11b ligation to occur, the protein must be 'immobilised'. This 'immobilisation' un-masks a cryptic binding site in the γ-chain C domain of the protein ($\gamma^{377-395}$) that allows FG-CD11b ligation (Lishko et al. 2002). Adams and colleagues use 'immobilised' fibrinogen as a model of fibrin deposition (Adams et al. 2007a). The main criticism of this model would be that coverslips were coated in FG in order to immobilise the protein prior to culturing of microglia, preventing any initial resting phenotype required for a baseline culture activation state. Interestingly, the same group that discovered $\gamma^{377-395}$ as the cryptic binding site published another paper two years later identifying further binding sites in the FG molecule for CD11b (Lishko et al. 2004). Furthermore soluble FG has been shown to interact with CD11b on polymorphonuclear leukocytes, mediating phagocytosis (Rubel et al. 2002) and induce pro-inflammatory cytokine release from isolated peripheral mononuclear blood cells (Jensen et al. 2007).

3.5.5. Caspase involvement in FG- and FN-mediated responses

Caspase activation is a classic hallmark of apoptotic cell death (Yuan et al. 2003; Danial & Korsmeyer 2004). Due to differing observations in our lab, ICC studies were performed on primary microglial cultures to identify whether cleaved caspase-3, the classic executioner caspase, was upregulated after treatment with FG and FN. As expected, treatment of microglial cultures with staurosporine induced significant expression of cleaved-caspase-3. Interestingly, caspase-3 cleavage after LPS treatment was significantly above that observed in control cultures however no significant increase in cells displaying an apoptotic nuclear morphology was observed. In the context of data presented here, this suggests caspase-3 cleavage can occur in microglia after LPS treatment as part of a non-apoptotic pathway. In support of these findings, Burguillos and colleagues published a paper earlier this year, providing strong evidence for LPS-induced, non-apoptotic induction of caspase-8 and caspase-3/7 in microglia that was involved purely with cellular activation (Burguillos et al. 2011). Caspase-3 cleavage in microglial cultures also occurred after FG- and FN-treatment. FN-mediated induction was associated with an increase in death, although it seemed to be necrotic cell death as previously described. FG-mediated caspase-3 cleavage was not associated with an increase in apoptotic morphology, in line with the LPS data. However, longer incubations may reveal that significant apoptosis does occur and timecourse analyses and the use of biochemical assays, such as the LDH assay would provide more conclusive data. Finally it is shown here that inhibition of caspase activation, specifically in microglia, is sufficient to attenuate FG- and FN-mediated neurotoxicity. However, it is possible that the pan-caspase inhibitor used to inhibit microglial caspase activation was transferred to the CGCs in the MGCM that was administered, providing direct protection rather than via microglial down-regulation. Protein silencing techniques specifically in microglia would remove this particular caveat and provide more robust data.

Together, these data suggest that caspase-3 cleavage in microglia can no longer confirm cellular apoptosis. Other markers such as Annexin V or caspase-3/7 expression in parallel with poly(ADP-ribose) polymerase (PARP-1) expression, a nuclear substrate of caspase-3, that is also involved in caspase-independent apoptosis (Hong et al. 2004), must be performed to truly identify whether apoptosis is occurring. Conversely, only using apoptotic morphology as a marker, as presented here, it cannot be comprehensively concluded that apoptosis in microglial cultures after treatment with FG or LPS does not occur.

3.5.6. Modelling FG- and FN-mediated neuronal toxicity – involvement of microglia

The loss of neurons underlies cognitive decline in neurodegenerative disorders (Alzheimer et al. 1995; Qiang et al. 2011). Whether this is due to indirect inflammation, intrinsic neuronal vulnerability, or a combination of both is yet to be elucidated with numerous arguments for and against each paradigm (Wyss-Coray & Mucke 2002; Saxena & Caroni 2011). It is therefore important to understand whether extravasation of blood-borne proteins, including FG, into the CNS parenchyma due to blood brain barrier dysfunction, and the subsequent deposition of FN can directly affect neuronal integrity.

Significant apoptotic morphology after FG treatment for only 24 hours in CGC cultures was observed here, whereas FN- and LPS-mediated toxicity was not present until 48 hours of exposure. These data suggest an early potently toxic effect of FG in neuronal cultures. Previous data suggesting administration of high molecular weight proteins, such as FG, can produce a hypertonic ‘extracellular’ culture medium that causes cell shrinkage (Horie et al. 1989) led us to check the ‘apoptotic’ morphology observed. The use of live Annexin V-FITC, live caspase-3/7, fixed caspase-3 ICC and lactate dehydrogenase release here provided strong support for apoptotic pathways being induced by FG and FN with ICC of caspase-3 expression supporting a neuronal

specific induction of the caspase, with respect to the observed apoptosis. These data suggest a more potently neurotoxic role for FG than previously published data that suggests inhibition of neurite outgrowth occurs in the presence of FG, but not significant neuronal death (Schachtrup et al. 2007).

As recently suggested, with respect to microglial activation (Burguillos et al. 2011), non-apoptotic roles for caspases have also been identified in neuronal cells, from *in vitro* drosophila neuronal models (Kuo et al. 2006), to mouse models of Alzheimer's disease (D'Amelio et al. 2011). Significant non-apoptotic caspase-3 activation in long term depression (LTD) and long term potentiation (LTP) (Li et al. 2010; Jo et al. 2011), phenomena associated with learning and memory (Malenka & Bear 2004), have also been observed. However with the range of staining protocols, morphological changes and biochemical assays, data presented here strongly suggests classical apoptosis and neuronal toxicity is occurring after FG and FN treatment of CGC cultures

Within the CNS, LPS induces its neurotoxicity primarily through activation of microglia, with a positive correlation being observed between abundance of microglia and sensitivity to LPS-induced neurotoxicity (Kim et al. 2000) so, it was expected that LPS treatment of neuronal cultures would not induce toxicity unless microglia were present. However, data presented here shows that after 48 hours of LPS treatment, significant apoptotic morphology occurs in the CGC cultures. These data suggest that either LPS can mediate direct neurotoxic effects, or that immune-competent cells such as microglia are present in the neuronal cultures, and chronic exposure (>24 h) of the 'contaminating' microglia to LPS is able to induce indirect neurotoxicity.

Manipulation of the neuronal cultures to specifically deplete 'contaminating' microglia using leucine-methyl-ester enabled us to identify the important role for microglia in LPS-mediated responses including TNFα release and neurotoxicity in CGC cultures. It also provided an opportunity to model and manipulate other responses hypothesised to be due to microglia. Leucine-methyl-ester (LME) as a phagocyte-specific executioner

has been used previously in our laboratory to deplete microglia from primary cultures (Morgan et al. 2004) with other groups using the compound to deplete microglia from astrocyte cultures (Hamby et al. 2006). Also, the compound has been used. LME is a lysosomotropic agent originally used to selectively destroy macrophages (Thiele et al. 1983). Here, it is shown that LPS-mediated neurotoxicity observed after 48 hours, could be ablated if microglia were depleted. The observed increase in apoptotic morphology seen after 24 hours exposure of the CGC cultures to FG could also be attenuated by LME pre-treatment, suggesting this initial early toxicity is indirect via a microglial-dependent mechanism. This protection via microglia depletion was lost however, after 48 hours of exposure. These data suggested that FG has direct neurotoxic capabilities, or that the protein is cleaved in culture to FN, which in turn could have direct neurotoxic effects. Studies identifying thrombin gene expression coupled with pharmacological manipulation of the enzyme suggested that FG is cleaved to FN in the cultures and it is the presence of FN that induces the later neurotoxicity.

This direct neurotoxicity was also observed if microglia were depleted prior to FN exposure for 24 hours, suggesting microglia were competently protecting neurons from FN-mediated toxicity for at least 24 hours, *in vitro*. However, a loss of this protection was observed here if FN exposure was prolonged. These observations suggest that microglia can cope with ‘acute’ (≤24 h) FN exposure, but not ‘chronic’ (>24 h) exposure, due possibly to phagocytic degradation pathways becoming saturated after chronic exposure, or microglia number significantly decreasing due to direct FN-mediated toxicity. This hypothesis certainly fits with the ED-1 expression profile after FN treatment of CGC cultures, showing a significant drop in expression after 48 hours of treatment. Interestingly, FG treatment gave a bi-phasic ED-1 expression profile, with significant drops observed after 4 and 48 hours of exposure. These decreases in ED-1 expression could correlate with early FG-mediated toxicity (≤ 24h) and late FG-

mediated toxicity (>24h), with the latter due to conversion to FN. Microglial senescence is also a possibility (Streit 2006) with chronic activation enhancing cell loss.

3.5.7. Preliminary ligand-receptor elucidation

Identification of the initial protein-cellular interactions that are responsible for the observed cytokine release and neurotoxicity would be important findings possibly enabling early attenuation of these responses. Involvement of CD11b in FN-, but not FG-mediated TNFα and IL-6 release further supports the requirement of protein immobilisation prior to receptor ligation, as previously described. Further studies on the role of scavenger receptor A (SRA) in FG- and FN-mediated responses yielded similar results, with no significant change in FG-mediated TNFα release or toxicity. Scavenger receptors are involved in mediating cell adhesion to, and endocytosis of, various native and pathologically modified substances (Husemann et al. 2002), including interactions with fibrillar $A\beta_{1-42}$ (El Khoury et al. 1996). Also, the receptor has been shown to be involved in chromogranin A-induced microglial stress and neurotoxicity (Hooper et al. 2009a) Interestingly, SRA-inhibition with fucoidan, attenuated FN-mediated iNOS expression but not TNFα release in CGC cultures. The inhibitory activity of fucoidan may reflect its capacity to mask sites on ligands, which interact with SRA, rather than masking the receptor itself (Husemann et al. 2002). Therefore, the observed differential attenuation of iNOS activity and TNFα release may in part be due to preferential masking of a binding motif associated with iNOS activity and not TNFα release.

3.5.8. No role for NADPH oxidase in attenuation of FG- or FN-mediated responses

Both FG and FN, at high concentrations, induced significant superoxide staining in microglia present in the CGC cultures, which was dependent on NADPH oxidase activity. This microglia associated increase in superoxide was comparable to data produced in our laboratory using BV2 microglia cells in an optimised biochemical assay (E. Mead, unpublished observations). Inhibition of NADPH oxidase activity did not affect FN- or FG-induced TNFα release or neurotoxicity. It was therefore decided that

this area of research would not be pursued for this thesis however, more elegant silencing of the NADPH oxidase enzyme using siRNA (Loane et al. 2009) or genetic knockouts would be an interesting avenue to pursue in future especially as the treatment. did significantly induce superoxide production.

3.5.9. TNFα synthesis, but not iNOS activity is involved in FG- and FN-mediated toxicity

Finally, pharmacological inhibition of factors here identified to be significantly induced by FG and FN treatment of cultures was performed. Here, TNFα synthesis but not iNOS activity was significantly associated with FG- and FN-mediated apoptosis. Furthermore it was shown that microglia are significantly involved in the observed neurotoxicity with MGCM experiments supporting these suggestions. The use of MGCM allowed identification of whether stable soluble factors released from microglia are involved in any observed toxicity. Using MGCM inhibition of TNFα release, specifically in microglia, is shown here to be sufficient to attenuate FG- and FN-mediated neurotoxicity. Furthermore, concentrating the FG-MGCM and immuno-blotting allowed us to show FG transfer in the MGCM to the CGCs was minimal and below levels shown to be neurotoxic. However, transfer of the inhibitors could not be ruled out.

3.5.10. Conclusions

These data provide initial characterisation of toxicity in microglial and CGC cultures after exposure to FG or FN, identifying a vital role for microglia in FG-mediated neurotoxicity, and are summarized in **Figure 3.5.1**. It seems FN deposition is highly toxic to the microglia and neurons, with data suggesting an induction of necrotic cell death as well as nitric oxide and TNFα release. However, inhibition of iNOS activity could not attenuate FN-mediated neurotoxicity in CGC cultures. FG treatment induced lower concentrations of TNFα with limited iNOS expression also observed. However exposure of microglia to FG can still induce activation and, in CGC cultures early

potent activation of microglia to a neurotoxic phenotype occurred. These data provide a platform to further identify mechanisms by which FG induces neurotoxicity and how microglia are involved.

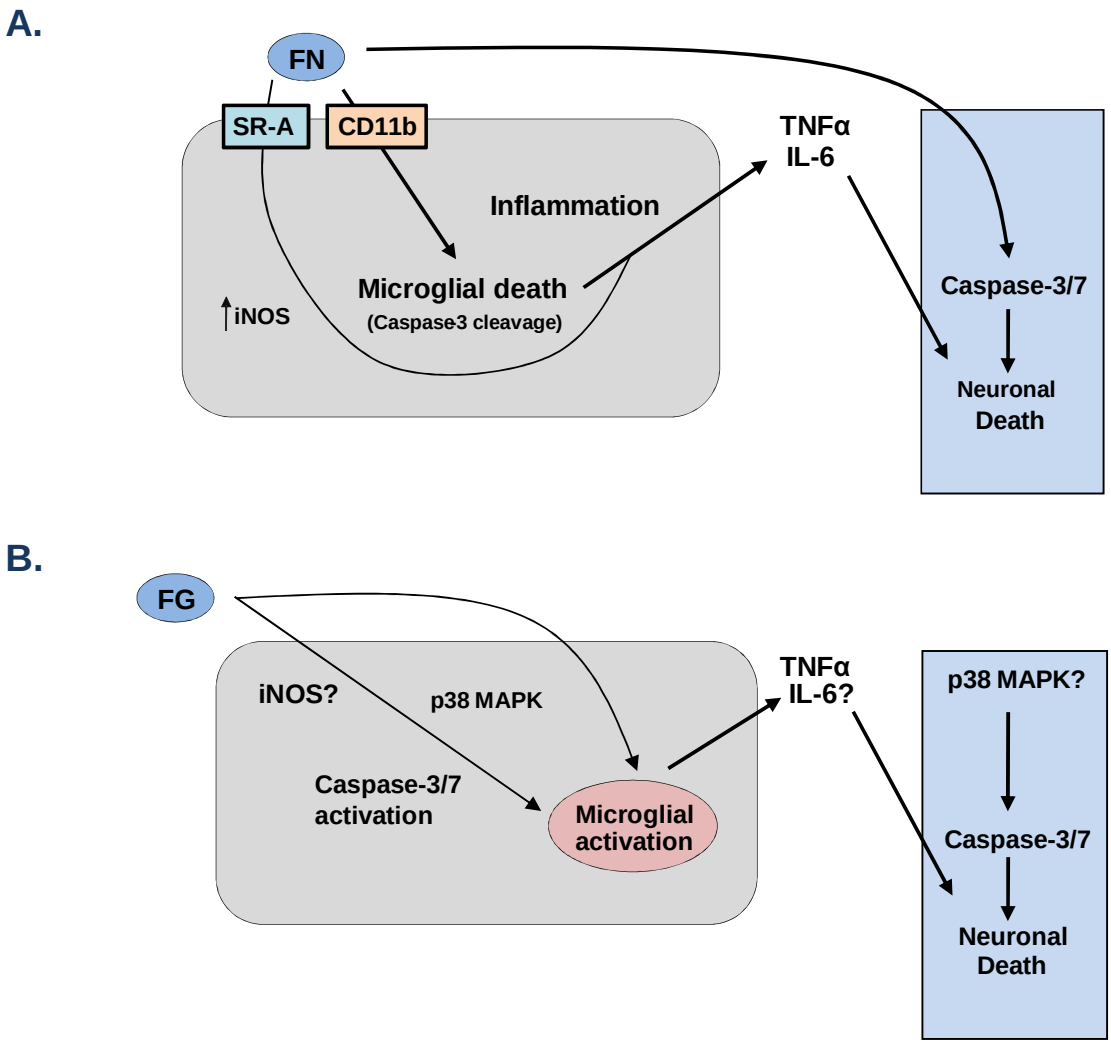

Figure 3.5.1. Summary of results obtained in chapter 3

A. Fibrin treatment of microglia led an increase in iNOS expression, toxicity and death via activation of CD11b and/or scavenger receptor A (SR-A). This led to the release of pro-inflmmatory cytokines, TNFα and IL-6 that, in the case of TNFα, participated in neuronal death via caspase-3/7 activation. Direct treatment of neurons with FN in the absence of microglia also induced death with dependence on caspase-3/7. **B.** Fibrinogen treatment of microglia led to an increase in iNOS expression in serum-free conditions but not serum-containing conditions. Caspase-3/7 activation occurred that did not seem to induce apoptosis, rather activation, which was also dependent on p38 MAPK-dependent pathways. FG-mediated microglial activation also led to the release of pro-inflammatory cytokines, in particular TNFα, with FG-mediated neuronal death being highly dependent on the observed TNFα release from microglia, as well as possible involvement from p38-MAPK pathways and activation of caspase-3/7.

4. Identifying and coupling a role for Endoplasmic Reticulum Stress in fibrinogen-mediated neuronal apoptosis

4.1. Introduction

This chapter focuses primarily on the involvement of the endoplasmic reticulum (ER) in FG-induced toxicity in neurons and microglia. Stressing of the ER is now widely accepted as an important pathological event in many diseases ranging from neurological disorders to cancers, diabetes, and atherosclerosis (Kim et al. 2008). Cells respond to ER stress by activation of the unfolded protein response (UPR), a cellular process that increases transcription of genes encoding ER-resident chaperones to facilitate protein folding and removal of mis-folded and mutant proteins (Imaizumi et al. 2001; Benn & Woolf 2004; Szegezdi et al. 2006). However, if mis-folding of proteins or expression of mutant proteins become chronic events such as in many neurodegenerative disorders (Saxena & Caroni 2011), ER stress can induce apoptotic cascades and death can occur. Initially, the discovery of an ER localised caspase in mice, caspase-12, was a significant suggestion that this organelle could be involved in cellular apoptosis (Nakagawa et al. 2000). Furthermore, Nakagawa and colleagues suggested β-amyloid-mediated neurotoxicity was dependent on ER stress involving caspase-12 cleavage.

4.1.1. ER stress in disease

In the last decade, much research has shown involvement of ER stress in neurodegenerative and neuroinflammatory disorders (Lindholm et al. 2006), including Alzheimer's disease (Salminen et al. 2009), Parkinson's disease (Wang & Takahashi 2007), amyotrophic lateral sclerosis (Kanekura et al. 2009) and multiple sclerosis (Mháille et al. 2008). Mutant presenilin-1 over expression as a model of Alzheimer's disease has been shown to down-regulate the UPR and also hyper-sensitise neurons to ER stress-mediated apoptosis (Katayama et al. 1999; Terro et al. 2002). In Parkinson's disease, mutant α-synuclein has been shown to induce ER stress

associated toxicity in neurons (Smith et al. 2005). Data recently published suggests parkin is involved in interorganellar crosstalk between the ER and mitochondria and increased expression of the protein is observed after both ER and mitochondrial stress (Bouman et al. 2011). Furthermore this group showed transcriptional regulation of parkin by ATF4, a transcription factor of the UPR. These data coupled with reports showing parkin-mediated suppression of UPR-mediated cell death (Imai et al. 2000), suggest loss of function mutants of parkin could enhance ER and mitochondrial stresses contributing to disease pathogenesis.

In an attempt to link fibrinogen extravasation into the CNS to induction of ER stress in neurons and microglia, literature from atherosclerosis research was studied. As previously stated, ER stress is prominent in atherosclerosis (Kim et al. 2008) with fibrinogen identified as a prominent feature of proliferative atherosclerotic lesions, constantly deposited and lysed (Bini et al. 1989; Smith et al. 1992) and degradation of fibrin has been suggested to induce macrophage migration enabling plaque removal (Smith et al. 1992). These observations coupled with ER stress dependent macrophage apoptosis in atherosclerosis (Tabas et al. 2009; Hotamisligil 2010a Hotamisligil 2010b), it was suggested that the study of fibrinogen-mediated ER stress in microglia and neurons could provide some interesting results.

4.1.2. Modelling ER stress, *in vitro*

Investigating ER stress *in vitro* has been suggested to be dissimilar to the actual process *in vivo*, with cultured cells displaying the full UPR repertoire upon induction of stress (Saxena & Caroni 2011), not seen *in vivo*. However, this induction *in vitro* has been suggested as another function of the UPR, independent of protein mis-folding induction, involved in regulating basal cellular homeostasis (Rutkowski & Hegde 2010). Here live cell staining, ICC and Western blotting were used to show FG and FN treatment of neurons and microglia can increase expression of ER stress markers, and inhibition of ER stress can attenuate observed toxicity. It is also shown that FG-

mediated induction of ER stress-related markers is dependent on microglia, supporting an indirect mechanism of toxicity with further elucidation of the pathway.

4.2. Exposure of CGC cultures to fibrinogen or fibrin induces expression of endoplasmic reticulum stress markers

Initially CGC cultures were treated with either thapsigargin or tunicamycin, time-dependently, as positive controls for caspase-12 cleavage, which occurs in cells undergoing ER stress (Nakagawa et al. 2000). Thapsigargin initiates ER stress by inhibiting the sarco-ER calcium-ATPase (SERCA), causing calcium dyshomeostasis, and tunicamycin can induce ER stress by inhibiting protein *N*-glycosylation (Takano et al. 2007). Treatment of CGCs with thapsigargin (Th) induced a significant increase in cleaved caspase-12 expression over time (**Figure 4.2.1 A**). Tunicamycin (Tu) treatment also induced a significant increase in cleaved caspase-12 expression, but only after 24 hours exposure with more variability being observed at the earlier time points (**Figure 4.2.1 B**). Therefore, thapsigargin was chosen as the main positive control for ER stress responses, however, where possible tunicamycin treatment was also performed.

4.2.1. Differential induction of caspase-12 activation is observed after fibrinogen and fibrin treatment

To identify if FG or FN exposure could induce significant caspase-12 cleavage, Western blotting was performed. Treatment of CGCs with FG induced significant cleavage of caspase-12 when compared with control levels, after 12 hours (**Figure 4.2.2 A**). Furthermore, significant time-dependent increases in the caspase-12 cleavage product were observed in FG-treated cultures at all time points tested post 12 hours of exposure. Conversely, FN treatment of CGC cultures did not give the same time-dependent increases in caspase-12 cleavage. Only 48 hours of exposure gave an observable increase in expression of the 36 kDa active form (**Figure 4.2.2 B**), suggesting any ER stress due to FN exposure is not the initial mediator of the observed

cell toxicity. Finally, administration of other treatments to CGCs gave variable responses. Treatment for 48 hours with LPS caused significant cleavage of caspase-12 compared with control levels (**Figure 4.2.3**). Treatment with staurosporine for 4 hours, the positive control used in previous experiments for induction of the classic intrinsic apoptotic pathway, did not significantly induce caspase-12 cleavage, as previously shown (Nakagawa et al. 2000) (**Figure 4.2.3**).

To further support these Western blotting data, live cell staining was performed on CGC cultures with a fluorescently tagged peptide that covalently binds to the active form of caspase-12 (**Figure 4.2.4 A**). The fluorescence intensity after treatment was quantified and compared with non-treated control cultures (**Figure 4.2.4 B**). Treatment with either thapsigargin or tunicamycin for 24 hours significantly increased the fluorescence intensity when compared with non-treated controls. These increases in fluorescence could be attributed to caspase activation as pre-treatment with the pan-caspase inhibitor, z-VAD-FMK, significantly attenuated fluorescence intensity (**Figure 4.2.4 B**).

Live cell staining on cultures that had been treated with FG or FN for 48 hours also showed a significant increase in fluorescence intensity compared with control. Comparable with the positive control-mediated induction, the increase in fluorescence due to FG treatment was dependent on caspase activation as pre-treatment with z-VAD-FMK attenuated the observed fluorescence intensity (**Figure 4.2.4 B**). Cultures were also exposed to FG for 24 hours and these data also show significant increases in fluorescence intensity that was dependent on caspase activation. The FN-mediated increase in fluorescence intensity could not be significantly attenuated by z-VAD-FMK pre-treatment. The high variability in the FN cultures could explain this observation and will be discussed further. Finally, in support of the Western blotting data, treatment of cultures with staurosporine for 8 hours did not induce a significant increase in fluorescence intensity although significant PI staining was observed, supporting the toxic effect of the compound in an ER-stress-independent manner (**Figure 4.2.4**). To

further support the significant impact of z-VAD-FMK pre-treatment, cleaved caspase-12 expression in lysates from cultures exposed to FG, FN, or thapsigargin after z-VAD-FMK treatment were compared with thapsigargin-mediated expression. Cultures with z-VAD-FMK pre-treatment showed significantly less cleaved caspase-12 expression when compared with thapsigargin treatment (**Figure 4.2.5**). Interestingly, FN-mediated expression was completely attenuated with z-VAD-FMK pre-treatment, suggesting a caveat in the live cell staining methodology, which will be discussed further.

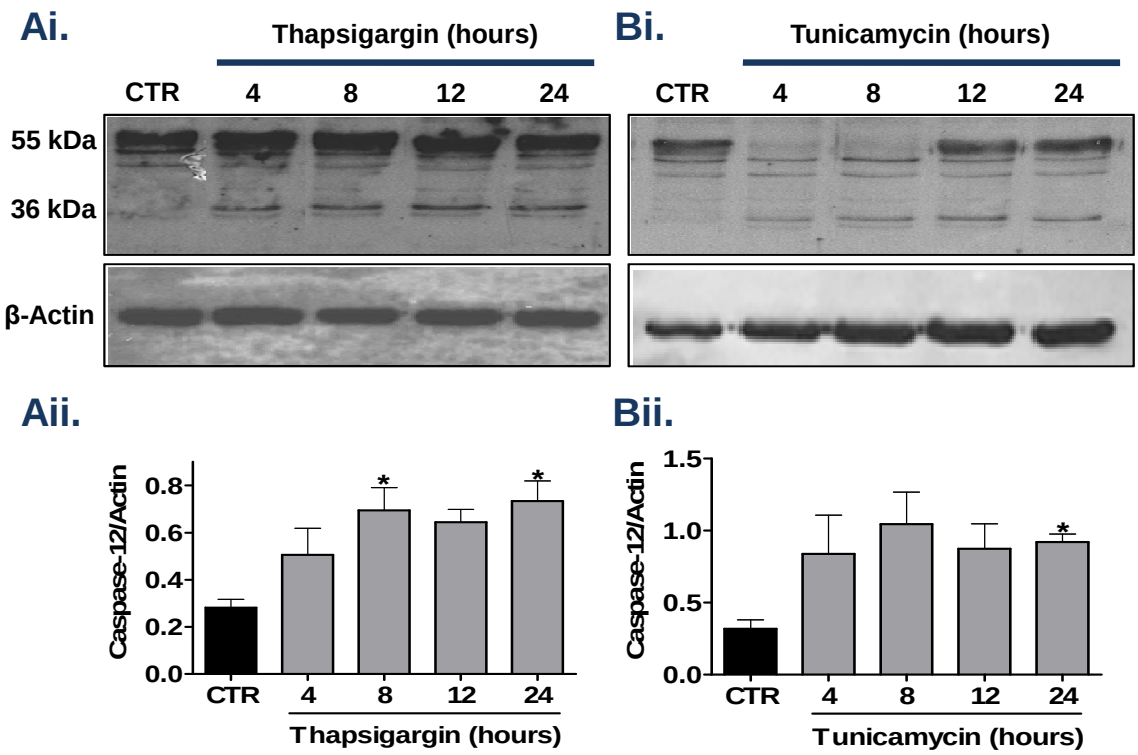

Figure 4.2.1. Thapsigargin and tunicamycin induce cleavage of caspase-12 in CGCs

Ai. Representative Western blots for caspase-12 and β-actin expression in CGC cultures after treatment with thapsigargin (Th; 2 µM) for 4-24 hours. **Aii.** Quantification of the time-dependent cleavage of caspase-12 expression by thapsigargin, with respect to β-actin expression as represented in **Ai**. **Bi.** Representative Western blots for caspase-12 and β-actin expression in CGC cultures after treatment with tunicamycin (Tu; 1 µg/ml) for 4-24 hours. **Bii.** Quantification of the time dependent cleavage of caspase-12 expression by tunicamycin, with respect to β-actin expression as represented in **Bi**. Experiments were repeated on 3 independent occasions. One way ANOVA with Dunnett's post-test was performed to compare control levels with each time-point. Levels of significance were: non-significant $p>0.05$, * $p<0.05$.

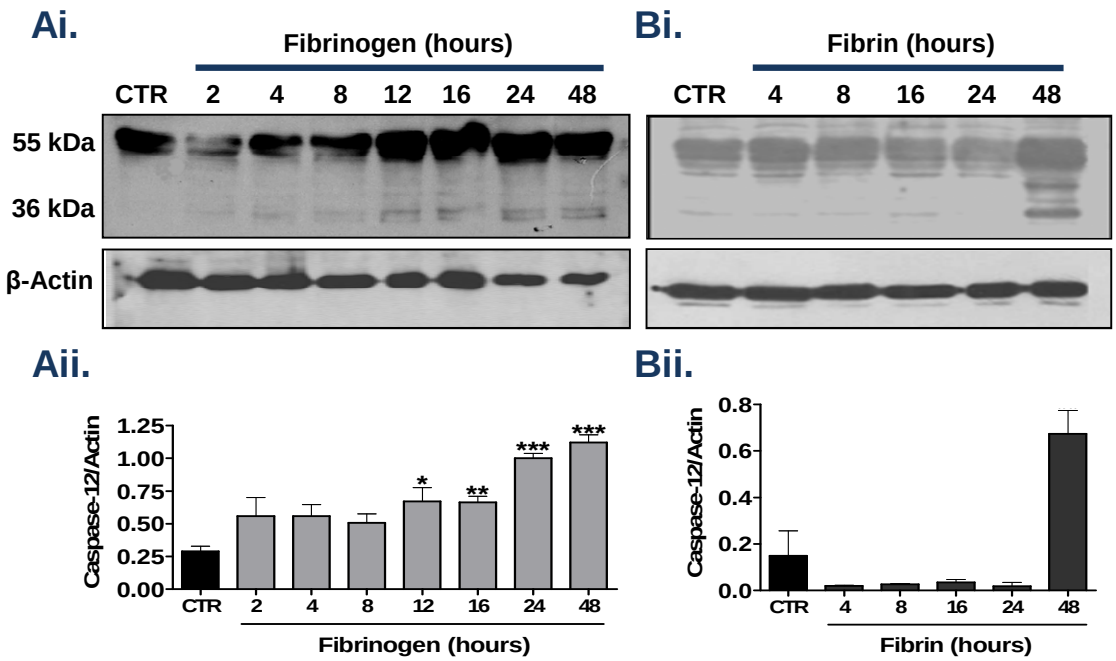

Figure 4.2.2. FG and FN induce time-dependent cleavage of caspase-12 in CGCs

Ai. Representative Western blots for caspase-12 and β-actin expression in CGC cultures after treatment with fibrinogen (FG; 2.5 mg/ml) for 2-48 hours. **Aii.** Quantification of the time-dependent cleavage of caspase-12 expression by FG, with respect to β-actin expression as represented in **Ai**. **Bi.** Representative Western blots for caspase-12 and β-actin expression in CGC cultures after treatment with fibrin (FN; 1 mg/ml) for 2-48 hours. **Bii.** Quantification of the time dependent cleavage of caspase-12 expression by FN, with respect to β-actin expression as represented in **Bi**. FG Western blotting was repeated on 3 independent occasions, and FN Western blotting was repeated on 2 independent occasions. One way ANOVA with Dunnett's post-test was performed to compare control levels with each time-point in the FG treatment studies. Levels of significance were: non-significant $p>0.05$, * $p<0.05$, ** $p<0.01$, *** $p<0.001$.

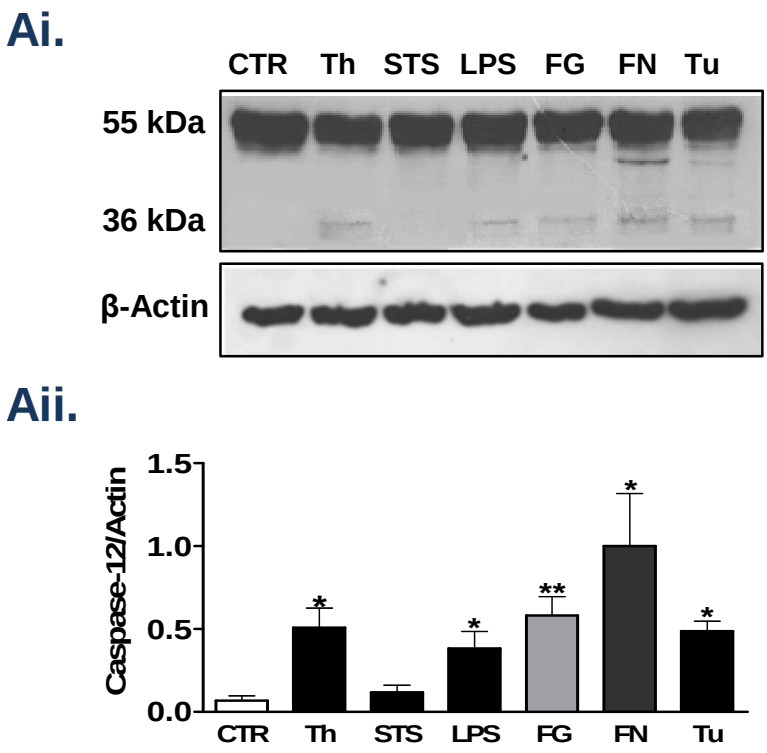

Figure 4.2.3. LPS but not Staurosporine induces cleavage of caspase-12 in CGCs

Ai. Representative Western blots for caspase-12 and β-actin expression in CGC cultures after treatment with thapsigargin (Th; 2 µM; 24 hours), staurosporine (STS; 0.5 µM; 8 hours), LPS (1 µg/ml; 48 hours), FG (2.5 mg/ml; 24 hours), FN (1 mg/ml; 48 hours) or tunicamycin (Tu; 1 µg/ml; 24 hours). **Aii.** Quantification of cleaved caspase-12 expression, with respect to β-actin expression, after treatments as outlined in **Ai**. Experiments were repeated on 3 independent occasions. One way ANOVA with Dunnett's post-test was performed to compare control levels with each treatment. Levels of significance were: non-significant $p>0.05$, * $p<0.05$, ** $p<0.01$.

Figure 4.2.4

A.

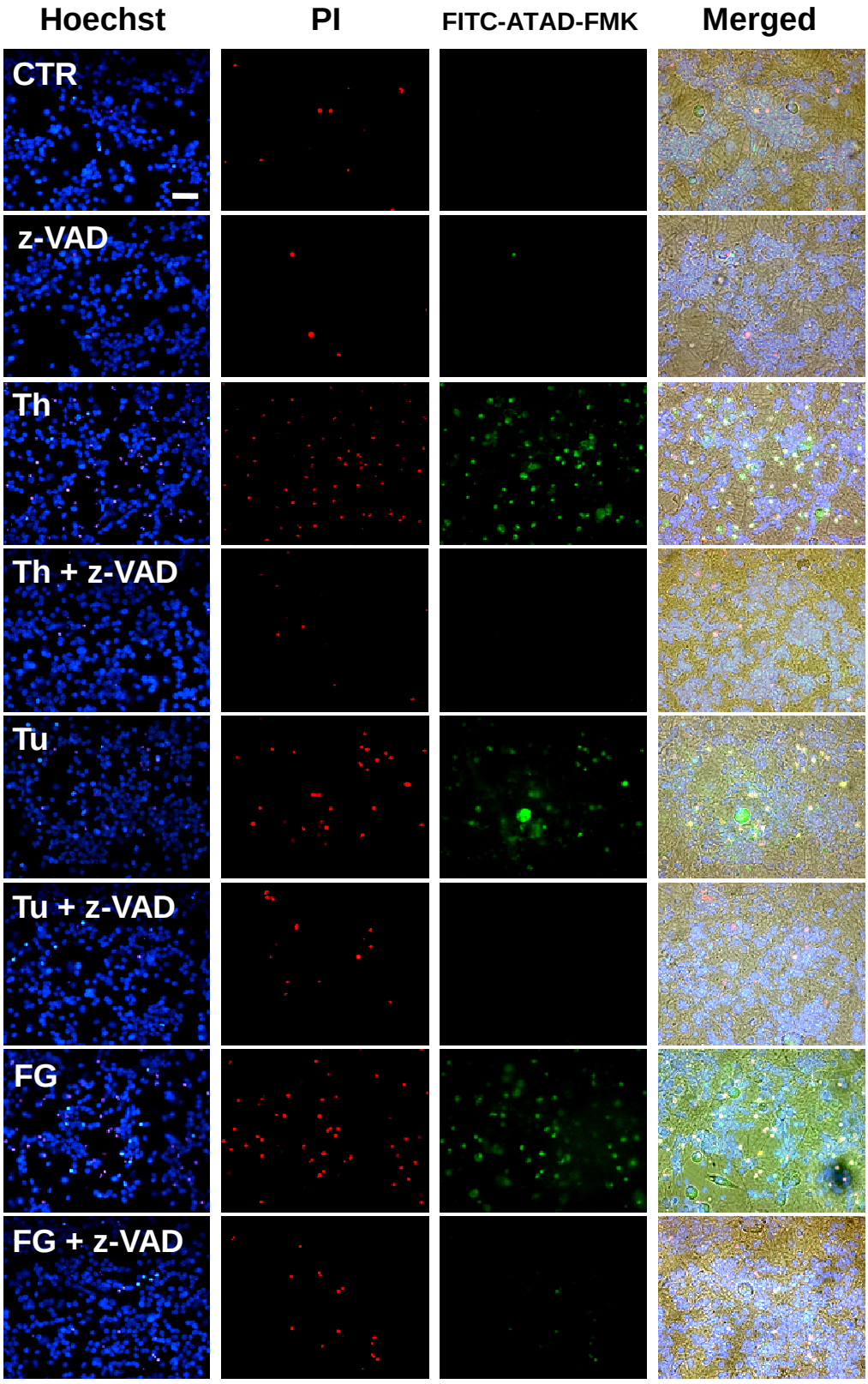
Hoechst
PI
FITC-ATAD-FMK
Merged
CTR
z-VAD
Th
Th + z-VAD
Tu
Tu + z-VAD
FG
FG + z-VAD

Figure 4.2.4

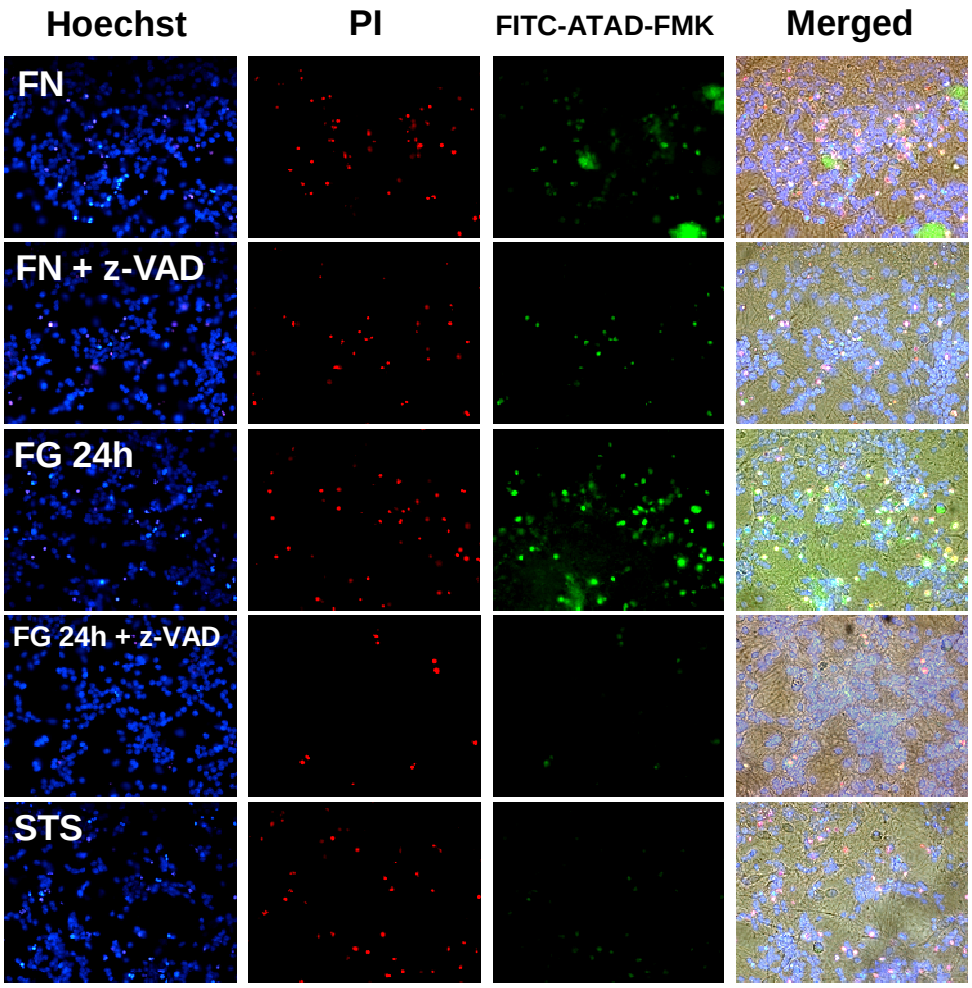
Hoechst
PI
FITC-ATAD-FMK
Merged
FN
FN + z-VAD
FG 24h
FG 24h + z-VAD
STS

B.

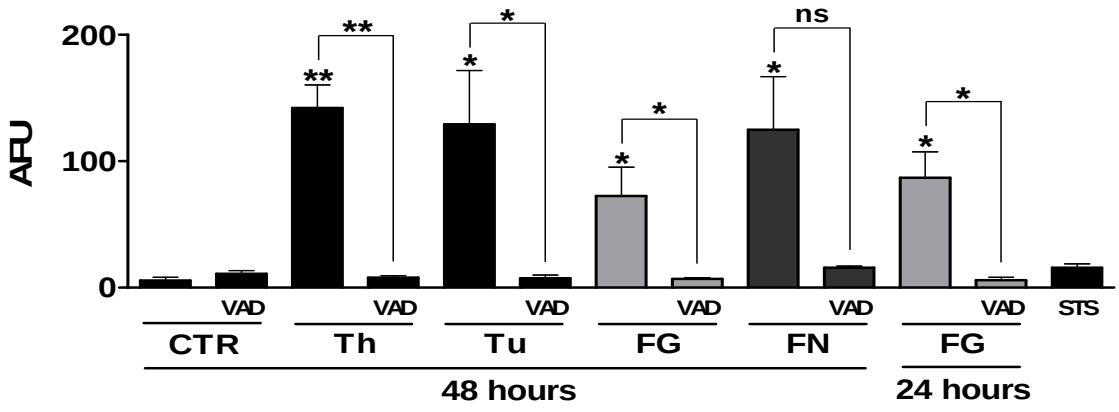
AFU
200
100
0
**
**
*
*
*
*
*
ns
*
*
VAD
VAD
VAD
VAD
VAD
VAD
STS
CTR
Th
Tu
FG
FN
FG
48 hours
24 hours

Figure 4.2.4. FG induces an increase in activated caspase-12-associated fluorescence, dependent on caspase activation

A. Panel of representative images of live cell staining experiments in CGC cultures after treatment with Th (2 µM; 24 hours), Tu (1 µg/ml; 24 hours), FG (2.5 mg/ml; 24 hours), FN (1 mg/ml; 48 hours) or STS (0.5 µM; 8 hours), alone or in combination with z-VAD-FMK (1 µg/ml). Live cell staining was performed with Hoechst-33342 for nucleus identification, propidium iodide (PI; red) for total cell death, and FITC-ATAD-FMK (green) for active caspase-12. Original magnification: x40, scale bar: 40 µm. **B.** Quantification of the relative active caspase-12 fluorescence intensity/cell in CGC cultures after administration of treatments stated in **A**. Data are presented in arbitrary fluorescence units (AFU). Treatments were in triplicate and data were analysed from 3 independent experiments. To compare AFU of control levels and treatments, a one way ANOVA was performed with Dunnett's post-test. To compare specific treatments with caspase inhibition, paired two-tailed Student's *t*-tests were performed. Levels of significance were: non-significant $p>0.05$, * $p<0.05$, ** $p<0.01$, *** $p<0.001$.

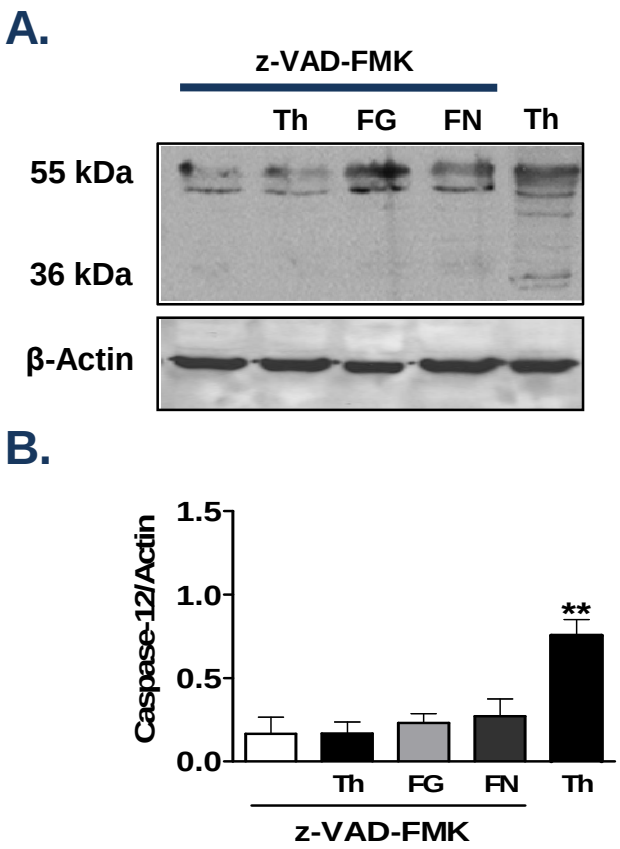

Figure 4.2.5. FG- and FN-mediated caspase-12 cleavage is dependent on caspase activation

A. Representative Western blots for caspase-12 and β-actin expression in CGC cultures after co-treatment with FG (2.5 mg/ml; 24 hours) or FN (1 mg/ml; 48 hours) with z-VAD-FMK (1 µg/ml), or treatment with thapsigargin (Th; 2 µM; 24 hours) alone or in combination with z-VAD-FMK. **B.** Quantification of cleaved caspase-12 expression, with respect to β-actin expression, after treatments outlined in **A**. The experiment was repeated on 3 independent occasions. Paired two-tailed Student's *t*-tests were performed to compare Th-mediated expression levels with each 'inhibited' treatment. Levels of significance were: non-significant $p>0.05$, ** $p<0.01$.

4.2.2. Fibrinogen- but not fibrin-mediated caspase-12 expression is dependent on the presence of microglia in CGC cultures

Following on from the earlier studies that identified a significant role for microglia in FG- and FN-mediated responses, CGC cultures were pre-treated with LME and live cell staining for the active form of caspase-12 were performed. Treatment of cultures for 24 hours with thapsigargin or tunicamycin significantly induced caspase-12 cleavage, which was not attenuated by microglial depletion. However, FG treatment induced significant expression of active caspase-12 after 24 hours and this could be prevented if microglia were depleted from the cultures (**Figure 4.2.6**). In line with the earlier observations suggesting FN and LPS did not induce significant toxicity after 24 hours, no significant increase in caspase-12 activation was seen in either treatment groups at this time point (**Figure 4.2.6**). However, if FN-treated cultures were depleted of microglia, significant increases in caspase-12 activation were observed, following a similar pattern to the increase in toxicity staining with PI. Following on from these data, caspase-12 cleavage was quantified in cultures after 48 hours of treatment, again using fluorescence intensity. As expected, thapsigargin and tunicamycin induced significant increases in caspase-12 cleavage which was independent of microglia (**Figure 4.2.7**). FG treatment for 48 hours induced significant induction of caspase-12 cleavage to a level similar to that seen in positive control treated cultures. Depletion of microglia from these cultures prior to FG treatment caused a drop in caspase-12 cleavage, however, this was not a significant decrease and cell toxicity staining was still significantly increased above control levels (**Figure 4.2.7**), in line with earlier observations (**Figure 3.3.1**). FN treatment for 48 hours also induced significant increases in the active form of caspase-12 and as predicted, microglial depletion did not inhibit this induction. Finally, LPS treatment for 48 hours induced significant caspase-12 induction with depletion of microglia causing a drop in cleavage close to significance (**Figure 4.2.7**).

Western blotting was performed on lysates from cultures pre-treated with LME to support the live cell staining data. Thapsigargin treatment for 24 hours increased the expression of the cleaved fragment of caspase-12 (36 kDa) and in support of the live cell staining data, depletion of microglia did not attenuate the expression (**Figure 4.2.8**). Also in line with the live staining data, FG treatment for 24 hours induced cleaved caspase-12 expression that seemed to be inhibited in cultures depleted of microglia. Finally, FN treatment for 48 hours increased expression of the cleaved form of caspase-12. However, no obvious modulation in FN-mediated caspase-12 cleavage was observed after pre-treatment with LME (**Figure 4.2.8**).

Figure 4.2.6

A.

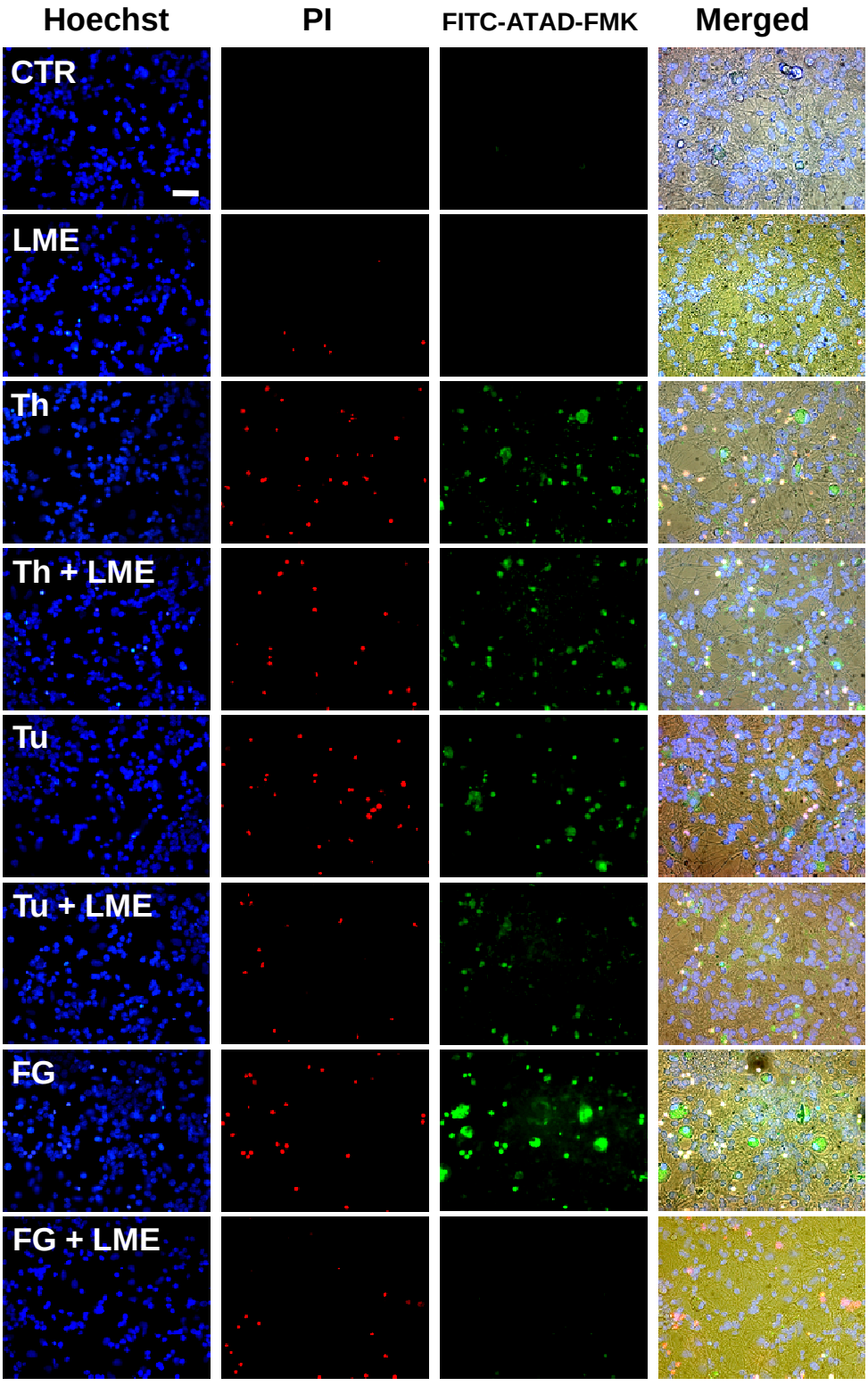
Hoechst
PI
FITC-ATAD-FMK
Merged
CTR
LME
Th
Th + LME
Tu
Tu + LME
FG
FG + LME

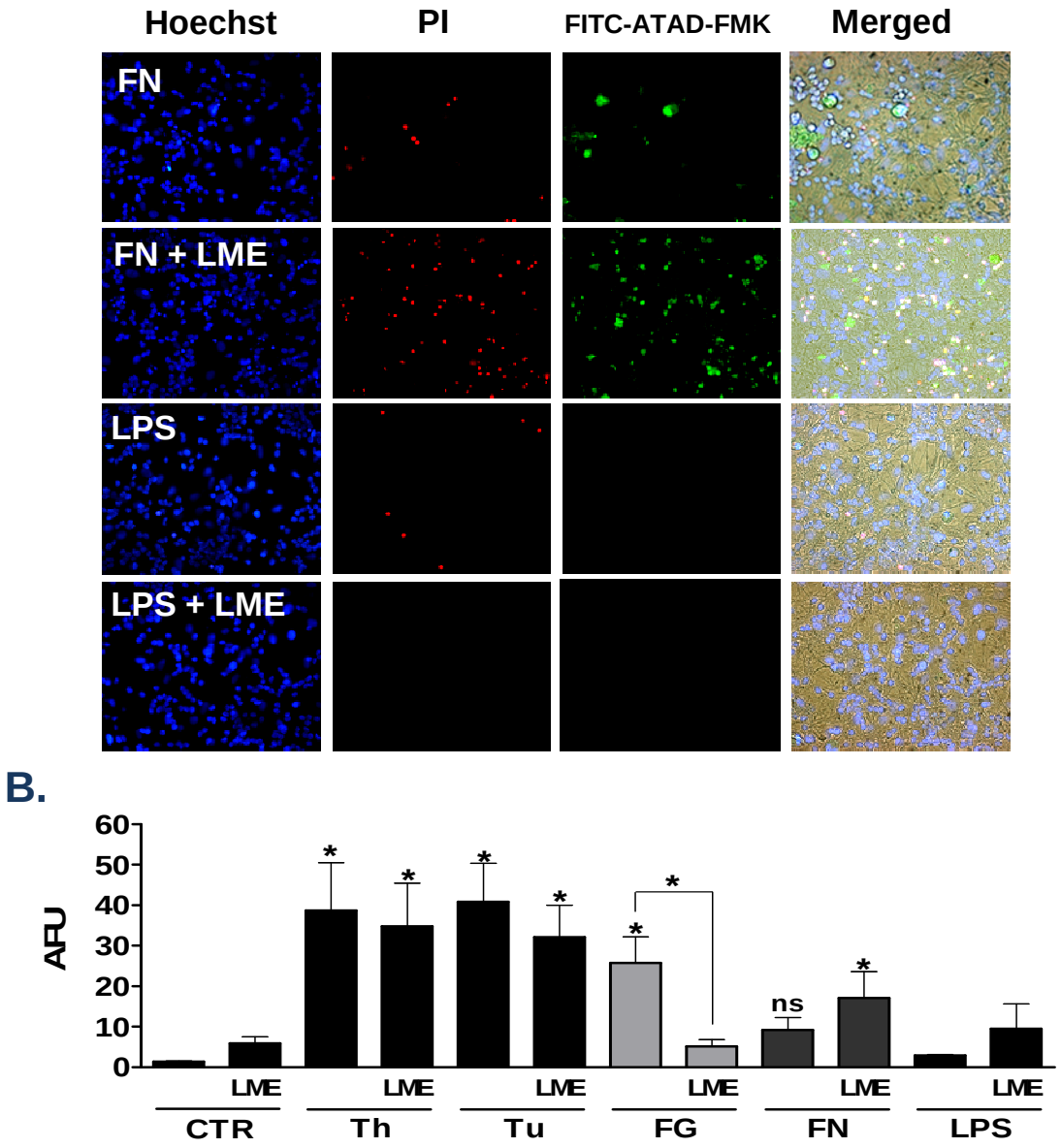

Figure 4.2.6. FG induces an increase in activated caspase-12-associated fluorescence in CGC cultures, dependent on the presence of microglia

A. Panel of representative images from live cell staining experiments in CGC cultures after treatment with Th (2 µM), Tu (1 µg/ml), FG (2.5 mg/ml), FN (1 mg/ml) or LPS (1 µg/ml) for 24 hours, +/- LME pre-treatment for the depletion of microglia (LME). Live cell staining was performed using Hoechst-33342 for nucleus identification, propidium iodide (PI; red) for total cell death, and FITC-ATAD-FMK (green) for active caspase-12. Original magnification: x40, scale bar: 40 µm. **B.** Quantification of the relative active caspase-12 fluorescence intensity/cell in CGC cultures after administration of treatments outlined in **A**. Data are presented in arbitrary fluorescence units (AFU). Treatments were in triplicate and data were analysed from 3 independent experiments. To compare the AFU of control levels and treatments, a one way ANOVA was performed with Dunnett's post-test. To compare specific treatments on cultures where microglia were present or removed, paired two-tailed Student's *t*-tests were performed. Levels of significance were: non-significant $p>0.05$, * $p<0.05$.

Figure 4.2.7

A.

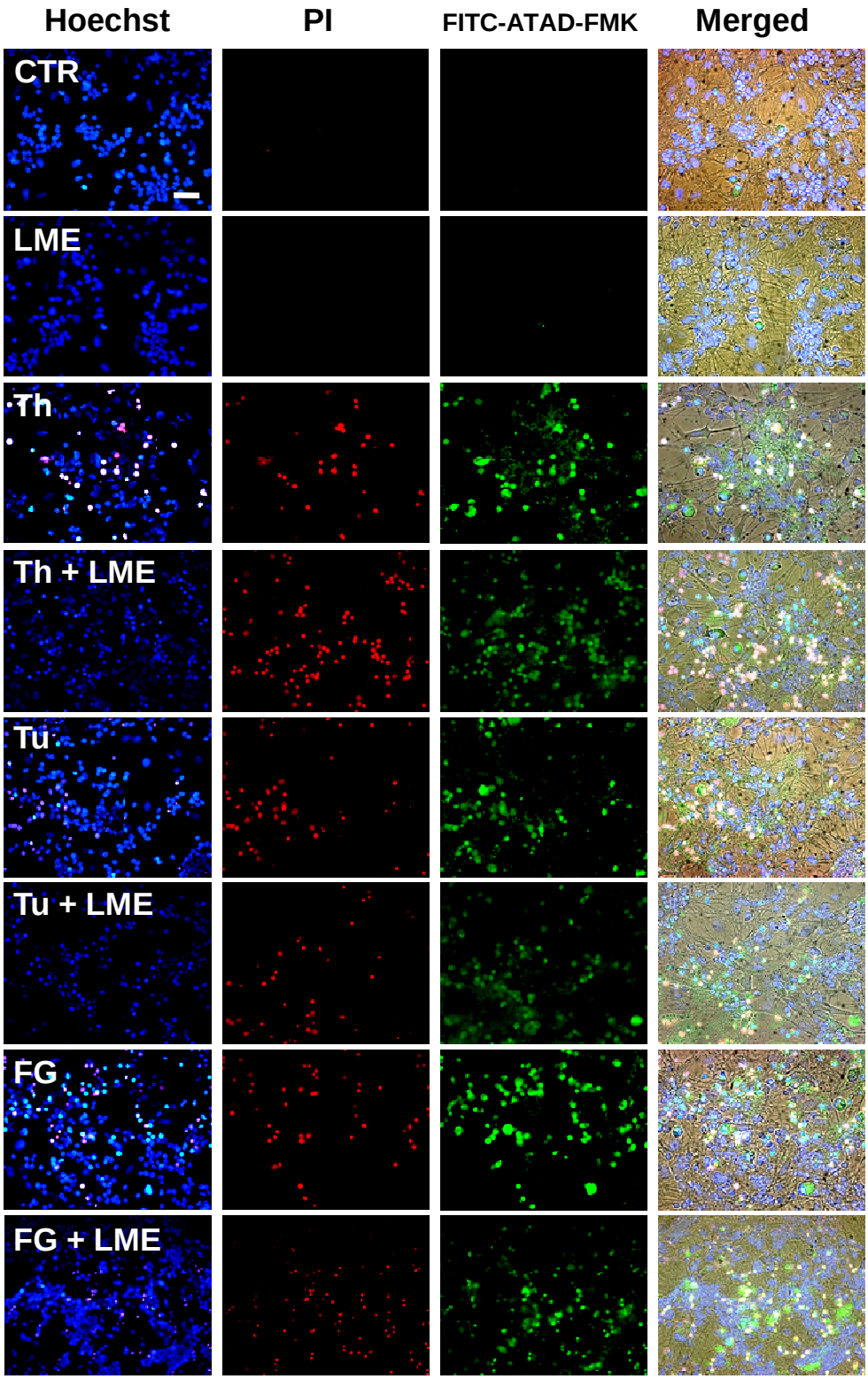
Hoechst
PI
FITC-ATAD-FMK
Merged
CTR
LME
Th
Th + LME
Tu
Tu + LME
FG
FG + LME

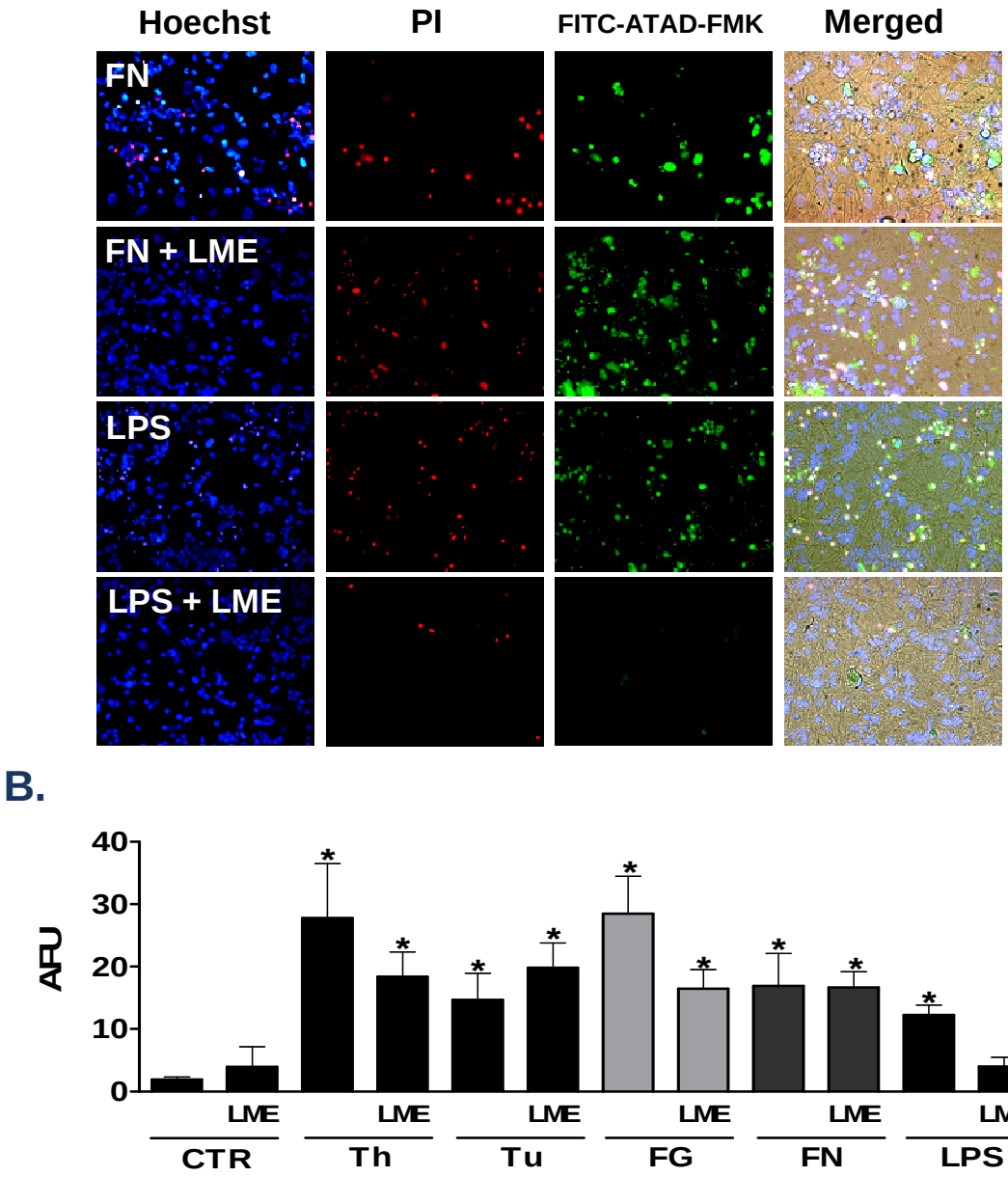

Figure 4.2.7. Microglial-associated dependence of FG-mediated caspase-12 cleavage in CGC cultures is time-dependent

A. Panel of representative images from live cell staining experiments in CGC cultures after treatment with Th (2 µM), Tu (1 µg/ml), FG (2.5 mg/ml), FN (1 mg/ml) or LPS (1 µg/ml) for 48 hours, +/- LME pre-treatment for the depletion of microglia (LME). Live cell staining was performed using Hoechst-33342 for nucleus identification, propidium iodide (PI; red) for total cell death, and FITC-ATAD-FMK (green) for active caspase-12. Original magnification: x40, scale bar: 40 µm. **B.** Quantification of the relative active caspase-12 fluorescence intensity/cell in CGC cultures after administration of treatments outlined in **A**. Data are presented in arbitrary fluorescence units (AFU). Treatments were in triplicate and data were analysed from 3 independent experiments. To compare the AFU of control levels and treatments, a one way ANOVA was performed with Dunnett's post-test. Levels of significance were: non-significant $p>0.05$, * $p<0.05$.

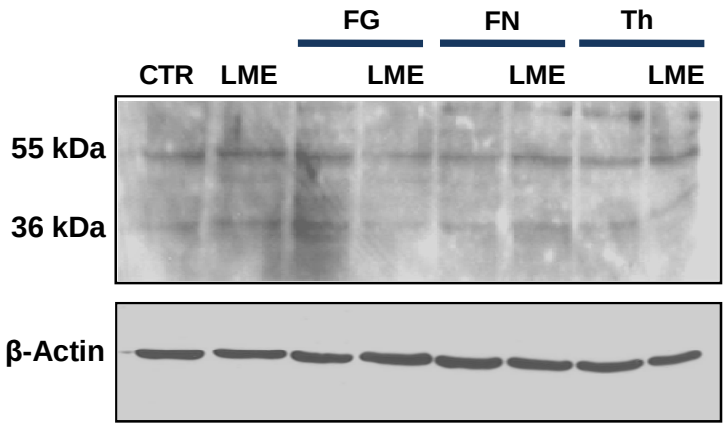

Figure 4.2.8. FG-mediated expression of the cleaved form of caspase-12 in CGC cultures seems to be dependent on the presence of microglia

Representative Western blots for caspase-12 and β-actin expression in CGC cultures after treatment with FG (2.5 mg/ml; 24 hours), FN (1 mg/ml; 48 hours) or Th (2 µM; 24 hours) +/- LME depletion of microglia (LME). The experiment was repeated on 2 independent occasions.

4.2.3. Fluorescence associated with fibrinogen- and thapsigargin-induced activated caspase-12 in microglia, present in CGC cultures, was not due to phagocytosis of the dye

It was observed that some of the caspase-12 staining appeared most intense in the microglia present in the cultures. Microglia are the phagocytes of the brain (Kreutzberg 1996). It could therefore be hypothesised that these significant increases in microglia expression of caspase-12 were partly due to the fluorescently-tagged peptide being recognised as a foreign pathogen and the microglia phagocytosing the dye creating a false positive increase in expression. Previously published studies have run control experiments at decreased temperatures to inhibit the mechanism of phagocytosis or internalisation (Tosello-Trampont et al. 2001; Gronski et al. 2009), therefore cultures treated with either thapsigargin or FG were incubated with the fluorescent caspase-12 tag at 4℃ for 30 minutes to observe whether the FITC-ATAD-FMK expression in the microglia was in fact due to phagocytosis and not microglial ER stress. Microglia were identified by morphology and quantified as being caspase-12 positive or negative.

A large number of the microglia in the CGC cultures displayed FITC-ATAD-FMK fluorescence after 24 hours of thapsigargin treatment at 37℃ and probe incubation at 4℃, when compared with control cultures (**Figure 4.2.9**). Similarly, FG treatment for 24 hours at 37℃ induced increased fluorescence above control levels after probe incubation at 4℃, with a larger numbers of microglia displaying FITC-ATAD-FMK fluorescence when compared with control cultures. Therefore, these data suggest the fluorescence observed in the microglia is due to binding to active caspase-12 and not due to internalisation/phagocytosis (**Figure 4.2.9**).

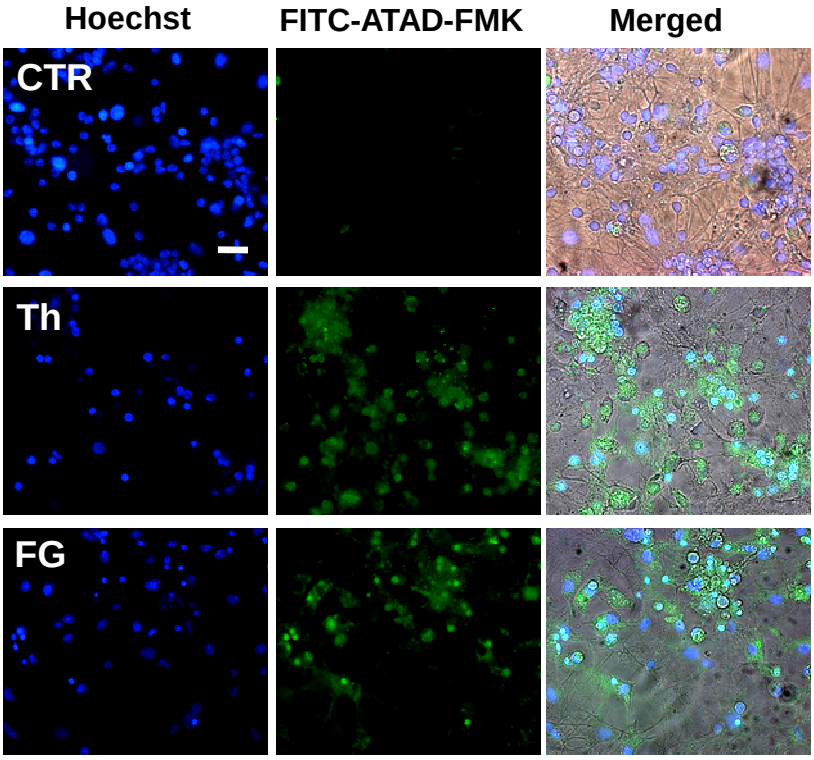

Figure 4.2.9. The observed fluorescence induction after treatments is not due to phagocytosis of FITC-ATAD-FMK

Panel of representative images from live cell staining experiments in CGC cultures after treatment with Th (2 µM) or FG (2.5 mg/ml) for 24 hours, followed by FITC-ATAD-FMK (green) dye incubation at 4℃ for 20 minu tes. Hoechst-33342 (blue) staining was also performed. Original magnification: x40, scale bar: 40 µm.

4.2.4. Fibrinogen and fibrin significantly increase expression of CHOP in primary microglial cultures

Caspase-12 has been shown to be activated by ER stress in rodents (Nakagawa et al. 2000). However, the argumentation cannot be reversed and an assumption made that caspase-12 activation implies ER stress. Therefore, to support the caspase-12 data, expression of CHOP/GADD153, the major pro-apoptotic transcription factor induced by ER stress (Salminen et al. 2009) was targeted.

Following on from the observations that caspase-12 activation is present in microglia in the CGC cultures, immunocytochemistry was performed on primary microglial cultures for expression of CHOP. Treatment of cultures with thapsigargin or tunicamycin for 24 hours increased the number of microglia staining positive for CHOP expression when compared with control cultures. Furthermore, FG or FN treatment of the microglial cultures for 24 hours also increased the number of cells displaying CHOP expression when compared with control levels (**Figure 4.2.10**).

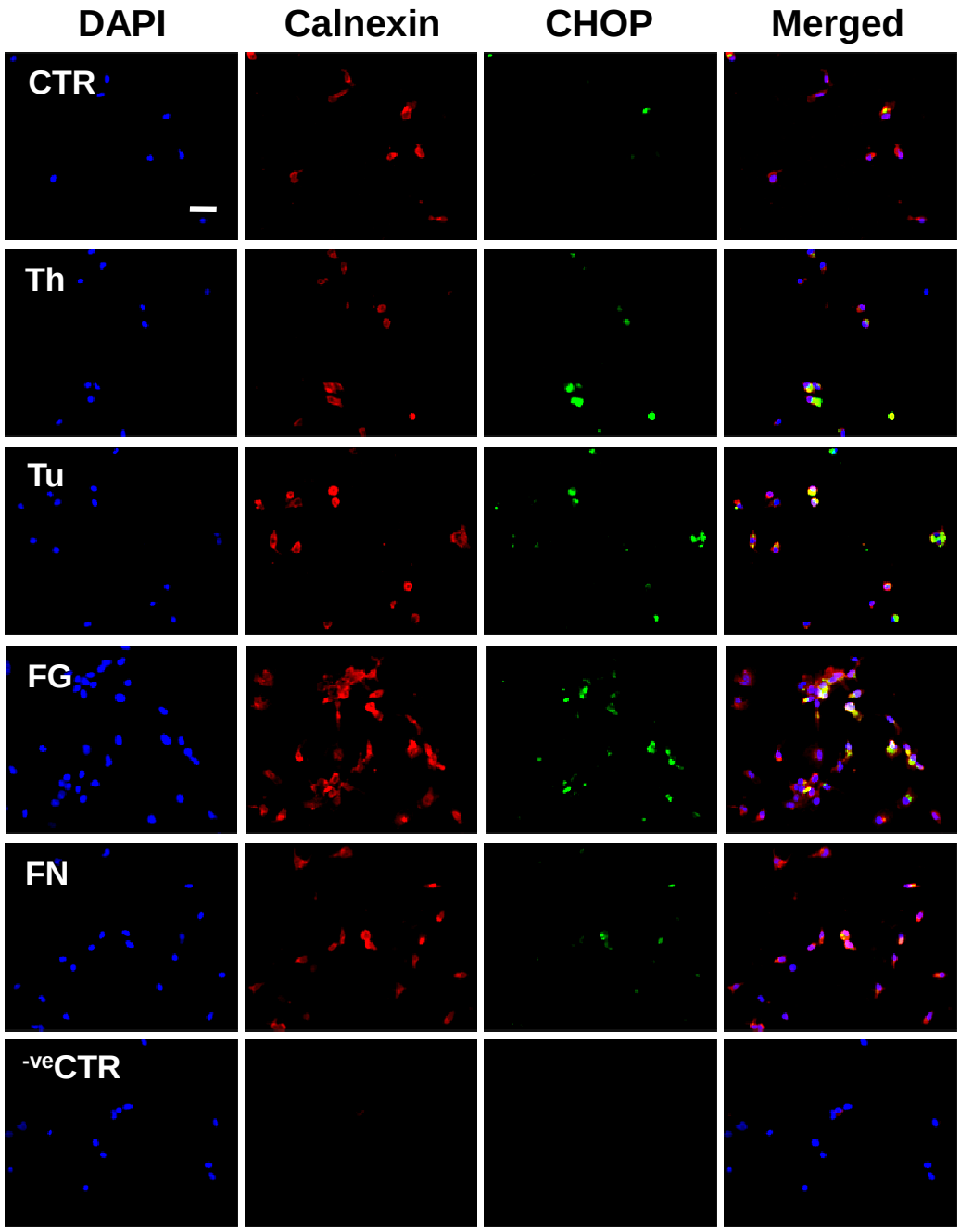

Figure 4.2.10. FG and FN induce expression of CHOP in primary microglial cultures

Representative images from primary microglial cultures after treatment with Th (2 µM), Tu (1 µg/ml), FG (2.5 mg/ml) or FN (1 mg/ml) for 24 hours. Cultures were stained with DAPI for quantification of cell number and probed with anti-Calnexin-TRITC (red) for staining of cellular ER and anti-CHOP (green), except in negative control cultures, where primary antibodies were omitted. Original magnification: x40, scale bar: 40 µm.

4.2.5. Fibrinogen-mediated responses can be attenuated through inhibition of an ER stress pathway

It was hypothesised that caspase-12 activation by FG or FN treatment would be downstream of any unfolded protein response (UPR) induced in the presence of these protein preparations. Therefore, inhibiting pathways activated during the UPR could prevent significant cleavage of caspase-12 and possibly increase cytoprotection. The compound salubrinal (Sal) has been shown to protect cultures from ER stress mediated by tunicamycin and other inducers by inhibiting the dephosphorylation of eukaryotic initiation factor 2α (eIF2α) (Boyce et al. 2005). The PKR-like endoplasmic reticulum kinase (PERK) is an eIF2α kinase that is activated during the UPR. The kinase phosphorylates eIF2α to attenuate mRNA translation, reducing the burden of protein substrate for the ER-folding and -degradation machinery (Yan et al. 2002). Pre-treatment of salubrinal therefore increases the expression of the phosphorylated form of eIF2α by inhibiting dephosphorylation, providing a more robust, prolonged protection against ER stress inducers.

The CGC cultures were treated with salubrinal prior to thapsigargin, FG, or FN treatment and cleaved caspase-12 expression was compared with cultures with no salubrinal pre-treatment by Western blotting. Salubrinal treatment alone did not modulate caspase-12 expression (**Figure 4.2.11**). However, the FG-mediated expression of cleaved caspase-12 after 24 hours of exposure was observably attenuated with salubrinal pre-treatment. Cleavage above the control was still observed in these cultures, suggesting the involvement of other pathways. Interestingly, FN-mediated cleaved caspase-12 expression after 48 hours of treatment was not attenuated by salubrinal pre-treatment, suggesting other pathways may be involved in FN-mediated caspase-12 expression, or as previously suggested, the observed caspase-12 expression is secondary and FN-mediated toxicity is due primarily to other stress pathways. However, these data are preliminary and require further clarification.

To further support a role for ER stress in FG-mediated microglial activation, live cell staining for cleaved caspase-3/7 was performed on primary microglial cultures in the presence or absence of salubrinal pre-treatment. This experiment was performed in line with recent studies suggesting significant non-apoptotic roles for caspase-3/7 in microglial activation. Obviously it wouldn't be possible to rule out with 100% certainty, the classical apoptotic roles of caspase-3/7; however quantification of morphological changes attributed to cells undergoing apoptosis provided a strong indicator of whether any observed increase in fluorescence associated with caspase-3/7 cleavage is apoptosis-dependent or –independent.

Treatment of the cultures with staurosporine (STS) for 4 hours induced significant active caspase-3/7 associated fluorescence, as expected (**Figure 4.2.12**). Also it was likely this activation of caspase-3/7 was primarily apoptotic-dependent with a significant increase cells displaying apoptotic morphology when compared with control cultures (**Figure 4.2.12 Aiii**). Similarly, treatment of cultures with FG for 24 hours induced a significant increase in active caspase-3/7 associated fluorescence. However, the observed cellular morphology in FG-treated cultures seemed healthy with little or no significant apoptotic morphology when compared with control cultures, in line with previous observations (**Figure 3.2.8**), suggesting these observed increases in caspase-3/7 could be apoptosis-independent (**Figure 4.2.12 Aiii**). Furthermore, treatment of cultures with salubrinal prior to FG exposure completely ablated the said caspase-3/7 expression, suggesting ER stress via the PERK-eIF2α axis is involved in the downstream cleavage of caspase-3/7 in microglia after FG treatment. FN-treatment of the microglial cultures for 24 hours was also able to induce significant caspase-3/7 activation (**Figure 4.2.12 Aii**); however salubrinal pre-treatment could not significantly attenuate the activation, although there was a trend towards attenuation. This suggests the observed expression could be due to both apoptosis-dependent and -independent cleavage of the caspases. In line with the apoptotic-mediated activation, the percentage of cells displaying apoptotic morphology in the FN-treated cultures was

significantly higher than in non-treated control cultures (**Figure 4.2.12 Aiii**). Finally, LPS treatment was analysed for its ability to induce caspase-3/7 activation in the microglia. As shown previously (**Figure 3.2.8**), LPS significantly induced active caspase-3/7 expression after 24 hours. Pre-treatment with salubrinal did attenuate the caspase-3/7 expression, however, not significantly, suggesting that either the caspase-3/7 expression was apoptotic or induced in a non-apoptotic fashion independent of ER stress pathways. The percentage of cells displaying apoptotic morphology in LPS treated cultures was not significantly different to control cultures suggesting a non-apoptotic role for caspase-3/7 that was independent of ER stress induction.

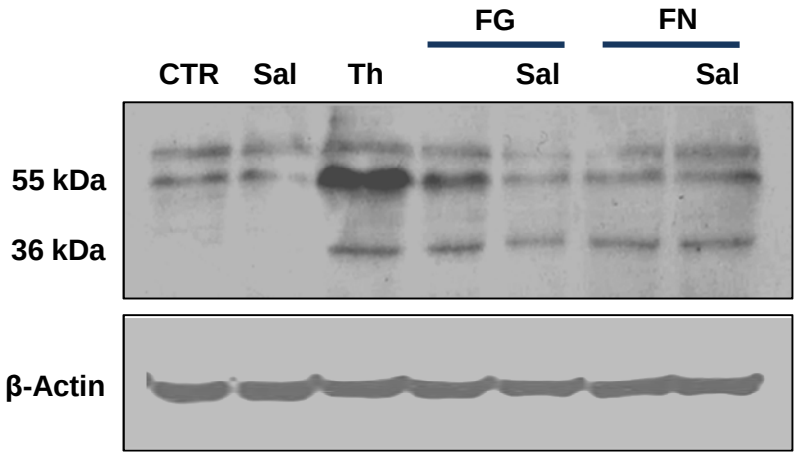

Figure 4.2.11. FG-mediated expression of the cleaved form of caspase-12 in CGC cultures can be inhibited with salubrinal treatment

Representative Western blots for caspase-12 and β-actin expression in CGC cultures after treatment with Th (2 µM; 24 hours), FG (2.5 mg/ml; 24 hours), or FN (1 mg/ml; 48 hours) alone or in combination with salubrinal (Sal; 100 nM). The experiment was repeated on 2 independent occasions.

Figure 4.2.12

Ai.

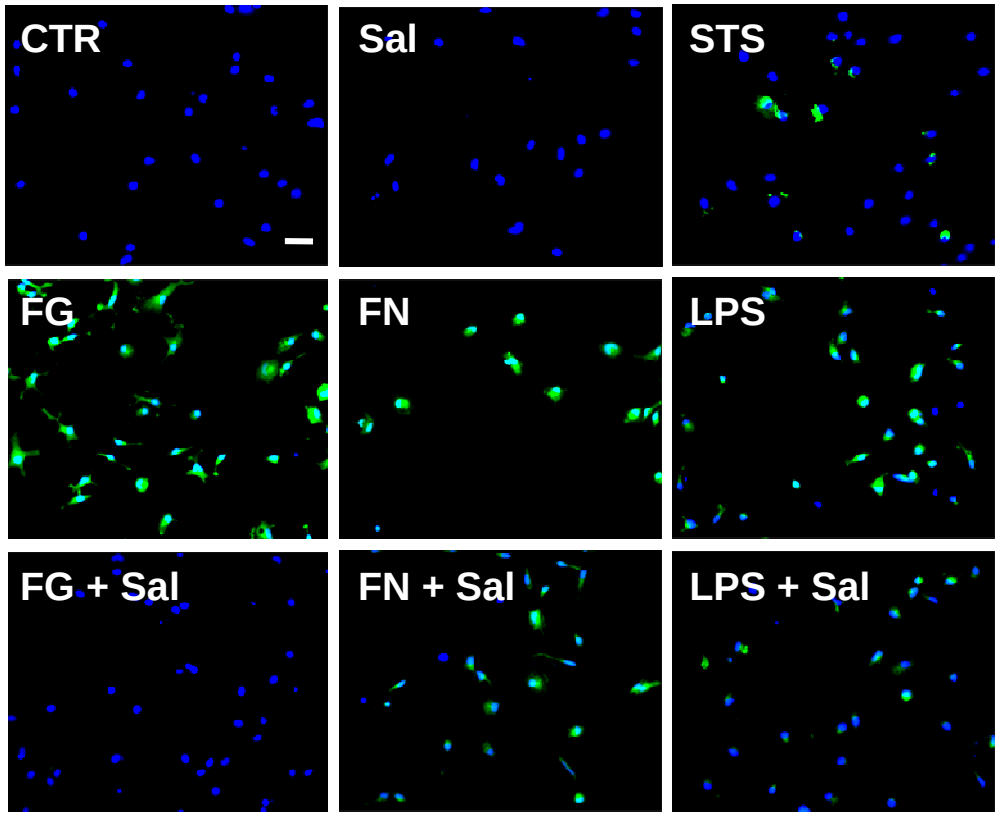

Aii.

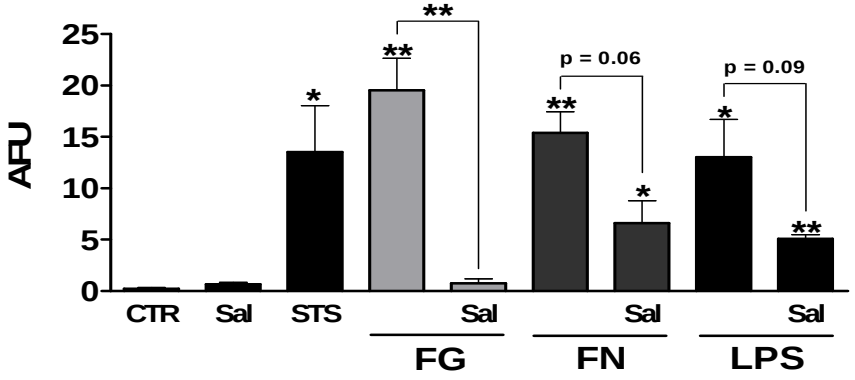

Aiii.

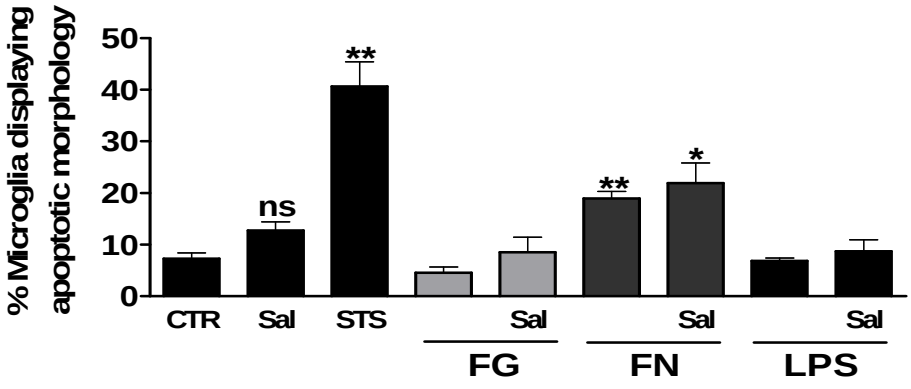

Figure 4.2.12. FG-mediated caspase-3/7 cleavage in microglia can be attenuated by inhibition of an ER stress-associated pathway

Ai. Panel of representative images from live cell staining experiments in primary microglial cultures after treatment with STS (0.5 µM; 8 hours), FG (2.5 mg/ml), FN (1 mg/ml) or LPS (1 µg/ml), for 24 hours. Live cell staining was performed using Hoechst-33342 for nucleus identification and FAM-DEVD-FMK (green) for active caspase-3/7. Original magnification: x40, scale bar: 40 µm. **Aii.** Quantification of the relative active caspase-3/7 fluorescence intensity/cell in microglial cultures after administration of treatments as outlined in **Ai**. Data are present in arbitrary fluorescence units (AFU) **Aiii.** Quantification of the percentage of microglia present that displayed classical apoptotic morphology after administration of treatments as outlined in **Ai**. Treatments were in duplicate and data were analysed from 3 experiments. One-way ANOVA was performed to compare control levels of AFU or apoptotic morphology to each treatment. Paired two-tailed Student's *t*-tests were performed to compare specific treatments in the absence and presence of inhibition. Levels of significance were: non-significant $p>0.05$, * $p<0.05$, ** $p<0.01$.

Turning the focus to the caspase-12 cleavage observed in the cerebellar granule neurons and to attempt to identify pathways involved in said cleavage, MGCM experiments were performed. Primary microglia were treated with thapsigargin or FG in the absence or presence of a range of pathway inhibitors for 24 hours, the medium was removed and administered to the CGC cultures depleted of microglia and caspase-12 expression was assayed by Western blotting. Administration of media from thapsigargin-treated microglial cultures to CGC cultures induced an increase in expression of the active, cleaved form of caspase-12 (36 kDa) (**Figure 4.2.13**), suggesting ER stress in microglia can induce extracellular signalling that can lead to neuronal vulnerability also with an ER stress component. Administration of media from FG-treated microglial cultures to the microglia-depleted CGC cultures also induced significant expression of the cleaved caspase-12, to a level similar to that seen with Th-MGCM (**Figure 4.2.13**) again suggesting microglial dysfunction or activation can lead to ER stress pathway activation in the neurons.

Previous data from ELISAs showed activation of the p38-MAPK pathway in FG-mediated TNFα release (**Figure 3.2.5**). Therefore, in an attempt to further elucidate the pathways in microglia responsible for the FG-mediated caspase-12 activation in the neurons, pathway inhibitors were administered to the microglial cultures prior to FG exposure for 24 hours. Pre-treatment of microglia with the specific inhibitor of p38-MAPK, SB203580 (SB) markedly decreased FG-MGCM-mediated caspase-12 cleavage in the neuronal cultures (**Figure 4.2.13**). This again suggests a role for this MAPK pathway in FG-mediated responses. Interestingly and conversely to the TNFα release data, pre-treatment of the microglial cultures with the phosphoinositide 3-kinase (PI3K) pathway inhibitor, wortmannin (Wort), also markedly attenuated the FG-mediated caspase-12 cleavage in the neuronal cultures. No observable modulation of caspase-12 cleavage occurred in the neuronal cultures after pre-treatment of the microglial cultures with the ERK1/2 specific inhibitor, PD98059 (PD) or the CD11b blocking antibody (CD11b). Finally, pre-treatment of the microglial cultures with

salubrinal did not attenuate the FG-MGCM-mediated caspase-12 cleavage observed in the neuronal cultures (**Figure 4.2.13**). This suggests FG-mediated microglial activation independent of the PERK-eIF2α axis of ER stress is sufficient to induce ER stress in neurons. These data however require clarification as the experiment was only performed on one occasion and the quality is poor.

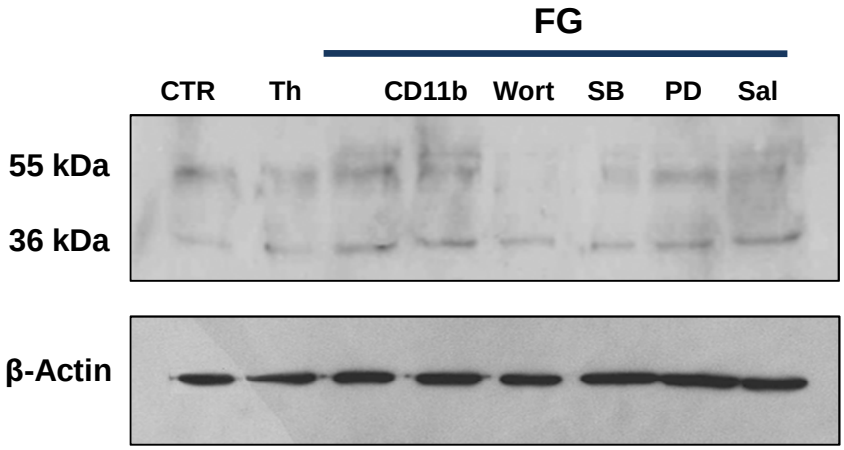

Figure 4.2.13. Expression of the cleaved form of caspase-12 in CGC cultures can be induced by FG-treated MGCM with involvement from MAPK pathways

Western blots for caspase-12 and β-actin expression in CGC cultures after treatment with MGCM from FG-treated microglial cultures alone or in combination with anti-CD11b blocking antibody (10 µg/ml), wortmannin (Wort; 100 nM), SB203580 (SB; 10 µM), PD98059 (PD; 10 µM) or salubrinal (Sal; 100 nM) for 24 hours. The experiment was performed on 1 occasion.

4.3. TNFα synthesis is involved in fibrinogen- and fibrin-mediated induction of endoplasmic reticulum stress marker activation in microglia and neuronal cultures

It was hypothesised from previous observations that soluble factors released from microglia could be responsible for the observed caspase-12 cleavage and subsequent cellular stress in the neurons, and therefore, pharmacological inhibition of iNOS activity or TNFα synthesis was performed. Addition of either AMT-HCl (iNOS activity inhibitor) or thalidomide (TNFα synthesis inhibitor) had no significant effect on fluorescence intensity attributed to caspase-12 activity, when compared with control levels (**Figure 4.3.1**). Similarly, pre-treatment of cultures with either AMT-HCl or thalidomide had no significant effect on caspase-12 activity induced by thapsigargin or tunicamycin treatment for 24 hours, as expected. FG-mediated induction of caspase-12 cleavage after 24 hours could not be attenuated by pre-treatment with AMT-HCl, in line with previous findings (**Figure 3.4.2 & 3.4.3**). However, exposure of the cultures to thalidomide prior to FG treatment for 24 hours significantly attenuated the fluorescence intensity attributed to caspase-12 activity (**Figure 4.3.1**). Modulation of the FN-mediated caspase-12 activity after 48 hours of treatment yielded similar, yet insignificant inhibition in the case of thalidomide pre-treatment, to that observed in FG treated cultures. Also, similarly to the FG-treated cultures, pre-treatment with AMT-HCl failed to attenuate FN-mediated caspase-12 activity (**Figure 4.3.1**). The presence of auto-fluorescent insoluble aggregates of FN in the cultures have been touched on previously, and could be manipulating, in a false-positive fashion, the fluorescence intensity data producing high variability between quantified fields and repetitions. To clarify these fluorescence findings, Western blotting was performed. In support of the thapsigargin-mediated induction of caspase-12 activity after 24 hours observed in the live cell staining experiments, significant expression of the cleaved form of caspase-12 (36 kDa), when compared with control levels, was observed (**Figure 4.3.2**).

Furthermore, pre-treatment with thalidomide failed to inhibit this significant cleavage. Again, in line with the fluorescence intensity analysis of the live cell staining, FG induced significant cleavage of caspase-12 after 24 hours, which could be significantly inhibited by thalidomide pre-treatment (**Figure 4.3.2**). Finally, FN-mediated induction of caspase-12 cleavage could not be inhibited by thalidomide pre-treatment, suggesting the quantified fluorescence intensity attributed to caspase-12 activity was correct. Interestingly, previous observations suggested treatment of cultures with thalidomide prior to FN for 48 hours protected the cultures from toxicity. This observation seemed to be supported in the caspase-12 live cell staining experiment by a significantly lower percentage of cells staining for propidium iodide (PI), further supporting the hypothesis that caspase-12 activity is not primarily required for FN-mediated toxicity.

These findings could also be replicated in primary microglial cultures, with FN treatment for 24 hours inducing cleavage that could not be inhibited after a pre-treatment of cultures with thalidomide (**Figure 4.3.3**). Furthermore, significant caspase-12 cleavage induced by FG treatment for 24 hours could be inhibited by thalidomide treatment.

Figure 4.3.1

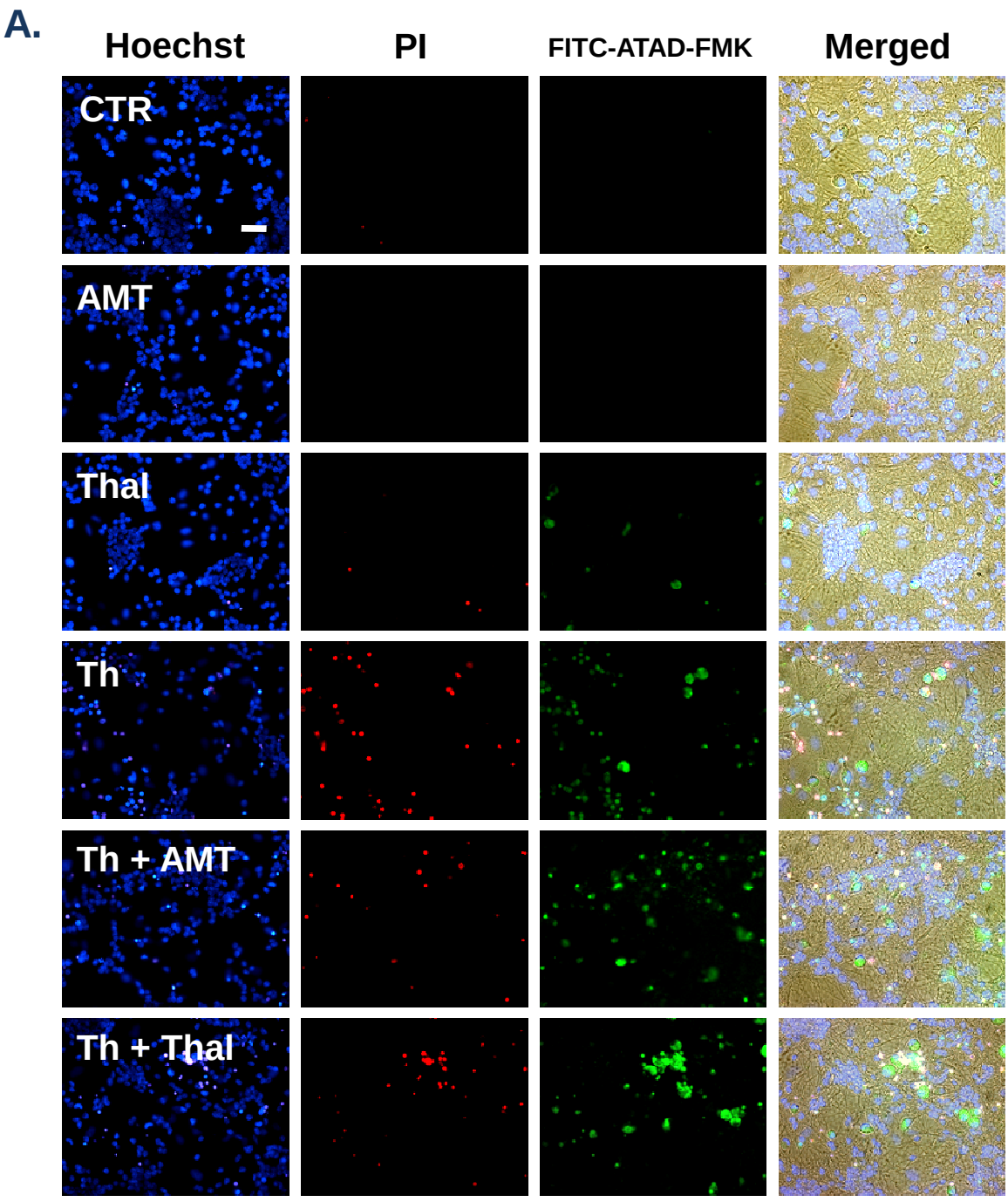
A.
Hoechst
PI
FITC-ATAD-FMK
Merged
CTR
AMT
Thal
Th
Th + AMT
Th + Thal

Figure 4.3.1A continued

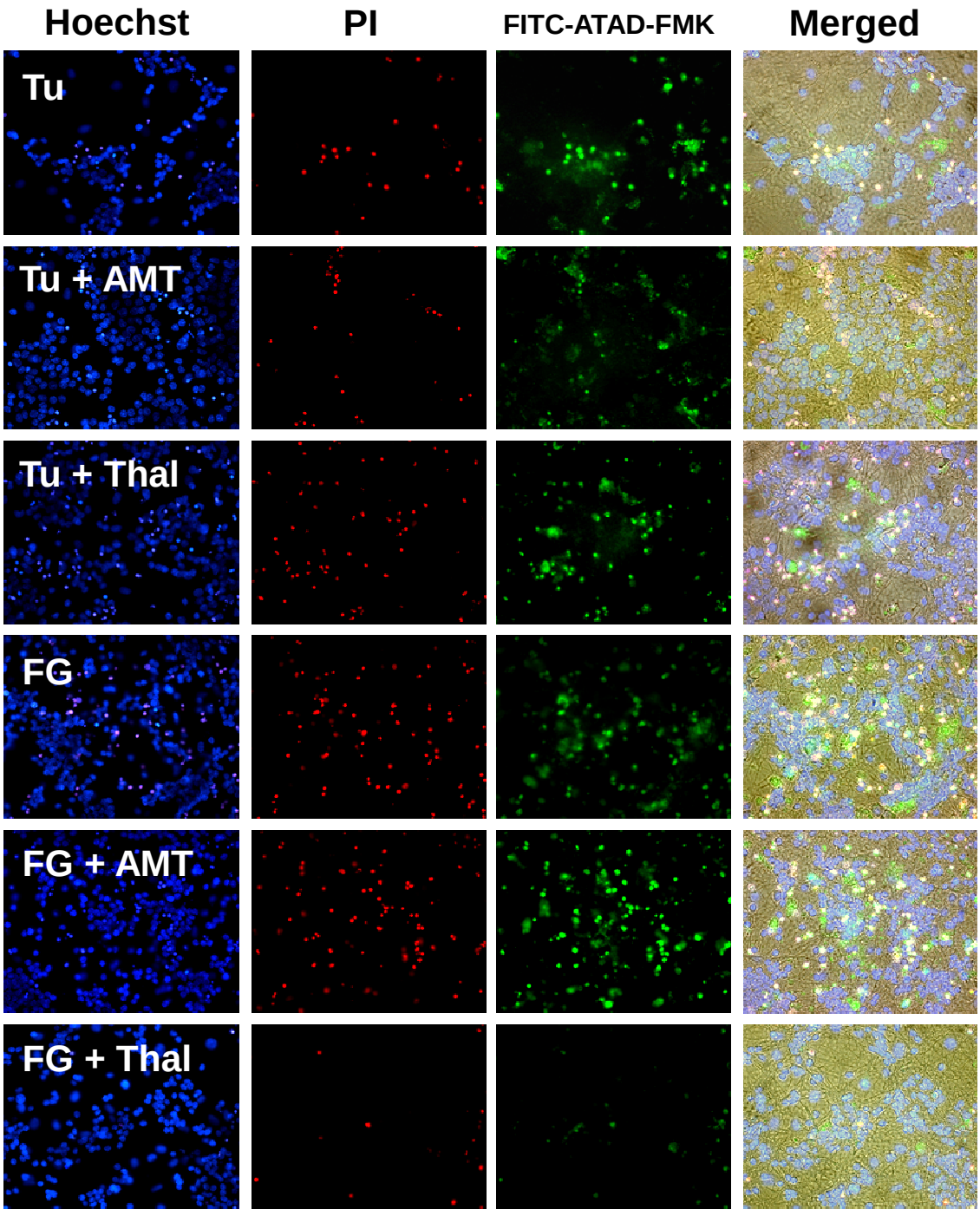

Figure 4.3.1A continued

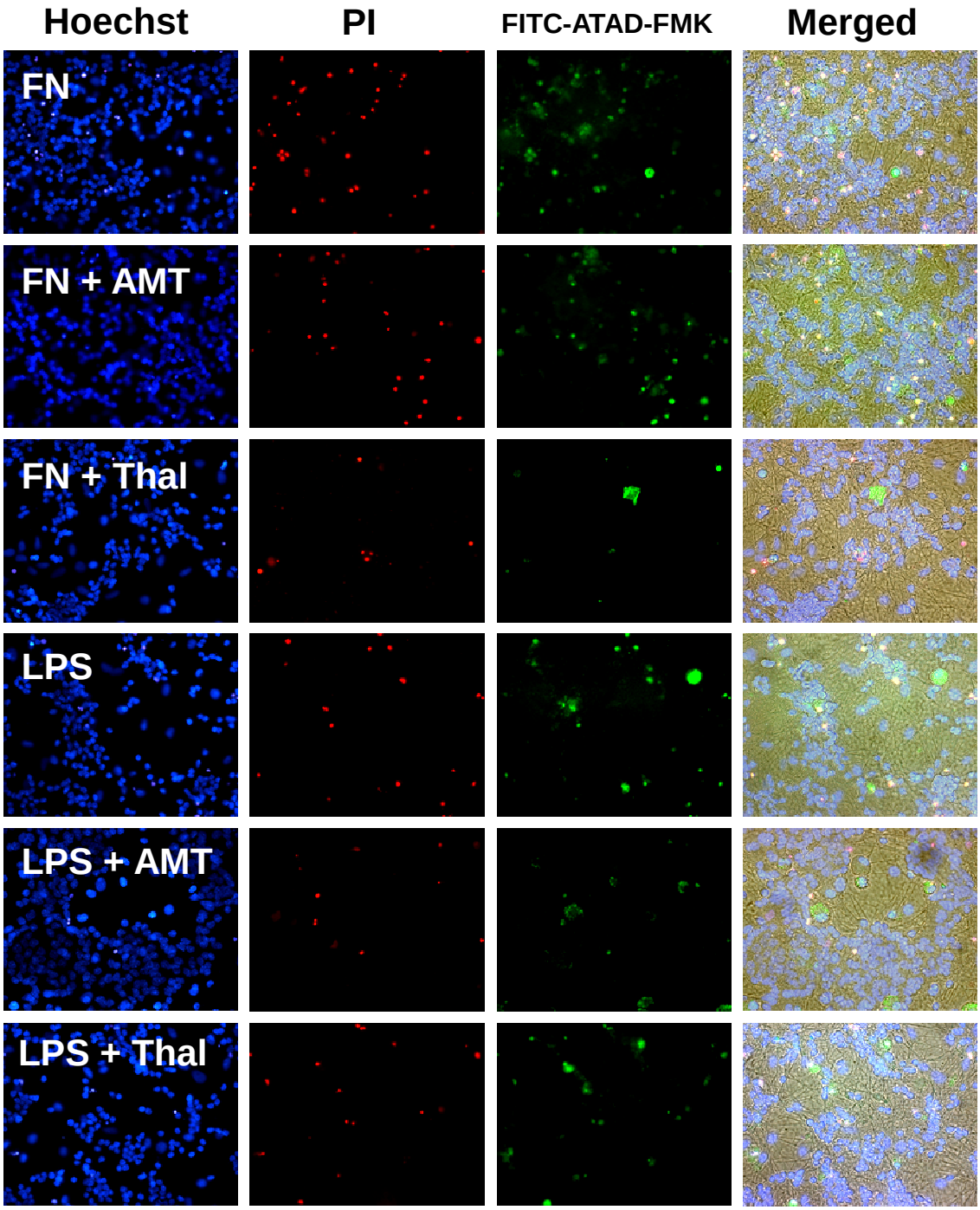

B.

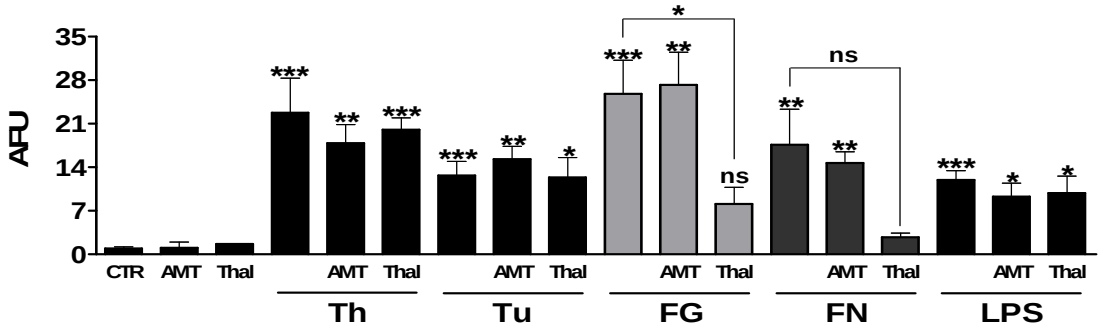

Figure 4.3.1. FG-induced caspase-12-associated fluorescence in CGC cultures is attenuated by inhibition of TNFα synthesis

A. Panel of representative images from live cell staining experiments in CGC cultures after treatment with Th (2 µM; 24 hours), Tu (1 µg/ml; 24 hours), FG (2.5 mg/ml; 24 hours), FN (1 mg/ml; 48 hours) or LPS (1 µg/ml; 48 hours) alone or in combination with AMT-HCl (AMT; 150 nM) or thalidomide (Thal; 10 µg/ml). Live cell staining was performed using Hoechst-33342 for nucleus identification, propidium iodide (PI; red) for total cell death, and FITC-ATAD-FMK (green) for active caspase-12. Original magnification: x40, scale bar: 40 µm. **B.** Quantification of the relative active caspase-12 fluorescence intensity/cell in CGC cultures after administration of treatments outlined in **A**. Data are presented in arbitrary fluorescence units (AFU). Treatments were in duplicate and data were analysed from 3 independent experiments. To compare the AFU of control levels to all other treatments, a one way ANOVA was performed with Dunnett's post-test. To compare specific treatments with treatments + inhibitors, paired two-tailed Student's *t*-tests were performed. Levels of significance were: non-significant $p>0.05$, * $p<0.05$, ** $p<0.01$, *** $p<0.001$.

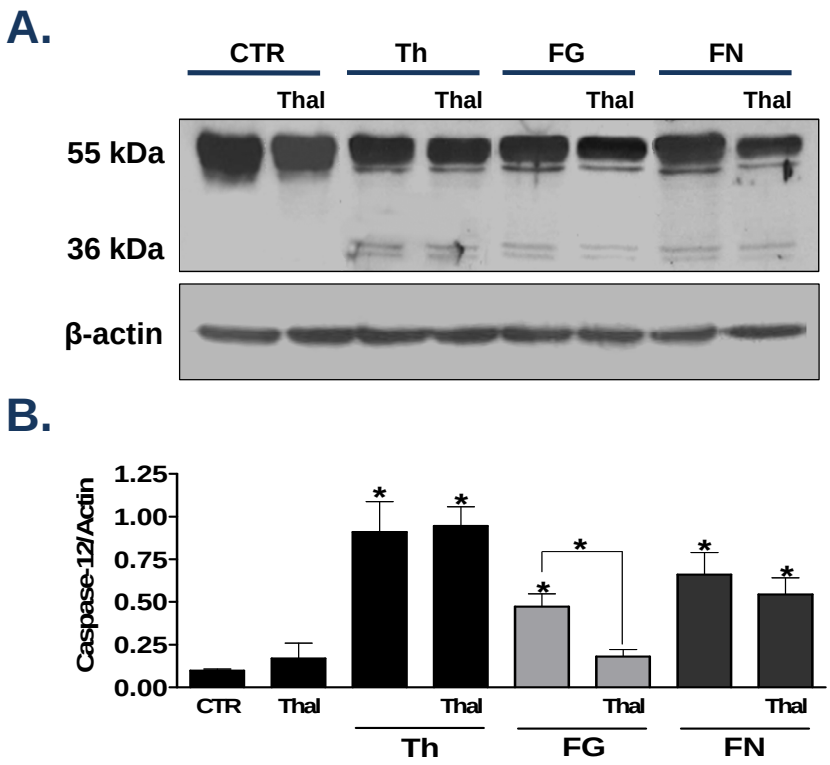

Figure 4.3.2. FG-mediated expression of the cleaved form of caspase-12 in CGC cultures is dependent on TNFα synthesis

A. Representative Western blots for caspase-12 and β-actin expression in CGC cultures after treatment with Th (2 µM; 24 hours), FG (2.5 mg/ml; 24 hours) or FN (1 mg/ml; 48 hours) alone or in combination with Thal (10 µg/ml). **B.** Quantification of cleaved caspase-12 expression, with respect to β-actin expression, after treatments as outlined in **A**. Experiments were repeated on 3 independent occasions. One-way ANOVA with Dunnett's post test was performed to compare control levels with each treatment and paired two-tailed Student's *t*-tests were performed to compare specific treatments with microglia present or absent. Levels of significance were: non-significant $p>0.05$, * $p<0.05$.

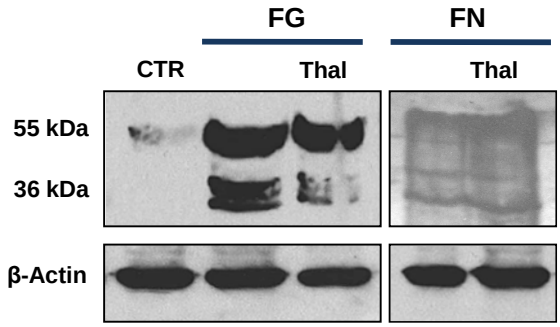

Figure 4.3.3. FG-mediated expression of the cleaved form of caspase-12 in CGC cultures seems to be dependent on TNFα synthesis

Representative Western blots for caspase-12 and β-actin expression in primary microglial cultures after treatment with FG (2.5 mg/ml) or FN (1 mg/ml) alone or in combination with Thal (10 µg/ml) for 24 hours. The FG treatment was performed on 2 independent occasions and FN treatment was performed on 1 occasions.

4.3.1. Fibrinogen- and fibrin-mediated CHOP expression in microglia is dependent on TNFα synthesis and fibrinogen-mediated TNFα release is dependent on ER stress induction

As explained previously, caspase-12 activation alone cannot confirm ER stress. Therefore, further support of the ER stress hypothesis, and involvement of TNFα signalling, was achieved by immunocytochemistry for CHOP expression in microglial cultures after treatment with FG and FN in the presence or absence of inhibition of TNFα signalling. Treatment with AMT-HCl or thalidomide alone did not induce an increase in CHOP-positive microglia, when compared with control cultures (**Figure 4.3.4**). As expected, treatment with thapsigargin for 24 hours induced an increase in the percentage of CHOP-positive microglia, when compared with control cultures. In line with previous observations, FG treatment for 24 hours also increased the percentage of CHOP-positive microglia, when compared with control cultures (**Figure 4.3.4**). AMT-HCl had no effect on FG-mediated CHOP expression however thalidomide pre-treatment markedly decreased the percentage of CHOP-positive microglia in FG-treated cultures. Exposure of cultures to FN for 24 hours increased the percentage of CHOP-positive cells, when compared with controls, in line with previous observations (**Figure 4.2.10**). Treatment of cultures with AMT-HCl prior to FN exposure for 24 hours did not modulate the percentage of CHOP-positive microglia. However, unlike the caspase-12 expression profile, thalidomide pre-treatment did decrease the number of CHOP-positive microglia in FN-treated cultures (**Figure 4.3.4**). Finally, FG-mediated TNFα release could be significantly attenuated by co-treatment with salubrinal, although significant TNFα release was still observed, when compared to control levels suggesting partial ER stress-dependent induction of TNFα release from microglia (**Figure 4.3.5**).

Figure 4.3.4

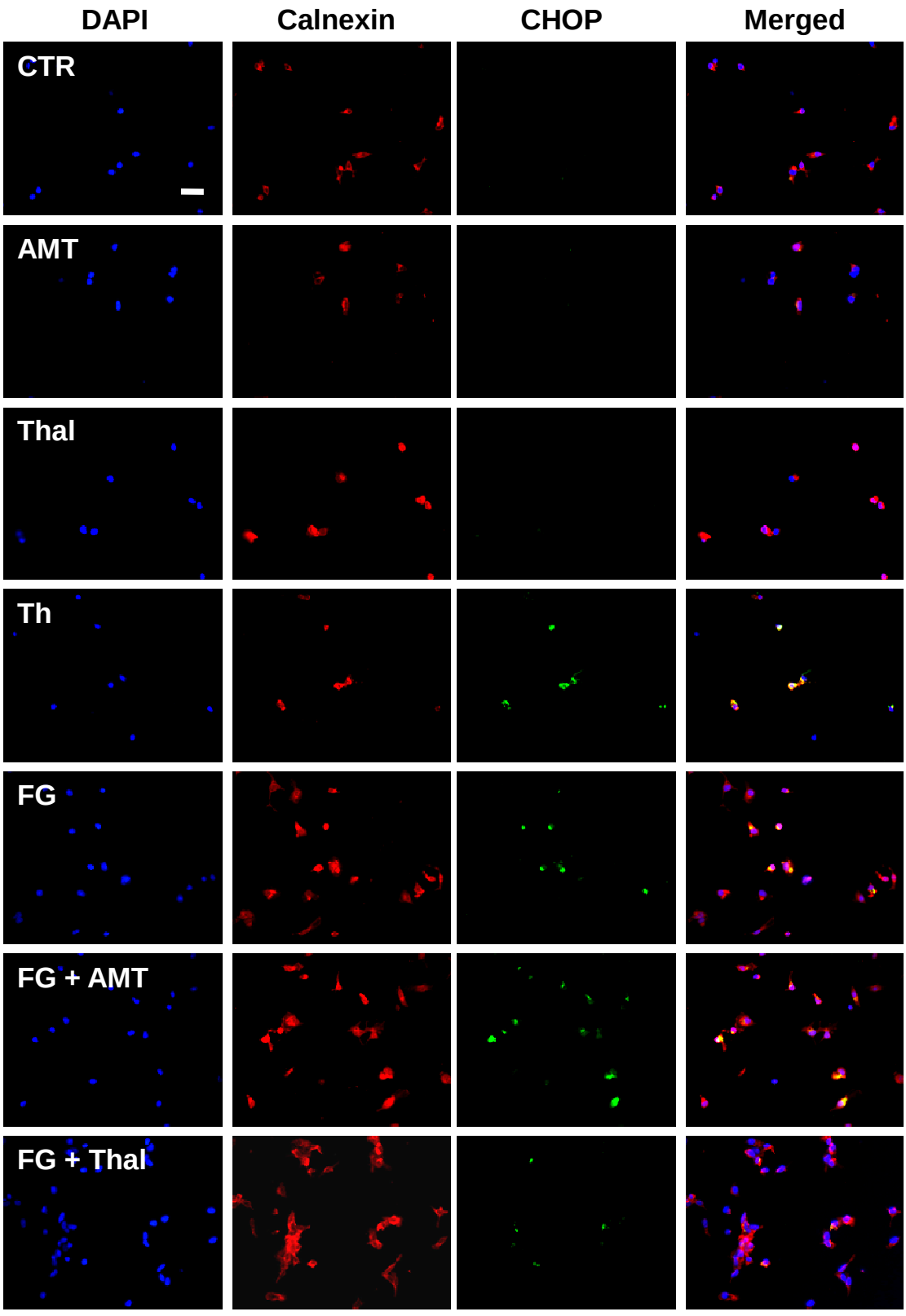

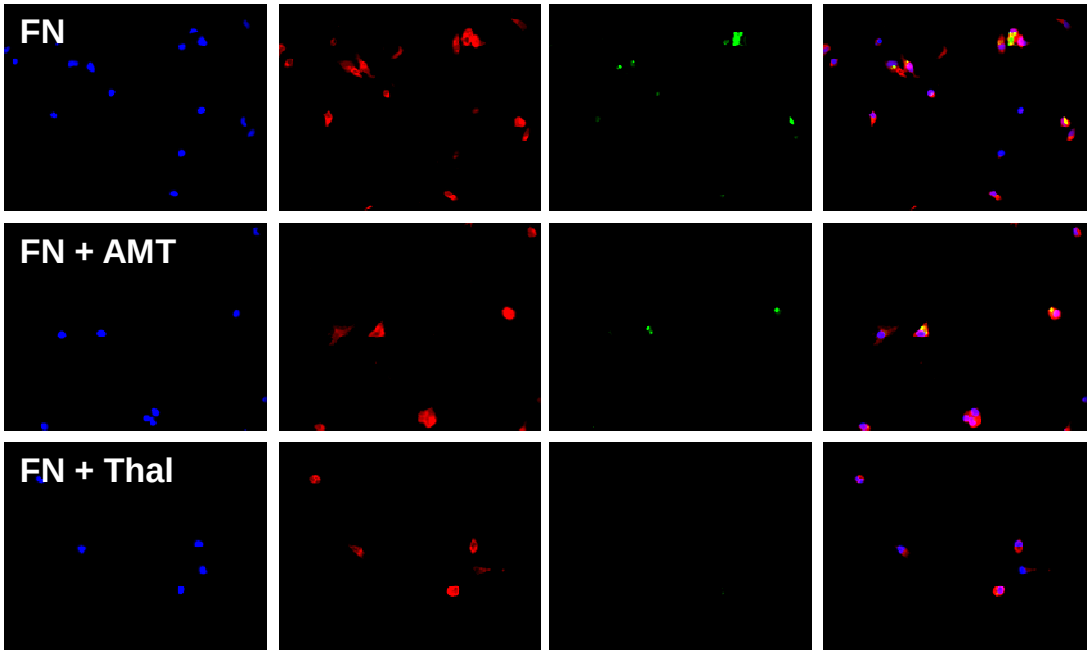

Figure 4.3.4. FG- and FN-mediated induction of CHOP expression in microglia is attenuated by TNFα synthesis inhibition

Representative images from primary microglial cultures after treatment with Th (2 µM, FG (2.5 mg/ml) or FN (1 mg/ml) alone or in combination with AMT (150 nM) or Thal (10 µg/ml), for 24 hours. Cultures were stained with DAPI for quantification of cell number and probed with anti-Calnexin-TRITC (red) for staining of cellular ER and anti-CHOP (green), except in negative control cultures, where primary antibodies were omitted. Original magnification: x40, scale bar: 40 µm. Treatments were in triplicate, n = 1.

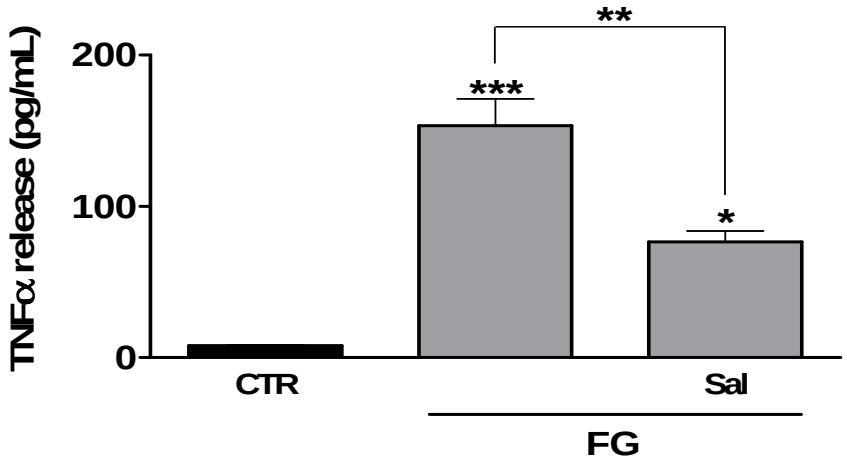

Figure 4.3.5. FG- mediated TNFα release from microglia is partially attenuated by ER stress inhibition

ELISA analysis of TNFα release from primary microglia cultures after treatment with FG (2.5 mg/ml) alone or in combination with salubrinal (100 nM) for 24 hours. Treatments were in duplicate in each experiment and data were analysed from 3 independent experiments. To compare multiple treatments to non-treated control levels an ANOVA with Dunnett's post-test was performed. Paired two-tailed Student's *t*-tests were performed between specific treatments. Levels of significance were: non-significant $p>0.05$, * $p<0.05$, ** $p<0.01$, *** $p<0.001$

4.4. Fibrinogen treatment causes calcium dyshomeostasis in microglia

Due to the more interesting and robust findings, it was decided the majority of subsequent ER stress related data would focus on FG-mediated responses. Alteration in calcium homeostasis is a contributing factor in ER stress (Lindholm et al. 2006). Therefore, it was hypothesised that suppressing any FG-mediated alterations in microglial calcium concentration would allow us to identify whether FG exposure modulated calcium homeostasis, in turn inducing ER stress pathways.

4.4.1. High concentrations of BAPTA-AM induce microglial apoptosis

Initially, previously published concentrations (50 µm; Hoffmann et al. 2003) of the well characterised calcium chelator, BAPTA-AM were tested, however almost total death was observed in the microglial cultures. Therefore a concentration titration was performed on the cultures and the percentage of apoptotic and amoeboid morphology was quantified. BAPTA-AM (5-10,000 nM) was incubated with microglial cultures for 24 hours to mimic the duration required for FG-treatment. Only the top concentration (10,000 nM) was able to induce observable levels of apoptotic morphology when compared with control levels (**Figure 4.4.1**). With previously published effective concentrations ranging from 10-50 µM, it was decided to use the highest concentration that did not induce an increase in apoptotic and amoeboid morphology,

Figure 4.4.1

A.

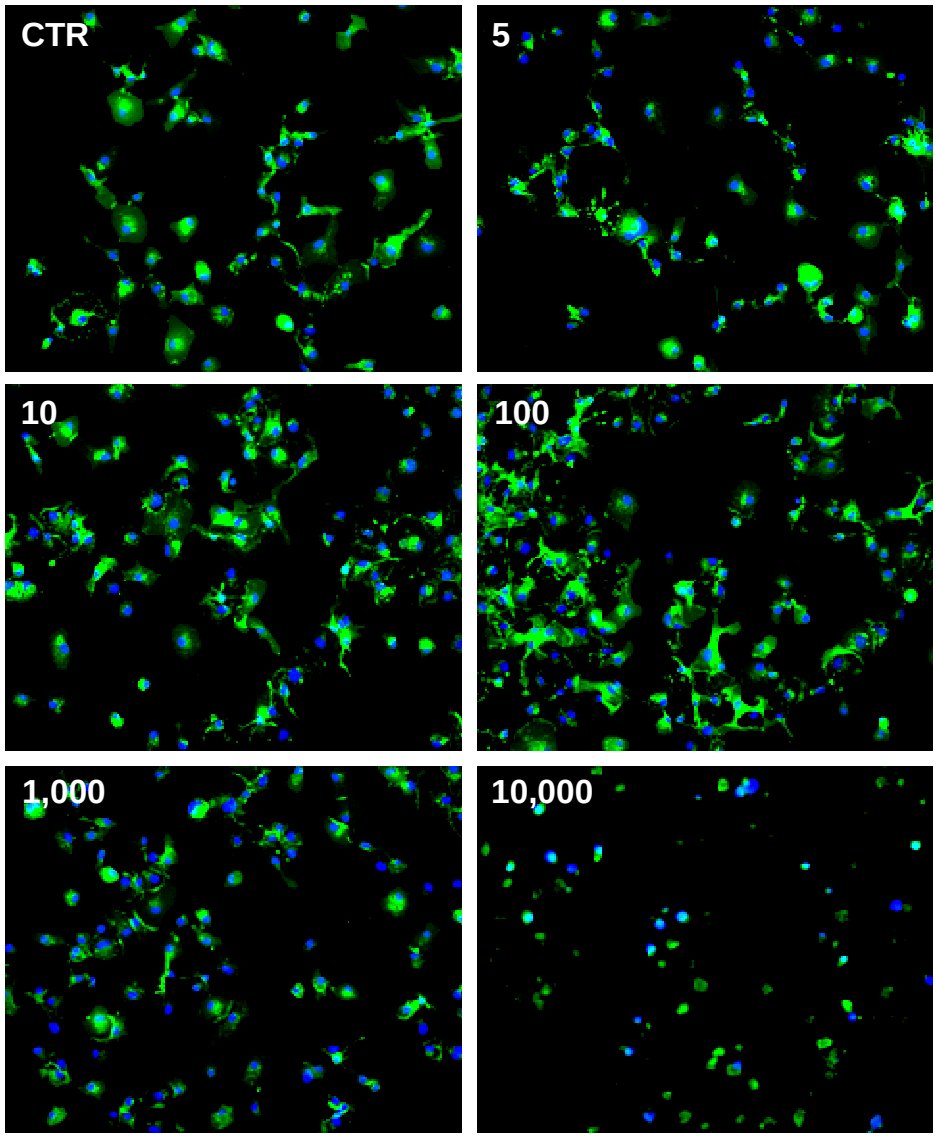

B.

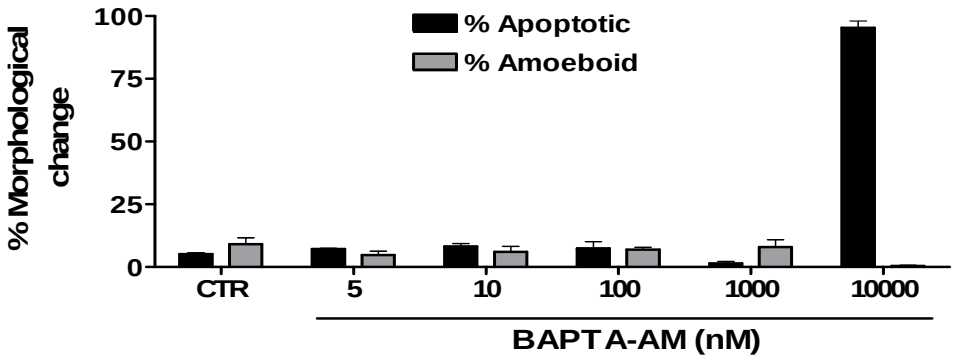

Figure 4.4.1. BAPTA-AM titration on primary microglial cultures – analysis of activated and apoptotic morphology

A. Panel of representative images from live cell staining experiments in primary microglial cultures after treatment with BAPTA-AM (5 – 10,000 nM). Live cell staining was performed using Hoechst-33342 for identification of nuclear apoptotic morphology and isolectin-B_4 (IB_4; green) for microglial identification and used for the quantification of amoeboid morphology. Original magnification: x20. **B.** Quantification of morphological changes in microglia (apoptotic and amoeboid after treatment as outlined in **A**. Data are presented as a percentage of the total number in each field analysed. Treatments were in triplicate, n = 1.

4.4.2. Co-treatment of microglia with fibrinogen and BAPTA induces significant apoptosis

Live cell staining was performed on microglial cultures to identify whether FG-mediated caspase-12 activation was modulated if free calcium was chelated. Treatment with BAPTA-AM alone for 24 hours did not induce caspase-12 activation or significant cell death. As previously shown, FG treatment for 24 hours significantly increased fluorescence intensity attributed to caspase-12 activation when compared with control intensity, and also in line with previous findings, the cultures did not show a significant percentage of cells staining positive for PI, when compared with control cultures (**Figure 4.4.2**). BAPTA-AM co-treatment with FG for 24 hours inhibited the FG-mediated increase in caspase-12 activity (**Figure 4.4.2**), however the cultures showed a significant increase in cells staining positive for PI, when compared with control cultures, suggesting strong toxicity of co-treatment is responsible for the lack of caspase-12 activity rather than an inhibitory effect mediated by BAPTA-AM. These findings support a vital role for calcium in FG-mediated caspase-12 activation in microglia.

Live cell staining for caspase-3/7 activation was performed on the microglial cultures after treatment with FG in the absence and presence of BAPTA-AM. Interestingly, BAPTA-AM treatment alone for 24 hours did not induce a significant increase in fluorescence intensity attributed to caspase-3/7 activity (**Figure 4.4.3**), further supporting a non-toxic induction of caspase-12 cleavage. Also, in line with previous experiments, no significant increase in death was observed, when compared with control cultures. FG treatment alone for 24 hours induced a significant in fluorescence, but no significant increase in death, when compared with control cultures (**Figure 4.4.3**). Finally, BAPTA-AM treatment prior to FG exposure for 24 hours induced significant death, when compared with control cultures and these data were further supported by a significant increase in caspase-3/7 attributed fluorescence (**Figure 4.4.3**).

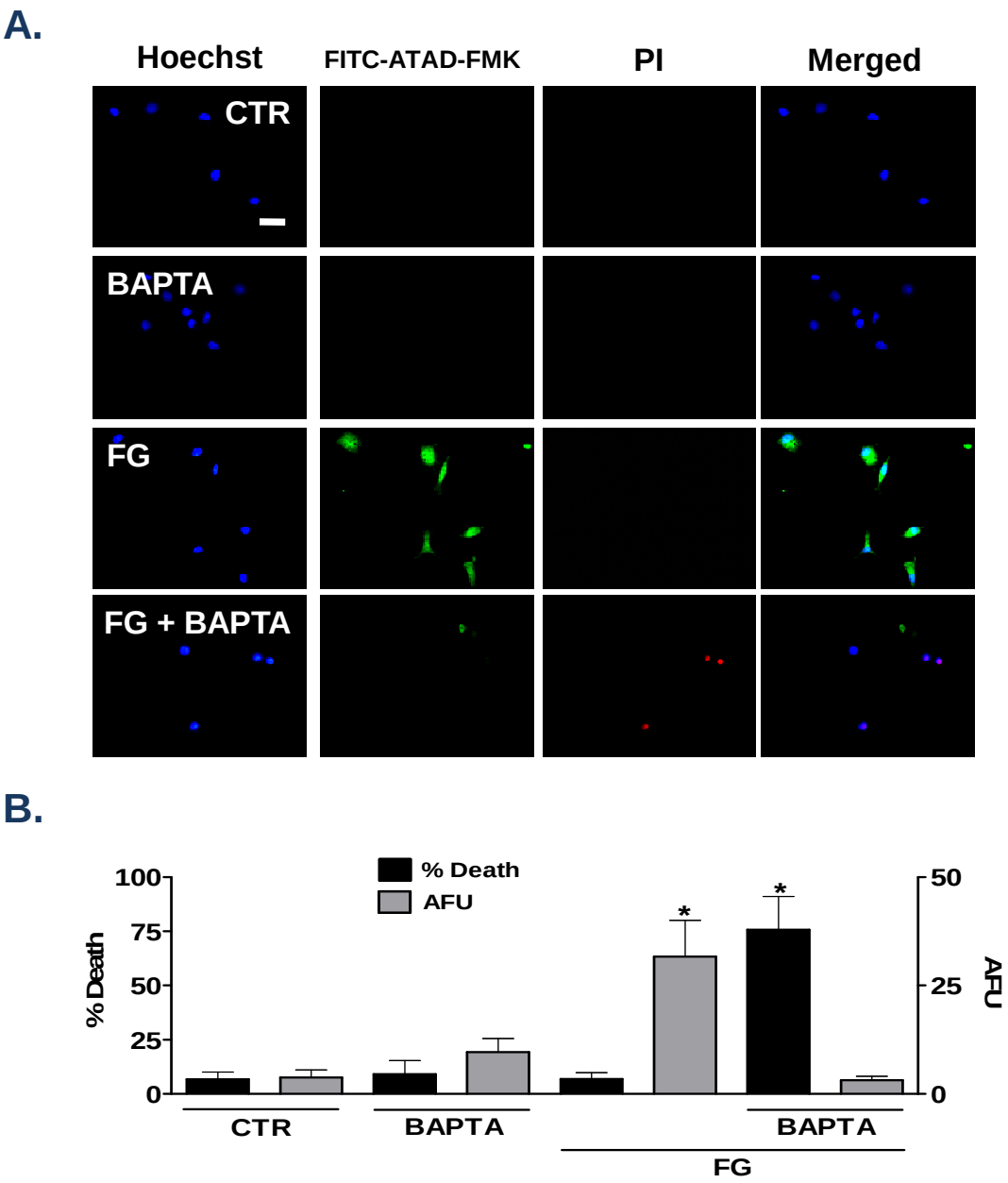

Figure 4.4.2. Co-treatment of microglia with FG and BAPTA-AM attenuates caspase-12 activation, but enhances cell death

A. Panel of representative images from live cell staining experiments in primary microglial cultures after treatment with BAPTA-AM (BAPTA; 1 µM) or FG (2.5 mg/ml), alone or in combination for 24 hours. Live cell staining was performed using Hoechst-33342 for nucleus identification, propidium iodide (PI; red) for total cell death, and FITC-ATAD-FMK (green) for active caspase-12. Original magnification: x40, scale bar: 40 µm. **B.** Quantification of cell death presented as a percentage of cells staining positive for PI (black bars) and quantification of the relative active caspase-12 fluorescence intensity/cell in microglial cultures (grey bars) after administration of treatments as outlined in **A**. Data are presented in arbitrary fluorescence units (AFU). Treatments were in triplicate and data were analysed from 3 independent experiments. To compare the % cell death and AFU of control levels and treatments, a one way ANOVA was performed with Dunnett's post-test. Levels of significance were: non-significant $p>0.05$, ** $p<0.01$, *** $p<0.001$.

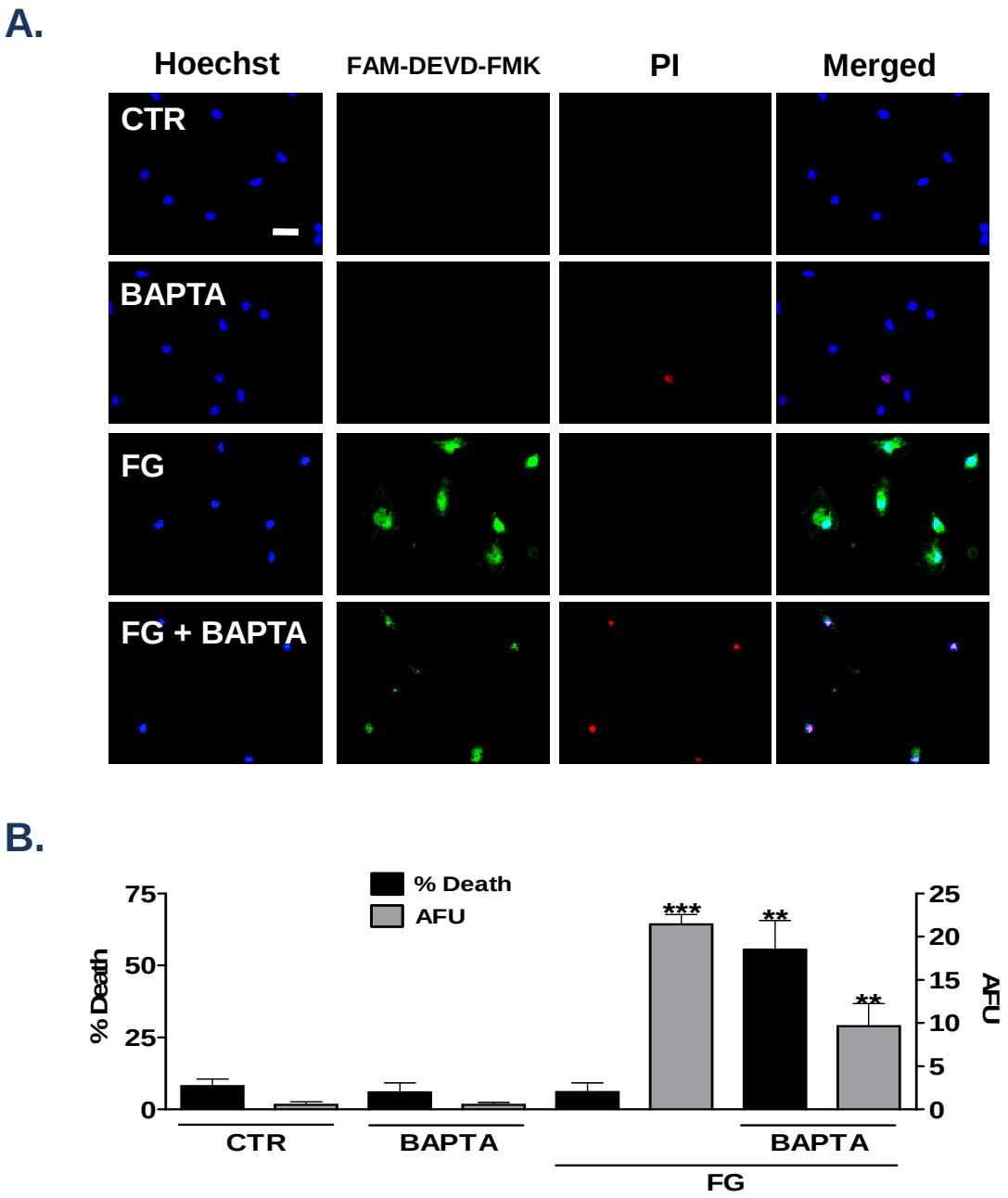

Figure 4.4.3. Co-treatment of microglia with FG and BAPTA-AM induces apoptotic cell death

A. Panel of representative images from live cell staining experiments in primary microglial cultures after treatment with BAPTA-AM (BAPTA; 1 µM) or FG (2.5 mg/ml), alone or in combination. Live cell staining was performed using Hoechst-33342 for nucleus identification, propidium iodide (PI; red) for total cell death, and FAM-DEVD-FMK (green) for active caspase-3/7. Original magnification: x40, scale bar: 40 µm. **B.** Quantification of cell death presented as a percentage of cells staining positive for PI (black bars) and quantification of the relative active caspase-3/7 fluorescence intensity/cell in microglial cultures (grey bars) after administration of treatments as outlined in **A**. Data are presented in arbitrary fluorescence units (AFU). Treatments were in triplicate and data were analysed from 3 independent experiments. To compare the % cell death and AFU of control levels and treatments, a one way ANOVA was performed with Dunnett's post-test. Levels of significance were: non-significant $p>0.05$, ** $p<0.01$, *** $p<0.001$.

4.4.3. Fibrinogen mediates early calpain activity in a microglial cell line

To further study the role of calcium in FG-mediated responses, calpain activity was analysed. Calpains are calcium activated cysteine proteases. To date, there are 6 members, divided into subfamilies by ubiquitous or tissue-specific expression. Two ubiquitously expressed members are the most comprehensively characterised, known as μ-calpain and m-calpain (Saido et al. 1994; Nakagawa & Yuan 2000). These calpains are distinguishable from each other by their differential *in vitro* calcium concentration requirement for activation, with μ-calpain dependent on micromolar calcium and m-calpain on millimolar (Nakagawa & Yuan 2000), hence the respective names. Furthermore it has been suggested that m-calpain may be responsible for procaspase-12 cleavage to the active form and that disturbances in intracellular calcium storage as a result of amyloid-β peptide cytotoxicity may induce apoptosis through calpain-mediated caspase-12 activation (Nakagawa & Yuan 2000). Therefore, it was decided, due to lack of calcium imaging facilities that characterisation of the activity of this protease family could allow us to further support a significant role for calcium in FG-mediated responses.

Initial optimisation and characterisation of the calpain activity assay adapted from D'Amelio et al., 2011, is shown in **Figure 4.4.4** and described in methodology **Section 2.9**. After optimisation was completed, a timecourse of FG-mediated calpain activity in the BV2 microglia cell line was performed as it was hypothesised that due to previous findings (Nakagawa & Yuan 2000), the calpain activity/activation would occur prior to any significant caspase-12 cleavage had occurred (i.e. < 12 hours; **Figure 4.2.2**). Ionomycin treatment for 30 minutes significantly increased calpain activity, when compared with control, and this increase could be inhibited by calpastatin pre-treatment (**Figure 4.4.5**). Longer exposure (1 hour) to ionomycin did not significantly increase calpain activity when compared with control. There was a highly significant increase in FG-mediated calpain activity after only 1 hour, when compared with control activity that was significantly attenuated by calpastatin pre-treatment. However, after 2-4 hours,

variability was observed and any significant increase of calpain activity was not inhibited by calpastatin pre-treatment, in fact at 2 hours, pre-treatment with calpastatin actually enhanced FG-mediated calpain activity (**Figure 4.4.5**). At 8 hours of FG treatment however, a highly significant increase in calpain activity was observed that could be inhibited by calpastatin pre-treatment (**Figure 4.4.5**). The signal window when compared with control activity was the largest observed, therefore 8 hours of FG treatment was used in subsequent calpain activity assays. Finally, it was noted that no significant increase in calpain activity was observed after 12 hours of treatment. This supports the idea that activity of this protease occurs primarily before significant caspase-12 cleavage.

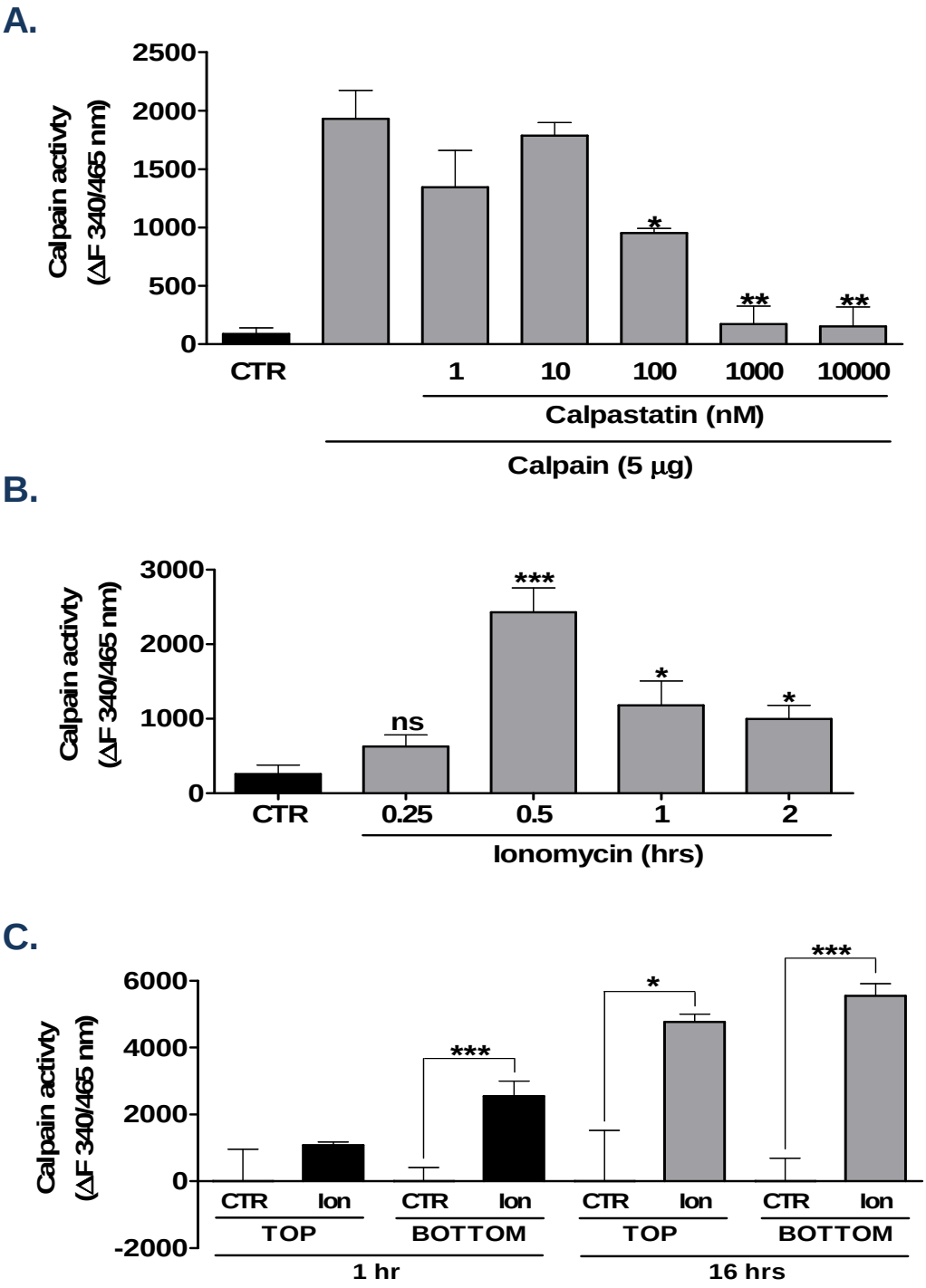

Figure 4.4.4. Calpain activity assay optimisation

A. Titration of calpastatin-mediated inhibition of calpain activity identified 1 µM calpastatin as the optimum concentration to be used in subsequent experiments. **B.** Optimisation of Ionomycin (Ion; 2 µM) incubation period shows 30 minutes provides the largest increase in calpain activity when compared with control and will therefore be used in subsequent experiments. **C.** Optimisation of the dye incubation period and fluorescence readout position shows 16 hours with the readout performed from the bottom of the well is the most effective.

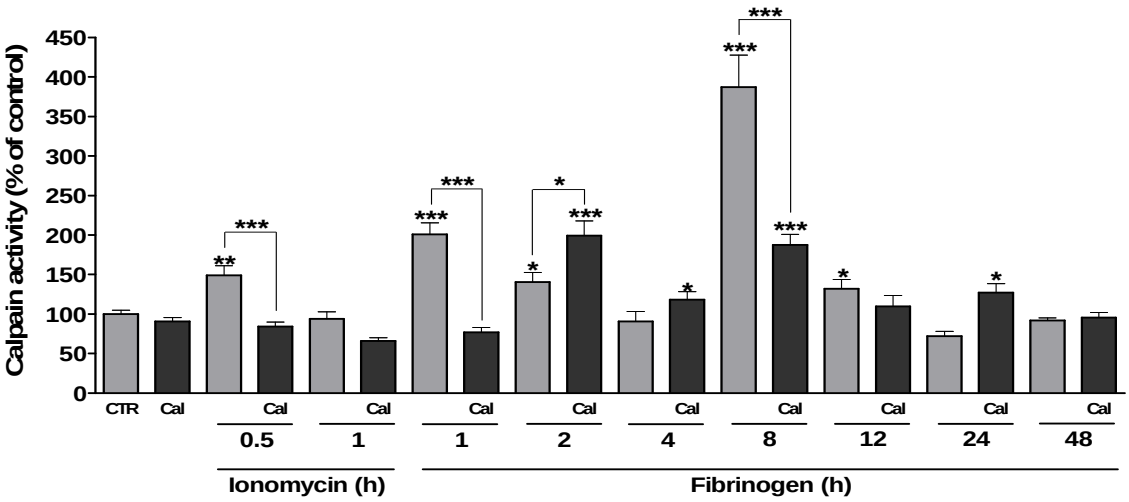

Figure 4.4.5. FG treatment of BV2 microglia induces a significant increase in calpain activity

Calpain activity assay performed on BV2 microglia lysates treated with ionomycin (2 µM) for 0.5 – 1 hours or FG (2.5 mg/ml) for 1 – 48 hours, alone or in combination with calpastatin (Cal; 1 µM). Data are presented as the percentage of calpain activity in relation to control levels. Treatments were in triplicate and data were analysed from 3 independent experiments. To compare calpain activity between control and all treatments, a one way ANOVA was performed with Dunnett's post-test. Paired two-tailed Student's *t*-tests were performed for comparisons between treatments with and without calpastatin 'inhibition'. Levels of significance were: non-significant $p>0.05$, * $p<0.05$, ** $p<0.01$, *** $p<0.001$.

4.4.4. Fibrinogen-mediated calpain activity has dependence on iNOS activity

It was hypothesised that inhibiting TNFα would not affect FG-mediated calpain activity after 8 hours. This was due to TNFα release data from FG-treated microglia (**Figure 3.2.3 A**) that identified the concentration of TNFα that is released after 8 hours of FG treatment to be significantly lower than the concentrations shown previously to be effective (Taylor et al. 2005). It was also suggested that iNOS activity would not be involved in any FG-mediated calpain responses due to lack of data supporting a role for the enzyme in any of the previously observed FG responses. As expected, treatment of cultures with ionomycin for 30 minutes significantly increased calpain activity, when compared with control (**Figure 4.4.6**). This increase in activity was significantly inhibited by pre-treatment of cultures with calpastatin. Also, treatment with either AMT-HCl or thalidomide alone for 8 hours did not significantly modulate calpain activity. In agreement with the first hypothesis, pre-treatment of cultures with thalidomide did not induce significant modulation of FG-mediated calpain responses after 8 hours. Interestingly however, treatment of cultures with AMT-HCl prior to FG exposure for 8 hours did significantly inhibit FG-mediated activity (**Figure 4.4.6**), suggesting an early role for iNOS activity in FG-mediated responses. Finally, in line with previous observations, treatment of cultures with calpastatin prior to FG exposure for 8 hours significantly inhibited calpain activity.

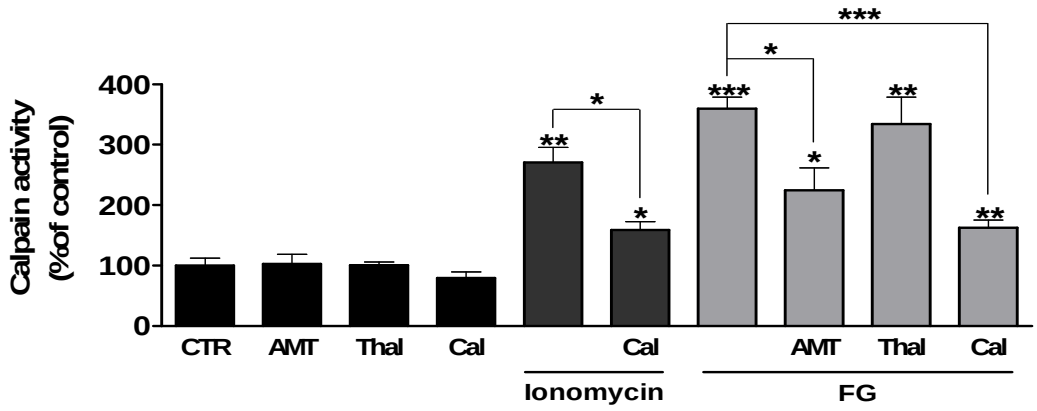

Figure 4.4.6. FG-mediated calpain activity in BV2 microglia is partially dependent on iNOS activity

Calpain activity assay performed on BV2 microglia lysates treated with ionomycin (2 µM) for 0.5 hours or FG (2.5 mg/ml) for 8 hours, alone or in combination with AMT-HCl (AMT; 150 nM), thalidomide (Thal; 10 µg/ml) or calpastatin (Cal; 1 µM). Data are presented as the percentage of calpain activity in relation to control levels. Treatments were in triplicate and data were analysed from 3 independent experiments. To compare calpain activity between control and all treatments, a one way ANOVA was performed with Dunnett's post-test. Paired two-tailed Student's *t*-tests were performed for comparisons between treatments with and without inhibitors. Levels of significance were: non-significant $p>0.05$, * $p<0.05$, ** $p<0.01$, *** $p<0.001$.

The involvement of calpain activity in FG-mediated cleavage of caspase-12 and TNFα expression was then assayed as these events have been shown to occur chronologically later than the significant calpain activity. Western blotting for caspase-12 and TNFα expression was performed in BV2 lysates after treatment with calpastatin prior to FG exposure for 24 hours (**Figure 4.4.7**). Treatment of cultures with thapsigargin for 24 hours significantly increased cleaved caspase-12 expression and TNFα expression. Also in line with previous experiments, treatment of cultures with FG induced significant cleaved caspase-12 and TNFα expression, and these increases in expression could be inhibited by calpastatin pre-treatment (**Figure 4.4.7**), suggesting calpain activity is upstream of FG-mediated caspase-12 cleavage and TNFα expression, which have been shown to be involved in subsequent neuronal toxicity.

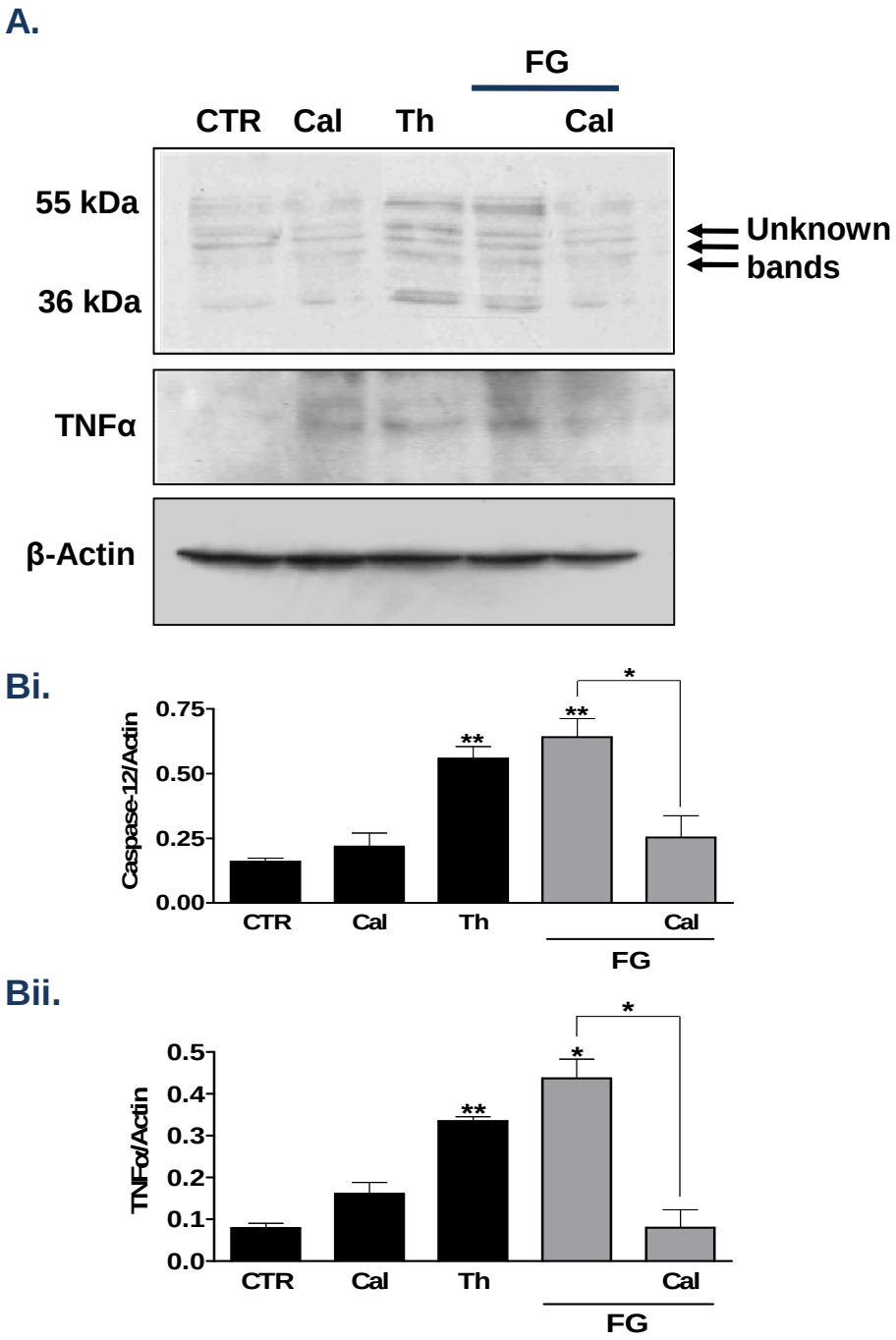

Figure 4.4.7. FG-mediated expression of the cleaved form of caspase-12 and TNFα in BV2 microglia is dependent on calpain activity

A. Representative Western blots for caspase-12, TNFα and β-actin expression in BV2 microglia lysates after treatment with Thapsigargin (2 µM) or FG (2.5 mg/ml) for 24 hours, alone or in combination with calpastatin (Cal; 1 µM). **B.** Quantification of cleaved caspase-12 expression (**Bi**) and TNFα expression (**Bii**), with respect to β-actin expression, after treatments as stated in **A**. Experiments were repeated on 3 independent occasions. One-way ANOVA with Dunnett's post test was performed to compare control levels with each treatment and paired two-tailed Student's *t*-tests were performed to compare FG with and without calpastatin inhibition. Levels of significance were: non-significant $p>0.05$, * $p<0.05$, ** $p<0.01$.

4.5. Pharmacological manipulation of ER stress-associated pathways significantly reduces fibrinogen-mediated apoptosis

Following on from these experiments showing a range of ER- and calcium-dependent responses, it was hypothesised that manipulation of these pathways could protect against microglial-mediated neurotoxicity. Initially, CGC cultures were treated with z-ATAD-FMK, a caspase-12 specific inhibitor, prior to FG or FN exposure for 24 or 48 hours, respectively. Staurosporine (STS) was used as a positive control for significant apoptosis but via a caspase-12 independent pathway, and tunicamycin and thapsigargin were used as positive controls for significant apoptosis via caspase-12 dependent pathways. As expected, STS treatment for 8 hours induced a significant increase in apoptotic morphology when compared with control levels, and this significant increase could not be inhibited by pre-treatment with z-ATAD-FMK (**Figure 4.5.1**). Both tunicamycin and thapsigargin administration for 24 hours induced significant increases in apoptotic morphology, when compared with control cultures. Interestingly however, pre-treatment with z-ATAD-FMK could only significantly inhibit tunicamycin-mediated apoptosis and not thapsigargin induction (**Figure 4.5.1**), suggesting caspase-12 independent pathways are involved in thapsigargin-mediated cellular toxicity or the thapsigargin concentration used was too high for effective inhibition by z-ATAD-FMK. FG treatment induced a significant increase in apoptotic morphology, as previously shown, which could be significantly inhibited by z-ATAD-FMK pre-treatment. However, the significant FN-mediated increase in apoptotic morphology could not be significantly inhibited by z-ATAD-FMK pre-treatment, further supporting the idea that caspase-12 is not primarily involved in FN-mediated cellular toxicity.

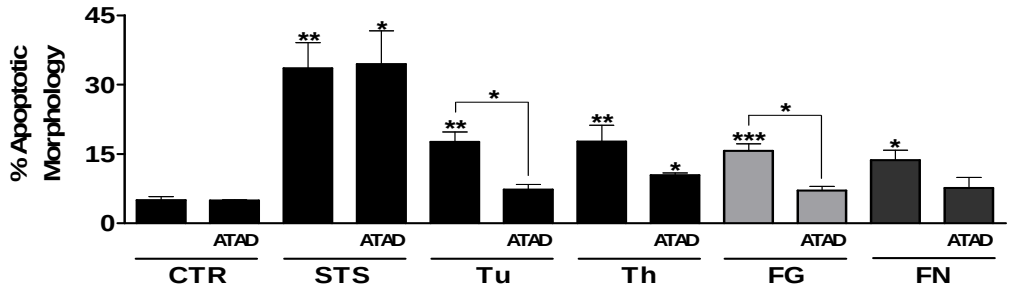

Figure 4.5.1. Inhibition of caspase-12 activation attenuates FG-mediated neuronal death, but not FN-mediated neuronal death

Quantification of apoptotic morphology in CGC cultures after direct treatment with STS (0.5 µM; 8 hours), Tunicamycin (Tu; 1 µg/ml; 24 hours), Thapsigargin (Th; 2 µM; 24 hours), FG (2.5 mg/ml; 24 hours) or FN (1 mg/ml; 48 hours), alone or in combination with z-ATAD-FMK (ATAD: 1 µg/ml). Cell staining was performed using Hoechst-33342 for nuclear morphology analysis. Treatments were in duplicate and data were analysed from 3 independent experiments. To compare between control levels and all other treatments, a one way ANOVA was performed with Dunnett's post-test. For direct comparison treatments with and without caspase-12 inhibition, paired two-tailed Student's *t*-tests were performed. Levels of significance were: non-significant $p>0.05$, * $p<0.05$, ** $p<0.01$, *** $p<0.001$.

4.5.1. Microglial specific ER stress is involved in fibrinogen-mediated neurotoxicity

To identify if microglial-specific ER stress induced by FG was involved in subsequent neuronal toxicity, primary microglial cultures were treated with salubrinal prior to FG or FN treatment for 24 hours. Microglial conditioned medium (MGCM) from these cultures was then administered to neuronal cultures depleted of microglia and Hoechst-33342 staining was employed to quantify apoptotic morphology (**Figure 4.5.2**). Treatment of CGCs with thapsigargin-MGCM induced a significant increase in apoptotic morphology, when compared with cultures treated with non-treated control-MGCM. FG-MGCM administered to CGCs also significantly increased the percentage of cells displaying apoptotic morphology when compared with control-MGCM treatment. MGCM from cultures treated with salubrinal prior to FG treatment induced significantly less apoptosis, however the percentage of apoptotic morphology in FG + Sal-MGCM-treated cultures was still significant above control levels (**Figure 4.5.2**). Finally, FN-MGCM administered to CGC cultures significantly increased the percentage of cells displaying apoptotic characteristics. However, pre-treatment of microglia with salubrinal did not significantly inhibit the FN-mediated increase in apoptotic morphology (**Figure 4.5.2**).

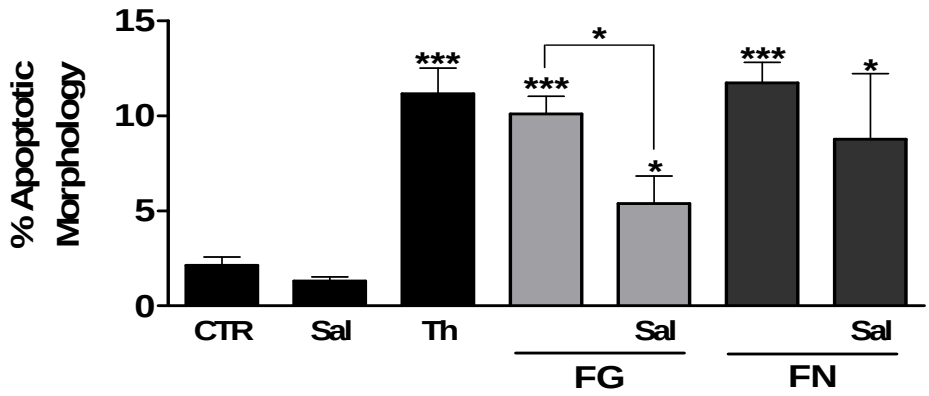

Figure 4.5.2. Inhibition of FG-mediated ER stress in microglia attenuates FG-mediated neurotoxicity

Quantification of apoptotic morphology in CGC cultures after exposure to microglial condition medium (MGCM) from cultures treated with Th (2 µM), FG (2.5 mg/ml) or FN (1 mg/ml), alone or in combination with Salubrinal (Sal; 100 nM), for 24 hours. Cell staining was performed using Hoechst-33342 for nuclear morphology analysis. Treatments were in duplicate and data were analysed from 3 independent experiments. To compare between control levels and all other treatments, a one way ANOVA was performed with Dunnett's post-test. For direct comparison between treatments with or without salubrinal inhibition, paired two-tailed Student's *t*-tests were performed. Levels of significance were: non-significant $p>0.05$, * $p<0.05$, *** $p<0.001$.

4.5.2. Inhibition of calpain activity in neurons and microglia can attenuate fibrinogen-mediated neurotoxicity

Previous data has suggested a significant role for calpain activity in FG-mediated responses (**Figure 4.4.4 – 4.4.6**). To identify if the inhibition of calpain activity could attenuate FG-mediated neurotoxicity, experiments with MGCM were performed (**Figure 4.5.3**). As previously described, CGC cultures were depleted of microglia prior to the addition of MGCM. As expected, administration of FG-MGCM significantly increased neuronal apoptosis. Interestingly, this observed increase in toxicity could be significantly attenuated if CGCs were pre-treated directly with calpastatin, when compared with FG-MGCM alone, suggesting a prominent role for neuronal calpain activity in FG-mediated neurotoxicity via microglia (**Figure 4.5.3**). Finally, the administration of MGCM from FG and calpastatin-treated cultures also attenuated neurotoxicity, when compared with FG-MGCM alone. This further suggests a significant role for microglial calpain activity in the release of neurotoxic factors.

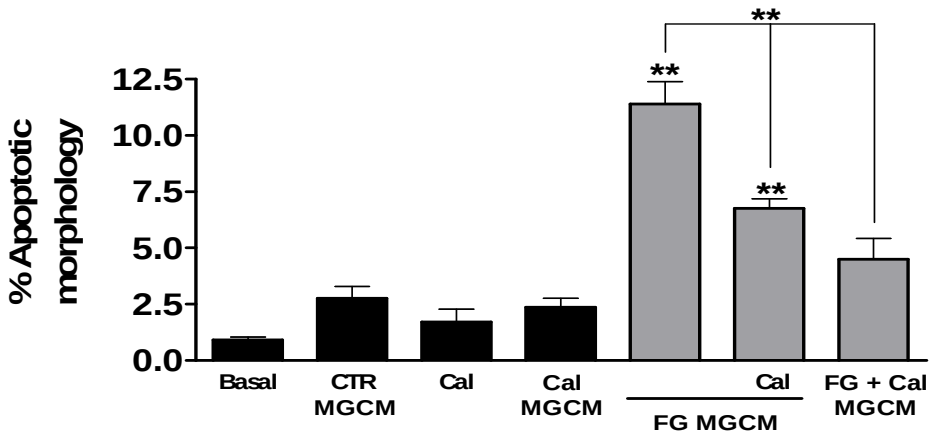

Figure 4.5.3. Inhibition of calpain activity in neurons and microglia can attenuate FG-mediated neurotoxicity

Quantification of apoptotic morphology in CGC cultures after exposure for 24 hours to microglial condition medium (MGCM) from cultures treated with FG (2.5 mg/ml) alone or in combination with calpastatin (Cal; 1 µM) for 24 hours. Some neuronal cultures were treated directly with calpastatin in the presence or absence of FG-MGCM. Cell staining was performed using Hoechst-33342 for nuclear morphology analysis. Treatments were in duplicate and data were analysed from 3 independent experiments. To compare between control levels and all other treatments, a one way ANOVA was performed with Dunnett's post-test. For direct comparison between treatments with or without salubrinal inhibition, paired two-tailed Student's *t*-tests were performed. Levels of significance were: non-significant $p>0.05$, ** $p<0.01$.

4.6. Discussion

This chapter focuses on the role of endoplasmic reticulum stress in the observed FG- and FN-mediated neurotoxicity. Here, significant induction of ER stress in both microglia and neurons after treatment was observed, with FG-mediated induction in neuronal cultures being dependent on microglia. Furthermore, data present here suggests up-stream involvement of a calcium dependent enzyme in FG-mediated induction of caspase-12 and TNFα expression and subsequent neuronal apoptosis, with contributions from other ER stress related pathways also being observed.

4.6.1. Caspase-12 involvement in fibrinogen-mediated neuronal death

Caspase-12 has been identified in rodents as an ER-residing caspase responsible for ER-stress-induced apoptosis (Nakagawa et al. 2000). Furthermore, Nakagawa and colleagues show amyloid-β induces neurotoxicity with dependence on ER stress and caspase-12. Therefore studies were undertaken to identify if FG or FN-mediated neurotoxicity was also dependent on caspase-12. Initial studies to identify if caspase-12 cleavage occurred in CGC cultures after treatment with known ER stress inducers were performed and both thapsigargin and tunicamycin induced caspase-12 cleavage differentially. Thapsigargin induces ER stress by inhibiting the sarco-ER calcium-ATPase (SERCA), causing calcium dyshomeostasis, whereas tunicamycin induces ER stress by inhibiting protein *N*-glycosylation (Takano et al. 2007). These differences in induction of ER stress may support the observed differential cleavage of caspase-12.

It was found that FG and FN could induce expression of the cleaved/active form of caspase-12 in the CGCs. Interestingly, FN-mediated induction occurred only after 48 hours of treatment whereas FG induced significant time-dependent caspase-12 cleavage from 12 hours of treatment. Given the lack of FN-mediated toxicity until 48 hours of exposure, if microglia were present in CGC cultures (**Section 3.3.2**), this late significant increase in caspase-12 cleavage suggests it is not primarily involved in the previously observed toxicity. However significant cleavage after 12 hours in FG-treated

cultures does suggest potential involvement in the previously observed toxicity (**Section 3.3.1 – 3.3.2**). These expression data were supported by live cell staining of CGCs, however, only FG-, and not FN-mediated increases in active caspase-12 fluorescence could be inhibited by pre-treatment of cultures with the pan-caspase inhibitor z-VAD-FMK suggesting that the fluorescence observed in FN-treated cultures was not due to caspase activation. However, with the use of Western blotting, it is shown that both FG and FN-mediated caspase-12 cleavage was due to caspase activation. Therefore, this anomaly in the fluorescence intensity experiments is most probably due to the auto-fluorescence of insoluble aggregates of FN present in the cultures contributing to the overall fluorescence intensity reading, making this experiment in this particular instance, unreliable.

To identify if microglia present in CGC cultures were important in FG-mediated caspase-12, LME depletion experiments were performed. It is shown that FG-mediated caspase-12 cleavage is dependent on the presence of microglia in the CGC cultures. It was suggested that this significant drop in active caspase-12 could have been due to the loss of microglia-specific caspase-12 activation, decreasing the fluorescence intensity. However, scrutiny of the fluorescent images shows neuronal/neurite expression of caspase-12 is lost when microglia are depleted. This suggests a requirement for microglia in neuronal-specific caspase-12 cleavage after FG treatment. Furthermore, Western blotting shows significant attenuation of caspase-12 cleavage after microglia are depleted. Finally, in support of a significant role for caspase-12 activation in FG-mediated neurotoxicity, it is shown here that inhibition of caspase-12 can significantly attenuate FG-induced death.

Briefly, in support of a protective role for microglia after FN exposure, cultures depleted of microglia had a significant increase in caspase-12 cleavage after 24 hours. However scrutiny of the images shows almost complete co-localisation of active caspase-12

staining with PI, potentially suggesting false-positive fluorescence due to channel cross-over and not an actual induction of caspase-12 cleavage.

4.6.2. CHOP up-regulation and cross-talk with caspase-12 activation strengthens a role for ER stress after fibrinogen treatment

Because caspase-12 cleavage has been shown to be occur after treatment with known ER stressors in rodents (Nakagawa et al. 2000), it has been assumed to this point that caspase-12 cleavage implies ER stress has occurred. However this assumption requires further support as caspase-12 activation alone does not imply ER stress. Furthermore it has been suggested, although data presented here disagrees, that pan-caspase inhibitors do not protect against ER stress-mediated apoptosis (Sanges & Marigo 2006), suggesting caspase-12 activation may not be wholly responsible for the observed neuronal toxicity. Therefore, to support a role for ER stress in toxicity after FG treatment in particular, expression of CHOP/GADD153 (CHOP) was analysed in microglia. CHOP has been identified as a major pro-apoptotic transcription factor that is induced by ER stress (Salminen et al. 2009). Furthermore, whereas caspase-12 activation is part of the m-calpain-caspase-12-caspase-3/7 axis of ER stress-mediated apoptosis, CHOP is part of the PERK-eIF2α-CHOP axis that down-regulates Bcl-2 and induces apoptosis (Lai et al. 2007), thus providing strong, dual pathway evidence of the induction of ER stress.

Here it is shown that both FG and FN treatment of microglia induced significant CHOP expression, comparable to thapsigargin or tunicamycin treatment, providing further support for ER stress induction. Furthermore, data presented here suggests that inhibition of the PERK-eIF2α-CHOP axis by salubrinal, a compound that inhibits dephosphorylation of eIF2α (Boyce et al. 2005), significantly inhibited caspase-12 cleavage CGC cultures after FG treatment, suggesting cross-talk between the two ER stress pathways under investigation. In support of this observation, caspase-12 cleavage has previously been inhibited by salubrinal treatment during identification of

ER stress involvement in excitotoxicity (Sokka et al. 2007). Interestingly, significant cleavage above control was still observed in FG-treated CGCs pre-treated with salubrinal suggesting salubrinal only partially inhibits caspase-12 cleavage. Salubrinal is also shown to inhibit FG-mediated TNFα release and caspase-3/7 activation in primary microglial cultures with no significant increase in apoptotic morphology. These data suggest that FG-mediated induction of inflammation, characterised by TNFα release, is dependent on ER stress supporting previously published literature (Hu et al. 2006; Martinon et al. 2010) that identifies novel roles for UPR and ER stress associated factors in macrophage inflammatory activation. Furthermore, if caspase-3/7 cleavage in microglia mediates cellular activation rather than apoptosis (Burguillos et al. 2011), these data also suggest ER stress is occurring up-stream of this activation.

It was hypothesised that if this observed down-regulation of caspase-3/7-associated activation in microglia by salubrinal is important in FG-mediated neurotoxicity, then medium from these microglial cultures (FG+Sal-MGCM) would attenuate stress marker expression in neuronal cultures, when compared with FG-MGCM. However it is shown here that FG+Sal-MGCM could not attenuate caspase-12 cleavage, when compared with FG-MGCM. These data suggest that inhibition of the PERK-eIF2α-CHOP axis of ER stress induced by FG in the microglial cultures is not sufficient to prevent the release of stable soluble factors that can induce neuronal caspase-12 cleavage, further supporting the involvement of other pathways in FG-mediated neurotoxicity. However, these data are of poor quality and require clarification through repetition. Interestingly, FG-MGCM-mediated neuronal apoptosis could be inhibited if microglial cultures were co-treated with salubrinal, suggesting caspase-12 activation is not solely responsible for FG-mediated neurotoxicity. In further support of this, significant levels of apoptosis were still observed.

Finally, inhibition of p38 MAPK and PI3K pathways in microglia attenuated indirect FG-mediated caspase-12 cleavage in neurons, supporting a significant role of p38 MAPK in FG-mediated responses via microglia. Again, these data are of poor quality and

require clarification through repetition, but coupled with previous data (**Figure 3.2.5**) showing inhibition of p38-MAPK attenuated FG-mediated TNFα release, a role for TNFα release in FG-mediated caspase-12 cleavage can be initially proposed.

4.6.3. TNFα synthesis is involved in fibrinogen-mediated ER stress induction

Following on from these preliminary MGCM data, live cell staining, Western blotting and ICC support a significant role for TNFα in FG-mediated ER stress in CGC and primary microglial cultures. It is shown here that FG-induced caspase-12 activation was down-regulated after pre-treatment with thalidomide. Furthermore, FG induction of CHOP expression in microglia was down-regulated if cultures were pre-treated with thalidomide. Conversely, it is shown that FN-induced caspase-12 activation in CGC and microglial cultures could not be inhibited by thalidomide pre-treatment however PI-positive nuclei in CGC cultures were significantly decreased, further supporting a primary role for TNFα, but a secondary role for caspase-12 activation in FN-mediated toxicity. Interestingly FN-mediated CHOP expression could be down-regulated by thalidomide suggesting an ER stress pathway independent of caspase-12 could be involved in FN-mediated responses. No significant involvement of iNOS activity was observed in any of these responses. Published literature shows ER stress can lead to expression of TNFα (Hu et al. 2006). Together these data suggest microglial ER stress can induce TNFα release leading to either autocrine activation or neuronal toxicity.

4.6.4. Calcium and iNOS involvement in early fibrinogen-mediated responses

Calcium dyshomeostasis is a contributing factor in ER stress (Lindholm et al. 2006). Therefore, it was hypothesised that suppressing any FG-mediated induction of calcium dyshomeostasis would further support a significant role for ER stress in the observed toxicity. BAPTA-AM, the well documented fast calcium chelator (Hoffmann et al. 2003; Hooper et al. 2005), was optimised for use on the microglial cultures and co-treated with FG to identify whether caspase-12 and -3/7 induction was dependent on calcium. It was found that co-treatment of microglia with FG and BAPTA-AM induced significant

death with a loss of caspase-12 activation, probably due to apoptosis. This was supported by significant caspase-3/7 induction associated with PI staining. Therefore ablation of free calcium by BAPTA-AM prevents microglial activation due to FG treatment leading to death. The use of BAPTA-AM as a tool in culture is ideal for acute ablation of free calcium, i.e. during calcium imaging protocols. However a chronic incubation, such as here, provides an extreme un-physiological environment meaning no great insights can be concluded from these data furthermore, this particular finding brings previously published data under scrutiny (Hoffmann et al. 2003). Future experiments should utilise calcium chelators with slower binding kinetics which may prevent the massive increase in death induced by the acute nature of BAPTA-AM-mediated calcium chelation. It was therefore decided that investigation into calpain activity would provide more valuable data into the involvement of calcium in FG-mediated responses.

Calpains are calcium activated cysteine proteases and it has been suggested that m-calpain may be responsible for procaspase-12 cleavage to the active form and that disturbances in intracellular calcium storage as a result of amyloid-β peptide cytotoxicity may induce apoptosis through calpain-mediated caspase-12 activation (Nakagawa & Yuan 2000). Furthermore, calpastatin over-expression in neurons significantly decreased Aβ-associated toxicity in neuronal-like PC12 cells (Vaisid et al. 2008), with further support for the regulation of Aβ-induced neurotoxicity by calpains being observed in primary cultured neurons (Wei et al. 2008).

To model calcium-mediated calpain activation and subsequent ER stress, the ionophore, Ionomycin that depletes intracellular calcium stores, increasing the availability of cytoplasmic calcium (Pocock & Nicholls 1992) was utilised. A significant induction in FG-mediated calpain activity was observed after only 1 hour suggesting calcium involvement in any FG-mediated response is early and up-stream of caspase-12 activation and TNFα release. Furthermore, the lack of any further significant calpain activity after 12 hours of FG treatment further supports the idea that the event is early

and up-stream of other responses observed so far. In line with this hypothesis pre-treatment of cultures with thalidomide could not attenuate FG-mediated calpain activity after 8 hours. However, iNOS activity inhibition could significantly attenuate calpain activity. Inhibitors of calpains have been shown to inhibit the induction of iNOS in macrophages (Griscavage et al. 1996) however no studies have been published that suggest inhibition of iNOS activity can attenuate calpain activity. It is possible that the observed attenuation of calpain activity by AMT-HCl is a non-specific action of the compound and the use of other iNOS activity inhibitors or protein silencing experiments would potentially provide more conclusive data for this perceived mechanism of action.

Calpain activity was also shown to be involved in upstream events including FG-mediated expression of cleaved caspase-12 and TNFα. This data led us to investigate the role of calpain activity in FG-mediated neurotoxicity. It is shown that inhibition of calpain activity in neurons provided protection form FG-MGCM, suggesting calpain activity in neurons plays an important role in FG-mediated neurotoxicity induced via activation of microglia. Recent studies suggest microglial cytokine release can induce calpain activation in neurons (McDowell et al. 2011) Furthermore, if calpain activity was inhibited in microglia treated with FG, significant neuronal protection was also observed suggesting calpain activity in microglia is responsible for FG-mediated release of neurotoxic factors. Previous studies identify an increase in calpain expression in the microglia in an inflammatory model (Shields et al. 1998). Together these data suggest that regulation of this family of enzymes may provide significant attenuation of neuronal loss due to microglial dependent and independent mechanisms of neurotoxicity.

4.6.5. Conclusions

Here, a significant role for ER stress in FG-mediated neuronal toxicity has been identified. Data presented here, summarized in **Figure 4.6.1**, suggest that FG can induce significant ER stress in both microglia and neurons. However, the significance and complete mechanisms require further elucidation. It seems that FG induces ER stress in microglia via calpain-associated pathways leading to TNFα release, which in

turn can induce further microglial activation in an autocrine fashion. Interestingly caspase-12 has been identified as having a prominent role in inflammation, with caspase-12 deficient mice showing enhanced bacterial clearance and sepsis resistance (Saleh et al. 2006), suggesting FG exposure could induce an inflammatory response in microglia leading to TNFα release which subsequently induces ER stress and toxicity in neurons via calpain activity.

Another important point that must be raised is that caspase-12 has been shown to have acquired deleterious mutations including the presence of a frameshift mutation that results in premature stop codons in the gene, suggesting the lack of a functional caspase (Fischer et al. 2002). However, active caspases generally undergo post-translational modifications (Earnshaw et al. 1999) and caspase-12 has been shown to mediate ER-stress associated neuronal death in human variant Creutzfeldt-Jakob disease (vCJD), a prion protein-associated neurodegenerative disease (Hetz et al. 2003) and human AD (Lee et al. 2010), suggesting a functional caspase-12 protein can occur in humans that mediates similar functions. Other studies have proposed that human caspase-4, which is homologous to mouse caspase-12, is performing the ER stress functions of caspase-12 in humans (Hitomi et al. 2004). It was shown that caspase-4 cleavage is specifically induced by ER stress but not by other apoptotic signals, and knockdown of caspase-4 decreases ER stress-induced apoptosis.

The suggestion that ER stress occurs in both microglia and neurons after FG treatment has been significantly strengthened by data here that shows significant CHOP expression in microglia but also pharmacological inhibition of the PERK-eIF2α-CHOP axis in CGC cultures, which significantly modulated FG-mediated responses. Furthermore, the early involvement of calpains in the FG-mediated activation of microglia proposes that calcium dyshomeostasis occurs upstream of the microglial-associated ER stress that is involved in TNFα release and subsequent neurotoxicity. Finally, calpain activity in neurons has also been implicated in the FG-mediated toxicity cascade.

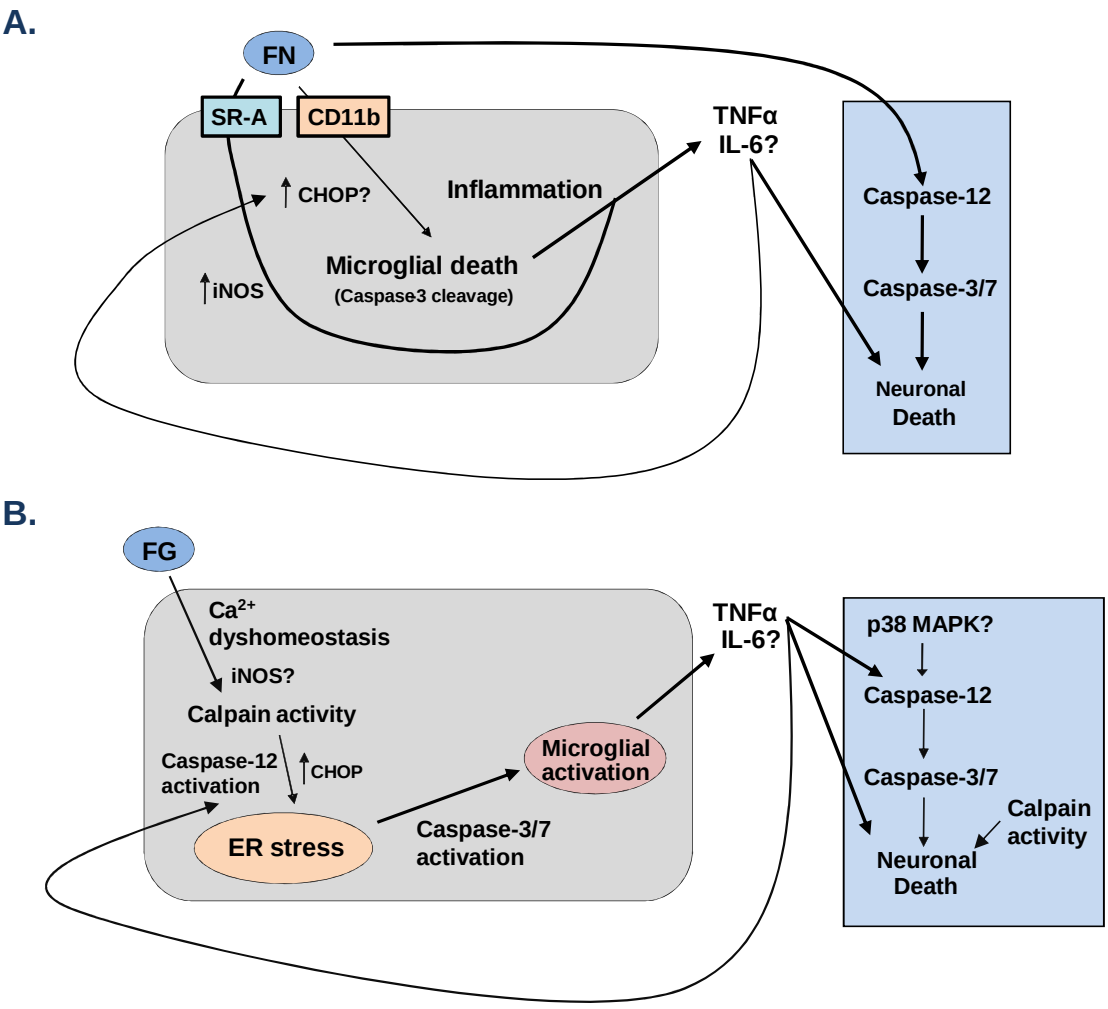

Figure 4.6.1. Summary of results obtained in chapter 4

A. Fibrin treatment of microglia led to an increase in CHOP expression suggesting some involvement of ER stress mechanisms in the earlier observations of toxicity. Treatment of neuronal cultures with FN caused a significant increase in caspase-12 activation, again suggesting a possible role for ER stress in the observed neurotoxicity. However, this involvement seemed to be minimal and potentially post-induction of significant toxicity via other pathways. **B.** Fibrinogen treatment of microglia led to an increase in the calpain activity suggesting modulation of calcium, with dependence on iNOS activity. Furthermore, CHOP and caspase-12 expression were increased with regulation from TNFα and calpain activity. FG-mediated microglial activation also led to an increase in neuronal caspase-12 and calpain activity, both of which were involved in the observed neuronal death.

5. Characterisation of mGluR agonist-mediated neuroprotection from fibrinogen-mediated toxicity

5.1. Introduction

In this chapter, experiments were performed to determine whether activation of particular metabotropic glutamate receptors (mGluRs) could provide neuroprotection from FG- and FN-induced neurotoxicity, with a particular focus on microglial-mediated toxicity. Activation of mGluRs on microglia can induce both neurotoxic and neuroprotective phenotypes, depending on the group or receptor activated (Pocock & Kettenmann 2007). Previous studies in our laboratory have attributed protective and toxic effects to the activation of specific group II and III mGluRs (Taylor et al. 2002; Taylor et al. 2003; Taylor et al. 2005). However, limited research has been performed on the role of group I mGluRs (mGluR1/5) on microglia.

5.1.1. Blood-borne proteins and mGluRs

A review of the published literature suggests little or no research has been performed on the relationship, if any, between fibrinogen and mGluRs. Interestingly however, thrombin, the proteolytic enzyme for fibrinogen immobilisation has been shown to down-regulate astrocytic mGluR5 (Miller et al. 1996).

5.1.2. The roles of mGluRs in disease

The diversity and heterogeneous distribution of mGluR subtypes throughout the CNS provides opportunities for selective targeting of particular subtypes in particular regions making them, as a group, an attractive therapeutic target. Furthermore, a vast array of pre-clinical studies suggests that ligands targeted at specific mGluR subtypes could provide potential treatments in numerous CNS disorders, some of which are listed below:

- Antagonism of mGluR2/3 and/or 5 in depression (Pilc et al. 2008)

- Agonism of mGluR2/3 and antagonism of mGluR5 in anxiety and stress disorders (Swanson et al. 2005)
- Agonism of mGluR2/3 or 5 in Schizophrenia (Moghaddam 2004)
- Antagonism of mGluR2 in Epilepsy (Alexander & Godwin 2006)
- Agonism of group II and III mGluRs in Alzheimer's disease (Lee et al. 2004b)
- Antagonism of mGluR5 in Parkinson's disease (Conn et al. 2005)

Allosteric modulation of mGluRs is an intense new area of research for the development of efficacious compounds for the treatment of a wide range of CNS disorders. This class of compound has been shown to provide high selectivity and novel modes of efficacy, which are desirable characteristics for compounds targeted at the CNS (Conn et al. 2009). Negative allosteric modulation of mGluR5 has been implicated as a promising therapeutic in fragile X syndrome, chronic pain and depression, with positive allosteric modulation of mGluR5 identified as a potent anti-psychotic with possible therapeutic benefits in other disorders that involve impaired cognitive function (Niswender & Conn 2010).

Data presented here suggests that positive allosteric modulation of mGluR5 can protect against FG-mediated neurotoxicity. Furthermore, it is shown that by specifically targeting microglial mGluR5, FG-mediated neurotoxicity can be attenuated.

5.2. Effects of mGluR agonists on fibrinogen-induced microglial reactivity

5.2.1. Fibrinogen-induced iNOS expression and TNFα expression and release can be attenuated by mGluR agonist treatment

To identify whether activation of mGluRs can modulate the FG-induced activated microglial phenotype, ICC, ELISA and live cell staining was performed. As previously shown in serum-free conditions, FG treatment induced iNOS expression in primary microglia (**Figure 5.2.1**). Therefore, as a measure of microglial reactivity, iNOS and ED-1 expression ICC was performed on primary microglial cultures after treatment with LPS or FG, in the absence or presence of mGluR agonists. Treatment with the group I agonist (*S*)-3,5-Dihydroxyphenylglycine (DHPG) at a previously published concentration (Macek et al. 1996) or the specific mGluR5 agonist 3-Cyano-*N*-(1,3-diphenyl-1*H*-pyrazol-5-yl)benzamide (CDPPB) at the published EC_{50} value (Stauffer 2011) did not significantly increase iNOS expression, when compared with control. However, a significant increase in ED-1 expression was observed (**Figure 5.2.1 A & B**). In line with previously published data (Taylor et al. 2005), treatment with the group II agonist (2*S*,2'*R*,3'*R*)-2-(2',3'-Dicarboxycyclopropyl)glycine (DCGIV) or the specific mGluR3 agonist N-acetyl-L-aspartyl-L-glutamate (NAAG) did not significantly increase expression of iNOS in primary microglial cultures. However, treatment with NAAG, but not DCGIV induced a significant increase in ED-1 expression (**Figure 5.2.1 A &B**). Furthermore, in line with previously published data (Taylor et al. 2003; Taylor et al. 2005), treatment with the group III (mGluR4/5/6/7) agonist (L)-2-amino-4-phosphono-butyric acid (L-AP4) did not significantly modulate iNOS or ED-1 expression, compared with relevant control levels (**Figure 5.2.1 A &B**).

LPS treatment of primary microglia induced a strong significant increase in iNOS and ED-1 expression levels, when compared with control levels (**Figure 5.2.1 A & B**). Co-treatment of cultures with any of the mGluR agonists tested could not down-regulate

the LPS-mediated increases in iNOS and ED-1 expression. Conversely, FG-induced increases in iNOS and ED-1 expression could be significantly attenuated by co-treatment with CDPPB, suggesting a role for mGluR5 in this activated microglial phenotype (**Figure 5.2.1 A & B**). Furthermore, only DCGIV treatment induced a significant increase in cells displaying apoptotic morphology, suggesting the CDPPB-associated attenuation of iNOS and ED-1 was not due to toxicity (**Figure 5.2.1 C**).

LPS or FG treatment of microglia can induce significant release of TNFα (**Section 3.2.1**). Therefore expression and release of the pro-inflammatory cytokine was assessed by Western blotting and ELISA analysis after FG or LPS treatment in the absence and presence of mGluR agonists. In line with the iNOS/ED-1 data, co-treatment with mGluR agonists could not attenuate LPS-mediated TNFα expression in BV2 microglia (**Figure 5.2.2 A**). FG-mediated TNFα expression in BV2 microglia could be attenuated by co-treatment with CDPPB. Furthermore, co-treatment with DHPG could also significantly attenuate TNFα expression (**Figure 5.2.2 B**). Expression of TNFα suggests functionality however release of the cytokine provides stronger evidence for involvement in downstream cascades, therefore a TNFα ELISA system was used. Treatment with DCGIV induced significant TNFα release from primary microglial cultures, when compared with non-treated controls as previously described (Taylor et al. 2005) (**Figure 5.2.2 C**). Similarly, LPS induced a significant increase in TNFα release from primary microglial cultures, when compared with non-treated controls, as previously shown (**Section 3.2.1**). In line with the expression data, LPS-induced TNFα release could not be attenuated by co-treatment with mGluR agonists ($p>0.05$; **Figure 5.2.2 C**). However, significant FG-induced TNFα release could be attenuated by co-treatment with either DHPG or CDPPB (**Figure 5.2.2 C**), further suggesting a role for group I mGluRs in down-regulating FG-mediated microglial activation

Figure 5.2.1

A.

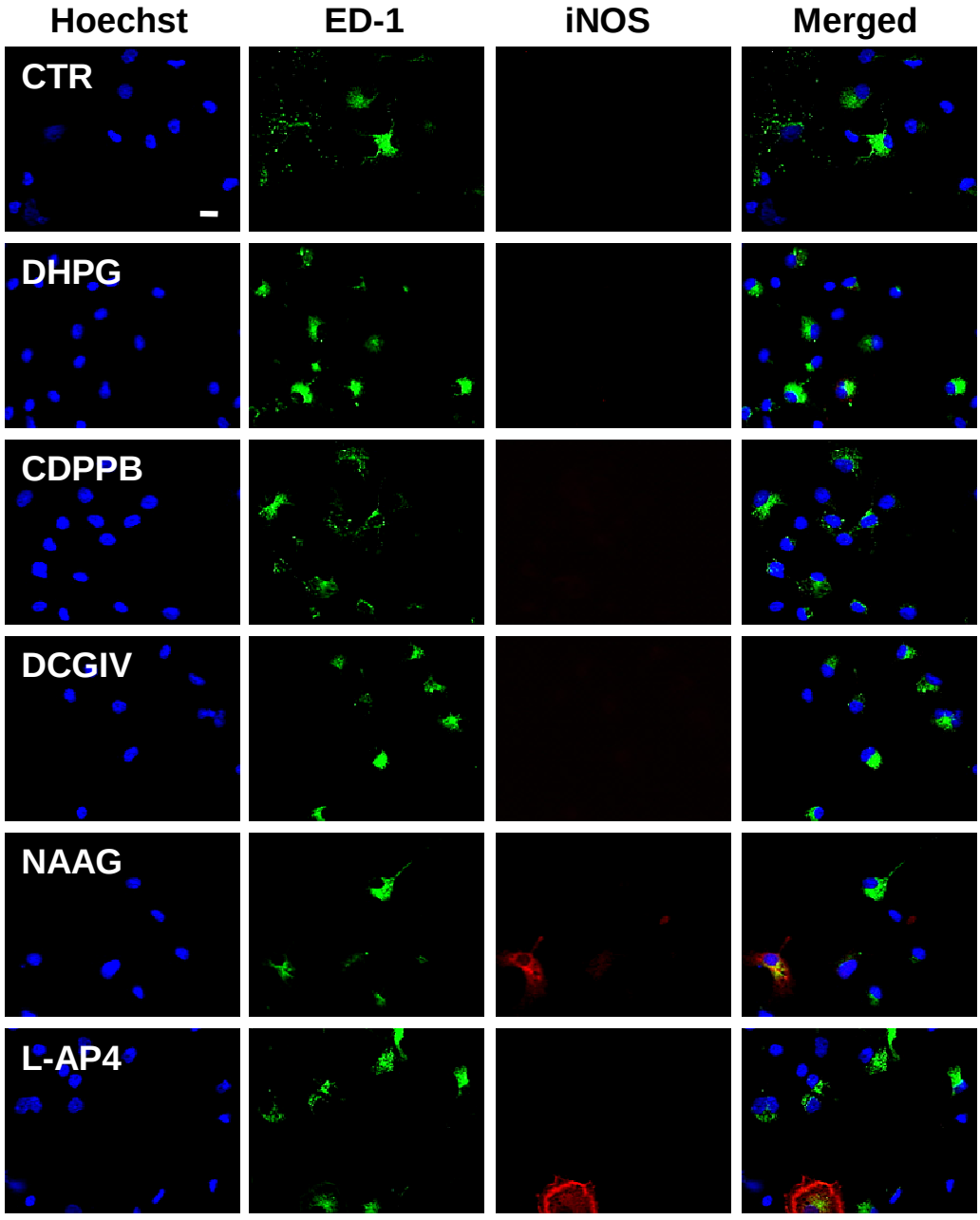

Figure 5.2.1

A cont.

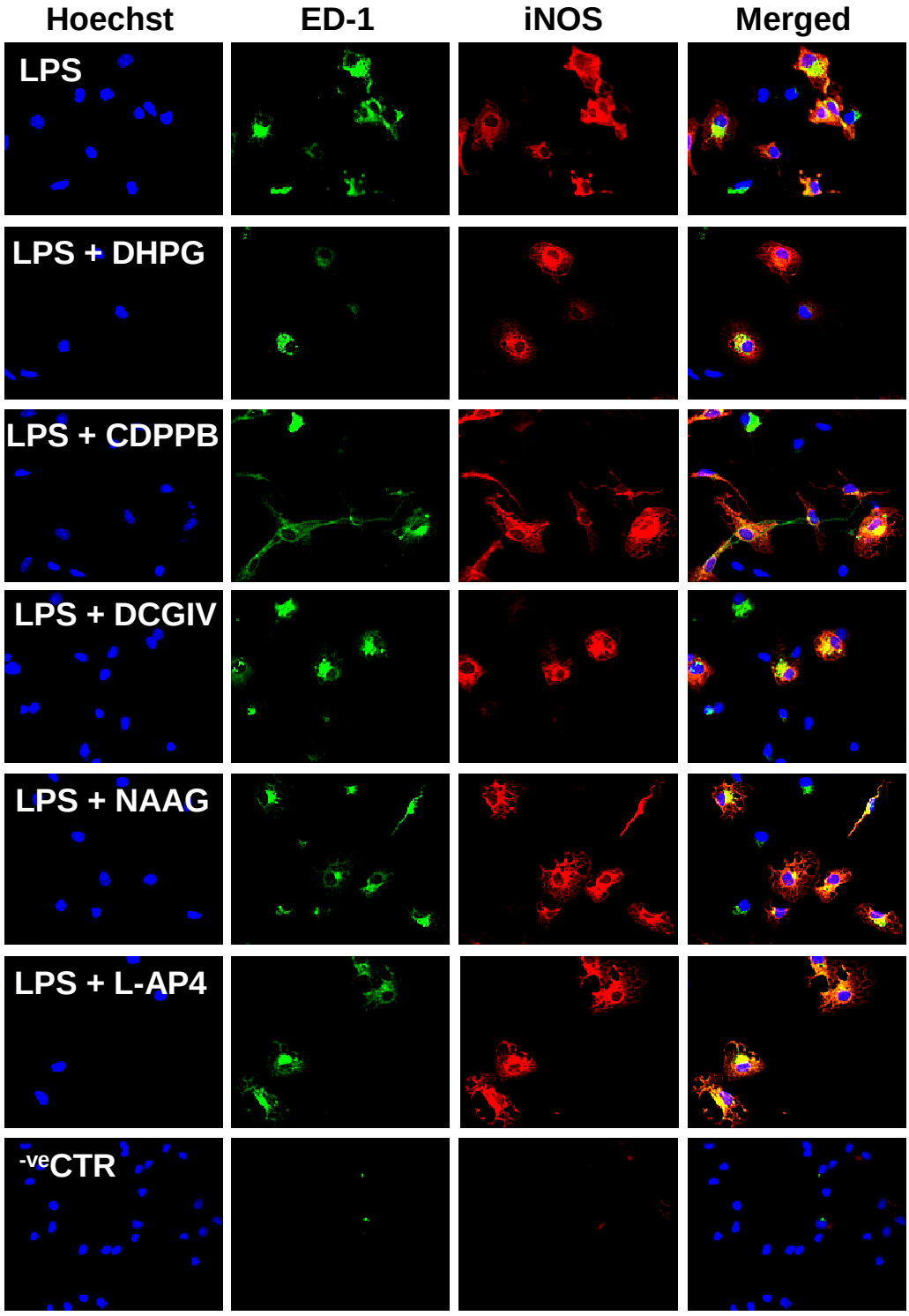

Figure 5.2.1

A cont.

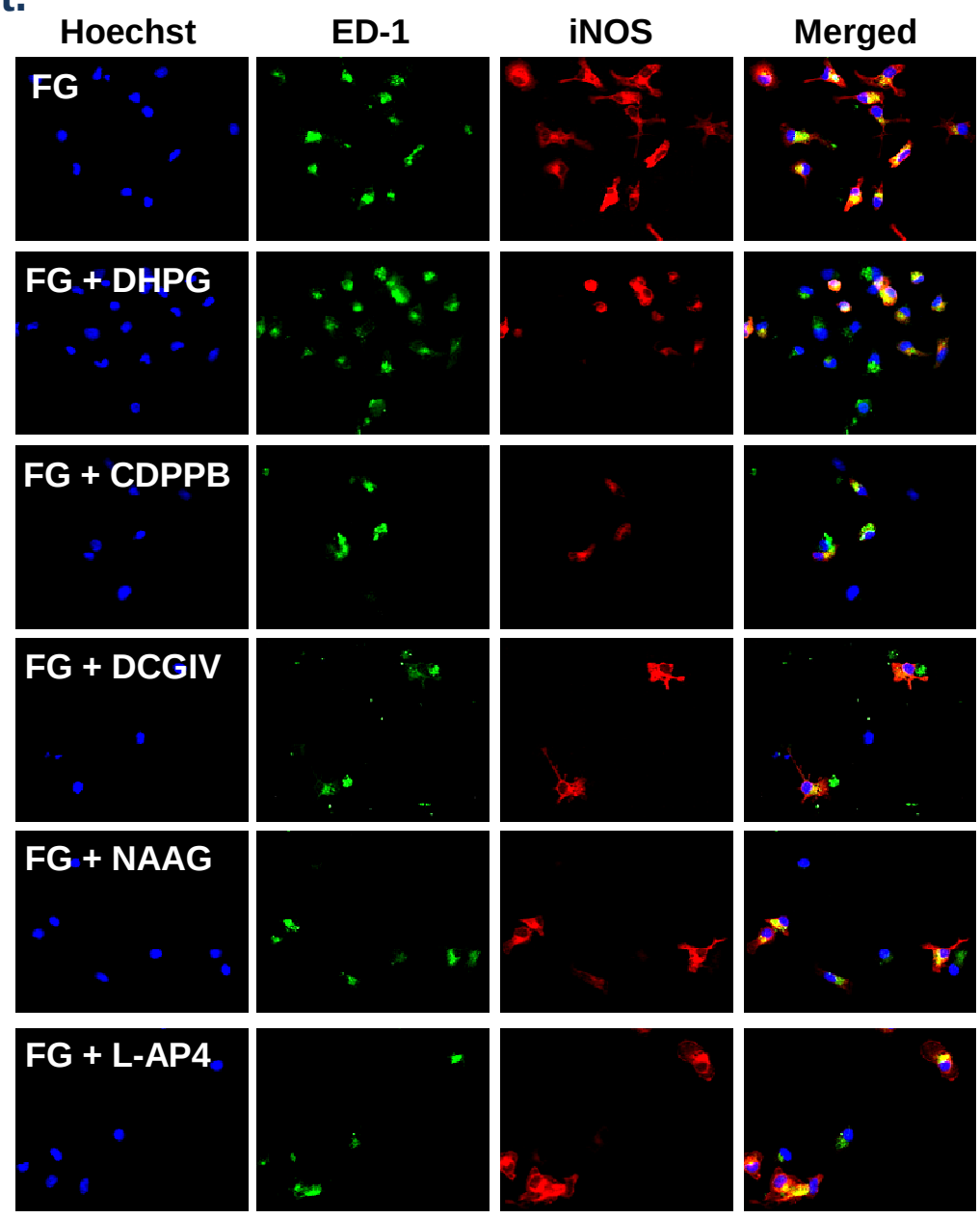

B.

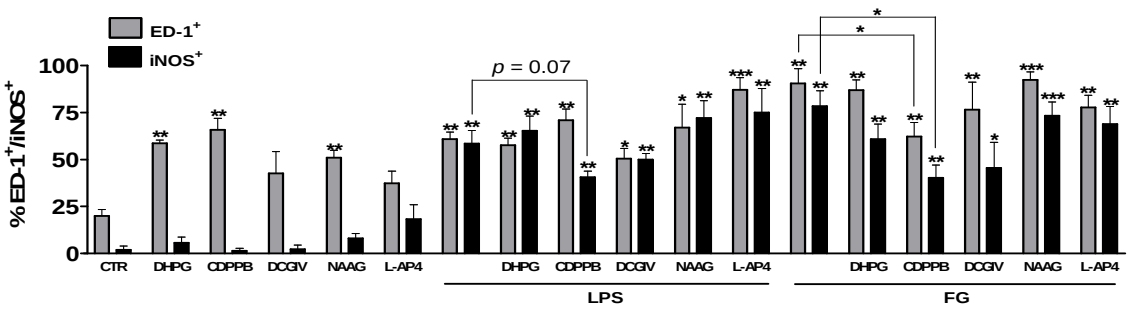

C.

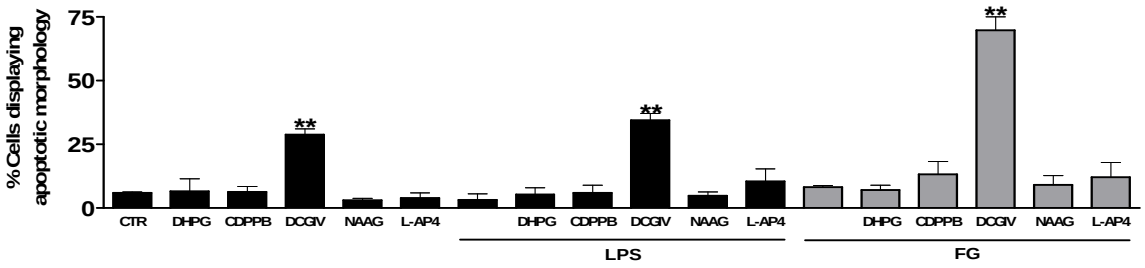

Figure 5.2.1. FG-induced microglial iNOS expression in serum-free conditions can be attenuated by co-treatment with CDPPB

A. Representative images of serum-free primary microglial cultures after 24 hours of treatment with FG (2.5 mg/ml) or LPS (1 µg/ml), and co-treatment with DHPG (100 µM), CDPPB (100 nM), DCGIV (500 nM), NAAG (50 µM) or L-AP4 (100 µM). Cultures were co-stained with DAPI for quantification of cell number and probed with anti-ED1 (green) for identification of activated microglia and anti-iNOS (red), except in negative control cultures, where primary antibodies were omitted. Original magnification: x40, scale bar: 10 µm. **B.** Quantification of ED-1^{+} and iNOS^{+} microglia after administration of treatments stated in **A**. **C.** Quantification of cells displaying apoptotic morphology after administration of treatments stated in **A**. Data in **B** and **C** is presented as a percentage of total microglial number. Treatments were in duplicate in each experiment and data were analysed from 3 independent experiments. To compare the expression of ED-1 or iNOS in multiple treatment groups to control levels a one way ANOVA was performed with Dunnett's post-test. Direct comparison of specific treatments was analysed using paired two-tailed Student's *t*-tests. Levels of significance were: non-significant $p>0.05$, * $p<0.05$, ** $p<0.01$, *** $p<0.001$.

Figure 5.2.2

Ai.

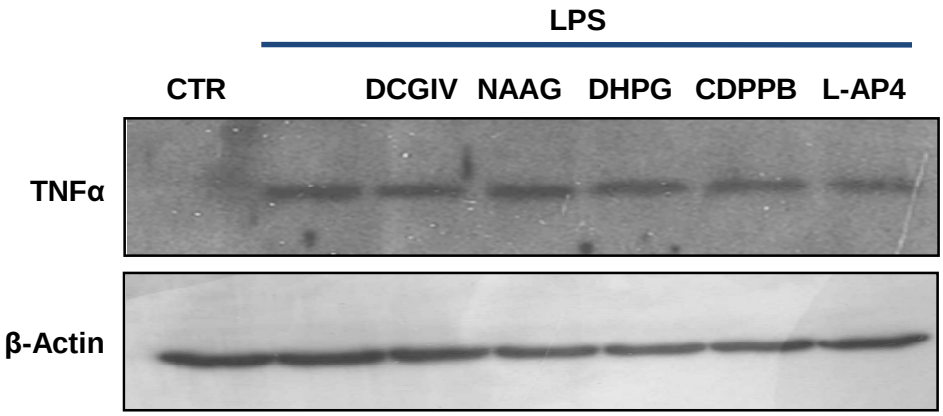

Aii.

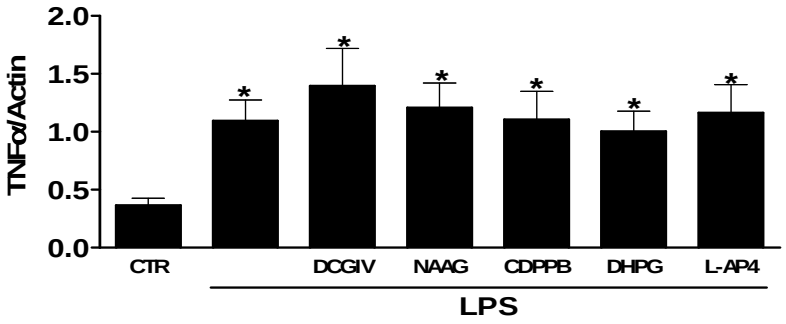

Bi.

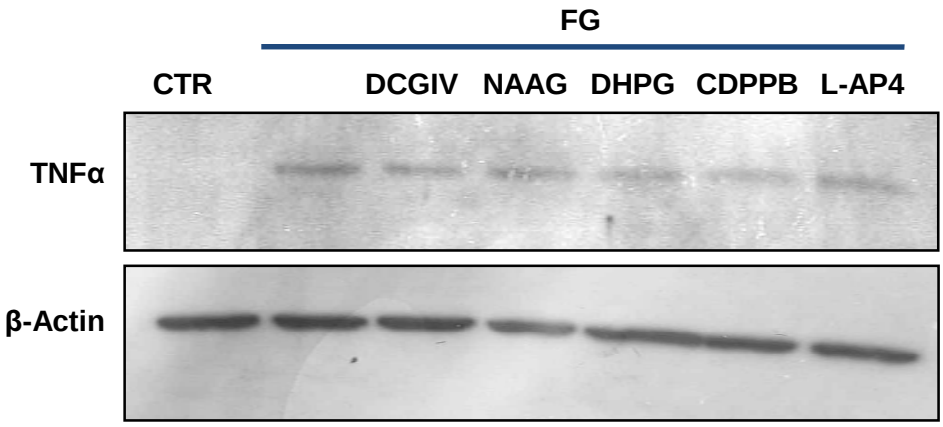

Bii.

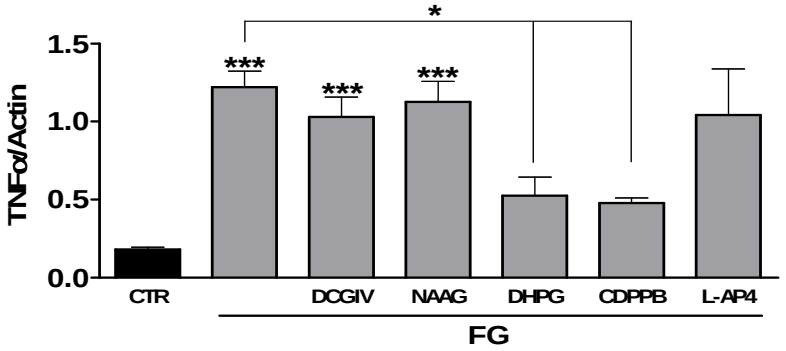

C.

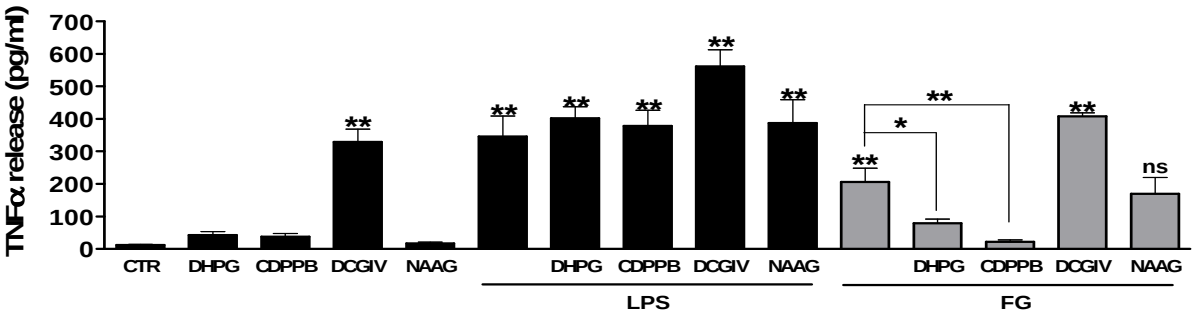

Figure 5.2.2. FG-induced microglial TNFα expression and release in serum-free conditions can be attenuated by co-treatment with DHPG or CDPPB

A and B. Representative Western blots for TNFα and β-actin expression in BV2-microglial cultures after treatment with LPS (1 µg/ml) (**Ai**) or FG (2.5 mg/ml) (**Bi**), and co-treatment with DHPG (100 µM), CDPPB (100 nM), DCGIV (500 nM), NAAG (50 µM) or L-AP4 (100 µM) for 24 hours. Quantification of TNFα expression was performed with respect to the β-actin loading control for LPS (**Aii**) and FG (**Bii**), respectively. **C.** ELISA quantification of TNFα release after treatments as outlined in **A**, except for L-AP4 co-treatment, which was omitted. For the ELISA system, treatments were in duplicate in each experiment and data were analysed from 3 independent experiments. Western blotting was also performed on 3 independent occasions. To compare TNFα expression or release in multiple treatment groups to control levels a one way ANOVA was performed with Dunnett's post-test. Direct comparison of specific treatments was analysed using paired two-tailed Student's *t*-tests. Levels of significance were: non-significant $p>0.05$, * $p<0.05$, ** $p<0.01$, *** $p<0.001$.

5.2.2. Fibrinogen-mediated caspase activity can be attenuated by mGluR agonist treatment

To identify whether mGluR agonist treatment could modulate FG-induced caspase activation in microglia, live cell staining was performed. Treatment of primary microglia with FG for 24 hours induced significant caspase-12 activation with no significant induction of cell death (**Figure 5.2.3 A, B & E**). Co-treatment of cultures with CDPPB or NAAG significantly attenuated FG-mediated caspase-12 activation (**Figure 5.2.3 A & B**), with no significant modulation of cell death (**Figure 5.2.3 E**). Co-treatment with DCGIV however did not attenuate caspase-12 activity, but did induce significant cell death, compared with control levels. Treatment with mGluR agonists alone did not induce significant caspase-12 activation, however, as expected, DCGIV treatment significantly increased cell death (**Figure 5.2.3 E**). FG induced a significant increase in caspase-3/7 induction. In line with the caspase-12 data, co-treatment with CDPPB or NAAG significantly attenuated the FG-mediated increase in caspase-3/7 induction (**Figure 5.2.3 C & D**). Furthermore, in line with previously published data (Taylor et al. 2005), treatment of primary microglial cultures with DCGIV significantly increased caspase-3/7 expression, whereas NAAG or CDPPB treatment had no effect (**Figure 5.2.3 C & D**).

Figure 5.2.3

A.

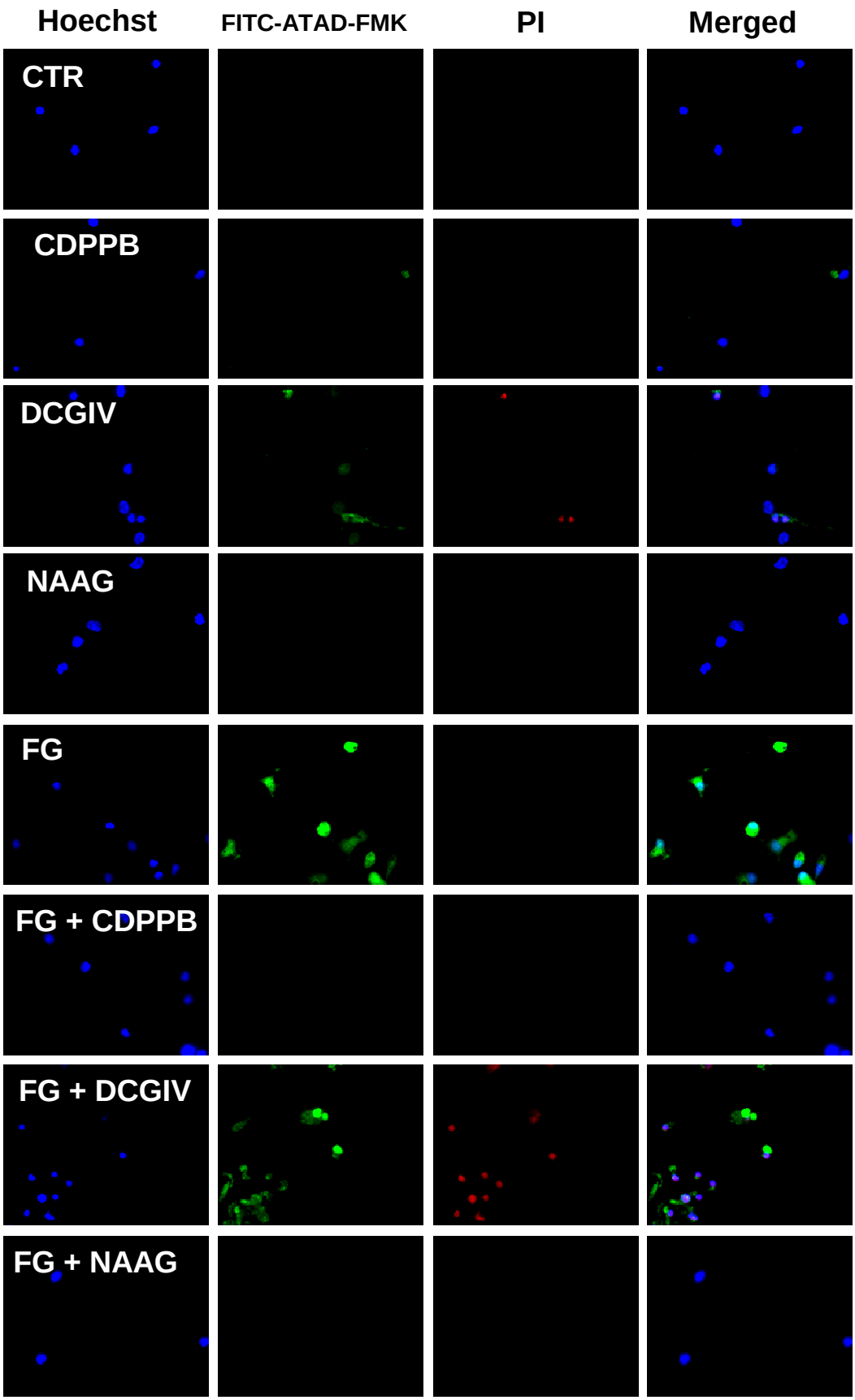
Hoechst
FITC-ATAD-FMK
PI
Merged
CTR
CDPPB
DCGIV
NAAG
FG
FG + CDPPB
FG + DCGIV
FG + NAAG

Figure 5.2.3

B.

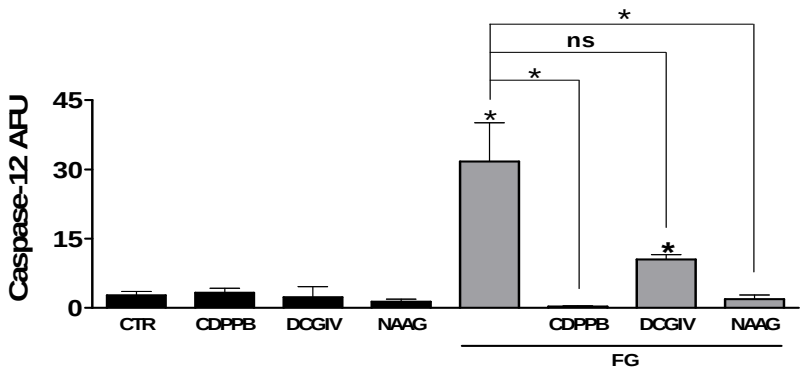
Caspase-12 AFU
45
30
15
0
*
ns
*
*
*
CTR
CDPPB
DCGIV
NAAG
CDPPB
DCGIV
NAAG
FG

Figure 5.2.3

C.

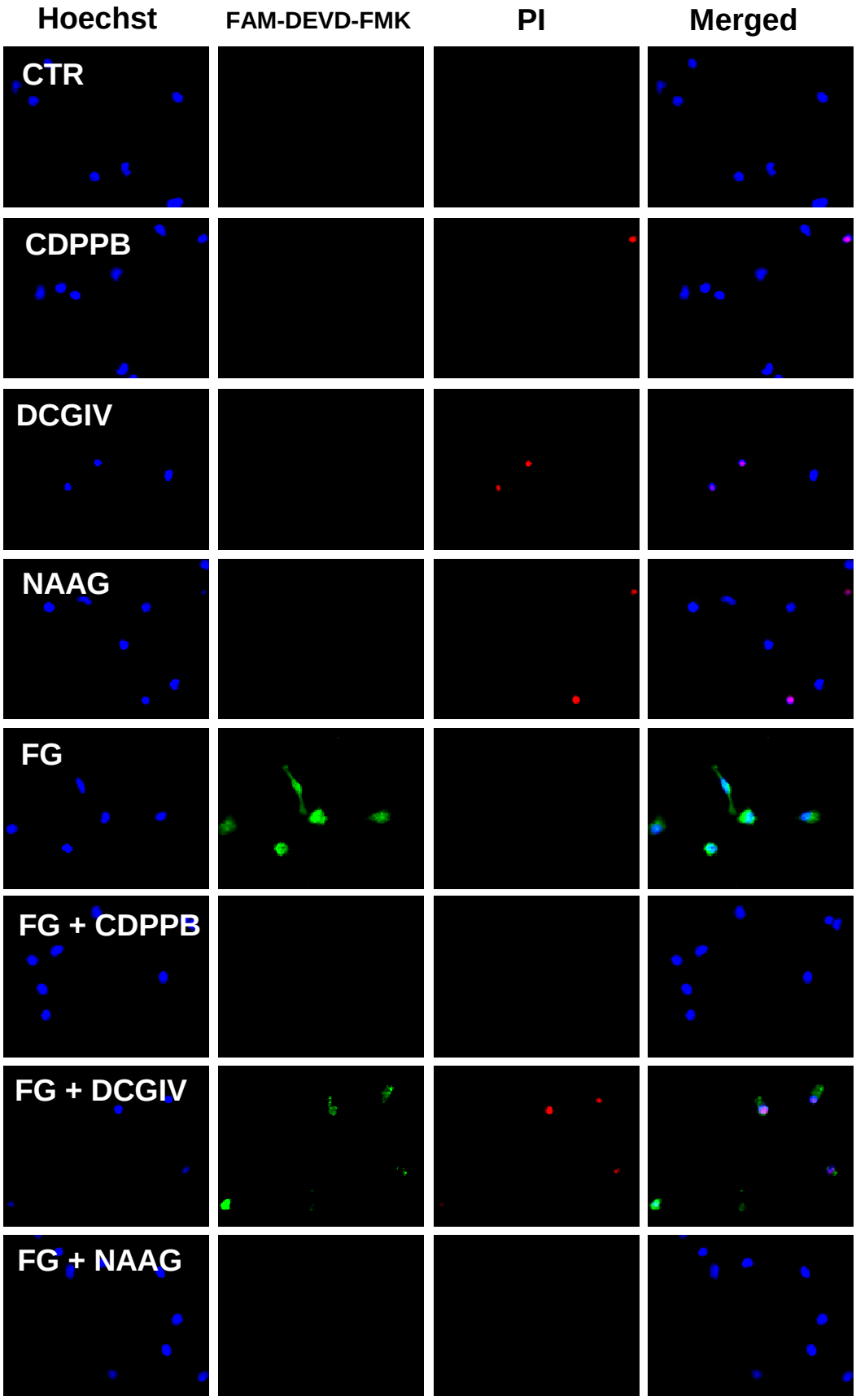
Hoechst
FAM-DEVD-FMK
PI
Merged
CTR
CDPPB
DCGIV
NAAG
FG
FG + CDPPB
FG + DCGIV
FG + NAAG

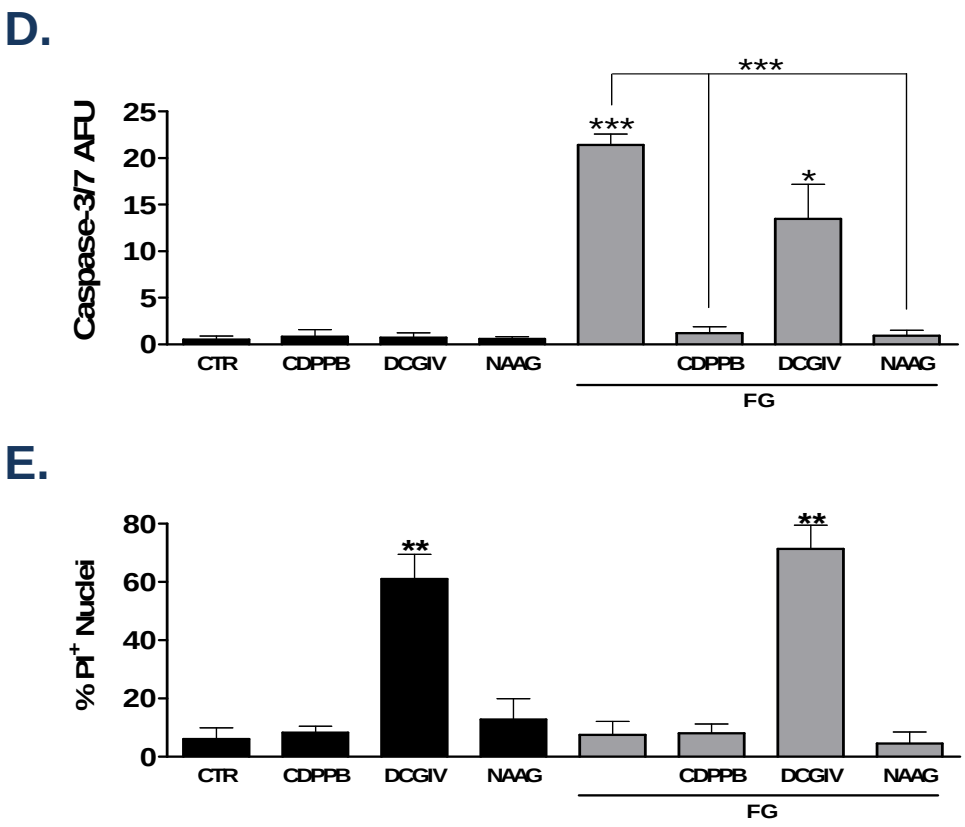

Figure 5.2.3. FG-induced caspase-12 and -3/7 activation in microglia can be attenuated by co-treatment with CDPPB or NAAG

A. Representative images from live cell staining experiments to identify caspase-12 activation in primary microglial cultures after treatment with FG (2.5 mg/ml), CDPPB (100 nM), DCGIV (500 nM) or NAAG (50 µM) alone or in combination for 24 hours. Live cell staining was performed using Hoechst-33342 for nucleus identification, propidium iodide (PI; red) for total cell death, and FITC-ATAD-FMK (green) for active caspase-12. Original magnification: x40. **B.** Quantification of the relative active caspase-12 fluorescence intensity/cell in primary microglial cultures after administration of treatments outlined in **A**. **C.** Representative images from live cell staining experiments to identify caspase-3/7 activation in primary microglial cultures after treatment as outlined in **A**. **D.** Quantification of the relative active caspase-3/7 fluorescence intensity/cell in primary microglial cultures after administration of treatments outlined in **A**. Data in **B** and **D** is presented in arbitrary fluorescence units (AFU). **E.** Quantification of PI^+ cells to identify levels of cell death after treatment outlined in **A**. Treatments were in duplicate in each experiment and data were analysed from 3 independent experiments. To compare caspase-12 or -3/7 expression or PI^+ nuclei in multiple treatment groups to control levels one way ANOVA were performed with Dunnett's post-test. Direct comparison of specific treatments was analysed using paired two-tailed Student's *t*-tests. Levels of significance were: non-significant $p>0.05$, * $p<0.05$, ** $p<0.01$, *** $p<0.001$.

5.2.3. Fibrinogen- and fibrin-mediated neurotoxicity can be attenuated by mGluR agonist treatment – dependence on microglia

The role of microglia in the CGC cultures with respect to mGluR agonist modulation of FG- and FN-mediated responses was investigated. Initially, apoptotic morphology in CGC cultures was quantified both in the presence and absence of microglia using the LME pre-treatment protocol (**Section 2.5.2**). With respect to the mGluR agonists, only DCGIV treatment alone induced significant neuronal apoptosis, which was dependent on microglia (**Figure 5.2.4 A**), similar to previously published data (Taylor et al. 2005).

FN induced a significant increase in apoptosis after 48 hours of treatment, when compared with control levels (**Figure 5.2.4 B**). Depletion of microglia had no significant effect on the observed toxicity, as previously shown (**Figure 3.3.4**). Co-treatment of cultures with DHPG, CDPPB, or NAAG significantly attenuated FN-mediated apoptosis (**Figure 5.2.4 B**) however, depletion of microglia prior to these treatments prevented the observed attenuation, suggesting significant involvement of microglia in the observed neuroprotection. Co-treatment of CGCs with FN and DCGIV or L-AP4 had no significant effect on the observed toxicity (**Figure 5.2.4 B**).

FG treatment for 24 hours significantly increased apoptosis in the CGC cultures, when compared with control levels. This significant increase was dependent on the presence of microglia (**Figure 5.2.4 C**) as previously shown (**Figure 3.3.4**). In the presence of microglia co-treatment of cultures with CDPPB significantly attenuated FG-mediated apoptosis. A significant attenuation was also observed if microglia were depleted, suggesting a microglial-independent neuroprotective role for mGluR5 allosteric modulation. Interestingly, co-treatment with DHPG could not attenuate FG-mediated apoptosis, with no significant modulation observed in cultures depleted of microglia. Furthermore, no significant modulation of FG-mediated apoptosis was observed if cultures were co-treated with DCGIV, however co-treatment with NAAG significantly attenuated the observed toxicity in the presence and absence of microglia (**Figure**

5.2.4 C). Interestingly, the previously published protective role of L-AP4 was not reciprocated here (Taylor et al. 2003), however culture conditions differed.

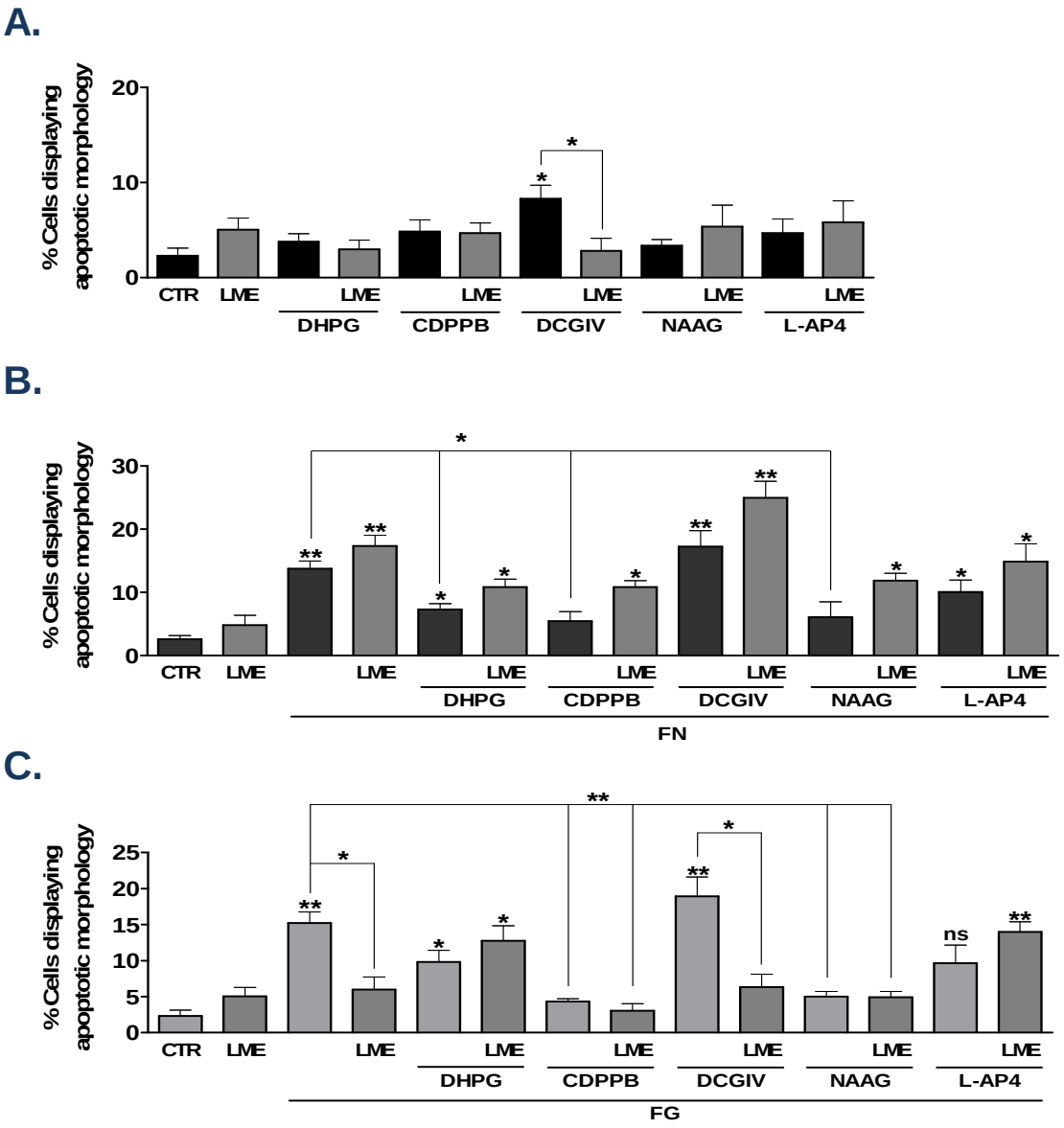

Figure 5.2.4. FN-mediated neurotoxicity can be down-regulated by a range of mGluR agonists in the presence of microglia, whereas attenuation of FG-induced neurotoxicity only occurs after CDPPB treatment in the presence of microglia

Hoechst-33342 staining of fixed CGC cultures for the quantification of apoptotic nuclear morphology. Some cultures were depleted of microglia prior to treatment with LME. Cultures were treated with DHPG (100 µM), CDPPB (100 nM), DCGIV (500 nM), NAAG (50 µM) or L-AP4 (100 µM) for 24 hours (**A**), FN alone and in combination with the stated mGluR agonists for 48 hours (**B**) or FG alone and in combination with the stated mGluR agonists for 24 hours (**C**). Treatments were in triplicate in each experiment and data were analysed from 3 independent experiments. To compare the percentage of apoptotic morphology in multiple treatment groups to control levels one way ANOVA were performed with Dunnett's post-test. Direct comparison of specific treatments was analysed using paired two-tailed Student's *t*-tests. Levels of significance were: non-significant $p>0.05$, * $p<0.05$, ** $p<0.01$.

5.2.4. Activation of mGluRs modulates fibrinogen-mediated ERK1/2 phosphorylation

The phosphorylation of p42/44 MAPK (ERK1/2) is generally associated with pro-survival pathways (Cheung & Slack 2004), although studies have been published suggesting neuronal ERK1/2 phosphorylation is detrimental to neurons after oxidative injury (Chu et al. 2004), with chronic activation playing a role in neurodegeneration (Colucci-D'Amato et al. 2003). Furthermore, phosphorylation of ERK1/2 has been shown to be involved in microglial activation (Kim et al. 2004; Hooper & Pocock 2007). To observe changes in ERK1/2 phosphorylation after FG and mGluR agonist treatment, Western blotting of CGC culture lysates was performed with microglia present or depleted. Treatment of CGCs with DCGIV significantly enhanced expression of phospho-ERK1/2 independent of the presence of microglia (**Figure 5.2.5 Ai**). FG also induced significant expression of phospho-ERK1/2 independent of the presence of microglia. In the presence of microglia, co-treatment of CGC cultures with FG and DCGIV also significantly induced phospho-ERK1/2 expression when compared with control, however if microglia were depleted prior to this co-treatment phospho-ERK1/2 expression was significantly attenuated (**Figure 5.2.5 Ai**).

Treatment of CGC cultures with CDPPB alone did not induce significant expression of phospho-ERK1/2 above control levels whether microglia were present or not. However, FG-mediated induction of phospho-ERK1/2 expression could be significantly attenuated by co-treatment of cultures with CDPPB, if microglia were present (**Figure 5.2.5 Aii**), further suggesting specific positive allosteric modulation of microglial mGluR5 is associated with down-regulation of FG-mediated responses.

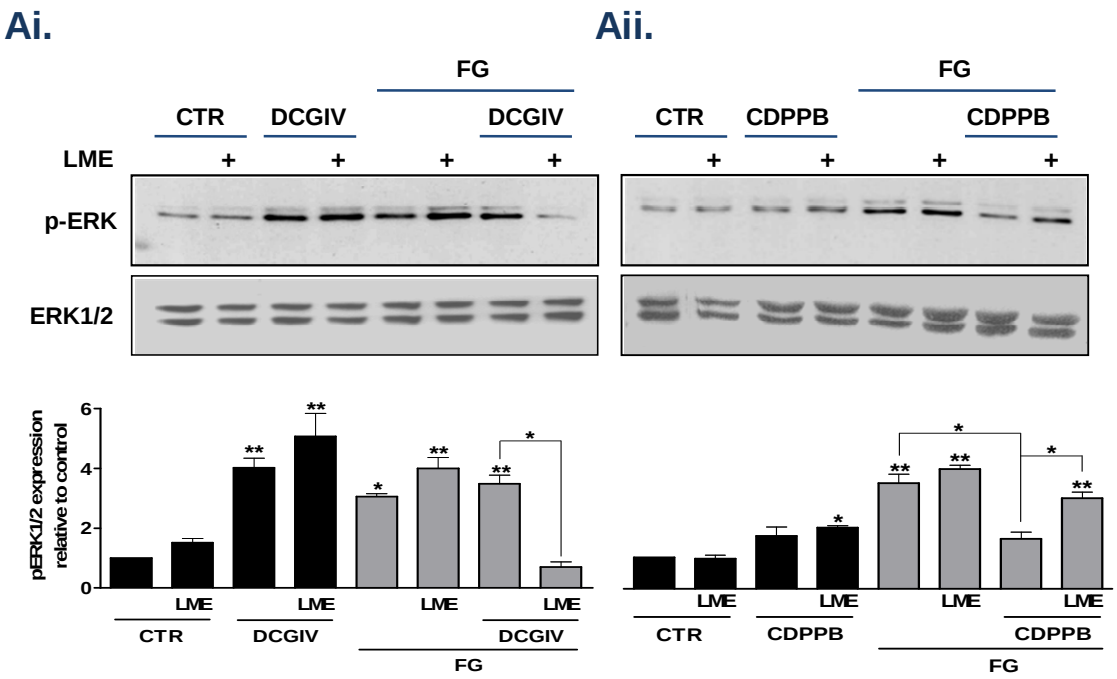

Figure 5.2.5. FG-induced phosphorylation of ERK1/2 can be down-regulated by CDPPB co-treatment if microglia are present

Representative Western blots and quantification of pERK1/2 and total ERK1/2 expression in CGC cultures in the presence or absence (denoted '+' on blots or 'LME' on quantification) of microglia after treatment with FG (2.5 mg/ml) and DCGIV (500 nM), alone or in combination (**Ai**), or FG and CDPPB (100 nM), alone or in combination (**Aii**) for 24 hours. Quantification of pERK1/2 expression was performed with respect to background intensity. Western blotting was also performed on 3 independent occasions. To compare pERK1/2 expression in multiple treatment groups to control levels a one way ANOVA was performed with Dunnett's post-test. Direct comparison of specific treatments was analysed using paired two-tailed Student's *t*-tests. Levels of significance were: non-significant $p>0.05$, * $p<0.05$, ** $p<0.01$.

5.2.5. Fibrinogen-mediated caspase-3 cleavage in neuronal cultures is attenuated by activation of group I mGluRs

Cleaved caspase-3 expression by Western blotting was performed after FG treatment of CGCs with co-treatment from mGluR agonists. FG induced significant expression of cleaved caspase-3, when compared with control levels, as previously shown (**Figure 3.3.2**). Interestingly, whether microglia were present or depleted, co-treatment of cultures with DHPG or CDPPB significantly attenuated FG-mediated caspase-3 cleavage (**Figure 5.2.6 A**). No significant attenuation was observed if cultures were co-treated with either NAAG or DCGIV, suggesting a limited role for group II in FG-mediated caspase-3 activity. Further support for neuronal caspase-3 cleavage being attenuated in the CGC cultures was provided by ICC. Caspase-3 cleavage after FG treatment was observed in CGC cultures in association with NeuN expression, suggesting neuronal caspase-3 activation is occurring (**Figure 5.2.6 B**). In line with the Western blotting data, expression of caspase-3 seems to be down regulated in the CDPPB co-treated cultures. However unlike the Western blotting data complete attenuation of FG-mediated caspase-3 activity was not observed in cultures co-treated with DHPG (**Figure 5.2.6 B**).

Figure 5.2.6

Ai.

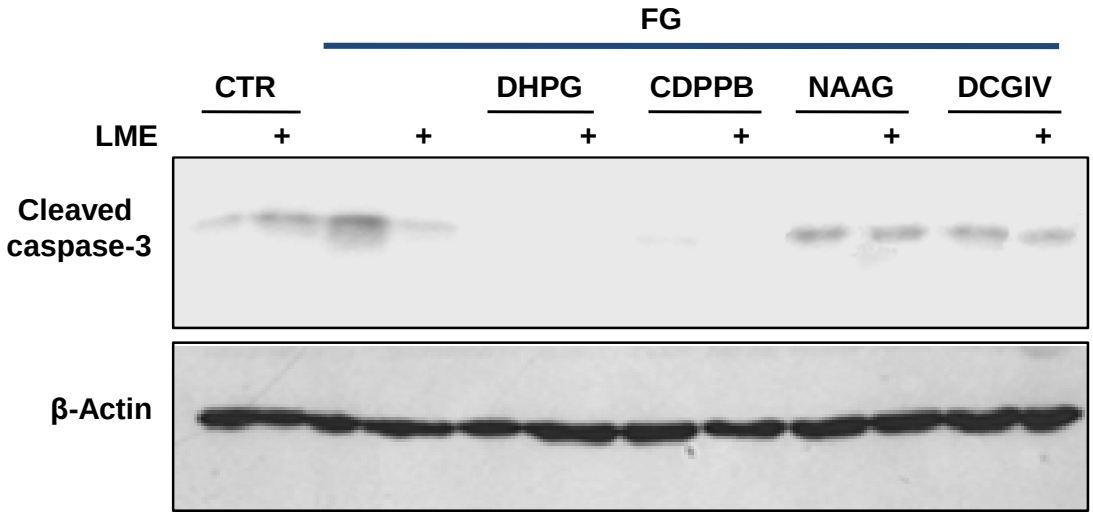

Aii.

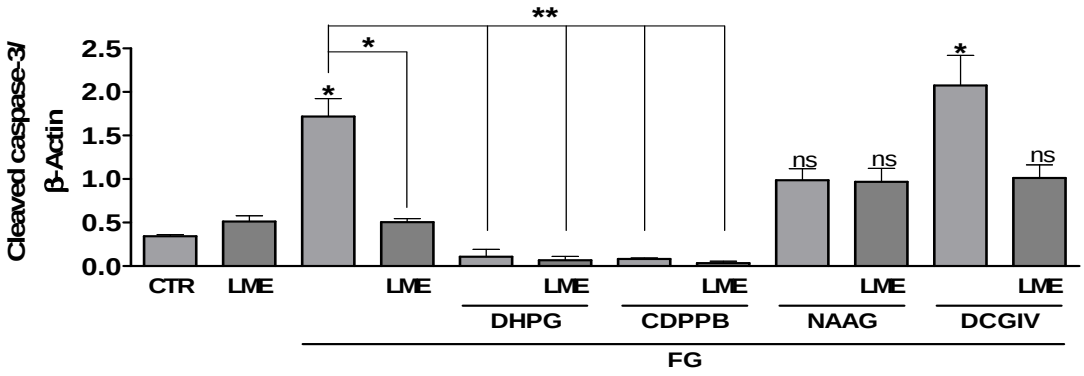

B.

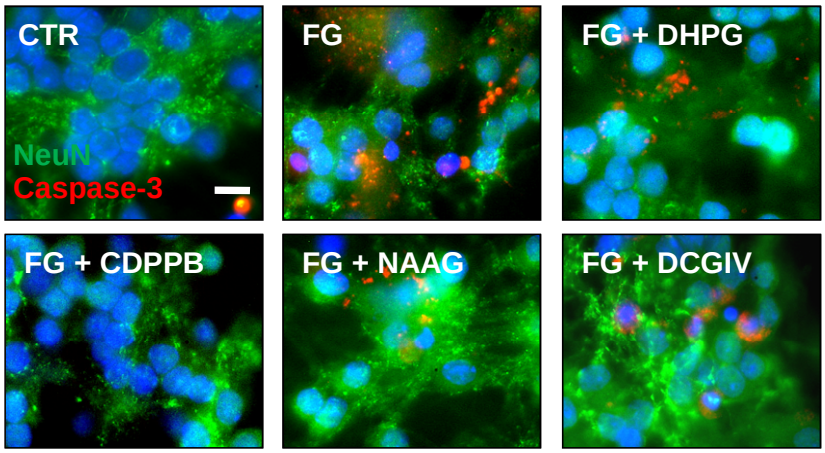

Figure 5.2.6. FG-mediated caspase-3 cleavage can be attenuated by group I mGluR agonists

Ai. Representative Western blots of cleaved caspase-3 and β-actin expression in CGC cultures in the presence or absence (LME) of microglia after treatment with FG (2.5 mg/ml) alone or in combination with DHPG (100 µM), CDPPB (100 nM), DCGIV (500 nM) or NAAG (50 µM) for 24 hours. Quantification of cleaved caspase-3 expression was performed with respect to β-actin loading control expression (**Aii**). Localisation of caspase-3 expression in CGC cultures was performed using ICC (**B**). After treatment as outlined in **Ai**, cultures were fixed and probed with anti-NeuN (green) for neuronal identification and anti-cleaved caspase-3 (red). Western blotting was performed on 3 independent occasions. To compare cleaved caspase-3 expression in multiple treatment groups to control levels a one way ANOVA was performed with Dunnett's post-test. Direct comparison of specific treatments was analysed using paired two-tailed Student's *t*-tests. Levels of significance were: non-significant $p>0.05$, * $p<0.05$, ** $p<0.01$.

5.2.6. Microglial mGluR5 activation attenuates fibrinogen-mediated neurotoxicity

Finally, to investigate the role of microglia in the observed neuroprotection by group I mGluR agonists, MGCM experiments were performed on CGC cultures initially depleted of contaminating microglia. In addition to agonist treatment, administration of the selective mGluR5 allosteric antagonist 3-((2-Methyl-4-thiazolyl)ethynyl)pyridine (MTEP) was performed in certain treatment groups. MGCM from cultures treated with DCGIV significantly increased apoptotic morphology in the CGC cultures when compared with non-treated controls (**Figure 5.2.7 A**), as previously described (Taylor et al. 2005). None of the other mGluR agonists or MTEP induced significant apoptosis ($p>0.05$) when administered alone.

As previously shown (**Figure 3.4.3**), FN-MGCM induced significant apoptosis in CGC cultures, when compared with control (**Figure 5.2.7 B**). MGCM from cultures co-treated with FN and mGluR agonists did not significantly modulate FN-mediated apoptosis (**Figure 5.2.7 Bii**). Interestingly antagonism of mGluR5 significantly enhanced FN-mediated toxicity, further suggesting an important role for mGluR5 in microglial reactivity.

FG-MGCM induced significant apoptosis in CGC cultures, when compared with control levels (**Figure 5.2.7 C**), similar to data previously reported (**Figure 3.4.3**). MGCM from cultures co-treated with FG and CDPPB or DHPG did not significantly induce CGC culture apoptosis (**Figure 5.2.7 Cii**) suggesting significant protective roles for group I mGluRs on microglia. Furthermore, if MGCM from cultures treated with FG, CDPPB and MTEP was applied to CGC cultures, significant apoptosis was observed when compared with control levels (**Figure 5.2.7 Cii**) supporting specific activation of microglial mGluR5 in the observed neuroprotection. Significant toxicity was observed if CGCs were treated with FG-DCGIV or FG-NAAG MGCM. However, as previously reported, L-AP4 activation of microglial group III mGluRs induced neuroprotection (Taylor et al. 2003) from FG-mediated toxicity (**Figure 5.2.7 Cii**).

In support of the microglial mGluR5-mediated protection, ICC was performed on CGC cultures after treatment with MGCM. FG-MGCM induced an increase in neuronal-associated caspase-3 cleavage, which was not present in CGC cultures treated with FG-CDPPB-MGCM. In line with the apoptotic morphology quantification, caspase-3 cleavage was observed after administration of MGCM from cultures co-treated with FG, CDPPB and MTEP (**Figure 5.2.7 D**).

To identify whether it was purely microglial mGluR5 activation that could modulate FG-mediated neurotoxicity, apoptosis was quantified in CGCs depleted of microglia and directly treated with mGluR agonists in the presence of FG-MGCM. As expected, FG-MGCM alone induced significant apoptosis, when compared with CTR-MGCM induction. Direct treatment of cultures with CDPPB but not DHPG significantly attenuated FG-mediated toxicity, supporting the ability of microglial independent activation mGluR5 to mediate protection (**Figure 5.2.8**). Direct treatment of CGCs with DCGIV and NAAG could not attenuate FG-MGCM induced neurotoxicity, suggesting any neuroprotective effect observed with NAAG treatment depends on activation of microglial mGluR3 rather neuronal or astrocytic receptors (**Figure 5.2.8**). These data are in contrast to data shown in **Figure 5.2.4 C**, suggesting microglia are not required for NAAG-mediated protection from toxicity induced by direct FG treatment.

To support the apoptotic morphology quantification and caspase-3 expression data, LDH assays were performed on CGC cultures treated with MGCM. As expected, DCGIV-MGCM treatment significantly increased LDH release above control levels (**Figure 5.2.9**). FG-MGCM treatment also significantly increased LDH release above control levels. Furthermore, in line with the apoptotic morphology quantification, LDH release was significantly attenuated in cultures treated with FG+DHPG-MGCM or FG+CDPPB-MGCM, with co-administration of MTEP significantly inhibiting DHPG- and CDPPB-mediated attenuation (**Figure 5.2.9**). No significant modulation of FG-MGCM-mediated LDH release was observed after co-treatment with group II agonists.

Figure 5.2.7

Ai.

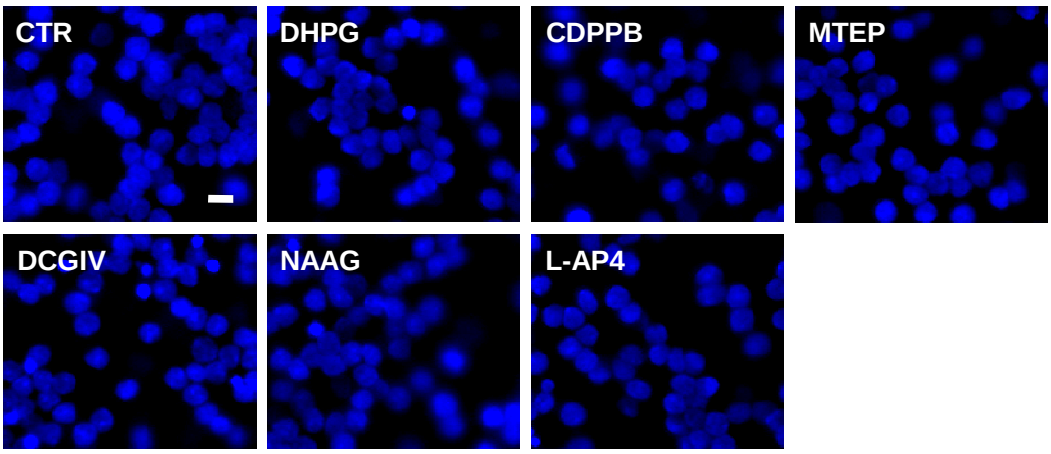

Aii.

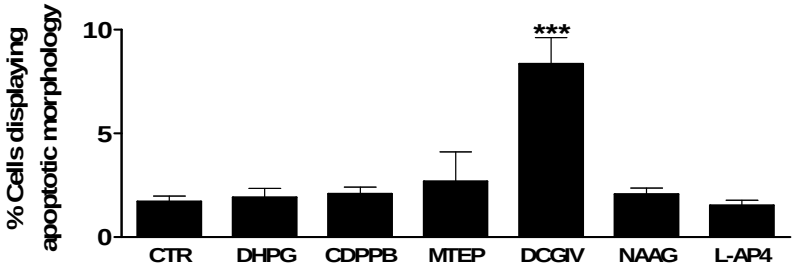

Bi.

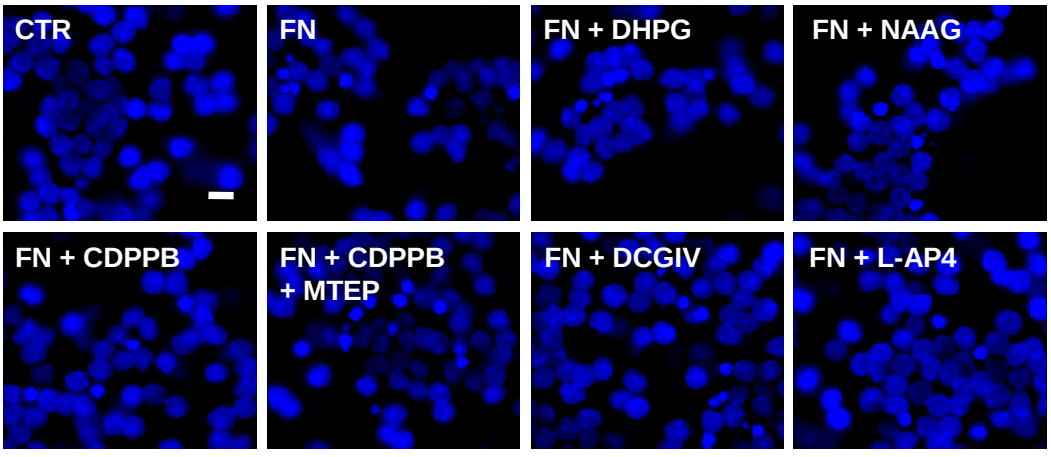

Bii.

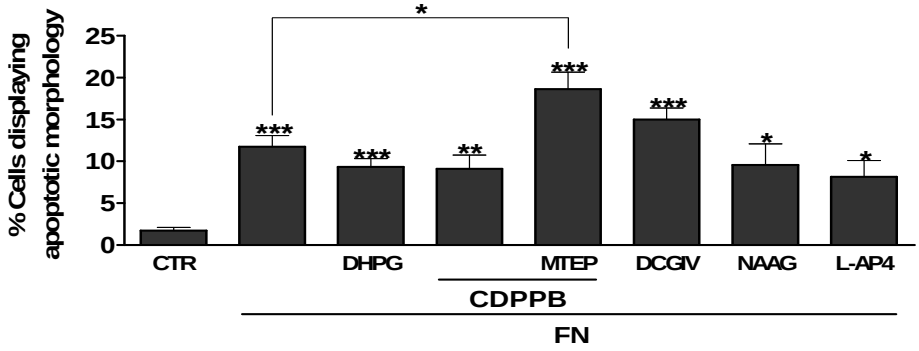

Figure 5.2.7

Ci.

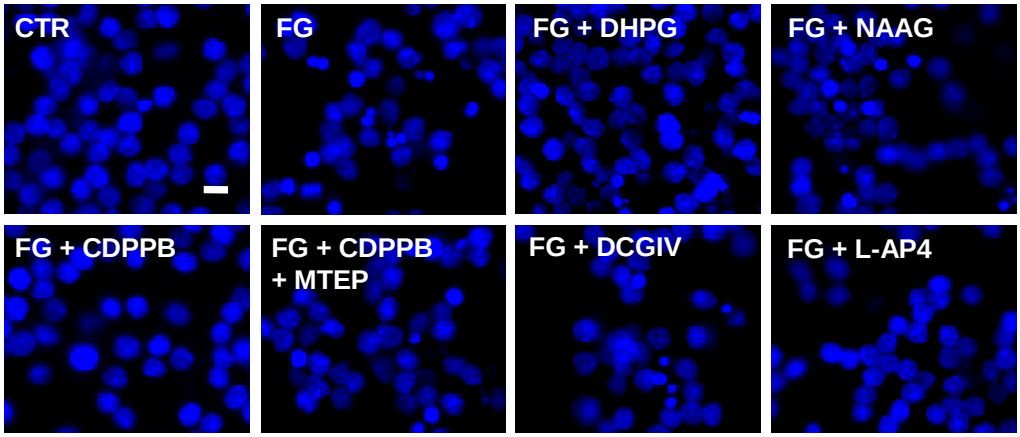

Cii.

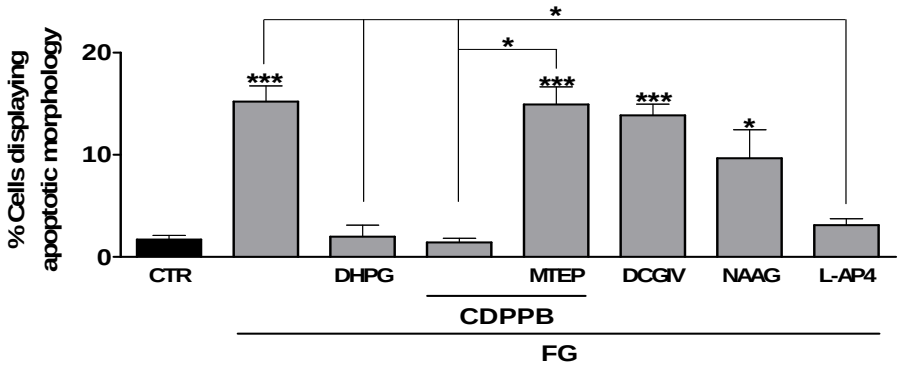

D.

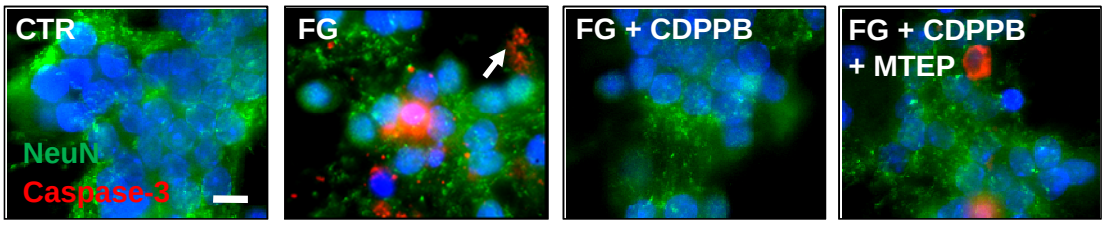

Figure 5.2.7. FG-MGCM induced neurotoxicity was attenuated by activation of microglial group I and III mGluRs

Ai. Representative images from Hoechst-33342 staining experiments on fixed CGC cultures for quantification of apoptotic morphology after treatment for 24 hours with MGCM from cultures treated with DHPG (100 µM), CDPPB (100 nM) MTEP (100 µM), DCGIV (500 nM), NAAG (50 µM) or L-AP4 (100 µM) for 24 hours. **Bi.** Representative images from Hoechst-33342 staining of CGC cultures after treatment with FN and mGluR compound MGCM for 24 hours. **Ci.** Representative images from Hoechst-33342 staining of CGC cultures after treatment with FG and mGluR compound MGCM for 24 hours as detailed in **A**. Quantification of apoptotic morphology was performed for each treatment group, i.e. mGluR compounds alone (**Aii**), FN and mGluR compounds (**Bii**) and FG and mGluR compounds (**Cii**). **D.** Expression and localisation of caspase-3 expression in CGC cultures treated with FG and mGluR5 compound MGCM was performed using ICC. After treatment with MGCM from FG-, FG + CDPPB- or FG + CDPPB + MTEP-treated microglial cultures, CGC cultures were fixed and incubated with anti-NeuN (green) for neuronal identification and anti-cleaved caspase-3 (red). Scale bars = 10 µm. All experiments were performed on 3 independent occasions. To compare the levels of apoptotic morphology in multiple treatment groups to control levels one way ANOVA were performed with Dunnett's post-test. Direct comparison of specific treatments was analysed using paired two-tailed Student's *t*-tests. Levels of significance were: non-significant $p>0.05$, * $p<0.05$, ** $p<0.01$, *** $p<0.001$.

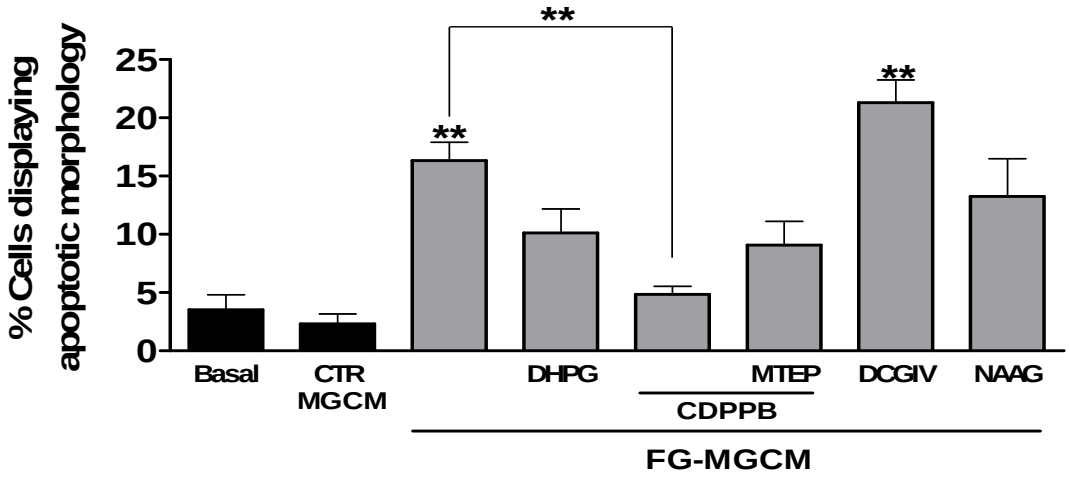

Figure 5.2.8. FG-MGCM-induced neurotoxicity could be prevented by direct treatment of neuronal cultures with CDPPB

Quantification of apoptotic morphology using Hoechst-33342 staining in fixed CGC cultures after treatment for 24 hours with FG-MGCM in the absence or presence of direct DHPG (100 µM), CDPPB (100 nM) MTEP (100 µM), DCGIV (500 nM), or NAAG (50 µM) treatment of neuronal cultures. Treatments were in duplicate and experiments were performed on 3 independent occasions. To compare the levels of apoptotic morphology in multiple treatment groups to control levels a one way ANOVA was performed with Dunnett's post-test. Direct comparison of specific treatments was analysed using paired two-tailed Student's *t*-tests. Levels of significance were: non-significant $p>0.05$, ** $p<0.01$.

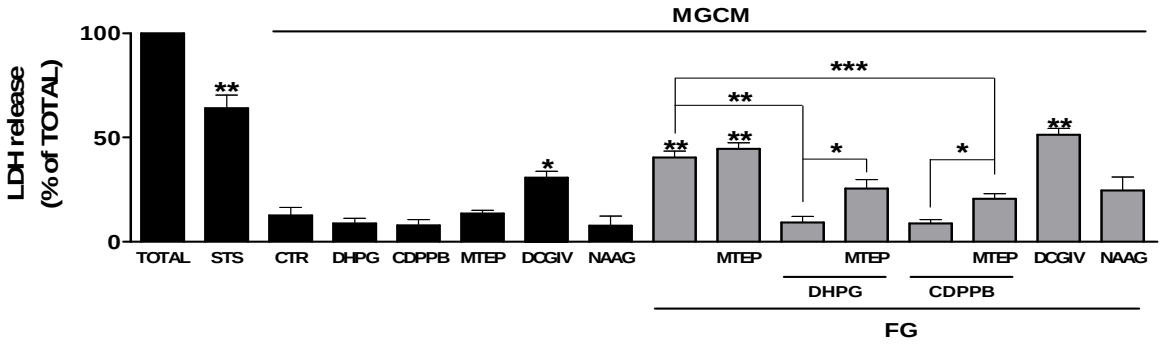

Figure 5.2.9. FG-MGCM-induced LDH release could be attenuated by activation of microglial mGluR5

Quantification of LDH release from CGC cultures after 24 hours of treatment with MGCM from cultures treated for 24 hours with DHPG (100 µM), CDPPB (100 nM) MTEP (100 µM), DCGIV (500 nM), or NAAG (50 µM), in the absence or presence of FG (2.5 mg/ml) treatment. Treatments were in triplicate and experiments were performed on 3 independent occasions. To compare the levels of LDH release in multiple treatment groups to control levels a one way ANOVA was performed with Dunnett's post-test. Direct comparison of specific treatments was analysed using paired two-tailed Student's *t*-tests. Levels of significance were: non-significant $p>0.05$, ** $p<0.01$.

5.3. Discussion

This chapter provides data suggesting neuroprotection from FG can be afforded by activating group I mGluRs present on microglia or by activating neuronal or astrocytic mGluR3 & 5. Furthermore, it is shown that FN-mediated toxicity in CGC cultures can be attenuated by activation of group I mGluRs or mGluR3. However, specific activation of these particular receptors on microglia does not protect against microglial-associated FN-induced neurotoxicity.

It is shown that positive allosteric modulation of microglial mGluR5 can provide strong neuroprotection from FG-induced toxicity. It is also important to note that microglial-independent mGluR3-dependent neuroprotection from FG was observed suggesting that protection from FG-mediated toxicity could be provided by activation of allosteric modulation of microglial mGluR5 and orthosteric agonism of neuronal mGluR3.

5.3.1. Classical microglial activation markers are down-regulated by mGluR agonist treatment

Treatment with the group I agonist DHPG (mGluR1 and 5) and the mGluR5 positive allosteric modulator CDPPB induced significant microglial activation shown by an increase in ED-1 expression, but not iNOS expression. Previous studies using DHPG treatment alone show little or no change in microglial morphology using OX-42 (CD11b) (Farso et al. 2009), another marker of microglial activation (**Figure 3.2.2**). Little research has been performed on the role of positive allosteric modulation of microglial mGluR5, however orthosteric agonism of microglial mGluR5 with (RS)-2-chloro-5-hydroxyphenylglycine (CHPG) does not significantly increase reactive oxygen species (ROS) or nitric oxide (NO) levels in microglia (Byrnes et al. 2009a; Loane et al. 2009), providing lose support for the lack of iNOS activity we observe here.

Treatment with group II agonists (DCGIV or NAAG) did not significantly increase iNOS expression, supporting previously published work from the laboratory (Taylor et al. 2005). However, treatment with mGluR3 specific agonist NAAG significantly increased

ED-1 expression, which does not concur with previously published data (Taylor et al. 2005; Pinteaux-Jones et al. 2008). This observed variability could be due to differences in the serum content of culture medium. Both Taylor et al (2005) and Pinteaux-Jones et al (2008) used serum-containing conditions, whereas here, serum-free conditions were used allowing FG-mediated iNOS expression to be used as a marker of activation. Therefore, higher microglial sensitivity in serum-free conditions could lower the activation threshold. However, no significant increase in ED-1 or iNOS expression was observed after treatment with the group III agonist, L-AP4, similar to the previously published data (Taylor et al. 2003; Taylor et al. 2005), suggesting mGluR3 but not group III activation is more sensitive to iNOS activity in serum-free conditions.

Orthosteric agonism of mGluR5 has been shown to reduce LPS-mediated microglia activation, identified by reductions in nitric oxide, reactive oxygen species, and TNFα production (Byrnes et al. 2009a; Loane et al. 2009). Findings presented here show no attenuation of LPS-induced iNOS and ED-1 expression and TNFα expression and release when co-treated with mGluR5 positive allosteric modulator, CDPPB. These data suggest allosteric modulation is less effective than orthosteric agonism in down-regulating LPS-mediated microglial activation. Further scrutiny of Byrnes et al (2009a) and Loane et al (2009), reveals the use of lower LPS concentrations (in both cases, 10 times lower), which could simply suggest that the concentration utilised here is insurmountable in terms of mGluR5 allosteric modulation. In contrast to LPS, the potency of positive allosteric mGluR5 modulation on reducing FG-evoked responses suggests that mGluR5 coupling to this pathway is highly robust. This further supports the suggestion that differential pathways are induced after LPS and FG treatments. Interestingly, co-treatment of microglia with DHPG could also significantly attenuate FG-mediated TNFα expression and release, suggesting important down-regulatory roles for both group I agonists in TNFα-associated responses. However, further reading provides data suggesting microglia only express mGluR5 and not mGluR1 (Biber et al. 1999). This in turn suggests that here, classical orthosteric agonism of mGluR5 is able

to down-regulate FG-mediated TNFα responses as well as positive allosteric modulation of the receptor.

5.3.2. Modulation of ER-associated caspase-12 and caspase-3/7 activation with mGluR agonists

Due to limited availability of the caspase-12 and -3/7 fluorescently tagged peptides, only a small number of treatments were analysed. Co-treatment of cultures with CDPPB or NAAG significantly attenuated FG-mediated caspase-12 and -3/7 activation. Involvement of mGluR3 or mGluR5 activation in down-regulation of ER stress is a novel idea and one which has received little or no attention. These data suggest FG-mediated caspase-12 expression due to ER stress can be prevented if cultures are co-treated with CDPPB or NAAG. MGluR5 is predominantly coupled to G_q/G_{11} proteins leading to activation of phospholipase C_β, which results in calcium mobilisation (Niswender & Conn 2010). The role of calcium dyshomeostasis in FG-mediated microglial activation has already been alluded to (**Section 4.4**) and these data coupled with the mGluR5 activation data here allow one to hypothesise that mGluR5 activation can regulate calcium levels possibly returning cellular homeostasis after FG-mediated dyshomeostasis has occurred. Western blotting for caspase-12 and/or caspase-3 activation would enable further clarification of these data.

NAAG treatment has been shown to down-regulate caspase-3 activation in neurons in excitotoxic conditions (Spillson & Russell 2003), however this microglial caspase-3/7 activation is not associated with enhanced cellular toxicity, suggestive on non-apoptotic caspase activation (Burguillos et al. 2011). These data therefore suggest that mGluR3 agonism can down-regulate FG-mediated microglial activation, which is at odds with the iNOS and ED-1 expression data and the TNFα expression and release data, implying differential pathways for iNOS, ED-1 and TNFα induction and caspase-3/7 activation, although this is at odds with Burguillos et al (2011), who show in BV2 microglia that inhibition of caspase-3/7 attenuates LPS-induced morphological changes

and iNOS expression, further confusing the data collected here associated with mGluR3 activation. Therefore, much greater, in depth studies with NAAG are required to understand the compounds' mechanism of action with respect to down-regulation of caspase activity in microglia. Microglial cultures treated with CDPPB down-regulated the FG-induced caspase-3/7 'activation' supporting the iNOS and ED-1 expression data and the TNFα expression and release data.

5.3.3. Modulation of neurotoxicity induced after direct treatment with fibrinogen or fibrin by mGluR agonists

The roles of specific mGluR activation in FG- and FN-mediated neuronal apoptosis were investigated. Initially, support for previously published data (Taylor et al. 2005) suggesting DCGIV treatment alone can induce death that is dependent on microglia is shown. No other mGluR agonists tested induced significant death when administered alone. Co-treatment of cultures with DHPG, CDPPB, or NAAG significantly attenuated FN-mediated apoptosis if microglia were present. However, prior depletion of microglia prevented the observed attenuation. These data suggest that the presence of microglia are required and potentially involved in group I and mGluR3-mediated neuroprotection from FN, further supporting a protective role for NAAG although later MGCM studies suggested otherwise.

FG-mediated neurotoxicity could be attenuated by CDPPB co-treatment but not DHPG, although co-treatment with DHPG could significantly inhibit caspase-3 cleavage in CGC cultures. Removal of microglia had no effect on the mGluR5-associated attenuation of the FG-induced apoptosis however we propose this is not due to neuronal specific modulation of mGluR5 but due to the previous observations made in **section 3.3.2**, that suggest that FG induces its neurotoxic effects via a microglial dependent mechanism. This is supported by cleaved caspase-3 expression in CGCs in the presence and absence of microglia. Previously published studies have shown that activation of group I mGluRs can significantly attenuate neuronal apoptosis induced by

staurosporine but in turn increase necrotic cell death (Allen et al. 2000). These data support the lack of significant attenuation of FG-mediated neuronal toxicity by DHPG co-treatment, which could be due to quantification of apoptotic-like necrotic cell death, further supported by the significant inhibition of caspase-3 cleavage. No significant modulation of FG-mediated apoptosis by co-treating with DCGIV was observed unless microglia were removed. However, co-treatment with NAAG significantly attenuated the observed FG-mediated toxicity in the presence of microglia. These data support previously published data from our laboratory identifying differential roles for the microglial group II mGluRs (Taylor et al. 2005). Caspase-3 cleavage data however suggests no significant modulation occurs in cultures where microglia were depleted, although, in the case of NAAG co-treatment in particular, the expression of caspase-3 cleavage is trending towards an attenuation and further repetitions would ascertain whether this treatment does in fact inhibit FG-mediated caspase-3 cleavage. In conclusion these data suggest varying mechanisms of cell death induced by particular treatments that would have otherwise been missed had these experiments been performed independently on homogenous cultures.

5.3.4. MAPK pathway modulation by mGluR agonists

Phosphorylation of p42/44 MAPK (ERK1/2) is generally associated with pro-survival pathways (Cheung & Slack 2004), although studies have been published suggesting neuronal ERK1/2 phosphorylation is detrimental to neurons after oxidative injury (Chu et al. 2004), with chronic activation playing a role in neurodegeneration (Colucci-D'Amato et al. 2003). Furthermore, phosphorylation of ERK1/2 has been shown to be involved in microglial activation (Kim et al. 2004; Hooper & Pocock 2007). Data presented here suggests that treatment of CGCs with DCGIV significantly enhanced expression of phospho-ERK1/2, independent of the presence of microglia, suggesting group II mGluR activation in neurons and astrocytes involves ERK1/2-associated pathways, which has recently been observed in striatal lysates using a different mGluR2/3 agonist (LY379268) (Di Liberto et al. 2011). We also show significant

expression of phospho-ERK1/2 independent of the presence of microglia after FG treatment suggesting FG is able to signal via other cells present in the cultures as shown previously (Schachtrup et al. 2007; Schachtrup et al. 2010). In the presence of microglia it is shown that co-treatment of CGC cultures with FG and DCGIV significantly induced phospho-ERK1/2 expression, however, if microglia were depleted prior to this co-treatment phospho-ERK1/2 expression was significantly attenuated, suggesting microglial involvement in this induction of phospho-ERK1/2.

Positive allosteric modulation of mGluR5 alone did not induce significant phosphorylation of ERK1/2 unless microglia were depleted. However FG-mediated induction of phospho-ERK1/2 expression could be significantly attenuated by co-treatment of cultures with CDPPB, if microglia were present. FG has been shown to suppress apoptosis in neutrophils during inflammation via activation of Akt and ERK1/2 pathways, which prolongs the inflammatory response (Pluskota et al. 2008). These published data coupled with observations here suggest mGluR5 modulation can down-regulate the FG-mediated prolongation of activation. However, due to the vast signalling capabilities of ERK1/2, at this stage it is impossible to know for certain. What is important is that CDPPB can down-regulate the FG-mediated phosphorylation of ERK1/2, with dependence on microglia, suggesting significant modulatory capabilities of the compound with respect to FG-induced responses.

5.3.5. Modulation of fibrinogen-induced microglial-mediated neurotoxicity by mGluR5

To further strengthen the notion of microglial dependence in mediating both FG toxicity and protection, MGCM studies were undertaken. Data presented here provides significant support for positive allosteric modulation of mGluR5 on microglia as a protective mechanism against FG-mediated neurotoxicity. Initially it is shown that only DCGIV treatment of microglia can induce neurotoxicity, supporting the microglial depletion data and previously published data (Taylor et al. 2005). Similarly to Taylor et

al (2005), no other mGluR agonist tested induced neurotoxicity via microglial-dependent release of soluble factors. In direct treatment studies it was shown that the presence of microglia in the CGCs was a requirement for group I- and mGluR3-mediated neuroprotection from FN. However, down-regulation of the activated microglial phenotype with DHPG, CDPPB and NAAG could not prevent microglial-mediated FN-induced neurotoxicity. These data suggest that FN is still able to induce the release of neurotoxic factors from microglia at a concentration high enough to induce neurotoxicity, which is feasible when reviewing the extent of TNFα release from microglia (**Figure 3.2.3**), compared with LPS or FG, where FG-mediated release is much lower. Alternatively, significant transfer of FN in the MGCM could have occurred that is able to induce direct neurotoxicity. This is a significant caveat to these experiments and is difficult to test in a similar manner to FG (**Section 2.4.2**) due to the insolubility of FN.

In the case of protection from FG-mediated neurotoxicity, activation of group I mGluRs and group III mGluRs afforded protection from FG. These data suggest it is not only mGluR5 on microglia that is able to protect against FG-mediated neurotoxicity. Group III mGluRs comprises of mGluR4/6/7/8, but rat microglia only express mRNA and receptor protein for mGluR4, mGluR6, and mGluR8, not mGluR7 (Taylor et al. 2003). Previously, activation of this group of receptors has been shown to mediate protection from LPS, chromogranin A, $A\beta_{25-35}$ (Taylor et al. 2003), myelin (Pinteaux-Jones et al. 2008) and excitotoxicity in neurons (Lafon-Cazal et al. 1999), suggesting the group is a promising target for pharmaceutical development. However, further investigation needs to be performed to identify if a particular receptor is specifically responsible for mediating this neuroprotection. This will enable the development of more specific agonists avoiding non-specific interactions with other group members.

As previously suggested, DHPG treatment of microglia will only agonise mGluR5 due to the lack of functional mGluR1 on microglia (Biber et al. 1999). Here it is shown that

DHPG treatment significantly attenuated FG-mediated neurotoxicity as assessed by quantification of apoptotic morphology as well as LDH release assays. Furthermore, co-administration of MTEP, the mGluR5 negative allosteric modulator, significantly inhibited the DHPG-mediated attenuation of FG-mediated LDH release, supporting mGluR5 specific activation by DHPG on microglia. This MTEP inhibition was also observed in CDPPB-treated microglia, with further data presented here showing an inhibition of CDPPB-mediated downregulation of cleaved caspase-3 in CGC cultures treated with MGCM. Finally, when cultures were directly treated with CDPPB then exposed to FG-MGCM, significant attenuation was again observed, which could not be reciprocated by DHPG direct treatment, supporting published data identifying differential toxicity profiles for the group I receptors present on neurons (Allen et al. 2000). These data also suggest that specific allosteric modulation of mGluR5 both on microglia and other cell types including neurons and astrocytes could provide protection against FG-induced toxicity.

5.3.6. Conclusions

Together these data provide evidence for a prominent role for the activation of specific mGluRs in mediating neuroprotection from FG and possibly FN, as summarized in **Figure 5.3.1**. The significant attenuation of FG-MGCM-mediated neurotoxicity by co-administering CDPPB direct to the CGCs provides strong support, in a more physiologically viable model, for a prominent role for mGluR5 in neuroprotection, as previously suggested in Alzheimer's disease and spinal cord injury models (Movsesyan et al. 2004; Byrnes et al. 2009b). Finally, these data provide support for the hypothesis that combating early FG extravasation before FN deposition will attenuate the accelerated neuronal loss observed in neurodegenerative disorders.

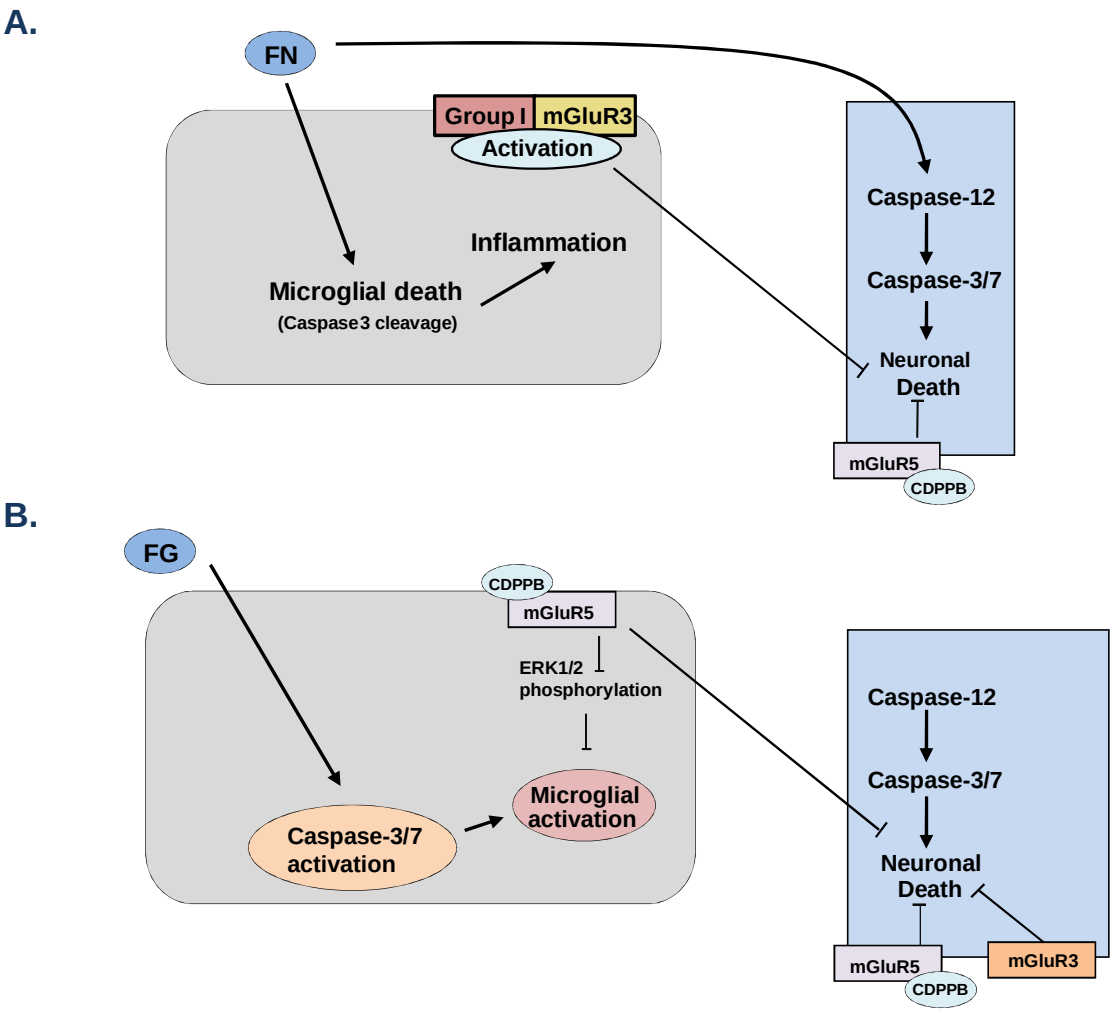

Figure 5.3.1. Summary of results obtained in chapter 5

A. Co-treatment of microglia with FN and either group I mGluR agonists or an mGluR3 agonist provided significant protection from FN-mediated neurotoxicity. Furthermore, specific activation of mGluR5 on neurons also provided protection from FN-mediated neurotoxicity. **B.** Fibrinogen-mediated microglial activation and subsequent neurotoxicity could be attenuated by co-treatment of microglial cultures with an mGluR5 agonist. Direct treatment of neuronal cultures with either an mGluR3 or mGluR5 agonist provided neuroprotection from FG mediated toxicity via microglial activation.

6. Initial translation of findings using a human model of phagocytes, *in vitro*

6.1. Introduction

To identify whether the significant microglial findings described in chapters 3-5 would translate to a human model, the *in vitro* monocyte-derived macrophage model (MDM or hMΦ) was selected. To date hMΦ are the closest culture available to model human pre-mortem microglial signalling *in vitro*, if human foetal microglia are discounted due to ethical and lawful reasons limiting their use. One of the most important aspects of the hMΦ cultures is how they are prepared *in vitro*. By isolating pure monocytes from the blood and differentiating them to macrophages in culture the desired cell type is not wrestled from its homeostatic environment, rather the macrophages are differentiated in the cell culture system, the only environment they are ever exposed to.

Early studies identified that the hMΦ share similar morphological and immunological features with microglia, such as the ruffled cell membrane and the expression of surface antigens including MHC class II and complement receptor 3 (CR3; MAC-1, CD11b) (Bauer et al. 1991). More recent studies using hMΦ in tandem with human foetal microglia showed that fibrillary Aβ can induce ROS and H_2O_2 to a similar extent in both models (Coraci et al. 2002).

Limited studies have been performed to characterise the hMΦ with respect to rodent microglia, studies which would provide invaluable data and hopefully support for the use of these cells. The identification of a subset of monocyte-derived microglia in rodent models (Bechmann et al. 2005; Mildner et al. 2007) suggests that studies to identify particular transcription regulators and the relevant extrinsic support factors that enable this differentiation *in vivo* could allow refinement of the hMΦ model to further mimic microglia however, species differences could create some difficulties. Some limited microarray studies have been performed which have identified some correlation

between the genes upregulated upon activation of the hMΦ and rodent microglia. Albright and colleagues (2004) compared the upregulation of genes in hMΦ to those in rat-derived mixed glial cultures (containing ~ 60% microglia) and found 180 genes were commonly upregulated, equating to approximately 24% of the total hMΦ genes and 20% of the total mixed glial genes that were upregulated. The obvious and rather large caveat in these experimental procedures is the use of mixed glia containing 40% non-microglial cells rather than using purified cultures with a purity of 90-99%. These non-microglial cells could be responsible for the greater number of genes that were shown to upregulated in the mixed glia cultures when compared with the hMΦ cultures (747 in hMΦ and 914 in mixed glia) (Albright & González-Scarano 2004). Furthermore, non-cell autonomous communication could be manipulating the gene expression in the microglia present in these cultures.

Here, using gene and protein expression techniques support is provided for studies suggesting a limited role for iNOS activity in human macrophages after activation and also significant support for the identification of pro-inflammatory cytokine induction upon FG treatment with regulation by ER stress.

6.2. Fibrinogen or fibrin treatment of hMΦ induces expression of TNFα, but only fibrinogen treatment is associated with ER stress

To ascertain whether FG and FN treatment of human macrophages (hMΦ) induced a similar profile to that seen in rat microglia studies, gene expression analysis for previously used markers was performed. Interestingly, no treatment tested induced significant iNOS gene expression in the hMΦ cultures, a result that supports previous suggestions that human macrophages lack the high output iNOS-mediated NO release that is observed in rodent cells (Peterson et al. 1994), although later studies disagree (Ding et al. 1997) (**Figure 6.2.1A & Bi**). However all treatments tested, apart from thapsigargin, induced significant increases in TNFα gene expression, suggesting strong activation of these cells also occurs after FG and FN treatment with little or no involvement from iNOS-dependent pathways (**Figure 6.2.1A & Bii**). Finally, to identify if ER stress pathways were being induced, CHOP gene expression was analysed after the same treatments. FG but not FN treatment significantly induced CHOP expression above that seen in control cultures (**Figure 6.2.1A & Biii**).

Live cell staining studies with the hMΦ cultures supported an induction of ER stress pathways after FG treatment for 24 hours with significant enhancement of caspase-12 cleavage that was not dependent on cell death (**Figure 6.2.2**). The positive control for ER stress induction, thapsigargin, also significantly enhanced caspase-12 cleavage in the hMΦ cultures after 24 hours. However, a significant increase in cell death was also observed.

Inhibition of the PERK-eIF2α-ATF4 axis of ER stress with salubrinal completely attenuated FG-mediated caspase-12 cleavage (**Figure 6.2.2**), supporting an ER stress-dependent cleavage of caspase-12. Interestingly however, salubrinal treatment could not significantly attenuate thapsigargin-induced caspase-12 cleavage, although a

significant attenuation of thapsigargin-mediated cell death was observed, when compared with thapsigargin treatment alone; **Figure 6.2.2**).

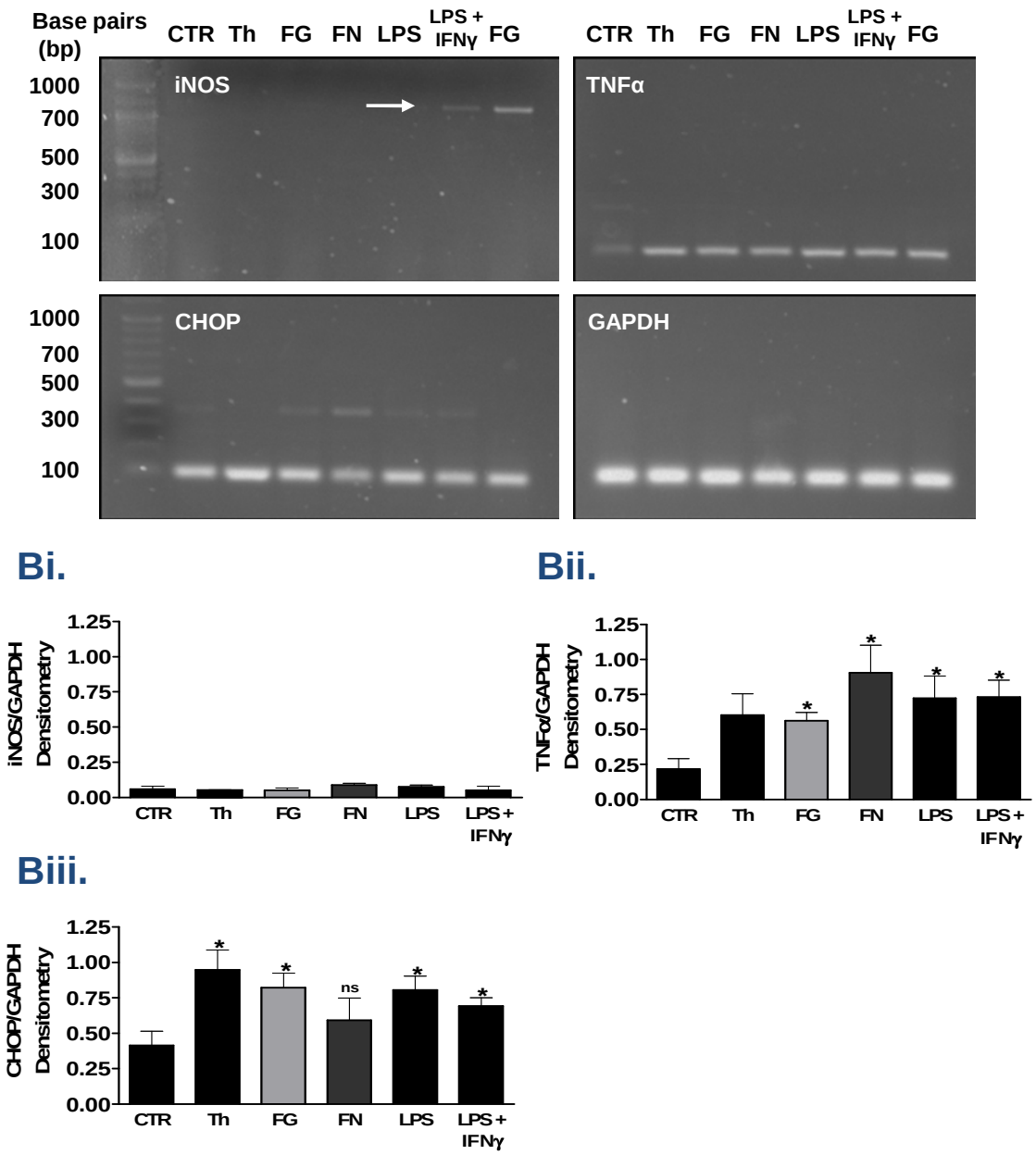

Figure 6.2.1. FG and FN treatment of human macrophages induces TNFα gene expression but only FG can induce CHOP gene expression

A. Representative PCR blots for iNOS (70 bp), TNFα (123 bp), CHOP (95 bp) and GAPDH (66 bp) gene expression after Thapsigargin (Th; 2 µM), FG (2.5 mg/ml), FN (1 mg/ml), LPS (1 µg/ml) or LPS + IFNγ (100 U/ml) treatment of hMΦ for 24 hours. Arrow indicates non-specific bands. Quantification of iNOS (**Bi**), TNFα (**Bii**) and CHOP (**Biii**) gene expression in hMΦ cultures with respect to gene expression of GAPDH. Quantified data were analysed from 3 independent experiments. To compare between control levels and multiple treatments, one way ANOVA were performed with Dunnett's post-test. Levels of significance were: non-significant, $p>0.05$, * $p<0.05$.

Figure 6.2.2

A.

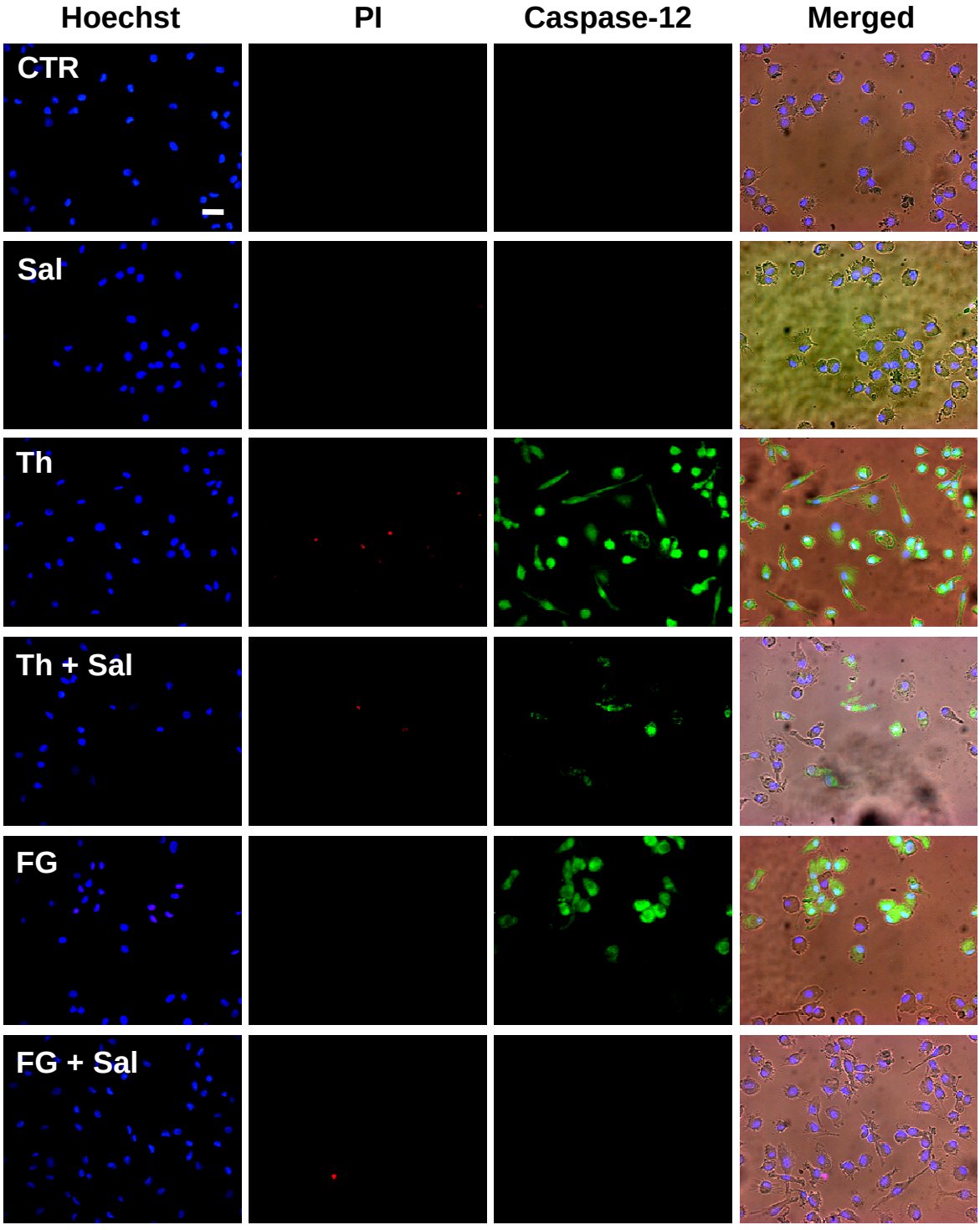

B.

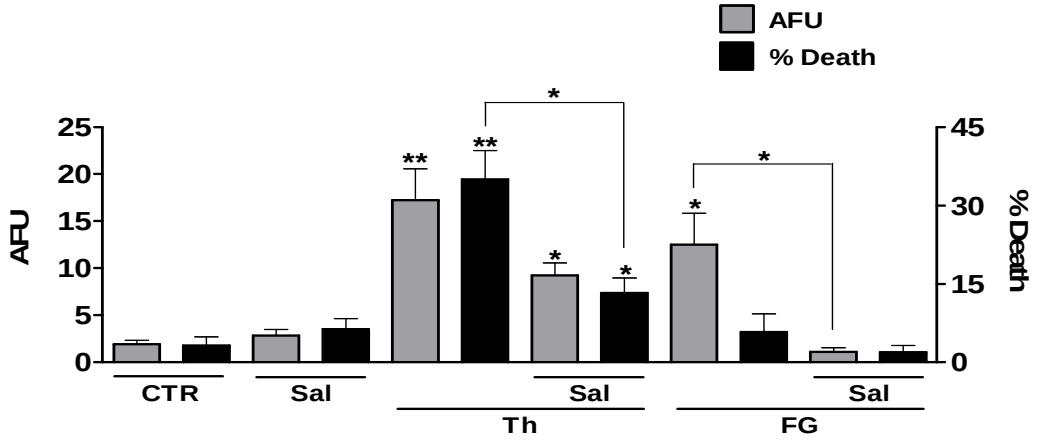

Figure 6.2.2. FG induces an increase in activated caspase-12-associated fluorescence in hMΦ cultures that is dependent on ER stress

A. Panel of representative images of live cell staining experiments in hMΦ cultures after treatment with Th (2 µM) or FG (2.5 mg/ml) alone or in combination with Sal (100 nM). Live cell staining was performed with Hoechst-33342 for nucleus identification, propidium iodide (PI; red) for total cell death, and FITC-ATAD-FMK (green) for active caspase-12. Original magnification: x40, scale bar: 30 µm. **B.** Quantification of the relative active caspase-12 fluorescence intensity/cell and % death in the population (by quantification of PI-positive cells) in hMΦ cultures after administration of the treatments outlined in **A**. Caspase-12 fluorescence data are presented in arbitrary fluorescence units (AFU). Treatments were in triplicate and data were analysed from 3 independent experiments. To compare multiple treatments to control levels, one way ANOVA were performed with Dunnett's post-test. To compare specific treatments with ER stress inhibited treatments, paired two-tailed Student's *t*-tests were performed. Levels of significance were: non-significant $p>0.05$, * $p<0.05$, ** $p<0.01$.

6.3. Inhibition of an ER stress pathway attenuates fibrinogen-mediated upregulation of TNFα gene expression and caspase-3 cleavage

To identify whether the observed induction of ER stress in the hMΦ cultures was upstream or downstream of TNFα expression, PCR was performed. Initially, CHOP gene expression was analysed and as previously shown (**Figure 6.2.1 Biii**), both thapsigargin and FG treatment enhanced gene expression. Interestingly, co-treatment of cultures with salubrinal did not attenuate the observed increase in expression (**Figure 6.3.1 A & Bi**).

As previously shown (**Figure 6.2.1 Bii**), thapsigargin treatment for 24 hours could not induce significant TNFα expression (**Figure 6.3.1 A & Bii**). However, FG treatment of the cultures for 24 hours induced significant TNFα expression that was attenuated if cultures had been treated with salubrinal (**Figure 6.3.1 A & Bii**). These data suggest that ER stress occurs prior to any significant induction of TNFα expression.

Induction of caspase-3 cleavage after FG, FN or thapsigargin treatment for 24 hours was then quantified from ICC experiments. Thapsigargin induced significant caspase-3 cleavage, which correlated to a significant increase in cell death characterised by apoptotic morphology (**Figure 6.3.2. A & B**). FN treatment also induced significant caspase-3 cleavage in parallel with a significant increase in cell death. In support of previous studies with rat microglia (**Section 3.2.3**), FG treatment significantly increased caspase-3 cleavage in the hMΦ cultures without a significant increase in cell death (**Figure 6.3.2 A & B**), suggesting caspase-3 involvement macrophage activation (Burguillos et al. 2011). Furthermore, this non-apoptotic cleavage of caspase-3 could be completely attenuated if cultures were co-treated with salubrinal (**Figure 6.3.2 A & B**), further suggesting ER stress as an initial mechanism in hMΦ activation.

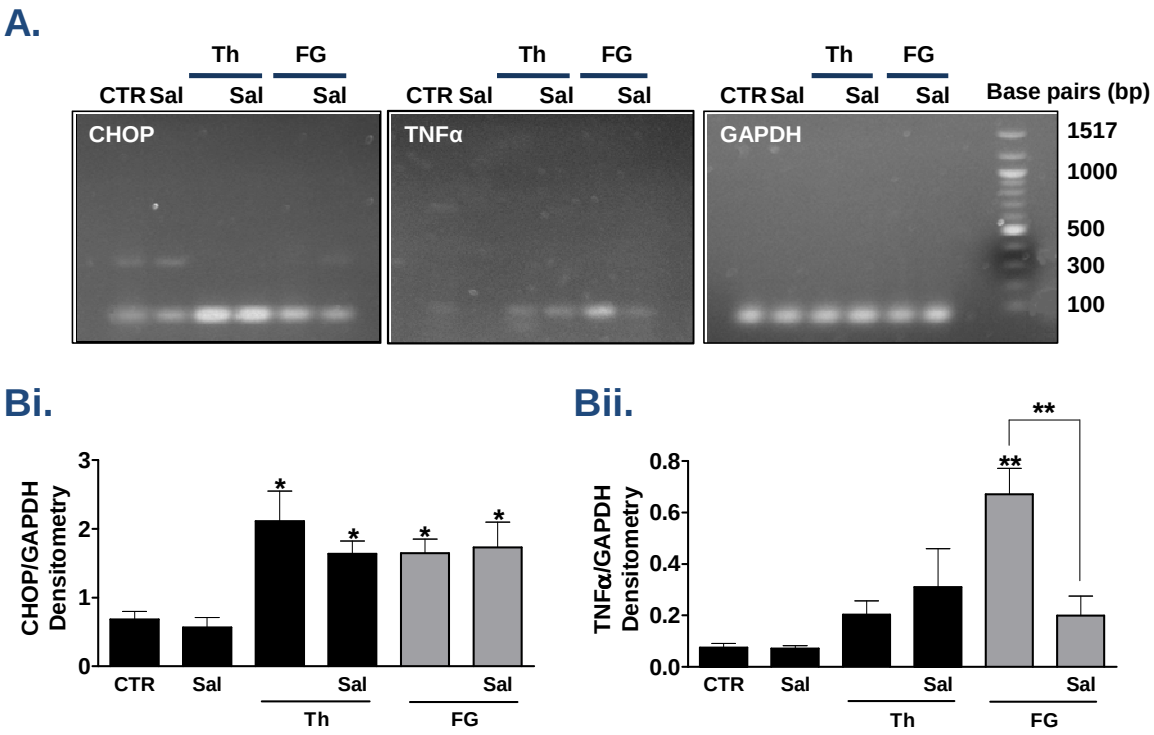

Figure 6.3.1. FG-mediated TNFα gene expression in hMΦ can be attenuated by inhibition of ER stress

A. Representative PCR blots for CHOP (95 bp), TNFα (123 bp) and GAPDH (66 bp) gene expression after Thapsigargin (Th; 2 µM) or FG (2.5 mg/ml) treatment for 24 hours, alone or in combination with salubrinal (Sal; 100 nM). Quantification of CHOP (**Bi**) and TNFα (**Bii**) gene expression in hMΦ cultures with respect to gene expression of GAPDH. Quantified data were analysed from 3 independent experiments. To compare between control levels and multiple treatments, one way ANOVA were performed with Dunnett's post-test. Paired two-tailed Student's *t*-tests were performed to compare specific treatments. Levels of significance were: non-significant p>0.05, * p<0.05, ** p<0.01.

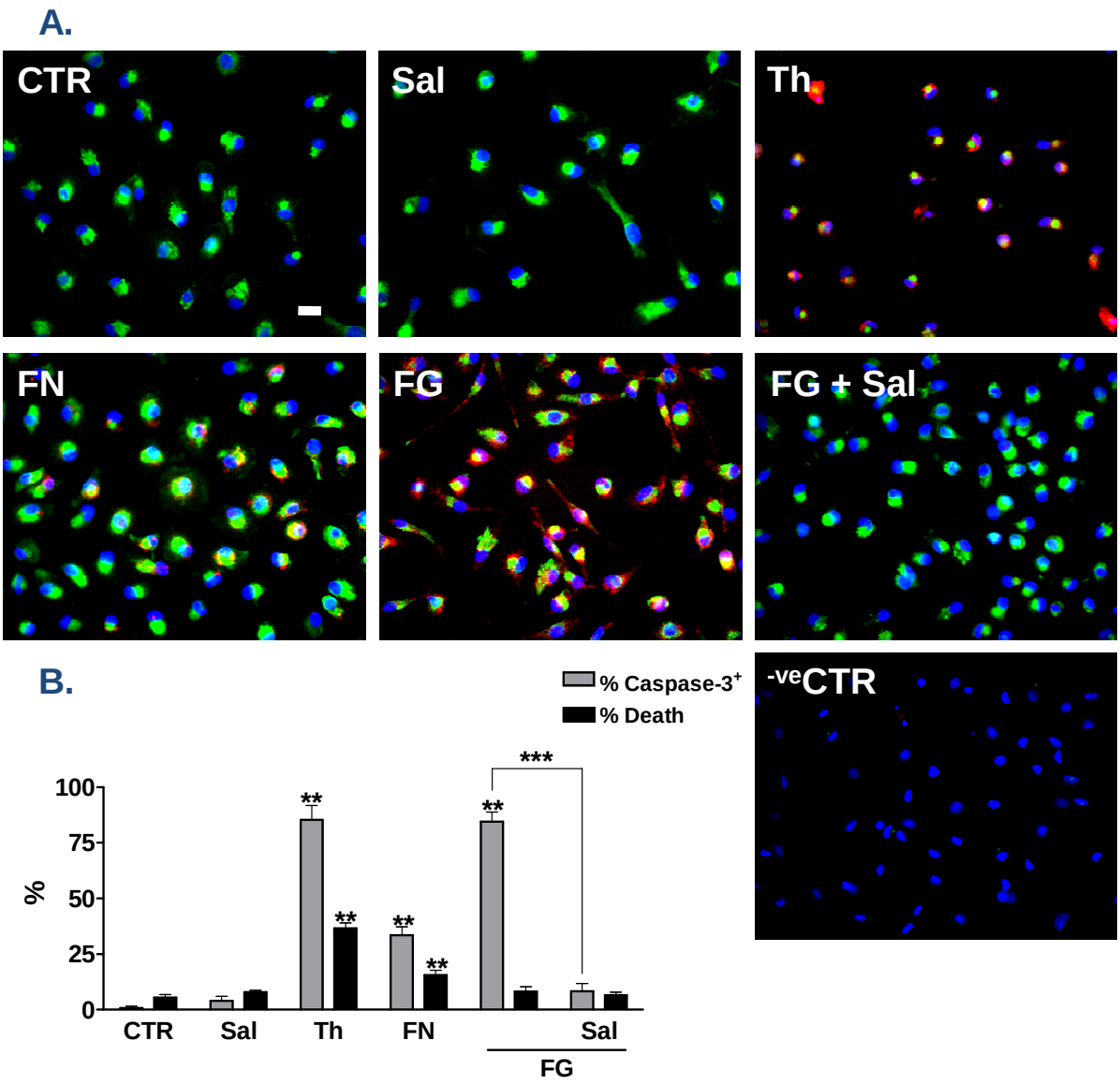

Figure 6.3.2. FN and FG induce caspase-3 cleavage in hMΦ with inhibition of ER stress attenuating the FG-mediated cleavage

A. Representative images of hMΦ cultures after 24 hours of treatment with Sal (100 nM), Th (2 µM), FN (1 mg/ml), FG (2.5 mg/ml) or FG + Sal. Cultures were stained with DAPI for quantification of cell number and probed with anti-CD68 (green) for identification of hMΦ and anti-cleaved caspase-3 (red), except in negative control cultures, where primary antibodies were omitted. Original magnification: x40, scale bar: 20 µm. **B.** Quantification of cleaved caspase-3-positive hMΦ (grey bars) and death in the hMΦ population (quantified by apoptotic morphology; black bars) after administration of treatments outlined in **A**. Data are presented as percentages of total hMΦ number. Treatments were in duplicate in each experiment and data were analysed from 3 independent experiments. To compare % cleaved caspase-3 cells or % death in multiple treatment groups to control levels one way ANOVA were performed with Dunnett's post-test. Direct comparison of specific treatments was analysed using paired two-tailed Student's *t*-tests. Levels of significance were: non-significant $p>0.05$, ** $p<0.01$, *** $p<0.001$.

6.4. Discussion

This final results chapter focuses on preliminary data from translational experiments performed to identify whether the novel rat microglial data reported in previous chapters in this thesis could be replicated in a human cell culture model. The majority of markers utilised in the hMΦ culture model correlated with previously presented rat data suggesting robust and evolutionarily conserved signalling pathways are involved in FG-mediated activation of phagocytes.

6.4.1. Human macrophage responses generally mimic those of rat microglia

The only marker tested that did not correlate to the rat data was the expression of iNOS, which was previously shown in similar serum-free conditions to be significantly enhanced by FG, FN, and LPS treatment (**Section 3.2.2**). Furthermore, potent co-treatment of hMΦ with LPS and IFNγ could not significantly enhance iNOS expression. Although studies have been published suggesting iNOS-mediated NO production does occur in human microglia and macrophages (Colasanti et al. 1995; Ding et al. 1997), data presented here are in support of the vast majority of studies published that have suggested human macrophage and microglial activation is independent of significant iNOS expression and NO release (Peterson et al. 1994; Denis 1994; Colton et al. 2000; Carter & Dick 2003). Furthermore, murine macrophages produce the large amounts of NO and L-citrulline from L-arginine via iNOS catalysis due to their capability of synthesising the obligatory cofactor tetrahydrobiopterin (BH4), essential for the stabilization and function of iNOS. However, human macrophages along with a number of other species are not able to synthesise BH4 and therefore have limited NOS activity (Schneemann & Schoeden 2007).

A significant conclusion from the primary rat culture data presented here was that inhibition of iNOS activity with AMT-HCl failed to attenuate FG- or FN-mediated responses including caspase activation and subsequent neuronal death. These observations correlate with the lack of involvement of iNOS in the hMΦ signalling after

treatment, further supporting the idea that there is little or no involvement of this enzymatic pathway in the execution of FG and FN toxicity cascades. Interestingly, some researchers even suggest that the lack of this high output iNOS-mediated NO release may actually exacerbate human disorders (Colton et al. 2000).

The expression of TNFα after FG and FN treatment in the hMΦ cultures correlated with the rat data suggesting significant expression and release after treatment. These data are in line with previous studies suggesting LPS and IFNγ can induce TNFα release from human retinal microglia independent of iNOS activity (Carter & Dick 2003) and LPS treatment of human macrophages downregulates CD4, a protein with a role in immune function, via an endogenous TNFα-dependent mechanism (Herbein et al. 1995). Limited research has been performed on the identification of FG-mediated TNFα from human macrophages. One paper does identify a significant induction of TNFα and IL-6 from human peripheral blood mononuclear cells (PBMCs) (Jensen et al. 2007), the pre-cursors to the hMΦ used here, with earlier studies using the same cells (PBMCs) identifying a significant induction of IL-1β after culturing with FG gels (Perez & Roman 1995). A significant induction of IL-6 release from human macrophages has been identified after exposure to FG via a TLR4-dependent mechanism and when FG was administered to a HEK293-CD14-MD2 cell line that expresses TLR4 significant induction of TNFα was also observed (Hodgkinson et al. 2008). The lack of thapsigargin-induced TNFα gene expression is at odds with the BV2-microlgial data that showed a significant increase in protein expression after treatment (**Figure 4.4.6**). However, an increase was certainly observed and a review of the raw data shows one assay significantly skewed the analysis suggesting further repetitions could provide statistical significance.

Significant CHOP gene expression was observed after treatment of hMΦ with thapsigargin, FG, LPS, and LPS and IFNγ, but not FN. These data were again broadly in line with the rat primary microglial data. However, rat data showed FN treatment of

primary microglia could induce a significant increase in CHOP protein expression (**Figure 4.2.10**) suggesting discrepancies between the two models with respect to FN-induced pathways. Further time-dependent studies must be undertaken however, as FN treatment induced significant toxicity in rat primary microglia after 24 hours, the same incubation period used in these hMΦ experiments, suggesting CHOP expression levels may be significantly induced at earlier time-points.

Interestingly, although a significant induction of CHOP gene expression was observed after FG treatment of hMΦ, no significant increase in death was observed. Previous studies have shown LPS treatment can induce non-apoptotic CHOP gene expression in a macrophage cell line (Nakayama et al. 2010), whereas recent protein expression studies suggest that LPS treatment of macrophages decreases CHOP protein levels (Woo et al. 2009; Martinon et al. 2010), a mechanism that may induce a significant increase in CHOP gene expression. However, further studies are required to unravel this complicated mechanism, again with timecourse analyses potentially providing clearer data.

6.4.2. ER stress pathways are mobilised in hMΦ in response to fibrinogen – regulation of cellular activation

The rest of the chapter focused on ER stress pathways in hMΦ cultures after FG treatment in particular. Live cell staining studies supported an induction of ER stress pathways after FG treatment with significant enhancement of caspase-12 cleavage being observed, with limited cell death. Furthermore, in support of ER stress-associated caspase-12 cleavage, an intensely debated topic in human disease progression, pre-treatment of hMΦ cultures with salubrinal, an inhibitor of the PERK-eIF2α-ATF4 axis of ER stress completely attenuated FG-mediated caspase-12 cleavage. These data support caspase-12 association with ER stress in humans (Hetz et al. 2003; Mandic et al. 2003; Lee et al. 2010) and further support the notion that FG can induce ER stress in phagocytes. Interestingly, thapsigargin-mediated caspase-12

cleavage could not be significantly attenuated by salubrinal pre-treatment even though a significant attenuation of cell death was observed. Furthermore, thapsigargin- and FG-mediated CHOP gene expression could not be attenuated by salubrinal pre-treatment. These data follow a similar pattern to recently published work suggesting salubrinal can significantly attenuate ER stress-mediated apoptosis but does not down-regulate pro-apoptotic factors, including CHOP, associated with ER stress after induction by thapsigargin (Kitamura et al. 2011).

In my view the most interesting data in this chapter identifies a potential role for ER stress in the regulation of macrophage activation. As previously described, FG treatment of the hMΦ cultures induced significant TNFα gene expression. However, expression could be attenuated if cultures were pre-treated with salubrinal. Furthermore, FG treatment could induce significant caspase-3 cleavage in the hMΦ, independent of apoptosis at the time-point tested, which could also be attenuated by pre-treatment of the cultures with salubrinal. Taken together with the assumption that the non-apoptotic caspase-3 cleavage observed was associated with activation as previously described (Burguillos et al. 2011; Venero et al. 2011), these data suggest that FG association with hMΦ induces ER stress-dependent pathways that in turn regulate activation via the release of TNFα. Recent elegant studies have suggested that TLR signalling specifically activates the ER stress sensor kinase IRE1α and the downstream transcription factor, XBP1 which is required for optimal production of pro-inflammatory cytokines including TNFα in macrophages (Martinon et al. 2010). These data support the hypothesis that the UPR has prominent roles in regulating cellular homeostasis as well as its classical role in protein quality control (Rutkowski & Hegde 2010).

6.4.3. Conclusions

Continuing research to couple ER stress pathways to macrophage and microglial activation cascades in general would potentially provide mechanisms that could be

manipulated for therapeutic benefit. Furthermore, complete elucidation of FG-mediated interaction with macrophages and microglia is likely to accelerate our understanding of how this protein is inducing the observed responses.

The data presented in this chapter, although preliminary, provide novel signalling pathways with respect to FG that require further elucidation. What is also promising is the relative consistency of the data produced in these hMΦ cultures with respect to the primary rat microglial data and further characterisation of the hMΦ cultures coupled with the use of human microglial cell lines and human tissue samples as well as the rapid development of pluripotent stem cell technology, could render rodent cultures obsolete.

7. Final Discussion

Blood brain barrier dysfunction leads to extravasation of fibrinogen into the CNS parenchyma followed by enhanced inflammation and cognitive decline in animal models of neurodegenerative diseases (Paul et al. 2007; Cortes-Canteli & Strickland 2009; Cortes-Canteli et al. 2010), as well as being a hallmark of human AD pathology (Fiala et al. 2007; Ryu & McLarnon 2009). In addition to exacerbating Aβ load in animal models of AD, fibrinogen has been shown to bind to microglia inducing a phagocytic phenotype with significant involvement in EAE disease progression (Adams et al. 2007a; Cortes-Canteli et al. 2010). Research into microglial involvement in neurodegeneration suggests these cells are intrinsically coupled to disease progression through chronic inflammation leading to an acceleration of degeneration in a self-perpetuating loop (Block et al. 2007; Glass et al. 2010). This thesis aimed to further elucidate the signalling capabilities of fibrinogen, and the cleavage product fibrin, through microglia.

The first aim of the study was to characterise microglial responses to FG and FN and how these responses manifested with respect to neuronal integrity and viability. It was hypothesised that FG and FN would induce inflammation and toxicity in microglial cultures due to previous observations in the laboratory (E. East, I. Sevastou, and J.M. Pocock, unpublished observations). Although both treatments induced significant responses associated with inflammation, only treatment with FN induced significant morphological changes that were associated with toxicity at the time points tested. In neuronal cultures, it was initially shown that direct FG treatment induced neurotoxicity after 48 hours of exposure. However, PCR analysis coupled with pharmacological manipulation of thrombin suggested that intra-culture conversion of FG to FN was responsible for the direct neurotoxicity at this time-point.

Interestingly, the identification of caspase-3 cleavage in microglial cultures after FG treatment initially suggested apoptosis. However, a non-significant increase in

apoptotic nuclear morphology was observed and recent studies have identified non-apoptotic cleavage of caspase-8, -3 and -7 is involved in microglial activation rather than apoptosis, with RNAi studies that targeted the implicated caspases causing a down-regulation of microglial-mediated inflammatory responses after TLR signalling (Burguillos et al. 2011; Venero et al. 2011). Data presented here suggest that FG-mediated microglial activation also involved non-apoptotic cleavage of caspases which therefore potentially suggests involvement of TLR signalling. Previous studies in our laboratory has suggested that blockage of TLR4 actually enhances FG-mediated iNOS expression in microglia (I. Sevastou & J.M. Pocock, unpublished observations). Furthermore published literature has suggested that fibrinogen can bind to TLR4 on macrophages and a HEK293 cell line inducing significant induction of pro-inflammatory cytokines (Hodgkinson et al. 2008). These data coupled with observations here suggesting FG does not induce pro-inflammatory cytokine release through CD11b suggests further investigation into the FG-TLR4-proinflammatory cytokine release pathway could yield some interesting and potentially useful results.

Comparison of FG- and FN-induced inflammatory responses to those of LPS suggested FN induced a similar response potentially via a similar pathway. However, published literature has identified LPS (endotoxin) contamination in other blood borne protein preparations stating that only 40 pg/ml of LPS (endotoxin) is required to induce microglial activation (Weinstein et al. 2008). It was therefore suggested that contamination of FN may be responsible for the observed activation. However, studies here using the endotoxin inhibitor PMX strongly suggested that the FG- and FN-mediated responses were not due to endotoxin contamination. Furthermore, co-treatment of FG- and FN-treated cultures with LPS supported the hypothesis that differential pathways were initiated by the blood borne proteins when compared with LPS induction. Other contaminants, however, cannot be ruled out.

One of the most interesting initial observations was that the serum composition of the culture medium could be used to manipulate FG-mediated responses. In serum-free conditions FG could induce iNOS expression and significantly greater cytokine release when compared with serum-containing conditions. These observations suggest serum components can down-regulate the FG-mediated inflammatory response, which in physiological conditions could prevent acute dyshomeostasis by desensitising the signalling capacity of FG. However data here suggests that chronic extravasation of FG into the CNS parenchyma that leads to saturation of degradation pathways, coupled with chronic inflammation and the subsequent release of toxic factors, including cytokines, can overcome this serum-associated protective mechanism.

The development and optimisation of a microglial-depletion technique for use on neuronal cultures provided a cell culture system in which modelling of microglial responses in an enriched neuronal culture could be performed. Using this technique it was possible to support the idea that LPS-mediated inflammatory responses and subsequent neurotoxicity occurs through microglia and not through astrocytes, *in vitro* (Lee et al. 1993). Furthermore, the FG-mediated neurotoxicity observed after only 24 hours *in vitro*, which was initially assumed to be a direct interaction, was shown to depend on microglia. It also enabled the identification of an acute neuroprotective mechanism afforded by microglia with respect to FN exposure. Microglia in the CGC cultures were also shown to respond differentially to FG or FN exposure shown by the analysis of ED-1 expression, which suggested that FG can induce a bi-phasic expression of ED-1, the marker of microglial activation, whereas FN induces prolonged expression with an early plateau followed by a late decline, correlating to neuronal death. These data support a role for microglia in FG- and FN-mediated responses in the neuronal cultures with the bi-phasic expression observed after FG treatment correlating to the immobilisation and conversion of FG to FN, in culture.

Modelling microglial responses within the CGC cultures provided a more physiological environment. However, the use of microglial conditioned medium treatment of microglial-depleted neuronal cultures also allowed us to identify the importance of soluble secreted factors, in particular TNFα (Taylor et al. 2005), in subsequent neurotoxicity, supporting the use of differing models in the investigation of microglial-mediated responses. The investigations here were performed in an attempt to characterise microglial- and neuronal-associated responses after exposure to FG or FN, *in vitro*, and how these responses were coupled. However, it is possible that other cells including astrocytes, which have been associated with FG signalling (Schachtrup et al. 2010), could be involved in the regulation of the observed responses and further investigations into the specific roles of other cell types should be performed.

Broadly speaking this initial characterisation of FG- and FN-mediated responses suggests indirect (microglial) FN-mediated neurotoxicity is predominantly due to microglial death whereas indirect FG-mediated neurotoxicity is due to pro-inflammatory activation of microglia.

The second section of this thesis describes the involvement of ER stress in FG- and FN-mediated neurotoxicity. ER stress is increasingly recognised as an integral part of the pathophysiology of many neurodegenerative diseases (Hetz et al. 2003; Lindholm et al. 2006; Unterberger et al. 2006; Mháille et al. 2008; Zhang & Kaufman 2008; Kim et al. 2008; Salminen et al. 2009). Research on atherosclerosis suggests an association between fibrinogen, a prominent feature of proliferative atherosclerotic lesions (Bini et al. 1989; Smith et al. 1992), and macrophage-specific ER stress (Tabas et al. 2009; Hotamisligil 2010a; Hotamisligil 2010b). The connections between FG, phagocytic cells and ER stress, and the mounting evidence for ER stress induction in neurodegeneration suggested that investigations into whether FG- or FN-mediated microglial activation and subsequent neurotoxicity involved ER stress could provide interesting findings.

Induction of ER stress, identified by caspase-12 and CHOP expression, was observed in microglia and neurons, preferentially after treatment with FG, particularly in the case of caspase-12 activation. Furthermore, a dependence on microglia with respect to FG-mediated caspase-12 expression in neurons was observed, which was not surprising considering the earlier data suggesting microglial-dependent induction of neurotoxicity by FG. Inhibition of TNFα synthesis could downregulate the FG-mediated caspase-12 and CHOP expression in the CGC and microglial cultures. Conversely, inhibition of ER stress downregulated FG-mediated TNFα release from microglial cultures. These data support previous work linking autocrine TNFα signalling to ER stress pathways (Hu et al. 2006; Martinon et al. 2010). Coupled to this observed ER stress-mediated regulation of TNFα signalling are further observations here that suggest FG-mediated 'non-apoptotic' caspase-3/7 activation in microglia can be attenuated by salubrinal treatment. Taken together, with the assumption that the non-apoptotic caspase-3/7 cleavage is associated with microglial activation (Burguillos et al. 2011; Venero et al. 2011), these data could provide an additional upstream factor in this still novel signalling cascade.

It was decided that calpain activity after treatment with FG would be investigated due to the suggestion that m-calpain may be responsible for procaspase-12 cleavage to the active form and that disturbances in intracellular calcium may induce neuronal apoptosis through calpain-mediated caspase-12 activation (Nakagawa & Yuan 2000). The assay was developed and optimised using a similar methodology to that performed by D'Amelio et al (2010) for the identification of caspase activity. Interestingly, FG-mediated calpain activity was attenuated by iNOS activity inhibition. This modulation of the early FG-mediated induction of calpain activity by iNOS suggests expression may occur prior to the incubation period previously tested (i.e. < 24 hours). A timecourse analysis of FG-mediated iNOS expression was subsequently attempted using lysates from serum-containing BV2-microglia but no significant expression was observed at any timepoint. These data suggest a potential non-specific role for AMT-HCl in the

regulation of calpain activity or via inhibition of fluorescence however, further studies are required. Finally, pharmacological inhibition of calpain activity in microglia prevented FG-mediated neurotoxicity. Furthermore, inhibition of calpain activity in the neuronal cultures (depleted of microglia) also afforded protection from FG-mediated neurotoxicity (via MGCM), suggesting prominent calcium dyshomeostasis also occurs in the neurons after induction of intracellular signalling cascades by inflammatory factors released from microglia. Together, these data suggest interesting additions to the FG-mediated activation of microglia including possible calcium signalling that leads to calpain-mediated ER stress which in turn regulates TNFα release leading to the loss of neuronal integrity (**Figure 7.1.1**).

In the past our laboratory has identified neurotoxic and neuroprotective roles for metabotropic glutamate receptors, dependent on the activation or inhibition of receptors in specific groups (Taylor et al. 2002; Taylor et al. 2003; Taylor et al. 2005; Pinteaux-Jones et al. 2008). However, little research has been performed on the role of the group I receptors in mediating neuroprotection or toxicity. Other laboratories have identified group I mGluR5 activation as a neuroprotective mechanism in culture models of microglial-mediated inflammation (Byrnes et al. 2009a; Loane et al. 2009), glutamate excitotoxicity (Montoliu et al. 1997), and Aβ-mediated neurotoxicity (Movsesyan et al. 2004), as well as *in vivo* spinal cord injury studies (Byrnes et al. 2009b). The third section of my thesis relates to studies performed to identify if the FG- and FN-mediated neurotoxicity could be attenuated by specific mGluR activation.

The majority of repeated studies here supported the previous work, in particular the observation that activation of all group II mGluRs induced significant microglial death as well as enhanced neuronal toxicity, but sole activation of group II mGluR3 was protective (Taylor et al. 2005). As previously discussed, FG-mediated iNOS expression could be induced if cultures were treated in serum-free conditions. Therefore, this manipulation of culture conditions was used to identify whether activation of mGluRs

could modulate the iNOS and ED-1 expression induced by FG in serum-free conditions. In contrast to previously published findings (Byrnes et al. 2009a; Loane et al. 2009), mGluR5 activation did not downregulate LPS-mediated microglial activation. However, this may be due to the mechanism of action of CDPPB, used here, which is a positive allosteric modulator of mGluR5 rather than a classic orthosteric agonist such as (*RS*)-2-chloro-5-hydroxyphenylglycine (CHPG), used in the cited studies (Byrnes et al. 2009a; Loane et al. 2009), although significant down-regulation was observed with DHPG, a group I orthosteric agonist.

As well as identifying possible neuroprotection from FG- and FN-mediated toxicity via activation of mGluR3, it was shown that FG-mediated neurotoxicity could be attenuated by positive allosteric modulation of mGluR5. Furthermore, unlike orthosteric binding sites which are often highly conserved across members of a single GPCR subfamily, making it difficult to achieve high selectivity for specific GPCR subtypes, allosteric binding sites (through which CDPPB acts) are highly specific for receptor subtypes meaning the ligands require greater selectivity and provide novel modes of efficacy (Conn et al. 2009). These ligand-receptor characteristics make these compounds very attractive from a pharmaceutical point of view.

What is also interesting with respect to these data is that specific positive allosteric modulation of microglial mGluR5 attenuated FG-mediated toxicity, suggesting that if it were possible to target only microglial mGluR5 sufficient neuroprotection may be afforded. This kind of cell-specific targeting would also decrease any non-specific effects of chronic mGluR5 activation on neurons and other cell types. Finally, data presented here provides support for previous studies that suggest microglia express mGluR5 but not mGluR1 of the group I receptors (Biber et al. 1999).

Translation of animal data to human models is, in many cases, an enormous hurdle. Due to contrasting data from genetic and system based studies, identification of whether certain characteristics of FG- and FN-mediated rat microglial activation could

be translated to a human phagocyte model in the form of monocyte-derived macrophages was performed. As previously described, caspase-12-associated ER stress is a controversial mechanism in humans due to acquired mutations in the caspase-12 gene (Fischer et al. 2002). However, active caspases generally undergo post-translational modification (Earnshaw et al. 1999) and studies have shown caspase-12 mediated ER stress in human models (Hetz et al. 2003), suggesting functionality can occur (Hetz et al. 2003; Lee et al. 2010). Here, data suggests that caspase-12 activation is associated with ER stress in human macrophages. Furthermore, FG can induce TNFα expression and caspase-3 cleavage, which is shown to be regulated by ER stress, correlating with to the previously presented rat microglia data. Researching ER stress mechanisms *in vitro* has received critism due to culture systems, upon stress induction, inducing the full UPR repertoire (Saxena & Caroni 2011), which is not seen *in vivo*. However, this more extensive UPR induction *in vitro* has been suggested as another function of the UPR involved in regulating basal cellular homeostasis, independent of the classic induction via protein mis-folding (Rutkowski & Hegde 2010). This is supported by recent studies that identified an ER stress associated transcription factor was regulating TLR signalling, with genetic ablation attenuating LPS-mediated cytokine expression in macrophages (Woo et al. 2009; Martinon et al. 2010).

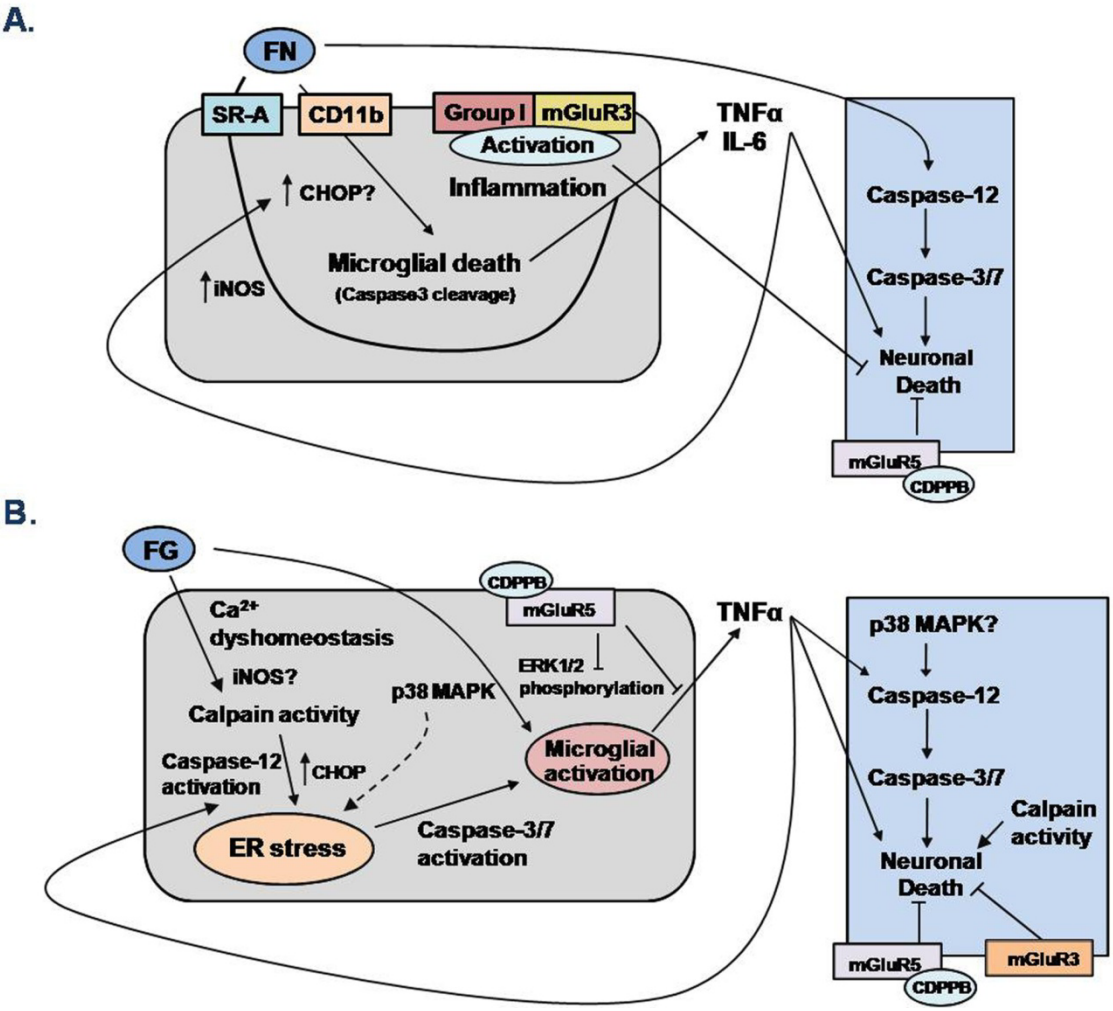

Figure 7.1.1. Summary of results

A. Overview of the proposed mechanism by which FN deposits induce the observed detrimental effects. FN can induce microglial death leading to an increase in inflammation through an increase in iNOS activity and the release of TNFα and IL-6, which in turn may mediate the observed neuronal death. These effects may be mediated through CD11b and scavenger receptor-A ligation. Activation of microglial group I mGluRs and mGluR3 but also neuronal positive allosteric modulation of mGluR5 can mediate neuroprotection. FN also induces direct neurotoxicity in the absence of microglia.

B. Overview of the proposed mechanisms by which soluble FG mediates the observed microglial activation and subsequent neurotoxicity. FG induced significant calpain activation upstream of ER stress pathway activation, identified via caspase-12 and CHOP induction, which in turn was found to be upstream of non-apoptotic microglial caspase-3/7 activation and subsequent TNFα release leading to neuronal death, with some dependence on MAPK pathway activation. Positive allosteric modulation of microglial mGluR5, but also neuronal mGluR5 and orthosteric agonism of mGluR3 could mediate neuroprotection. Question marks are associated with specific areas of the pathways that gave conflicting data or that would require much greater in depth investigation before concluding significant involvement.

7.1. Future work

The observations made here that FG-mediated induction of an activated microglial phenotype with regulation from ER stress are novel and require further characterisation. Listed below are future studies that would enable greater understanding of the pathways induced in microglia after FG treatment:

- Extensive calcium imaging to identify the role of this signalling molecule in both FG-mediated microglial activation and the subsequent loss of neuronal integrity
- Microarray studies on primary rat microglia and human macrophage cultures after fibrinogen treatment to allow full correlation analysis between the culture models with the added benefit of potentially uncovering further intrinsic members of the activation signalling cascades
- Initial elucidation of the mechanisms by which soluble fibrinogen interacts with microglia, i.e. with respect to the induced cytokine release, does fibrinogen signal through the TLRs?
- Studies focussing on the role of mitochondria in the observed signalling pathways
- Development and optimisation of RNAi studies to enable functional knockdown of proteins of interest in microglia without the use of pharmacology and all its non-specific effects
- Further characterisation of the hMΦ preparation including studies to identify transcription regulators and the relevant extrinsic support factors that could potentially allow greater refinement of the culture to further mimic human microglia. This could lead to studies comparing healthy human ‘microglia’ to diseased ‘microglia’, using simple phlebotomy allowing characterisation of microglia at all stages of disease rather than just end-stage, with respect to post-mortem cultures.

- Following on from the last point, research published on the conversion of human fibroblasts or somatic cells back to pluripotent stem cells that could be differentiated (Takahashi et al. 2007; Yu et al. 2007), suggests that upon acquiring the relevant transcription regulator and extrinsic support factor knowledge it could be possible to induce microglia from healthy as well as diseased individuals for comprehensive signalling analysis.

7.2. Conclusions

In conclusion, this thesis has provided, for the first time, characterisation of soluble fibrinogen-mediated microglial activation, a mechanism with potentially important consequences. Specifically it is shown here that FG- and FN-mediated toxicity is independent of iNOS activity, an important point with respect to the translation of these data to human studies. Identification of non-apoptotic caspase cleavage is also a novel mechanism, which was subsequently reported earlier this year (Burguillos et al. 2011; Venero et al. 2011). However, FG induction of non-apoptotic caspase activation is described here for the first time. The development of a microglial depletion technique for use on the CGC cultures allowed us to perform more physiologically relevant studies and enabled us to show the significant potency of a small population of microglia with respect to mediated neurotoxicity. ER stress mechanisms have also been identified and coupled to the FG-mediated activation of microglia, as well as suggestions that this stress pathway is also induced in neurons possibly after calcium dyshomeostasis due to non-cell autonomous factors. Furthermore, regulation of FG-mediated cytokine expression and release has been afforded to ER stress induction in rat microglia which was translated in hMΦ studies. Finally data presented here shows for the first time that specific positive allosteric modulation of the mGluR5 receptor can protect neurons from microglial-dependent FG-mediated toxicity.

It is understood that basic neuroscience does not directly or immediately offer therapeutic benefit to suffers of neurodegenerative disease however, it is hoped that

further elucidation of pathways such as those described in this thesis will lead to a greater understanding of neurodegenerative disease pathogenesis which in turn could lead to more effective and efficacious treatments for patients suffering from an array of diseases that encompass common pathological events.

8. References

Abbott, N.J., Rönnbäck, L. & Hansson, E., 2006. Astrocyte-endothelial interactions at the blood-brain barrier. *Nature Reviews. Neuroscience*, 7(1), pp.41-53.

Abbott, N.J. et al., 2010. Structure and function of the blood-brain-barrier. *Neurobiology of Disease*, 37(1), pp.13-25.

Abram, C.L. & Lowell, C.A., 2009. The ins and outs of leukocyte integrin signaling. *Annual Review of Immunology*, 27, pp.339-362.

Adams, R.A. et al., 2004. Fibrin mechanisms and functions in nervous system pathology. *Molecular Interventions*, 4(3), pp.163-76.

Adams, R.A. et al., 2007a. The fibrin-derived gamma377-395 peptide inhibits microglia activation and suppresses relapsing paralysis in central nervous system autoimmune disease. *The Journal of Experimental Medicine*, 204(3), pp.571-82.

Adams, R.A. et al., 2007b. Fibrinogen signal transduction as a mediator and therapeutic target in inflammation: lessons from multiple sclerosis. *Current Medicinal Chemistry*, 14(27), pp.2925-36.

Agnati, L F et al., 1995. Intercellular communication in the brain: wiring versus volume transmission. *Neuroscience*, 69(3), pp.711-726.

Akassoglou, K et al., 2000. Tissue plasminogen activator-mediated fibrinolysis protects against axonal degeneration and demyelination after sciatic nerve injury. *The Journal of Cell Biology*, 149(5), pp.1157-1166.

Akassoglou, K. & Strickland, S, 2002. Nervous system pathology: the fibrin perspective. *Biological Chemistry*, 383(1), pp.37-45.

Akassoglou, K. et al., 2002. Fibrin Inhibits Peripheral Nerve Remyelination by Regulating Schwann Cell Differentiation. *Neuron*, 33(6), pp.861-875.

Akassoglou, K. et al., 2004. Fibrin depletion decreases inflammation and delays the onset of demyelination in a tumor necrosis factor transgenic mouse model for multiple sclerosis. *Proceedings of the National Academy of Sciences of the United States of America*, 101(17), pp.6698-703.

Akiyama, H. & McGeer, P.L., 1990. Brain microglia constitutively express beta-2 integrins. *Journal of Neuroimmunology*, 30(1), pp.81-93.

Akiyama, H. et al., 2000. Inflammation and Alzheimer's disease. *Neurobiology of Aging*, 21(3), pp.383-421. Alafuzoff, I. et al., 1987. Blood-brain barrier in Alzheimer dementia and in non-demented elderly. An immunocytochemical study. *Acta Neuropathologica*, 73(2), pp.160-166.

Alberts, B. et al., 2008. *Molecular Biology of the Cell* 5th ed., Garland Science.

Albright, A.V. & González-Scarano, F., 2004. Microarray analysis of activated mixed glial (microglia) and monocyte-derived macrophage gene expression. *Journal of Neuroimmunology*, 157(1-2), pp.27-38.

Alexander, G.M. & Godwin, D.W., 2006. Metabotropic glutamate receptors as a strategic target for the treatment of epilepsy. *Epilepsy Research*, 71(1), pp.1-22.

Allen, J.W., Knoblach, S.M. & Faden, A.I., 2000. Activation of group I metabotropic glutamate receptors reduces neuronal apoptosis but increases necrotic cell death in vitro. *Cell Death and Differentiation*, 7(5), pp.470-476.

Alzheimer, A. et al., 1995. An English translation of Alzheimer's 1907 paper, "Uber eine eigenartige Erkankung der Hirnrinde." *Clinical Anatomy (New York, N.Y.)*, 8(6), pp.429-431.

Arai, T. et al., 2006. Thrombin and prothrombin are expressed by neurons and glial cells and accumulate in neurofibrillary tangles in Alzheimer disease brain. *Journal of Neuropathology and Experimental Neurology*, 65(1), pp.19-25.

Atkin, J.D. et al., 2006. Induction of the unfolded protein response in familial amyotrophic lateral sclerosis and association of protein-disulfide isomerase with superoxide dismutase 1. *The Journal of Biological Chemistry*, 281(40), pp.30152-30165.

Banati, R.B., 2002. Visualising microglial activation in vivo. *Glia*, 40(2), pp.206-217.

Barres, B., 2008. The Mystery and Magic of Glia: A Perspective on Their Roles in Health and Disease. *Neuron*, 60(3), pp.430-440.

Bartels, A.L., van Berckel, B.N.M., et al., 2008a. Blood-brain barrier P-glycoprotein function is not impaired in early Parkinson's disease. *Parkinsonism & Related Disorders*, 14(6), pp.505-508.

Bartels, A.L., Willemsen, A T M, et al., 2008b. Decreased blood-brain barrier P-glycoprotein function in the progression of Parkinson's disease, PSP and MSA. *Journal of Neural Transmission*, 115(7), pp.1001-1009.

Bauer, J et al., 1991. In-vitro matured human macrophages express Alzheimer's Î²A4-amyloid precursor protein indicating synthesis in microglial cells. *FEBS Letters*, 282(2), pp.335-340.

Bechmann, I. et al., 2005. Circulating monocytic cells infiltrate layers of anterograde axonal degeneration where they transform into microglia. *The FASEB Journal: Official Publication of the Federation of American Societies for Experimental Biology*, 19(6), pp.647-649.

Bechmann, I., Galea, I. & Perry, V.H., 2007. What is the blood-brain barrier (not)? *Trends in Immunology*, 28(1), pp.5-11.

Beers, D.R. et al., 2006. Wild-type microglia extend survival in PU.1 knockout mice with familial amyotrophic lateral sclerosis. *Proceedings of the National Academy of Sciences of the United States of America*, 103(43), pp.16021-16026.

Bell, R.D. & Zlokovic, B.V., 2009. Neurovascular mechanisms and blood-brain barrier disorder in Alzheimer's disease. *Acta Neuropathologica*, 118(1), pp.103-113.

Benimetskaya, L. et al., 1997. Mac-1 (CD11b/CD18) is an oligodeoxynucleotide-binding protein. *Nature Medicine*, 3(4), pp.414-420.

Benn, S.C. & Woolf, C.J., 2004. Adult neuron survival strategies [mdash] slamming on the brakes. *Nat Rev Neurosci*, 5(9), pp.686-700.

Berezovska, O. et al., 2005. Familial Alzheimer's Disease Presenilin 1 Mutations Cause Alterations in the Conformation of Presenilin and Interactions with Amyloid Precursor Protein. *The Journal of Neuroscience*, 25(11), pp.3009 -3017.

Berger, T. et al., 1992. GABA- and glutamate-activated currents in glial cells of the mouse corpus callosum slice. *Journal of Neuroscience Research*, 31(1), pp.21-27.

Betarbet, R et al., 2000. Chronic systemic pesticide exposure reproduces features of Parkinson's disease. *Nature Neuroscience*, 3(12), pp.1301-1306.

Bhat, N.R. et al., 1998. Extracellular Signal-Regulated Kinase and p38 Subgroups of Mitogen-Activated Protein Kinases Regulate Inducible Nitric Oxide Synthase and Tumor Necrosis Factor-α Gene Expression in Endotoxin-Stimulated Primary Glial Cultures. *The Journal of Neuroscience*, 18(5), pp.1633 -1641.

Biber, K. et al., 1999. Expression and signaling of group I metabotropic glutamate receptors in astrocytes and microglia. *Journal of Neurochemistry*, 72(4), pp.1671-1680.

Bini, A. et al., 1989. Identification and distribution of fibrinogen, fibrin, and fibrin(ogen) degradation products in atherosclerosis. Use of monoclonal antibodies. *Arteriosclerosis, Thrombosis, and Vascular Biology*, 9(1), pp.109 -121.

Björkqvist, M. et al., 2008. A novel pathogenic pathway of immune activation detectable before clinical onset in Huntington's disease. *The Journal of Experimental Medicine*, 205(8), pp.1869-1877.

Blinzinger, K. & Kreutzberg, G., 1968. Displacement of synaptic terminals from regenerating motoneurons by microglial cells. *Zeitschrift Für Zellforschung Und Mikroskopische Anatomie (Vienna, Austria: 1948)*, 85(2), pp.145-157.

Block, M.L., Zecca, L. & Hong, J.-S., 2007. Microglia-mediated neurotoxicity: uncovering the molecular mechanisms. *Nature Reviews. Neuroscience*, 8(1), pp.57-69.

Boillée, S., Vande Velde, C. & Cleveland, D.W., 2006a. ALS: a disease of motor neurons and their nonneuronal neighbors. *Neuron*, 52(1), pp.39-59.

Boillée, S., Yamanaka, K., et al., 2006b. Onset and progression in inherited ALS determined by motor neurons and microglia. *Science*, 312(5778), pp.1389-1392.

Bornemann, K.D. et al., 2001. Aβ-Induced Inflammatory Processes in Microglia Cells of APP23 Transgenic Mice. *The American Journal of Pathology*, 158(1), pp.63-73.

Bouman, L. et al., 2011. Parkin is transcriptionally regulated by ATF4: evidence for an interconnection between mitochondrial stress and ER stress. *Cell Death and Differentiation*, 18(5), pp.769-782.

Boyce, M. et al., 2005. A Selective Inhibitor of eIF2α Dephosphorylation Protects Cells from ER Stress. *Science*, 307(5711), pp.935 -939.

Braak, H. et al., 2006. Stanley Fahn Lecture 2005: The staging procedure for the inclusion body pathology associated with sporadic Parkinson's disease reconsidered. *Movement Disorders*, 21(12), pp.2042-2051.

Bradford, M.M., 1976. A rapid and sensitive method for the quantitation of microgram quantities of protein utilizing the principle of protein-dye binding. *Analytical Biochemistry*, 72(1-2), pp.248-254.

Bradl, M. & Lassmann, H., 2010. Oligodendrocytes: biology and pathology. *Acta Neuropathologica*, 119(1), pp.37-53.

Brück, W, Brück, Y. & Friede, R.L., 1992. TNF-alpha suppresses CR3-mediated myelin removal by macrophages. *Journal of Neuroimmunology*, 38(1-2), pp.9-17.

Bsibsi, M. et al., 2002. Broad expression of Toll-like receptors in the human central nervous system. *Journal of Neuropathology and Experimental Neurology*, 61(11), pp.1013-21.

Burguillos, M. A. et al., 2011. Caspase signalling controls microglia activation and neurotoxicity. *Nature*, 472(7343), pp.319-324.

Byrnes, K.R., Stoica, B., Loane, D.J., et al., 2009a. Metabotropic glutamate receptor 5 activation inhibits microglial associated inflammation and neurotoxicity. *Glia*, 57(5), pp.550-560.

Byrnes, K.R., Stoica, B., Riccio, A., et al., 2009b. Activation of metabotropic glutamate receptor 5 improves recovery after spinal cord injury in rodents. *Annals of Neurology*, 66(1), pp.63-74.

Béraud, D. et al., 2011. α-Synuclein Alters Toll-Like Receptor Expression. *Frontiers in Neuroscience*, 5(80).

Carbonell, W.S. et al., 2005. Infiltrative microgliosis: activation and long-distance migration of subependymal microglia following periventricular insults. *Journal of Neuroinflammation*, 2(1), p.5.

Carter, D.A. & Dick, A.D., 2003. Lipopolysaccharide/interferon-gamma and not transforming growth factor beta inhibits retinal microglial migration from retinal explant. *The British Journal of Ophthalmology*, 87(4), pp.481-487.

Cecconi, F et al., 1998. Apaf1 (CED-4 homolog) regulates programmed cell death in mammalian development. *Cell*, 94(6), pp.727-37.

Charles, A.C. et al., 1991. Intercellular signaling in glial cells: calcium waves and oscillations in response to mechanical stimulation and glutamate. *Neuron*, 6(6), pp.983-992.

Chaudhuri, A. & Behan, P.O., 2004. Multiple sclerosis is not an autoimmune disease. *Archives of Neurology*, 61(10), pp.1610-1612.

Chen, H. et al., 2008. Peripheral inflammatory biomarkers and risk of Parkinson's disease. *American Journal of Epidemiology*, 167(1), pp.90-95.

Cheung, E.C.C. & Slack, R.S., 2004. Emerging role for ERK as a key regulator of neuronal apoptosis. *Science's STKE: Signal Transduction Knowledge Environment*, 2004(251), p.PE45.

Choi, S.-H. et al., 2003. Thrombin-induced microglial activation produces degeneration of nigral dopaminergic neurons in vivo. *The Journal of Neuroscience: The Official Journal of the Society for Neuroscience*, 23(13), pp.5877-5886.

Chomczynski, P. & Sacchi, N., 1987. Single-step method of RNA isolation by acid guanidinium thiocyanate-phenol-chloroform extraction. *Analytical Biochemistry*, 162(1), pp.156-159.

Christie, R.H., Freeman, M. & Hyman, B T, 1996. Expression of the macrophage scavenger receptor, a multifunctional lipoprotein receptor, in microglia associated with senile plaques in Alzheimer's disease. *The American Journal of Pathology*, 148(2), pp.399-403.

Chu, C.T. et al., 2004. Oxidative neuronal injury. *European journal of biochemistry / FEBS*, 271(11), pp.2060-2066.

Colasanti, M. et al., 1995. Induction of Nitric Oxide Synthase mRNA Expression. *Journal of Biological Chemistry*, 270(45), pp.26731 -26733.

Cole, G.M. & Ard, M.D., 2000. Influence of lipoproteins on microglial degradation of Alzheimer's amyloid beta-protein. *Microscopy Research and Technique*, 50(4), pp.316-324.

Colton, C.A. et al., 2000. Microglial contribution to oxidative stress in Alzheimer's disease. *Annals of the New York Academy of Sciences*, 899, pp.292-307.

Colucci-D'Amato, L., Perrone-Capano, C. & di Porzio, U., 2003. Chronic activation of ERK and neurodegenerative diseases. *BioEssays: News and Reviews in Molecular, Cellular and Developmental Biology*, 25(11), pp.1085-1095.

Combs, C K et al., 2000. Inflammatory mechanisms in Alzheimer's disease: inhibition of beta-amyloid-stimulated proinflammatory responses and neurotoxicity by PPARgamma agonists. *The Journal of Neuroscience: The Official Journal of the Society for Neuroscience*, 20(2), pp.558-567.

Combs, C. K., Karlo, J. C. et al., 2001. β-Amyloid Stimulation of Microglia and Monocytes Results in TNFα-Dependent Expression of Inducible Nitric Oxide Synthase and Neuronal Apoptosis. *The Journal of Neuroscience*, 21(4), pp.1179 -1188.

Compston, A. et al., 2005. *McAlpine's Multiple Sclerosis* 4th ed., Churchill Livingstone.

Conn, P. J. et al., 2005. Metabotropic glutamate receptors in the basal ganglia motor circuit. *Nature Reviews. Neuroscience*, 6(10), pp.787-798.

Conn, P. J., Christopoulos, A. & Lindsley, C.W., 2009. Allosteric modulators of GPCRs: a novel approach for the treatment of CNS disorders. *Nature reviews. Drug discovery*, 8(1), pp.41-54.

Contestabile, A., 2002. Cerebellar granule cells as a model to study mechanisms of neuronal apoptosis or survival in vivo and in vitro. *Cerebellum (London, England)*, 1(1), pp.41-55.

Coraci, I.S. et al., 2002. CD36, a Class B Scavenger Receptor, Is Expressed on Microglia in Alzheimer's Disease Brains and Can Mediate Production of Reactive Oxygen Species in Response to β-Amyloid Fibrils. *The American Journal of Pathology*, 160(1), pp.101-112.

Cornell-Bell, A.H. et al., 1990. Glutamate induces calcium waves in cultured astrocytes: long-range glial signaling. *Science (New York, N.Y.)*, 247(4941), pp.470-473.

Cortes-Canteli, M & Strickland, S, 2009. Fibrinogen, a possible key player in Alzheimer's disease. *Journal of Thrombosis and Haemostasis: JTH*, 7 Suppl 1, pp.146-150.

Cortes-Canteli, M. et al., 2010. Fibrinogen and beta-amyloid association alters thrombosis and fibrinolysis: a possible contributing factor to Alzheimer's disease. *Neuron*, 66(5), pp.695-709.

Cunnea, P. et al., 2011. Expression profiles of endoplasmic reticulum stress-related molecules in demyelinating lesions and multiple sclerosis. *Multiple Sclerosis (Houndmills, Basingstoke, England)*, 17(7), pp.808-818.

Cunningham, O. et al., 2009. Microglia and the urokinase plasminogen activator receptor/uPA system in innate brain inflammation. *Glia*, 57(16), pp.1802-1814.

Czapski, G.A. et al., 2007. Role of nitric oxide in the brain during lipopolysaccharide-evoked systemic inflammation. *Journal of Neuroscience Research*, 85(8), pp.1694-1703.

Damoiseaux, J.G. et al., 1994. Rat macrophage lysosomal membrane antigen recognized by monoclonal antibody ED1. *Immunology*, 83(1), pp.140-147.

Daneman, R. et al., 2010. Pericytes are required for blood-brain barrier integrity during embryogenesis. *Nature*, 468(7323), pp.562-566.

Danial, N.N. & Korsmeyer, S.J., 2004. Cell Death: Critical Control Points. *Cell*, 116(2), pp.205-219.

Davalos, D. et al., 2005. ATP mediates rapid microglial response to local brain injury in vivo. *Nature Neuroscience*, 8(6), pp.752-758.

Davenport, C.M. et al., 2010. Inhibiting p53 pathways in microglia attenuates microglial-evoked neurotoxicity following exposure to Alzheimer peptides. *Journal of Neurochemistry*, 112(2), pp.552-563.

Degterev, A, Boyce, M & Yuan, J, 2001. The channel of death. *The Journal of Cell Biology*, 155(5), pp.695-698.

Degterev, A. & Yuan, J. 2008. Expansion and evolution of cell death programmes. *Nature Reviews. Molecular Cell Biology*, 9(5), pp.378-390.

Denis, M., 1994. Human monocytes/macrophages: NO or no NO? *Journal of Leukocyte Biology*, 55(5), pp.682-684.

Desai, B.S. et al., 2007. Blood-brain barrier pathology in Alzheimer's and Parkinson's disease: implications for drug therapy. *Cell Transplantation*, 16(3), pp.285-299.

Dietzmann, K. et al., 2000. Expression of the plasminogen activator system and the inhibitors PAI-1 and PAI-2 in posttraumatic lesions of the CNS and brain injuries following dramatic circulatory arrests: an immunohistochemical study. *Pathology, Research and Practice*, 196(1), pp.15-21.

Di Liberto, V., Mudò, G. & Belluardo, N., 2011. mGluR2/3 agonist LY379268, by enhancing the production of GDNF, induces a time-related phosphorylation of RET receptor and intracellular signaling Erk1/2 in mouse striatum. *Neuropharmacology*, 61(4), pp.638-645.

Dinarello, C.A., 2000. Proinflammatory cytokines. *Chest*, 118(2), pp.503-508.

Ding, M. et al., 1997. Inducible Nitric-oxide Synthase and Nitric Oxide Production in Human Fetal Astrocytes and Microglia. *Journal of Biological Chemistry*, 272(17), pp.11327 - 11335.

Dore-Duffy, P. & LaManna, J.C., 2007. Physiologic angiodynamics in the brain. *Antioxidants & Redox Signaling*, 9(9), pp.1363-1371.

Drake, C.T. & Iadecola, C., 2007. The Role of Neuronal Signaling in Controlling Cerebral Blood Flow. *Brain and Language*, 102(2), pp.141-152.

Drożdzik, M. et al., 2003. Polymorphism in the P-glycoprotein drug transporter MDR1 gene: a possible link between environmental and genetic factors in Parkinson's disease. *Pharmacogenetics*, 13(5), pp.259-263.

Du, Y. et al., 2001. Minocycline prevents nigrostriatal dopaminergic neurodegeneration in the MPTP model of Parkinson's disease. *Proceedings of the National Academy of Sciences of the United States of America*, 98(25), pp.14669-14674.

D'Amelio, M. et al., 2011. Caspase-3 triggers early synaptic dysfunction in a mouse model of Alzheimer's disease. *Nature Neuroscience*, 14(1), pp.69-76.

D'Mello, S.R. et al., 1993. Induction of apoptosis in cerebellar granule neurons by low potassium: inhibition of death by insulin-like growth factor I and cAMP. *Proceedings of the National Academy of Sciences of the United States of America*, 90(23), pp.10989-10993.

Earnshaw, W.C., Martins, L.M. & Kaufmann, S.H., 1999. Mammalian caspases: structure, activation, substrates, and functions during apoptosis. *Annual Review of Biochemistry*, 68, pp.383-424.

East, E. et al., 2005. A role for the plasminogen activator system in inflammation and neurodegeneration in the central nervous system during experimental allergic encephalomyelitis. *The American Journal of Pathology*, 167(2), pp.545-554.

East, E. et al., 2008. Chronic relapsing experimental allergic encephalomyelitis (CREAE) in plasminogen activator inhibitor-1 knockout mice: the effect of fibrinolysis during neuroinflammation. *Neuropathology and Applied Neurobiology*, 34(2), pp.216-230.

Edison, P. et al., 2008. Microglia, amyloid, and cognition in Alzheimer's disease: An [11C](R)PK11195-PET and [11C]PIB-PET study. *Neurobiology of Disease*, 32(3), pp.412-419.

Ehlers, M.R.W., 2000. CR3: a general purpose adhesion-recognition receptor essential for innate immunity. *Microbes and Infection*, 2(3), pp.289-294.

Ehrlich, P., 1904. Ueber die beziehungen von chemischer constitution, verteilung und pharmakologischer wirkung. *Gesammelte Arbeiten zur Immunitaetsforschung*, 574.

El Khoury, J. et al., 1996. Scavenger receptor-mediated adhesion of microglia to beta-amyloid fibrils. *Nature*, 382(6593), pp.716-719.

Elovaara, I. et al., 1985. CSF in Alzheimer's disease. Studies on blood-brain barrier function and intrathecal protein synthesis. *Journal of the Neurological Sciences*, 70(1), pp.73-80.

Engelhardt, J.I. & Appel, S H, 1990. IgG reactivity in the spinal cord and motor cortex in amyotrophic lateral sclerosis. *Archives of Neurology*, 47(11), pp.1210-1216.

Etminan, M., Gill, S. & Samii, A., 2003. Effect of non-steroidal anti-inflammatory drugs on risk of Alzheimer's disease: systematic review and meta-analysis of observational studies. *BMJ (Clinical Research Ed.)*, 327(7407), p.128.

Fadok, V.A. et al., 1992. Exposure of phosphatidylserine on the surface of apoptotic lymphocytes triggers specific recognition and removal by macrophages. *Journal of Immunology (Baltimore, Md.: 1950)*, 148(7), pp.2207-2216.

Fan, S.T. & Edgington, T.S., 1991. Coupling of the adhesive receptor CD11b/CD18 to functional enhancement of effector macrophage tissue factor response. *The Journal of Clinical Investigation*, 87(1), pp.50-7.

Fan, S.T. & Edgington, T.S., 1993. Integrin regulation of leukocyte inflammatory functions. CD11b/CD18 enhancement of the tumor necrosis factor-alpha responses of monocytes. *Journal of Immunology (Baltimore, Md.: 1950)*, 150(7), pp.2972-80.

Farso, M.C., O'Shea, R.D. & Beart, P.M., 2009. Evidence group I mGluR drugs modulate the activation profile of lipopolysaccharide-exposed microglia in culture. *Neurochemical Research*, 34(10), pp.1721-1728.

Ferretti, M.T. et al., Intracellular A[beta]-oligomers and early inflammation in a model of Alzheimer's disease. *Neurobiology of Aging*, In Press, Corrected Proof. Available at: http://www.sciencedirect.com/science/article/pii/S0197458011000091 [Accessed June 22, 2011].

Fiala, M et al., 2002. Cyclooxygenase-2-positive macrophages infiltrate the Alzheimer's disease brain and damage the blood-brain barrier. *European Journal of Clinical Investigation*, 32(5), pp.360-371.

Fiala, M., Cribbs, D.H., Rosenthal, M. & Bernard, G. 2007. Phagocytosis of amyloid-beta and inflammation: two faces of innate immunity in Alzheimer's disease. *Journal of Alzheimer's Disease: JAD*, 11(4), pp.457-463.

Fillit, H. et al., 1991. Elevated circulating tumor necrosis factor levels in Alzheimer's disease. *Neuroscience Letters*, 129(2), pp.318-320.

Fischer, H. et al., 2002. Human caspase 12 has acquired deleterious mutations. *Biochemical and Biophysical Research Communications*, 293(2), pp.722-726.

Franklin, R.J. et al., 1995. Differentiation of the O-2A progenitor cell line CG-4 into oligodendrocytes and astrocytes following transplantation into glia-deficient areas of CNS white matter. *Glia*, 13(1), pp.39-44.

Gallo, V. et al., 1982. Selective release of glutamate from cerebellar granule cells differentiating in culture. *Proceedings of the National Academy of Sciences of the United States of America*, 79(24), pp.7919-7923.

Gallo, V. et al., 1987. The role of depolarization in the survival and differentiation of cerebellar granule cells in culture. *The Journal of Neuroscience*, 7(7), pp.2203 -2213.

Garbuzova-Davis, S. et al., 2007. Ultrastructure of blood-brain barrier and blood-spinal cord barrier in SOD1 mice modeling ALS. *Brain Research*, 1157, pp.126-137.

Gatz, M. et al., 2006. Role of Genes and Environments for Explaining Alzheimer Disease. *Arch Gen Psychiatry*, 63(2), pp.168-174.

Gay, F.W. et al., 1997. The application of multifactorial cluster analysis in the staging of plaques in early multiple sclerosis. Identification and characterization of the primary demyelinating lesion. *Brain: A Journal of Neurology*, 120 (Pt 8), pp.1461-1483.

Ge, W.-P. et al., 2006. Long-term potentiation of neuron-glia synapses mediated by Ca2+-permeable AMPA receptors. *Science (New York, N.Y.)*, 312(5779), pp.1533-1537.

Gebicke-Haerter, P.J., 2001. Microglia in neurodegeneration: molecular aspects. *Microscopy Research and Technique*, 54(1), pp.47-58.

Genoud, S. et al., 2002. Notch1 control of oligodendrocyte differentiation in the spinal cord. *The Journal of Cell Biology*, 158(4), pp.709-718.

Germain, M., Mathai, J.P. & Shore, G.C., 2002. BH-3-only BIK functions at the endoplasmic reticulum to stimulate cytochrome c release from mitochondria. *The Journal of Biological Chemistry*, 277(20), pp.18053-60.

Girouard, H. & Iadecola, C., 2006. Neurovascular coupling in the normal brain and in hypertension, stroke, and Alzheimer disease. *Journal of Applied Physiology (Bethesda, Md.: 1985)*, 100(1), pp.328-335.

Giulian, D., Vaca, K. & Corpuz, M., 1993. Brain glia release factors with opposing actions upon neuronal survival. *The Journal of Neuroscience: The Official Journal of the Society for Neuroscience*, 13(1), pp.29-37.

Glass, C.K. et al., 2010. Mechanisms underlying inflammation in neurodegeneration. *Cell*, 140(6), pp.918-934.

Glezer, I., Lapointe, A. & Rivest, S., 2006. Innate immunity triggers oligodendrocyte progenitor reactivity and confines damages to brain injuries. *The FASEB Journal: Official Publication of the Federation of American Societies for Experimental Biology*, 20(6), pp.750-752.

Goate, A. et al., 1991. Segregation of a missense mutation in the amyloid precursor protein gene with familial Alzheimer's disease. *Nature*, 349(6311), pp.704-706.

Goldmann, E., 1913. Vitalfarbung am zentralnervensystem. *Abhandl Konigl preuss Akad Wiss*, 1, pp.1-60.

Gowing, G. et al., 2006. Absence of tumor necrosis factor-alpha does not affect motor neuron disease caused by superoxide dismutase 1 mutations. *The Journal of Neuroscience: The Official Journal of the Society for Neuroscience*, 26(44), pp.11397-11402.

Graeber, M B, Bise, K. & Mehraein, P., 1993. Synaptic stripping in the human facial nucleus. *Acta Neuropathologica*, 86(2), pp.179-181.

Graeber, M.B. & Streit, W.J. 2009. Microglia: biology and pathology. *Acta Neuropathologica*, 119(1), pp.89-105.

Greenberg, S.M. et al., 2004. Amyloid angiopathy-related vascular cognitive impairment. *Stroke; a Journal of Cerebral Circulation*, 35(11 Suppl 1), pp.2616-2619.

Grewal, R.P. et al., 1997. Scavenger receptor mRNAs in rat brain microglia are induced by kainic acid lesioning and by cytokines. *Neuroreport*, 8(5), pp.1077-1081.

Griscavage, J.M., Wilk, S. & Ignarro, L J, 1996. Inhibitors of the proteasome pathway interfere with induction of nitric oxide synthase in macrophages by blocking activation of transcription factor NF-kappa B. *Proceedings of the National Academy of Sciences of the United States of America*, 93(8), pp.3308-3312.

Gronski, M.A. et al., 2009. An essential role for calcium flux in phagocytes for apoptotic cell engulfment and the anti-inflammatory response. *Cell Death Differ*, 16(10), pp.1323-1331.

Gross, A., McDonnell, J.M. & Korsmeyer, S J, 1999. BCL-2 family members and the mitochondria in apoptosis. *Genes & Development*, 13(15), pp.1899-911.

Gyllensten, L. & Malmfors, T., 1963. Myelinization of the Optic Nerve and its Dependence on Visual Function— A Quantitative Investigation in Mice. *Journal of Embryology and Experimental Morphology*, 11(1), pp.255 -266.

Haass, C. & Selkoe, D.J., 2007. Soluble protein oligomers in neurodegeneration: lessons from the Alzheimer's amyloid beta-peptide. *Nature Reviews. Molecular Cell Biology*, 8(2), pp.101-112.

Halliday, G.M. & Stevens, C.H., 2011. Glia: initiators and progressors of pathology in Parkinson's disease. *Movement Disorders: Official Journal of the Movement Disorder Society*, 26(1), pp.6-17.

Hamby, M.E. et al., 2006. Characterization of an improved procedure for the removal of microglia from confluent monolayers of primary astrocytes. *Journal of Neuroscience Methods*, 150(1), pp.128-137.

Hamza, T.H. et al., 2010. Common genetic variation in the HLA region is associated with late-onset sporadic Parkinson's disease. *Nature Genetics*, 42(9), pp.781-785.

Hanisch, U.K. et al., 2004. The microglia-activating potential of thrombin: the protease is not involved in the induction of proinflammatory cytokines and chemokines. *The Journal of Biological Chemistry*, 279(50), pp.51880-7.

Hardy, J & Allsop, D., 1991. Amyloid deposition as the central event in the aetiology of Alzheimer's disease. *Trends in Pharmacological Sciences*, 12(10), pp.383-388.

Hardy, J. 2006. A hundred years of Alzheimer's disease research. *Neuron*, 52(1), pp.3-13.

Harold, D. et al., 2009. Genome-wide association study identifies variants at CLU and PICALM associated with Alzheimer's disease. *Nature Genetics*, 41(10), pp.1088-1093.

Haydon, P.G., 2001. GLIA: listening and talking to the synapse. *Nature Reviews. Neuroscience*, 2(3), pp.185-193.

Hemmer, B., Archelos, J.J. & Hartung, H.P., 2002. New concepts in the immunopathogenesis of multiple sclerosis. *Nature Reviews. Neuroscience*, 3(4), pp.291-301.

Henkel, J S et al., 2009. Decreased mRNA expression of tight junction proteins in lumbar spinal cords of patients with ALS. *Neurology*, 72(18), pp.1614-1616.

Heppner, F.L. et al., 2005. Experimental autoimmune encephalomyelitis repressed by microglial paralysis. *Nature Medicine*, 11(2), pp.146-152.

Herbein, G. et al., 1995. Lipopolysaccharide (LPS) down-regulates CD4 expression in primary human macrophages through induction of endogenous tumour necrosis factor (TNF) and IL-1 beta. *Clinical and Experimental Immunology*, 102(2), pp.430-437.

Hetier, E. et al., 1988. Brain macrophages synthesize interleukin-1 and interleukin-1 mRNAs in vitro. *Journal of Neuroscience Research*, 21(2-4), pp.391-397.

Hetz, C. et al., 2003. Caspase-12 and endoplasmic reticulum stress mediate neurotoxicity of pathological prion protein. *The EMBO Journal*, 22(20), pp.5435-5445.

Hewett, J.A. et al., 1999. Inducible nitric oxide synthase expression in cultures enriched for mature oligodendrocytes is due to microglia. *Journal of Neuroscience Research*, 56(2), pp.189-198.

Hickey, W.F. & Kimura, H., 1988. Perivascular microglial cells of the CNS are bone marrow-derived and present antigen in vivo. *Science (New York, N.Y.)*, 239(4837), pp.290-292.

Hill, K.E. et al., 2004. Inducible nitric oxide synthase in chronic active multiple sclerosis plaques: distribution, cellular expression and association with myelin damage. *Journal of Neuroimmunology*, 151(1-2), pp.171-179.

Hirt, U.A. & Leist, M., 2003. Rapid, noninflammatory and PS-dependent phagocytic clearance of necrotic cells. *Cell Death Differ*, 10(10), pp.1156-1164.

Hitomi, J. et al., 2004. Involvement of caspase-4 in endoplasmic reticulum stress-induced apoptosis and Aβ-induced cell death. *The Journal of Cell Biology*, 165(3), pp.347-356.

Hitomi, J. et al., 2008. Identification of a molecular signaling network that regulates a cellular necrotic cell death pathway. *Cell*, 135(7), pp.1311-1323.

Hodgkinson, C.P., Patel, K. & Ye, S., 2008. Functional Toll-like receptor 4 mutations modulate the response to fibrinogen. *Thrombosis and Haemostasis*, 100(2), pp.301-307.

Hoffmann, A. et al., 2003. Elevation of Basal Intracellular Calcium as a Central Element in the Activation of Brain Macrophages (Microglia): Suppression of Receptor-Evoked Calcium Signaling and Control of Release Function. *The Journal of Neuroscience*, 23(11), pp.4410 -4419.

Holler, N. et al., 2000. Fas triggers an alternative, caspase-8-independent cell death pathway using the kinase RIP as effector molecule. *Nature Immunology*, 1(6), pp.489-495.

Honda, M. et al., 1998. Immunohistochemical evidence for a macrophage scavenger receptor in Mato cells and reactive microglia of ischemia and Alzheimer's disease. *Biochemical and Biophysical Research Communications*, 245(3), pp.734-740.

Hong, Dawson, T.M. & Dawson, V.L., 2004. Nuclear and mitochondrial conversations in cell death: PARP-1 and AIF signaling. *Trends in Pharmacological Sciences*, 25(5), pp.259-264.

Hooper, C., Taylor, D.L. & Pocock, J.M., 2005. Pure albumin is a potent trigger of calcium signalling and proliferation in microglia but not macrophages or astrocytes. *Journal of Neurochemistry*, 92(6), pp.1363-1376.

Hooper, C. & Pocock, J.M., 2007. Chromogranin A activates diverse pathways mediating inducible nitric oxide expression and apoptosis in primary microglia. *Neuroscience Letters*, 413(3), pp.227-232.

Hooper, C., Fry, V.A.H., et al., 2009a. Scavenger receptor control of chromogranin A-induced microglial stress and neurotoxic cascades. *FEBS Letters*, 583(21), pp.3461-3466.

Hooper, C., Pinteaux-Jones, F., et al., 2009b. Differential effects of albumin on microglia and macrophages; implications for neurodegeneration following blood–brain barrier damage. *Journal of Neurochemistry*, 109(3), pp.694-705.

Horie, H. et al., 1989. Adaptation of cultured mammalian neurons to a hypotonic environment with age-related response. *Brain Research*, 477(1-2), pp.233-240.

van Horssen, J. et al., 2007. The blood-brain barrier in cortical multiple sclerosis lesions. *Journal of Neuropathology and Experimental Neurology*, 66(4), pp.321-328.

Horvath, R.J. et al., 2008. Differential migration, LPS-induced cytokine, chemokine, and NO expression in immortalized BV2 and HAPI cell lines and primary microglial cultures. *Journal of Neurochemistry*, 107(2), pp.557-569.

Hotamisligil, G.S., 2010a. Endoplasmic Reticulum Stress and the Inflammatory Basis of Metabolic Disease. *Cell*, 140(6), pp.900-917.

Hotamisligil, G.S., 2010b. Endoplasmic reticulum stress and atherosclerosis. *Nature Medicine*, 16(4), pp.396-399.

Houen, G., Bruun, L. & Barkholt, V., 1997. Combined immunostaining and Coomassie Brilliant Blue staining of polyvinylidene difluoride membranes without organic solvent. *ELECTROPHORESIS*, 18(5), pp.701-705.

Hu, P. et al., 2006. Autocrine tumor necrosis factor alpha links endoplasmic reticulum stress to the membrane death receptor pathway through IRE1alpha-mediated NF-kappaB activation and down-regulation of TRAF2 expression. *Molecular and Cellular Biology*, 26(8), pp.3071-3084.

Hu, X. et al., 2010. β2-Integrins in demyelinating disease: not adhering to the paradigm. *Journal of Leukocyte Biology*, 87(3), pp.397 -403.

Huang, F. et al., 1999. Elimination of the Class A Scavenger Receptor Does Not Affect Amyloid Plaque Formation or Neurodegeneration in Transgenic Mice Expressing Human Amyloid Protein Precursors. *The American Journal of Pathology*, 155(5), pp.1741-1747.

Husemann, J & Silverstein, S C, 2001. Expression of scavenger receptor class B, type I, by astrocytes and vascular smooth muscle cells in normal adult mouse and human brain and in Alzheimer's disease brain. *The American Journal of Pathology*, 158(3), pp.825-832.

Husemann, J. et al., 2002. Scavenger receptors in neurobiology and neuropathology: their role on microglia and other cells of the nervous system. *Glia*, 40(2), pp.195-205.

Iadecola, C., 2004. Neurovascular regulation in the normal brain and in Alzheimer's disease. *Nature Reviews. Neuroscience*, 5(5), pp.347-360.

Ifuku, M. et al., 2007. Bradykinin-induced microglial migration mediated by B1-bradykinin receptors depends on Ca2+ influx via reverse-mode activity of the Na+/Ca2+ exchanger. *The Journal of Neuroscience: The Official Journal of the Society for Neuroscience*, 27(48), pp.13065-13073.

Imai, Y, Soda, M. & Takahashi, R, 2000. Parkin suppresses unfolded protein stress-induced cell death through its E3 ubiquitin-protein ligase activity. *The Journal of Biological Chemistry*, 275(46), pp.35661-35664.

Imai, Y & Takahashi, R., 2004. How do Parkin mutations result in neurodegeneration? *Current Opinion in Neurobiology*, 14(3), pp.384-389.

Imaizumi, K et al., 2001. The unfolded protein response and Alzheimer's disease. *Biochimica Et Biophysica Acta*, 1536(2-3), pp.85-96.

Jack, C.S. et al., 2005. TLR signaling tailors innate immune responses in human microglia and astrocytes. *Journal of Immunology (Baltimore, Md.: 1950)*, 175(7), pp.4320-30.

Jacobs, D M & Morrison, D C, 1977. Inhibition of the mitogenic response to lipopolysaccharide (LPS) in mouse spleen cells by polymyxin B. *Journal of Immunology (Baltimore, Md.: 1950)*, 118(1), pp.21-27.

Jensen, T. et al., 2007. Fibrinogen and fibrin induce synthesis of proinflammatory cytokines from isolated peripheral blood mononuclear cells. *Thrombosis and Haemostasis*, 97(5), pp.822-829.

Jo, J. et al., 2011. Aβ(1-42) inhibition of LTP is mediated by a signaling pathway involving caspase-3, Akt1 and GSK-3β. *Nature Neuroscience*, 14(5), pp.545-547.

Johnson, G.L. & Lapadat, R., 2002. Mitogen-activated protein kinase pathways mediated by ERK, JNK, and p38 protein kinases. *Science (New York, N.Y.)*, 298(5600), pp.1911-1912.

Kajikawa, T. et al., 1986. Induction by heterologous fibrinogen of release of TNF-like cytotoxic factor from murine macrophages. *Journal of Biological Response Modifiers*, 5(4), pp.283-287.

Kalaria, R.N. & Kroon, S.N., 1992. Complement inhibitor C4-binding protein in amyloid deposits containing serum amyloid P in Alzheimer's disease. *Biochemical and Biophysical Research Communications*, 186(1), pp.461-466.

Kanekura, K. et al., 2009. ER stress and unfolded protein response in amyotrophic lateral sclerosis. *Molecular Neurobiology*, 39(2), pp.81-89.

Kaplan, M.R. et al., 1997. Induction of sodium channel clustering by oligodendrocytes. *Nature*, 386(6626), pp.724-728.

Kaplan, M.R. et al., 2001. Differential control of clustering of the sodium channels Na(v)1.2 and Na(v)1.6 at developing CNS nodes of Ranvier. *Neuron*, 30(1), pp.105-119.

Katayama, T et al., 1999. Presenilin-1 mutations downregulate the signalling pathway of the unfolded-protein response. *Nature Cell Biology*, 1(8), pp.479-485.

Kaul, M., Garden, G.A. & Lipton, Stuart A., 2001. Pathways to neuronal injury and apoptosis in HIV-associated dementia. *Nature*, 410(6831), pp.988-994.

Kaushal, V. & Schlichter, L.C., 2008. Mechanisms of microglia-mediated neurotoxicity in a new model of the stroke penumbra. *The Journal of Neuroscience: The Official Journal of the Society for Neuroscience*, 28(9), pp.2221-2230.

Kawahara, K. et al., 2001. Induction of CHOP and apoptosis by nitric oxide in p53-deficient microglial cells. *FEBS Letters*, 506(2), pp.135-139.

Keizman, D. et al., 2009. Low-grade systemic inflammation in patients with amyotrophic lateral sclerosis. *Acta Neurologica Scandinavica*, 119(6), pp.383-389.

Kermode, A.G. et al., 1990. Breakdown of the blood-brain barrier precedes symptoms and other MRI signs of new lesions in multiple sclerosis. Pathogenetic and clinical implications. *Brain: A Journal of Neurology*, 113 (Pt 5), pp.1477-89.

Kerr, J.F.R., Wyllie, A.H. & Currie, A.R., 1972. Apoptosis: A Basic Biological Phenomenon with Wide-ranging Implications in Tissue Kinetics. *British Journal of Cancer*, 26(4), pp.239-257.

Kettenmann, H. et al., 2011. Physiology of microglia. *Physiological Reviews*, 91(2), pp.461-553.

Kiernan, J.A, 2009. *Barr's The Human Nervous System: An Anatomical Viewpoint* 9th ed., Lippincott Williams & Wilkins.

Kim, W.G. et al., 2000. Regional Difference in Susceptibility to Lipopolysaccharide-Induced Neurotoxicity in the Rat Brain: Role of Microglia. *The Journal of Neuroscience*, 20(16), pp.6309 -6316.

Kim, K.Y. et al., 2002. Thrombin induces IL-10 production in microglia as a negative feedback regulator of TNF-alpha release. *Neuroreport*, 13(6), pp.849-852.

Kim, S.H., Smith, C.J. & Van Eldik, L.J., 2004. Importance of MAPK pathways for microglial pro-inflammatory cytokine IL-1 beta production. *Neurobiology of Aging*, 25(4), pp.431-439.

Kim, I., Xu, W. & Reed, J.C., 2008. Cell death and endoplasmic reticulum stress: disease relevance and therapeutic opportunities. *Nature Reviews Drug Discovery*, 7(12), pp.1013-1030.

Kim, E.K. & Choi, E.J., 2010. Pathological roles of MAPK signaling pathways in human diseases. *Biochimica Et Biophysica Acta*, 1802(4), pp.396-405.

Kingham, P.J., Cuzner, M L & Pocock, J M, 1999. Apoptotic pathways mobilized in microglia and neurones as a consequence of chromogranin A-induced microglial activation. *Journal of Neurochemistry*, 73(2), pp.538-47.

Kingham, P.J. & Pocock, J M, 2000. Microglial apoptosis induced by chromogranin A is mediated by mitochondrial depolarisation and the permeability transition but not by cytochrome c release. *Journal of Neurochemistry*, 74(4), pp.1452-62.

Kitamura, M et al., 2011. Aberrant, differential and bidirectional regulation of the unfolded protein response towards cell survival by 3'-deoxyadenosine. *Cell Death and Differentiation*. Available at: http://www.ncbi.nlm.nih.gov/pubmed/21597460 [Accessed September 27, 2011].

Klegeris, A. et al., 2008. Alpha-synuclein activates stress signaling protein kinases in THP-1 cells and microglia. *Neurobiology of Aging*, 29(5), pp.739-752.

Klintworth, H., Garden, G. & Xia, Z., 2009. Rotenone and Paraquat do not Directly Activate Microglia or Induce Inflammatory Cytokine Release. *Neuroscience letters*, 462(1), pp.1-5.

Koenigsknecht, J. & Landreth, Gary, 2004. Microglial phagocytosis of fibrillar beta-amyloid through a beta1 integrin-dependent mechanism. *The Journal of Neuroscience: The Official Journal of the Society for Neuroscience*, 24(44), pp.9838-9846.

Koh, J.Y. & Choi, D.W., 1987. Quantitative determination of glutamate mediated cortical neuronal injury in cell culture by lactate dehydrogenase efflux assay. *Journal of Neuroscience Methods*, 20(1), pp.83-90.

Kondo, T. & Raff, M., 2000. Oligodendrocyte precursor cells reprogrammed to become multipotential CNS stem cells. *Science (New York, N.Y.)*, 289(5485), pp.1754-1757.

Kortekaas, Rudie et al., 2005. Blood-brain barrier dysfunction in parkinsonian midbrain in vivo. *Annals of Neurology*, 57(2), pp.176-179.

Kreutzberg, G.W., 1996. Microglia: a sensor for pathological events in the CNS. *Trends in Neurosciences*, 19(8), pp.312-318.

Kroemer, G. et al., 2008. Classification of cell death: recommendations of the Nomenclature Committee on Cell Death 2009. *Cell Death and Differentiation*, 16(1), pp.3-11.

Kuno, R. et al., 2005. Autocrine activation of microglia by tumor necrosis factor-alpha. *Journal of Neuroimmunology*, 162(1-2), pp.89-96.

Kuo, C.T. et al., 2006. Identification of E2/E3 ubiquitinating enzymes and caspase activity regulating Drosophila sensory neuron dendrite pruning. *Neuron*, 51(3), pp.283-290.

Kurokawa, M. & Kornbluth, S., 2009. Caspases and kinases in a death grip. *Cell*, 138(5), pp.838-854.

Kwon, E.E. & Prineas, J.W., 1994. Blood-brain barrier abnormalities in longstanding multiple sclerosis lesions. An immunohistochemical study. *Journal of Neuropathology and Experimental Neurology*, 53(6), pp.625-636.

Ladeby, R. et al., 2005. Microglial cell population dynamics in the injured adult central nervous system. *Brain Research Reviews*, 48(2), pp.196-206.

Laemmli, U.K., 1970. Cleavage of Structural Proteins during the Assembly of the Head of Bacteriophage T4. *Nature*, 227(5259), pp.680-685.

Lafon-Cazal, M. et al., 1999. mGluR7-like metabotropic glutamate receptors inhibit NMDA-mediated excitotoxicity in cultured mouse cerebellar granule neurons. *The European Journal of Neuroscience*, 11(2), pp.663-672.

Lai, E., Teodoro, T. & Volchuk, A., 2007. Endoplasmic Reticulum Stress: Signaling the Unfolded Protein Response. *Physiology*, 22(3), pp.193 -201.

Lalo, U. et al., 2006. NMDA receptors mediate neuron-to-glia signaling in mouse cortical astrocytes. *The Journal of Neuroscience: The Official Journal of the Society for Neuroscience*, 26(10), pp.2673-2683.

Lambert, J.C. et al., 2009. Genome-wide association study identifies variants at CLU and CR1 associated with Alzheimer's disease. *Nature Genetics*, 41(10), pp.1094-1099.

Lau, A. & Tymianski, M., 2010. Glutamate receptors, neurotoxicity and neurodegeneration. *Pflügers Archiv: European Journal of Physiology*, 460(2), pp.525-542.

Lauber, K. et al., 2001. The Adapter Protein Apoptotic Protease-activating Factor-1 (Apaf-1) Is Proteolytically Processed during Apoptosis. *J. Biol. Chem.*, 276(32), pp.29772-29781.

Lee, S., Liu, W., et al., 1993. Cytokine production by human fetal microglia and astrocytes. Differential induction by lipopolysaccharide and IL-1 beta. *The Journal of Immunology*, 150(7), pp.2659 -2667.

Lee, J C et al., 1994. A protein kinase involved in the regulation of inflammatory cytokine biosynthesis. *Nature*, 372(6508), pp.739-746.

Lee, P. et al., 2001. NO as an autocrine mediator in the apoptosis of activated microglial cells: correlation between activation and apoptosis of microglial cells. *Brain Research*, 892(2), pp.380-385.

Lee, G. & Bendayan, R., 2004. Functional expression and localization of P-glycoprotein in the central nervous system: relevance to the pathogenesis and treatment of neurological disorders. *Pharmaceutical Research*, 21(8), pp.1313-1330.

Lee, C.G.L., Tang, K., et al., 2004a. MDR1, the blood-brain barrier transporter, is associated with Parkinson's disease in ethnic Chinese. *Journal of Medical Genetics*, 41(5), p.e60.

Lee, H., Zhu, Z. et al., 2004b. The role of metabotropic glutamate receptors in Alzheimer's disease. *Acta Neurobiologiae Experimentalis*, 64(1), pp.89-98.

Lee, J.W. et al., 2007. Fibrinogen gamma-A chain precursor in CSF: a candidate biomarker for Alzheimer's disease. *BMC Neurology*, 7, p.14.

Lee, J.H. et al., 2010. Induction of the unfolded protein response and cell death pathway in Alzheimer's disease, but not in aged Tg2576 mice. *Experimental & Molecular Medicine*, 42(5), pp.386-394.

Lees, A.J., Hardy, J. & Revesz, T., 2009. Parkinson's disease. *Lancet*, 373(9680), pp.2055-2066.

Lehnardt, S. et al., 2003. Activation of innate immunity in the CNS triggers neurodegeneration through a Toll-like receptor 4-dependent pathway. *Proceedings of the National Academy of Sciences of the United States of America*, 100(14), pp.8514-8519.

Leonardi, A. et al., 1984. Cerebrospinal fluid (CSF) findings in amyotrophic lateral sclerosis. *Journal of Neurology*, 231(2), pp.75-78.

Lequin, R.M., 2005. Enzyme Immunoassay (EIA)/Enzyme-Linked Immunosorbent Assay (ELISA). *Clin Chem*, 51(12), pp.2415-2418.

Ley, K. et al., 2007. Getting to the site of inflammation: the leukocyte adhesion cascade updated. *Nature Reviews. Immunology*, 7(9), pp.678-689.

Li, Z. et al., 2010. Caspase-3 activation via mitochondria is required for long-term depression and AMPA receptor internalization. *Cell*, 141(5), pp.859-871.

Liberatore, G.T. et al., 1999. Inducible nitric oxide synthase stimulates dopaminergic neurodegeneration in the MPTP model of Parkinson disease. *Nature Medicine*, 5(12), pp.1403-1409.

Lien, E. et al., 2000. Toll-like receptor 4 imparts ligand-specific recognition of bacterial lipopolysaccharide. *The Journal of Clinical Investigation*, 105(4), pp.497-504.

Lin, S.C. et al., 2005. Climbing fiber innervation of NG2-expressing glia in the mammalian cerebellum. *Neuron*, 46(5), pp.773-785.

Lindholm, D, Wootz, H. & Korhonen, L, 2006. ER stress and neurodegenerative diseases. *Cell Death and Differentiation*, 13(3), pp.385-392.

Lindsten, T., Zong, W.-X. & Thompson, C.B., 2005. Defining the role of the Bcl-2 family of proteins in the nervous system. *The Neuroscientist: A Review Journal Bringing Neurobiology, Neurology and Psychiatry*, 11(1), pp.10-5.

Lishko, V.K. et al., 2002. Regulated unmasking of the cryptic binding site for integrin alpha M beta 2 in the gamma C-domain of fibrinogen. *Biochemistry*, 41(43), pp.12942-12951.

Lishko, V.K. et al., 2004. Multiple binding sites in fibrinogen for integrin alphaMbeta2 (Mac-1). *The Journal of Biological Chemistry*, 279(43), pp.44897-44906.

Loane, D.J. et al., 2009. Activation of metabotropic glutamate receptor 5 modulates microglial reactivity and neurotoxicity by inhibiting NADPH oxidase. *The Journal of Biological Chemistry*, 284(23), pp.15629-15639.

Lobsiger, C.S. & Cleveland, D.W., 2007. Glial cells as intrinsic components of non-cell-autonomous neurodegenerative disease. *Nature Neuroscience*, 10(11), pp.1355-1360.

Lopez-Talavera, J.C. et al., 1996. Thalidomide inhibits tumor necrosis factor alpha, decreases nitric oxide synthesis, and ameliorates the hyperdynamic circulatory syndrome in portal-hypertensive rats. *Hepatology (Baltimore, Md.)*, 23(6), pp.1616-1621.

Lukiw, W.J., 2004. Gene expression profiling in fetal, aged, and Alzheimer hippocampus: a continuum of stress-related signaling. *Neurochemical Research*, 29(6), pp.1287-1297.

Macek, T.A. et al., 1996. Differential involvement of group II and group III mGluRs as autoreceptors at lateral and medial perforant path synapses. *Journal of Neurophysiology*, 76(6), pp.3798 -3806.

Maezawa, I. et al., 2011. Amyloid-β Protein Oligomer at Low Nanomolar Concentrations Activates Microglia and Induces Microglial Neurotoxicity. *Journal of Biological Chemistry*, 286(5), pp.3693 -3706.

Malenka, R.C. & Bear, M.F., 2004. LTP and LTD: an embarrassment of riches. *Neuron*, 44(1), pp.5-21.

Man, S., Ubogu, E.E. & Ransohoff, R.M, 2007. Inflammatory cell migration into the central nervous system: a few new twists on an old tale. *Brain Pathology (Zurich, Switzerland)*, 17(2), pp.243-250.

Mandic, A. et al., 2003. Cisplatin Induces Endoplasmic Reticulum Stress and Nucleus-independent Apoptotic Signaling. *Journal of Biological Chemistry*, 278(11), pp.9100 - 9106.

Marco, S. & Skaper, S.D., 2006. Amyloid beta-peptide1-42 alters tight junction protein distribution and expression in brain microvessel endothelial cells. *Neuroscience Letters*, 401(3), pp.219-224.

Martinon, F. et al., 2010. TLR activation of the transcription factor XBP1 regulates innate immune responses in macrophages. *Nature Immunology*, 11(5), pp.411-418.

McCarthy & De Vellis, 1980. Preparation of separate astroglial and oligodendroglial cell cultures from rat cerebral tissue. *The Journal of Cell Biology*, 85(3), pp.890-902.

McCoy, M.K. & Tansey, M.G., 2008. TNF signaling inhibition in the CNS: implications for normal brain function and neurodegenerative disease. *Journal of Neuroinflammation*, 5, p.45.

McDonald, D.R. et al., 1998. beta-Amyloid fibrils activate parallel mitogen-activated protein kinase pathways in microglia and THP1 monocytes. *The Journal of Neuroscience: The Official Journal of the Society for Neuroscience*, 18(12), pp.4451-4460.

McDowell, M.L. et al., 2011. Neuroprotective effects of genistein in VSC4.1 motoneurons exposed to activated microglial cytokines. *Neurochemistry International*, 59(2), pp.175-184.

McKimmie, C.S. & Fazakerley, J.K., 2005. In response to pathogens, glial cells dynamically and differentially regulate Toll-like receptor gene expression. *Journal of Neuroimmunology*, 169(1-2), pp.116-25.

Mháille, A.N. et al., 2008. Increased expression of endoplasmic reticulum stress-related signaling pathway molecules in multiple sclerosis lesions. *Journal of Neuropathology and Experimental Neurology*, 67(3), pp.200-211.

Micheau, O. & Tschopp, J., 2003. Induction of TNF receptor I-mediated apoptosis via two sequential signaling complexes. *Cell*, 114(2), pp.181-90.

Mildner, A. et al., 2007. Microglia in the adult brain arise from Ly-6ChiCCR2+ monocytes only under defined host conditions. *Nature Neuroscience*, 10(12), pp.1544-1553.

Miller, S. et al., 1996. Exposure of astrocytes to thrombin reduces levels of the metabotropic glutamate receptor mGluR5. *Journal of Neurochemistry*, 67(4), pp.1435-1447.

Miller, S.D. et al., 2007. Antigen presentation in the CNS by myeloid dendritic cells drives progression of relapsing experimental autoimmune encephalomyelitis. *Annals of the New York Academy of Sciences*, 1103, pp.179-191.

Minagar, A. & Alexander, J.S., 2003. Blood-brain barrier disruption in multiple sclerosis. *Multiple Sclerosis (Houndmills, Basingstoke, England)*, 9(6), pp.540-549.

Miyazaki, K. et al., 2011. Disruption of neurovascular unit prior to motor neuron degeneration in amyotrophic lateral sclerosis. *Journal of Neuroscience Research*, 89(5), pp.718-728.

Moghaddam, B., 2004. Targeting metabotropic glutamate receptors for treatment of the cognitive symptoms of schizophrenia. *Psychopharmacology*, 174(1), pp.39-44.

Montoliu, C. et al., 1997. Activation of the metabotropic glutamate receptor mGluR5 prevents glutamate toxicity in primary cultures of cerebellar neurons. *The Journal of Pharmacology and Experimental Therapeutics*, 281(2), pp.643-647.

Morgan, S.C., Taylor, D.L & Pocock, J.M, 2004. Microglia release activators of neuronal proliferation mediated by activation of mitogen-activated protein kinase, phosphatidylinositol-3-kinase/Akt and delta-Notch signalling cascades. *Journal of Neurochemistry*, 90(1), pp.89-101.

Morishima, N., et al., 2002. An endoplasmic reticulum stress-specific caspase cascade in apoptosis. Cytochrome c-independent activation of caspase-9 by caspase-12. *The Journal of Biological Chemistry*, 277(37), pp.34287-34294.

Morrison, D.C. & Jacobs, D.M., 1976. Binding of polymyxin B to the lipid A portion of bacterial lipopolysaccharides. *Immunochemistry*, 13(10), pp.813-818.

Mosesson, M.W., 2005. Fibrinogen and fibrin structure and functions. *Journal of Thrombosis and Haemostasis: JTH*, 3(8), pp.1894-1904.

Mosley, K. & Cuzner, M L, 1996. Receptor-mediated phagocytosis of myelin by macrophages and microglia: effect of opsonization and receptor blocking agents. *Neurochemical Research*, 21(4), pp.481-487.

Mount, M.P. et al., 2007. Involvement of interferon-gamma in microglial-mediated loss of dopaminergic neurons. *The Journal of Neuroscience: The Official Journal of the Society for Neuroscience*, 27(12), pp.3328-3337.

Movsesyan, V.A., Stoica, B.A. & Faden, A.I., 2004. MGLuR5 activation reduces β-amyloid-induced cell death in primary neuronal cultures and attenuates translocation of cytochrome c and apoptosis-inducing factor. *Journal of Neurochemistry*, 89(6), pp.1528-1536.

Möller, T, Hanisch, U.K. & Ransom, B R, 2000. Thrombin-induced activation of cultured rodent microglia. *Journal of Neurochemistry*, 75(4), pp.1539-1547.

Möller, T., Weinstein, J.R. & Hanisch, U.K., 2006. Activation of microglial cells by thrombin: past, present, and future. *Seminars in Thrombosis and Hemostasis*, 32 Suppl 1, pp.69-76.

Nagata, T. et al., 2007. Increased ER stress during motor neuron degeneration in a transgenic mouse model of amyotrophic lateral sclerosis. *Neurological Research*, 29(8), pp.767-771.

Nakagawa, T. & Yuan, J, 2000. Cross-talk between two cysteine protease families. Activation of caspase-12 by calpain in apoptosis. *The Journal of Cell Biology*, 150(4), pp.887-894.

Nakagawa, T. et al., 2000. Caspase-12 mediates endoplasmic-reticulum-specific apoptosis and cytotoxicity by amyloid-beta. *Nature*, 403(6765), pp.98-103.

Nakajima, K. et al., 2004. Protein kinase C[alpha] requirement in the activation of p38 mitogen-activated protein kinase, which is linked to the induction of tumor necrosis factor [alpha]

in lipopolysaccharide-stimulated microglia. *Neurochemistry International*, 44(4), pp.205-214.

Nakamura, K. et al., 2000. Changes in endoplasmic reticulum luminal environment affect cell sensitivity to apoptosis. *The Journal of Cell Biology*, 150(4), pp.731-740.

Nakayama, Y. et al., 2010. Molecular mechanisms of the LPS-induced non-apoptotic ER stress-CHOP pathway. *Journal of Biochemistry*, 147(4), pp.471-483.

Nedergaard, M., Ransom, B. & Goldman, S.A., 2003. New roles for astrocytes: Redefining the functional architecture of the brain. *Trends in Neurosciences*, 26(10), pp.523-530.

Newman, E.A., 2003. New roles for astrocytes: regulation of synaptic transmission. *Trends in Neurosciences*, 26(10), pp.536-542.

Nguyen, M.D., Julien, J.-P. & Rivest, S., 2002. Innate immunity: the missing link in neuroprotection and neurodegeneration? *Nat Rev Neurosci*, 3(3), pp.216-227.

Nimmerjahn, A., Kirchhoff, F. & Helmchen, F., 2005. Resting microglial cells are highly dynamic surveillants of brain parenchyma in vivo. *Science (New York, N.Y.)*, 308(5726), pp.1314-1318.

Nishiyama, A. et al., 2009. Polydendrocytes (NG2 cells): multifunctional cells with lineage plasticity. *Nature Reviews. Neuroscience*, 10(1), pp.9-22.

Niswender, C.M. & Conn, P Jeffrey, 2010. Metabotropic glutamate receptors: physiology, pharmacology, and disease. *Annual Review of Pharmacology and Toxicology*, 50, pp.295-322.

Noseworthy, J.H. et al., 2000. Multiple sclerosis. *The New England Journal of Medicine*, 343(13), pp.938-952.

van Oijen, M. et al., 2005. Fibrinogen is associated with an increased risk of Alzheimer disease and vascular dementia. *Stroke; a Journal of Cerebral Circulation*, 36(12), pp.2637-2641.

Oltvai, Z.N., Milliman, C.L. & Korsmeyer, S J, 1993. Bcl-2 heterodimerizes in vivo with a conserved homolog, Bax, that accelerates programmed cell death. *Cell*, 74(4), pp.609-619.

Oyadomari, S. et al., 2001. Nitric oxide-induced apoptosis in pancreatic beta cells is mediated by the endoplasmic reticulum stress pathway. *Proceedings of the National Academy of Sciences of the United States of America*, 98(19), pp.10845-10850.

Oyadomari, S. & Mori, M, 2003. Roles of CHOP//GADD153 in endoplasmic reticulum stress. *Cell Death and Differentiation*, 11(4), pp.381-389.

Pacher, P., Beckman, J.S. & Liaudet, L., 2007. Nitric Oxide and Peroxynitrite in Health and Disease. *Physiological Reviews*, 87(1), pp.315 -424.

Pan, X.D. et al., 2011. Microglial phagocytosis induced by fibrillar β-amyloid is attenuated by oligomeric β-amyloid: implications for Alzheimer's disease. *Molecular Neurodegeneration*, 6, p.45.

Panaro, M.A. et al., 2003. Evidences for iNOS expression and nitric oxide production in the human macrophages. *Current Drug Targets. Immune, Endocrine and Metabolic Disorders*, 3(3), pp.210-221.

Park, K.W. & Jin, B.K., 2008. Thrombin-induced oxidative stress contributes to the death of hippocampal neurons: Role of neuronal NADPH oxidase. *Journal of Neuroscience Research*, 86(5), pp.1053-1063.

Paul, J., Strickland, S. & Melchor, J.P., 2007. Fibrin deposition accelerates neurovascular damage and neuroinflammation in mouse models of Alzheimer's disease. *J. Exp. Med.*, 204(8), pp.1999-2008.

Pei, Z. et al., 2007. MAC1 mediates LPS-induced production of superoxide by microglia: the role of pattern recognition receptors in dopaminergic neurotoxicity. *Glia*, 55(13), pp.1362-73.

Perea, G. & Araque, A., 2010. GLIA modulates synaptic transmission. *Brain Research Reviews*, 63(1-2), pp.93-102.

Perez, R.L. & Roman, J., 1995. Fibrin enhances the expression of IL-1 beta by human peripheral blood mononuclear cells. Implications in pulmonary inflammation. *Journal of Immunology (Baltimore, Md.: 1950)*, 154(4), pp.1879-1887.

Perez, R.L., Ritzenthaler, J.D. & Roman, J., 1999. Transcriptional regulation of the interleukin-1beta promoter via fibrinogen engagement of the CD18 integrin receptor. *American Journal of Respiratory Cell and Molecular Biology*, 20(5), pp.1059-66.

Perry, V.H., Cunningham, C. & Holmes, C., 2007. Systemic infections and inflammation affect chronic neurodegeneration. *Nature Reviews. Immunology*, 7(2), pp.161-7.

Perry, V.H. & O'Connor, V., 2010. The role of microglia in synaptic stripping and synaptic degeneration: a revised perspective. *ASN Neuro*, 2(5). Available at: http://www.ncbi.nlm.nih.gov/pubmed/20967131 [Accessed September 15, 2011].

Peterson, P.K. et al., 1994. Nitric oxide production and neurotoxicity mediated by activated microglia from human versus mouse brain. *The Journal of Infectious Diseases*, 170(2), pp.457-460.

Pettmann, B. & Henderson, C.E., 1998. Neuronal cell death. *Neuron*, 20(4), pp.633-647.

Pfrieger, F.W. & Barres, B.A., 1997. Synaptic Efficacy Enhanced by Glial Cells in Vitro. *Science*, 277(5332), pp.1684 -1687.

Pilc, A. et al., 2008. Mood disorders: regulation by metabotropic glutamate receptors. *Biochemical Pharmacology*, 75(5), pp.997-1006.

Pinteaux-Jones, F. et al., 2008. Myelin-induced microglial neurotoxicity can be controlled by microglial metabotropic glutamate receptors. *Journal of Neurochemistry*, 106(1), pp.442-454.

Pluskota, E. et al., 2008. Neutrophil apoptosis: selective regulation by different ligands of integrin alphaMbeta2. *Journal of Immunology (Baltimore, Md.: 1950)*, 181(5), pp.3609-3619.

Pocock, J.M. & Nicholls, D.G., 1992. A toxin (Aga-GI) from the venom of the spider Agelenopsis aperta inhibits the mammalian presynaptic Ca2+ channel coupled to glutamate exocytosis. *European Journal of Pharmacology: Molecular Pharmacology*, 226(4), pp.343-350.

Pocock, J.M. & Kettenmann, H., 2007. Neurotransmitter receptors on microglia. *Trends in Neurosciences*, 30(10), pp.527-35.

Politis, M.J. & Houle, J.D., 1985. Effect of cytosine arabinofuranoside (AraC) on reactive gliosis in vivo. An immunohistochemical and morphometric study. *Brain Research*, 328(2), pp.291-300.

Porcheray, F. et al., 2005. Macrophage activation switching: an asset for the resolution of inflammation. *Clinical and Experimental Immunology*, 142(3), pp.481-489.

Purves, D., 2008. *Neuroscience, Fourth Edition* 4th ed., Sinauer Associates, Inc.

Puthalakath, H. et al., 2007. ER Stress Triggers Apoptosis by Activating BH3-Only Protein Bim. *Cell*, 129(7), pp.1337-1349.

Qiang, L. et al., 2011. Directed Conversion of Alzheimer's Disease Patient Skin Fibroblasts into Functional Neurons. *Cell*, 146(3), pp.359-371.

Quaegebeur, A., Lange, C. & Carmeliet, P., 2011. The neurovascular link in health and disease: molecular mechanisms and therapeutic implications. *Neuron*, 71(3), pp.406-424.

Raff, M.C., Miller, R.H. & Noble, M., 1983. A glial progenitor cell that develops in vitro into an astrocyte or an oligodendrocyte depending on culture medium. *Nature*, 303(5916), pp.390-396.

Ralph, G.S. et al., 2005. Silencing mutant SOD1 using RNAi protects against neurodegeneration and extends survival in an ALS model. *Nature Medicine*, 11(4), pp.429-433.

Ransohoff, R.M., Kivisäkk, P. & Kidd, G., 2003. Three or more routes for leukocyte migration into the central nervous system. *Nature Reviews. Immunology*, 3(7), pp.569-581.

Rao, R.V. et al., 2002. Coupling endoplasmic reticulum stress to the cell death program. An Apaf-1-independent intrinsic pathway. *The Journal of Biological Chemistry*, 277(24), pp.21836-21842.

Richardson, J.A. & Burns, D.K., 2002. Mouse models of Alzheimer's disease: a quest for plaques and tangles. *ILAR Journal / National Research Council, Institute of Laboratory Animal Resources*, 43(2), pp.89-99.

Rio-Hortega, P del, 1932. Microglia. In *Cytology & Cellular Pathology of the Nervous System*. Hocker, New York, pp. 481-534.

Rubel, C. et al., 2002. Soluble fibrinogen modulates neutrophil functionality through the activation of an extracellular signal-regulated kinase-dependent pathway. *Journal of Immunology (Baltimore, Md.: 1950)*, 168(7), pp.3527-3535.

Rutkowski, D.T. & Hegde, R.S., 2010. Regulation of basal cellular physiology by the homeostatic unfolded protein response. *The Journal of Cell Biology*, 189(5), pp.783 - 794.

Ryu, E.J. et al., 2002. Endoplasmic reticulum stress and the unfolded protein response in cellular models of Parkinson's disease. *The Journal of Neuroscience: The Official Journal of the Society for Neuroscience*, 22(24), pp.10690-10698.

Ryu, J.K. & McLarnon, J.G., 2009. A leaky blood-brain barrier, fibrinogen infiltration and microglial reactivity in inflamed Alzheimer's disease brain. *Journal of Cellular and Molecular Medicine*, 13(9A), pp.2911-2925.

Sagare, A. et al., 2007. Clearance of amyloid-[beta] by circulating lipoprotein receptors. *Nature Medicine*, 13(9), pp.1029-1031.

Saido, T., Sorimachi, H. & Suzuki, K., 1994. Calpain: new perspectives in molecular diversity and physiological- pathological involvement. *The FASEB Journal*, 8(11), pp.814 -822.

Saijo, K. et al., 2009. A Nurr1/CoREST Pathway in Microglia and Astrocytes Protects Dopaminergic Neurons from Inflammation-Induced Death. *Cell*, 137(1), pp.47-59.

Saleh, M. et al., 2006. Enhanced bacterial clearance and sepsis resistance in caspase-12-deficient mice. *Nature*, 440(7087), pp.1064-1068.

Salińska, E., Danysz, W. & Łazarewicz, J.W., 2005. The role of excitotoxicity in neurodegeneration. *Folia Neuropathologica / Association of Polish Neuropathologists and Medical Research Centre, Polish Academy of Sciences*, 43(4), pp.322-339.

Salminen, A. et al., 2009. ER stress in Alzheimer's disease: a novel neuronal trigger for inflammation and Alzheimer's pathology. *Journal of Neuroinflammation*, 6, p.41.

Sandoval, K.E. & Witt, K.A., 2008. Blood-brain barrier tight junction permeability and ischemic stroke. *Neurobiology of Disease*, 32(2), pp.200-219.

Sanges, D. & Marigo, V., 2006. Cross-talk between two apoptotic pathways activated by endoplasmic reticulum stress: differential contribution of caspase-12 and AIF. *Apoptosis*, 11(9), pp.1629-1641.

Santacruz, K. et al., 2005. Tau suppression in a neurodegenerative mouse model improves memory function. *Science (New York, N.Y.)*, 309(5733), pp.476-481.

Sappino, A.P. et al., 1993. Extracellular proteolysis in the adult murine brain. *The Journal of Clinical Investigation*, 92(2), pp.679-685.

Sato, S. et al., 2005. Essential function for the kinase TAK1 in innate and adaptive immune responses. *Nature Immunology*, 6(11), pp.1087-1095.

Saura, J., 2007. Microglial cells in astroglial cultures: a cautionary note. *Journal of Neuroinflammation*, 4, p.26.

Sawada, M., Imamura, K. & Nagatsu, T., 2006. Role of cytokines in inflammatory process in Parkinson's disease. *Journal of Neural Transmission. Supplementum*, (70), pp.373-381.

Saxena, S., Cabuy, E. & Caroni, P., 2009. A role for motoneuron subtype-selective ER stress in disease manifestations of FALS mice. *Nature Neuroscience*, 12(5), pp.627-636.

Saxena, S. & Caroni, P., 2011. Selective Neuronal Vulnerability in Neurodegenerative Diseases: from Stressor Thresholds to Degeneration. *Neuron*, 71(1), pp.35-48.

Schachtrup, C. et al., 2007. Fibrinogen inhibits neurite outgrowth via beta 3 integrin-mediated phosphorylation of the EGF receptor. *Proceedings of the National Academy of Sciences of the United States of America*, 104(28), pp.11814-9.

Schachtrup, C. et al., 2010. Fibrinogen triggers astrocyte scar formation by promoting the availability of active TGF-beta after vascular damage. *The Journal of Neuroscience: The Official Journal of the Society for Neuroscience*, 30(17), pp.5843-5854.

Schiefer, J. et al., 1999. Microglial motility in the rat facial nucleus following peripheral axotomy. *Journal of Neurocytology*, 28(6), pp.439-453.

Schneemann, M. & Schoeden, G., 2007. Macrophage biology and immunology: man is not a mouse. *Journal of Leukocyte Biology*, 81(3), p.579.

Schulz, B. et al., 2007. β-Amyloid (Aβ40, Aβ42) binding to modified LDL accelerates macrophage foam cell formation. *Biochimica et Biophysica Acta (BBA) - Molecular and Cell Biology of Lipids*, 1771(10), pp.1335-1344.

Schummers, J., Yu, H. & Sur, M., 2008. Tuned responses of astrocytes and their influence on hemodynamic signals in the visual cortex. *Science (New York, N.Y.)*, 320(5883), pp.1638-1643.

Schuurs, A.H.W.M. & Van Weemen, B.K., 1977. Enzyme-immunoassay. *Clinica Chimica Acta*, 81(1), pp.1-40.

Seal, R.P. & Edwards, R.H., 2006. Functional implications of neurotransmitter co-release: glutamate and GABA share the load. *Current Opinion in Pharmacology*, 6(1), pp.114-119.

Sherer, T.B. et al., 2003. Subcutaneous Rotenone Exposure Causes Highly Selective Dopaminergic Degeneration and alpha-Synuclein Aggregation. *Experimental Neurology*, 179(1), pp.9-16.

Shi, Y., 2002. Mechanisms of caspase activation and inhibition during apoptosis. *Molecular Cell*, 9(3), pp.459-470.

Shields, D.C. et al., 1998. Increased calpain expression in activated glial and inflammatory cells in experimental allergic encephalomyelitis. *Proceedings of the National Academy of Sciences of the United States of America*, 95(10), pp.5768-5772.

Simón-Sánchez, J. et al., 2009. Genome-wide association study reveals genetic risk underlying Parkinson's disease. *Nature Genetics*, 41(12), pp.1308-1312.

Slee, E.A. et al., 1999. Ordering the Cytochrome c–initiated Caspase Cascade: Hierarchical Activation of Caspases-2, -3, -6, -7, -8, and -10 in a Caspase-9–dependent Manner. *The Journal of Cell Biology*, 144(2), pp.281-292.

Smiley, S.T., King, J.A. & Hancock, W.W., 2001. Fibrinogen Stimulates Macrophage Chemokine Secretion Through Toll-Like Receptor 4. *Journal of Immunology*, 167(5), pp.2887-2894.

Smith, E.B. et al., 1992. Fibrinogen/fibrin in Atherogenesis. *European Journal of Epidemiology*, 8, pp.83-87.

Smith, R.G. et al., 1994. Cytotoxicity of immunoglobulins from amyotrophic lateral sclerosis patients on a hybrid motoneuron cell line. *Proceedings of the National Academy of Sciences of the United States of America*, 91(8), pp.3393-3397.

Smith, W.W. et al., 2005. Endoplasmic reticulum stress and mitochondrial cell death pathways mediate A53T mutant alpha-synuclein-induced toxicity. *Human Molecular Genetics*, 14(24), pp.3801-3811.

Sofroniew, M.V. & Vinters, H.V., 2010. Astrocytes: biology and pathology. *Acta Neuropathologica*, 119(1), pp.7-35.

Sokka, A.-L. et al., 2007. Endoplasmic reticulum stress inhibition protects against excitotoxic neuronal injury in the rat brain. *The Journal of Neuroscience: The Official Journal of the Society for Neuroscience*, 27(4), pp.901-908.

Spillson, A.B. & Russell, J.W., 2003. Metabotropic glutamate receptor regulation of neuronal cell death. *Experimental Neurology*, 184 Suppl 1, pp.S97-105.

Stauffer, S.R., 2011. Progress toward Positive Allosteric Modulators of the Metabotropic Glutamate Receptor Subtype 5 (mGlu5). *ACS Chemical Neuroscience*, 2(8), pp.450-470.

Streit, W.J., 1990. An improved staining method for rat microglial cells using the lectin from Griffonia simplicifolia (GSA I-B4). *Journal of Histochemistry and Cytochemistry*, 38(11), pp.1683-1686.

Streit, W.J., 2004. Microglia and Alzheimer's disease pathogenesis. *Journal of Neuroscience Research*, 77(1), pp.1-8.

Streit, W.J., 2006. Microglial senescence: does the brain's immune system have an expiration date? *Trends in Neurosciences*, 29(9), pp.506-510.

Strick, P.L., Dum, R.P. & Fiez, J.A., 2009. Cerebellum and nonmotor function. *Annual Review of Neuroscience*, 32, pp.413-434.

Sun, X.J. et al., 1999. Insulin-induced insulin receptor substrate-1 degradation is mediated by the proteasome degradation pathway. *Diabetes*, 48(7), pp.1359-1364.

Suzuki, N. et al., 1994. An increased percentage of long amyloid beta protein secreted by familial amyloid beta protein precursor (beta APP717) mutants. *Science*, 264(5163), pp.1336 -1340.

Swanson, C.J. et al., 2005. Metabotropic glutamate receptors as novel targets for anxiety and stress disorders. *Nature Reviews. Drug Discovery*, 4(2), pp.131-144.

Szegezdi, E., Fitzgerald, U. & Samali, A., 2003. Caspase-12 and ER-stress-mediated apoptosis: the story so far. *Annals of the New York Academy of Sciences*, 1010, pp.186-194.

Szegezdi, E. et al., 2006. Mediators of endoplasmic reticulum stress-induced apoptosis. *EMBO Reports*, 7(9), pp.880-885.

Tabas, I. et al., 2009. Macrophage Apoptosis in Advanced Atherosclerosis. *Annals of the New York Academy of Sciences*, 1173, p.E40-E45.

Takahashi, Kazutoshi et al., 2007. Induction of pluripotent stem cells from adult human fibroblasts by defined factors. *Cell*, 131(5), pp.861-872.

Takano, Y. et al., 2007. Suppression of cytokine response by GATA inhibitor K-7174 via unfolded protein response. *Biochemical and Biophysical Research Communications*, 360(2), pp.470-475.

Takeuchi, O. & Akira, S., 2010. Pattern Recognition Receptors and Inflammation. *Cell*, 140(6), pp.805-820.

Tanner, C.M. & Aston, D.A., 2000. Epidemiology of Parkinson's disease and akinetic syndromes. *Current Opinion in Neurology*, 13(4), pp.427-430.

Tanzi, R E, Moir, R.D. & Wagner, S.L., 2004. Clearance of Alzheimer's Abeta peptide: the many roads to perdition. *Neuron*, 43(5), pp.605-608.

Tanzi, R.E. & Bertram, L., 2005. Twenty years of the Alzheimer's disease amyloid hypothesis: a genetic perspective. *Cell*, 120(4), pp.545-555.

Tarkowski, E. et al., 1999. Intracerebral production of tumor necrosis factor-alpha, a local neuroprotective agent, in Alzheimer disease and vascular dementia. *Journal of Clinical Immunology*, 19(4), pp.223-230.

Tartaglia, L.A., Pennica, D. & Goeddel, D.V., 1993. Ligand passing: the 75-kDa tumor necrosis factor (TNF) receptor recruits TNF for signaling by the 55-kDa TNF receptor. *The Journal of Biological Chemistry*, 268(25), pp.18542-18548.

Taylor, D L et al., 2002. Activation of group II metabotropic glutamate receptors underlies microglial reactivity and neurotoxicity following stimulation with chromogranin A, a peptide up-regulated in Alzheimer's disease. *Journal of Neurochemistry*, 82(5), pp.1179-1191.

Taylor, D.L, Diemel, L.T & Pocock, J.M., 2003. Activation of microglial group III metabotropic glutamate receptors protects neurons against microglial neurotoxicity. *The Journal of Neuroscience*, 23(6), pp.2150-60.

Taylor, D.L. et al., 2005. Stimulation of Microglial Metabotropic Glutamate Receptor mGlu2 Triggers Tumor Necrosis Factor-alpha-Induced Neurotoxicity in Concert with Microglial-Derived Fas Ligand. *The Journal of Neuroscience*, 25(11), pp.2952-2964.

von Tell, D., Armulik, A. & Betsholtz, C., 2006. Pericytes and vascular stability. *Experimental Cell Research*, 312(5), pp.623-629.

Terro, F. et al., 2002. Neurons overexpressing mutant presenilin-1 are more sensitive to apoptosis induced by endoplasmic reticulum-Golgi stress. *Journal of Neuroscience Research*, 69(4), pp.530-539.

Thal, D.R., Griffin, W.S.T. & Braak, H., 2008. Parenchymal and vascular Abeta-deposition and its effects on the degeneration of neurons and cognition in Alzheimer's disease. *Journal of Cellular and Molecular Medicine*, 12(5B), pp.1848-1862.

Thiele, D., Kurosaka, M. & Lipsky, P., 1983. Phenotype of the accessory cell necessary for mitogen-stimulated T and B cell responses in human peripheral blood: delineation by its

sensitivity to the lysosomotropic agent, L-leucine methyl ester. *Journal of Immunology*, 131(5), pp.2282-2290.

Timmann, D. et al., 2010. The human cerebellum contributes to motor, emotional and cognitive associative learning. A review. *Cortex; a Journal Devoted to the Study of the Nervous System and Behavior*, 46(7), pp.845-857.

Tobiume, K. et al., 2001. ASK1 is required for sustained activations of JNK/p38 MAP kinases and apoptosis. *EMBO Reports*, 2(3), pp.222-228.

de la Torre, J C, 2002. Alzheimer disease as a vascular disorder: nosological evidence. *Stroke; a Journal of Cerebral Circulation*, 33(4), pp.1152-1162.

de la Torre, J.C., 2004. Is Alzheimer's disease a neurodegenerative or a vascular disorder? Data, dogma, and dialectics. *Lancet Neurology*, 3(3), pp.184-190.

de la Torre, J.C., 2006. How do heart disease and stroke become risk factors for Alzheimer's disease? *Neurological Research*, 28(6), pp.637-644.

Tosello-Trampont, A.C., Brugnera, E. & Ravichandran, K.S., 2001. Evidence for a conserved role for CRKII and Rac in engulfment of apoptotic cells. *The Journal of Biological Chemistry*, 276(17), pp.13797-13802.

Trapp, B.D. et al., 1998. Axonal transection in the lesions of multiple sclerosis. *The New England Journal of Medicine*, 338(5), pp.278-285.

Ugarova, T P & Yakubenko, V P, 2001. Recognition of fibrinogen by leukocyte integrins. *Annals of the New York Academy of Sciences*, 936, pp.368-85.

Unterberger, U. et al., 2006. Endoplasmic reticulum stress features are prominent in Alzheimer disease but not in prion diseases in vivo. *Journal of Neuropathology and Experimental Neurology*, 65(4), pp.348-357.

Vaisid, T., Barnoy, S. & Kosower, N.S., 2008. Calpastatin overexpression attenuates amyloid-beta-peptide toxicity in differentiated PC12 cells. *Neuroscience*, 156(4), pp.921-931.

van der Valk, P. & Amor, S., 2009. Preactive lesions in multiple sclerosis. *Current Opinion in Neurology*, 22(3), pp.207-213.

Vegeto, E. et al., 2001. Estrogen Prevents the Lipopolysaccharide-Induced Inflammatory Response in Microglia. *The Journal of Neuroscience*, 21(6), pp.1809 -1818.

Venero, J L et al., 2011. The executioners sing a new song: killer caspases activate microglia. *Cell Death and Differentiation*. Available at: http://www.ncbi.nlm.nih.gov/pubmed/21836616 [Accessed September 2, 2011].

Venters, H.D. et al., 1999. A new mechanism of neurodegeneration: a proinflammatory cytokine inhibits receptor signaling by a survival peptide. *Proceedings of the National Academy of Sciences of the United States of America*, 96(17), pp.9879-9884.

Verkhratsky, A. & Butt, A., 2007. *Glial Neurobiology* 1st ed., Wiley.

Vlad, S.C. et al., 2008. Protective effects of NSAIDs on the development of Alzheimer disease. *Neurology*, 70(19), pp.1672-1677.

Wajant, H., Pfizenmaier, K. & Scheurich, P., 2003. Tumor necrosis factor signaling. *Cell Death and Differentiation*, 10(1), pp.45-65.

Wang, H.-Q. & Takahashi, Ryosuke, 2007. Expanding insights on the involvement of endoplasmic reticulum stress in Parkinson's disease. *Antioxidants & Redox Signaling*, 9(5), pp.553-561.

Watanabe, K. & Jaffe, E.A., 1993. Comparison of the potency of various serotypes of E. coli lipopolysaccharides in stimulating PGI2 production and suppressing ace activity in cultured human umbilical vein endothelial cells. *Prostaglandins, Leukotrienes and Essential Fatty Acids*, 49(6), pp.955-958.

Watkins, T.A. et al., 2008. Distinct stages of myelination regulated by gamma-secretase and astrocytes in a rapidly myelinating CNS coculture system. *Neuron*, 60(4), pp.555-569.

Weggen, S., Rogers, M. & Eriksen, J., 2007. NSAIDs: small molecules for prevention of Alzheimer's disease or precursors for future drug development? *Trends in Pharmacological Sciences*, 28(10), pp.536-543.

Wei, Z. et al., 2008. Role of calpain and caspase in beta-amyloid-induced cell death in rat primary septal cultured neurons. *Neuropharmacology*, 54(4), pp.721-733.

Weinstein, J.R. et al., 2008. Lipopolysaccharide is a frequent and significant contaminant in microglia-activating factors. *Glia*, 56(1), pp.16-26.

Weydt, P. et al., 2004. Increased cytotoxic potential of microglia from ALS-transgenic mice. *Glia*, 48(2), pp.179-182.

Whitlock, B.B. et al., 2000. Differential roles for alpha(M)beta(2) integrin clustering or activation in the control of apoptosis via regulation of akt and ERK survival mechanisms. *The Journal of Cell Biology*, 151(6), pp.1305-20.

Wilkinson, B.L. & Landreth, G.E., 2006. The microglial NADPH oxidase complex as a source of oxidative stress in Alzheimer's disease. *Journal of Neuroinflammation*, 3, p.30.

Williams, K. et al., 1994. Activation of adult human derived microglia by myelin phagocytosis in vitro. *Journal of Neuroscience Research*, 38(4), pp.433-443.

Wolburg, H. et al., 2003. Localization of claudin-3 in tight junctions of the blood-brain barrier is selectively lost during experimental autoimmune encephalomyelitis and human glioblastoma multiforme. *Acta Neuropathologica*, 105(6), pp.586-592.

Wollmer, M.A. et al., 2001. ATP and adenosine induce ramification of microglia in vitro. *Journal of Neuroimmunology*, 115(1-2), pp.19-27.

Wong, K.T. et al., 2010. Association of fibrinogen with Parkinson disease in elderly Japanese-American men: a prospective study. *Neuroepidemiology*, 34(1), pp.50-54.

Woo, C.W. et al., 2009. Adaptive suppression of the ATF4-CHOP branch of the unfolded protein response by toll-like receptor signalling. *Nat Cell Biol*, 11(12), pp.1473-1480.

Wyss-Coray, T. & Mucke, L., 2002. Inflammation in neurodegenerative disease--a double-edged sword. *Neuron*, 35(3), pp.419-432.

Xu, G. et al., 2008. Plasma fibrinogen is associated with cognitive decline and risk for dementia in patients with mild cognitive impairment. *International Journal of Clinical Practice*, 62(7), pp.1070-1075.

Yabe, T., Wilson, D. & Schwartz, J.P., 2001. NFkappaB activation is required for the neuroprotective effects of pigment epithelium-derived factor (PEDF) on cerebellar granule neurons. *The Journal of Biological Chemistry*, 276(46), pp.43313-43319.

Yan, W. et al., 2002. Control of PERK eIF2α kinase activity by the endoplasmic reticulum stress-induced molecular chaperone P58IPK. *Proceedings of the National Academy of Sciences*, 99(25), pp.15920 -15925.

Yang, Y., Tian, S. et al., 2011a. Fibrinogen depleting agent batroxobin has a beneficial effect on experimental autoimmune encephalomyelitis. *Cellular and Molecular Neurobiology*, 31(3), pp.437-448.

Yang, C.N., Shiao, Y.J., et al., 2011b. Mechanism mediating oligomeric Aβ clearance by naïve primary microglia. *Neurobiology of Disease*, 42(3), pp.221-230.

Yu, J. et al., 2007. Induced pluripotent stem cell lines derived from human somatic cells. *Science (New York, N.Y.)*, 318(5858), pp.1917-1920.

Yuan, J et al., 1993. The C. elegans cell death gene ced-3 encodes a protein similar to mammalian interleukin-1 beta-converting enzyme. *Cell*, 75(4), pp.641-52.

Yuan, J., Lipinski, M. & Degterev, A., 2003. Diversity in the Mechanisms of Neuronal Cell Death. *Neuron*, 40(2), pp.401-413.

Zhang, D. et al., 2011. Microglial MAC1 receptor and PI3K are essential in mediating β-amyloid peptide-induced microglial activation and subsequent neurotoxicity. *Journal of Neuroinflammation*, 8(1), p.3.

Zhang, G. et al., 1997. Early detection of apoptosis using a fluorescent conjugate of annexin V. *BioTechniques*, 23(3), pp.525-531.

Zhang, K. & Kaufman, R.J., 2008. From endoplasmic-reticulum stress to the inflammatory response. *Nature*, 454(7203), pp.455-462.

Zhong, Z. et al., 2008. ALS-causing SOD1 mutants generate vascular changes prior to motor neuron degeneration. *Nature Neuroscience*, 11(4), pp.420-422.

Zhu, S. et al., 2002. Minocycline inhibits cytochrome c release and delays progression of amyotrophic lateral sclerosis in mice. *Nature*, 417(6884), pp.74-78.

Ziegler, U. & Groscurth, P., 2004. Morphological Features of Cell Death. *Physiology*, 19(3), pp.124 -128.

Zlokovic, B.V., 2005. Neurovascular mechanisms of Alzheimer's neurodegeneration. *Trends in Neurosciences*, 28(4), pp.202-208.

Zlokovic, B.V., 2008. The blood-brain barrier in health and chronic neurodegenerative disorders. *Neuron*, 57(2), pp.178-201.

9. Drug Glossary

Drug Name	Abbreviation	Action
2-Amino-5,6-dihydro-6-methyl-4H-1,3-thiazine hydrochloride	**AMT-HCl or AMT**	iNOS activity inhibitor
Apocynin	**APO**	NADPH oxidase inhibitor
1,2-*Bis*(2-aminophenoxy)ethane-*N*,*N*,*N*',*N*'-tetraacetic acid tetrakis(acetoxymethyl ester)	**BAPTA-AM or BAPTA**	Ca^{2+} chelator
Calpastatin	**Cal**	Calpain inhibitor
Anti-CD11b antibody	**CD11b**	CD11b receptor blocking antibody
3-Cyano-*N*-(1,3-diphenyl-1*H*-pyrazol-5-yl)benzamide	**CDPPB**	mGluR5 positive allosteric modulator (agonist; group I)
(2*S*,2'*R*,3'*R*)-2-(2',3'-Dicarboxycyclopropyl)glycine	**DCGIV**	Group II mGluR agonist
(*S*)-3,5-Dihydroxyphenylglycine	**DHPG**	Group I mGluR agonist
Fucoidan	**Fu**	Scavenger receptor A ligand
Hirudin	**Hi**	Thrombin activity inhibitor
Interferon-γ	**IFNγ**	Pro-inflammatory cytokine – activator of microglia
Ionomycin	**Ion**	Ca^{2+} ionophore
(L)-2-amino-4-phosphono-butyric acid	**L-AP4**	Group III mGluR agonist
Leucine-methyl-ester	**LME**	Lysosomatropic agent inducing toxicity in phagocytes
Lipopolysachharide	**LPS**	Classical microglial inflammatory activator
3-((2-Methyl-4-thiazolyl)ethynyl)pyridine	**MTEP**	mGluR5 antagonist
N-acetyl-L-aspartyl-L-glutamate	**NAAG**	mGluR3 agonist (group II)
PD98059	**PD**	ERK1/2 inhibitor

Phorbol 12-myristate 13-acetate	**PMA**	NADPH oxidase activator
Polymyxin B	**PMX**	LPS activity inhibitor
Salubrinal	**Sal**	ER stress inhibitor via eIF2α-associated pathways
SB203580	**SB**	P38 MAPK inhibitor
Staurosporine	**STS**	Inducer of the intrinsic pathway of apoptosis
Thapsigargin	**Th**	ER stress activator via inhibition of Ca^{2+}/ATPase
Thalidomide	**Thal**	TNFα synthesis inhibitor
Tunicamycin	**Tu**	ER stress activator via inhibition of *N*-glycosylation
Wortmannin	**Wort**	PI3K inhibitor
carbobenzoxy-Val-Ala-Asp(OME)-fluoromethylketone	**z-VAD-FMK or z-VAD**	Caspase-3/7 inhibitor
carbobenzoxy -Ala-Thr-Ala-Asp(OME)-fluoromethylketone	**z-ATAD-FMK or z-ATAD**	Caspase-12 inhibitor

10. List of Publications and Conferences

Publications

- Hirano, K., **Piers, T M.,** Searle, K L., Miller, N D., Rutter, A R., and Chapman P F. 2009. Procognitive 5-HT_6 antagonists in the rat forced swimming test: Potential therapeutic utility in mood disorders associated with Alzheimer's disease. *Life Sciences*. 10;84(15-16):558-62
- **Piers, T M.,** Heales, S J., and Pocock J M. 2011. Positive allosteric modulation of metabotropic glutamate receptor 5 down-regulates fibrinogen-activated microglia providing neuronal protection. *Neuroscience Letters. In Press*
- **Piers, T M.,** East, E., Sevastou, I G., Traeger, U., Tabrizi, S J., Heales, S J., and Pocock, J M. 2011. Fibrinogen triggers microglial activation and ER stress-mediated neurotoxicity. *Under Review: Neurobiology of Aging*

Conferences

- **Alzheimer's Research UK (ARUK) annual meeting, Leeds, March 2011**
  Invited to present my research, the talk was entitled:
  'Fibrinogen-induced neuronal apoptosis involves microglia and ER stress'
  A poster was also displayed on the same work
- **Department of Neuroinflammation MS Symposium, London, October 2010**
  Invited to present my research, the talk was entitled:
  'Identifying fibrinogen-mediated microglial signalling pathways leading to neuroinflammation and degeneration'
- **Queens Square Symposium, London, May 2010**
  Presented a poster entitled:
  'ER stress is potentially involved in fibrinogen-mediated neuronal apoptosis'
- **Society for Neuroscience Meeting, Chicago, October 2009**
  Presented a poster entitled:
  'Fibrin and fibrinogen contribute to neuron non-cell autonomous degeneration'
- **9th European Meeting on Glial Cells in Health and Disease, Paris, September 2009**
  Presented the poster above (S*f*N)
- **Blood brain barrier Symposium, Biopolis, Singapore, October 2007**